The morphology and evolution of adult head structures in Trichoptera (Insecta)

Dissertation

zur Erlangung des akademischen Grades

doctor rerum naturalium

(Dr. rer. nat.)

vorgelegt dem

Fach-Promotionsausschuss Biologie

an der Fakultät für Mathematik, Informatik und Naturwissenschaften

Fachbereich Biologie

der Universität Hamburg

von

M.Sc. (Biologie) Martin Kubiak

geboren am 14. August 1984 in Wolmirstedt

Hamburg

2016

Gutachter:

1. Prof. Dr. Susanne Dobler

(Universität Hamburg)

2. Dr. Frank Friedrich

(Universität Hamburg)

Tag der Einreichung: 13. Oktober 2016

Tag der Disputation: 18. November 2016

Table of Contents

1. Introduction[1] 1
1.1. General appearance, biology and ecology of Trichoptera 1
1.2. Systematics and phylogeny of Trichoptera 7
1.3. Morphological studies of Trichoptera 11
1.4. Aims of the study 12

2. Material and methods 15
2.1. List of taxa examined 15
2.2. Morphological techniques 15
2.2.1. Synchrotron radiation based micro-computer tomography (SR-µCT) 15
2.2.2. Confocal laser scanning microscopy (CLSM) 17
2.2.3. Scanning electron microscopy (SEM) 17
2.2.4. Light microscopy imaging 17
2.2.5. Histology 18
2.2.6. Computer-based 3D-reconstruction 19
2.3. Illustration 20
2.4. Terminology 20
2.5. Phylogenetic analyses 20

3. Results 21
3.1. The adult head morphology of *Philopotamus ludificatus* McLachlan, 1878 * ... 21
3.1.1. General appearance 21
3.1.2. Head capsule 21
3.1.3. Tentorium 24
3.1.4. Eyes 25
3.1.5. Antenna 26
3.1.6. Labrum 28
3.1.7. Mandible 28
3.1.8. Maxilla 29
3.1.9. Labium 33
3.1.10. Epipharynx and hypopharynx 37
3.1.11. Haustellum 40
3.1.12. Salivarium 41
3.1.13. Cephalic food tract 42

3.1.14. Central nervous system (CNS) 42

3.1.15. Stomatogastric nervous system 44

3.1.16. Hypocerebral complex 44

3.1.17. Circulatory system 47

3.1.18. Tracheal system 48

3.1.19. Fat body 48

3.2. Comparative analysis of adult head structures 48

3.2.1. Tentorium 48
- 3.2.1.1. General appearance 48
- 3.2.1.2. Anterior tentorial arms 48
- 3.2.1.3. Posterior tentorial arms 50
- 3.2.1.4. Dorsal tentorial arms 50

3.2.2. Antenna 51
- 3.2.2.1. General appearance 51
- 3.2.2.2. Extrinsic musculature of the antenna 55

3.2.3. Anteclypeolabrum 58
- 3.2.3.1. General appearance 58
- 3.2.3.2. Musculature of the anteclypeolabrum 58

3.2.4. Epipharynx and hypopharynx 58
- 3.2.4.1. General appearance 58
- 3.2.4.2. Musculature of epipharynx and hypopharynx 59

3.2.5. Mandible 60
- 3.2.5.1. General appearance 60
- 3.2.5.2. Musculature of the mandible 60

3.2.6. Cephalic food tract 62
- 3.2.6.1. General appearance 62
- 3.2.6.2. Musculature of the cephalic food tract 62

3.2.7. Maxilla 64
- 3.2.7.1. General appearance 64
- 3.2.7.2. Musculature of the maxilla 66

3.2.8. Labium 67
- 3.2.8.1. General appearance 67
- 3.2.8.2. Musculature of the labium 67

3.2.9. Salivarium 69
- 3.2.9.1. General appearance 69
- 3.2.9.2. Musculature of the salivarium 69

3.2.10. Haustellum 69
- 3.2.10.1. General appearance 69
- 3.2.10.2. Haustellar surface structures 71

3.3. Morphology of the pupal mouthparts in Trichoptera 71

3.3.1. General appearance 71

3.3.2. Anteclypeolabrum 72

3.3.3. Mandible 74
3.4. Phylogenetically relevant characters 76
3.4.1. Adult head characters....76
3.4.2. Pupal head characters....85
3.5. Phylogenetic evaluation....86
3.5.1. Cladistic analyses of adult and pupal head characters 86
3.5.2. Character mapping on phylogenetic hypotheses 91
4. Discussion 104
4.1. Morphology and terminology * 104
4.1.1. Frontopostclypeus 104
4.1.2. Anteclypeolabrum....105
4.1.3. Gena and occiput 107
4.1.4. Tentorium....107
4.1.5. Setal warts....108
4.1.6. Photoreceptors 108
4.1.7. Antenna 109
4.1.8. Mandible 109
4.1.9. Preoral cavity and mouth opening 110
4.1.10. Maxilla.... 111
4.1.11. Haustellum....112
4.1.12. Salivarium 112
4.1.13. Labium....113
4.1.14. Nervous system....113
4.2. Phylogenetic implications.... 114
4.3. Ground plan reconstruction.... 119
4.4. Evolution of head structures in Trichoptera....123
5. Summary 125
6. Zusammenfassung 127
7. References....131
8. Acknowledgements 143

Table of Figures

Figure 1: Merolimnic life cycle of *Halesus radiatus* (Curtis, 1834) (Limnephilidae) 2

Figure 2: Life history stages of Trichoptera (larva, pupa, and adult of Limnephilidae) 3

Figure 3: Postulated hypotheses of higher level phylogenetic relationships of Trichoptera 8

Figure 4: Head of *Philopotamus ludificatus* McLachlan, 1878, anterior view, light-microscopy 22

Figure 5: Head of *Philopotamus ludificatus* McLachlan, 1878, lateral and posterior view, light-microscopy 23

Figure 6: The tentorium of *Philopotamus ludificatus* McLachlan, 1878, 3D-reconstruction based on SR-μCT data 25

Figure 7: Details of head capsule of *Philopotamus ludificatus* McLachlan, 1878, scanning electron microscopy 25

Figure 8: Compound eye and immaginal stemma of *Philopotamus ludificatus* McLachlan, 1878, histological cross-section 26

Figure 9: The antenna of *Philopotamus ludificatus* McLachlan, 1878, scanning electron microscopy 27

Figure 10: Mouthparts of *Philopotamus ludificatus* McLachlan, 1878, scanning electron microscopy 29

Figure 11: Dorsal view on mouthparts of *Philopotamus ludificatus* McLachlan, 1878, scanning electron microscopy 30

Figure 12: The galeolacinia of *Philopotamus ludificatus* McLachlan, 1878, histological cross-section 31

Figure 13: Head of *Philopotamus ludificatus* McLachlan, 1878, posterior view, line drawing based on SR-μCT data 32

Figure 14: Mouthparts of *Philopotamus ludificatus* McLachlan, 1878, scanning electron microscopy 33

Figure 15: Head of *Philopotamus ludificatus* McLachlan, 1878, anterior and posterior view, 3D-reconstruction based on SR-μCT data 35

Figure 16: Head of *Philopotamus ludificatus* McLachlan, 1878, parasagittal and sagittal section, 3D-reconstruction based on SR-μCT data 36

Figure 17: Head of *Philopotamus ludificatus* McLachlan, 1878, lateral view, scanning electron microscopy 37

Figure 18: Internal head structures of *Philopotamus ludificatus* McLachlan, 1878, histological cross-sections 39

Figure 19: Details of internal head structures of *Philopotamus ludificatus* McLachlan, 1878, histological cross-sections 41

Figure 20: Nervous system and gut with attached musculature of *Philopotamus ludificatus* McLachlan, 1878, 3D-reconstruction based on SR-μCT data 43

Figure 21: Structures of the antennal base of adult of *Micropterix calthella* (Linnaeus, 1761) (Lepidoptera), based on confocal laser scanning microscopy 51

Figure 22: Structures of the antennal base in adult trichopterans, volume rendering based on confocal laser scanning microscopy..53

Figure 23: Extrinsic antennal musculature of adult trichopterans, line drawing based on SR-µCT data 55

Figure 24: Extrinsic musculature of the adult antenna of *Limnephilus flavicornis* (Fabricius, 1787) (Limnephilidae), line drawing based on SR-µCT data.............55

Figure 25: Head of *Limnephilus flavicornis* (Fabricius, 1787), anterior view, scanning electron microscopy 70

Figure 26: The haustellum of *Limnephilus flavicornis* (Fabricius, 1787), anterior view, scanning electron microscopy...71

Figure 27: Head of the pharate adult of *Philopotamus ludificatus* McLachlan, 1878, anterior view, light-microscopy 72

Figure 28: Head of the pharate adult of *Philopotamus ludificatus* McLachlan, 1878, anterior view, 3D-reconstruction based on SR-µCT data 73

Figure 29: The pupal mandible of *Rhyacophila fasciata* Hagen, 1859 and *Limnephilus flavicornis* (Fabricius, 1787), confocal laser scanning microscopy 74

Figure 30: Pupal and enclosed adult mandible of *Philopotamus ludificatus* McLachlan, 1878, 3D-reconstruction based on SR-µCT data 75

Figure 31: The pupal mandible of Trichoptera, line drawing based on volume rendering of confocal laser scanning microscopy 75

Figure 32: Phylogenetic tree obtained in the cladistic analysis of the adult and pupal head character data set 88

Figure 33: Majority-rule consensus tree obtained in the cladistics analysis of the adult and pupal head character data set...88

Figure 34: Phylogenetic hypothesis after Wiggins & Wichard (1989): Spicipalpia form the sistergroup of a clade comprising Annulipalpia and Integripalpia 90

Figure 35: Phylogenetic hypothesis after Weaver & Morse (1986): Spicipalpia and Annulipalpia form the sister group of Integripalpia 90

Figure 36: Phylogenetic hypothesis after Kjer et al. (2002): Spicipalpia and Integripalpia form the sister group of Annulipalpia 92

Figure 37: Phylogenetic hypothesis after Ross (1967): Paraphyletic ‘Spicipalpia’ and Integripalpia form the sister group of Annulipalpia 92

Figure 38: Phylogenetic hypothesis after Kjer et al. (2016): Paraphyletic ‘Spicipalpia’ and Integripalpia form the sister group of Annulipalpia 94

Figure 39: Phylogenetic hypothesis after Schmid (1989): Paraphyletic ‘Spicipalpia’ and Annulipalpia form the sister group of Integripalpia 94

Figure 40: Phylogenetic hypothesis after Malm et al. (2013): Paraphyletic ‘Spicipalpia’ as sister group to a clade comprising Annulipalpia and Integripalpia..................96

Figure 41: Phylogenetic hypothesis after Frania & Wiggins (1997): Polyphyletic ‘Spicipalpia’ 96

List of tables

Table 1: The recent systematics of Trichoptera with numbers of extant genera and species as well as their global distribution 5-6

Table 2: Taxon sampling and applied techniques 16

Table 3: Summary of SR-µCT data acquisition at beamlines BW2 and P05 at the German Electron Synchrotron Facility (DESY) Hamburg 18

Table 4: Terminology and homology of the trichopteran adult head musculature........45-47

Table 5: The tentorium of adult Trichoptera 49-50

Table 6: External morphological features of the adult antenna of Trichoptera..................52

Table 7: Antennal musculature in the adult head of Trichoptera......................................56

Table 8: Epipharyngeal and hypopharyngeal muscles in the adult head of Trichoptera...61

Table 9: Musculature of the food tract in the adult head of Trichoptera 63

Table 10: Musculature of the trichopteran maxilla 65

Table 11: Musculature of the trichopteran labium and salivarium.......................................68

Table 12: Overview of external features of the trichopteran pupal head.............................72

Table 13: Overview of the morphological terminology applied to sclerites of the adult head capsule and to selected mouthpart structures 106

1. Introduction[1]

1.1. General appearance, biology and ecology of Trichoptera

The taxon Trichoptera (caddisflies) comprises approximately 15,000 species (Holzenthal et al. 2011) in 49 extant families (Tab. 1) and represents one of the most species-rich insect groups with primarily aquatic larvae (Grimaldi & Engel 2005; Malm et al. 2013). Within the mega-diverse Endopterygota (= Holometabola), Trichoptera is the only order in which both, the larval development and the pupation take place almost exclusively submerged (Wichard et al. 1995) (Fig. 1A–F). However, a few exceptions from the general pattern occur in the integripalpian families Limnephilidae and Apataniidae, i.e., in the terrestrial limnephilid genus *Enoicyla* (Europe) and the apataniid genus *Manophylax* (North America) which pupate in the semiaquatic terrestrial habitat of their larvae (e.g., Malicky 1973; Chuluunbat et al. 2010; Wichard & Wagner 2015). Furthermore, Flint (1958) reported larvae of the North American limnephilid species *Ironoquia parvula* (Banks, 1900) leaving their aquatic habitat to pupate onshore.

In general, caddisflies are merolimnic insects (Fig. 1) which means that they inhabit freshwater biotopes. Few exceptions, e.g., the family Chathamiidae can be found in marine costal waterbodies (i.e., marine intertidal rock pools) in eastern Australia and New Zealand (e.g., Riek 1976; Winterbourn & Anderson 1980; De Moor & Ivanov 2008). The merolimnic life cycle of Trichoptera also includes a terrestrial adult life stage (Fig. 1I). Adult caddisflies resemble small moths, with brown, grey, yellow or even black body and wing color shades predominating. In contrast to Lepidoptera which possess scales on their wings, the two wing pairs of caddisflies are usually covered by a very dense, regular vestiture of setae inducing the inconspicuous color patterns (Fig. 2C). Kirby (1815) first introduced the scientific group name ‘Trichoptera’ based on this typical feature of adult caddisflies (i.e., from the Greek words θρίξ – thrix, ‘hair’, and πτερόν – pteron, ‘wing’). Additionally, adult caddisflies are characterized by roof-like folded wings in resting position and a specifically modified structure of the mouth parts, the haustellum, which is used for the uptake of liquids (e.g., Crichton 1957; Holzenthal et al. 2007a). The terrestrial adult stage plays an important role in terms of dispersal, swarming behavior, mating, and oviposition in the life cycle of caddisflies (e.g., Ehlert 2009). Usually adults live only for a few weeks (e.g., Barnard & Ross 2012). Exceptions occur in species of the family Limnephilidae which inhabit temporal water bodies and live up to several weeks or even a few months (e.g., Hickin 1967). Females of these species are characterized by a seasonal imaginal diapause allowing them to colonize temporal water bodies in the larval stage which usually dry out during the summer months (e.g., Novak & Sehnal 1963; Wichard 1989). After mating the egg clutches are deposited by the females directly in (e.g., Hydropsychidae, Rhyacophilidae, Brachycentridae, Phryganeidae, and Leptoceridae)

---

[1] Some chapters of the present study were already published in Kubiak, M., Beckmann, F., Friedrich, F. (2015): The adult head of the annulipalpian caddisfly *Philopotamus ludificatus* McLachlan, 1878 (Philopotamidae), mouthpart homologies, and implications on the ground plan of Trichoptera. Arthropod Systematics & Phylogeny 73 (3): 351–384. These sections are in the following marked by an asterisk (*) in the heading (see also Declaration of oath at the end of the thesis).

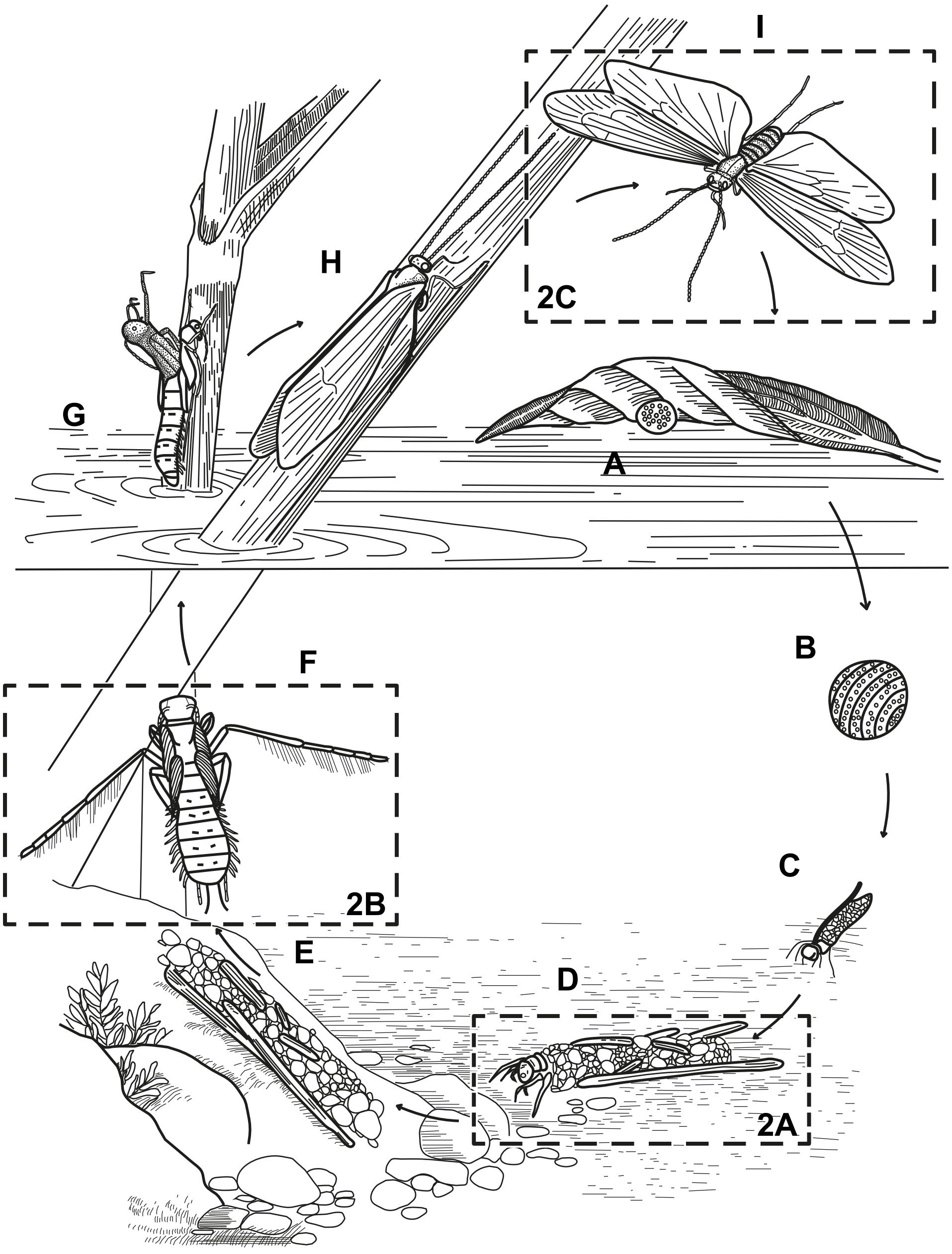

Figure 1: Merolimnic life cycle of *Halesus radiatus* (Curtis, 1834) (Integripalpia: Limnephilidae [true-case makers]). **A**: Gelatinous egg clutch above the water surface; **B**: egg clutch sinking to the bottom of the water body; **C**: first instar larva with larval shelter; **D**: fifth instar larva crawls to the waterside; **E**: pupation – pupal shelter near the waterside; **F**: pupa swimming actively to the water surface; **G**: eclosion of the pharate adult from the pupa in the riparian vegetation of the water body; **H**: imago in resting position with wings characteristically roof-like folded over the abdomen; **I**: female searching for a partner and oviposition site. (Redrawn after Moretti 1973)

or near by the potential aquatic habitat of the larvae, i.e., directly in the terrestrial vicinity like the riparian vegetation (e.g., Goeridae, most Limnephilidae; Fig. 1A) (Silvenius 1906; Ehlert 2009).

First instar larvae hatch after a time period of approximately 20 to 40 days in most species (fig. 2-6 in Wichard & Wagner 2015). In the postembryonic stage most species of caddisflies pass through five larval instars (Fig. 1C–E) (Malicky 1973; Waringer & Graf 2011). However, Becker (2011) demonstrated

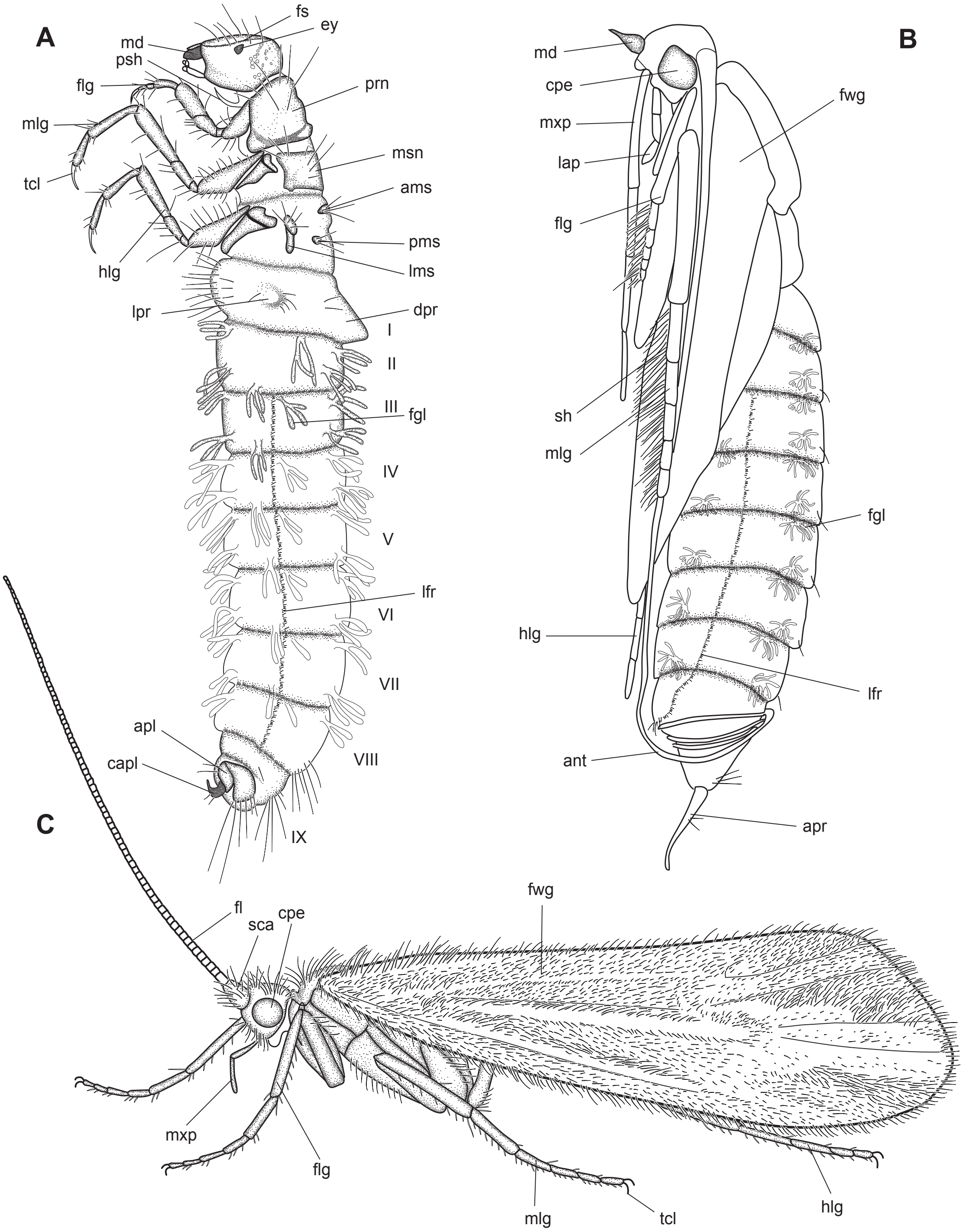

Figure 2: Life history stages of Trichoptera. **A**: Larva of *Halesochila taylori* (Banks, 1904) (Integripalpia-Limnephilidae); **B**: pupa of *Ceraclea* sp. (Integripalpia-Leptoceridae); **C**: adult of *Hesperophylax designatus* (Walker, 1852) (Integripalpia-Limnephilidae). Abbreviations: **ams** – anterior metadorsal sclerite, **ant** – antenna, **apl** – anal proleg, **apr** – anal process, **capl** – claw of anal proleg, **cpe** – compound eye, **dpr** – dorsal protuberance of 1st abdominal segment, **ey** – larval eye, **fgl** – filament gill, **fl** – flagellomere, **flg** – foreleg, **fs** – frontal suture, **fwg** – forewing, **hlg** – hindleg, **lap** – labial palp, **lfr** – lateral fringe, **lms** – lateral metadorsal sclerite, **lpr** – lateral protuberance of 1st abdominal segment, **md** – mandible, **mlg** – midleg, **msn** – mesonotum, **mxp** – maxillary palp, **pms** – posterior metadorsal sclerite, **prn** – pronotum, **psh** – prosternal horn, **sca** – scapus, **sh** – swimming hairs, **tcl** – tarsal claw, **I–IX** – number of abdominal segment. (Redrawn after Holzenthal et al. (2007a)) (Scales bars not given by Holzenthal et al. (2007a))

the presence of seven larval instars in the glossosomatid species *Agapetus fuscipes* Curtis, 1834. The number of larval instars is also multiplied in species of the integripalpian family Sericostomatidae (e.g., Resh et al. 1981; Wagner 1990).

Larvae of Trichoptera inhabit a broad variety of lentic (e.g., ponds, lakes, fens, and bogs) and lotic (e.g., springs, small creeks and rivers, streams) freshwater biotopes and differ remarkably in their ecological preferences (e.g., Mackay & Wiggins 1979; Graf et al. 2008). Consequently, caddisflies are well-established biological indicator organisms for water and habitat quality in freshwater ecosystems (e.g., Holzenthal et al. 2007a; De Moor & Ivanov 2008). Furthermore, caddisfly larvae play an important role in the decomposition of organic matter in aquatic habitats. Most species of the integripalpian family Limnephilidae for example are shredders of leaf litter (Wichard & Wagner 2015). According to Unzicker et al. (1982) five feeding types can be distinguished between the larvae of caddisflies. Beside the shredding habit of most limnephilids, other caddisfly species are passive filter feeders (e.g., Philopotamidae, Hydropsychidae), scrapers (e.g., Glossosomatidae), piercers (e.g., Hydroptilidae), or even predators (e.g., Rhyacophilidae).

In the aquatic food web the larvae of caddisflies represent an important food source for other aquatic invertebrates (e.g., larvae of Plecoptera or Coleoptera [Malicky 1973]), and especially for many species of freshwater fishes (e.g., Moretti et al. 1981) and water birds (e.g., Wiggins 2004). Adults are also an important food source for many bird and bat species (e.g., Malicky 1973).

Most species of Trichoptera construct portable cases (Integripalpia and the spicipalpian families Glossosomatidae and Hydroptilidae) or fixed retreats (Annulipalpia) in the larval life stage. Only representatives of the spicipalpian families Rhyacophilidae and Hydrobiosidae possess completely ‘free-living’ larvae due to their predaceous feeding style (e.g., Waringer & Graf 2011).

Caddisfly larvae are equipped with a pair of anal prolegs distinguishing their juvenile stages from those of any other aquatic insect group (e.g., Wallace et al. 2003; Fig. 2A). In contrast to their adults, larvae of Trichoptera possess well developed and functional mouth-parts. The larval body is divided into the heavily sclerotized head capsule, the thorax, and the mainly membranous abdomen which often bears abdominal gills (e.g., Holzenthal et al. 2007a; Fig. 2A). Generally, the larvae of caddisflies can be subdivided into two morphological subgroups. On the one hand larvae of case bearing species (e.g., Integripalpia) are characterized by a stout and almost cylindrical body shape (eruciform type) and an orthognathous head position (fig. 2-8a in Wichard & Wagner 2015; Fig. 2A). On the other hand most representatives of Annulipalpia and the ‘free-living’ spicipalpian families Rhyacophilidae and Hydrobiosidae possess larvae with a slender, elongated body (campodeid type) and a prognathous head position (fig. 2-8b in Wichard & Wagner 2015). Similar to caterpillars of the sister group Lepidoptera caddisfly larvae are equipped with strongly developed salivary glands which produce silk and enable the larvae of Trichoptera to build retreats or portable cases (see above; Fig. 1C–E) (Malicky 1973; Mackay & Wiggins 1979). This capability of silk production was a major driver in caddisfly diversification allowing for the development of an enormous array of morphological adaptations to the life in freshwater (e.g., De Moor & Ivanov 2008).

The larval stage is subsequently followed

Table 1: The following list shows the recent systematics of Trichoptera. Additionally, numbers of extant genera and species are given. The original distribution within the major biogeographical regions of the world of each of these families is also shown to illustrate their range (modified after Holzenthal et al. (2011) and De Moor & Ivanov (2008)). Abbreviations: **AT** – Afrotropical, **AU** – Australasian, **EP** – East Palearctic, **NA** – Nearctic, **nb.** – number, **NT** – Neotropical, **OL** – Oriental, **WP** – West Palearctic.

Suborder	Superfamily	Family	Nb. of genera	Nb. of species	Distribution
Annulipalpia	Philopotamoidea Stephens, 1829	Philopotamidae Stephens, 1829	19	1168	WP-EP-NA-AT-NT-OL-AU
Annulipalpia	Philopotamoidea Stephens, 1829	Stenopsychidae Martynov, 1924	3	94	EP-AT-NT-OL-AU
Annulipalpia	Psychomyioidea Walker, 1852	Dipseudopsidae Ulmer, 1904	5	114	WP-EP-NA-AT-OL-AU
Annulipalpia	Psychomyioidea Walker, 1852	Ecnomidae Ulmer, 1903	9	469	WP-EP-NA-AT-NT-OL-AU
Annulipalpia	Psychomyioidea Walker, 1852	Kambaitipsychidae Malicky, 1992	1	2	OL
Annulipalpia	Psychomyioidea Walker, 1852	Polycentropodidae Ulmer, 1903	16	806	WP-EP-NA-AT-NT-OL-AU
Annulipalpia	Psychomyioidea Walker, 1852	Pseudoneureclipsidae Ulmer, 1951	2	116	WP-EP-AT-OL
Annulipalpia	Psychomyioidea Walker, 1852	Psychomyiidae Walker, 1852	11	522	WP-EP-NA-AT-OL-AU
Annulipalpia	Psychomyioidea Walker, 1852	Xiphocentronidae Ross, 1949	7	172	EP-NA-AT-NT-OL
Annulipalpia	Hydropsychoidea Curtis, 1835	Hydropsychidae Curtis, 1835	37	1808	WP-EP-NA-AT-NT-OL-AU
'Spicipalpia'	Glossosomatoidea Wallengren, 1891	Glossosomatidae Wallengren, 1891	22	682	WP-EP-NA-AT-NT-OL-AU
'Spicipalpia'	Hydroptiloidea Stephens, 1836	Hydroptilidae Stephens, 1836	72	2124	WP-EP-NA-AT-NT-OL-AU
'Spicipalpia'	Hydroptiloidea Stephens, 1836	Ptilocolepidae Martynov, 1913	2	16	WP-EP-NA-OL
'Spicipalpia'	Rhyacophiloidea Stephens, 1836	Hydrobiosidae Ulmer, 1905	50	407	EP-NA-NT-OL-AU
'Spicipalpia'	Rhyacophiloidea Stephens, 1836	Rhyacophilidae Stephens, 1836	5	774	WP-EP-NA-OL-AU
Integripalpia	Leptoceroidea Leach, 1815	Atriplectidae Neboiss, 1977	4	6	AT-NT-AU
Integripalpia	Leptoceroidea Leach, 1815	Calamoceratidae Ulmer, 1905	8	182	WP-EP-NA-AT-NT-OL-AU
Integripalpia	Leptoceroidea Leach, 1815	Molannidae Wallengren, 1891	2	41	WP-EP-NA-OL
Integripalpia	Leptoceroidea Leach, 1815	Leptoceridae Leach, 1815	48	2020	WP-EP-NA-AT-NT-OL-AU
Integripalpia	Leptoceroidea Leach, 1815	Limnocentropodidae Tsuda, 1942	1	15	EP-OL
Integripalpia	Leptoceroidea Leach, 1815	Odontoceridae Wallengren, 1891	15	154	WP-EP-NA-NT-OL-AU
Integripalpia	Leptoceroidea Leach, 1815	Philorheithridae Mosely, 1936	9	30	NT-AU
Integripalpia	Leptoceroidea Leach, 1815	Kokiriidae McFarlane, 1964	6	15	NT-AU

Table 1 continued.

Suborder	Superfamily	Family	Nb. of genera	Nb. of species	Distribution
Integripalpia	Sericostomatoidea Stephens, 1836	Anomalopsychidae Flint, 1981	2	27	NT
Integripalpia	Sericostomatoidea Stephens, 1836	Antipodoeciidae Ross, 1967	1	1	AU
Integripalpia	Sericostomatoidea Stephens, 1836	Barbarochthonidae Scott, 1985	1	1	AT
Integripalpia	Sericostomatoidea Stephens, 1836	Beraeidae Wallengren, 1891	7	57	WP-EP-NA, AT
Integripalpia	Sericostomatoidea Stephens, 1836	Calocidae Ross, 1967	7	23	AU
Integripalpia	Sericostomatoidea Stephens, 1836	Chathamiidae Tillyard, 1925	2	5	AU
Integripalpia	Sericostomatoidea Stephens, 1836	Conoesucidae Ross, 1967	11	43	AU
Integripalpia	Sericostomatoidea Stephens, 1836	Helicophidae Mosely, 1953	9	44	NT-AU
Integripalpia	Sericostomatoidea Stephens, 1836	Helicopsychidae Ulmer, 1906	2	279	WP-EP-NA-AT-NT-OL-AU
Integripalpia	Sericostomatoidea Stephens, 1836	Hydrosalpingidae Scott, 1985	1	1	AT
Integripalpia	Sericostomatoidea Stephens, 1836	Petrothrincidae Scott, 1985	1	14	AT
Integripalpia	Sericostomatoidea Stephens, 1836	Sericostomatidae Stephens, 1836	19	107	WP-EP-NA-AT-NT-OL
Integripalpia	Tasimioidea Riek, 1968	Tasimiidae Riek, 1968	4	9	NT-AU
Integripalpia	Limnephiloidea Kolenati, 1848	Apataniidae Wallengren, 1886	21	203	WP-EP-NA-OL
Integripalpia	Limnephiloidea Kolenati, 1848	Goeridae Ulmer, 1903	11	180	WP-EP-NA-AT-OL-AU
Integripalpia	Limnephiloidea Kolenati, 1848	Limnephilidae Kolenati, 1848	99	880	WP-EP-NA-NT-OL-AU
Integripalpia	Limnephiloidea Kolenati, 1848	Rossianidae Gall, 1996	2	2	NA
Integripalpia	Limnephiloidea Kolenati, 1848	Thremmatidae Martynov, 1935	3	52	WP-EP-NA-OL
Integripalpia	Limnephiloidea Kolenati, 1848	Uenoidae Iwata, 1927	4	31	WP-EP-NA-OL
Integripalpia	Phryganeoidea Leach, 1815	Brachycentridae Ulmer, 1903	7	111	WP-EP-NA-OL
Integripalpia	Phryganeoidea Leach, 1815	Lepidostomatidae Ulmer, 1903	7	471	WP-EP-NA-AT-NT-OL
Integripalpia	Phryganeoidea Leach, 1815	Oeconesidae Tillyard, 1921	6	18	AU
Integripalpia	Phryganeoidea Leach, 1815	Phryganeidae Leach, 1815	17	84	WP-EP-NA-OL
Integripalpia	Phryganeoidea Leach, 1815	Phryganopsychidae Wiggins, 1959	1	4	EP-OL
Integripalpia	Phryganeoidea Leach, 1815	Pisuliidae Ross, 1967	2	19	AT
Integripalpia	Phryganeoidea Leach, 1815	Plectrotarsidae Mosely, 1953	3	5	AU

by the pupal stage which takes approximately two to four weeks in most caddisfly species (Wichard & Wagner 2015). The pupal stage is a quite critical period in the life of Trichoptera and other holometabolous insects. During this time the insect is mainly immobile and very susceptible to variations in several physical factors, especially in freshwater biotopes (e.g., oxygen content, osmosis). Therefore, many semiaquatic insect groups, as water beetles have to leave their larval habitat before pupation. In contrast, Trichoptera is the only taxon in which almost all representatives pupate submerged (Fig. 1F) (Hinton 1949; Wichard et al. 1995). Consequently, the caddisfly pupa shows several specific adaptations to life in freshwater. All trichopteran representatives construct pupal shelters enclosing the permeable (e.g., Hydropsychidae [Annulipalpia], Limnephilidae [Integripalpia]), or semipermeable silken pupal cocoon (e.g., Rhyacophilidae [‘Spicipalpia’]) (Wichard et al. 1995), which allows the trichopteran pupa to overcome osmotic limits of the aquatic environment. Furthermore, the caddisfly pupa is equipped with strong and functional mandibles (i.e., decticous pupa) enabling the pharate adult (i.e., imago enclosed by the pupal cuticle) to bite through the silken cocoon (Fig. 2B). Its body appendages are free (i.e., exarate), which means that wings and legs are not soldered to the body wall enabling the pupa of Trichoptera to swim actively to the water surface before eclosion (Fig. 1F) (Hinton 1946). The hatching and swimming activity of the pharate adult is supported by several morphological features of the pupa (e.g., fringes of long hairs along the legs, backwardly directed spines on some of the abdominal tergites) (Hinton 1949; Fig. 2B).

In summary, Trichoptera is one of the most species rich insect groups in freshwater ecosystems. The group has evolved a broad variety of adaptations to life in freshwater, which cover the larval and also the pupal life stages enabling Trichoptera to fill numerous ecological niches in limnic habitats. However, many underlying evolutionary processes and functional consequences of structural modifications within the trichopteran lineage are not fully understood until now.

1.2. Systematics and phylogeny of Trichoptera

Although Trichoptera and Lepidoptera differ remarkably in their live histories, both insect groups form one of the best supported sister group relationships in insect phylogeny (Hennig 1969: 298; Kristensen 1999; see also Misof et al. 2014). The monophyly of Amphiesmenoptera (i.e., Trichoptera + Lepidoptera) is well supported by several apomorphic characters (e.g., Hennig 1969; Kristensen 1981, 1991; Weaver 1984). Furthermore, Weaver (1984), Morse (1997), and Holzenthal et al. (2007a) provided several apomorphic characters which substantiate a monophyletic trichopteran lineage.

In contrast, the intraordinal relationships of the 49 extant families have been subject of discussion for decades (e.g., Ross 1956, 1967; Weaver 1984; Schmid 1989; Frania & Wiggins 1997; Kjer et al. 2002, 2016; Holzenthal et al. 2007b; Malm et al. 2013) (Fig. 3). Initially, Martynov (1924) subdivided the taxon Trichoptera into two major lineages, and termed them Annulipalpia (fixed-retreat makers) and Integripalpia (true-case makers).

Weaver (1984) recognized several morphological features (e.g., shape of adult maxillary palp, mobile feeding strategies of larvae) delineating the four families Rhyacophilidae, Hydrobiosidae (both free-living), Glossosomatidae (saddle-case makers), and Hydroptilidae (purse-case makers) from all other representatives of Annulipalpia.

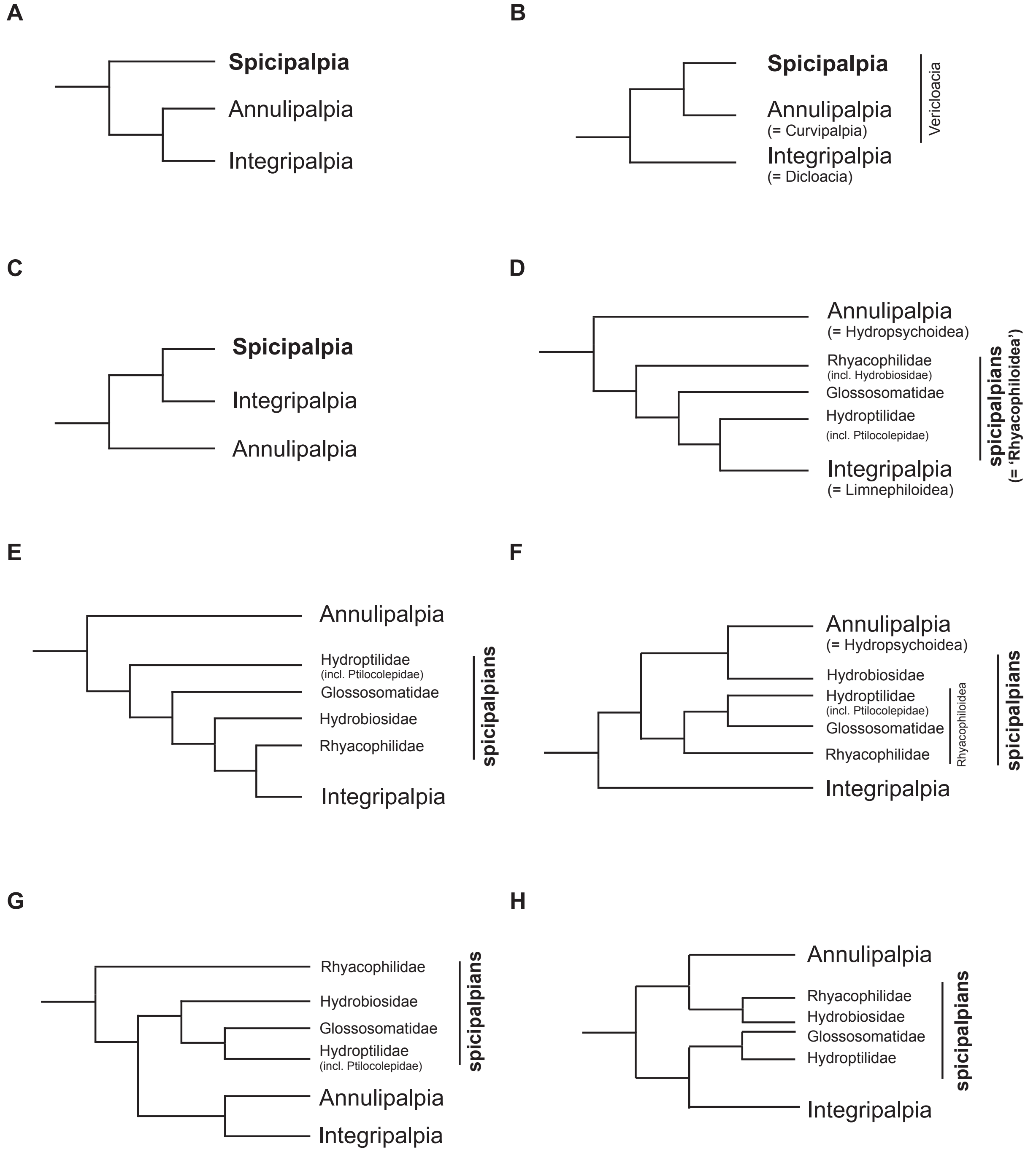

Figure 3: Postulated hypotheses of higher level phylogenetic relationships of Trichoptera. **A**: Monophyletic Spicipalpia as sister group of a clade comprising Annulipalpia and Integripalpia (after Wiggins & Wichard 1989); **B**: monophyletic Spicipalpia + monophyletic Annulipalpia (= Curvipalpia) as sister group of Integripalpia (= Dicloacia) (after Weaver 1984; Weaver & Morse 1986); **C**: monophyletic Spicipalpia + monophyletic Integripalpia as sister group of Annulipalpia (after Kjer et al. 2002); **D**: Paraphyletic 'Spicipalpia' (= 'Rhyacophiloidea') and monophyletic Integripalpia (= Limnephiloidea) form the sister group of Annulipalpia (= Hydropsychoidea) (after Ross 1967); **E**: Paraphyletic 'Spicipalpia' and monophyletic Integripalpia form the sister group of Annulipalpia (after Kjer et al. 2016); **F**: Paraphyletic 'Spicipalpia' and monophyletic Annulipalpia (= Hydropsychoidea) form the sister group of Integripalpia (after Schmid 1989); **G**: Paraphyletic 'Spicipalpia' at the base of a clade comprising monophyletic Annulipalpia and Integripalpia (after Malm et al. 2013); **H**: Polyphyletic 'Spicipalpia' (after Frania & Wiggins 1997).

Subsequently, he splits off these four families forming the sister group to the remaining annulipalpian families and introduced the scientific name Spicipalpia.

Afterwards, Malicky (2000) transferred the hydroptilid subfamily Ptilocolepinae to family rank. Therefore, most recently the taxon 'Spicipalpia' comprises five families (Rhyacophilidae, Hydrobiosidae, Glossosomatidae, Ptilocolepidae, and Hydroptilidae).

The monophyly of Annulipalpia and Integripalpia is well supported by both morphological and molecular data (e.g., Ross 1956, 1964, 1967; Lepneva 1964; Schmid 1980, 1989; Weaver 1984; Ivanov 1993, 2002; Morse 1997; Frania & Wiggins 1997; Kristensen 1999; Kjer et al. 2001, 2002, 2016; Malm et al. 2013).

In contrast, the monophyly of the spicipalpian families is highly equivocal and the phylogenetic affinities of the groups are discussed controversially (e.g., Ross 1956; Schmid 1980; Frania & Wiggins 1997; Kjer et al. 2002; Holzenthal et al. 2007b; Malm et al. 2013). However, the monophyly of each spicipalpian family is well argued by several autapomorphies (Ross 1956; Schmid 1980, 1989; Holzenthal et al. 2007a). Nonetheless, the mainly unsolved placement of the spicipalpian families is a major problem in the higher level phylogeny of Trichoptera and greatly impedes the reconstruction of the basal branching pattern of the group. Hence, the spicipalpian families clearly represent key-taxa for the understanding of the evolution of major morphological and behavioral traits in Trichoptera.

Therefore, in the last decades several studies focused on the intraordinal relationships of Trichoptera with special reference to the placement of the spicipalpian families in regard to monophyletic Annulipalpia and Integripalpia:

- **Monophyletic Spicipalpia form the sister group of a clade comprising Annulipalpia and Integripalpia (Fig. 3A)**

The morphology and evolution of the pupal cocoon in caddisflies was extensively studied by Wiggins & Wichard (1989). Both authors demonstrated that the spicipalpian lineages are clearly separated from all other groups of Trichoptera by the construction of closed cocoons. In contrast, representatives of both, Annulipalpia and Integripalpia construct a pupal cell with open meshes at the end (i.e., permeable cocoon). Consequently, Wiggins & Wichard (1989) suggested a sister group relationship between Annulipalpia and Integripalpia, and both suborders co-ordinate to a third suborder Spicipalpia (Fig. 3A).

This hypotheses was corroborated by the studies of Wichard (1991), Wiggins (1992), and Wichard et al. (1993, 1997).

- **Monophyletic Spicipalpia and Annulipalpia form the sister group of Integripalpia (Fig. 3B)**

Weaver (1984, 1992a, b) was the first who postulated monophyletic Spicipalpia forming the sister group to monophyletic Annulipalpia (= Curvipalpia). He analyzed a quite limited number of external morphological structures covering all major body regions of both, adults and larvae. Furthermore, Weaver (1984) analyzed the morphological character matrix cladistically and explicitly stated apomorphic characters supporting the major clades of his phylogeny (e.g., Spicipalpia: 2nd segment of adult maxillary palp ovoid and about as long as the 1st; larvae specialized in freedom of movement, with monile feeding strategies for grazing or pursuing prey etc.).

Subsequently, Weaver & Morse (1986) analyzed feeding strategies in Trichoptera. Their results strongly support the monophyly of Spicipalpia and a sister group relationship to Annulipalpia as previously suggested by Weaver (1984).

- **Monophyletic Spicipalpia and Integripalpia form the sister group of Annulipalpia (Fig. 3C)**

Kjer et al. (2001, 2002) proposed a close relationship between monophyletic Spicipalpia and monophyletic Integripalpia based on a combined analysis of molecular (rRNA [18S and 28S], elongation factor 1 alpha [EF-1α], cytochrome c oxidase subunit I [COI]) and morphological (taken from Frania & Wiggins 1997) data (Fig. 3C).

However, Kjer et al. (2002) mentioned the quite low branch support of the spicipalpian clade rendering its monophyly unlikely.

- **Paraphyletic 'Spicipalpia' and Integripalpia form the sister group of Annulipalpia (Fig. 3D, E)**

A close relationship of paraphyletic 'Spicipalpia' and monophyletic Integripalpia was proposed by Ross (1956, 1964, 1967) (Fig. 3D), Holzenthal et al. (2007b), and Kjer et al. (2016) (Fig. 3E).

Ross (1956, 1964, 1967) analyzed a quite limited number of external morphological features including all live stages (altogether nine characters covering head, thorax and abdomen) (Fig. 3D).

Holzenthal et al. (2007b) extended the molecular data set of Kjer et al. (2001, 2002) (see above) in terms of taxa and sequence data. In contrast to Kjer et al. (2002) the monophyly of Spicipalpia could not be confirmed. Nonetheless, a monophyletic clade comprising paraphyletic 'Spicipalpia' and monophyletic Integripalpia was strongly supported.

Kjer et al. (2016) in the most recent phylogeny of Trichoptera performed a combined analysis of mitochondrial and nuclear DNA sequence data (rRNA [18S and 28S], elongation factor 1 alpha [EF-1α], cytochrome c oxidase subunit I [COI], and carbamoylphosphate synthethase [CAD]). Furthermore, Kjer et al. (2016) included also the morphological character matrix initially published by Frania & Wiggins (1997) into their combined analyses (Fig. 3E). The obtained results are quite similar compared to those in Holzenthal et al. (2007b).

- **Paraphyletic 'Spicipalpia' and Annulipalpia form the sister group of Integripalpia (Fig. 3F)**

A close relationship of paraphyletic 'Spicipalpia' and monophyletic Annulipalpia was proposed by Schmid (1980, 1989, 1998) (Fig. 3F). The phylogenetic scenario of Schmid (1989) was based on a limited number of external features of the adult head, thorax, and abdomen. Unfortunately, Schmid (1980, 1989, 1998) did not explicitly mention apomorphic features supporting his phylogenetic scenario. Consequently, the lack of data greatly impedes a critical reevaluation of his hypotheses.

- **Paraphyletic 'Spicipalpia' at the base of a clade comprising Annulipalpia and Integripalpia (Fig. 3G)**

Malm et al. (2013) proposed an ancestral placement of the spicipalpian lineages with respect to a clade comprising Annulipalpia and Integripalpia. Their phylogenetic scenario was based on the analysis of molecular data from three nuclear (carbamoylphosphate synthethase [CAD], isocitrate dehydrogenase [IDH], RNA polymerase II [POL]) and one mitochondrial (cytochrome oxidase I [COI]) protein coding genes (Fig. 3G).

- **Polyphyletic 'Spicipalpia' (Fig. 3H)**

A further phylogenetic hypothesis with 'Spicipalpia' turning out as a polyphyletic group was provided by Frania & Wiggins (1997) and Ivanov (1993, 1997, 2002). The two case-bearing spicipalpian families Glossosomatidae and Hydroptilidae are closely related to

Integripalpia, whereas the free-living groups Rhyacophilidae and Hydrobiosidae are closely related to Annulipalpia (Fig. 3H). Frania & Wiggins (1997) analyzed a comparatively large morphological dataset (70 external features) of both, larvae and adults covering all major lineages of Trichoptera (50 representatives).

Considering all these different scenarios of trichopteran phylogenetic relationships, it seems to be obvious that the higher-level phylogeny of Trichoptera remains mainly unresolved until now.

1.3. Morphological studies of Trichoptera

In the past century morphological studies in Trichoptera mainly focused on external features of the exoskeleton in both, the larval and adult life stages (e.g., Krafka 1923; Durand 1955; Lepneva 1964, 1966; Hickin 1967; Frania & Wiggins 1997; Chamorro & Holzenthal 2011). Most commonly comparative data is only available for taxonomic relevant external features like the male genitalia (e.g., Macan & Worthington 1973; Schmid 1998; Malicky 2004, 2010) or larval head features (e.g., shape and coloration of the frontoclypeus, mandibles etc.) (e.g., Pitsch 1993; Wallace et al. 2003; Waringer & Graf 2011).

Comprehensive studies on both, external and internal structures mainly focused on the larval stage (Pryor 1951; Winkler 1959; Badcock 1961; Fotius-Jaboulet 1961; Tindall 1963, 1964; Friedrich et al. 2015). In contrast, detailed studies on internal features of adult Trichoptera are quite scarce and cover only a single or very few representatives (e.g., Crichton 1957; Klemm 1966; Ivanov & Kozlov 1987; Friedrich & Beutel 2010a; Hünefeld et al. 2012). Additionally, the data availability varies considerably between the major body regions in adults.

Hünefeld et al. (2012) extensively studied the female postabdomen in several endopterygote representatives, providing also detailed information on internal features of the trichopteran lineage Rhyacophilidae (‘Spicipalpia’). Maki (1938) was the first who extensively studied the thoracic musculature of a trichopteran representative, *Stenopsyche griseipennis* McLachlan, 1866. Subsequently, Tindall (1965) provided another and extraordinary detailed study of external and internal thoracic features in Trichoptera. However, his description of thoracic features in *Limnephilus marmoratus* Curtis, 1834 covered an integripalpian representative (Limnephilidae) as well.

The first comparative study of the pterothoracic musculature of 16 representatives covering all major groups of Trichoptera was performed by Ivanov & Kozlov (1987). Most recently, Friedrich & Beutel (2010a) studied the thoracic morphology of several endopterygote lineages and provided another extensive description of external and internal features of the spicipalpian lineage Rhyacophilidae.

Comprehensive studies on internal head structures of Trichoptera are limited. Crichton (1957) superficially studied the external head morphology in adults of several caddisfly families. Additionally, he described the internal features (e.g., muscles, digestive tract) of the integripalpian family Phryganeidae in detail (*Phryganea bipunctata* (Retzius, 1783)). But as this taxon is apparently deeply subordinate phylogenetically (see e.g., Malm et al. 2013), the usefulness of the data for the reconstruction of the ordinal ground plan is quite limited. Subsequently, Klemm (1966) provided another comprehensive description of adult head structures for a spicipalpian representative (*Rhyacophila* spp.). This is the only study of a comparatively ‘ancestral’ trichopteran at hand.

Further early investigations focused on a limited number of external features and the published data (e.g., Cummings 1914; Demoulin 1960) are largely insufficient for comparative analyses and phylogenetic evaluation. However, beside the comprehensive studies of Crichton (1957) and Klemm (1966), information on anatomical features are almost completely lacking for the remaining caddisfly families (especially for the subgroup Annulipalpia comprising 5,271 species [= 37 %] of the extant trichopteran world fauna [see Tab. 1]). Only Deoras (1943), Durand (1955), Demoulin (1960), Chaudonneret (1990), Neboiss (1991), and Crichton (1992) provided additional data on a very limited number of external and internal adult head features. Surface structures of the cuticle in the adult head (i.e., setae and cuticular sensilla [see Beutel et al. 2014]) were comparatively studied by Faucheux (2004) and Melnitsky & Ivanov (2011).

Furthermore, detailed information on the pupal stage is also quite limited. Only Hinton (1946, 1949) provided comprehensive information about the pupa of *Rhyacophila dorsalis* (Curtis, 1834) with special reference to the function of its mouth parts. External pupal features are for example described by Cowley (1976) for several caddisfly families from New Zealand and by Spinelli Batta & Moretti (1987) for some European representatives.

Several studies (e.g., Beutel & Vilhelmsen 2007 [Hymenoptera]; Dressler & Beutel 2010 [Coleoptera]; Blanke et al. 2012 [Odonata]; Friedrich et al. 2013 [Mecoptera]; and Spangenberg et al. 2013 [Hemiptera]) demonstrated the high value of head features as character system in phylogenetic studies due to the concentration of sense organs, brain, mouthparts and anterior digestive tract (Beutel et al. 2014).

The lack of comprehensive and comparative morphological data of the skeleton and soft tissues in all body parts of Trichoptera but especially in head structures impede the reconstruction of a sophisticated trichopteran ground plan which is strongly needed in order to understand the evolution of major morphological and behavioral traits within the group.

1.4. Aims of the study

Topic I – Comparative analysis of external and internal head structures of 22 trichopteran representatives

Detailed information on the adult head anatomy of Trichoptera is quite limited (see above [1.3.]). In order to obtain a deeper understanding of the adult head structures a comparative analysis of the skeleto-muscular system of 22 representatives covering all major lineages of Trichoptera will be performed. A special focus is dedicated to the five spicipalpian lineages being of major importance for the reconstruction of the basal branching pattern in Trichoptera. Furthermore, detailed and comparative morphological information is strongly needed in order to understand the evolution of major morphological and behavioral traits within the group.

For the investigation of soft tissues and the skeleton of the head a combination of traditional and innovative morphological techniques will be applied (see Beutel et al. 2014), including micro-computed tomography (SR-μCT), confocal laser-scanning microscopy (CLSM), scanning electron microscopy (SEM), histological sectioning, and light microscopy.

Topic II – Detailed description of the adult head of a presumably ‘basalmost’ annulipalpian representative, *Philopotamus ludificatus* McLachlan, 1878 in order to introduce a consistent terminology of adult head structures in Trichoptera

The number of studies dealing with the adult head anatomy in Trichoptera is quite small (see above [1.3.]). Nonetheless, the terminology applied to cephalic structures is mainly inconsistent since the authors use different terminological systems to describe muscles, sclerites and other structures. Consequently, a direct comparison of the available information may lead to wrong homology hypothesis by using the same terms for different structures. In order to establish a consistent terminology for adult head features which is strongly needed as a solid reference for the comparative work (Topic I), the cephalic anatomy of a presumably basal trichopteran representative, *Philopotamus ludificatus* McLachlan, 1878 will be described in detail. Furthermore, a consistent terminology for the head musculature will be developed. Subsequently, the data for both species already described (*Phryganea bipunctata* (Retzius, 1783) [Crichton 1957]; *Rhyacophila* spp. [Klemm 1966]) will be re-evaluated by own investigations and the primarily described structures will be compared with those found in the reference species, *P. ludificatus*. Finally, the homology of specific structures (e.g., mouthparts) will be discussed evaluating the existing hypotheses.

Topic III – Comparative analysis of pupal head structures of seven trichopteran representatives

Comprehensive and detailed descriptions of the trichopteran pupal head morphology are quite scarce (see above [1.3.]). However, the head morphology of the terrestrial adults (e.g., structure and musculature of the adult mandible) seems to be closely associated with morphological features of the pupa used by the pharate adult during eclosion. For a deeper understanding of the adult head architecture detailed information of the external and internal morphology of the pupal stage is required. Consequently, a comparative analysis of the pupal head of seven trichopteran representatives covering all major trichopteran lineages will be performed.

Topic IV – Description and documentation of phylogenetically relevant character complexes of the adult and pupal head with considerations on the ordinal ground plan

Comprehensive and comparative morphological data on major structural complexes of the adult trichopteran head (e.g., the antenna) is mainly restricted to external features. Nonetheless, it could be demonstrated in several studies dealing with other endopterygote insect groups (e.g., Friedrich et al. 2013) that internal structures (e.g., muscles) represent also a valuable source of phylogenetically relevant characters. Consequently, the external and especially the internal morphology of the adult head appendages and the digestive tract in Trichoptera will be analyzed in detail. Subsequently, character complexes which might help to address major issues in the higher level phylogeny of Trichoptera will be identified and discussed. Furthermore, the detailed and comparative analyses of morphological structures covering all major trichopteran lineages and outgroup taxa (*Micropterix* [Lepidoptera], *Nannochorista* [Mecoptera]) will allow for a critical evaluation of cephalic ground plan features in Trichoptera, which will be subsequently worked out.

Topic V – Analysis and interpretation of a trichopteran head character matrix with respect to the major phylogenetic hypotheses published during the last decades

The higher level phylogenetic relationships of Trichoptera has been subject of discussion for decades (see above [1.2.]). One of the main goals of the present thesis is to answer the question whether head features can serve as an informative source to solve the basal branching pattern in Trichoptera. Consequently, the present data set of adult and pupal head structures will be analyzed cladistically. Subsequently, a cladistic analyses based on each of the eight phylogenetic hypotheses (see above [1.2.) published during the last decades will also be performed.

The results will allow for a critical evaluation of the major clades being in question (e.g., ‘Spicipalpia’, Psychomyioidea). Finally, potential apomorphic characters supporting major clades will be presented and discussed.

2. Material and methods

2.1. List of taxa examined

The external and internal adult head morphology of 24 taxa covering 18 caddisfly families and all major subgroups of Trichoptera was investigated in detail, including two representatives of non-trichopteran endopterygote insect groups (*Micropterix calthella* (Linnaeus, 1761) [Lepidoptera] and *Nannochorista* ssp. [Mecoptera]) for outgroup comparison. A special focus was dedicated to the five spicipalpian families which are represented by eight species. Additionally, the pupa and the enclosed pharate adult of seven trichopteran representatives was investigated in detail as well (Tab. 2). The majority of the examined material was collected by the author of this thesis. Furthermore, voucher material of some caddisfly families (mainly non-European) was donated by colleagues (Dr. Wolfram Mey [Museum für Naturkunde Berlin, Germany], Univ.-Prof. Dr. Hans Malicky [Lunz am See, Austria], Prof. Dr. Karl M. Kjer [University of California, Davis, USA], Dr. Alice Wells [Department of Sustainability, Water, Population and Communities, Canberra, Australia], and Brian J. Smith (National Institute of Water and Atmospheric Research, Hamilton, New Zealand]) (Tab. 2). Usually, the examined material was preserved in 70 % ethanol and is now deposited at the University of Hamburg, Centrum für Naturkunde (CeNak) – Zoologisches Museum Hamburg (ZMH), Germany.

2.2. Morphological techniques

For a detailed description of external and internal head features the complete set of techniques was applied to a limited number of species (e.g., *Philopotamus*, *Limnephilus*, *Ptilocolepus* [Tab. 2]). In contrast, only a subset of techniques was used for several representatives in order to investigate selected external or internal character complexes in detail (Tab. 2).

2.2.1. Synchrotron radiation based micro-computer tomography (SR-µCT)

The SR-µCT data of 17 caddisfly representatives (plus *Micropterix calthella* [Lepidoptera]) were obtained at beamlines BW2 (storage ring DORIS III) and P05 (storage ring PETRA III) at the German Electron Synchrotron Facility (DESY) Hamburg (Tab. 3).

For our studies we used a stable low photon energy beam (8 or 9 keV) and absorption contrast (for technical details of micro-tomography at beamlines BW2/P05, see Beckmann et al. 2006, 2008; Greving et al. 2014; Wilde et al. 2016). Before the SR-µCT scans were carried out, the appendages of the insect body (wings, antennae, and legs) were cut off proximally. This step greatly reduced the size of the scan window (field of view) and helps to maximize the obtained spatial resolution. Subsequently, the specimens were dehydrated in an ethanol series (20, 50, 75, 80, 90, 96, 100) and critical point dried (Balzers Critical Point Dryer, CPD 030) to avoid shrinking artifacts of soft tissues. Each sample was mounted with superglue on a metal rod and scanned in 180 ° or 360 ° rotation (usually 0.25 ° steps; 720 tomograms). The obtained image stacks revealed a physical resolution between 3.38 µm (voxel size app. 2.5 µm) (e.g., *Holocentropus*) and 8.06 µm (voxel size app. 3.9 µm) (e.g., *Limnephilus*) (Tab. 3), and allowed for easy discrimination of different tissue types.

The large sample of *Phryganea grandis*

Suborder	Family	Species	Technique applied	Reference
Annulipalpia	Philopotamidae	*Philopotamus ludificatus* McLachlan, 1878 *	diss., SR-µCT, SEM, hist., CLSM	Crichton 1957
Annulipalpia	Stenopsychidae	*Stenopsyche marmorata* Navas, 1920 [a]	diss., SR-µCT	-
Annulipalpia	Hydropsychidae	*Hydropsyche angustipennis* (Curtis, 1834) *	diss., SR-µCT, SEM, hist., CLSM	Durand 1955; Crichton 1957
Annulipalpia	Psychomyiidae	*Tinodes dives* (Pictet, 1834) [b]	diss., hist.	Durand 1955; Crichton 1957
Annulipalpia	Polycentropodidae	*Holocentropus dubius* (Rambur, 1842)	diss., SR-µCT, SEM, hist.	Crichton 1957
'Spicipalpia'	Rhyacophilidae	*Rhyacophila obliterata* McLachlan, 1863	SR-µCT, diss.	Durand 1955
'Spicipalpia'	Rhyacophilidae	*Rhyacophila fasciata* Hagen, 1859 [1, *]	diss., CLSM	Klemm 1966; Crichton 1957
'Spicipalpia'	Hydrobiosidae	*Apsilochorema sutshanum* Martynov, 1934 [c]	SR-µCT	-
'Spicipalpia'	Hydrobiosidae	*Hydrobiosis styracine* McFarlane, 1960 [f]	diss., hist., SR-µCT, CLSM	-
'Spicipalpia'	Glossosomatidae	*Glossosoma spinosum* Morse et Yang, 2005	diss., hist.	-
'Spicipalpia'	Glossosomatidae	*Agapetus fuscipes* Curtis, 1834 *	diss., SR-µCT, hist., CLSM	Durand 1955, Crichton 1957
'Spicipalpia'	Ptilocolepidae	*Ptilocolepus granulatus* (Pictet, 1834) [a]	diss., SR-µCT, SEM, hist., CLSM	-
'Spicipalpia'	Hydroptilidae	*Hydroptila scamandra* Neboiss, 1977 [d]	diss., hist., CLSM	-
'Spicipalpia'	Hydroptilidae	*Orthotrichia atraseta* Wells, 1979 [d]	diss., hist.	Durand 1955
Integripalpia	Phryganeidae	*Phryganea bipunctata* Retzius, 1783	diss.	Crichton 1957
Integripalpia	Phryganeidae	*Phryganea grandis* Linnaeus, 1758	SR-µCT, diss.	Durand 1955
Integripalpia	Phryganeidae	*Trichostegia minor* (Curtis, 1834)	SR-µCT, diss.	-
Integripalpia	Sericostomatidae	*Sericostoma personatum* Kirby et Spence, 1826	SR-µCT, diss.	Durand 1955; Crichton 1957
Integripalpia	Brachycentridae	*Brachycentrus subnubilus* Curtis, 1834 *	SR-µCT, diss.	Crichton 1957
Integripalpia	Limnephilidae	*Limnephilus flavicornis* (Fabricius, 1787) *	diss., SR-µCT, SEM, hist., CLSM	Durand 1955; Crichton 1957
Integripalpia	Goeridae	*Silo nigricornis* (Pictet, 1834) *	diss., SR-µCT, SEM, hist.	Durand 1955; Crichton 1957
Integripalpia	Conoesucidae	*Pycnocentria evecta* McLachlan, 1868 [f]	SR-µCT, diss.	-
Integripalpia	Molannidae	*Molanna angustata* Curtis, 1834	SR-µCT, diss.	Crichton 1957
Integripalpia	Leptoceridae	*Leptocerus tineiformis* Curtis, 1834	diss., hist., CLSM	Durand 1955; Crichton 1957
n.a. [Lepidoptera]	Micropterigidae	*Micropterix calthella* (Linnaeus, 1761)	SR-µCT, diss.	Hannemann 1956
n.a. [Mecoptera]	Nannochoristidae	*Nannochorista* Tillyard, 1917	diss., hist.	Beutel & Baum 2008

← **Table 2:** Taxon sampling and applied techniques, with additional information on literature containing detailed information on external [not underlined] and internal features [underlined references] of the adult head. Material preserved in 70 % ethanol. Abbreviations: **hist.** – histological section series, **SR-µCT** – synchrotron radiation based micro-computed tomography, **SEM** – scanning electron microscopy, **diss.** – dissection, **CLSM** – Confocal laser scanning microscopy. Symbols: '**-**' – no information available, **a**–**f** – indicates donation of material by colleagues (**a** – W. Mey, **b** – H. Malicky, **c** – K. M. Kjer, **d** – A. Wells, **f** – B. J. Smith; see Acknowledgements), **n.a.** – not applicable, **1** – pair of species in Klemm (1966): *Rhyacophila fasciata* Hagen, 1859 / *R. dorsalis* (Curtis, 1834), * – adult and pupal (i.e., pharate adult) life stage analyzed.

Linnaeus, 1758 was scanned using a desktop machine (Phoenix|X-ray nanotom®, GE Measurement & Control Solutions, Wunstorf, Germany) at Hasylab/DESY.

2.2.2. Confocal laser scanning microscopy (CLSM)

The degree of sclerotization of specific parts of the cuticle (e.g., pupal mandible, base of adult antenna) was investigated using CLSM.

The structures were prepared under a Leica M165 C stereomicroscope (Wetzlar, Germany) using small insect needles. Then, each sample was embedded into a drop of glycerine or gelatin between an object slide and a high precision cover glass to avoid movements of the delicate structures. A further advantage of these embedding media is that they can be easily washed out in 70 % ethanol or distilled water.

The scans were performed using a Leica TCS-SPE confocal laser scanning microscope (Wetzlar, Germany). The autofluorescence of the insect cuticle was induced with laser light at 488 nm (for details see Michels 2007). The green (500–570 nm) and red (580–960 nm) fluorescence spectra were chosen for recording the emitted light. The overlay of both channels in a maximal projection or volume rendering allows for easy and detailed discrimination of membranous (non-sclerotized) areas appearing green and sclerites which are colored yellowish-brown (Deans et al. 2012). Bitplane Imaris 6 software (Bitplane AG, Zürich, Switzerland) was used for 3D-reconstruction and for visualizing volume renderings.

2.2.3. Scanning electron microscopy (SEM)

The fine structure of the external head capsule and its appendages was studied and documented using SEM.

The head of male specimens of six trichopteran representatives (Tab. 2) were dehydrated in an ascending ethanol series (20, 50, 75, 80, 90, 96, 100), critical point dried (Balzers Critical Point Dryer, CPD 030), glued to a thin metal pin, and finally fixed to a specimen holder following the methods of Pohl (2010). The sample was evenly coated with platinum using a Polaron SC7650 Sputter Coater (Polaron Ltd., Watford, United Kingdom).

SEM images were taken with a LEO 1525 scanning electron microscope (Carl Zeiss SMT, Jena, Germany) at 5 or 10 keV. Helicon Focus Pro X64 (Helicon Soft Ltd.) was used to combine the partially focused SEM images.

2.2.4. Light microscopy imaging

Light microscopy imaging represents a useful tool for the documentation of coloration

Table 3: Summary of SR-µCT data acquisition at beamlines BW2 and P05 at the German Electron Synchrotron Facility (DESY) Hamburg with the resulting scan resolution and voxel size. Abbreviations: **BW2** – beamline BW2 of storage ring DORIS III, **P05** – beamline P05 of storage ring PETRA III, **NNT** – nanotom® Phoenix|X-ray, **n.a.** – not applicable.

Species	Beam line	Photon energy	Physical resolution [µm]	Magnification	Voxel size [µm]
Philopotamus ludificatus McLachlan, 1878	BW2	9 keV	5.68	3.909	2.3054
Stenopsyche marmorata Navas, 1920	BW2	9 keV	4.80	3.912	2.3036
Hydropsyche angustipennis (Curtis, 1834)	BW2	9 keV	4.61	3.900	2.3107
Holocentropus dubius (Rambur, 1842)	P05	8 keV	3.38	9.486	2.5300
Rhyacophila obliterata McLachlan, 1863	BW2	8 keV	3.74	3.461	2.6038
Apsilochorema sutshanum Martynov, 1934	P05	8 keV	5.46	19.657	1.2210
Hydrobiosis styracine McFarlane, 1960	P05	8 keV	5.46	19.657	1.2210
Agapetus fuscipes Curtis, 1834	P05	8 keV	5.46	19.657	1.2210
Ptilocolepus granulatus (Pictet, 1834)	P05	8 keV	5.46	19.657	1.2210
Phryganea grandis Linnaeus, 1758	NNT	33 keV	n.a.	n.a.	3.5000
Trichostegia minor (Curtis, 1834)	P05	8 keV	3.38	9.486	2.5300
Brachycentrus subnubilus Curtis, 1834	BW2	8 keV	5.68	3.909	2.3054
Limnephilus flavicornis (Fabricius, 1787)	BW2	8 keV	8.06	2.295	3.9267
Silo nigricornis (Pictet, 1834)	BW2	9 keV	4.62	4.547	1.9819
Sericostoma personatum Kirby et Spence, 1826	BW2	9 keV	5.44	3.231	2.7890
Pycnocentria evecta McLachlan, 1868	P05	8 keV	8.06	2.295	3.9267
Molanna angustata Curtis, 1834	BW2	9 keV	4.80	3.912	2.3036
Leptocerus tineiformis Curtis, 1834	P05	8 keV	5.46	19.657	1.2210
Micropterix clathella (Linnaeus, 1761)	BW2	8 keV	4.44	4.507	1.9995

pattern and allows for easy discrimination of membranous and well-sclerotized areas of the insect body.

The head of a male specimen of *Philopotamus ludificatus* McLachlan, 1878 was dehydrated in an ascending ethanol series (20, 50, 75, 80, 90, 96, 100) and critical point dried (Balzers Critical Point Dryer, CPD 030). Subsequently, it was glued on a small insect pin for imaging in standard morphological views. Photographs were taken using a Passport II Imaging System built by Visionary Digital™ (now Dun Inc.), equipped with a Canon EOS 6D digital camera and a 65 mm Canon compact macro-lens.

Helicon Focus Pro X64 (Helicon Soft Ltd.) was used to combine the partially focused images.

2.2.5. Histology

Adult heads of 13 trichopteran representatives (Tab. 2) were embedded in epoxy resin (usually Araldite® CY212 kit; Plano, Wetzlar, Germany) and cut at 1 µm with a Microm Microtome (HM 360) (Walldorf, Germany) with diamond knife or a Reichert-Jung Ultracut E microtome (Wien, Austria) with glass knives.

The obtained cross sections were transferred to adhesion microscope slides and subsequently stained with a mixture of toluidine blue-O (1 % solution), Borax (1 % solution), and pyronin-G (exposure time: 30 s). Finally, the stained cross sections were embedded in Euparal® and covered by a microscope cover slip.

Digitalization was carried out using a Leica DM6000 microscope (Wetzlar, Germany) with semiautomatic slide scanning option (based on MetaMorph software). The photographed sections were edited in Adobe® Photoshop® CS6 software (Adobe Systems, San José, USA) applying general imaging enhancement tools (contrast, brightness, sharpness).

Subsequently, the cross sections were automatically aligned and processed using Visage Imaging Amira 5.4–6.0® software (FEI, Berlin, Germany).

2.2.6. Computer-based 3D-reconstruction

A combination of different software packages (Visage Imaging Amira® 5.4–6.0 [(FEI, Berlin, Germany)], Bitplane Imaris 6 [Bitplane AG, Zürich, Switzerland], and Autodesk® Maya 2014 [Autodesk GmbH, München, Germany]) was applied to reconstruct the head morphology of 22 trichopteran representatives based on µCT- and histological image data three-dimensionally.

Amira software in combination with a Wacom Cintiq 22HD interactive pen display (Saitama, Japan) was used for semiautomatic segmentation of raw image data by applying the ‚brush‘ and ‚magic wand‘ tools. Due to high density resolution of the SR-µCT scans, different types of soft tissue such as muscles, glands, nerves, and also the sclerotization of the skeleton could be easily distinguished. The segmentation process delivered a ‚labels‘ data object for each specific structure allowing for the assignment of voxels from the original data to selected materials (i.e., different tissues). The ‚arithmetic‘ function in Amira software was used in order to generate separate volume datasets for different structures (for details see Kleinteich et al. 2008).

The image stack series obtained for each segmented structure was subsequently transferred into Bitplane Imaris 6 software for automatic creation of surface objects. In Bitplane Imaris 6 software, the work space (region of interest) for the processing of volume data into surface objects was adjusted to the object limits using the ‚select‘ tool. This step remarkably reduced the computation time during the surface creation. Subsequently, the ‚smooth‘ option was applied to remove minor surface artifacts (applied surfaces area detail level between 300 and 600 µm). The obtained Imaris surface files (.iv) were converted into object files (.obj) using the Transform2 64 bit software (Heiko Stark, Jena, Germany; URL: http://starkrats.de). This file format allowed for the final post processing in Maya 2014 software.

The Maya 2014 software package was mainly used for modeling of minor surface artifacts and file size reduction. For this purpose a combination of several options like ‚reduce polygon‘, ‚average‘, and ‚smooth‘ was applied. The ‚smoothing‘ process did not noteably change the general shape and the arrangement of structures. Finally, surface renderings were also created in Maya 2014 software.

2.3. Illustration

Adobe® Photoshop® CS6 software (Adobe Systems, San José, USA) was used for editing the obtained images by adjusting contrast, brightness, and sharpness. Image plates were assembled with Adobe® Illustrator® CS6 software (Adobe Systems, San José, USA), which was also used for creating line drawings.

2.4. Terminology

The terminology of the skeleton is mainly based on Snodgrass (1935) and Beutel et al. (2014). Sensilla are named and homologized after Melnitsky & Ivanov (2011). The names of muscles are designated by the areas of their origin and insertion sites (abbreviations used in the text: O = origin, I = insertion). If this alone is ambiguous, the topographical orientation (e.g., ventralis vs. dorsalis, etc.) is added. Furthermore, the muscles are homologized with the terminologies used by Hannemann (1956), von Kéler (1955), and Wipfler et al. (2011) (Tab. 4). The musculature of other trichopteran species investigated in the present study or taken from the literature (Crichton 1957; Klemm 1966) is also summarized in Table 4.

The systematics follows Weaver (1984) and Holzenthal et al. (2011) (exceptions are referenced in the text). Nomenclature for trichopteran taxa is adopted from Malicky (2005) (Europe) and Neboiss (1986) (Australia and New Zealand).

2.5. Phylogenetic analyses

Morphological character evolution of adult and pupal head features in Trichoptera was studied using eight different phylogenetic hypotheses proposed by Ross (1967), Weaver & Morse (1986), Wiggins & Wichard (1989), Schmid (1989), Frania & Wiggins (1997), Kjer et al. (2002, 2016), and Malm et al. (2013).

Initially, tree topologies were created manually by using Mesquite software (version 3.0.4; Maddison & Maddison 2011). In this software package tree topologies can be easily edited by hand using the ‚With Tree To Edit by Hand‘ option. Subsequently, the character matrix (App. 8; 37 characters) with respect to the above mentioned phylogentic scenarios was analyzed using a parsimony approach in Mesquite software as well. For the data analysis the following options were applied: ‘Trace Character History Source’, ‘Reconstruct Ancestral States’, and ‘Parsimony Ancestral States’ option. The treelength for each topology was calculated using the ‘Values for current Tree‘ and ‘Treelength‘ option.

Subsequently, the character matrix and the manually created tree topologies were transferred as data file (.ss) to Winclada software (Nixon 1999-2002). Winclada software was used for quantitative characterization of data fitting and also for vizualization of apomorphic characters (non-homoplasious and homoplasious) on eight different phylogenetic scenarios extracted from the literature (see above). The following options were applied: ‘Map Characters’ and ‘Number hashmarks’ option. The resulting phylogenetic trees were edited using Adobe® Illustrator® CS6 software.

Additionally, the complete adult and pupal head data set (App. 8; 37 characters) was independently analyzed using Winclada software (presets: heuristic search, multiple TBR + TBR, unconstrained search, number of replicates: 1000, starting trees per replicate: 500) as well.

3. Results

3.1. The adult head morphology of *Philopotamus ludificatus* McLachlan, 1878 *

3.1.1. General appearance

The mean body length of adults of *P. ludificatus* is 8.2 mm (6.2–10.2 mm; n = 25) for males and 9.9 mm (8.0–11.7 mm; n = 25) for females. The body color of the adults is dark brown. The ovate forewings are brown with large, evenly distributed yellowish to ochre spots. The hindwings are uniformly light brown. The wings are held roof-like folded above the abdomen when the living insect is at rest. Large parts of the body and especially the forewings have a dense vestiture of setae and microtrichia. The tibia of all three pairs of legs bear large, ochre spurs (spur formula 2,4,4).

3.1.2. Head capsule

The head is orthognathous and largely covered by a dense vestiture of minute microtrichia (Fig. 9A,B). The margin of the antennal foramen is slightly reinforced by the circumantennal sulcus[2] (‘antennal socket’ sensu Snodgrass 1935; Fig. 4). The antennal socket is ventrally suspended by a large extension (antennifer = atf, in Figs. 4, 9A), which is continuous with the dorsal end of the strong frontogenal sulcus (fgs, Fig. 4), interconnecting the ventral margin of the antennal socket and the base of the anterior tentorial arm (anterior tentorial pit = atp, in Figs. 4, 9A). The frontal sulci (fs) diverge anteriorly from the median coronal sulcus (cs) directly behind the median ocellus (Fig. 4). They run ventrolaterally in a straight line toward the antennal socket (obliterated at level of the frontal setal warts [fsw, Fig. 4]; see below). The coronal sulcus extends backwards toward the occipital foramen. The dorsal part of the head capsule represents the vertex (ve, Fig. 4). It is not distinctly bordered laterally, but continuous with the gena (ge, Fig. 5A) and the occiput (occ, Fig. 15B). Halfway between the lateral ocelli and the occiput a postfrontal sulcus (pfs, Fig. 4) arises from the coronal sulcus, runs laterad of the lateral ocellus anteriorly and meets the antennal socket dorsally. Below the median ocellus a very distinct, curved interantennal sulcus (ias, Fig. 4) runs ventrolaterad toward the frontoclypeal setal wart (see below) (Fig. 4).

The triangular facial area, dorsally and laterally delimited by the frontal sulcus and the frontogenal sulcus, respectively, is a frontopostclypeus without any external demarcation of a frontoclypeal boundary (i.e., epistomal sulcus) (Fig. 4); the area above a line connecting the anterior tentorial pits bears a smooth median depression.

The lower facial region is subdivided into ante- and postclypeus by a conspicuous horizontal furrow (hf, Figs. 4, 15A). The head capsule areas adjacent to this horizontal furrow are less pigmented than elsewhere. Furthermore, the originating muscles indicate a clypeal nature of this area and the apical (/ventral) part must include a labral component (see below). Therefore, the lower facial area can conveniently be termed postclypeus (i.e., frontopostclypeus, fpc, Fig.

---

[2] The term ‘sulcus‘ refers to any line of cuticular inflection forming internal ridges. In contrast, the term ‘suture‘ is only used for unsclerotized lines between two adjacent sclerotized areas, which are not present in the adult head capsule of caddisflies (see Snodgrass 1963: 9; Kristensen 2003: 39).

Figure 4: *Philopotamus ludificatus* McLachlan, 1878: head, light-microscopic image, anterior view. Abbreviations: **acl(d)** – distal part of anteclypeolabrum, **acl(p)** – proximal part of anteclypeolabrum, **as** – antennal socket, **atf** – antennifer, **atp** – anterior tentorial pit, **cpe** – compound eye, **cs** – coronal sulcus, **fcsw** – frontoclypeal setal wart, **fgs** – frontogenal sulcus, **fl** – flagellomere, **fo** – fossa of subgenal process, **fpc** – frontopostclypeus, **fs** – frontal sulcus, **fsw** – frontal setal wart, **ge** – gena, **gp** – subgenal process, **hf** – horizontal furrow between frontopostclypeus and anteclypeolabrum, **hst** – haustellum, **ias** – interantennal sulcus, **lap** – labial palp, **loc** – lateral ocellus, **md(m)** – membranous part of mandible, **md(s)** – mandibular sclerite, **moc** – median ocellus, **mxp** – maxillary palp, **ped** – pedicellus, **pfs** – postfrontal sulcus, **sca** – scapus, **srts** – smooth ribbed trichoid sensillum, **ve** – vertex, **vsw(a)** – anterior setal wart of vertex, **vsw(p)** – posterior setal wart of vertex, **I**–**V** – number of palpomere. (Scale bar: 250 µm)

4) and anteclypeolabrum (acl(p)/acl(d), Fig. 4), respectively. The upper/dorsal part (acl(p)) of the anteclypeolabrum has a sparse vestiture of strong smooth ribbed trichoid sensilla and a few placoid sensilla (Fig. 10A), while the lower/apical part (acl(d)) is weakly sclerotized and pigmented (Fig. 4). The lateral parts of the head capsule, enclosing the compound eyes,

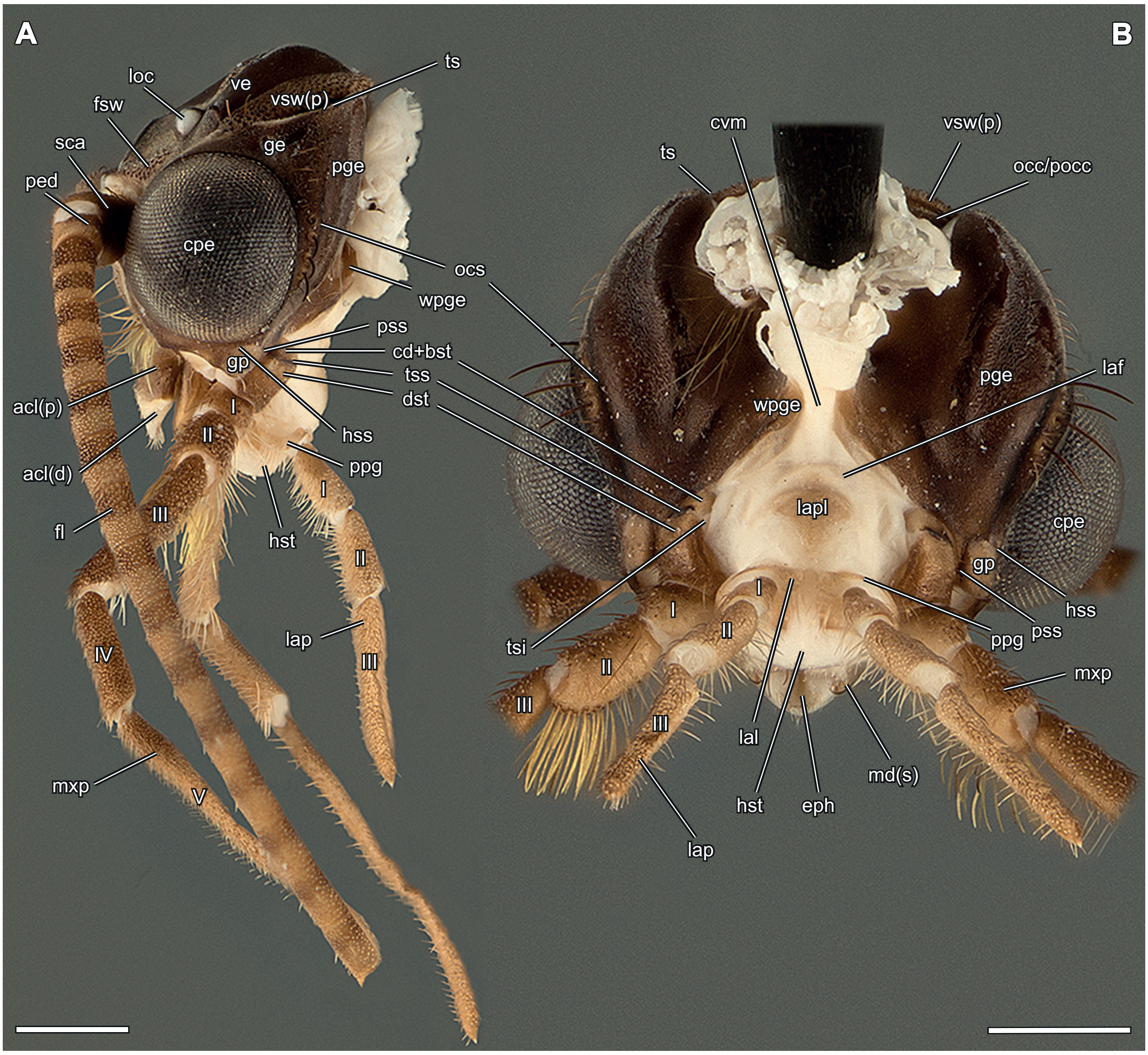

Figure 5: *Philopotamus ludificatus* McLachlan, 1878: head, light-microscopic images. **A**: lateral view; **B**: posterior view. Abbreviations: **acl(d)** – distal part of anteclypeolabrum, **acl(p)** – proximal part of anteclypeolabrum, **bst** – basistipes, **cd** – cardo, **cpe** – compound eye, **cvm** – cervical membrane, **dst** – dististipes, **eph** – epipharynx, **fl** – flagellomere, **fsw** – frontal setal wart, **ge** – gena, **gp** – subgenal process, **hss** – hypostomal sulcus, **hst** – haustellum, **laf** – semicircular fold of labium, **lal** – labial lobe, **lap** – labial palp, **lapl** – central plate of labium, **loc** – lateral ocellus, **md(s)** – mandibular sclerite, **mxp** – maxillary palp, **occ** – occiput, **ocs** – occipital sulcus, **ped** – pedicellus, **pge** – postgena, **pocc** – postocciput, **ppg** – palpiger, **pss** – pleurostomal sulcus, **sca** – scapus, **ts** – temporal suture, **tsi** – triangular membranous incision of stipes, **tss** – transstipital sulcus, **ve** – vertex, **vsw(p)** – posterior setal wart of vertex, **wpge** – wing-shaped extension of postgena, **I–V** – number of palpomere. (Scale bars: 250 µm)

are formed by the genae (ge, Fig. 5A). Each gena bears a row of five strong dentate and ribbed trichoid sensilla behind the compound eye (Fig. 5A,B). Three basiconic sensilla (bs, Fig. 9A) are located on its anterior surface between the frontogenal sulcus and the anterior margin of the compound eye. Posteriorly, the gena is delimited from the postgenal region by an incomplete occipital sulcus (ocs, Fig. 5A,B). This sulcus disappears dorsally (behind the compound eye), but ventrally splits into an anterior pleurostomal sulcus (pss) and a posterior hypostomal sulcus (hss) (both in Fig. 5A,B). The two latter sulci demarcate the dorsal margin of the small subgena, which forms a strong, heavily sclerotized process lateral to the base of the mandible. The subgenal process (gp, Figs. 4, 5A,B) is enforced by a strong sulcus and bears an oval fossa (fo, Fig. 4) apically. This structure forms the articular surface of the posterior joint of the pupal mandible.

The posteroventral parts of the head capsule are formed by the postgenae (pge, Fig. 5A,B), which are dorsally delimited from the occiput/postocciput by a strong sulcus ('sulcus temporalis' sensu Klemm 1966, ts, Fig. 5A). The mesal halves of the postgenae are bent posteriorly and form wing-shaped extensions (wpge, Fig. 5B) connected with the extensive cervical membrane (cvm, Fig. 5B). A ventral closure of the head capsule (e.g., postgenal bridge, gula) is absent (Fig. 5B).

Occipital and postoccipital regions are inseparable. Dorsolaterally to the tentorial bridge a prominent process forming the median margin of the postoccipital component of the composite occipital and postoccipital region ('condylus occipitalis' sensu Snodgrass 1935, cocc, Fig. 15B) is developed on each side of the occipital foramen, articulating with the lateral cervical sclerite.

The foramen occipitale is divided by the tentorial bridge into a broad, trapezoid upper part (about ⅔ of the opening) and a smaller lower part (about ⅓ of the opening). The lower opening has the margins reinforced by a strong sulcus laterally, but is ventrally just closed by the cervical membrane (Fig. 15B).

The head capsule bears a vestiture of strong dentate ribbed trichoid sensilla densely clustered on bulged setal warts (after Oláh & Johanson [2007]). One slightly raised frontoclypeal setal wart (fcsw, Figs. 4, 9A) is located on the lateral frontopostclypeal region (fpc, Fig. 4) between the anterior tentorial pit and the antennal socket (Fig. 9A). Three closely adjacent setal warts (two lateral and one median) are arranged in a broad w-shaped pattern in the frontal region (= frontal setal wart, fsw, Figs. 4, 9A) bordered anteriorly by the median ocellus, laterally by the postfrontal sulcus and posteriorly by the frontal sulcus and the lateral ocelli. A pair of large triangular setal warts (= anterior setal wart of vertex, vsw(a), Fig. 4) is located on the vertex between the lateral ocelli and the meeting point of coronal sulcus and postfrontal sulcus. The posterolateral regions of the vertex bear extremely large, strongly bulged setal warts (= posterior setal wart of vertex, vsw(p), Figs. 5A, 15B). These areas are posteriorly reinforced by strong internal sulci at their anterior and lateral margins.

A shallow furrow (tf(p), Fig. 7B) is located directly behind the dorsal setal wart of the vertex. Its surface is tubercular and lacks microtrichia. A similarly structured but slightly bulged field (tf(a), Fig. 7A) is located laterally behind the lateral ocellus. The nature of these fields (secretory or sensory) could not be identified in histological sections.

3.1.3. Tentorium

The tentorium is X-shaped with very short, but stout posterior tentorial arms (pta, Fig. 6A,B) enforcing the ventrolateral margin of the alaforamen toward the condyli occipitales (Fig. 15B). The posterior tentorial pit (ptp, Fig. 15B) is located in the postoccipital sulcus. It is directed laterad (Fig. 15B).

A stout tentorial bridge (tb, Fig. 6A,B) connects the posterior tentorial arms. The posterior-most parts of the anterior tentorial arms are mesally fused, forming a plate-like corpotentorium (cot, Fig. 6A,B) posteriorly continuous with the tentorial bridge.

The anterior tentorial arm (ata, Fig. 6A,B) is well-developed and originates in a large, rounded anterior tentorial pit located about half

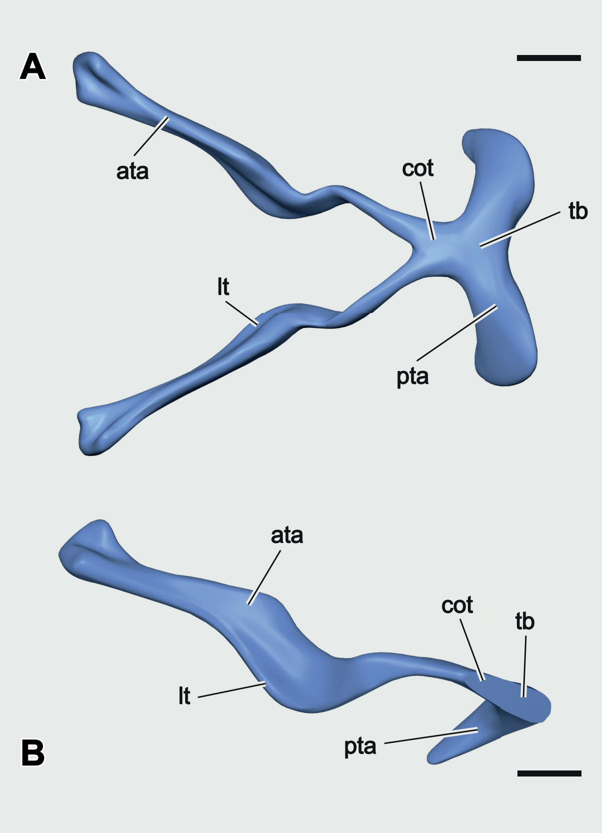

Figure 6: *Philopotamus ludificatus* McLachlan, 1878: tentorium, 3D-reconstruction based on µCT data. **A**: dorsal view; **B**: sagittal section (Dorsal tentorial arm not shown; see Fig. 19C). Abbreviations: **ata** – anterior tentorial arm, **cot** – corpotentorium, **lt** – laminatentorium, **pta** – posterior tentorial arm, **tb** – tentorial bridge. (Scale bars: 100 µm)

the distance between the base of the antenna and the anteclypeolabrum (atp, Figs. 4, 15A). The part of the anterior arm directly adjacent to the head capsule or the tentorial bridge is well sclerotized. Between these areas the arm becomes medio-laterally flattened with the lateral side weakly sclerotized. In this region a flattened and weakly sclerotized ventromesally directed process (laminatentorium) is developed (lt, Fig. 6A,B). The margin of the anterior tentorial pit is reinforced by the dorsally directed frontogenal sulcus (fgs, Figs. 4, 18A).

A dorsal tentorial arm is weakly developed and is represented by a short peak directed dorsad (dta, Fig. 19C).

3.1.4. Eyes

The large circular compound eye (cpe, Figs. 4, 8) protrudes laterally beyond the head capsule. Along its internal margin it is supported by a well-sclerotized circumocular sulcus (cos, Figs. 8, 18A) with a keyhole-shaped aperture.

Each compound eye consists of app. 1,500 ommatidia. The ommatidia are covered by a dense vestiture of very fine, rounded corneal nipples (after Bernhard & Miller 1962) (ca. 130 nm in diameter). Few interommatidial trichoid sensilla are irregularly spread on the surface of

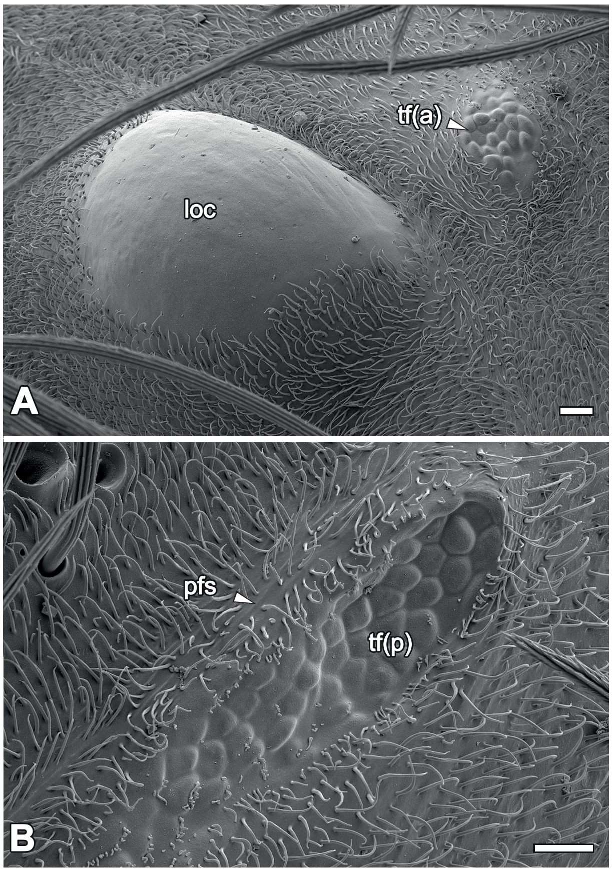

Figure 7: *Philopotamus ludificatus* McLachlan, 1878: details of head capsule, SEM images. **A**: dorsal view on lateral ocellus with adjacent tubercular field (tubercular field marked by arrow head); **B**: detail of tubercular field behind the postfrontal sulcus (postfrontal sulcus marked by arrow head). Abbreviations: **loc** – lateral ocellus, **pfs** – postfrontal sulcus, **tf(a)** – anterior tubercular field of vertex, **tf(p)** – posterior tubercular field of vertex. (Scale bars: 10 µm)

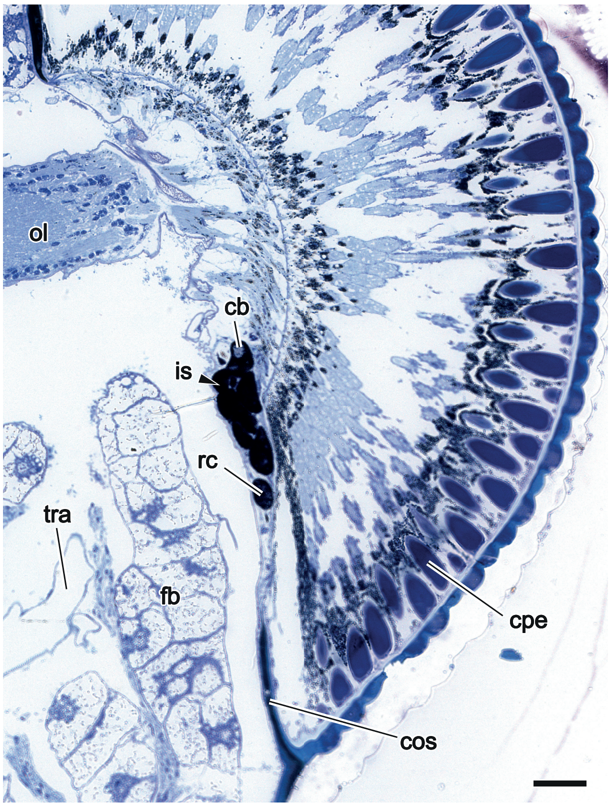

Figure 8: *Philopotamus ludificatus* McLachlan, 1878: head, cross-section of compound eye and immaginal stemma (marked by arrow head). Abbreviations: **cb** – crystalline body, **cos** – circumocular sulcus, **cpe** – compound eye, **fb** – fat body, **is** – immaginal stemma, **ol** – optical lobe of protocerebrum, **rc** – retinula cell, **tra** – trachea. (Scale bar: 10 µm)

the compound eye.

Two lateral ocelli (loc, Fig. 4) are located mesally, slightly behind the midline of the compound eyes. A median ocellus (moc, Fig. 4) is located half the distance between the dorsal antennal edges.

An internalized imaginal stemma (is, Fig. 8) is located posteroventrally adjacent to the retinula cells of the compound eye between the optic lobe of the brain (ol, Fig. 8) and the inner edge of the circumocular sulcus (cos, Fig. 8). It is visible as a wedge-shaped assemblage of several pigment cells (rc) and at least one cone cell (cb, Fig. 8).

3.1.5. Antenna

The filiform antenna is almost as long as the body. It comprises on average 53 antennomeres in both sexes (49–55; n = 50). The general coloration is light brown. Scapus (sca), pedicellus (ped), and the first 24–27 flagellomeres (fl, all in Fig. 4) show a dark brown band in the proximal half (Figs. 4, 5A). The width of the band decreases along the antenna from proximal to distal. The scapus is the largest antennomere. It is almost as long as wide (sca, Figs. 4, 15A). The pedicellus (ped, Figs. 4, 15A) is the smallest antennomere (half of the size of the scapus). Flagellomeres 1 and 2 are smaller than the remaining flagellomeres. The terminal flagellomere is apically pointed.

All antennomeres, except the scapus, are irregularly covered by numerous dentate ribbed trichoid (drts) and fungiform pseudoplacoid sensilla (fps) (both in Fig. 9B). Additionally, each flagellomere is equipped with a few and irregularly distributed coronary sensilla (mainly in the proximal half on the dorsal side) (crs, Fig. 9E), numerous helical trichoid sensilla (distal half) (hts, Fig. 9C), and very few small basiconic sensilla (distal half). The ventrolateral side of the scapus is equipped with two basiconic sensilla (Fig. 9D). Proximally, the scapus bears two groups of sensilla chaetica A (after Drilling & Klass 2010; scA, Fig. 9A) flanking the articulation of the antennifer.

The antenna is attached dorsolaterally between the compound eye and the median ocellus. It is articulated with the antennifer situated at the ventral margin of the broad antennal socket (Fig. 9A). Scapus and pedicellus are similarly articulated. A ventromesal process of the scapus corresponds with a small furrow at the base of the pedicellus. The position of this articulation is shifted by 55° in relation to the antennifer (Fig. 4). There are no specific articulations between the flagellomeres, which are separated by very short membranous areas.

Musculature (Figs. 15A, 16A, 18A,B, 19C–F): **Musculus tentorio-scapalis anterior** [te-sc(a)]: long, together with te-sc(l) the largest antennal muscle, O: mesal side of the anterior tentorial arm and laminatentorium, I: ventromesally at the scapal base with strong tendon (mesal of antennifer); **M. tentorio-scapalis posterior** [te-sc(p)]: slender, O: dorsally at the anterior tentorial arm (between te-sc(a)/(l)), I: dorsomesal margin of the scapal base; **M. tentorio-scapalis lateralis** [te-sc(l)]: two adjacent bundles, O: lateral face of the anterior tentorial arm and the laminatentorium (opposite to te-sc(a)), I: ventrolaterally at the scapal base (lateral of antennifer), posterior bundle with short tendon; **M. tentorio-scapalis medialis** [te-sc(m)]: comparatively short, O: dorsally on the anterior tentorial arm close to the head capsule (close to fr-ph(l)), distinctly anterior to the other antennal muscles, I:

---

[3] Lateral and medial reflects the relative position of the muscles to the scapo-pedicellar joint.

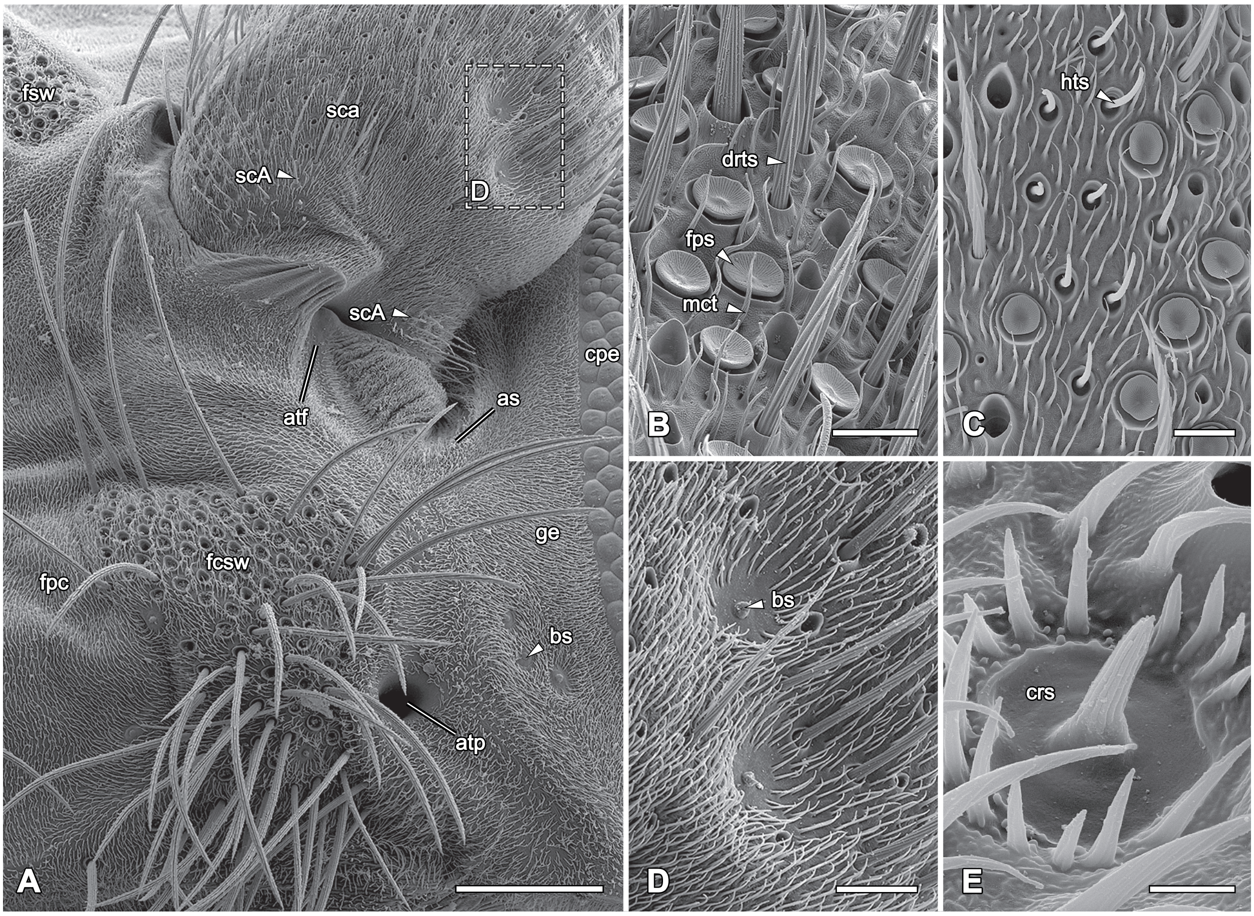

Figure 9: *Philopotamus ludificatus* McLachlan, 1878: antenna, SEM images. **A**: anterior view on frontoclypeus and antennal base; **B**: detail of antennal sensilla and microtrichia; **C**: detail of sensory field on sixth flagellomere; **D**: detail of scapal sensilla; **E**: detail of sensillum basiconicum surrounded by a ring of microtrichia. Abbreviations: **as** – antennal socket, **atf** – antennifer, **atp** – anterior tentorial pit, **bs** – sensillum basiconicum, **cpe** – compound eye, **crs** – coronary sensillum, **drts** – dentate ribbed trichoid sensillum, **fcsw** – frontoclypeal setal wart, **fpc** – frontopostclypeus, **fps** – fungiform pseudoplacoid sensillum, **fsw** – frontal setal wart, **ge** – gena, **hts** – helical trichoid sensillum, **mct** – microtrichium, **sca** – scapus, **scA** – sensillum chaeticum A. (Scale bars: A: 100 µm; D: 20 µm; B, C: 10 µm; E: 2 µm)

mesal margin of the scapal base; **M. scapo-pedicellaris medialis** [sc-pe(m)][3]: comprises three bundles: two lateral: O: dorsal and ventromesal areas of scapal base, I: both bundles together mesally at the pedicellar base (mesal of scapo-pedicellar articulation); one dorsal: O: between the first two bundles on the mesal face of the scapus, I: dorsally at the proximal margin of the pedicellus (almost opposite to scapo-pedicellar articulation); **M. scapo-pedicellaris lateralis** [sc-pe(l)]: two bundles, O: ventromesal and ventrolateral margin of scapal base (enclosing the scapal joint with the head capsule) I: large parts of ventral and ventrolateral margin of the pedicellus (lateral of scapo-pedicellar articulation).

3.1.6. Labrum

The labrum and anteclypeus together form a structural and functional unit (anteclypeolabrum, acl, Fig. 4; see above); the two components are inseparable since a clypeolabral articulation and the cranial flexor muscle (M. fronto-labralis) of the labrum are absent. The anteclypeolabrum is triangular and divided into a large, strongly sclerotized proximal part (acl(p)) and a short, membranous distal section (acl(d)) forming a rounded tip (Fig. 4).

Musculature: **Musculus labro-epipharyngalis** [lb-eph]: absent. **M. fronto-labralis** [fr-lb]: absent.

3.1.7. Mandible

The mandible (md) is largely membranous in its lateral half (md(m), Figs. 4, 10A), which is mesally continuous with the moderately sclerotized mandibular sclerite (md(s), Figs. 4, 10A). The short, lobe-like mandibular sclerite is antero-posteriorly flattened and lacks any teeth. The inner rims of the mandibular sclerites form blunt edges, which do not overlap, but touch each other at mid-length. Proximally, the mandibular sclerites enclose the bulged mid-part of the hypopharynx (Fig. 18D). The mandibular sclerites are almost completely covered by the anteclypeolabrum and hung into distinct concavities of the latter (Fig. 18D). There are no true articulations with the head capsule. The extensive adductor tendon (adte, Fig. 18C) is largely formed by non-sclerotized cuticle and has a broad origin at the proximomesal edge of the mandible (Fig. 18C); the cuticle is not particularly thickened in this area. The abductor tendon (abte, Fig. 18D) is not connected to the mandibular sclerite, but attaches to an invagination, which forms a distinct pit in the lateral mandibular membrane (Fig. 10A). This configuration does not allow notable movements of the mandible in the post-pharate stage (see also Discussion).

Musculature (Figs. 15A,B, 16A,B, 18A–D, 19D,E): **Musculus cranio-mandibularis medialis** [cr-md(m)]: the largest muscle of the head (fills app. ½ of the head capsule volume), composed of several bundles, which aggregate toward the adductor tendon, O: large parts of the dorsal and lateral head capsule (occipital/postoccipital region, postgena and vertex posterior to postfrontal sulcus), I: adductor tendon of the mandible; **M. cranio-mandibularis lateralis** [cr-md(l)]: large, but only app. ¼ of cr-md(m), O: with several bundles on the lateral area of the postgena and dorsolateral on gena and circumocular sulcus (partly between attachment areas of cr-md(m)), I: laterally at the membranous part of the mandible (close to the subgenal process) by means of the long abductor tendon; **M. hypopharyngo-mandibularis** [hy-md]: absent; **M. tentorio-mandibularis** [te-md]: extremely thin, composed of 2−3 fibers, closely

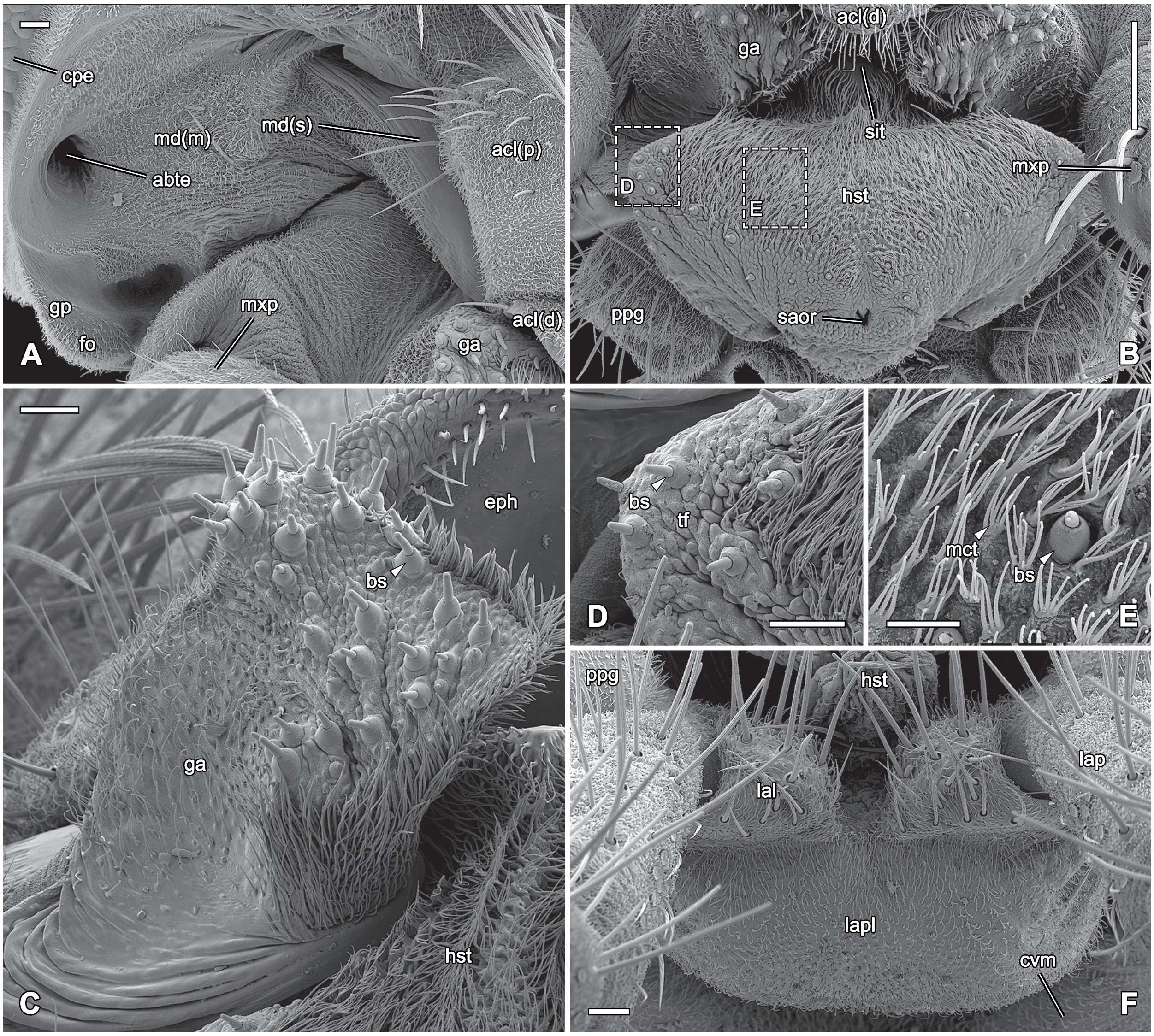

Figure 10: *Philopotamus ludificatus* McLachlan, 1878: mouthparts, SEM images. **A**: anterior view on base of mandible; **B**: anterior view on haustellum; **C**: anterior view on galeolacinia; **D**: detail of surface of haustellum; **E**: detail of sensilla and microtrichia of haustellum; **F**: anterior view on labium. Abbreviations: **abte** – tendon of abductor muscle of mandible (M. cranio-mandibularis lateralis), **acl(d)** – distal part of anteclypeolabrum, **acl(p)** – proximal part of anteclypeolabrum, **bs** – sensillum basiconicum, **cpe** – compound eye, **cvm** – cervical membrane, **eph** – epipharynx, **fo** – fossa of subgenal process, **ga** – galea, **gp** – subgenal process, **hst** – haustellum, **lal** – labial lobe, **lap** – labial palp, **lapl** – central plate of labium, **mct** – microtrichium, **md(m)** – membranous part of mandible, **md(s)** – mandibular sclerite, **mxp** – maxillary palp, **ppg** – palpiger, **saor** – salivary orifice, **sit** – sitophore plate, **tf** – tubercular field. (Scale bars: B: 100 µm; A, C, D, F: 20 µm; E: 10 µm)

adjacent with the mandibular nerve, O: anterior tentorial arm, covered by the anterior bundle of te-sc(l), I: mesally on the inner wall of the mandibular sclerite (with a long and very thin tendon).

3.1.8. Maxilla

The maxilla is composed of a composite basal sclerite (i.e., cardo + basistipes, dististipes), a composite galeolacinia, and a 5-segmented maxillary palp.

The small cardo (cd, Figs. 5A,B, 13) forms the basal-most part of the maxilla. Distally, the cardo is completely fused with the considerably larger stipes. A strong oblique sulcus (tss, Figs. 5A,B, 13), externally visible as a dark brown stripe, separates the stipes into a proximal basistipes (bst, Figs. 5A,B, 13), which is continuous with the cardo and an apical dististipes (dst, Figs. 5A,B, 13). The lateral end of this sulcus forms a distinct dorsal apodeme serving as attachment area of the cranial muscle of the stipes, whereas the mesal end is only slightly pointed. The proximolateral angle of the cardo meets the subgena close to the adjacent postgena without forming a distinct articulation.

The proximal margin of the dististipes is almost completely fused with the composite basal piece formed by the cardo and the basistipes. It is only mesally separated by a short triangular membranous incision (tsi, Fig. 5B). The mesal margin of the trough-shaped stipes is somewhat more strongly sclerotized than the remaining parts and forms a short distal process (msp, Fig. 13) at ⅔ of its length. The sclerite slightly widens distally bearing two terminal appendages, the large maxillary palp (mxp, Figs. 4, 5A,B) laterally and an endite lobe, which presumably represents a composite structure formed by a galea and a mainly incorporated lacinia mesally (i.e., a galeolacinia, see Discussion).

Most parts of the galea (ga, Figs. 11, 12A–C) are weakly sclerotized and quite flexible. Only the lateral margin is more strongly sclerotized. The lobe-like structure is dorso-ventrally flattened and apically blunt (Fig. 11). A membranous area around the base of the galea allows for substantial movements of the appendage (Fig. 10C). A small, slightly bulged lobe is located on the lower inner wall of the galea. It is separated from the latter by a small invagination of comparatively weakly sclerotized cuticle, whereas its inner wall is heavily sclerotized (Fig. 12A–C). This inner lobe of the galea may represent the remnants of a lacinia (lac, Figs. 11, 12B), see Discussion), and hence this structure should be termed as a galeolacinia.

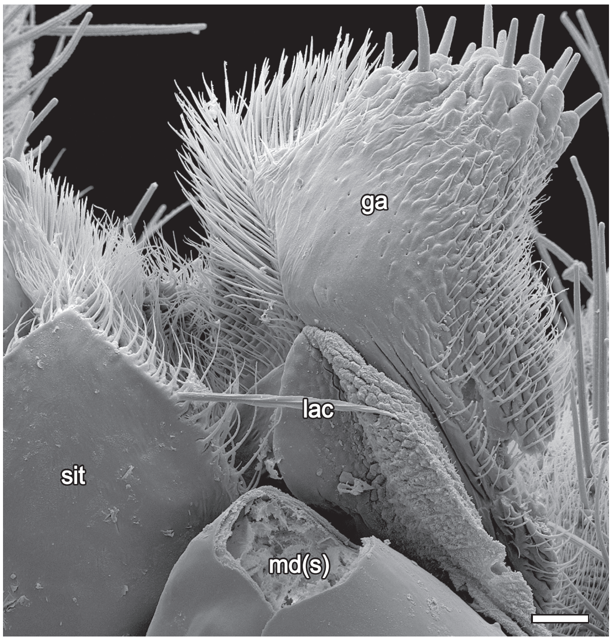

Figure 11: *Philopotamus ludificatus* McLachlan, 1878: dorsal view on mouthparts with mandible partly removed, SEM images. Abbreviations: **ga** – galea, **lac** – lacinia, **md(s)** – mandibular sclerite, **sit** – sitophore plate. (Scale bar: 20 µm)

The galeolacinia is located between the base of the haustellum and the maxillary palp (Fig. 10B). Its surface is densely covered by different types of sensilla. The granulose terminal face lacks microtrichia, but bears several large basiconic sensilla (bs, Fig. 10C). The mesal wall is covered by a very dense vestiture of outwards directed microtrichia.

The large maxillary palp (mxp, Fig. 4) is 5-segmented in both sexes. It is about three times longer than the overall length of the head capsule. The 1st and 2nd palpomeres are comparatively short (together as long as the 3rd). The 3rd and the 4th palpomere are of equal length. The tapering 5th palpomere is by far the longest (almost as long as the other palpomeres together) (Fig. 4). The diameter of the palpomeres constantly decreases toward the apex. All are covered by a dense vestiture of short, dentate ribbed trichoid and fungiform pseudoplacoid sensilla (same condition as in labial palp; drts, fps in Fig. 14A,E). Additionally, the 1st and 2nd palpomeres are equipped with numerous strong, smooth ribbed trichoid sensilla (mainly on the mesal faces) (srts, Fig. 4). The 4th palpomere bears proximomesally a distinctly delimited sensory field composed of numerous sensilla with stout, peg-shaped trichoms (ps, Fig. 14C). The 5th palpomere is apically equipped with three basiconic sensilla. A large central sensillum basiconicum (bs) is mesally and laterally flanked by three-time shorter sensilla of this type (same ratio as in labial palp; Fig. 14D).

Musculature (Figs. 12A,B, 13, 15A,B, 16A, 18E): **Musculus cranio-cardinalis** [cr-cd]: flattened, fan-shaped, O: ventrolaterally at the postgena, immediately mesally to the occipital sulcus, I: ventromesally at the proximal margin of the cardostipital sclerite (i.e., cardo + basistipes); **M. cranio-stipitalis** [cr-st]: long and slender, intersects with cr-prm(l), O: postgena, ventrally of base of the posterior tentorial arm (between cr-prm(l) and cr-prm(m)), I: distal process of mesal dististipital margin (msp) (together with te-st); **M. tentorio-cardinalis** [te-cd]: strong, slightly tapering, O: laterally at the mid part of the anterior tentorial arm, I: mesally at the distal margin of the cardostipital sclerite (i.e., cardo + basistipes); **M. tentorio-stipitalis** [te-st]: equally sized and shaped as te-cd, O: broadly at the ventral face of the laminatentorium, I: distal process of mesal dististipital margin (msp) (together with cr-st); **M. cranio-lacinialis** [cr-lc]: long and slender, O: postgena (dorsally to cr-cd), I: laterally at the small inner lobe (i.e., lacinia) of the galeolacinia; **M. stipito-lacinialis** [st-lc]: absent; **M. stipito-galealis** [st-ga]: absent; **M. cardo-palpalis dorsalis** [cd-mp(d)]: strong (app. two times stronger than st-mp(d)), O: proximomesal angle of the cardostipital sclerite, I: dorsolaterally at the base of the 1st palpomere; **M. cardo-palpalis ventralis** [cd-mp(v)]: compact, O: cardostipital sclerite,

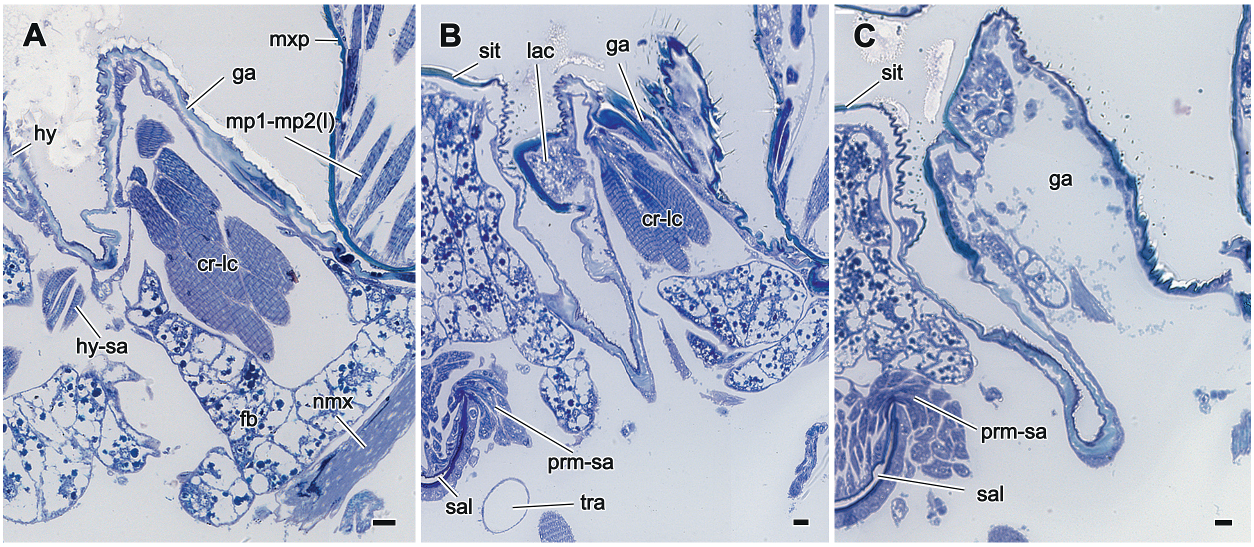

Figure 12: *Philopotamus ludificatus* McLachlan, 1878: head, cross-section of galeolacinia. **A**: proximal part of galea; **B**: galea with incorporated lacinia; **C**: distal part of galea. Abbreviations: **cr-lc** – M. cranio-lacinialis, **fb** – fat body, **ga** – galea, **lac** – lacinia, **hy** – hypopharynx, **hy-sa** – M. hypopharyngo-salivarialis, **mp1-mp2(l)** – M. palpo-palpalis maxillae primus lateralis, **mxp** – maxillary palp, **nmx** – maxillary nerve, **prm-sa** – M. praemento-salivarialis, **sal** – salivarium, **sit** – sitophore plate, **tra** – trachea. (Scale bars: 100 µm)

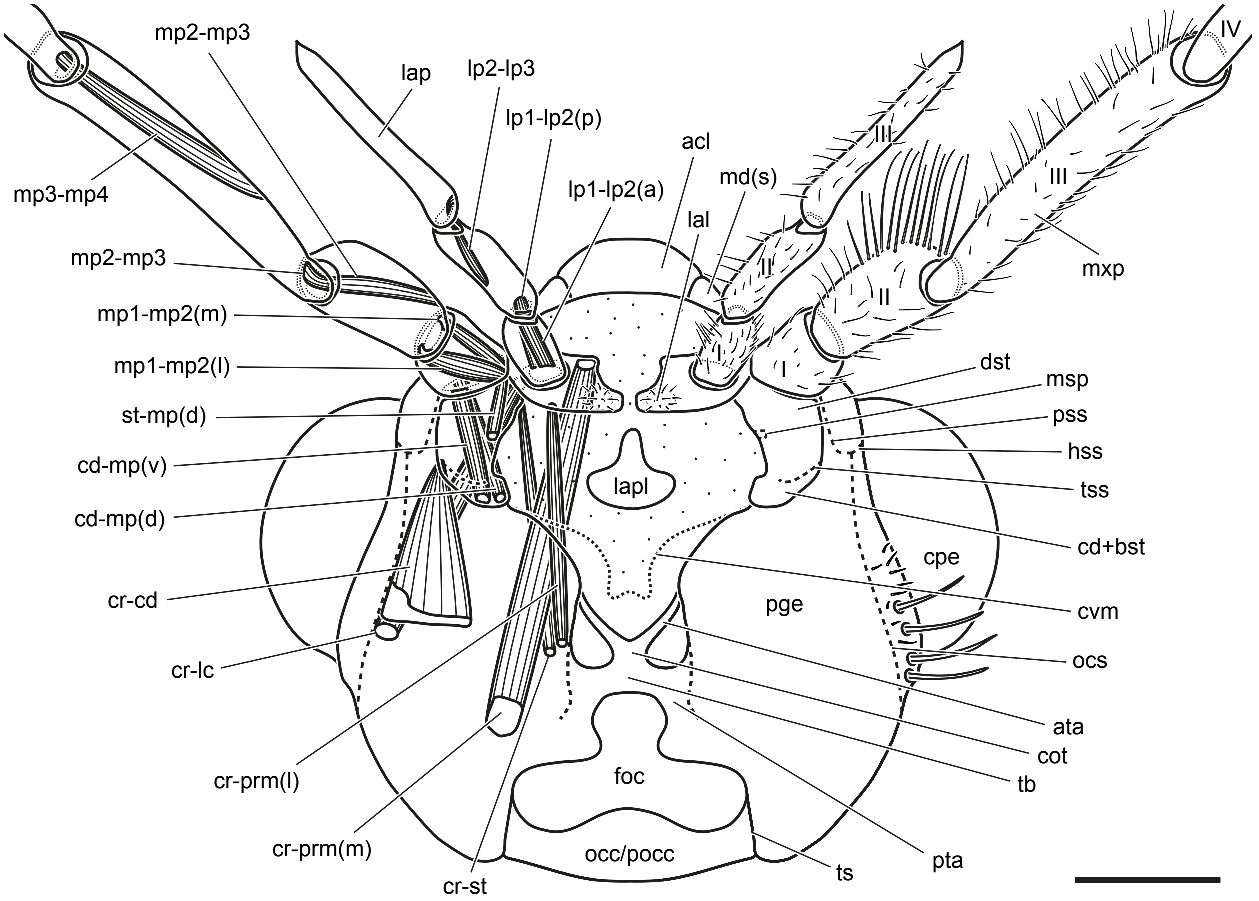

Figure 13: *Philopotamus ludificatus* McLachlan, 1878: head, posterior view. Abbreviations: **acl** – anteclypeolabrum, **ata** – anterior tentorial arm, **bst** – basistipes, **cd** – cardo, **cd-mp(d)** – M. cardo-palpalis dorsalis, **cd-mp(v)** – M. cardo-palpalis ventralis, **cot** – corpotentorium, **cpe** – compound eye, **cr-cd** – M. cranio-cardinalis, **cr-lc** – M. cranio-lacinialis, **cr-prm(l)** – M. cranio-praementalis lateralis, **cr-prm(m)** – M. cranio-praementalis medialis, **cr-st** – M. cranio-stipitalis, **cvm** – cervical membrane, **dst** – dististipes, **foc** – foramen occipitale, **hss** – hypostomal sulcus, **lal** – labial lobe, **lap** – labial palp, **lapl** – labial plate, **lp1-lp2(a)** – M. palpo-palpalis labii primus anterior, **lp1-lp2(p)** – M. palpo-palpalis labii primus posterior, **lp2-lp3** – M. palpo-palpalis labii secundus, **md(s)** – mandibular sclerite, **mp1-mp2(l)** – M. palpo-palpalis maxillae primus lateralis, **mp1-mp2(m)** – M. palpo-palpalis maxillae primus medialis, **mp2-mp3** – M. palpo-palpalis maxillae secundus, **mp3-mp4** – M. palpo-palpalis maxillae tertius, **mxp** – maxillary palp, **msp** – mesal process of dististipes, **occ** – occiput, **ocs** – occipital sulcus, **pge** – postgena, **pocc** – postocciput, **pss** – pleurostomal sulcus, **pta** – posterior tentorial arm, **st-mp(d)** – M. stipito-palpalis dorsalis, **tb** – tentorial bridge, **ts** – temporal sulcus, **tss** – transstipital sulcus, **I–IV** – number of palpomere. (Scale bar: 250 μm)

laterally of cd-mp(d), I: ventral margin of the 1st palpomere (opposite cd-mp(d)); **M. stipito-palpalis dorsalis** [st-mp(d)]: compact, O: mesally on the proximal half of the dististipes, I: mesally at the dorsal margin of the 1st palpomere (medially of cd-mp(d)); **M. palpo-palpalis maxillae primus lateralis** [mp1-mp2(l)]: two adjacent bundles, O: mesal margin of the base of palpomere 1, I: ventrolaterally at the proximal margin of palpomere 2; **M. palpo-palpalis maxillae primus medialis** [mp1-mp2(m)]: short, slightly tapering, O: mesal wall of palpomere 1 (distally of mp1-mp2(l)), I: dorsomesally at the base of palpomere 2; **M. palpo-palpalis maxillae secundus** [mp2-mp3]: compact, flattened, O: dorsal wall of palpomere 2, I: dorsolaterally at the base of palpomere 3; **M. palpo-palpalis maxillae**

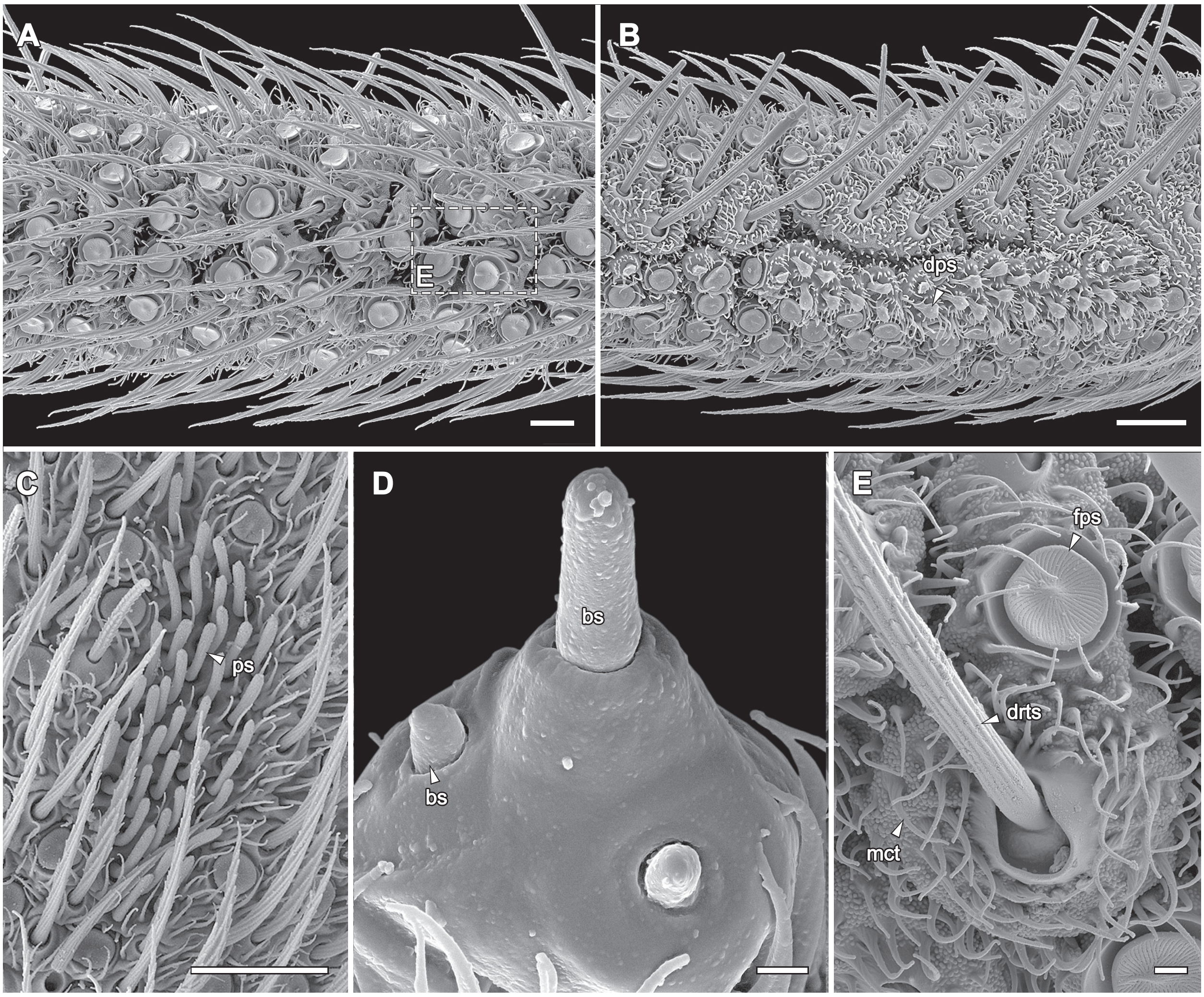

Figure 14: *Philopotamus ludificatus* McLachlan, 1878: mouthparts, SEM images. **A**: lateral wall of third palpomere of labial palp; **B**: mesal wall of third palpomere of labial palp with sensory field of dentate pseudoplacoid sensilla; **C**: lateral wall of maxillary palp with sensory field of peg-like sensilla; **D**: tip of labial palp with basiconic sensilla; **E**: detail of sensilla and microtrichia of labial palp. Abbreviations: **bs** – sensillum basiconicum, **dps** – dentate pseudoplacoid sensillum, **drts** – dentate ribbed trichoid sensillum, **fps** – fungiform pseudoplacoid sensillum, **mct** – microtrichium, **ps** – peg-like sensillum. (Scale bars: B, C: 20 μm; A: 10 μm; E: 2 μm; D: 1 μm)

tertius [mp3-mp4]: slender, O: dorsally at the middle of the mesal wall of palpomere 3, I: ventromesally at the base of palpomere 4; **M. palpo-palpalis maxillae quartus** [mp4-mp5]: very thin, O: dorsomesally on the distal half of palpomere 4, I: ventromesally at the base of palpomere 5.

3.1.9. Labium

The main body of the labium is bulged, pillow-shaped and weakly sclerotized (Figs. 5B, 10F). Posteriorly, it is continuous with the cervical membrane (cvm, Fig. 5B). A non-pigmented central labial plate (lapl, Fig. 5B) is delimited from the cervix by a semicircular fold (laf, Fig. 5B). This fold might represent the posterior margin of the labium, but the homology of the central plate is problematic (see Discussion). The degree of sclerotization increases from

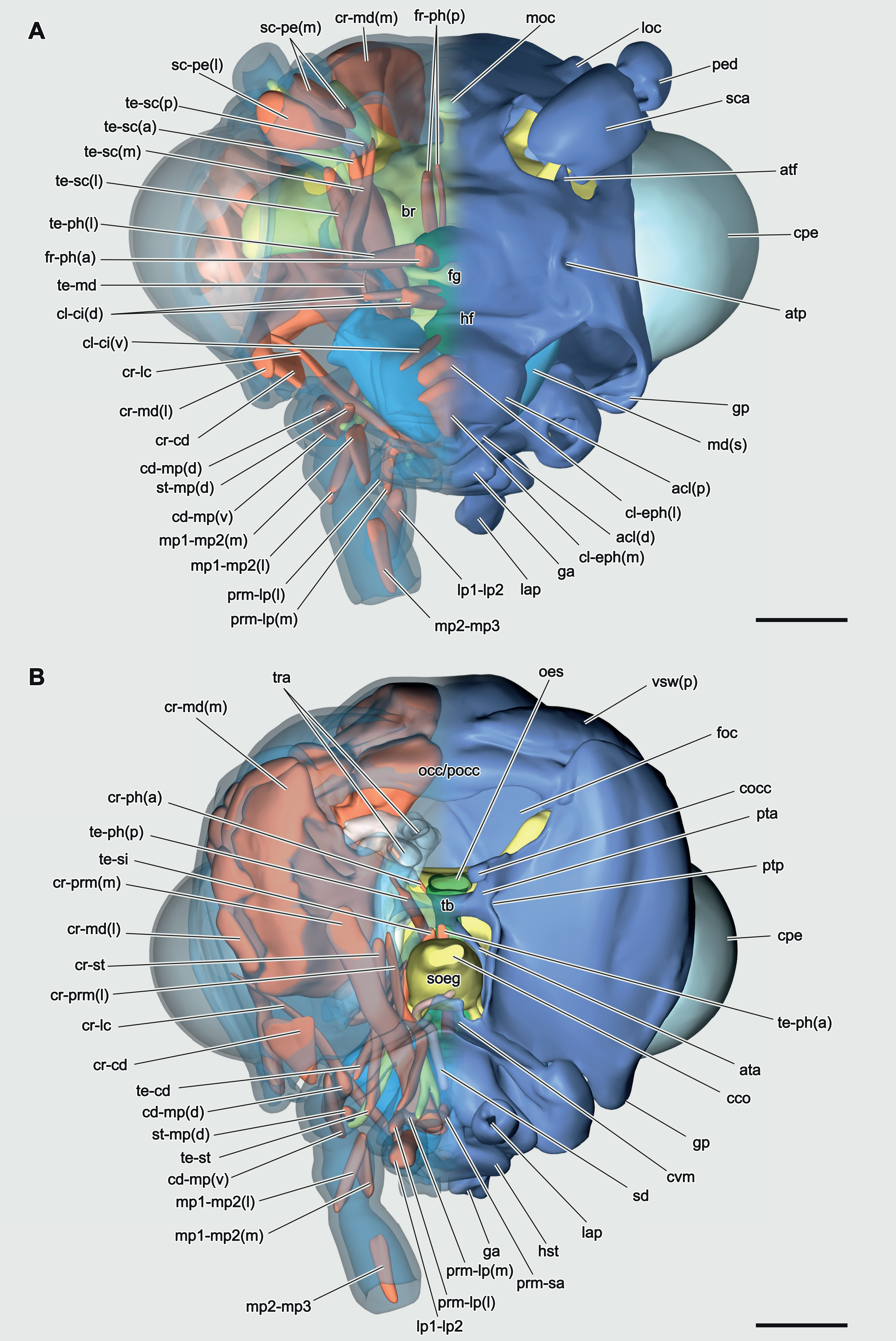
A
sc-pe(m)
cr-md(m)
fr-ph(p)
moc
loc
ped
sc-pe(l)
sca
te-sc(p)
te-sc(a)
te-sc(m)
atf
te-sc(l)
br
cpe
te-ph(l)
fr-ph(a)
fg
te-md
cl-ci(d)
hf
atp
cl-ci(v)
cr-lc
cr-md(l)
gp
md(s)
cr-cd
cd-mp(d)
acl(p)
st-mp(d)
cl-eph(l)
cd-mp(v)
acl(d)
mp1-mp2(m)
cl-eph(m)
mp1-mp2(l)
ga
lp1-lp2
lap
prm-lp(l)
prm-lp(m)
mp2-mp3
B
tra
oes
vsw(p)
cr-md(m)
foc
occ/pocc
cr-ph(a)
cocc
pta
te-ph(p)
te-si
ptp
cr-prm(m)
tb
cr-md(l)
cpe
cr-st
soeg
cr-prm(l)
te-ph(a)
cr-lc
ata
cr-cd
cco
te-cd
cd-mp(d)
gp
st-mp(d)
cvm
te-st
sd
cd-mp(v)
mp1-mp2(l)
lap
mp1-mp2(m)
ga
hst
prm-lp(m)
prm-sa
mp2-mp3
prm-lp(l)
lp1-lp2

← **Figure 15:** *Philopotamus ludificatus* McLachlan, 1878: head, 3D-reconstruction based on µCT data. **A**: anterior view; **B**: posterior view. Colors: blue – skeleton (sclerotized), light blue – eyes, green – gut, orange – musculature, rose – glands, yellow – nervous system. Abbreviations: **acl(d)** – distal part of anteclypeolabrum, **acl(p)** – proximal part of anteclypeolabrum, **ata** – anterior tentorial arm, **atf** – antennifer, **atp** – anterior tentorial pit, **br** – brain, **cco** – cervical connective, **cd-mp(d)** – M. cardo-palpalis dorsalis, **cd-mp(v)** – M. cardo-palpalis ventralis, **cl-ci(d)** – M. clypeo-cibarialis dorsalis, **cl-ci(v)** – M. clypeo-cibarialis ventralis, **cl-eph(l)** – M. clypeo-epipharyngalis lateralis, **cl-eph(m)** – M. clypeo-epipharyngalis medialis, **cocc** – condyli occipitales, **cpe** – compound eye, **cr-cd** – M. cranio-cardinalis, **cr-lc** – M. cranio-lacinialis, **cr-md(l)** – M. cranio-mandibularis lateralis, **cr-md(m)** – M. cranio-mandibularis medialis, **cr-ph(a)** – M. cranio-pharyngalis anterior, **cr-prm(l)** – M. cranio-praementalis lateralis, **cr-prm(m)** – M. cranio-praementalis medialis, **cr-st** – M. cranio-stipitalis, **cvm** – cervical membrane, **foc** – foramen occipitale, **fg** – ganglion frontale, **fr-ph(a)** – M. fronto-pharyngalis anterior, **fr-ph(p)** – M. fronto-pharyngalis posterior, **ga** – galea, **gp** – subgenal process, **hst** – haustellum, **lap** – labial palp, **loc** – lateral ocellus, **lp1-lp2** – M. palpo-palpalis labii primus [lp1-lp2(a) and lp1-lp2(p) together], **md(s)** – mandibular sclerite, **moc** – median ocellus, **mp1-mp2(l)** – M. palpo-palpalis maxillae primus lateralis, **mp1-mp2(m)** – M. palpo-palpalis maxillae primus medialis, **mp2-mp3** – M. palpo-palpalis maxillae secundus, **occ** – occiput, **oes** – oesophagus, **ped** – pedicellus, **pocc** – postocciput, **prm-lp(l)** – M. praemento-palpalis lateralis, **prm-lp(m)** – M. praemento-palpalis medialis, **prm-sa** – M. praemento-salivarialis, **pta** – posterior tentorial arm, **ptp** – posterior tentorial pit, **sc-pe(l)** – M. scapo-pedicellaris lateralis, **sc-pe(m)** – M. scapo-pedicellaris medialis, **sca** – scapus, **sd** – salivary duct, **soeg** – suboesophageal ganglion, **st-mp(d)** – M. stipito-palpalis dorsalis, **tb** – tentorial bridge, **te-cd** – M. tentorio-cardinalis, **te-md** – M. tentorio-mandibularis, **te-ph(a)** – M. tentorio-pharyngalis anterior, **te-ph(l)** – M. tentorio-pharyngalis lateralis, **te-ph(p)** – M. tentorio-pharyngalis posterior, **te-sc(a)** – M. tentorio-scapalis anterior, **te-sc(l)** – M. tentorio-scapalis lateralis, **te-sc(m)** – M. tentorio-scapalis medialis, **te-sc(p)** – M. tentorio-scapalis posterior, **te-si** – M. tentorio-sitophorialis, **te-st** – M. tentorio-stipitalis, **tra** – trachea, **vsw(p)** – posterior setal wart of vertex. (Scale bars: 250 µm) (General features of nervous system shown, for details see Fig. 20)

the proximal to the distal parts (Fig. 5B). There are no traces of subdivision. Laterally it is not distinctly delimited from the surrounding membrane. The distal face of the labial plate bears a small lobe (lal, Fig. 10F) mesally to the base of the labial palp (lap, Figs. 10F, 13). This lobe is covered with several stout smooth ribbed trichoid sensilla and is not equipped with intrinsic muscles. Laterally, the prementum forms a moderately sclerotized palpiger (ppg, Fig. 10B). This sclerite surrounds the base of the labial palp forming the anterolateral edge of the labium. The surface of the palpiger is equipped with stout smooth ribbed trichoid sensilla.

The labial palp is 3-segmented in both sexes and located distally on the premental palpiger. Both elements are distinctly separated by an extensive articulary membrane; no specific skeletal articulation is developed. The 2nd palpomere is almost as long as the 1st. The tapering 3rd palpomere is as long as segments 1 and 2 together (Fig. 4). All labial palpomeres are covered by a dense vestiture of short dentate ribbed trichoid and fungiform pseudoplacoid sensilla (drts, fps, Fig. 14 A,E). A discrete, elongate sensory field composed of ca. 30 dentate pseudoplacoid sensilla is located mesally in the proximal half of the 3rd palpomere (Fig. 14B). The tip of the 3rd palpomere bears four basiconic sensilla: a large central sensillum is surrounded by three smaller ones (Fig. 14D).

Musculature (Figs. 13, 15A,B, 16A,B, 18D–F): **Musculus cranio-praementalis medialis** [cr-prm(m)]: strong, composed of two more or less distinct bundles, O: both bundles closely adjacent mesally at the postgena

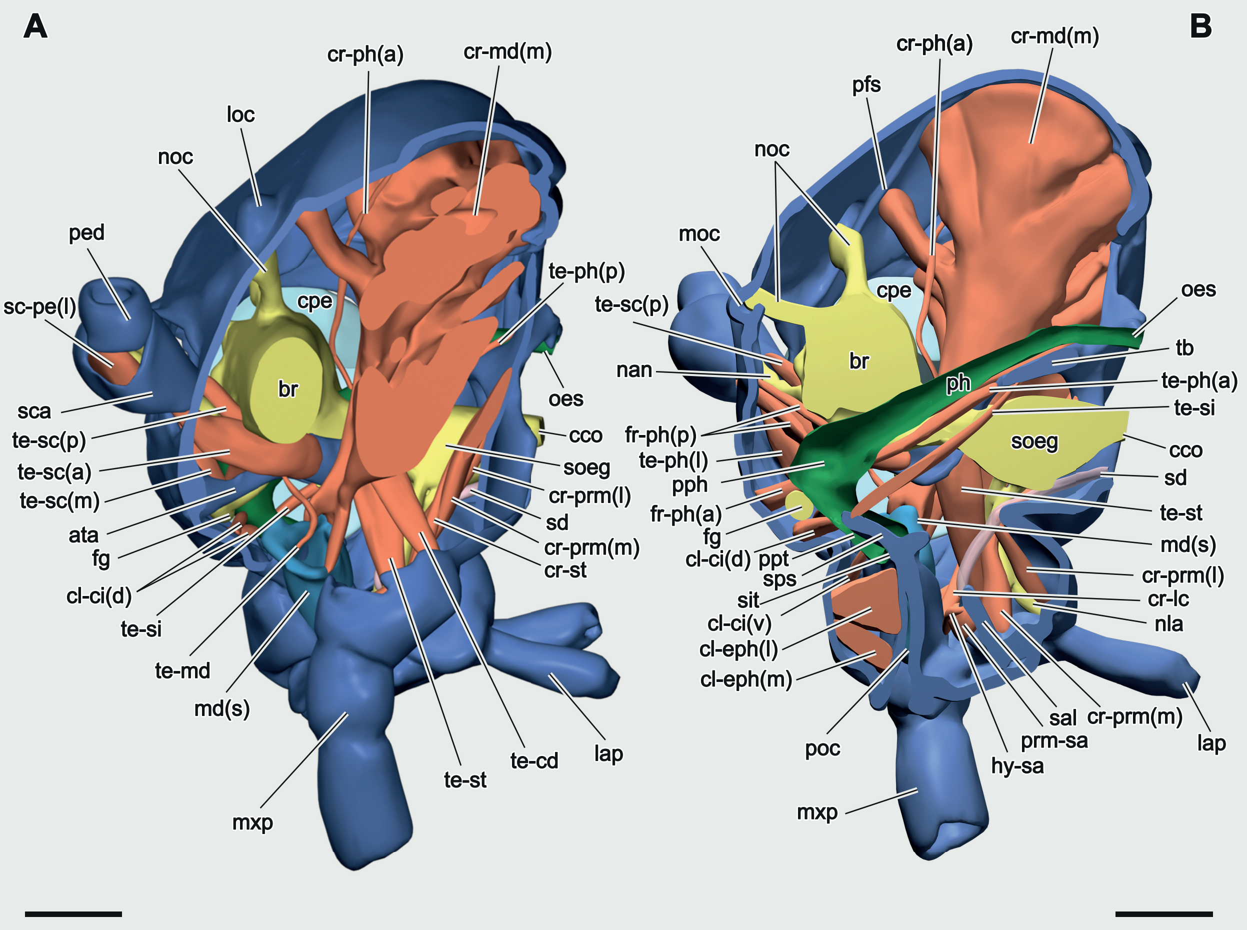

Figure 16: *Philopotamus ludificatus* McLachlan, 1878: head, 3D-reconstruction based on µCT data. **A**: parasagittal section (level of anterior tentorial pit); **B**: sagittal section. Colors: blue – skeleton (sclerotized), light blue – eyes, green – gut, orange – musculature, rose – glands, yellow – nervous system. Abbreviations: **ata** – anterior tentorial arm, **br** – brain, **cco** – cervical connective, **cl-ci(d)** – M. clypeo-cibarialis dorsalis, **cl-ci(v)** – M. clypeo-cibarialis ventralis, **cl-eph(l)** – M. clypeo-epipharyngalis lateralis, **cl-eph(m)** – M. clypeo-epipharyngalis medialis, **cpe** – compound eye, **cr-lc** – M. cranio-lacinialis, **cr-md(m)** – M. cranio-mandibularis medialis, **cr-ph(a)** – M. cranio-pharyngalis anterior, **cr-prm(l)** – M. cranio-praementalis lateralis, **cr-prm(m)** – M. cranio-praementalis medialis, **cr-st** – M. cranio-stipitalis, **fg** – ganglion frontale, **fr-ph(a)** – M. fronto-pharyngalis anterior, **fr-ph(p)** – M. fronto-pharyngalis posterior, **hy-sa** – M. hypopharyngo-salivarialis, **lap** – labial palp, **loc** – lateral ocellus, **md(s)** – mandibular sclerite, **moc** – median ocellus, **mxp** – maxillary palp, **nan** – nervus antennalis, **nla** – labial nerve, **noc** – ocellar nerve, **oes** – oesophagus, **ped** – pedicellus, **pfs** – postfrontal sulcus, **ph** – pharynx, **poc** – preoral cavity, **pph** – precerebral pharynx, **ppt** – prepharyngeal tube, **prm-sa** – M. praemento-salivarialis, **sal** – salivarium, **sca** – scapus, **sc-pe(l)** – M. scapo-pedicellaris lateralis, **sd** – salivary duct, **sit** – sitophore plate, **soeg** – suboesophageal ganglion, **sps** – spoon-shaped process of sitophore plate, **tb** – tentorial bridge, **te-cd** – M. tentorio-cardinalis, **te-md** – M. tentorio-mandibularis, **te-ph(a)** – M. tentorio-pharyngalis anterior, **te-ph(l)** – M. tentorio-pharyngalis lateralis, **te-ph(p)** – M. tentorio-pharyngalis posterior, **te-sc(a)** – M. tentorio-scapalis anterior, **te-sc(m)** – M. tentorio-scapalis medialis, **te-sc(p)** – M. tentorio-scapalis posterior, **te-si** – M. tentorio-sitophorialis, **te-st** – M. tentorio-stipitalis. (Scale bars: 250 µm) (General features of nervous system shown, for details see Fig. 20)

(laterally of posterior tentorial pits, dorsolaterally of cr-st), I: broadly at the distal part of the prementum, bundles more or less distinctly separated mesally and laterally of prm-lp(m); **M. cranio-praementalis lateralis** [cr-prm(l)]: long, slender (app. ⅔ thinner as cr-prm(m)), O: postgena, ventrally of posterior tentorial pit and directly mesally of cr-st, I: lateral rim of palpiger; **M. submento-praementalis** [smt-prm]: absent; **M. praemento-paraglossalis** [prm-pgl]: absent; **M. praemento-glossalis** [prm-gl]: absent; **M. praemento-palpalis medialis** [prm-lp(m)]: slender, comparatively long, O: mesally at the dorsal face of the prementum (close to the base of haustellum, between bundles of cr-prm(m)), I: laterally at the proximal margin of palpomere 1; **M. praemento-palpalis lateralis** [prm-lp(l)]: compact, O: proximolaterally on palpiger, I: laterally at the proximal margin of palpomere 1 (close to prm-lp(m)); **M. palpo-palpalis labii primus anterior** [lp1-lp2(a)]: O: anterolaterally at the base of palpomere 1, I: anteriorly at the base of palpomere 2; **M. palpo-palpalis labii primus posterior** [lp1-lp2(p)]: O: posteriorly at the base of palpomere 1, I: posteriorly at the base of palpomere 2; **M. palpo-palpalis labii secundus** [lp2-lp3]: thin, O: anterolaterally at the distal half of palpomere 2, I: laterally at the proximal margin of palpomere 3.

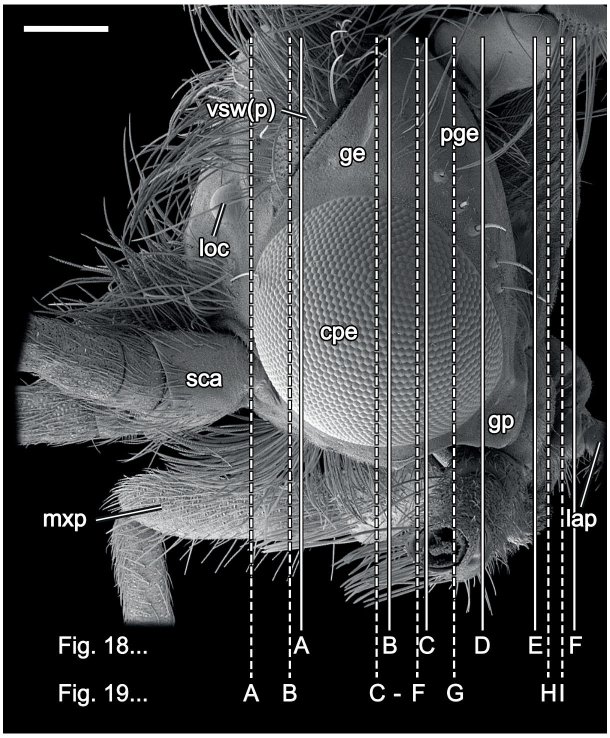

Figure 17: *Philopotamus ludificatus* McLachlan, 1878: head, SEM image. Lateral view with section planes of Figs. 18 (continuous lines) and 19 (dashed lines) marked. Abbreviations: **cpe** – compound eye, **ge** – gena, **gp** – subgenal process, **lap** – labial palp, **loc** – lateral ocellus, **mxp** – maxillary palp, **pge** – postgena, **sca** – scapus, **vsw(p)** – posterior setal wart of vertex. (Scale bar: 200 µm)

3.1.10. Epipharynx and hypopharynx

The epipharynx (eph, Figs. 10C, 18D), representing the inner wall of the anteclypeolabrum, is strongly sclerotized and positioned between the mandibles in its ventral half, forming the roof of the preoral cavity (= cibarium) (poc, Fig. 16B). The narrow, somewhat bulged epipharynx is only continuous with the sclerotized lateral margin of the anteclypeolabrum at its distal end. It is laterally surrounded by membranous regions in the other parts. The epipharyngeal sclerite terminates dorsally at the beginning of the closed prepharyngeal tube (see below)

.

The hypopharynx is composed of a mainly membranous, ventral section (i.e., anterior surface of the haustellum between the functional mouth opening and the salivary orifice) and the dorsal sitophore plate (sensu Chaudonneret 1990). The ventral part of the sitophore (sit, Figs. 11, 18C) is broadly underlying the distal half of the mandibles (Fig. 18D). It narrows dorsally and bulges between the mandibular bases. Before the beginning of the prepharyngeal tube (i.e., the lateral union of hypo- and epipharynx) (ppt, Figs. 16B, 18C) the sitophore plate is deeply transversely folded and continues toward the anatomical mouth opening (below the frontal ganglion) (Fig. 19F). This part of the sitophore plate forms the sclerotized floor of the prepharynx terminating in a spoon-shaped median process (sps, Fig. 16B), which projects into the prepharyngeal

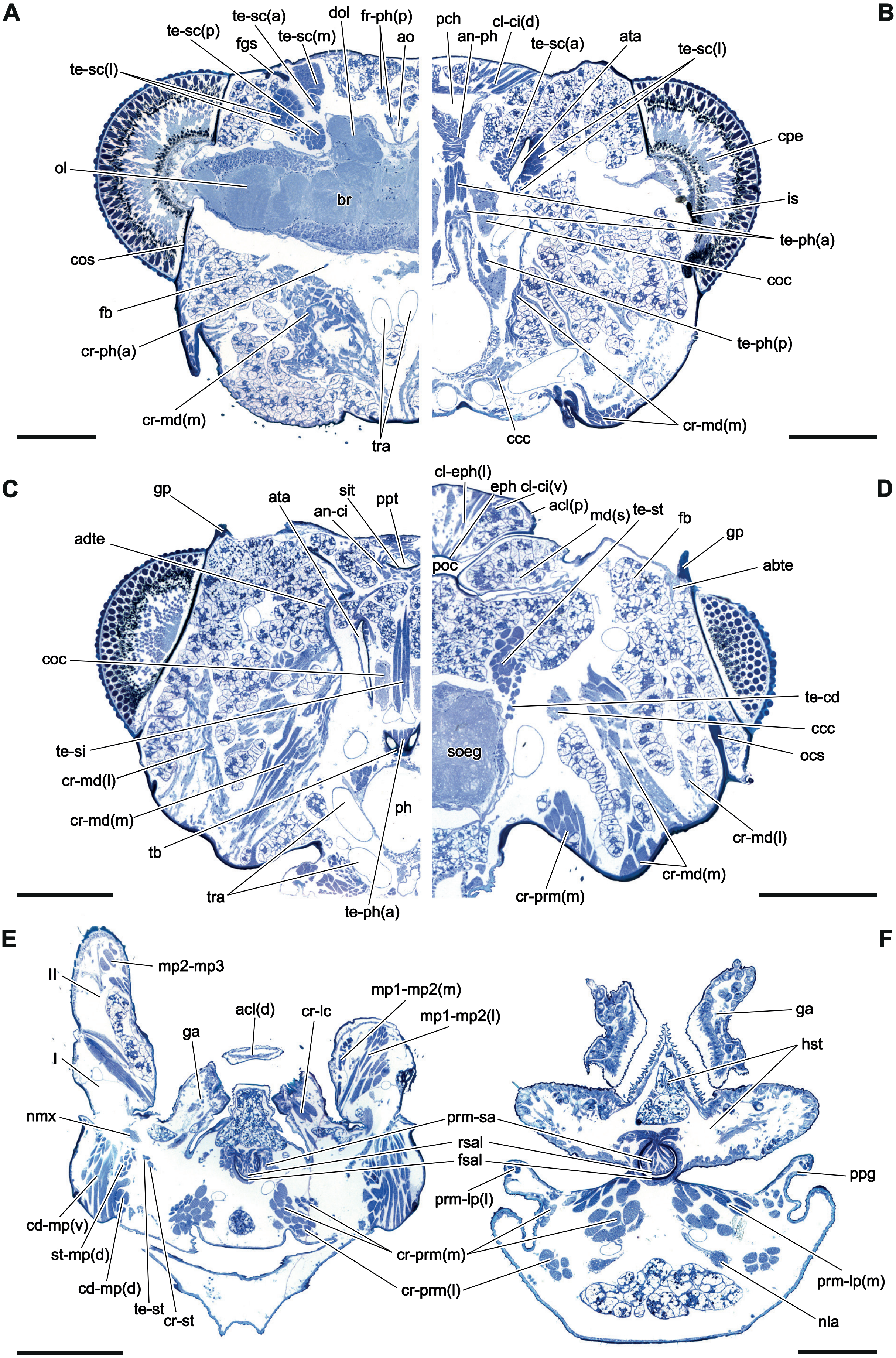
A
te-sc(p)
te-sc(a)
fgs
te-sc(m)
dol
fr-ph(p)
ao
te-sc(l)
ol
br
cos
fb
cr-ph(a)
cr-md(m)
tra
B
pch
an-ph
cl-ci(d)
te-sc(a)
ata
te-sc(l)
cpe
is
te-ph(a)
coc
te-ph(p)
cr-md(m)
ccc
C
gp
ata
sit
an-ci
ppt
adte
coc
te-si
cr-md(l)
cr-md(m)
tb
ph
tra
te-ph(a)
D
cl-eph(l)
eph
cl-ci(v)
acl(p)
md(s)
te-st
fb
gp
poc
abte
soeg
te-cd
ccc
ocs
cr-md(l)
cr-md(m)
cr-prm(m)
E
ll
mp2-mp3
l
acl(d)
cr-lc
mp1-mp2(m)
mp1-mp2(l)
ga
nmx
prm-sa
rsal
fsal
prm-lp(l)
cd-mp(v)
st-mp(d)
cd-mp(d)
te-st
cr-st
cr-prm(m)
cr-prm(l)
F
ga
hst
ppg
prm-lp(m)
nla

← **Figure 18:** *Philopotamus ludificatus* McLachlan, 1878: head, cross-sections. **A–F**: Cross-sections in dorsal-ventral sequence. Abbreviations: **abte** – tendon of abductor muscle of mandible (M. cranio-mandibularis lateralis), **acl(d)** – distal part of anteclypeolabrum, **acl(p)** – proximal part of anteclypeolabrum, **adte** – tendon of adductor muscle of mandible (M. cranio-mandibularis medialis), **an-ci** – M. anularis cibarialis, **an-ph** – M. anularis pharyngalis, **ao** – aorta, **ata** – anterior tentorial arm, **br** – brain, **ccc** – corpora cardiaca & corpora allata complex, **cd-mp(d)** – M. cardo-palpalis dorsalis, **cd-mp(v)** – M. cardo-palpalis ventralis, **cl-ci(d)** – M. clypeo-cibarialis dorsalis, **cl-ci(v)** – M. clypeo-cibarialis ventralis, **cl-eph(l)** – M. clypeo-epipharyngalis lateralis, **coc** – circumoesophageal commissure, **cos** – circumocular sulcus, **cpe** – compound eye, **cr-lc** – M. cranio-lacinialis, **cr-md(l)** – M. cranio-mandibularis lateralis, **cr-md(m)** – M. cranio-mandibularis medialis, **cr-ph(a)** – M. cranio-pharyngalis anterior, **cr-prm(l)** – M. cranio-praementalis lateralis, **cr-prm(m)** – M. cranio-praementalis medialis, **cr-st** – M. cranio-stipitalis, **dol** – deutocerebral olfactory lobe, **eph** – epipharynx, **fb** – fat body, **fgs** – frontogenal sulcus, **fsal** – floor of salivarium, **fr-ph(p)** – M. fronto-pharyngalis posterior, **ga** – galea, **gp** – subgenal process, **hst** – haustellum, **is** – immaginal stemma, **md(s)** – mandibular sclerite, **mp1-mp2(l)** – M. palpo-palpalis maxillae primus lateralis, **mp1-mp2(m)** – M. palpo-palpalis maxillae primus medialis, **mp2-mp3** – M. palpo-palpalis maxillae secundus, **nla** – labial nerve, **nmx** – maxillary nerve, **ocs** – occipital sulcus, **ol** – optical lobe of protocerebrum, **pch** – precerebral pumping chamber, **ph** – pharynx, **poc** – preoral cavity, **ppg** – palpiger, **ppt** – prepharyngeal tube, **prm-lp(l)** – M. praemento-palpalis lateralis, **prm-lp(m)** – M. praemento-palpalis medialis, **prm-sa** – M. praemento-salivarialis, **rsal** – floor of salivarium, **sit** – sitophore plate, **soeg** – suboesophageal ganglion, **st-mp(d)** – M. stipito-palpalis dorsalis, **tb** – tentorial bridge, **te-cd** – M. tentorio-cardinalis, **te-ph(a)** – M. tentorio-pharyngalis anterior, **te-ph(p)** – M. tentorio-pharyngalis posterior, **te-sc(a)** – M. tentorio-scapalis anterior, **te-sc(l)** – M. tentorio-scapalis lateralis, **te-sc(m)** – M. tentorio-scapalis medialis, **te-sc(p)** – M. tentorio-scapalis posterior, **te-si** – M. tentorio-sitophorialis, **te-st** – M. tentorio-stipitalis, **tra** – trachea, **I**, and **II** – number of palpomere of maxillary palp. (Section planes marked in Fig. 17, continuous lines) (Scale bars: A–E: 250 μm; F: 100 μm)

lumen (Figs. 16B, 19F). The sitophore lacks any sensilla (i.e., chemoreceptors) along its entire surface. The membranous roof of the prepharyngeal tube is formed by the epipharynx. The prepharynx is encircled by a thick layer of ring muscle fibers (Fig. 18C).

Musculature (Figs. 15A,B, 16A,B, 18A−C, 19C,D,F,G): **Musculus clypeo-epipharyngalis medialis** [cl-eph(m)]: compact, fan-shaped, O: central at the beginning of the sclerotized part of the anteclypeolabrum, I: median at the distal end of the epipharynx; **M. clypeo-epipharyngalis lateralis** [cl-eph(l)]: strong, compact, O: laterally at proximal half of the anteclypeolabrum (between cl-eph(m) and horizontal furrow), I: mesally at the epipharynx dorsad cl-eph(m); **M. clypeo-cibarialis ventralis** [cl-ci(v)]: slender, O: dorsolaterally at the anteclypeolabrum (dorsally of cl-eph(l)), I: preoral cavity at the ventralmost part of the prepharyngeal tube (dorsally of epipharyngeal sclerite), between prepharyngeal ring muscle fibers; **M. clypeo-cibarialis dorsalis** [cl-ci(d)]: two distinct bundles, compact median bundle app. two times larger than the slender lateral bundle, O: mesally (median bundle) and laterally (lateral bundle) at the frontopostclypeus, dorsally to the horizontal furrow, I: lateral bundle: proximal edge of the membranous (epipharyngeal) part of the prepharyngeal tube, directly below the ganglion frontale, median bundle: ventromesally of lateral bundle; **M. tentorio-sitophorialis** [te-si]: slender, O: paramedian on the ventral side of the tentorial bridge (between the anterior tentorial arms), I: dorsal end of the sitophore plate (below the spoon-shaped process), opposite to cl-ci(v); **M. anularis cibarialis** [an-ci]: series of ring muscle fibers covering the prepharynx, dorsally not delimited from the pharyngeal ring musculature (an-ph).

3.1.11. Haustellum

The distal region of the hypopharynx is fused with the labium, forming an extensive, largely membranous and eversible lobe, the haustellum (hst, Figs. 4, 10B,C). The haustellum is located between the galeolaciniae (dorsolateral), the bases of the maxillary and labial palps (ventrolateral) and the labial lobes (posterior) (Figs. 10B, 18F). It is dorsally continuous with

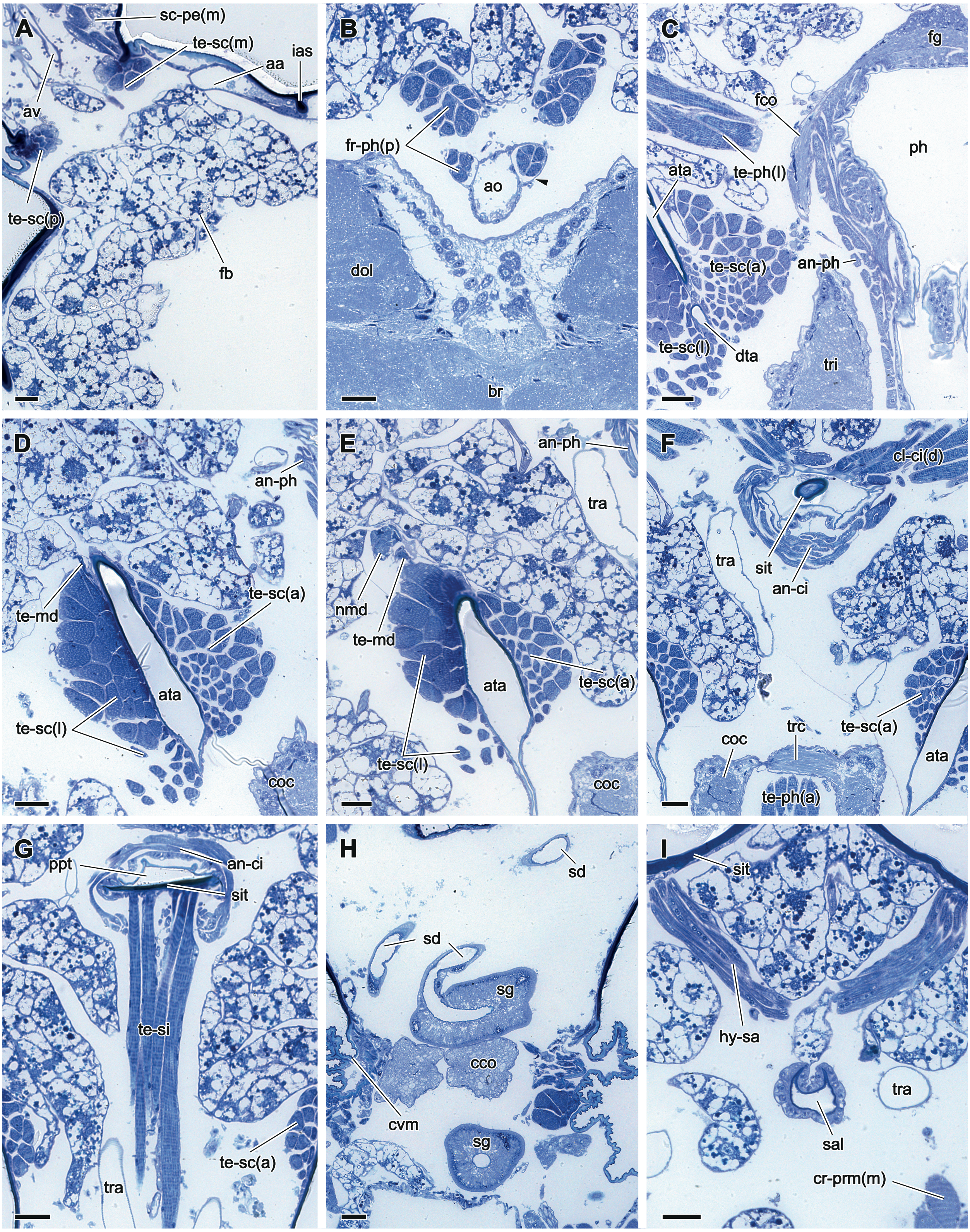

the sitophore (see above) and below it forms a keel between the galeolaciniae (Fig. 10C). Behind the galeolaciniae the haustellum extends laterally till the bases of the maxillary and labial palps. This anterior, upper area is densely covered by multi-branched, irregularly distributed microtrichia (mct, Fig. 10E) more or less directed toward the preoral cavity.

A regular system of channels on the surface of the haustellum is not present (Figs. 10B–E). The posterior part of the haustellum converges towards the labial lobes (Fig. 10F). Its lower surface is glabrous and tubercular (Fig. 10D). Centrally on this anterior area the salivarium terminates (see below). A median crest with a moderately dense set of microtrichia connects the salivary orifice and the preoral cavity (Fig. 10C). Basiconic sensilla (bs, Fig. 10E) of different sizes are randomly distributed on the whole face of the haustellum.

3.1.12. Salivarium

The long, tubular salivary glands (sg, Fig. 19H) extend into the cervical and prothoracic regions. Anteriorly two thin salivary ducts (sd, Fig. 19H) enter the head capsule through the lower section of the occipital foramen (below the suboesophageal ganglion) and unite at the beginning of the unpaired salivarium (sal, Figs. 16B, 19I).

The sclerotized salivarium is U-shaped in cross section and rapidly increases its circumference in the proximal half (Fig. 18E,F). The distal part (after the muscle insertion areas) is tapering toward the orifice. Its strongly concave floor (fsal, Fig. 18E,F) is heavily sclerotized. The less sclerotized pestle-like roof (rsal, Fig. 18E,F) is inserted into the concavity of the floor.

The salivary orifice is located on the lower, anterior edge of the haustellum (saor, Fig. 10B). The opening is surrounded by numerous small, two- to three-branched microtrichia.

Musculature (Figs. 16B, 18E,F, 19I): **Musculus hypopharyngo-salivarialis** [hy-sa]: compact, slender, O: laterally at the ventral half of the sitophore, close to the base of the galeolacinia, I: proximally on the roof of the salivarium; **M. praemento-salivarialis** [prm-

---

← **Figure 19:** *Philopotamus ludificatus* McLachlan, 1878: head, cross-sections in dorsal-ventral sequence. **A**: base of antenna with antennal ampulla; **B**: head aorta accompanied by bundles of posterior fronto-pharyngeal muscle (marked by arrow) in front of the brain; **C**: precerebral pharynx at level of the ganglion frontale; **D**: mid part of the anterior tentorial arm with origin of tentorio-antennal muscles and M. tentorio-mandibularis (extremely thin); **E**: region short distance ventrad from (**D**) with M. tentorio-mandibularis accompanied by mandibular nerve; **F**: prepharyngeal tube below the frontal ganglion with dorsal margin of the sitophore plate; **G**: sitophore plate short distance below (**F**); **H**: cervical region with salivary glands; **I**: proximal part of salivarium. Abbreviations: **aa** – antennal ampulla, **an-ci** – M. anularis cibarialis, **an-ph** – M. anularis pharyngalis, **ao** – aorta, **ata** – anterior tentorial arm, **av** – antennal vessel, **br** – brain, **cco** – cervical connective, **cl-ci(d)** – M. clypeo-cibarialis dorsalis, **coc** – circumoesophageal commissure, **cr-prm(m)** – M. cranio-praementalis medialis, **cvm** – cervical membrane, **dol** – deutocerebral olfactory lobe, **dta** – dorsal tentorial arm, **fb** – fat body, **fco** – frontal connective, **fg** – ganglion frontale, **fr-ph(p)** – M. fronto-pharyngalis posterior, **hy-sa** – M. hypopharyngo-salivarialis, **ias** – interantennal sulcus, **nmd** – mandibular nerve, **ph** – pharynx, **ppt** – prepharyngeal tube, **sal** – salivarium, **sc-pe(m)** – M. scapo-pedicellaris medialis, **sd** – salivary duct, **sg** – salivary gland, **sit** – sitophore plate, **te-md** – M. tentorio-mandibularis, **te-ph(a)** – M. tentorio-pharyngalis anterior, **te-ph(l)** – M. tentorio-pharyngalis lateralis, **te-sc(a)** – M. tentorio-scapalis anterior, **te-sc(l)** – M. tentorio-scapalis lateralis, **te-sc(m)** – M. tentorio-scapalis medialis, **te-sc(p)** – M. tentorio-scapalis posterior, **te-si** – M. tentorio-sitophorialis, **tra** – trachea, **trc** – tritocerebral commissure, **tri** – tritocerebrum. (Section planes marked in Fig. 17, dashed lines) (Scale bars: 100 µm) sa]: ventral part of the prementum (close to prm-lp(m) and the mesal bundle of cr-prm(m)), I: proximal half of the roof of the salivarium (immediately laterally and before hy-sa); **M. intra-salivarialis** [i-sa]: absent.

3.1.13. Cephalic food tract

The cephalic food tract comprises a distinctly widened precerebral pumping chamber (pch, Fig. 20A) (= buccal cavity, i.e. a composite formation of the prepharyngeal tube [ppt] and the precerebral pharynx [pph, Fig. 16B]). The border between both elements, i.e., the anatomical mouth opening, is marked by the position of the ganglion frontale (fg, Figs. 16B, 20A). The precerebral pumping chamber is moved by strong cibarial and pharyngeal dilator muscles. Posteriorly, the pharynx (ph, Fig. 16B) tapers distinctly before passing the tritocerebral commissures (trc, Fig. 20B).

The straight intra-/postcerebral pharyngeal regions have a constant, comparatively small width (⅓ of diameter of the precerebral pharynx) (Fig. 16B).

Musculature of the precerebral pharynx (Figs. 15A, 16A,B, 18A–C, 19B,C, 20A): **Musculus fronto-pharyngalis anterior** [fr-ph(a)]: compact, O: central region of frontopostclypeus, between the anterior tentorial pits, I: mesally at the anterolateral corner of the precerebral pumping chamber, directly behind the ganglion frontale; **M. fronto-pharyngalis posterior** [fr-ph(p)]: two distinct bundles, ventral bundle app. two times larger than dorsal bundle, both bundles are closely associated with the precerebral part of the cephalic aorta, O: frons, mesally of interantennal sulcus, I: dorsally at the posterodorsal face of the pharyngeal pumping chamber, just in front of the brain; **M. tentorio-pharyngalis lateralis** [te-ph(l)]: strong, O: broad area of the distal half of the anterior tentorial arm, I: dorsolaterally at the pharyngeal pumping chamber; **M. tentorio-pharyngalis anterior** [te-ph(a)]: two long and slender bundles, O: mesally on the base of the anterior tentorial arm, I: ventrally at the posterior end of the pharyngeal pumping chamber (opposite to fr-ph(p)).

Musculature of the postcerebral pharynx (Figs. 16B, 18A–C, 20A): **M. tentorio-pharyngalis posterior** [te-ph(p)]: slender, O: posterior tentorial arm, I: ventrally at the postcerebral pharynx, slightly behind the brain, opposite to cr-ph(a); **M. cranio-pharyngalis anterior** [cr-ph(a)]: very thin, composed of very few fibers, O: vertex, mesally of postgenal sulcus (posteriorly of lateral ocellus), I: dorsally on postcerebral pharynx, directly behind the brain; **M. cranio-pharyngalis posterior** [cr-ph(p)]: absent.

Musculature of the entire pharynx (pre- and postcerebral regions) (Figs. 18B,C, 19C,F): **M. anularis pharyngalis** [an-ph]: series of ring muscles covering the surface of the entire pharynx, most heavily developed around the precerebral pharyngeal pumping chamber; forming a distinctly thinner layer along the postcerebral pharynx. **M. longitudinalis pharyngalis** [lo-ph]: series of longitudinal muscle fibers stretching between the surface of the pharynx and an-ph, the layer is of constant thickness in the pre- and postcerebral regions.

3.1.14. Central nervous system (CNS)

The brain is located in the dorsal half of the head capsule between the large compound eyes. The large protocerebrum forms laterally the optical lobes (ol, Fig. 18A), which are of similar diameter as the rest of the brain (Fig. 20A,B). One compact anteromedian nerve

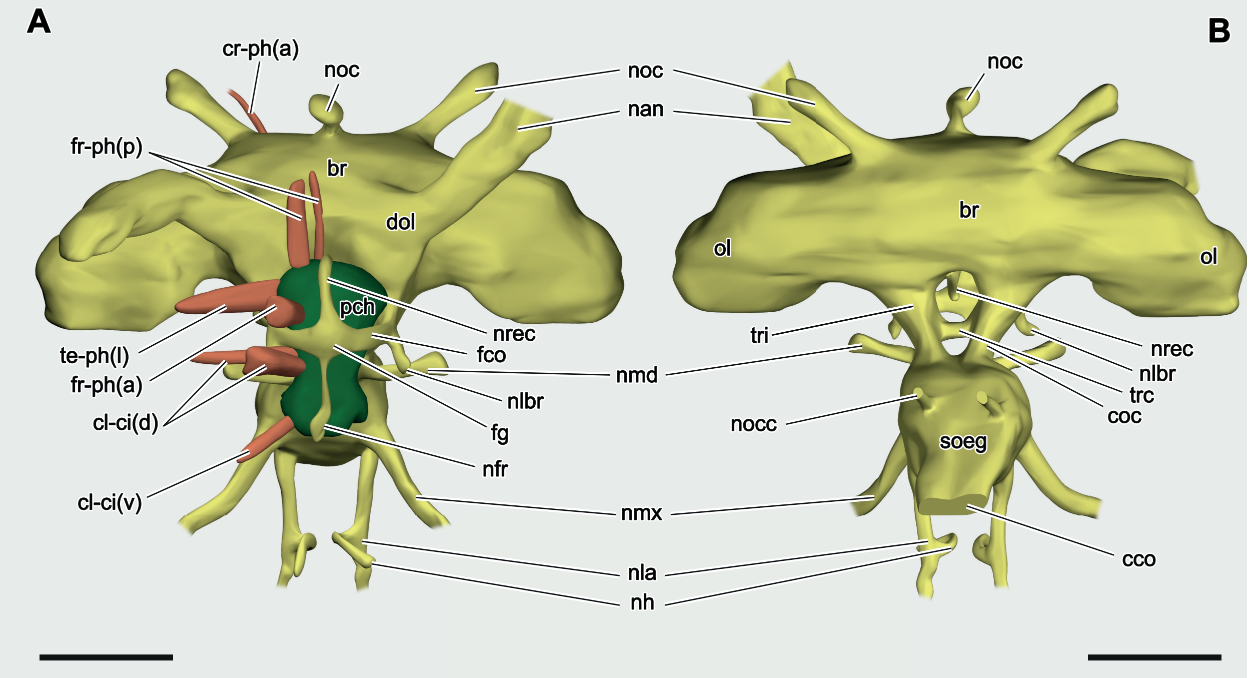

Figure 20: *Philopotamus ludificatus* McLachlan, 1878: nervous system and gut with attached musculature (removed in B), 3D-reconstruction based on µCT data. **A**: anterior view; **B**: posterior view. Colors: green – gut, orange – musculature, yellow – nervous system. Abbreviations: **br** – brain, **cco** – cervical connective, **cl-ci(d)** – M. clypeo-cibarialis dorsalis, **cl-ci(v)** – M. clypeo-cibarialis ventralis, **coc** – circumoesophageal commissure, **cr-ph(a)** – M. cranio-pharyngalis anterior, **dol** – deutocerebral olfactory lobe, **fco** – frontal connective, **fg** – ganglion frontale, **fr-ph(a)** – M. fronto-pharyngalis anterior, **fr-ph(p)** – M. fronto-pharyngalis posterior, **nan** – nervus antennalis, **nfr** – nervus frontalis, **nh** – nerve of the haustellum, **nla** – labial nerve, **nlbr** – labral nerve, **nmd** – mandibular nerve, **nmx** – maxillary nerve, **noc** – ocellar nerve, **nocc** – occipital nerve, **nrec** – nervus recurrens, **ol** – optical lobe of protocerebrum, **pch** – precerebral pumping chamber, **soeg** – suboesophageal ganglion, **te-ph(l)** – M. tentorio-pharyngalis lateralis, **trc** – tritocerebral commissure, **tri** – tritocerebrum. (Scale bars: 250 µm)

and two posterolateral nerves arising from the dorsal protocerebral surface supply the median ocellus and the lateral ocelli, respectively (Fig. 20A).

The deutocerebral olfactory lobe (dol, Fig. 18A) is located paramedially on the anterodorsal edge of the brain. It is not externally delimited from the deutocerebrum (Figs. 19B, 20A). The strong antennal nerve (nan, Fig. 20A,B) proximally innervates the tentorio-scapal muscles with thin nerve fibers before entering the scapus. It splits into two equally strong branches at the base of the antenna.

The ventral portion of the brain is formed by the tritocerebrum, which is also not externally delimited from the other parts. The tritocerebrum forms the anterior lobes and the circumoesophageal connectives (coc, Fig. 20B) of the CNS. They are interconnected by a short free tritocerebral commissure (trc, Fig. 20B) below the pharynx, extending between the tentorial muscles of the sitophore plate and the ventral pharynx (te-si, te-ph(a), Figs. 20F, 21B). A thin nervus tegumentalis emerges from the posterolateral face of the dorsal part of the tritocerebrum. It runs dorsolaterally into the large posterolateral setal wart of the vertex.

The somewhat egg-shaped suboesophageal ganglion (soeg, Figs. 16B, 20B) is located below the postpharynx, between the posterior margin of the brain and the neuroforamen. Its posterior end is continuous with the paired cervical connectives (cco, Fig. 20B). The comparatively thin mandibular nerve arises at its anterior edge. The mandibular nerve (nmd, Fig. 20A,B) passes the mesal side of the anterior tentorial arm (at level of the laminatentorium) and splits into several bundles associated with the mandibular muscles. The thickest branch runs into the mandible closely accompanied by the extremely thin tentorio-mandibular muscle (te-md, see above, Fig. 19E). The strong maxillary nerve (nmx, Fig. 20A,B) originates from the ventral side of the suboesophageal ganglion, distinctly behind the mandibular nerve. It runs into the maxilla innervating its muscles with very thin branches. The major part of the maxillary nerve forms the sensory branch, which enters the sensilla-rich palps.

Shortly behind the maxillary nerve originates its almost equally thick labial counterpart (nla, Fig. 20A,B). It innervates the labial and salivary muscles. Analogous to the conditions of the maxilla, the main part of the labial nerve continues into the labial palp to receive information of the large array of different sensory setae (see above). A smaller branch (nh, Fig. 20A,B) is send to the sensilla of the haustellum.

3.1.15. Stomatogastric nervous system

The stomatogastric nervous system innervates the preoral and pharyngeal musculature. The moderately sized frontal ganglion is connected with the anterior tritocerebral lobes by strong frontal connectives (fco, Figs. 19C, 20A). At the base of each connective originate the labro-frontal nerves, rapidly splitting up into two discrete fine branches. The very thin frontal nerves run downwards, merge after a short distance and proceed as an unpaired nervus frontalis (nfr, Fig. 20A) in front of the ganglion frontale downwards. The labral nerve (nlbr, Fig. 20A) runs more laterally, posterior to the ganglion frontale downwards sending branches to the clypeolabral dilator muscles.

An unpaired nervus connectivus linking the frontal ganglion with the protocerebrum is absent.

The nervus recurrens (nrec, Fig. 20A) originates from the hind face of the frontal ganglion. Subsequently, it runs between the pharyngeal ring musculature and the aorta backwards below the brain. Posteriorly, it proceeds into the hypocerebral ganglion which forms together with the corpora cardiaca a somewhat diffuse structure.

A thin occipital nerve (nocc, Fig. 20B) supplying the posterior part of the vertex, the occipital/postoccipital region, and the cervix, originates from the posterior end of the suboesophageal ganglion, immediately above the cervical connectives.

3.1.16. Hypocerebral complex

Paired, diffuse neural glands (corpora

→ **Table 4:** Terminology and homology of the trichopteran adult head musculature. Muscles are named by their areas of origin and insertion. The musculature described for *Philopotamus* (Annulipalpia) is homologized with muscles described for ‚Spicipalpia' (Klemm 1966: *Rhyacophila*), Integripalpia (Crichton 1957: *Phryganea*) and basal lepidopterans (Hannemann 1956: *Micropterix*). General nomenclatures of the insect head muscles (v. Kéler 1955; Wipfler et al. 2011) are also assigned. Squared brackets indicate that the muscle description was extracted from the literature, because it is absent in *Philopotamus*. Abbreviations: **X** = present, **−** = absent, **?** = uncertain homology, ***** = revised information taken from Kristensen 2003, **n.a.** = no information available.

Name	Abbrev.	Origin	Insertion	v. Kéler 1955	Wipfler et al. 2011	Hannemann 1956	Klemm 1966	Crichton 1957	present study
						Micropterix	*Rhyacophila*	*Phryganea*	*Philopotamus*
M. fronto-labralis	fr-lb	[mesally on frons]	[mesally on outer basal wall of labrum]	8	0lb1	19	–	–	–
M. fronto-epipharyngalis	fr-eph	[mesally on frons]	[basal labral wall]	9	0lb2	–	mlrp (?)	–	–
M. labro-epipharyngalis	lb-eph	[outer wall of labrum]	[epipharynx]	7	0lb5	21	–	–	–
M. clypeo-epipharyngalis medialis	cl-eph(m)	distomedian at anteclypeolabrum	distal at epipharynx	43, 7 (?)	0ci1, 0lb5 (?)	20	1cplr	1	X
M. clypeo-epipharyngalis lateralis	cl-eph(l)	lateral at anteclypeolabrum	epipharynx	43	0ci1	45	2cplr	2	X
M. clypeo-cibarialis ventralis	cl-ci(v)	proximal at anteclypeolabrum	anteroventral at cibarium	44 (?)	0bu1 (?)	–	2dlcb, 1dlcb (?)	21, 22 (?)	X
M. clypeo-cibarialis dorsalis	cl-ci(d)	frontoclypeus, directly below frontal ganglion	anteroventral at cibarium	44	0bu1	49 (?)	1dlphy, 1dlcb (?)	21, 22	X (two bundles)
M. tentorio-sitophorialis	te-si	tentorial bridge	dorsal margin of sitophore	48	0bu5	46	pdlcb	23	X
M. fronto-pharyngalis anterior	fr-ph(a)	frontoclypeus, directly behind frontal ganglion	dorsal at precerebral pharynx (anterior)	45	0bu2	48 (?)	4dlphy	24	X
M. fronto-pharyngalis posterior	fr-ph(p)	frontoclypeus	dorsal at precerbral pharynx (posterior), in front of supraoesophageal ganglion	46	0bu3	50	2dlphy	25	X (two bundles)
M. tentorio-pharyngalis lateralis	te-ph(l)	distal at anterior tentorial arm	lateral at precerbral pharynx	47 (?)	0hy2 (?)	48 (?)	3dlphy	26 (?)	X
M. tentorio-pharyngalis anterior	te-ph(a)	tentorial bridge	ventral at precerbral pharynx	50	0bu6	54	pdlphy1, 2 (?)	23, 28 (?)	X
M. tentorio-pharyngalis posterior	te-ph(p)	tentorial bridge or posterior tentorial arm	ventral / ventrolateral at precerebral pharynx	52, 54 (?)	0ph2 (?)	55	pdlphy 3, 4, 2dlpphy (?)	28 (?)	X
M. cranio-pharyngalis anterior	cr-ph(a)	vertex	dorsal at postcerbral pharynx, behind supraoesophageal ganglion	51	0ph1	51	1dlpphy	27	X
M. cranio-pharyngalis posterior	cr-ph(p)	[posterolateral at cranium]	[dorsolateral at postcerebral pharynx]	51, 53 (?)	0ph1, 0ph3 (?)	52, 53	2dlpphy (?)	28 (?)	–
M. anularis cibarialis	an-ci	ring muscle fibers covering the prepharynx		67	0hy9	X (*)	rm	29	X
M. anularis pharyngalis	an-ph	ring muscle fibers covering the entire pharynx		68	0st1	X (*)	rm	29	X
M. longitudinalis pharyngalis	lo-ph	longitudinal muscle fibers stretching between the surface of the pharynx and an-ph		69	0st2	47	lm	n.a.	X
M. tentorio-scapalis anterior	te-sc(a)	anterior tentorial arm	anterior basal margin of scapus	1	0an1	3	abant2	5	X
M. tentorio-scapalis posterior	te-sc(p)	anterior tentorial arm	posterior basal margin of scapus	2	0an2	4	adant2	3	X
M. tentorio-scapalis lateralis	te-sc(l)	anterior tentorial arm	lateral basal margin of scapus	3	0an3	2	abant1	4	X (two bundles)
M. tentorio-scapalis medialis	te-sc(m)	anterior tentorial arm	mesal basal margin of scapus	4	0an4	1	adant1	6	X
M. scapo-pedicellaris lateralis	sc-pe(l)	ventrolateral and ventromesal wall of scapus	ventral and ventrolateral basal margin of pedicellus	5	0an6	7, 8	adpde	n.a.	X (two bundles)
M. scapo-pedicellaris medialis	sc-pe(m)	dorsal and ventromesal wall of scapus	dorsal at proximal margin of pedicellus	6	0an7	5, 6	abpde	n.a.	X (three bundles)

Table 4 continued.

Name	Abbrev.	Origin	Insertion	v. Kéler 1955	Wipfler et al. 2011	Hannemann 1956	Klemm 1966	Crichton 1957	present study
						Micropterix	*Rhyacophila*	*Phryganea*	*Philopotamus*
M. cranio-mandibularis medialis	cr-md(m)	dorsal and lateral head capsule	adductor tendon of mandible	11	0md1	22	1admd	7	X
M. cranio-mandibularis lateralis	cr-md(l)	lateral at head capsule	abductor tendon of mandible	12	0md3	23	abmd	7	X
M. tentorio-mandibularis	te-md	anterior tentorial arm	mesally at inner wall of mandible	14	0md6	– (*)	2admd	–	X
M. hypopharyngo-mandibularis	hy-md	[hypopharyngeal sclerite]	[inner wall of mandible]	13	0md4	–	–	–	–
M. tentorio-cardinalis	te-cd	anterior tentorial arm	mesal process of 'cardo' (cardo + basistipes)	17	0mx3	26	adcd	9	X
M. tentorio-stipitalis	te-st	anterior tentorial arm	mesal margin of 'stipes' (dististipes)	18	0mx4	27	adst	–	X
M. cranio-cardinalis	cr-cd	postgena	proximolateral process of 'cardo' (cardo + basistipes)	15	0mx1	24	J	8	X
M. cranio-stipitalis	cr-st	postgena	distal process of mesal stipital margin (dististipes)	16	0mx1	25	–	–	X
M. cranio-lacinialis	cr-lc	postgena	laterally at composite endite lobe of maxilla	19	0mx2	29	flcc	10	X
M. stipito-lacinialis	st-lc	[mesal at stipes]	[basal edge of lacinia]	20	0mx6	28	flcs	11	–
M. stipito-galealis	st-ga	[stipes]	[basal edge of galea]	21	0mx7	30	–	–	–
M. cardo-palpalis dorsalis	cd-mp(d)	proximomesal angle of 'cardo' (cardo + basistipes)	dorsolateral at palpomere 1	–	–	–	lplp b	12, 13 (?)	X
M. stipito-palpalis dorsalis	st-mp(d)	mesally at proximal half of 'stipes' (dististipes)	mesal at dorsal margin of palpomere 1	23	0mx10	31	lplp a	12, 13 (?)	X
M. stipito-palpalis ventralis / M. cardo-palpalis ventralis	st-mp(v) / cd-mp(v)	lateral at 'cardo' (cardo + basistipes)	ventral basal margin of palpomere 1	22	0mx8	32	dplp	12, 13 (?)	X
M. palpo-palpalis maxillae primus medialis	mp1-mp2(m)	mesal wall of palpomere 1	dorsomesal of basal margin of palpomere 2	24 (?)	0mx12	33	X	X	X
M. palpo-palpalis maxillae primus lateralis	mp1-mp2(l)	mesal basal margin of palpomere 1	ventrolateral at basal margin of palpomere 2	24	0mx12	33	X	X	X
M. palpo-palpalis maxillae secundus	mp2-mp3	dorsal wall of palpomere 2	dorsolaterally at basal margin of palpomere 3	25	0mx13	34	X	X	X
M. palpo-palpalis maxillae tertius	mp3-mp4	dorsomesally at palpomere 3	ventromesally at basal margin of palpomere 4	26	0mx14	35	X	X	X
M. palpo-palpalis maxillae quartus	mp4-mp5	dorsomesal on distal half of palpomere 4	ventromesally at basal margin of palpomere 5	27	0mx15	36	X	X	X
M. hypopharyngo-salivarialis	hy-sa	lateral at ventral half of hypopharynx	proximally on the roof of the salivarium	37	0hy12	56, 57	–	–	X
M. intra-salivarialis	i-sa	[roof of salivarium]	[roof of salivarium]	37 (?)	–	–	1 (unpaired)	18	–
M. praemento-salivarialis	prm-sa	prementum	proximal half of the roof of the salivarium	38/39	0hy7, 0hy8 (?)	– (*)	2s	17	X
M. cranio-praementalis medialis	cr-prm(m)	postgena (together with cr-st)	mesally at distal part of prementum	30	0la6	39	1ablb, 2adlb	16	X (two bundles)
M. cranio-praementalis lateralis	cr-prm(l)	mesal at postgena	lateral rim of palpiger	29	0la5	40	rst	16	X

Table 4 continued.

Name	Abbrev.	Origin	Insertion	v. Kéler 1955	Wipfler et al. 2011	Hannemann 1956	Klemm 1966	Crichton 1957	present study
						Micropterix	*Rhyacophila*	*Phryganea*	*Philopotamus*
M. submento-praementalis	smt-pmt	[submentum or gula]	[prementum]	28	0la8	41(*)	-	-	-
M. praemento-paraglossalis	prm-pgl	[basal edge of prementum]	[paraglossa]	31	0la11	37	-	-	-
M. praemento-glossalis	prm-gl	[mesally on prementum]	[glossa]	32	0la12	38	-	-	-
M. praemento-palpalis medialis	prm-lp(m)	mesally at dorsal face of prementum	lateral at proximal margin of palpomere 1	33	0la13	42	lplp	19, 20 (?)	X
M. praemento-palpalis lateralis	prm-lp(l)	proximolateral on palpiger	lateral at proximal margin of palpomere 1	34	0la14	43	dplp	19, 20 (?)	X
M. palpo-palpalis labii primus anterior	lp1-lp2(a)	lateral at the base of palpomere 1	anteriorly at the base of palpomere 2	35	0la16	44a (*)	X	X	X
M. palpo-palpalis labii primus posterior	lp1-lp2(p)	posteriorly at the base of palpomere 1	posteriorly at the base of palpomere 2	35 (?)	0la16	44b (*)		X	X
M. palpo-palpalis labii secundus	lp2-lp3	anterolaterally at the distal half of palpomere 2	laterally at the proximal margin of palpomere 3	36	0la17	-	X	X	X

cardiaca and corpora allata; together ccc, Fig. 18B,D) are situated adjacent to the dorsal face of the postcerebral pharynx and the cephalic aorta with the comparatively small, rounded corpora cardiaca located directly behind the brain. They receive a thin and short nerve (nervus corpus cardiacus) from the brain. The considerably voluminous, elongated corpora allata are continuous with the corpora cardiaca and proceed into the neck region after receiving the nervus corpus allatum from the latter. A thin nerve originating laterally from the corpora allata connects it with the strong maxillary nerve.

3.1.17. Circulatory system

The cephalic aorta (ao, Figs. 18A, 19B) enters the head capsule through the alaforamen, directly dorsal of the pharynx. Its postcerebral part is voluminous, but constricts rapidly before the passage through the circumoesophageal connectives. In front of the brain, the aorta bents upwards and runs toward the area between the antennal sockets. It adheres to the posterior fronto-pharyngeal muscle (fr-ph(p)) (Fig. 19B) whose contractions may enhance the haemolymph flow. Between the antennae the aorta widens into a flat unpaired haemolymph sinus, reaching the median ocellus dorsally. Laterally, the sinus extends toward the antennal base, where it continues as a thin vessel extending into the antennae (av, Fig. 19A). This antennal vessel runs, accompanied by a trachea, into the distal part of the flagellum. Specific dilator muscles of the aorta or the antennal sinus are absent. However, the thickened wall of the sinus laterally to the interantennal sulcus may contain muscle fibers and may be contractile (muscles fibers could not be identified with certainty in histological sections at hand).

3.1.18. Tracheal system

Two pairs of main head tracheae (tra, Fig. 15B) pass through the alaforamen into the head capsule and flank the postcerebral pharynx dorsolaterally. The dorsal pair of stems splits into two branches. One runs dorsolaterally and supplies the mandibular muscles, whereas the second is almost exclusively associated with the brain and the antenna. The ventral stems proceed anterolaterally and split into numerous thin branches which supply the musculature of the ventral parts of the head capsule (mouthparts, cibarium, precerebral pharynx, etc.).

3.1.19. Fat body

Fat body aggregations take approximately two thirds of the free lumen of the head (space not filled with musculature or the nervous system) (fb, Fig. 18A–D). They are only absent directly around the digestive, circulatory, nervous, and tracheal systems. The entire antenna and the distal segments of the maxillary (3rd and following palpomeres) and labial palps (2nd and 3rd palpomere) are also free of fat body.

3.2. Comparative analysis of adult head structures

3.2.1. Tentorium

3.2.1.1. General appearance

The tentorium is X-shaped with anterior tentorial arms fused forming a distinct corpotentorium in Philopotamidae (Fig. 6).

A Π-shaped configuration with extremely short posterior tentorial arms and well separated anterior tentorial arms in front of the tentorial bridge is present in several not closely related lineages (Tab. 5).

Furthermore, the tentorium is H-shaped with posterior tentorial arms distinctly developed before reaching the tentorial bridge (anterior tentorial arms separated) in the spicipalpian lineages Rhyacophilidae, Glossosomatidae, Hydroptilidae as well as in some annulipalpians (e.g., Stenopsychidae, Hydropsychidae, Polycentropodidae, and Psychomyiidae; Tab. 5).

The tentorial bridge bears at its anterior margin small median ridges (= antero-mesal protuberance after Neboiss [1991]) in Hydrobiosidae and Sericostomatidae.

3.2.1.2. Anterior tentorial arms

Anterior tentorial arms (ata, Fig. 6) are well developed in all trichopteran lineages. They originate at the anterior tentorial pits and slightly converge towards the tentorial bridge (Fig. 6). Furthermore, they are usually distinctly separated before reaching the tentorial bridge (i.e., a corpotentorium is absent) in most groups of Trichoptera, except for Philopotamidae (see Tab. 5).

The anterior tentorial arms usually bear internally directed processes (= laminatentoria = lt, Fig. 6), which greatly differ in size and level of sclerotization among different lineages. They are comparatively large and heavily sclerotized in Hydrobiosidae (Fig. 23D), where they almost touch each other mesally. The laminatentoria of Hydropsychidae are also strongly developed, but they are clearly separated from each other mesally. In most other groups of Trichoptera the laminatentoria are much smaller (e.g., Philopotamidae, Fig. 6; Limnephilidae, Fig. 24) or even completely absent (e.g., Ptilocolepidae, Fig. 23F) (Tab. 5).

The anterior tentorial arms are connected

Table 5: The tentorium of adult Trichoptera. Abbreviations: **ata** – anterior tentorial arm, **cot** – corpotentorium, **dta** – dorsal tentorial arm, **H** – H-shaped configuration of the tentorium, **lt** – laminatentorium, **prot**. – protuberance, **pta** – posterior tentorial arm, **tb** – tentorial bridge, **tent**. – tentorium, **X** – X-shaped configuration of the tentorium, **Π** – Π-shaped configuration of the tentorium, **-** – absent, **+** – present, **n.a.** – not applicable, [**1**] – homology of dorso-lateral protuberance and dorsal tentorial arm uncertain, [**2**] – 'incomplete', dorsal tentorial arm not continuous with the head capsule, [**3**] – 'complete', dorsal tentorial arm continuous with the head capsule, **?** – uncertain.

Taxon	Shape of tent.	Presence of cot	Size and sclerotization of lt	Dorso-lateral prot. at ata	Dorsal tentorial arm	Origin of dta	Median prot. at tb	Size of pta
Philopotamus ludificatus McLachlan, 1878	X	+	small and weakly sclerotized	-	+ (vestigial)	in the middle of ata	-	well developed (2x longer than width)
Stenopsyche marmorata Navas, 1920	H	-	small and weakly sclerotized	-	+ (comparatively small)	in the anterior half of ata	-	well developed (2x longer than width)
Hydropsyche angustipennis (Curtis, 1834)	H	-	large and strongly sclerotized	+ [?]	- [?]	n.a. [1]	-	well developed (2x longer than width)
Tinodes dives (Pictet, 1834)	H	-	small and moderatly sclerotized	-	+ (vestigial)	in the middle of ata	-	well developed (2x longer than width)
Holocentropus dubius (Rambur, 1842)	H	-	large and strongly sclerotized	-	-	-	-	well developed (2x longer than width)
Rhyacophila obliterata McLachlan, 1863	H	-	large and moderatly sclerotized	-	+ (strong, 'incomplete' [2])	in the middle of ata	-	well developed (2x longer than width)
Apsilochorema sutshanum Martynov, 1934	Π	-	massive and strongly sclerotized	-	+ (strong, 'incomplete' [2])	in the middle of ata	+ [?]	short (as long as width)
Hydrobiosis styracine McFarlane, 1960	Π	-	massive and strongly sclerotized	-	+ (strong, 'incomplete' [2])	in the middle of ata	+	short (as long as width)
Glossosoma spinosum Morse et Yang, 2005	H	-	large and strongly sclerotized	-	+ (vestigial)	in the anterior half of ata	-	well developed (2x longer than width)
Agapetus fuscipes Curtis, 1834	H	-	large and strongly sclerotized	-	+ (vestigial)	in the anterior half of ata	-	well developed (2x longer than width)
Ptilocolepus granulatus (Pictet, 1834)	H	-	-	-	+ (vestigial)	in the anterior half of ata	-	well developed (2x longer than width)
Hydroptila scamandra Neboiss, 1977	H	-	-	-	-	-	-	well developed (> 3x longer than width)
Orthotrichia atraseta Wells, 1979	H	-	-	-	-	-	-	well developed (> 3x longer than width)
Phryganea grandis Linnaeus, 1758	Π	-	large and strongly sclerotized	-	+ (strong, 'complete' [3])	in the middle of ata	-	short (as long as width)
Trichostegia minor (Curtis, 1834)	H	-	large and strongly sclerotized	-	+ (strong, 'complete' [3])	in the middle of ata	-	well developed (2x longer than width)

Table 5 continued.

Taxon	Shape of tent.	Presence of cot	Size and sclerotization of lt	Dorso-lateral prot. at ata	Dorsal tentorial arm	Origin of dta	Median prot. at tb	Size of pta
Brachycentrus subnubilus Curtis, 1834	Π	-	large and strongly sclerotized	-	+ (strong, 'complete'[3])	in the middle of ata	-	extremely short
Limnephilus flavicornis (Fabricius, 1787)	Π	-	large and strongly sclerotized	-	+ (strong, 'complete'[3])	in the middle of ata	-	extremely short
Silo nigricornis (Pictet, 1834)	Π	-	large and strongly sclerotized	-	+ (strong, 'complete'[3])	in the middle of ata	-	extremely short
Sericostoma personatum Kirby et Spence, 1826	Π	-	small but strongly sclerotized	-	-	-	+	extremely short
Pycnocentria evecta McLachlan, 1868	Π	-	small but strongly sclerotized	-	-	-	-	extremely short
Molanna angustata Curtis, 1834	Π	-	small but strongly sclerotized	-	-	-	-	extremely short
Leptocerus tineiformis Curtis, 1834	Π	-	large and strongly sclerotized	-	+ (strong, 'incomplete'[2])	posterior half of ata	-	extremely short

with the circumantennal sulcus, in particular with the antennifer, by the frontogenal sulcus (fgs, Fig. 18A), which is strongly developed in most groups (e.g., Hydropsychidae). It is comparatively short and not continuous with the circumantennal sulcus or antennifer in the integripalpian lineage Plenitentoria.

The anterior tentorial arms of Hydropsychidae are equipped with large rounded protuberances on the dorsolateral wall.

3.2.1.3. Posterior tentorial arms

The posterior tentorial arms (pta, Fig. 13) originate close to the occipital foramen at the posterior tentorial pits. They are comparatively short, but strongly developed, in most groups of Trichoptera (e.g., Philopotamidae, Fig. 13; Glossosomatidae; Tab. 5). In contrast, they are extremely short in most Integripalpia and the spicipalpian lineage Hydrobiosidae (Tab. 5).

3.2.1.4. Dorsal tentorial arms

Representatives of Plenitentoria are equipped with strong dorsal tentorial arms which are continuous with the head capsule (e.g., Limnephilidae; dta, Fig. 24). Dorsal tentorial arms are also well-developed, but incomplete since they do not reach the head capsule in the breviteritorian lineage Leptoceridae. The arms originate along the posterior half of the anterior tentorial arms in this group.

Well-developed, but incomplete dorsal tentorial arms are also present in Hydrobiosidae (Fig. 23D). They are comparatively short, vestigial or even completely absent in all other trichopteran lineages (e.g., Philopotamidae, Fig. 19C; Glossosomatidae, Fig. 23E) (Tab. 5).

3.2.2. Antenna

3.2.2.1. General appearance

The adult antenna of Trichoptera is filiform. In most groups it is as long as the forewing in males (e.g., Philopotamidae, Hydropsychidae, Phryganeidae), but distinctly shorter in females (e.g., Hydropsychidae; Tab. 6). In the annulipalpian families Polycentropodidae, Psychomyiidae, and the phryganeid genus *Trichostegia* it is remarkably shorter than the length of the forewing in both sexes. In contrast, it is strikingly longer than the forewing in Leptoceridae.

The number of antennomers in males varies between an average of 27 in Hydroptilidae and Glossosomatidae-Agapetinae, and 100 in Leptoceridae (Tab. 6).

The number of antennomers in males and females is similar in most trichopteran groups (e.g., Philopotamidae, Hydropsychidae, Phryganeidae [i.e., *Trichostegia*]; Tab. 6), but varies between both sexes in Limnephilidae, Leptoceridae, Hydroptilidae, and in the phryganeid genus *Phryganea* as well (Tab. 6).

The adult antenna is inserted on the dorsolateral part of the head capsule between the anterior edges of the compound eyes. Its basal segment, the scapus, is situated in a membranous antennal foramen (af, Fig. 22A–I) and articulates with the antennifer (see Fig. 4A,B). The position and size of the antennifer varies considerably between different lineages of Trichoptera (Fig. 22A–I; Tab. 6). It is strongly developed and positioned at the ventral margin of the antennal socket in Annulipalpia (Fig. 22A,B) as well as in Rhyacophilidae (Fig. 22C), Glossosomatidae (Fig. 22E), and Ptilocolepidae (Fig. 22F).

In the ‚basal‘ lepidopteran lineage Micropterigidae (Fig. 21) the antennifer is comparatively small but also positioned at the ventral margin of the antennal foramen.

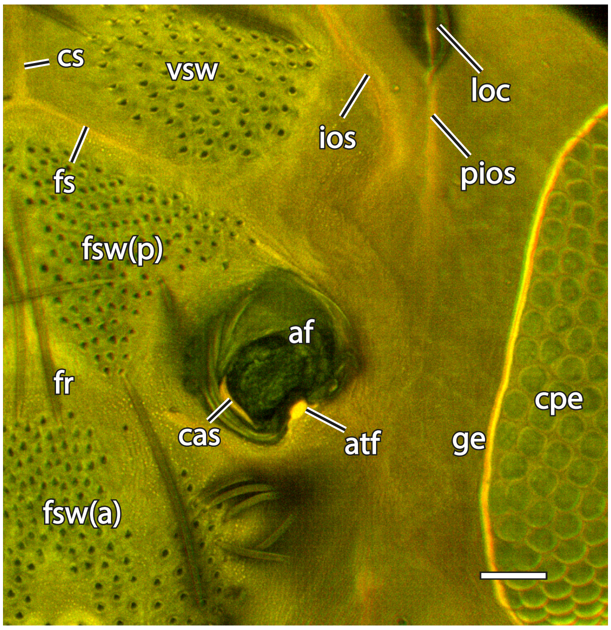

Figure 21: Structures of the antennal base of adult *Micropterix calthella* (Linnaeus, 1761) (Lepidoptera). Volume rendering based on confocal laser scanning microscopy (CLSM). Abbreviations: **af** – antennal foramen, **atf** – antennifer, **cas** – circumantennal sulcus, **cpe** – compound eye, **cs** – coronal sulcus, **fr** – frons, **fs** – frontal sulcus, **fsw(a)** – anterior setal wart of frons, **fsw(p)** – posterior setal wart of frons, **ge** – gena, **ios** – interocellar sulcus, **loc** – lateral ocellus, **pios** – postinterocellar sulcus, **vsw** – setal wart of vertex. (Scale bar: 30 µm)

In contrast, it is comparatively small and positioned at the ventrolateral to lateral parts of the antennal socket in Integripalpia (Fig. 22H). Furthermore, it is extremely small and located at the ventrolateral edge of the antennal socket in Hydrobiosidae (Fig. 22D).

In all known cases the scapus (sca, Fig. 4A,B) is the longest antennomere of Trichoptera (Tab. 6). In some groups it is up to four times longer than wide (e.g., Goeridae, Limnephilidae). It is followed by the small pedicellus (ped, Fig. 4A,B), which usually represents one of the smallest antennomeres. Both are articulated by a well-sclerotized scapal process, which articulates to a small furrow at the base of the pedicellus.

Table 6: External morphological features of the adult antenna of Trichoptera. Abbreviations: **atf** – antennifer, **cas** – circumantennal sulcus, **F** – female, **M** – male, **N** – sample size, **n.a.** – not applicable, **nb.** – number, **ped** – pedicellus, **sca** – scapus, **<** – length of antenna only slightly shorter than length of forewing, **<<** – length of antenna remarkably shorter than length of forewing, **≤** – length of antenna as long as or only slightly shorter than length of forewing.

Species	Length of antenna	Length of forewing		Nb. of antennomeres		Shape of sca	Length ratio (sca:ped)	Position of atf at cas
		M	F	M	F			
Philopotamus ludificatus McLachlan, 1878	≤ length of forewing (M & F)	8.2 mm (6.2–10.2 mm, N=25)	9.9 mm (8.0–11.7 mm, N=25)	53 (49–55, N=25)	53 (49–55, N=25)	largest antennomere (as long as wide)	2:1	ventral margin
Holocentropus dubius (Rambur, 1842)	< length of forewing (M) << length of forewing (F)	7.1 mm (6.7–8.5 mm, N=4)	8.4 mm (7.7–9.2 mm, N=6)	38 (37–39, N=4)	38 (37–39, N=6)	largest antennomere as long as wide	2:1	ventral margin
Hydropsyche angustipennis (Curtis, 1834)	≤ length of forewing (M) << length of forewing (F)	9.6 mm (9.2–10.2 mm, N=25)	11.6 mm (9.7–13.1 mm, N=25)	56 (53–58, N=25)	56 (51–59, N=25)	largest antennomere (as long as wide)	2:1	ventral margin
Tinodes dives (Pictet, 1834)	< length of forewing (M & F)	5.7 mm (5.0–6.3 mm, N=25)	5.7 mm (4.8–6.3 mm, N=25)	35 (34–37, N=25)	35 (33–37, N=25)	largest antennomere 2x longer than wide	2:1	ventral margin
Agapetus fuscipes Curtis, 1834	<< length of forewing (M)	4.2 mm (3.8–4.8 mm, N=8)	n.a.	27 (26–28, N=8)	n.a.	largest antennomere 2x longer than wide	2:1	ventral margin
Hydroptila scamandra Neboiss, 1977	<< length of forewing (M & F)	2.2 mm (1.9–2.4 mm, N=6)	2.2 mm (2.0–2.6 mm, N=4)	27 (25–28, N=6)	22 (21–23, N=4)	largest antennomere 2x longer than wide	2:1	lateral margin
Orthotrichia atraseta Wells, 1979	<< length of forewing (M & F)	3.5 mm (3.4–3.6 mm, N=3)	3.7 mm (3.6–3.7 mm, N=2)	31 (30–31, N=3)	26 (25–27, N=2)	largest antennomere 2x longer than wide	2:1	lateral margin
Phryganea grandis Linnaeus, 1758	≤ length of forewing (M) << length of forewing (F)	23.0 mm (21.0–25.0 mm, N=25)	27.0 mm (24.0–29.0 mm, N=25)	65 (60–71, N=25)	58 (55–63, N=25)	largest antennomere 2x longer than wide	3:1	lateral margin
Trichostegia minor Curtis, 1834	< length of forewing (M & F)	9.6 mm (8.5–10.3 mm, N=25)	10.9 mm (9.7–11.7 mm, N=25)	44 (39–47, N=25)	44 (41–49, N=25)	largest antennomere as long as wide	2:1	lateral margin
Limnephilus flavicornis (Fabricius, 1787)	< length of forewing (M & F)	16.9 mm (16.0–18.0 mm, N =25)	16.5 mm (15.0–18.0 mm, N=25)	68 (64–73, N=25)	44 (64–70, N=25)	largest antennomere 3x longer than wide	4–5:1	lateral margin
Leptocerus tineiformis Curtis, 1834	2–2.5 length of forewing (M) 1.5 length of forewing (F)	7.2 mm (6.4–7.7 mm, N =25)	7.3 mm (6.5–8.1 mm, N=25)	100 (94–106, N=25)	81 (71–86, N=25)	largest antennomere 3x longer than wide	4–5:1	lateral margin

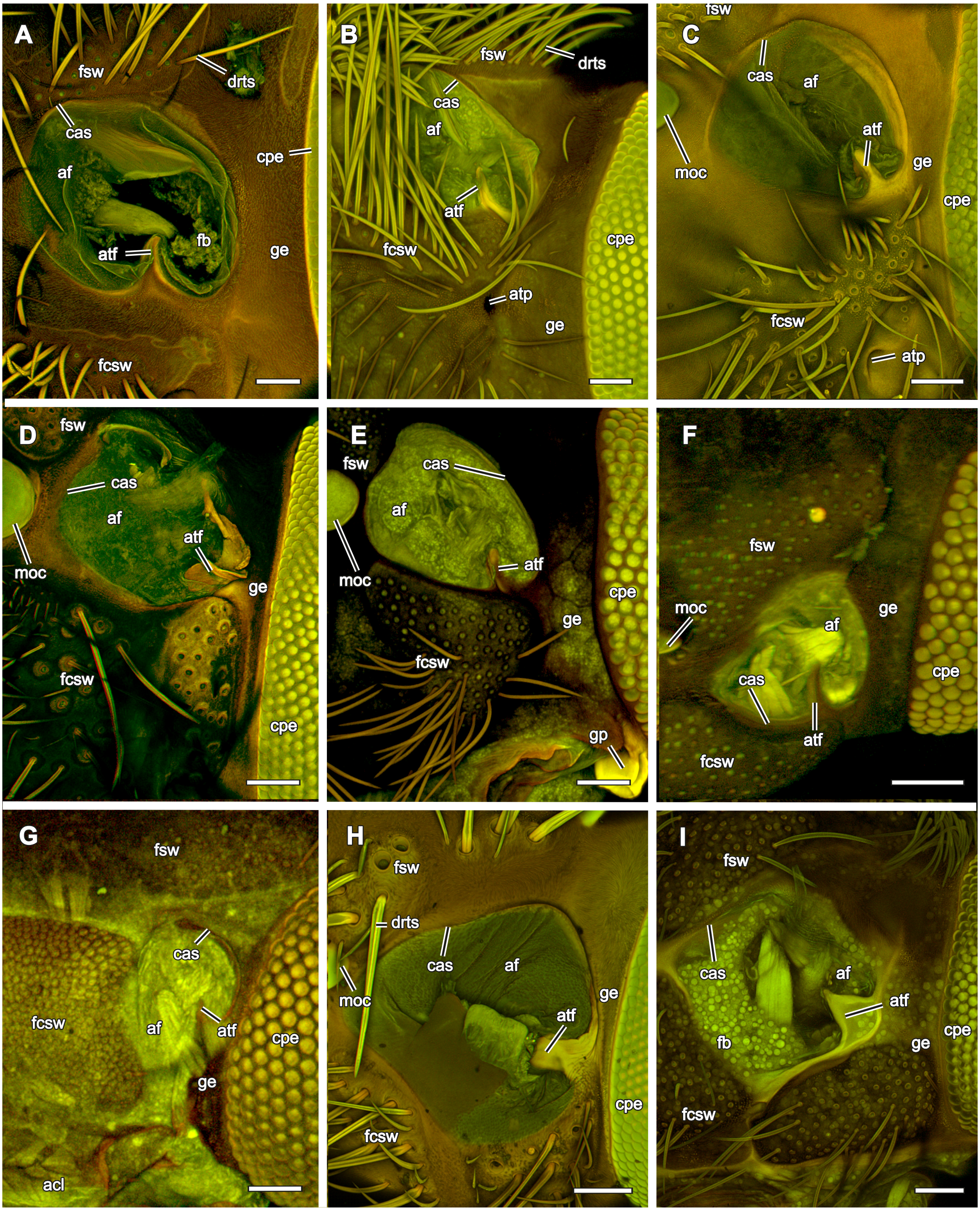

Figure 22: Structures of the antennal base in trichopterans. Volume renderings based on confocal laser scanning microscopy. Membranes: green, sclerites yellow to brown. **A**: *Philopotamus ludificatus* McLachlan, 1878; **B**: *Holocentropus dubius* (Rambur, 1842); **C**: *Rhyacophila fasciata* Hagen, 1859; **D**: *Hydrobiosis styracine* McFarlane, 1960; **E**: *Agapetus fuscipes* Curtis, 1834; **F**: *Ptilocolepus granulatus* (Pictet, 1834); **G**: *Hydroptila scamandra* Neboiss, 1977; **H**: *Limnephilus flavicornis* (Fabricius, 1787); **I**: *Leptocerus tineiformis* Curtis, 1834. Abbreviations: **acl** – anteclypeolabrum, **af** – antennal foramen, **atf** – antennifer, **atp** – anterior tentorial pit, **cpe** – compound eye, **cas** – circumantennal sulcus, **drts** – dentate ribbed trichoid sensillum, **fb** – fat body, **fcsw** – frontoclypeal setal wart, **fsw** – frontal setal wart, **ge** – gena, **gp** – subgenal process, **moc** – median ocellus. (Scale bars: H: 100 µm, C, D: 70 µm, A, B, F, I: 50 µm, E: 40 µm, G: 30 µm)

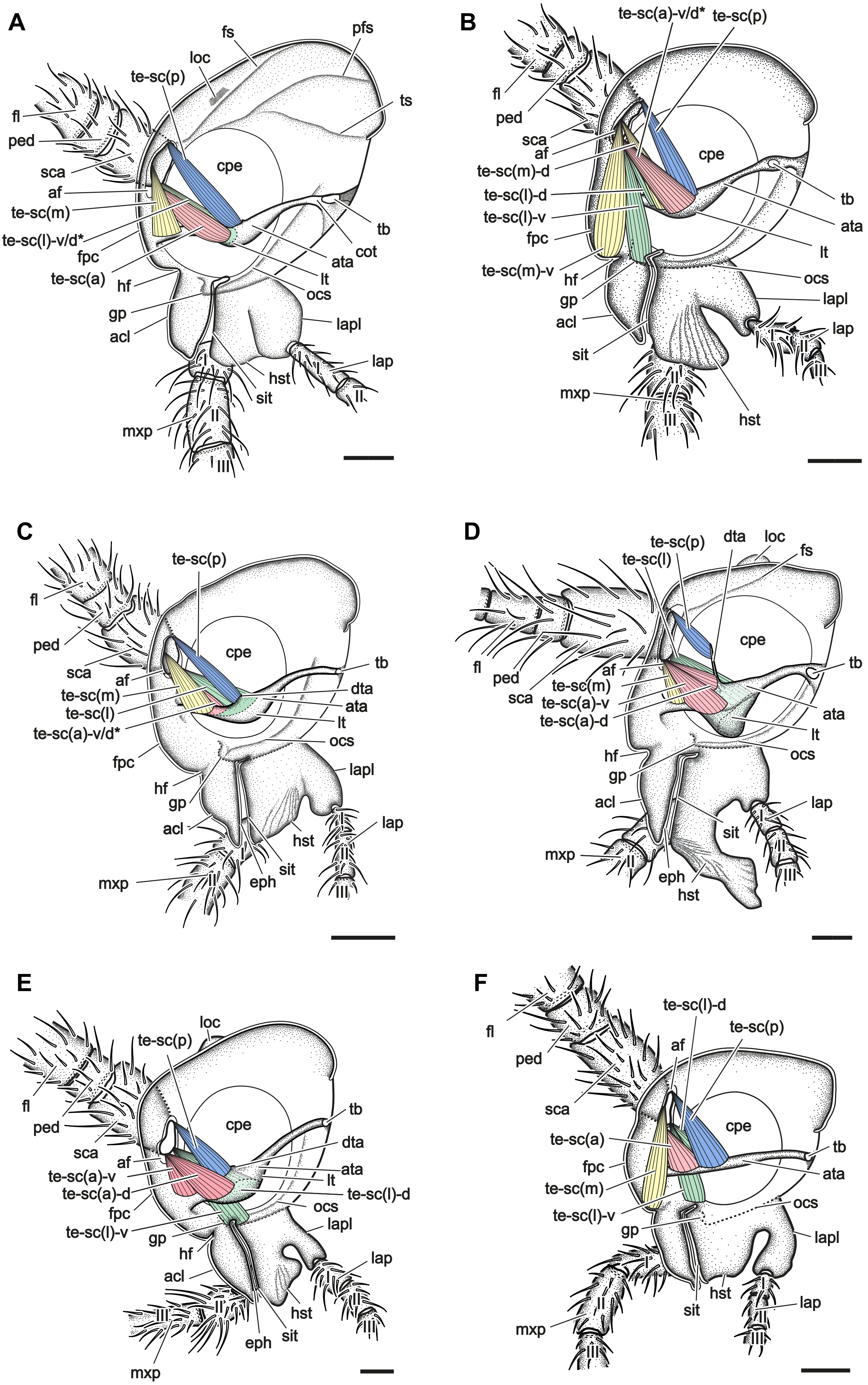
A
fs
pfs
loc
te-sc(p)
ts
fl
ped
sca
cpe
af
te-sc(m)
te-sc(l)-v/d*
fpc
te-sc(a)
tb
cot
ata
lt
ocs
hf
gp
acl
lapl
lap
hst
sit
mxp
I
II
III
B
te-sc(a)-v/d*
te-sc(p)
fl
ped
sca
af
te-sc(m)-d
cpe
te-sc(l)-d
te-sc(l)-v
fpc
te-sc(m)-v
tb
ata
lt
ocs
lapl
hf
gp
acl
lap
sit
mxp
hst
I
II
III
C
te-sc(p)
fl
ped
sca
af
te-sc(m)
te-sc(l)
te-sc(a)-v/d*
cpe
tb
dta
ata
lt
ocs
fpc
lapl
hf
gp
acl
lap
hst
mxp
eph
sit
I
II
III
D
te-sc(p)
dta
loc
fs
te-sc(l)
cpe
fl
ped
sca
af
te-sc(m)
te-sc(a)-v
te-sc(a)-d
tb
ata
lt
ocs
hf
gp
acl
lap
sit
mxp
eph
hst
I
II
III
E
loc
te-sc(p)
fl
ped
sca
cpe
tb
dta
af
ata
te-sc(a)-v
te-sc(a)-d
lt
te-sc(l)-d
fpc
ocs
te-sc(l)-v
lapl
gp
hf
acl
lap
hst
mxp
eph
sit
I
II
III
F
te-sc(l)-d
fl
te-sc(p)
af
ped
sca
cpe
te-sc(a)
tb
ata
fpc
te-sc(m)
te-sc(l)-v
ocs
gp
lapl
hst
sit
lap
mxp
I
II
III

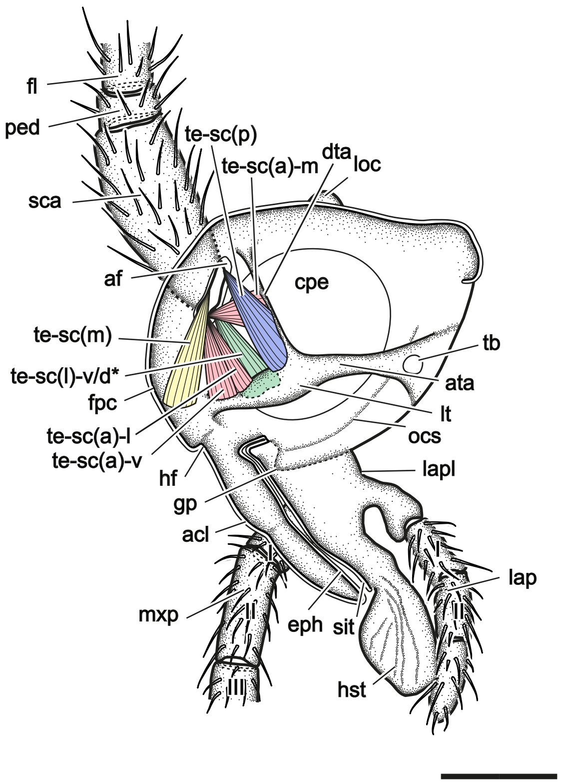

← **Figure 24:** Extrinsic musculature of the adult antenna of *Limnephilus flavicornis* (Fabricius, 1787) (Limnephilidae), line drawing based on µCT-data. Abbreviations: **acl** – anteclypeolabrum, **af** – antennal foramen, **ata** – anterior tentorial arm, **cpe** – compound eye, **dta** – dorsal tentorial arm, **eph** – epipharynx, **fl** – flagellomere, **fpc** – frontopostclypeus, **gp** – subgenal process, **hf** – horizontal furrow between frontopostclypeus and anteclypeolabrum, **hst** – haustellum, **lap** – labial palp, **lapl** – central plate of labium, **loc** – lateral ocellus, **lt** – laminatentorium, **mxp** – maxillary palp, **ocs** – occipital sulcus, **ped** – pedicellus, **sca** – scapus, **sit** – sitophore plate, **tb** – tentorial bridge, **te-sc(a)** – M. tentorio-scapalis anterior [**te-sc(a)-m** – median bundle of M. tentorio-scapalis anterior, **te-sc(a)-v** – ventral bundle of M. tentorio-scapalis anterior, **te-sc(a)-l** – lateral bundle of M. tentorio-scapalis anterior], **te-sc(l)** – M. tentorio-scapalis lateralis, **te-sc(m)** – M. tentorio-scapalis medialis, **te-sc(p)** – M. tentorio-scapalis posterior, **I–III** – number of palpomere. (Scale bar: 100 µm)

3.2.2.2. Extrinsic musculature of the antenna

The adult antenna of Trichoptera is equipped with four extrinsic muscles in most lineages (i.e., two abductor muscles [Musculus tentorio-scapalis anterior and M. tentorio-scapalis lateralis] and two adductor muscles [M. tentorio-scapalis posterior and M. tentorio-scapalis medialis]) (Tab. 7). As an exception the median adductor of the antenna (M. tentorio-scapalis medialis [te-sc(m)]) is absent in Glossosomatidae (Fig. 23E).

Usually, these muscles are attached to

← **Figure 23:** Extrinsic antennal musculature of adult trichopterans, line drawing based on µCT-data. **A**: *Philopotamus ludificatus* McLachlan, 1878 (Philopotamidae); **B**: *Holocentropus dubius* (Rambur, 1842) (Polycentropodidae); **C**: *Rhyacophila obliterata* McLachlan, 1863 (Rhyacophilidae); **D**: *Apsilochorema sutshanum* Martynov, 1934 (Hydrobiosidae); **E**: *Glossosoma spinosum* Morse et Yang, 2005 (Glossosomatidae); **F**: *Ptilocolepus granulatus* (Pictet, 1834) (Ptilocolepidae). Abbreviations: **acl** – anteclypeolabrum, **af** – antennal foramen, **ata** – anterior tentorial arm, **cot** – corpotentorium, **cpe** – compound eye, **dta** – dorsal tentorial arm, **eph** – epipharynx, **fl** – flagellomere, **fpc** – frontopostclypeus, **fs** – frontal sulcus, **gp** – subgenal process, **hf** – horizontal furrow between frontopostclypeus and anteclypeolabrum, **hst** – haustellum, **lap** – labial palp, **lapl** – central plate of labium, **loc** – lateral ocellus, **lt** – laminatentorium, **mxp** – maxillary palp, **ocs** – occipital sulcus, **ped** – pedicellus, **pfs** – postfrontal sulcus, **sca** – scapus, **sit** – sitophore plate, **tb** – tentorial bridge, **te-sc(a)** – M. tentorio-scapalis anterior, [**te-sc(a)-d** – dorsal bundle of M. tentorio-scapalis anterior, **te-sc(a)-v** – ventral bundle of M. tentorio-scapalis anterior], **te-sc(l)** – M. tentorio-scapalis lateralis [**te-sc(l)-d** – dorsal bundle of M. tentorio-scapalis lateralis, **te-sc(l)-v** – ventral bundle of M. tentorio-scapalis lateralis], **te-sc(m)** – M. tentorio-scapalis medialis [**te-sc(m)-d** – dorsal bundle of M. tentorio-scapalis medialis, **te-sc(m)-v** – ventral bundle of M. tentorio-scapalis medialis], **te-sc(p)** – M. tentorio-scapalis posterior, **ts** – temporal sulcus, **I–III** – number of palpomere, ***** – two closely adjacent bundles present, but these are not subdivided in this figure. (Scale bars: A: 200 µm, B–F: 100 µm)

Taxon	te-sc(a)	te-sc(p)	te-sc(l)	te-sc(m)
Philopotamus ludificatus McLachlan, 1878	1 ata/lt	1 ata	2 ata/lt	1 ata
Stenopsyche marmorata Navas, 1920	1 ata/dta [?]	1 dta	2 ata/ge	1 ata
Hydropsyche angustipennis (Curtis, 1834)	1 ata/lt	1 ata	2 ata/lt	2 lt/fpc
Tinodes dives (Pictet, 1834)	1 ata/lt	1 ata	2 ge/ata/lt	2 lt/fpc
Holocentropus dubius (Rambur, 1842)	2 ata/lt	1 ata	2 ge/ata/lt	2 lt/fpc
Rhyacophila obliterata McLachlan, 1863	2 ata/lt	1 dta	1 ata/lt	1 lt
Hydrobiosis styracine McFarlane, 1960	2 ata/lt/dta	1 dta	1 lt	1 ata
Apsilochorema sutshanum Martynov, 1934	2 ata/lt/dta	1 dta	1 ata/lt	1 ata
Glossosoma spinosum Morse et Yang, 2005	2 ata/lt	1 ata	2 ge/ata/lt	-
Agapetus fuscipes Curtis, 1834	2 ata/lt	1 ata/lt	2 dta/ata/lt	-
Ptilocolepus granulatus (Pictet, 1834)	1 ata	1 ata/dta	2 ge/ata	1 fpc
Hydroptila scamandra Neboiss, 1977	1 ata	1 ata	2 ata/ge	1 lt
Orthotrichia atraseta Wells, 1979	1 ata	1 ata	2 ata/ge	1 ata/lt
Phryganea grandis Linnaeus, 1758	3 ata/dta	1 dta	1 ata/lt	1 ata
Trichostegia minor Curtis, 1834	3 ata/lt/dta	1 dta	1 ata/lt	1 ata
Brachycentrus subnubilus Curtis, 1834	3 fpc/lt/dta	1 dta	1 ata/lt	1 ata/fpc
Limnephilus flavicornis (Fabricius, 1787)	3 ata/lt/dta	1 dta	2 ata/lt	1 ge
Silo nigricornis (Pictet, 1834)	3 ge/ata	1 dta	1 ge	1 ge
Sericostoma personatum Kirby et Spence, 1826	1 ata/lt	1 ata	1 ge	1 ge
Pycnocentria evecta McLachlan, 1868	3 ge/ata	1 ata	2 ge	1 ata/lt
Molanna angustata Curtis, 1834	3 ge/ata/fpc	1 ata	2 ge	1 fpc
Leptocerus tineiformis Curtis, 1834	3 ata/lt/dta	1 dta	2 pge	1 ata/lt

← **Table 7:** Antennal musculature in the adult head of Trichoptera with information on number of bundles and the origin sites. Abbreviations: **ata** – anterior tentorial arm, **dta** – dorsal tentorial arm, **fpc** – frontopostclypeus, **ge** – gena, **lt** – laminatentorium, **pge** – postgena, **te-sc(a)** – M. tentorio-scapalis anterior, **te-sc(l)** – M. tentorio-scapalis lateralis, **te-sc(m)** – M. tentorio-scapalis medialis, **te-sc(p)** – M. tentorio-scapalis posterior. (For detailed description see Appendix 2)

---

the tentorium, but in several cases bundles shifted their origin to the head capsule. The only exception is M. tentorio-scapalis posterior (te-sc(p)) which is exclusively attached to the tentorium (anterior or dorsal tentorial arm) (App. 2).

The anterior abductor muscle (M. tentorio-scapalis anterior [te-sc(a)]) is composed of a single bundle originating from the anterior tentorial arm and the laminatentorium in several not closely related groups (e.g., Philopotamidae, Fig. 23A; Ptilocolepidae, Fig. 23F; Hydroptilidae; and Sericostomatidae) (App. 2). Two closely adjacent bundles of te-sc(a) (ventral bundle: M. tentorio-scapalis anterior ventralis [te-sc(a)-v]; dorsal bundle: M. tentorio-scapalis anterior dorsalis [te-sc(a)-d]) are present in Polycentropodidae, Rhyacophilidae (Fig. 23C), Hydrobiosidae (Fig. 23D), and Glossosomatidae (Fig. 23E). Except for Sericostomatidae all integripalpian lineages investigated so far are equipped with three bundles of te-sc(a) (median bundle: M. tentorio-scapalis anterior medialis [te-sc(a)-m]; lateral bundle: M. tentorio-scapalis anterior lateralis [te-sc(a)-l]; ventral bundle: M. tentorio-scapalis anterior ventralis [te-sc(a)-v]) (e.g., Limnephilidae, Fig. 24).

M. tentorio-scapalis anterior originates from the mesal face of the anterior tentorial arm and the laminatentorium in most groups (App. 2). The median bundle is attached to the dorsal tentorial arm in most representatives of Plenitentoria (e.g., Limnephilidae, Fig. 24). Furthermore, the ventral bundle originates from the head capsule in some groups of Integripalpia (e.g., Conoesucidae, Tab. 7; App. 2).

M. tentorio-scapalis anterior inserts exclusively at the anterior margin of the scapal base directly mesal/below to the antennifer.

The posterior abductor muscle (M. tentorio-scapalis lateralis [te-sc(l)]) is composed of two bundles in Philopotamidae (Fig. 18A), Glossosomatidae (Fig. 23E), Ptilocolepidae (Fig. 23F), Hydroptilidae, and Leptoceridae. The muscle is formed by one bundle in all other trichopteran taxa (e.g., Rhyacophilidae, Fig. 23C; Hydrobiosidae, Fig. 24D; and Goeridae; Tab. 7).

M. tentorio-scapalis lateralis is attached to the lateral wall of the anterior tentorial arm and to the laminatentorium in various taxa (e.g., Rhyacophildae, Fig. 23C; Hydrobiosidae, Fig. 23D) (Tab. 7; App. 2). In contrast, the ventral bundle (M. tentorio-scapalis lateralis ventralis [te-sc(l)-v]) originates from the genal area of the head capsule in Psychomyiidae, Polycentropodidae (Fig. 23B), Glossosomatidae (partim, e.g. *Glossosoma*, Fig. 23E), Ptilocolepidae (Fig. 23F), Hydroptilidae, and Leptoceridae (Tab. 7; App. 2).

Usually, the muscle inserts laterally at the base of the scapus directly above/lateral to the antennifer. However, in the spicipalpian families Ptilocolepidae and Hydroptilidae the insertion site of the dorsal bundle (M. tentorio-scapalis lateralis dorsalis [te-sc(l)-d]) is located at the dorsolateral margin of the scapus, directly lateral to the insertion of M. tentorio-scapalis posterior.

The posterior adductor muscle of the

trichopteran adult antenna (M. tentorio-scapalis posterior [te-sc(p)]) consists of a single, usually comparatively small bundle originating from the anterior tentorial arm directly posterior to all other antennal muscles in most lineages of Trichoptera (e.g., Philopotamidae, Fig. 23A; Ptilocolepidae, Fig. 23F). In a few taxa it originates from the dorsal tentorial arm (e.g., Hydrobiosidae, Fig. 23D; Limnephilidae, Fig. 24) (Tab. 7, App. 2).

M. tentorio-scapalis posterior inserts at the posterior basal margin of the scapus in Trichoptera (Figs. 23A–F; 24).

The anterior adductor muscle of the antenna (M. tentorio-scapalis medialis [te-sc(m)]) is absent in Glossosomatidae (Fig. 23E). It is composed of one bundle in most lineages (e.g., Philopotamidae, Fig. 23A; Rhyacophilidae, Fig. 23C; Limnephilidae, Fig. 24) (Tab. 7; App. 2). Two bundles are only present in Polycentropodidae (Fig. 23B).

M. tentorio-scapalis medialis originates from the mesal wall of the anterior tentorial arm and the laminatentorium near the head capsule distinctly in front of the other antennal muscles in most groups of Trichoptera (e.g., Philopotamidae, Fig. 23A; Rhyacophilidae, Fig. 23C) (Tab. 7). In contrast, its origin site is completely located on the anterior or ventral regions of the gena in some integripalpians (e.g., Goeridae, Sericostomatidae; Tab. 7). Furthermore, the ventral bundle of M. tentorio-scapalis medialis (M. tentorio-scapalis medialis ventralis [te-sc(m)-v]) is also attached to the anterior face of the head capsule (i.e. frontopostclypeus above the anterior tentorial pit) in some Annulipalpia (e.g., Polycentropodidae, Fig. 23B).

M. tentorio-scapalis medialis usually inserts at the mesal basal margin of the scapus. Its insertion site is shifted to the anterior basal margin directly mesal to M. tentorio-scapalis anterior in Hydrobiosidae (Fig. 23D).

3.2.3. Anteclypeolabrum

3.2.3.1. General appearance

The anteclypeolabrum (acl, Fig. 4) is comparatively small and triangular in Annulipalpia (Fig. 4), all ‘Spicipalpia‘, and in Integripalpia-Brevitentoria. In contrast, it is remarkably elongated (Fig. 24) ventrally (app. 2–4 times longer than width) forming a rectangular plate in the integripalpian lineage Plenitentoria.

3.2.3.2. Musculature of the anteclypeolabrum

The anteclypeolabrum of Trichoptera lacks any extrinsic and intrinsic muscles usually present in the generalized insect condition (M. labro-epiharyngalis [lb-eph] and M. fronto-labralis [fr-lb] absent) (App. 1).

3.2.4. Epipharynx and hypopharynx

3.2.4.1. General appearance

The epipharyngeal sclerite of Trichoptera (eph, Fig. 10C) is narrow and heavily sclerotized. It is only slightly concave in cross section in Philopotamidae, Hydropsychidae, Psychomyiidae, Ptilocolepidae, Hydroptilidae, and some Brevitentoria, but distinctly widened mesally in several other lineages (e.g., all Plenitentoria, some Brevitentoria). The epipharynx is comparatively short in Glossosomatidae, Ptilocolepidae, and Hydroptilidae. In contrast, it is extremely elongated ventrally forming the roof of a long preoral tube in all lineages of Plenitentoria (Fig. 24). The sclerite is laterally surrounded by membranous areas and apically connected with the sclerotized wall of the anteclypeolabrum. The rather uniform trichopteran epipharynx forms the roof of the preoral cavity (poc, Fig. 18D), which is posteriorly delimited by the heavily sclerotized region of the hypopharynx, i.e., the sitophore plate (sit, Fig. 19G). The preoral cavity terminates dorsally at the beginning of the ring musculature (an-ci) of the prepharyngeal tube, distinctly below the insertion site of M. clypeo-cibarialis ventralis (cl-ci(v)). A strongly sclerotized and smooth (chemoreceptors absent) sitophore plate as part of the hypopharynx is usually present in Trichoptera. It terminates dorsally in a typical spoon-shaped process in many groups (e.g., Philopotamidae). Furthermore, the hypopharynx is membranous along its distal section and forms the anterior face of the haustellum which is comparatively large developed in all integripalpian lineages.

3.2.4.2. Musculature of epipharynx and hypopharynx

The epipharynx of Trichoptera is generally equipped with the strongly developed dilator muscles Mm. clypeo-epipharyngales medialis and lateralis [cl-eph(m)/(l)]; Figs. 15A, 16B) (App. 1).

The compact and fan-shaped ventral dilator (M. clypeo-epipharyngalis medialis) is composed of a single, unpaired bundle in almost all lineages of Trichoptera. The muscle uniformly originates from the central part of the anteclypeolabrum and inserts mesally at the distal end of the epipharynx as described for *Philopotamus* (see above [3.1.10.]).

The dorsal dilator muscle of the epipharynx, M. clypeo-epipharyngalis lateralis (cl-eph(l)), is attached to the median and lateral face of the anteclypeolabrum directly dorsal to its ventral counterpart and inserts at the proximal half of the epipharyngeal sclerite directly below the prepharyngeal tube in all trichopteran lineages (Fig. 16B). It is composed of a single, unpaired bundle in some lineages of Annulipalpia (e.g., Philopotamidae), some ‘Spicipalpia’ (e.g., Ptilocolepidae), and all Brevitentoria (Tab. 8). In contrast, the muscle is composed of two bundles (ventral [cl-eph(l)-v] and dorsal [cl-eph(l)-d] bundle) with distinct insertion sites along the proximal half of the epipharynx in Brachycentridae, Limnephilidae, and Goeridae (Tab. 8, App. 3).

The proximal section of the preoral cavity (= prepharyngeal tube) is encircled by pharyngeal ring musculature, but it is also equipped with two dilator muscles (Mm. clypeo-cibarialis ventralis and dorsalis [cl-ci(v)/(d)]; Fig. 15A).

The ventral dilator of the prepharyngeal tube (cl-ci(v)) originates either from the upper part of the anteclypeolabrum directly below the horizontal furrow (hf, Fig. 15A) (e.g., Philopotamidae, Fig. 15A) or from the lower frontopostclypeus above the horizontal furrow (e.g., Hydropsychidae; Molannidae; Tab. 8, App. 3). It inserts at the ventral half of the prepharyngeal tube, directly above of the epipharyngeal sclerite. Usually it is composed of one bundle (e.g., Philopotamidae, Fig. 20A). Two bundles are present in Polycentropodidae, Rhyacophilidae, Hydrobiosidae, and Glossosomatidae.

The dorsal dilator muscle of the prepharyngeal tube (cl-ci(d)) is composed of one (most ‘Spicipalpia’), two (several not closely related groups) or even three bundles (Tab. 8). The muscle has its origin (usually with all bundles) on the median or lateral face of the frontopostclypeus (fpc, Fig. 4) directly above the horizontal furrow in most groups of Trichoptera (App. 3). As an exception the lateral bundle of M. clypeo-cibarialis dorsalis (cl-ci(d)-l) originates from the anterior face of the gena directly above the sclerotized area of the mandible (md(m), Fig. 4) in Annulipalpia-

→ **Table 8:** Epipharyngeal and hypopharyngeal muscles in the adult head of Trichoptera with information on number of bundles and the origin sites. Abbreviations: **acl** – anteclypeolabrum, **cl-ci(d)** – M. clypeo-cibarialis dorsalis, **cl-ci(v)** – M. clypeo-cibarialis ventralis, **cl-eph(l)** – M. clypeo-epipharyngalis lateralis, **cl-eph(m)** – M. clypeo-epipharyngalis medialis, **fpc** – frontopostclypeus, **ge** – gena, **lt** – laminatentorium, **tb** – tentorial bridge, **te-si** – M. tentorio-sitophorialis. (For detailed description see Appendix 3)

Psychomyioidea. The insertion site of its bundles along the anterior and lateral face of the prepharyngeal tube (proximal half) is variable, but it is exclusively found below the frontal ganglion (fg, Fig. 20A).

The strongly sclerotized floor of the prepharyngeal tube is equipped with a strong dilator muscle (M. tentorio-sitophorialis [te-si]). It is uniformly composed of one bundle in all Trichoptera as described for *Philopotamus* (see above [3.1.10]; Fig. 18C, 19G).

3.2.5. Mandible

3.2.5.1. General appearance

The mandibles of adult Trichoptera are usually rather small and only moderately sclerotized. The general structure is quite similar to the conditions described for *Philopotamus* (see above for details [3.1.7.]).

Among the trichopteran lineages remarkable differences occur only in the level of sclerotization and the size of the mandibles. They are comparatively large and moderately sclerotized in Annulipalpia and ‘Spicipalpia’ (Fig. 4). In contrast, the mandibles are extremely small or vestigial and mainly membranous in all representatives of Integripalpia.

The mandibles are remarkably pointed antero-mesally in some annulipalpian and spicipalpian taxa (e.g., Psychomyiidae, Polycentropodidae, Hydroptilidae, but not in the hydroptilid representative *Orthotrichia*).

3.2.5.2. Musculature of the mandible

The adult mandible of Trichoptera is usually equipped with a large median adductor and a considerably smaller lateral abductor muscle (Mm. cranio-mandibulares medialis and lateralis [cr-md(m)/(l)]). Size and fine structure of both muscles vary considerably among the trichopteran lineages.

M. cranio-mandibularis medialis is by far the largest head muscle in most taxa examined filling about half of the head capsule volume in several not closely related groups (e.g., Philopotamidae, Fig. 16A,B). In contrast, it is absent in other trichopteran lineages (e.g., Hydrobiosidae) (App. 1). Additionally, in a few groups only highly degenerated muscle tissue or remnants of the adductor tendon could be observed.

The same pattern is recognizeable for the abductor muscle (M. cranio-mandibularis lateralis) (App. 1).

Besides the large muscles of the mandible an extremely thin adductor composed of only 2–3 fibers is found in several taxa. The M. tentorio-mandibularis (te-md) (Fig. 19E) is present in most Annulipalpia and ‘Spicipalpia’ (App. 1). It is always accompanied by a small nerve tract of the mandibular nerve. M. tentorio-mandibularis is absent in Integripalpia.

Furthermore, a hypopharyngo-mandibular muscle (hy-md) could not be observed in any trichopteran lineage.

Taxon	**cl-eph(m)**	**cl-eph(l)**	**cl-ci(v)**	**cl-ci(d)**	**te-si**
Philopotamus ludificatus McLachlan, 1878	1 - compact acl	1 - compact acl	1 acl	2 fpc	1 tb
Stenopsyche marmorata Navas, 1920	1 - compact acl	1 - compact acl	1 fpc	1 [?] fpc [?]	1 tb
Hydropsyche angustipennis (Curtis, 1834)	1 - compact acl	1 acl	1 fpc	2 fpc	1 tb
Tinodes dives (Pictet, 1834)	1 - compact acl	1 acl	1 fpc	2 fpc/ge	1 tb
Holocentropus dubius (Rambur, 1842)	1 - compact acl	1 acl	2 fpc	2 fpc/ge	1 tb
Rhyacophila obliterata McLachlan, 1863	1 - compact acl	1 acl	2 acl	1 fpc	1 tb
Hydrobiosis styracine McFarlane, 1960	1 - compact acl	1 - compact acl	1 acl	2 fpc	1 lt
Apsilochorema sutshanum Martynov, 1934	1 - compact acl	1 acl	2 acl	1 fpc	1 tb
Glossosoma spinosum Morse et Yang, 2005	1 - compact acl	1 - compact acl	2 acl	1 fpc	1 lt
Agapetus fuscipes Curtis, 1834	1 - compact acl	1 acl	1 acl	2 fpc	1 tb
Ptilocolepus granulatus (Pictet, 1834)	1 - compact acl	1 - compact acl	1 acl	1 fpc	1 lt
Hydroptila scamandra Neboiss, 1977	1 - compact acl	1 acl	1 acl	1 fpc	1 tb
Orthotrichia atraseta Wells, 1979	1 fiber acl	2 fibers acl	1 acl	1 fpc	1 lt
Phryganea grandis Linnaeus, 1758	1 - compact acl	1 - compact acl	1 fpc	2 fpc	1 tb
Trichostegia minor Curtis, 1834	1 - compact acl	1 - compact acl	1 fpc	2 fpc	1 lt
Brachycentrus subnubilus Curtis, 1834	1 - compact acl	2 - compact acl	1 acl	3 fpc	1 tb
Limnephilus flavicornis (Fabricius, 1787)	1 - compact acl	2 - compact acl	1 acl	3 fpc	1 lt
Silo nigricornis (Pictet, 1834)	1 - compact acl	2 - compact acl	1 fpc	3 fpc	1 tb
Sericostoma personatum Kirby et Spence, 1826	1 - compact acl	1 - compact acl	1 acl	2 fpc	1 lt
Pycnocentria evecta McLachlan, 1868	1 - compact acl	1 - compact acl	1 acl	2 [?] fpc	1 tb
Molanna angustata Curtis, 1834	1 - compact acl	1 - compact acl	1 fpc	2 fpc	1 lt
Leptocerus tineiformis Curtis, 1834	1 - compact acl	1 - compact acl	1 fpc	2 fpc	1 tb

→ **Table 9:** Musculature of the food tract in the adult head of Trichoptera with information on number of bundles and the origin sites. Abbreviations: **ata** – anterior tentorial arm, **cr-ph(a)** – M. cranio-pharyngalis anterior, **cr-ph(p)** – M. cranio-pharyngalis posterior, **fgs** – frontogenal sulcus, **fpc** – frontopostclypeus, **fr-ph(a)** – M. fronto-pharyngalis anterior, **fr-ph(p)** – M. fronto-pharyngalis posterior, **hc** – head capsule, **pta** – posterior tentorial arm, **tb** – tentorial bridge, **te-ph(a)** – M. tentorio-pharyngalis anterior, **te-ph(l)** – M. tentorio-pharyngalis lateralis, **te-ph(p)** – M. tentorio-pharyngalis posterior, **-** – absent, **?** – uncertain. (For detailed description see Appendix 4)

3.2.6. Cephalic food tract

3.2.6.1. General appearance

A distinctly widened precerebral pumping chamber (pch, Fig. 20A) is a typical morphological feature of the adult head in Trichoptera. Its general appearance is quite uniform throughout the order and no significant differences could be observed compared with the description of the precerebral pumping chamber in *Philopotamus* (see above [3.1.13]).

3.2.6.2. Musculature of the cephalic food tract

Four well developed dilator muscles are usually present in the precerebral pharynx of Trichoptera (Tab. 9).

M. fronto-pharyngalis anterior (fr-ph(a), Fig. 20A) originates on the mesal face of the frontopostclypeus and inserts at the anterior wall of the precerebral pharynx directly dorsally of the frontal ganglion. It is usually composed of one bundle, except for the spicipalpian family Glossosomatidae in which two bundles are present.

The posterior fronto-pharyngeal dilator muscle (M. fronto-pharyngalis posterior (fr-ph(p)) originates mesally on the frons (on vertex in *Orthotrichia* [Hydroptilidae]) and inserts at the dorsal wall of the precerebral pharynx in all lineages of Trichoptera. It is usually closely associated with the cephalic aorta (see Fig. 19B) and composed of two bundles. Three bundles occur in Hydropsychidae, Hydrobiosidae, and Hydroptilidae.

M. tentorio-pharyngalis lateralis (te-ph(l)) is composed of one bundle exclusively attached to the distal half of the anterior tentorial arm in some representatives of Annulipalpia (e.g., Philopotamidae) and the integripalpian lineage Leptoceroidea (e.g., Leptoceridae; Tab. 9, App. 4). In most other groups of Trichoptera the site of origin of te-ph(l) is located at the lateral face of the frontopostclypeus. Two bundles are present in Hydrobiosidae and Glossosomatidae, in which the mesal bundle originates from the lateral wall of the frontopostclypeus, whereas the lateral bundle is attached to the anterior tentorial arm near the head capsule. Furthermore, two bundles originating closely adjacent at the lateral wall of the frontopostclypeus above the anterior tentorial pit are present in Ptilocolepidae.

M. tentorio-pharyngalis posterior (te-ph(p)) is almost exclusively composed of two bundles; the only exception with one bundle is *Leptocerus* (Leptoceridae). The ventral dilator of the precerebral pharynx has its insertion site usually ventrally at the posterior end of the precerebral pumping chamber. Its origin site varies between not closely related groups (Tab. 9, App. 4).

The remarkably narrowed postcerebral pharynx is equipped with two dilator muscles (M. tentorio-pharyngalis posterior (te-ph(p) and M. cranio-pharyngalis anterior (cr-ph(a)) in most groups of Trichoptera (Tab. 9).

Taxon	**fr-ph(a)**	**fr-ph(p)**	**te-ph(l)**	**te-ph(a)**	**te-ph(p)**	**cr-ph(a)**	**cr-ph(p)**
Philopotamus ludificatus McLachlan, 1878	1 fpc	2 frons	1 ata	2 ata	1 pta	1 vertex	-
Stenopsyche marmorata Navas, 1920	1 fpc	1 [?] frons	1 ata	1 [?] ata	- [?]	- [?]	-
Hydropsyche angustipennis (Curtis, 1834)	1 fpc	3 frons	1 ata	2 ata	1 tb/pta	1 vertex	-
Tinodes dives (Pictet, 1834)	1 fpc	2 frons	1 fpc	2 ata	1 pta	1 vertex	-
Holocentropus dubius (Rambur, 1842)	1 fpc	2 frons	1 ata/fgs	2 ata	1 pta	1 vertex	1 pta
Rhyacophila obliterata McLachlan, 1863	1 fpc	2 frons	1 ata/fgs	2 ata/tb	1 ata	1 vertex	1 hc
Hydrobiosis styracine McFarlane, 1960	1 fpc	2 frons	2 fpc	2 ata/tb	1 pta	1 vertex	2 pta
Apsilochorema sutshanum Martynov, 1934	1 fpc	3 frons	2 fpc/ata/fgs	2 ata/tb	1 tb	1 vertex	2 [?] pta
Glossosoma spinosum Morse et Yang, 2005	2 fpc	2 frons	2 fpc/ata/fgs	2 ata/tb	1 tb	1 vertex	2 [?] pta
Agapetus fuscipes Curtis, 1834	1 fpc	1 [?] frons	2 fpc/ata/fgs	2 ata/tb	- [?]	1 vertex	1 [?] hc
Ptilocolepus granulatus (Pictet, 1834)	1 fpc	2 frons	2 fpc	2 ata	1 ata	1 vertex	1 hc
Hydroptila scamandra Neboiss, 1977	1 fpc	2 [?] frons	1 ata	2 ata/tb	1 ata	-	-
Orthotrichia atraseta Wells, 1979	1 fpc	3 [?] vertex	1 fpc	2 ata/tb	1 ata	-	-
Phryganea grandis Linnaeus, 1758	1 fpc	2 frons	1 fpc	2 [?] ata/tb	1 pta	1 vertex	-
Trichostegia minor Curtis, 1834	1 fpc	2 frons	1 fpc	2 ata/tb	1 pta	1 vertex	-
Brachycentrus subnubilus Curtis, 1834	1 fpc	2 frons	1 fpc	2 ata/tb	1 pta	1 vertex	-
Limnephilus flavicornis (Fabricius, 1787)	1 fpc	2 frons	1 fpc	2 tb/pta	1 pta	1 vertex	-
Silo nigricornis (Pictet, 1834)	1 fpc	2 [?] frons	1 fpc	2 [?] tb/pta	1 pta	1 vertex	-
Sericostoma personatum Kirby et Spence, 1826	1 fpc	2 frons	3 [?] fpc	2 tb/pta	1 pta	1 vertex	-
Pycnocentria evecta McLachlan, 1868	1 fpc	2 [?] frons	1 fpc	1 [?] ata	1 pta	1 vertex	-
Molanna angustata Curtis, 1834	1 fpc	2 frons	1 ata	2 ata/tb	1 pta	1 vertex	-
Leptocerus tineiformis Curtis, 1834	1 fpc	2 frons	1 ata	1 tb	- [?]	1 vertex	-

→ **Table 10:** Musculature of the trichopteran maxilla with information on number of bundles and the origin sites. Abbreviations: **ata** – anterior tentorial arm, **cd/st** – cardo-stipital sclerite, **cd-mp(d)** – M. cardo-palpalis dorsalis, **cd/st-mp(v)** – M. cardo-palpalis ventralis / M. stipito-palpalis ventralis, **cr-cd** – M. cranio-cardinalis, **cr-lc** – M. cranio-lacinialis, **cr-st** – M. cranio-stipitalis, **dst** – dististipes, **fgs** – frontogenal sulcus, **lt** – laminatentorium, **ocs** – occipital sulcus, **pge** – postgena, **pta** – posterior tentorial arm, **st-lc** – M. stipito-lacinialis, **te-cd** – M. tentorio-cardinalis, **st-mp(d)** – M. stipito-palpalis dorsalis, **te-st** – M. tentorio-stipitalis, **-** – absent, **?** – uncertain. (For detailed description see Appendix 5)

A third one, M. cranio-pharyngalis posterior (cr-ph(p)) is only present in 'Spicipalpia' (except for Hydroptilidae) and the annulipalpian family Polycentropodidae. It originates at the posterior tentorial arm or at the adjacent parts of the head capsule and inserts laterally at the posterior half of the postcerebral pharynx.

The dorsal dilator muscle of the postcerebral pharynx (M. cranio-pharyngalis anterior (cr-ph(a)) is usually present in Trichoptera (except for Hydroptilidae). In all cases it originates laterally at the head capsule and inserts dorsally at the postcerebral pharynx, directly behind the brain. The size of cr-ph(a) varies remarkably between the major groups of Trichoptera. It is strongly developed and composed of several bundles in Integripalpia and all spicipalpian lineages. In contrast, it is extremely thin and composed of only a single fiber in Annulipalpia.

M. tentorio-pharyngalis posterior (te-ph(p)) is present in most trichopteran groups (composed of one bundle), but it could not be observed in the spicipalpian representative *Agapetus* (Glossosomatidae-Agapetinae) and the integripalpian lineage Leptoceridae. Its origin site varies between distantly related groups (Tab. 9; App. 4). The surface of the entire pharynx is covered by ring muscle fibers (M. anularis pharyngalis [an-ph]). Furthermore, longitudinal muscle fibers (M. longitudinalis pharyngalis [lo-ph]) are present along the entire pharynx in all trichopteran lineages.

3.2.7. Maxilla

3.2.7.1. General appearance

The maxilla of Trichoptera is typically equipped with extremely long maxillary palps (Fig. 4). Always five palpomeres are present in females. Furthermore, five maxillary palpomeres are also present in males of Annulipalpia (Fig. 4), 'Spicipalpia', and some integripalpians (e.g., *Leptocerus* [Leptoceridae]). In contrast, sexual dimorphism occurs in the integripalpian lineage Plenitentoria with three palpomeres in males (four in Phryganeidae).

The terminal segment of the maxillary palp is remarkably long and flexible in all representatives of Annulipalpia. Here a system of regularly arranged cuticular 'clefts' of the surface results in an annulated appearance of the maxillary palp (Fig. 14). In contrast, the terminal segment is not distinctly longer than the preceding segment in all groups of 'Spicipalpia' and Integripalpia. The first and second segment of the maxillary palp are comparatively short in all trichopteran lineages. The third palpomere is as long as both preceding segments together.

The maxillary palps are usually densely covered by a large number of different types of sensilla. Strong smooth ribbed trichoid sensilla are present on the mesal wall of the first and second palpomere.

The base of the maxilla is formed by a large composite sclerite (see 3.1.8. for details). Cardo (small, cap-like), basistipes and dististipes (trough-like) are widely inseparable

Taxon	te-cd	te-st	cr-cd	cr-st	cr-lc	st-lc	cd-mp(d)	cd/st-mp(v)	st-mp(d)
Philopotamus ludificatus McLachlan, 1878	1 ata	1 lt	1 pge	1 pge	1 pge	-	1 cd/st sclerite	1 cd/st sclerite	1 dst
Stenopsyche marmorata Navas, 1920	1 ata	1 ata/lt	1 pge	1 pge	1 pge	-	1 cd/st sclerite	1 cd/st sclerite	1 dst
Hydropsyche angustipennis (Curtis, 1834)	1 ata/lt	1 ata/lt	1 pge-ocs	1 pge	1 pge-ocs	-	1 cd/st sclerite	1 cd/st sclerite	1 dst
Tinodes dives (Pictet, 1834)	1 ata	1 ata/lt	1 pge-ocs	1 pta	1 pge-ocs	-	1 cd/st sclerite	1 cd/st sclerite	1 dst
Holocentropus dubius (Rambur, 1842)	1 ata/lt	1 lt	1 pge	1 pge	1 pge	-	1 cd/st sclerite	1 cd/st sclerite	1 dst
Rhyacophila obliterata McLachlan, 1863	1 ata	1 ata/lt	1 pge	-	1 pge	1 dst	1 cd/st sclerite	1 cd/st sclerite	1 dst
Hydrobiosis styracine McFarlane, 1960	1 lt	1 lt	1 pge	-	1 pge	1 dst	1 cd/st sclerite	1 cd/st sclerite	1 cd/st sclerite
Apsilochorema sutshanum Martynov, 1934	1 ata/lt	1 ata	1 pge	-	1 pge	1 dst	1 cd/st sclerite	1 cd/st sclerite	1 cd/st sclerite
Glossosoma spinosum Morse et Yang, 2005	1 ata/lt	1 lt	1 pge	-	1 pge	-	1 cd/st sclerite	1 cd/st sclerite	1 dst
Agapetus fuscipes Curtis, 1834	1 lt	1 lt	1 pge	-	1 pge-ocs	1 dst	1 cd/st sclerite	1 cd/st sclerite	1 dst
Ptilocolepus granulatus (Pictet, 1834)	1 ata	1 ata	1 pge	-	1 pge	1 dst	1 cd/st sclerite	1 cd/st sclerite	1 dst
Hydroptila scamandra Neboiss, 1977	1 ata	1 ata	1 pge	-	1 pge	1 dst	1 cd/st sclerite	1 cd/st sclerite	- [?]
Orthotrichia atraseta Wells, 1979	1 ata	1 ata	1 pge	-	1 pge	1 dst	1 cd/st sclerite	1 cd/st sclerite	1 dst
Phryganea grandis Linnaeus, 1758	1 ata/lt	-	1 pge	-	1 pge	1 dst	1 cd/st sclerite	1 cd/st sclerite	1 dst
Trichostegia minor Curtis, 1834	1 ata/lt	-	1 pge	-	1 pge	1 dst	1 cd/st sclerite	1 cd/st sclerite	1 dst
Brachycentrus subnubilus Curtis, 1834	1 ata/fgs	1 ata	1 pge-ocs	-	1 pge	1 dst	1 cd/st sclerite	1 cd/st sclerite	1 dst
Limnephilus flavicornis (Fabricius, 1787)	1 ata/lt	1 lt	1 pge	-	1 pge-ocs	1 dst	1 cd/st sclerite	1 cd/st sclerite	1 dst
Silo nigricornis (Pictet, 1834)	1 ata/lt	1 lt	1 pge-ocs	-	1 pge-ocs	1 dst	2 cd/st sclerite	- [?]	- [?]
Sericostoma personatum Kirby et Spence, 1826	1 ata	1 ata/lt	1 pge	-	1 pge	-	1 cd/st sclerite	1 cd/st sclerite	1 dst
Pycnocentria evecta McLachlan, 1868	1 ata/lt	1 ata/lt	1 pge	-	1 pge	-	1 cd/st sclerite	1 cd/st sclerite	1 dst
Molanna angustata Curtis, 1834	1 ata/lt	1 lt	1 pge	-	1 pge	-	1 cd/st sclerite	1 cd/st sclerite	1 dst
Leptocerus tineiformis Curtis, 1834	1 ata/lt	1 ata/lt	1 pge	-	1 pge	-	1 cd/st sclerite	1 cd/st sclerite	1 dst

in all lineages. The composite cardostipital sclerite is remarkably elongated and ventrally directed in representatives of Plenitentoria.

The trichopteran maxilla is equipped with large endite lobes (i.e., galeolaciniae) including a well-developed galea and a quite smaller lacinia mesally. The latter is strongly sclerotized and distinctly separated from the membranous galea as described for *Philopotamus* (see above [3.1.8.] in Annulipalpia (Fig. 11) and 'Spicipalpia'. In contrast, it is remarkably reduced in size and level of sclerotization in all lineages of Integripalpia, especially in Integripalpia-Brevitentoria with only a small and moderately sclerotized crest present at the mesal wall of the galeolacinia. The mainly membranous galea is usually equipped with a large number of basiconic sensilla. It is remarkably large in representatives of the integripalpian lineage Plenitentoria.

3.2.7.2. Musculature of the maxilla

The cardostipital sclerite (i.e., cardo + basistipes and dististipes) is equipped with two large tentorial adductor muscles (Tab. 10).

M. tentorio-cardinalis (te-cd) is formed by a single bundle in all groups of Trichoptera. It always connects the ventral or mesal wall of the anterior tentorial arm with the distal margin of the 'basal' piece (i.e., cardo + basistipes) of the cardostipital sclerite.

The second tentorial adductor, M. tentorio-stipitalis (te-st), is also present in all Trichoptera except for the integripalpian lineage Phryganeidae (Tab. 10). It originates ventromesally at the anterior tentorial arm and at the laminatentorium, directly in front of te-cd. M. tentorio-stipitalis inserts at the mesal wall of the dististipital section of the cardostipital sclerite.

The 'basal' piece of the cardostipital sclerite is also moved by a cranial adductor muscle (M. cranio-cardinalis [cr-cd]) in all trichopteran representatives. Usually, the fan-shaped muscle originates ventrally at the postgena and inserts mesally at the proximal margin of the cardostipital sclerite. In contrast, it exclusively originates at the occipital sulcus in the annulipalpian lineages Hydropsychidae and Psychomyiidae.

A cranio-stipital adductor muscle (M. cranio-stipitalis [cr-st]) is only present in Annulipalpia (Figs. 16A, 19E). The comparatively long and slender muscle originates at the postgena and inserts mesally at the dististipital part of the cardostipital sclerite closely adjacent to the origin site of te-st.

The cranial flexor muscle of the lacinia (M. cranio-lacinialis [cr-lc]) is well-developed and attached to the maxillary lobe (i.e., galeolacinia) in all Trichoptera. It is composed of a single, long and slender bundle, which originates laterally at the postgena in several groups (Tab. 10). The muscle is attached to the mesal wall of the occipital sulcus in several not closely related taxa (e.g., Hydropsychidae; Glossosomatidae; Limnephilidae; Tab. 10; App. 5).

A second muscle attached to the galeolacinia is the stipital flexor, M. stipito-lacinialis (st-lc). The muscle is present in most lineages of 'Spicipalpia' and Integripalpia (Tab. 10). It is composed of a single small bundle, which has its site of origin mesally at the dististipital part of the cardostipital sclerite and inserts proximolaterally at the galeolacinia. In contrast, it is absent in Annulipalpia, as well as in the spicipalpian family Glossosomatidae and in the integripalpian lineage Sericostomatidae.

M. stipito-galealis (st-ga) is absent in Trichoptera.

Three extrinsic muscles of the maxillary palp originate from the cardostipital sclerite in most lineages of Trichoptera (Tab. 10). The origin and insertion sites of these muscles are quite similar to the conditions described for *Philopotamus* (see above [3.1.8.]). As an exception, M. stipito-palpalis dorsalis (st-mp(d)) is absent in Hydroptilidae and Goeridae.

The intrinsic musculature of the maxillary palp is also rather uniformly developed throughout the trichopteran lineages (Tab. 10; App. 1).

3.2.8. Labium

3.2.8.1. General appearance

The main part of the trichopteran labium is membranous. A moderately sclerotized labial plate (lapl, Fig. 5) is present in its distal half in all lineages. Prelabium and postlabium of the generalized insect head are not discriminable in trichopterans as extensively described at the beginning for *Philopotamus* (see above [3.1.9.]).

The labium of both sexes bears three-segmented labial palps. The third palpomere is by far the longest segment. It is longer as the preceding first and second segment together (Fig. 4). The labial palps are densely covered with different types of sensilla.

Its base is surrounded by moderately sclerotized palpigers (ppg, Fig. 5). Furthermore, the labium bears two unsegmented terminal lobes in all lineages of Annulipalpia investigated (lal, Fig. 10F). The homology of these endite lobes of the labium is uncertain since intrinsic muscles are completely absent (see below). The surface of the endite labial lobes is usually covered by several strong smooth ribbed trichoid sensilla (Fig. 10).

3.2.8.2. Musculature of the labium

The labium of Trichoptera is equipped with two strongly developed cranial adductor muscles (Tab. 11).

M. cranio-praementalis medialis (cr-prm(m)) is usually composed of two adjacent bundles. Both bundles originate posteriorly at the postgena near the base of the posterior tentorial arm in most lineages (e.g., Hydropsychidae; Ptilocolepidae; Goeridae). In some groups the dorsal bundle (M. cranio-praementalis medialis dorsalis [cr-prm(m)-d]) shifted its site of origin to the posterior tentorial arm (e.g., Glossosomatidae) or even to the proximal half of the anterior tentorial arm (e.g., Hydrobiosidae). Both bundles insert separately at the distal part of the labial sclerite near the origin site of M. praemento-palpalis medialis (prm-lp(m)).

M. cranio-praementalis lateralis (cr-prm(l)) is composed of a single, long and slender bundle in all trichopteran representatives investigated. It originates at the postgena near the base of the posterior tentorial arm, mesal to cr-prm(m) in most groups (App. 6) and inserts at the lateral margin of the palpiger.

The labial palp is moved by two extrinsic, single-bundled muscles (M. praemento-palpalis medialis [prm-lp(m)] and M. praemento-palpalis lateralis [prm-lp(l)]) in Trichoptera. Their origin and insertion sites form a quite uniform pattern throughout Trichoptera.

M. praemento-palpalis medialis (prm-lp(m)) originates mesally at the dorsal face of the premental area in most lineages (e.g., Philopotamidae, Fig. 19F; Tab. 11). It is shifted to the mesal margin of the palpiger in some groups (e.g., Psychomyiidae; Tab. 11). The muscle is generally inserted on the lateral basal margin of the first palpomere.

M. praemento-palpalis lateralis (prm-lp(l)) is attached to the lateral wall of the palpiger in all trichopteran representatives. It inserts dorsolaterally at the proximal margin of the first palpomere.

Further labial muscles of the generalized insect head (M. submento-praementalis [smt-prm]; M. praemento-paraglossalis [prm-pgl]; M. praemento-glossalis [prm-gl]) are absent in

Taxon	**hy-sa**	**i-sa**	**prm-sa**	**cr-prm(m)**	**cr-prm(l)**	**prm-lp(m)**	**prm-lp(l)**
Philopotamus ludificatus McLachlan, 1878	1 sit	-	1 prm	2 pge	1 pge	1 prm	1 ppg
Stenopsyche marmorata Navas, 1920	- [?]	-	1 [?] prm	1 [?] pge	1 pge	1 [?] prm	1 [?] ppg
Hydropsyche angustipennis (Curtis, 1834)	1 sit	-	2 prm	2 pge	1 pge	1 prm	1 ppg
Tinodes dives (Pictet, 1834)	-	-	2 prm	2 pge	1 pge	1 ppg	1 ppg
Holocentropus dubius (Rambur, 1842)	-	1 sal	-	2 pge	1 pge	1 prm	1 ppg
Rhyacophila obliterata McLachlan, 1863	-	1 sal	1 prm	2 pge/pta	1 pta	1 ppg	1 ppg
Hydrobiosis styracine McFarlane, 1960	-	-	1 prm	2 pge/pta	1 pge	1 prm	1 ppg
Apsilochorema sutshanum Martynov, 1934	-	-	1 prm	2 pge/ata	1 ata	1 prm	1 ppg
Glossosoma spinosum Morse et Yang, 2005	-	-	1 prm	2 pge/pta	1 pge	1 prm	1 ppg
Agapetus fuscipes Curtis, 1834	-	-	1 prm	2 pge	1 pge	1 prm	1 ppg
Ptilocolepus granulatus (Pictet, 1834)	-	-	1 prm	2 pge	1 pge	1 prm	1 ppg
Hydroptila scamandra Neboiss, 1977	-	-	1 prm	2 pge	1 pge	1 prm	1 ppg
Orthotrichia atraseta Wells, 1979	-	-	1 prm	2 pge	1 pge	1 prm	1 ppg
Phryganea grandis Linnaeus, 1758	-	1 [?] sal	1 prm	2 pge	1 pge	1 prm	1 ppg
Trichostegia minor Curtis, 1834	-	1 [?] sal	1 prm	2 pge	1 pge	1 prm	1 ppg
Brachycentrus subnubilus Curtis, 1834	-	1 sal	- [?]	2 pge	1 pge	1 prm	1 ppg
Limnephilus flavicornis (Fabricius, 1787)	-	1 [?] sal	- [?]	2 pge	1 pge	1 prm	1 ppg
Silo nigricornis (Pictet, 1834)	-	1 [?] sal	- [?]	2 pge	1 pge	1 prm	1 ppg
Sericostoma personatum Kirby et Spence, 1826	-	- [?]	1 prm	2 pge	1 pge	1 prm	1 ppg
Pycnocentria evecta McLachlan, 1868	-	-	1 prm	2 pge	1 pge	1 prm	1 ppg
Molanna angustata Curtis, 1834	-	1 sal	1 prm	2 pge	1 pge	1 prm	1 ppg
Leptocerus tineiformis Curtis, 1834			1 prm	2 [?] pge	1 pge	1 prm	1 ppg

← **Table 11:** Musculature of the trichopteran labium and salivarium with information on number of bundles and the origin sites. Abbreviations: **ata** – anterior tentorial arm, **cr-prm(l)** – M. cranio-praementalis lateralis, **cr-prm(m)** – M. cranio-praementalis medialis, **hy-sa** – M. hypopharyngo-salivarialis, **i-sa** – M. intra-salivarialis, **pge** – postgena, **ppg** – palpiger, **prm** – prementum, **prm-lp(l)** – M. praemento-palpalis lateralis, **prm-lp(m)** – M. praemento-palpalis medialis, **prm-sa** – M. praemento-salivarialis, **pta** – posterior tentorial arm, **sal** – salivarium, **sit** – sitophore plate, **-** – absent, **?** – uncertain. (For detailed description see Appendix 6)

Trichoptera.

The labial palp is equipped with three intrinsic muscles (M. palpo-palpalis labii primus anterior [lp1-lp2(a)]; M. palpo-palpalis labii primus posterior [lp1-lp2(p)]; M. palpo-palpalis labii secundus [lp2-lp3]) in all lineages of Trichoptera (see above [3.1.9.]). These muscles are morphologically very uniform throughout the investigated species (App. 1).

3.2.9. Salivarium

3.2.9.1. General appearance

The structure of the salivarium is quite uniform throughout Trichoptera (see above [3.1.12.]).

It is U-shaped in cross section and is proximally supplied by two thin salivary ducts. Its concave basis is strongly sclerotized (Fig. 19F), whereas the roof is pestle-like and is inserted into the concavity of the floor in all lineages. The salivarium is remarkably tapering towards its orifice.

The salivary orifice is located on the lower anterior part (e.g., Hydropsychidae) or the posteriorly directed surface of the haustellum (e.g., Leptoceridae).

3.2.9.2. Musculature of the salivarium

The arrangement of the salivary musculature in Trichoptera is highly variable (Tab. 11).

A hypopharyngeal dilator muscle, connecting the hypopharynx and the roof of the salivarium (M. hypopharyngo-salivarialis [hy-sa]), is only present in the annulipalpian lineages Philopotamidae (Fig. 19I) and Hydropsychidae.

In contrast, a strongly developed muscle enclosing the roof of the distal part of the salivarium (M. intra-salivarialis [i-sa]) is present in most lineages of Integripalpia (e.g., Brachycentridae; Molannidae; Tab. 11), the annulipalpian lineage Polycentropodidae, and in the spicipalpian taxon Rhyacophilidae (Tab. 11; App. 6).

Furthermore, a well-developed extensor muscle of the salivarium is present in most lineages of Trichoptera. In general, the single bundle of M. praemento-salivarialis (prm-sa) originates from the ventral part of the premental area (close to the insertion site of cr-prm(m)) and inserts at the proximal half of the salivary roof. The muscle is absent in the annulipalpian family Polycentropodidae and in some lineages of Integripalpia-Plenitentoria (e.g., Limnephilidae; Tab. 11).

3.2.10. Haustellum

3.2.10.1. General appearance

The flexible haustellum (hst, Fig. 10B) of Trichoptera is a composite, but distinctive structure formed by the distal region of the hypopharynx and the anterior wall of the prelabium (see above [3.1.11.]).

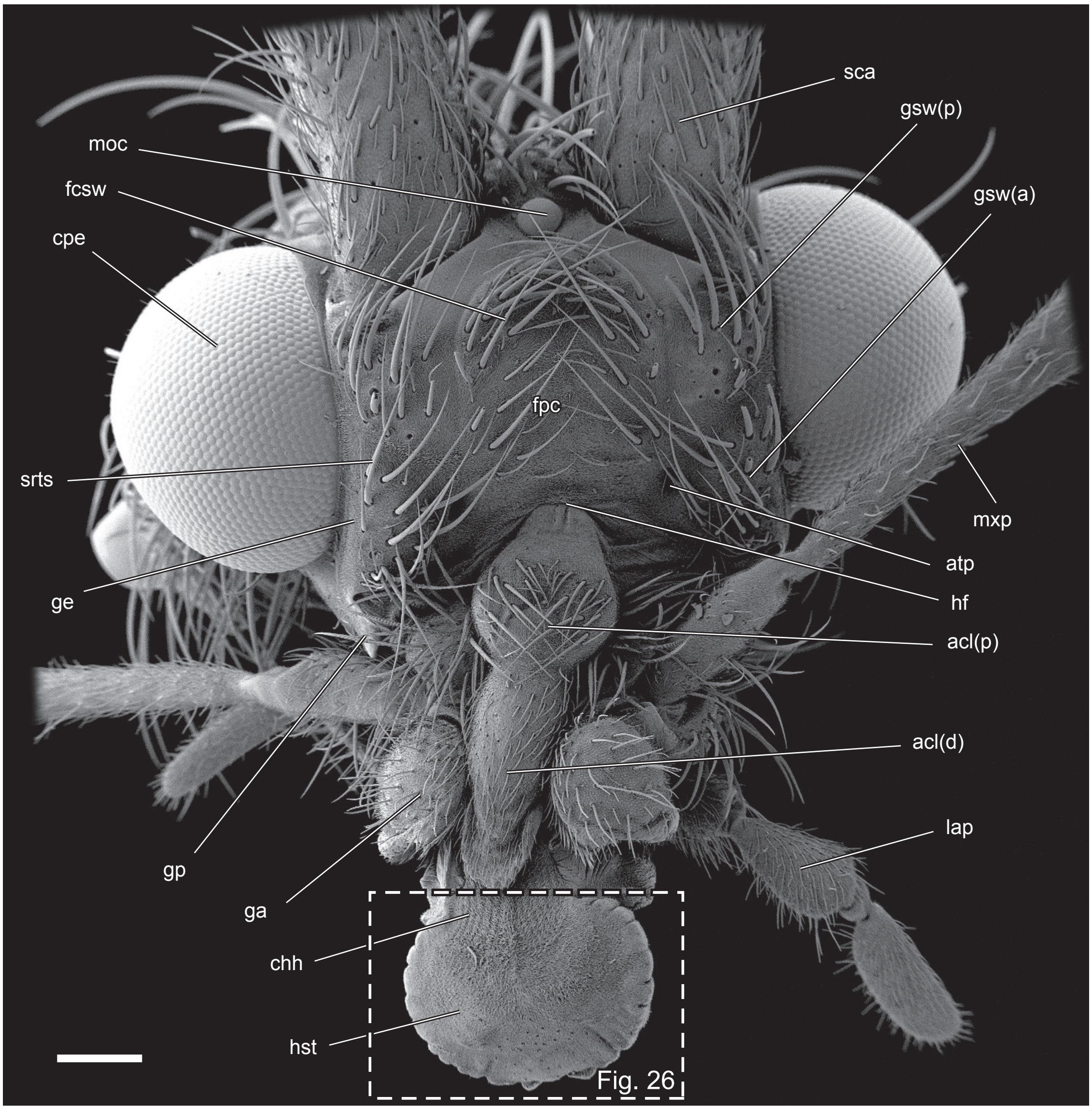

Figure 25: *Limnephilus flavicornis* (Fabricius, 1787): head – anterior view, SEM image. Abbreviations: **acl(d)** – distal part of anteclypeolabrum, **acl(p)** – proximal part of anteclypeolabrum, **atp** – anterior tentorial pit, **cpe** – compound eye, **fcsw** – frontoclypeal setal wart, **fpc** – frontopostclypeus, **ga** – galea (i.e. galeolacinia), **ge** – gena, **gsw(a)** – anterior setal wart of gena, **gsw(p)** – posterior setal wart of gena, **gp** – subgenal process, **hf** – horizontal furrow between frontopostclypeus and anteclypeolabrum, **hst** – haustellum, **lap** – labial palp, **moc** – median ocellus, **mxp** – maxillary palp, **sca** – scapus, **srts** – smooth ribbed trichoid sensillum, **I–III** – number of palpomere. (Scale bar: 200 µm)

It is mainly membranous, pillow-shaped and anteriorly continuous with the sitophore plate in all trichopterans. Posteriorly, it converges toward the labial lobes in Annulipalpia (Fig. 10F) or towards the labial palpigers in all other lineages. The haustellum is comparatively small and almost triangular-shaped in Annulipalpia (Fig. 10B) and ‘Spicipalpia’. In contrast, it is distinctly enlarged and tongue-like in all representatives of Integripalpia (Figs. 25, 26). In the integripalpian lineage Limnephilidae it is specifically rounded (Figs. 25, 26). Furthermore, it bears the salivary orifice (saor, Fig. 10B), which is well visible on the anterior surface of the haustellum in Annulipalpia (Fig. 10B) and all spicipalpian lineages. In contrast, the salivary orifice is covered by a salivary pleat in all integripalpians investigated. This semi-

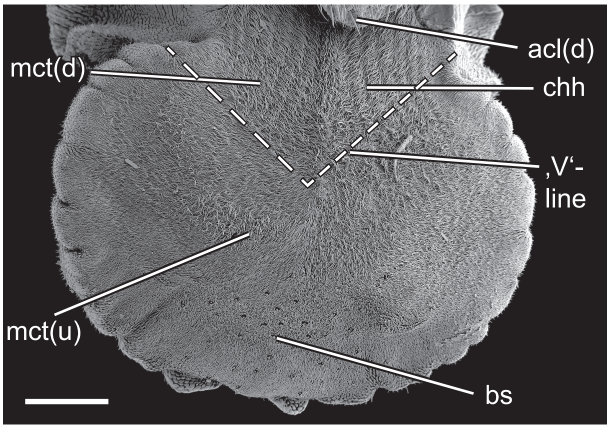

Figure 26: *Limnephilus flavicornis* (Fabricius, 1787): haustellum, anterior view, SEM image. Abbreviations: **acl(d)** – distal part of anteclypeolabrum, **bs** – basiconic sensillum, **chh** – regular channels on the surface of the haustellum, **mct(d)** – downward directed microtrichia, **mct(u)** – upward directed microtrichia. (Scale bar: 100 µm)

circular pleat is formed by the dorsally folded anterior wall of the haustellum. The trichopteran haustellum can be completely retracted and protruded using hemolymph pressure changes.

3.2.10.2. Haustellar surface structures

Large parts of the anterior surface of the haustellum are densely covered with multi-branched microtrichia remarkably differing in length and shape between species (Figs. 10B; 26). The microtrichia of Rhyacophilidae vary considerably from trichoid to knob- and leaf-like shape. A similar pattern was not observed in any of the other investigated species. Furthermore, basiconic sensilla are present on the haustellar surface in several not closely related groups (Figs. 10D,E, 26).

The haustellum of Integripalpia and of the annulipalpian lineage Polycentropodidae is equipped with a system of longitudinal channels formed by a regular arrangement of multibranched microtrichia (chh, Fig. 26). These channels converge towards the sitophore plate (i.e., mouth opening).

In contrast, a very dissimilar type of the haustellum with the surface structure being rather granulose is present in all remaining annulipalpian and spicipalpian lineages (Fig. 10B). The granulose surface of Glossosomatidae, Ptilocolepidae, and Hydroptilidae is quite unique among Trichoptera and differs from the mainly unstructured annulipalpian surface since it is produced by transverse grooves and ridges. In these groups the microtrichia are arranged in horizontal rows.

In all investigated lineages of Integripalpia the microtrichia on the proximal and distal half of the anterior haustellar surface show an opposing orientation distinctly separated by a V-shaped convergence line (Fig. 26). A V-shaped convergence line could not be observed in any annulipalpian or spicipalpian lineage.

3.3. Morphology of the pupal mouthparts in Trichoptera

3.3.1. General appearance

In the final stage of metamorphosis the pupal hull completely encloses the pharate adult as a comparatively thin layer of weakly sclerotized cuticle (Fig. 27). Invaginated structures of the adult body as trachea, fore- and hindgut are also lined with a sheet of pupal cuticle. The morphology of this hull strongly resembles the external features of the adult. Striking differences between the pharate adult and the pupal hull occur in structures used by the pupa during its live in the cocoon or during hatching from it. In the head region noteworthy differences were found in the shape and sclerotization of the mandibles and of the anteclypeolabrum. These structures are therefore described in detail below. However,

Table 12: Overview of external features of the trichopteran pupal head. Abbreviations: **acl** – anteclypeolabrum, **app.** – approximately, **nb.** – number, **?** – uncertain.

Taxon	Nb. of sts of acl	Surface of acl	Shape of mandible	Nb. of mandibular incisivi	Structure of mandibular cutting edge
Philopotamus ludificatus McLachlan, 1878	app. 15, scattered distribution	smooth, without any separation	falciform	4 (3 subapical + 1 apical)	with only a few scattered distributed
Hydropsyche angustipennis (Curtis, 1834)	> 50, acl densely covered	with proximo-lateral projection bearing numerous setae	falciform	5 (4 subapical + 1 apical)	comb-like with small teeth
Rhyacophila fasciata Hagen, 1859	app. 15, scattered distribution	small posterior band separated from anterior part by transverse groove	falciform	4 (3 subapical + 1 apical)	comb-like with small teeth
Agapetus fuscipes Curtis, 1834	app. 15, scattered distribution	posterior half weakly sclerotized, anterior half strongly sclerotized	falciform	3 (2 subapical + 1 apical)	comb-like with small teeth
Limnephilus flavicornis (Fabricius, 1787)	app. 15, separated groups	separated by deep transverse groove	proximal half broad, apically pointed	1 (apical)	comb-like with small teeth
Silo nigricornis (Pictet, 1834)	app. 15, separated groups	separated by deep transverse groove	proximal half broad, apically pointed	1 (apical)	comb-like with small teeth
Brachycentrus Curtis, 1834	app. 15, separated groups	smooth, without separation (?)	proximal half broad, apically pointed	1 (apical)	comb-like with small teeth

also thoracic (e.g., legs, wings) and abdominal structures (e.g., dorsal sclerites) are distinctly modified in the pupal stage.

3.3.2. Anteclypeolabrum

The pupal anteclypeolabrum is generally much more sclerotized than other regions of the pupal head capsule. Its lateral bases form a hinge-like articulation with the inner walls of the mandibles and can be moved by the adult anteclypeolabrum inside. In many lineages (e.g., Limnephilidae) it is subdivided into a less sclerotized posterior region and a more heavily sclerotized anterior section by a deep transverse fold (Tab. 12). In contrast, its surface is not subdivided in the annulipalpian lineages (e.g., Philopotamidae, Fig. 27).

The pupal anteclypeolabrum is covered by smooth trichoid sensilla in all investigated species. These sensilla can vary greatly in

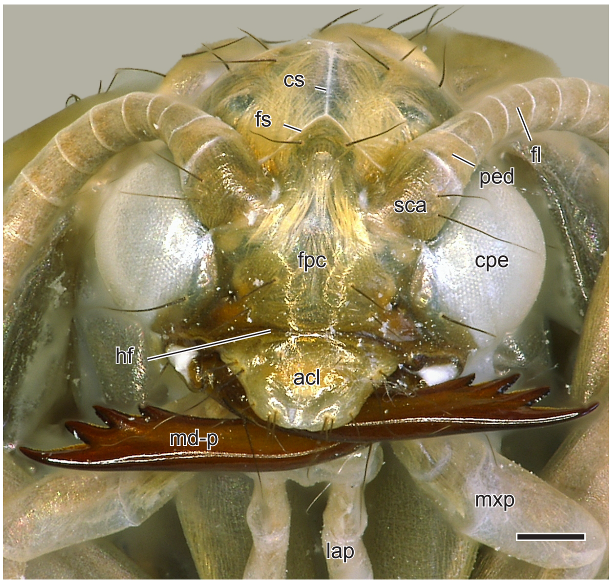

Figure 27: *Philopotamus ludificatus* McLachlan, 1878: head of pharate adult enclosed by pupal hull, light-microscopic image, anterior view. Abbreviations: **acl** – anteclypeolabrum, **cpe** – compound eye, **cs** – coronal sulcus, **fl** – flagellomere, **fpc** – frontopostclypeus, **fs** – frontal sulcus, **hf** – horizontal furrow between frontopostclypeus and anteclypeolabrum, **lap** – labial palp, **md-p** – pupal mandible, **mxp** – maxillary palp, **ped** – pedicellus, **sca** – scapus. (Scale bar: 250 µm)

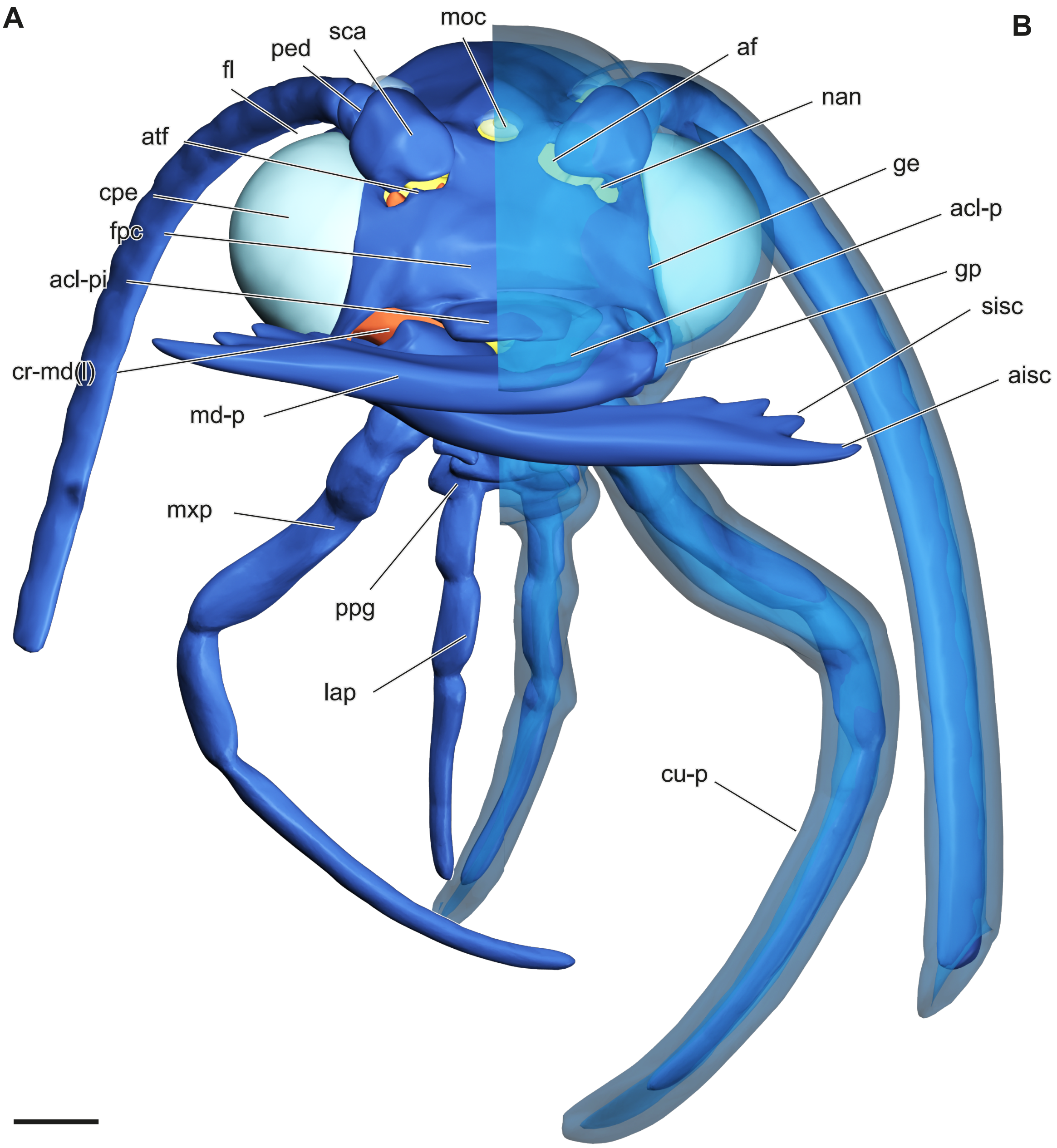

Figure 28: *Philopotamus ludificatus* McLachlan, 1878: head, 3D-reconstruction based on µCT data. **A**: pharate adult; **B**: pupal hull. Abbreviations: **acl-p** – anteclypeolabrum of pupa, **acl-pi** – anteclypeolabrum of pharate imago, **af** – antennal foramen, **aisc** – apical incisivus of pupal mandible, **atf** – antennifer, **cpe** – compound eye, **cr-md(l)** – M. cranio-mandibularis lateralis, **cu-p** – cuticle of pupa, **fl** – flagellomere, **ge** – gena, **gp** – subgenal process, **hf** – horizontal furrow, **lap** – labial palp, **md-p** – mandible of pupa, **moc** – median ocellus, **mxp** – maxillary palp, **nan** – nervus antennalis, **fpc** – frontopostclypeus, **ped** – pedicellus, **ppg** – palpiger, **sca** – scapus, **sisc** – subapical incisivus of pupal mandible, **I–V** – number of palpomere. (Scale bar: 250 µm)

number and size between different lineages (Tab. 12). In the annulipalpian lineage Hydropsychidae it bears a large number of comparatively small, smooth trichoid sensilla (e.g., > 50 in *Hydropsyche*). Only a few, but extremely strong trichoid sensilla are scattered distributed in Philopotamidae (< 15 in *Philopotamus*) and other groups of Trichoptera (e.g., *Agapetus* [‘Spicipalpia’: Glossosomatidae]; *Silo* [Integripalpia: Goeridae]). The strong trichoid sensilla are arranged in two comparatively weakly sclerotized fields in the anterior section of the anteclypeolabrum in *Limnephilus*. Each group consists of five sensilla. Additionally, the posterior region is equipped with two strong sensilla on each side and a large number of irregularly distributed minute trichoid sensilla.

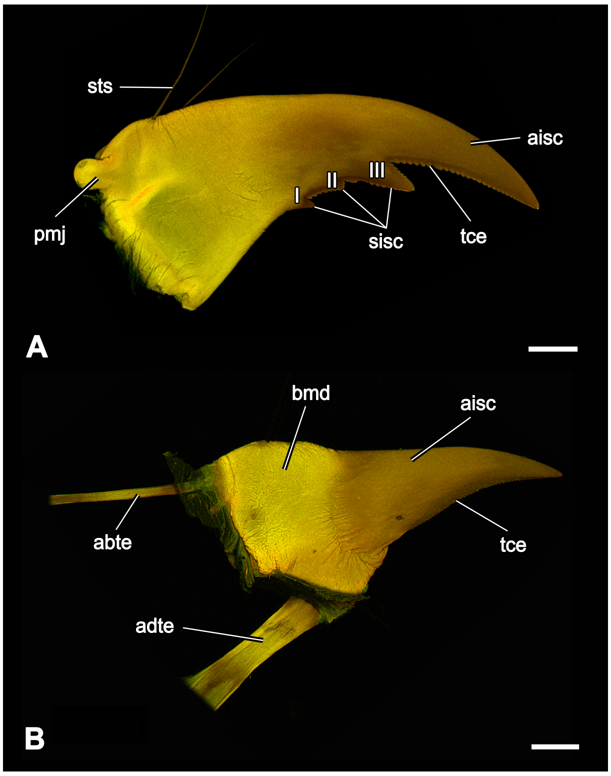

Figure 29: The pupal mandibles of two trichopteran representatives, volume rendering based on confocal laser scanning microscopy (CLSM). **A**: *Rhyacophila fasciata* Hagen, 1859 (Rhyacophilidae); **B**: *Limnephilus flavicornis* (Fabricius, 1787) (Limnephilidae). Abbreviations: **abte** – abductor tendon of mandible (M. cranio-mandibularis lateralis), **adte** – adductor tendon of mandible (M. cranio-mandibularis medialis), **aisc** – apical incisivus, **bmd** – basal piece of mandible, **pmj** – posterior primary mandibular joint, **sisc I–III**, – subapical incisivi **I–III**, **sts** – smooth trichoid sensillum, **tce** – tooth of mandibular cutting edge. (Scale bars: 100 µm)

3.3.3. Mandible

The pupal mandibles are strongly developed and heavily sclerotized in most trichopteran groups (Figs. 27; 28). Its general shape varies considerably. They are overall falciform, strongly curved, and apically narrowing in Annulipalpia and ‘Spicipalpia’. In these taxa the mandibles are not distinctly subdivided and only slightly bulged at the base (Figs. 28, 31A,B). In contrast, the mandibles are subdivided into a broad, bulged basal piece (bmd, Fig. 29B) and a strongly sclerotized and tapering apical incisivus (aisc, Fig. 29B) in all integripalpian lineages investigated. Additionally, the apical area is equipped with a distinctly concave mesal edge equipped with a fine, saw-like pattern (Fig. 31D).

The number of incisivi varies between different lineages (Figs. 29, 31). In Integripalpia it is equipped with only a single large apical incisivus (e.g., Limnephilidae, Fig. 29B; Goeridae, Fig. 31D). In addition to a single apical incisivus representatives of Rhyacophilidae and Glossosomatidae possess three (e.g., Rhyacophilidae, Fig. 29A) or two (Glossosomatidae, Fig. 31C) subapical incisivi. One apical incisivus and three (e.g., Philopotamidae, Figs. 28, 31A) or four subapical incisivi (e.g., Hydropsychidae, Fig. 31B) are present in Annulipalpia (Tab. 12). A distinct grinding area, i.e., a mola is absent in mandibles of all trichopterans.

The mesal surface of the pupal mandible forms a distinct cutting edge, which is equipped

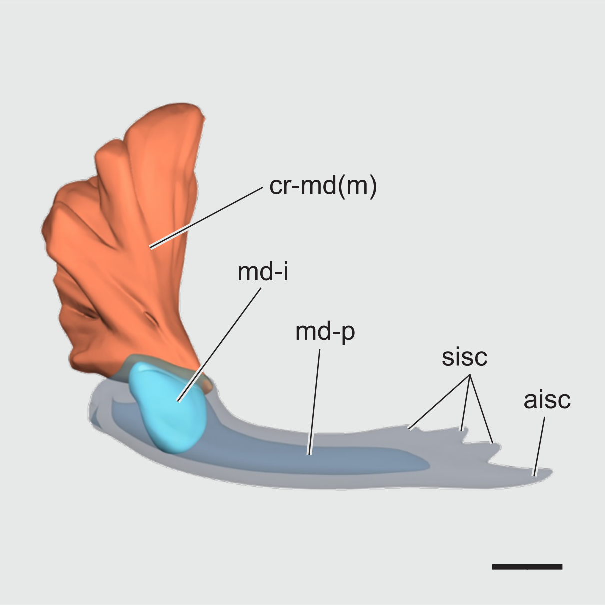

Figure 30: *Philopotamus ludificatus* McLachlan, 1878: Pupal and enclosed adult mandible with the large adductor muscle of the adult mandible (M. cranio-mandibularis medialis), 3D-reconstruction based on µCT-data. Abbreviations: **aisc** – apical incisivus, **cr-md(m)** – M. cranio-mandibularis medialis, **md-i** – mandible of the pharate imago, **md-p** – pupal mandible, **sisc** – subapical incisivi. (Scale bar: 200 µm)

with numerous comb-like arranged small teeth (tce, Figs. 29A; 31A–D). The teeth of the cutting edge are comparatively small and inconspicuous in Philopotamidae (Fig. 31A), but well-developed in the remaining taxa investigated (Figs. 29A, 31C,D). The lateral surface of the mandibular base usually bears straight trichoid sensilla (sts, Figs. 29A; 31A–C), which vary considerably in size and number between the different trichopteran groups. In several groups two strong straight trichoid sensilla are present (e.g., Philopotamidae, Glossosomatidae, and Limnephilidae; Fig. 31A,C). A comparatively large number of this type of sensilla is found in Hydropsychidae (e.g., > 10 in *Hydropsyche*, Fig. 31B).

The pupal mandible is articulated with the head capsule of the enclosed adult by two

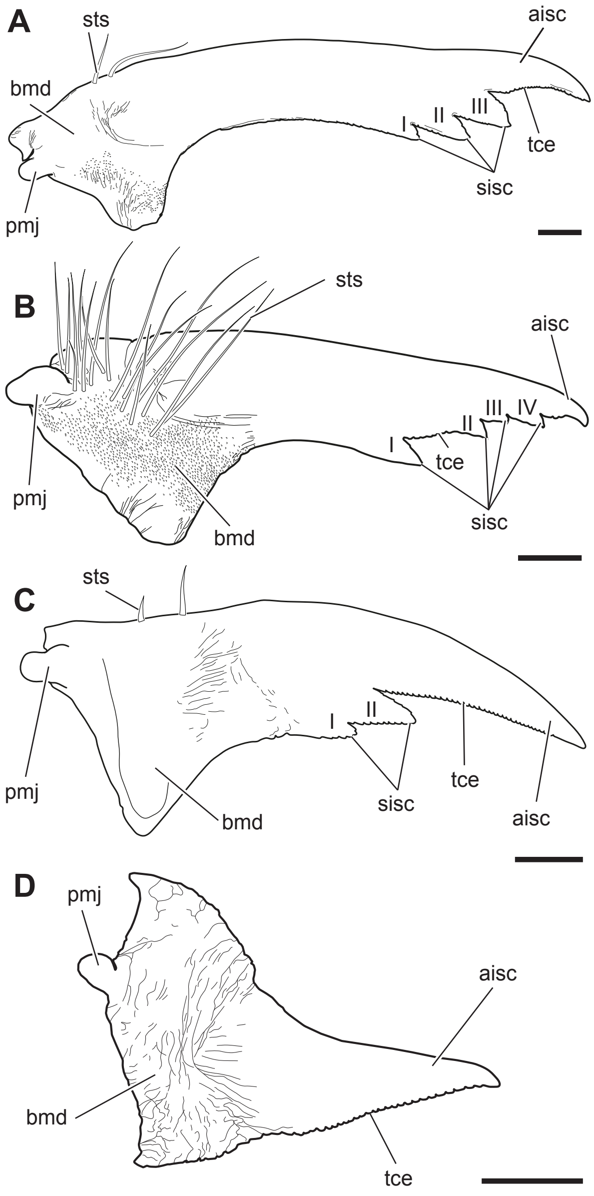

Figure 31: The pupal mandible of Trichoptera, line drawing based on confocal laser scanning microscopy (CLSM) data. **A**: *Philopotamus ludificatus* McLachlan, 1878 (Philopotamidae); **B**: *Hydropsyche angustipennis* (Curtis, 1834) (Hydropsychidae); **C**: *Agapetus fuscipes* Curtis, 1834 (Glossosomatidae); **D**: *Silo nigricornis* (Pictet, 1834) (Goeridae). Abbreviations: **aisc** – apical incisivus, **bmd** – basal piece of mandible, **pmj** – posterior primary mandibular joint, **sisc I–IV**, – subapical incisivi I–IV, **sts** – smooth trichoid sensillum, **tce** – tooth of mandibular cutting edge. (Scale bars: A,B: 100 µm; C,D: 50 µm)

strongly developed joints in all trichopterans investigated. Furthermore, the pupal mandible forms the ball head of the strong posterior / primary mandibular joint (pmj, Fig. 29A), which is hinged to the subgenal process of the adult (gp, Figs. 10, 28). The anterior / secondary mandibular joint is by way less distinctly developed. Here, the pupal mandible articulates in an area between the lateral edges of the anteclypeolabrum and the anterior margin of the frontopostclypeus of the adult. The small adult mandibles (md(s), Fig. 4) are inserted into concavities of the pupal counterparts (md-p, Fig. 30).

The pupal mandibles are moved by the strong mandibular muscles of the pharate adult (Fig. 30). The long, comparatively thin tendon of the abductor muscle (M. cranio-mandibularis lateralis) of the adult encloses its thin pupal counterpart, which continues towards the lateral-most margin of the pupal mandible (abte, Fig. 29B). The similar construction is realized for the very strong tendon of the adductor, M. cranio-mandibularis medialis (adte, Fig. 29B). It encases the distal half of the pupal adductor tendon inserting at the mesal margin of the mandible. Consequently, the pupal mandible lacks any own pupal mandibular musculature and is moved by the mandibular musculature of the pharate imago (see Fig. 30).

Live observations in *Philopotamus* (Philopotamidae) and *Hydropsyche* (Hydropsychidae) show that the mandibles of the pupa powered by the strongly developed muscles of the adult are used to cut its way out of the silken cocoon during hatching.

3.4. Phylogenetically relevant characters

3.4.1. Adult head characters

1. Ocelli: (0) present; (1) absent.

Three ocelli are present in Philopotamidae, Stenopsychidae (Malicky 2010) (both Annulipalpia), Rhyacophilidae, Hydrobiosidae (Neboiss 1986), Glossosomatidae, Ptilocolepidae (all 'Spicipalpia'), and in some integripalpian lineages (e.g., Limnephilidae).

Ocelli are absent in the annulipalpian lineages Hydropsychidae, Polycentropodidae, and Psychomyiidae, as well as in the integripalpian lineages Leptoceridae, Sericostomatidae, Goeridae, and Brachycentridae. Furthermore, ocelli are also absent in most representatives of the spicipalpian lineage Hydroptilidae (*Hydroptila*, *Orthotrichia*; Malicky 2004; pers. obs.). However, two lateral ocelli are present in the hydroptilid genus *Zumatrichia* (Malicky 1973: 35).

The median ocellus is also reduced in Lepidoptera (Kristensen 2003). Within Mecoptera three ocelli are well-developed in *Nannochorista* (Nannochoristidae; Beutel & Baum 2008), greatly reduced in size (e.g., *Boreus* [Beutel et al. 2008]), or completely absent in other groups (e.g., *Merope* [Friedrich et al. 2013], *Caurinus* [Beutel et al. 2008]).

2. Sexual dimorphism in number of maxillary palpomeres: (0) same number of maxillary palpomeres in both sexes; (1) number of maxillary palpomeres is reduced in males.

The number of maxillary palpomeres is the same in males and females of Annulipalpia, 'Spicipalpia', and some representatives of

Integripalpia-Brevitentoria.

The number of palpomeres is sexually dimorphic in Integripalpia-Plenitentoria (e.g., Limnephilidae; Uenoidae, Wiggins et al. 1985; Phryganopsychidae, Wiggins & Gall 1992; Rossianidae Schmid 1998).

Furthermore, the number of maxillary palpomeres is the same in males and females of Lepidoptera (Hannemann 1956; Kristensen 2003) and Mecoptera (Friedrich et al. 2013; Beutel & Baum 2008).

3. **Number of maxillary palpomeres in males: (0) five; (1) four; (2) three; (3) two; (4) one.**

The maxillary palp is five-segmented in males of Annulipalpia and 'Spicipalpia'. Furthermore, some representatives of Integripalpia-Brevitentoria are also equipped with a five-segmented maxillary palp in males (e.g., Leptoceridae, Crichton 1957; pers. obs.; Molannidae, Malicky 1973, 2004).

In contrast, the maxillary palp is three-segmented in some representatives of Integripalpia (e.g., Limnephilidae; Goeridae; and Brachycentridae). A four-segmented palp is present in males of the integripalpian families Phryganeidae and Phryganopsychidae (Wiggins & Gall 1992). Further reductions in the number of maxillary palpomeres occur in some other lineages of Integripalpia as for instance in Helicopsychidae (partim, e.g., *Helicopsyche sperata* McLachlan, 1876; Johanson & Pham 2011) with two palpomeres or in Lepidostomatidae with only one palpomere in males (partim, e.g., *Crunoecia irrorata* (Curtis, 1834); Malicky 1973, 2004).

Five maxillary palpomeres in males are also assigned to the ground plan of Lepidoptera (Kristensen 2003: 51) and Mecoptera (e.g., Friedrich et al. 2013).

4. **Fifth maxillary palpomere: (0) not elongated; (1) distinctly elongated.**

The fifth segment of the maxillary palp is distinctly elongated in Annulipalpia (e.g., Stenopsychidae; Philopotamidae, Fig. 4; see also Kristensen 2003: 51).

The fifth segment of all other trichopteran lineages investigated so far is as long as the preceding one (e.g., Rhyacophilidae, Klemm 1966: 7, fig. 3; Phryganeidae, Crichton 1957: 51, fig. 4; Leptoceridae).

The fourth segment of the maxillary palp is by far the longest in the 'basal' lepidopteran lineages (e.g., Micropterigidae, Hannemann 1956: 179, fig. 1). The terminal segment of the maxillary palp is only slightly elongated in Mecoptera (Beutel & Baum 2008; Friedrich et al. 2013).

5. **Integument of the terminal segment of maxillary palp: (0) highly flexible ('annulate') with regular cuticular clefts along the entire length of the segment; (1) smooth surface without regular cuticular clefts and restricted flexibility.**

The integument of the terminal maxillary palp is flexible with deep transverse cuticular clefts in Annulipalpia (see Fig. 14 A,B). The surface of the last maxillary palpomere is rather smooth, without a conspicious pattern and with reduced flexibility in all other lineages of Trichoptera.

The second last (fourth) maxillary palp segment of the lepidopteran non-glossatan families (e.g., Micropterigidae) is also flexible and equipped with deep transverse cuticular clefts, which are remarkably similar to the surface structures observed in annulipalpians (Kristensen 2003).

6. **Presence of labial endite lobes: (0) present; (1) absent.**

The labium bears small endite lobes between the labial palps in Annulipalpia (e.g., Philopotamidae, Fig. 10F) and in Rhyacophilidae (Klemm 1966; pers. obs.). Labial endite lobes are absent in all other trichopteran lineages investigated (see also Malicky 1973; Crichton 1957; Chaudonneret 1990).

The labium of Lepidoptera bears a composite formation, the 'ligula' (fused glossae after Kristensen 2003). Additionally, distinct paraglossae are present in the non-glossatan family Micropterigidae (e.g., Hannemann 1956; Kristensen 2003). A similar pattern (fused glossae ['ligula'] + paraglossae) occurs in Neuroptera (e.g., Randolf et al. 2014). Endite lobes of the labium are absent in Mecoptera (e.g., Beutel et al. 2008; Friedrich et al. 2013).

7. **Shape of anteclypeolabrum: (0) short and almost triangular; (1) remarkably elongated ventrally and somewhat rectangular shaped.**

The anteclypeolabrum is triangular and comparatively short in Annulipalpia (e.g., Philopotamidae, Fig. 4), Integripalpia-Brevitentoria (e.g., Leptoceridae), and all spicipalpian lineages (e.g., Rhyacophilidae, Klemm 1966: 5, fig. 1; Glossosomatidae, Durand 1955).

It is remarkably elongated ventrally and rectangular in Integripalpia-Plenitentoria (e.g., Phryganeidae, Crichton 1957: 49, fig. 1; Limnephilidae).

Clypeus and labrum are well separated structures in the head of Micropterigidae with the labrum almost triangular in shape (Hannemann 1956; Kristensen 2003; pers. obs.). The labrum of Mecoptera is also remarkably elongated ventrally (Nannochoristidae, Beutel & Baum 2008; pers. obs.; Meropeidae, Friedrich et al. 2013).

8. **Position of antennifer along the circumantennal margin: (0) ventral margin; (1) ventrolateral edge; and (2) lateral margin.**

The antennifer is formed by the ventral margin of the antennal foramen in Annulipalpia (see Fig. 22A; Durand 1955; Crichton 1957) and the spicipalpian lineages Rhyacophilidae, Glossosomatidae (Fig. 22E), and Ptilocolepidae (Fig. 22F). A ventrolateral position of the antennifer is only present in the spicipalpian lineage Hydrobiosidae (Fig. 22D). In contrast, it is formed by the lateral margin of the antennal foramen in Integripalpia (Fig. 22H; Crichton 1957: 69, fig. 33) and the spicipalpian family Hydroptilidae (Fig. 22G; Durand 1955: fig. 39).

A ventral position of the antennifer is also present in non-glossatan Lepidoptera (e.g., Micropterigidae, Fig. 21; Hannemann 1956: 179, fig. 2). Furthermore, it is positioned at the ventrolateral edge of the antennal foramen in most mecopterans (e.g., *Merope*, Friedrich et al. 2013), and Neuroptera (e.g., *Nevrorthus*, Randolf et al. 2014).

9. **Shape of tentorium: (0) Π-shaped; (1) H-shaped; (2) X-shaped.**

The tentorium is Π-shaped in Integripalpia (pers. obs.; see also Durand 1955; Neboiss 1991), some Annulipalpia (e.g., *Aethaloptera* [Hydropsychidae], Neboiss 1991), and the spicipalpian lineage Hydrobiosidae. A H-shaped configuration is present in most spicipalpian lineages (e.g., Rhyacophilidae; Glossosomatidae; Hydroptilidae), as well as in some annulipalpian groups (e.g., Stenopsychidae; Polycentropodidae; Psychomyiidae; see also Neboiss 1991). The presence of a corpotentorium (i.e. anterior tentorial arms fused before reaching the tentorial bridge) is a unique feature of Philopotamidae resulting in an X-shaped configuration of the tentorium (Fig. 6; see also Neboiss 1991; Kristensen 2003). In some hydropsychids (e.g., several *Hydropsyche* and *Austropsyche* species; see Neboiss 1991) the tentorium appears also X-shaped. However, in these cases the shape is caused by the closely adjacent insertions of the anterior tentorial arms on the tentorial bridge without forming a distinct corpotentorium.

A Π-shaped tentorium is a ground plan feature in Lepidoptera and Mecoptera (Kristensen 2003).

10. Dorsal tentorial arm: (0) absent; (1) present.

A dorsal tentorial arm is present in most lineages of Trichoptera (e.g., Philopotamidae, Fig. 23A; Hydrobiosidae, Fig. 23D; Limnephilidae, Fig. 24). It is absent in some lineages of Integripalpia-Brevitentoria (e.g., Conoesucidae; Molannidae; Neboiss 1991).

Well-developed dorsal tentorial arms are a typical feature of the head capsule in other endopterygote insect groups (e.g., Hymenoptera [Beutel & Vilhelmsen 2007], Neuroptera [Randolf et al. 2014], and Lepidoptera [Kristensen 2003]). It is present, but usually very thin in Mecoptera (Friedrich et al. 2013).

11. Length of dorsal tentorial arm: (0) vestigial; (1) short (not reaching the head capsule); (2) well-developed (continuous with head capsule).

The dorsal tentorial arm is strongly developed and continuous with the head capsule in Integripalpia-Plenitentoria (e.g., Limnephilidae, Fig. 24; Phryganeidae, Durand 1955: fig. 32; see also Neboiss 1991). It is short (i.e., not continuous with the head capsule) in the spicipalpian lineages Rhyacophilidae and Hydrobiosidae (Fig. 23D), as well as in a few integripalpian taxa (e.g., Leptoceridae, Neboiss 1991). The dorsal tentorial arm is vestigial in most annulipalpian taxa (e.g., Stenopsychidae; Hydropsychidae [*Diplectrona*], see Neboiss 1991; Philopotamidae, Fig. 23A), and in the spicipalpian families Glossosomatidae and Hydroptilidae (e.g., *Maydenoptila*, Neboiss 1991).

The dorsal tentorial arms of Lepidoptera are weakly developed or vestigial in the non-glossatan groups (e.g., Micropterigidae, Hannemann 1956), but well-developed in heteroneurous Glossata (fused with the head capsule in Acanthopteroctetidae; see Kristensen 2003). They are narrow but attached to the head capsule in Mecoptera (e.g., Friedrich et al. 2013: 75, fig. 5B).

12. Laminatentorium: (0) small to moderately sized and rather weakly sclerotized; (2) massively developed and strongly sclerotized.

The laminatentorium is strongly developed in the spicipalpian lineages Hydrobiosidae (Fig. 23D) and Glossosomatidae, as well as in few annulipalpians (e.g., Hydropsychidae). Furthermore, it is strongly developed in Integripalpia-Plenitentoria (e.g., Limnephilidae). The laminatentorium is comparatively small and only weakly sclerotized in the remaining annulipalpians (e.g., Philopotamidae; Psychomyiidae; and Polycentropodidae), the spicipalpian families Ptilocolepidae (Fig. 23F) and Hydroptilidae, and in Integripalpia-Brevitentoria (e.g., Molannidae).

The laminatentorium of micropterigid moths is comparatively tiny (Hannemann 1956; Kristensen 2003; pers. obs.). It is completely absent in *Nannochorista* (Beutel & Baum 2008), whereas it is well-developed in some other mecopterans (e.g., Meropeidae, Friedrich et al. 2013).

13. **Number of bundles of M. tentorio-scapalis anterior (te-sc(a)) (v. Kéler 1955: M. 1; Wipfler et al. 2011: 0an1): (0) one; (1) two; (2) three.**

Three bundles are present in all integripalpian families (see Fig. 24) with the single known exception of Sericostomatidae in which only one bundle is present. Crichton (1957) only mentioned the presence of te-sc(a) in *Phryganea bipunctata* without providing information on the number of bundles. Own observations revealed the presence of three bundles in other phryganeid species (*Phryganea grandis* and *Trichostegia minor*). Two bundles are present in the spicipalpian families Rhyacophilidae, Glossosomatidae (Fig. 23E), and Ptilocolepidae (Fig. 23F), and the annulipalpian family Polycentropodidae. In other investigated groups of Annulipalpia and 'Spicipalpia' only one bundle of te-sc(a) was found (see App. 2).

14. **M. tentorio-scapalis medialis (te-sc(m)) (v. Kéler 1955: M. 4; Wipfler et al. 2011: 0an4): (0) present; (1) absent.**

M. tentorio-scapalis medialis is absent in the investigated representatives of Glossosomatidae (Fig. 23E). The muscle is well-developed in all other trichopteran lineages investigated (see Fig. 23D).

It is also well-developed in the non-glossatan family Micropterigidae (Hannemann 1956; pers. obs.), and in Mecoptera (e.g., Nannochoristidae, Beutel & Baum 2008; pers. obs.).

15. **Number of bundles of M. tentorio-scapalis medialis (te-sc(m)) (v. Kéler 1955: M. 4; Wipfler et al. 2011: 0an4): (0) one; (1) two.**

One bundle is present in all integripalpian species investigated (see Fig. 24) and in most representatives of 'Spicipalpia' (e.g., Ptilocolepidae, Fig. 23F; Hydrobiosidae, Fig. 23D; see also App. 2). Two distinct bundles were observed in Hydropsychidae and Polycentropodidae (Fig. 23B).

The muscle consists of only a single bundle in Mecoptera (e.g., Meropeidae, Friedrich et al. (2013)) and Lepidoptera (e.g., Micropterigidae, Hannemann 1956; pers. obs.).

16. **Number of bundles of M. tentorio-scapalis lateralis (te-sc(l)) (v. Kéler 1955: M. 3; Wipfler et al. 2011: 0an3): (0) one; (1) two.**

M. tentorio-scapalis lateralis is composed of two bundles in Annulipalpia (Fig. 19D; App. 2), most spicipalpians (Glossosomatidae, Fig. 23E; Ptilocolepidae, Fig. 23F; Hydroptilidae), and a few integripalpians (e.g., Limnephilidae; Conoesucidae; see App. 2). One bundle is present in the spicipalpian lineages Rhyacophilidae, Hydrobiosidae, and in most integripalpian groups (e.g., Goeridae; Sericostomatidae; App. 2).

One bundle of M. tentorio-scapalis lateralis is described in basal lepidopterans (e.g., Micropterigidae; Hannemann 1956). The muscle is absent in Mecoptera (e.g., Beutel & Baum 2008; Friedrich et al. 2013; pers. obs.).

17. **Origin site of bundles of M. tentorio-scapalis lateralis (te-sc(l)-d/-v) (v. Kéler 1955: M. 3; Wipfler et al. 2011: 0an3): (0) both bundles exclusively on tentorium; (1) dorsal bundle on tentorium and ventral bundle on head capsule; (2) both bundles exclusively on head capsule.**

Both bundles of M. tentorio-scapalis lateralis originate exclusively on the mesal face of the anterior tentorial arm and the laminatentorium in the annulipalpian lineages Philopotamidae (Fig. 23A) and Hydropsychidae, as well as in the integripalpian family Limnephilidae (Fig. 24). In contrast, both bundles originate distinctly separated from each other from the tentorium and the head capsule in several annulipalpians (e.g., Stenopsychidae; Polycentropodidae, Fig. 23B), and in some spicipalpians (e.g., Glossosomatidae [*Glossosoma*], Fig. 23E; Ptilocolepidae, Fig. 23F; Hydroptilidae; see Tab. 7). Both bundles are exclusively attached to the head capsule in the integripalpian representative *Pycnocentria* (Conoesucidae).

Both bundles of M. tentorio-scapalis lateralis originate on the mesal face of the anterior tentorial arm in the non-glossatan moth family Micropterigidae (Hannemann 1956; pers. obs.). The muscle is absent in the mecopteran family Nannochoristidae (Beutel & Baum 2008; pers. obs.).

18. **Specific origin site of ventral bundle of M. tentorio-scapalis lateralis (te-sc(l)-v) (v. Kéler 1955: M. 3; Wipfler et al. 2011: 0an3): (0) anterior face of gena between frontopostclypeus and subgenal process; (1) ventral face of gena behind subgenal process.**

The ventral bundle of M. tentorio-scapalis lateralis (te-sc(l)-v) originates from the anterior face of the gena between the frontopostclypeus and the subgenal process in a few annulipalpians (e.g., Polycentropodidae, Fig. 23B) and in 'Spicipalpia' (e.g., Glossosomatidae, Fig. 23E; Ptilocolepidae, Fig. 23F; Hydroptilidae, see Tab. 7). It is attached to the ventral wall of the gena behind the subgenal process in *Pycnocentria* (Conoesucidae, see Tab. 7; App. 2).

19. **Origin of M. tentorio-scapalis posterior (te-sc(p)) (v. Kéler 1955: M. 2; Wipfler et al. 2011: 0an2): (0) anterior tentorial arm; (1) exclusively on dorsal tentorial arm.**

M. tentorio-scapalis posterior originates from the dorsal tentorial arm in the spicipalpian lineages Rhyacophilidae (Klemm 1966: 10, fig. 5; pers. obs.) and Hydrobiosidae (Fig. 23D). Furthermore, it is also attached to the dorsal tentorial arm in representatives of Integripalpia-Plenitentoria (e.g., Phryganeidae, Crichton 1957: 59, fig. 24; pers. obs.; Limnephilidae), as well as in Leptoceridae (Integripalpia-Brevitentoria; see App. 2). It is almost exclusively attached to the anterior tentorial arm in all other trichopteran lineages investigated (e.g., Polycentropodidae, Fig. 23B; Ptilocolepidae, Fig. 23E; Sericostomatidae; see App. 2).

M. tentorio-scapalis posterior is also

attached to the anterior tentorial arm in micropterigid lepidopterans (Hannemann 1956; pers. obs.) and in Mecoptera (e.g., Nannochoristidae, Beutel & Baum 2008; pers. obs.; Meropeidae, Friedrich et al. 2013).

20. Number of bundles of M. clypeo-epipharyngalis lateralis (cl-eph(l)) (v. Kéler 1955: M. 43; Wipfler et al. 2011: 0ci1): (0) one; (1) two with distinct insertion sites.

M. clypeo-epipharyngalis lateralis is composed of two bundles with distinctly separated insertion sites in the integripalpian lineage Limnephiloidea (e.g., Limnephilidae; Brachycentridae; and Goeridae). A compact, single bundle is present in all other trichopteran taxa investigated (e.g., Philopotamidae, Fig. 16; see Tab. 8).

The muscle is composed of a single bundle in micropterigid lepidopterans (Hannemann 1956; pers. obs.) and Nannochoristidae (Mecoptera; Beutel & Baum 2008; pers. obs.).

21. Number of bundles of M. clypeo-cibarialis dorsalis (cl-ci(d)) (v. Kéler 1955: M. 44; Wipfler et al. 2011: 0bu1): (0) one; (1) two; (2) three.

M. clypeo-cibarialis dorsalis consists of a single bundle in most representatives of ‘Spicipalpia’ (Tab. 8). It is composed of two distinct bundles in Annulipalpia (e.g., Philopotamidae, Fig. 20; Psychomyiidae) and in most lineages of Integripalpia (e.g., Phryganeidae; Molannidae; Tab. 8). In contrast, three bundles are present in the integripalpian families Limnephilidae, Brachycentridae, and Goeridae (= Limnephiloidea).

One bundle is present in the mecopteran family Nannochoristidae, as well as in the lepidopteran lineage Micropterigidae (App. 1).

22. Origin of M. clypeo-cibarialis dorsalis (cl-ci(d)) (v. Kéler 1955: M. 44; Wipfler et al. 2011: 0bu1): (0) exclusively at the median face of frontopostclypeus; (1) with at least one bundle at the gena above the sclerotized part of the mandible.

M. clypeo-cibarialis dorsalis originates exclusively from the frontopostclypeus in most lineages of Trichoptera (e.g., Philopotamidae, Fig. 15A; Rhyacophilidae; Sericostomatidae; see Tab. 8). The lateral bundle is attached to the anterior face of the gena directly above the sclerotized part of the mandible in representatives of the annulipalpian families Psychomyiidae and Polycentropodidae (Tab. 8).

It originates from the frons in Lepidoptera (e.g., Micropterigidae; Hannemann 1956; Kristensen 2003; pers. obs.) and Mecoptera (e.g., Nannochoristidae; Beutel & Baum 2008; pers. obs.).

23. Size of M. cranio-pharyngalis anterior (cr-ph(a)) (v. Kéler 1955: M. 51; Wipfler et al. 2011: 0ph1): (0) extremely thin, exclusively composed of a single fiber; (1) well-developed, composed of several bundles (at least in its proximal half).

M. cranio-pharyngalis anterior is strongly developed in ‘Spicipalpia’ (e.g., Rhyacophilidae, Klemm 1966: 20, fig. 9; pers. obs.) and Integripalpia (e.g., Phryganeidae, Crichton 1957: 61, fig. 26; pers. obs.). It is very thin and composed of a single fiber in all annulipalpians investigated (e.g., Philopotamidae, Fig. 18A; Hydropsychidae).

It is also well-developed and composed of at least two fibers in 'basal' lepidopterans (e.g., Micropterigidae, Hannemann 1956; pers. obs.). M. cranio-pharyngalis anterior is also strongly developed in nannochoristid mecopterans (Beutel & Baum 2008: 350, fig. 5; pers. obs.).

24. M. tentorio-mandibularis (te-md) (v. Kéler 1955: M. 14; Wipfler et al. 2011: 0md6): (0) present; (1) absent.

M. tentorio-mandibularis is present in Annulipalpia (e.g., Philopotamidae, Fig. 19E; Polycentropodidae), and most spicipalpian groups (e.g., Ptilocolepidae, Hydroptilidae, see App. 1). In contrast, it is absent in Integripalpia (App. 1).

The presence of this muscle is a ground plan feature of Lepidoptera (Kristensen 2003: 49) and Mecoptera (Beutel & Baum 2008; Friedrich et al. 2013).

25. M. cranio-pharyngalis posterior (cr-ph(p)) (v. Kéler 1955: M. 51/53 (?); Wipfler et al. 2011: 0ph1/0ph3 (?)): (0) present; (1) absent.

M. cranio-pharyngalis posterior is present in most spicipalpian lineages (e.g., Rhyacophilidae, Klemm 1966: 20, fig. 9; pers. obs.; Hydrobiosidae; Glossosomatidae; and Ptilocolepidae), and in the annulipalpian family Polycentropodidae. It is absent in all other trichopteran lineages investigated so far (see Tab. 9).

The muscle is well-developed in Lepidoptera (e.g., Micropterigidae, Hannemann 1956; Kristensen 2003; pers. obs.) and Mecoptera (Nannochoristidae, Beutel & Baum 2008; pers. obs.; Meropeidae, Friedrich et al. 2013).

26. M. cranio-stipitalis (cr-st) (v. Kéler 1955: M. 16; Wipfler et al. 2011: 0mx1): (0) present; (1) absent.

M. cranio-stipitalis is present in Annulipalpia (e.g., Philopotamidae, Fig. 18E, and Polycentropodidae; Tab. 10). It is absent in all other lineages of Trichoptera investigated so far (see Tab. 10).

The muscle is well-developed in some lineages of Lepidoptera (e.g., Micropterigidae, Hannemann 1956: 191, fig. 13; Kristensen 2003; pers. obs.), but absent in Mecoptera (Beutel & Baum; Friedrich et al. 2013; pers. obs.).

27. M. cranio-cardinalis (cr-cd) (v. Kéler 1955: M. 15; Wipfler et al. 2011: 0mx1): (0) present; (1) absent.

M. cranio-cardinalis is absent in the integripalpian family Phryganeidae. The muscle is present in all other trichopteran lineages investigated (e.g., Philopotamidae, Fig. 15B; Rhyacophilidae, Klemm 1966: 16, fig. 7; pers. obs.; Limnephilidae; see App. 5).

It is also present in Lepidoptera (e.g., Micropterigidae, Hannemann 1956; pers. obs.), but absent in Mecoptera (Beutel & Baum 2008; Friedrich et al. 2013; pers. obs.).

28. M. stipito-lacinialis (st-lc) (v. Kéler 1955: M. 20; Wipfler et al. 2011: 0mx6): (0) present; (1) absent.

M. stipito-lacinialis is present in all spicipalpian lineages and in Integripalpia-Plenitentoria (e.g., Phryganeidae, Crichton 1957: 61, 62, figs. 26, 27; pers. obs.; Goeridae; see Tab. 10). It is absent in Annulipalpia and in Integripalpia-Brevitentoria (e.g., Sericostomatidae; see Tab. 10).

M. stipito-lacinialis is present in the

lepidopteran groundplan (see Kristensen 2003). It is absent in Mecoptera (e.g., Nannochoristidae, Beutel & Baum 2008; pers. obs.; Meropeidae, Friedrich et al. 2013).

29. **Galea and lacinia: (0) lacinia present as small, distinctly separated structure; (1) lacinia and galea inseparable (forming galeolacinia).**

A distinct, small and heavily sclerotized lacinial lobe is attached to the large and mainly membranous galea in Annulipalpia (e.g., Philopotamidae, Fig. 12B), 'Spicipalpia' (e.g., Rhyacophilidae, Klemm 1966; pers. obs.; Glossosomatidae, Durand 1955; pers. obs.), and the integripalpian lineage Plenitentoria (e.g., Limnephilidae). The lacinia forms a small sclerotized crest on the mesal wall of the galea in Integripalpia-Brevitentoria (e.g., Leptoceridae).

The maxillary endite lobe of Lepidoptera is composed of a small, but distinct lacinia and a much larger galea in the non-glossatan groups (see Kristensen 2003). Lacinia and galea are well separated structures in most mecopterans (e.g., Meropeidae, Friedrich et al. 2013).

30. **Presence of longitudinal channels on the anterior surface of the haustellum: (0) absent; (1) present.**

A system of longitudinal channels formed by a regular arrangement of the haustellar microtrichia is present in Integripalpia (see e.g., Crichton 1957, 1989, 1992: 46, fig. 3; Chaudonneret 1990: 78, figs. 172, 179; Engvall 1993; pers. obs. [see Fig. 24]), and in the annulipalpian family Polycentropodidae (Engvall 1993). The haustellum is completely granulose without a regular system of longitudinal channels in the remaining annulipalpian representatives (e.g., *Philopotamus* [Philopotamidae], see Fig. 10B), and all spicipalpian families (Crichton 1957; Engvall 1993; pers. obs.).

31. **Presence of transverse line on the anterior surface of the haustellum: (0) present; (1) absent.**

A transverse line, i.e., a transition zone of different shaped/orientated types of microtrichia, is present in the annulipalpian lineage Polycentropodidae (e.g., *Plectrocnemia*, Engvall 1993), the spicipalpian family Rhyacophilidae (e.g., *Rhyacophila*), and in Integripalpia (Fig. 26; see also Engvall 1993). Such a line is absent in most spicipalpian (e.g., Glossosomatidae) and annulipalpian lineages. It is also absent in *Philopotamus* (Fig. 10B), but present in the philopotamid genus *Sortosa* (Engvall 1993).

32. **Shape of microtrichia along the transverse line: (0) different types; (1) microtrichia of same type, but with opposing orientation.**

A transverse transition zone from multi-branched to leaf-like shaped microtrichia is present in a few annulipalpian species (e.g., *Sortosa* [Philopotamidae], Engvall 1993: fig. 47) and the spicipalpian family Rhyacophilidae (Engvall 1993: fig. 39; pers. obs.). In contrast, it is formed by microtrichia of the same type (multi-branched) but with opposing orientation (V-line after Engvall 1993) in all Integripalpia (e.g., Leptoceridae, Engvall 1993: fig. 60; pers. obs.; Phryganeidae, Crichton 1957: 51, fig. 5; pers. obs.) and the annulipalpian taxon Polycentropodidae (e.g., *Plectrocnemia*, Engvall 1993). A transverse line of convergence is absent in most other Annulipalpia (e.g., *Philopotamus* [Philopotamidae], see Fig. 10), and 'Spicipalpia' (Engvall 1993).

33. **Salivary pleat on the distal surface of the haustellum: (0) absent; (1) present.**

    The salivary orifice is covered by a dorsal fold of the anterior haustellar wall in Integripalpia (e.g., Limnephilidae, Fig. 26; Engvall 1993). The orifice is not covered by cuticular outgrowths in Annulipalpia (e.g., Philopotamidae, Fig. 10B) and all spicipalpian groups (e.g., Rhyacophilidae; see Engvall 1993).

34. **M. hypopharyngo-salivarialis (hy-sa) (v. Kéler: M. 37; Wipfler et al. 2011: 0hy12): (0) interconnecting hypopharynx and salivarium; (1) forming sphincter of salivarium; (2) absent.**

    The muscle is attached to the hypopharynx in Philopotamidae (Fig. 19I). In contrast, a strongly developed and compact muscle specifically enclosing the roof of the distal part of the salivary tube ("Sekretformer" of Heddergott 1938) is present in Rhyacophilidae and Phryganeidae. The muscle is absent in the spicipalpian lineages Hydrobiosidae, Glossosomatidae, Ptilocolepidae, and Hydroptilidae (see Tab. 11).

    M. hypopharyngo-salivarialis is also attached to the hypopharynx in the mecopteran family Nannochoristidae (Beutel & Baum 2008; pers. obs.), in Lepidoptera (Micropterigidae, Kristensen 2003; pers. obs.), Siphonaptera (Wenk 1953), and most other holometabolan lineages (e.g., Röber 1942; Beutel & Vilhelmsen 2007; Schneeberg & Beutel 2011). It is enclosing the roof of the distal part of the salivary tube in the mecopteran families Panorpidae (Heddergott 1938), Meropeidae (Friedrich et al. 2013), Bittacidae, and Boreidae (Beutel et al. 2008).

35. **Mandibles: (0) moderately sized and sclerotized; (1) vestigial and mainly membranous.**

    The adult mandibles are comparatively large and moderately sclerotized in Annulipalpia (e.g., Philopotamidae, Fig. 4) and all spicipalpian lineages (e.g., Rhyacophilidae; Klemm 1966: 10, fig. 5; pers. obs.). Mandibles are vestigial and completely membranous in Integripalpia (e.g., Phryganeidae, Crichton 1957: 51, fig. 4; pers. obs.).

    Well developed and heavily sclerotized mandibles are present in non-glossatan moths (e.g., Micropterigidae, Hannemann 1956; Kristensen 2003) and in Mecoptera (Beutel & Baum 2008; Friedrich et al. 2013).

3.4.2. Pupal head characters

36. **Number of mandibular subapical teeth: (0) two; (1) three; (2) one; (3) four; (4) absent.**

    Three subapical teeth are present on the mandibles of Philopotamidae and Rhyacophilidae (Fig. 31A). Two subapical incisivi are present in the spicipalpian taxa Glossosomatidae (Fig. 31C), and Ptilocolepidae (e.g., *Ptilocolepus*, González et al. 2000). Four subapical incisivi are present in Hydropsychidae, (Fig. 31B; Cowley 1976). In contrast, subapical teeth are absent in the integripalpian lineages (e.g., Limnephilidae, Fig. 29B; Goeridae, Fig. 31D).

    Pupal mandibles are remarkably reduced in the micropterigid lepidopterans

(Kristensen 2003). In contrast, two subapical incisivi are present in the non-glossatan lepidopteran family Eriocraniidae (Busck & Böving 1914; Hinton 1946). Furthermore, two subapical incisivi are also present in Megaloptera (e.g., Hinton 1946: 286, fig. 4).

37. **Shape of pupal mandible: (0) elongated and falciform; (1) short and stout.**

    The pupal mandibles are remarkably elongated and falciform in Annulipalpia (e.g., Philopotamidae, Figs. 27; 31A; Hydropsychidae, Fig. 31B) and in all spicipalpian lineages (Rhyacophilidae, Figs. 29A, 31C; see also Hinton 1946; González et al. 2000). They are comparatively short and stout in integripalpian representatives (Limnephilidae, Fig. 29A).

3.5. Phylogenetic evaluation

3.5.1. Cladistic analyses of adult and pupal head characters

The analysis of the complete adult and pupal head data set (37 characters, 22 trichopteran ingroup taxa, 2 outgroup taxa) using Winclada software (heuristic search) yielded one parsimonious tree (91 steps, CI: 0.53, RI: 0.81; Fig. 32). The tree supports the monophyly of Annulipalpia, Integripalpia, a clade (Ptilocolepidae + Glossosomatidae) + (Hydroptilidae + Annulipalpia), and a clade Rhyacophilidae + (Hydrobiosidae + Integripalpia). Consequently, the monophyly of ‘Spicipalpia’ was not support. Apomorphies supporting clades are listed in the following (homoplasious changes in italics).

Trichoptera: 12.2. Laminatentorium strongly developed and heavily sclerotized (ACCTRAN optimization; reversal in Philopotamoidea and *Tinodes*); 34.2. M. hypopharyngo-salivarialis absent (reversal in Annulipalpia).

(*Ptilocolepus* + Glossosomatidae) + (Hydroptilidae + Annulipalpia): *9.1. Tentorium H-shaped (also in* Trichostegia *and* Rhyacophila*)*; *16.1. M. tentorio-scapalis lateralis composed of two bundles (also in* Pycnocentria *and* Limnephilus*)*; 17.1. Bundles of M. tentorio-scapalis lateralis originate separately on the head capsule and on the tentorium (ACCTRAN optimization; reversal in *Philopotamus*, *Hydropsyche*, and *Agapetus*).

***Ptilocolepus* + Glossosomatidae:** 36.0. Pupal mandible equipped with two subapical teeth (ACCTRAN optimization).

Hydroptilidae + Annulipalpia: *25.0. M. cranio-pharyngalis posterior absent (reversal in* Holocentropus*; also absent in Integripalpia).*

Annulipalpia: 4.1. 5th segment of maxillary palp distinctly elongated; 5.0. Integument of 5th maxillary palpomere with regular cuticular clefts, flexible; *6.0. Labium equipped with small endite labial lobes (also in* Rhyacophila*)*; *21.1. M. clypeo-cibarialis dorsalis composed of two bundles (also in* Agapetus*,* Hydrobiosis*, and Integripalpia)*; 23.0. M. cranio-pharyngalis anterior extremely thin, composed of a single fiber; *26.0. M. cranio-stipitalis present (also in* Micropterix*)*; *28.1. M. stipito-lacinialis absent (also in Brevitentoria)*; *34.0. M. hypopharyngo-salivarialis connecting hypopharynx and salivarium (reversal in Psychomyioidea and Integripalpia; also in* Nannochorista *and* Micropterix*).*

Philopotamoidea: *12.0. Laminatentorium small and weakly sclerotized (also in* Tinodes*,* Molanna*,* Sericostoma*, and* Pycnocentria*).*

Hydropsychoidea: 15.1. M. tentorio-scapalis medialis composed of two bundles.

Psychomyioidea: 22.1. M. clypeo-cibarialis dorsalis originates with one bundle at the anterior face of the gena above the non-sclerotized area of the adult mandible; *34.1. M. hypopharyngo-salivarialis forming sphincter of salivarium (also in Integripalpia)*.

Rhyacophilidae + (‘Hydrobiosidae’ + Integripalpia): 11.2. Dorsal tentorial arm not continuous with head capsule; *13.2. M. tentorio-scapalis anterior composed of two bundles (also in* Holocentropus *and Glossosomatidae)*; *19.1. M. tentorio-scapalis posterior originates exclusively from the dorsal tentorial arm (also in* Stenopsyche*; reversal in* Molanna*,* Sericostoma*, and* Pycnocentria*)*.

‘**Hydrobiosidae**’ **+ Integripalpia:** *8.2. Origin of antennifer at ventrolateral margin of circumantennal sulcus (also in* Nannochorista*)*; 24.1. M. tentorio-mandibularis absent.

Integripalpia: *8.2. Origin of antennifer at lateral margin of circumantennal sulcus (DELTRAN optimization)*; 12.1. Laminatentorium small but strongly sclerotized (reversal in *Molanna*, *Sericostoma*, and *Pycnocentria*); 13.2. M. tentorio-scapalis anterior composed of three bundles; *25.0. M. cranio-pharyngalis posterior absent (also in Hydroptilidae and Annulipalpia; reversal in* Holocentropus*)*; *30.1. Longitudinal channels on the anterior surface of haustellum present (also in* Holocentropus*)*; *31.1. Transverse line on the anterior surface of the haustellum present (also in* Rhyacophila *and* Holocentropus*)*; 33.1. Salivary pleat covering the salivary orifice; *34.1. M. hypopharyngo-salivarialis forming sphincter of salivarium (also in* Tinodes *and* Holocentropus*)*; *35.1. Adult mandible vestigial (also in Hydroptilidae)*; 37.1. Pupal mandible small and stout (DELTRAN optimization).

Brevitentoria: *1.1. Ocelli absent (also in Hydroptilidae, Hydropsychoidea,* Brachycentrus*, and* Silo*)*; *28.1. M. stipito-lacinialis absent (also in Annulipalpia)*; 29.1. Lacinia and galea completely inseparable.

Plenitentoria: *2.1. Number of maxillary palpomeres reduced in males (also in* Sericostoma *and* Pycnocentria*)*; *7.1. Anteclypeolabrum remarkably elongated ventrally (also in* Nannochorista*)*; *11.2. Dorsal tentorial arm well-developed and continuous with head capsule (ACCTRAN optimization; also in* Nannochorista*)*.

Phryganeoidea: 3.1. maxillary palp in males 4-segmented; *27.1. M. cranio-cardinalis absent (also in* Nannochorista*)*.

Limnephiloidea: *3.1. maxillary palp in males 3-segmented (also in* Sericostoma*)*; 20.1. M. clypeo-epipharyngalis lateralis composed of two bundles; 21.2. M. clypeo-cibarialis dorsalis composed of three bundles.

In a second analysis the outgroup taxon *Nannochorista* was excluded from the analysis in oder to evaluate the impact of mecopteran head features on the analysis. The analysis of the reduced data set yielded 13 equally parsimonious trees (86 steps, CI: 0.56, RI: 0.82; Fig. 33).

Apomorphies supporting clades are listed in the following (homoplasious changes in italics).

Annulipalpia: 4.1. 5th segment of maxillary palp distinctly elongated; 5.0. Integument of 5th maxillary palpomere with regular cuticular clefts, flexible; *21.1. M. clypeo-cibarialis dorsalis composed of two bundles (also in* Agapetus*,* Hydrobiosis*, and Integripalpia)*; 23.0. M. cranio-pharyngalis anterior extremely

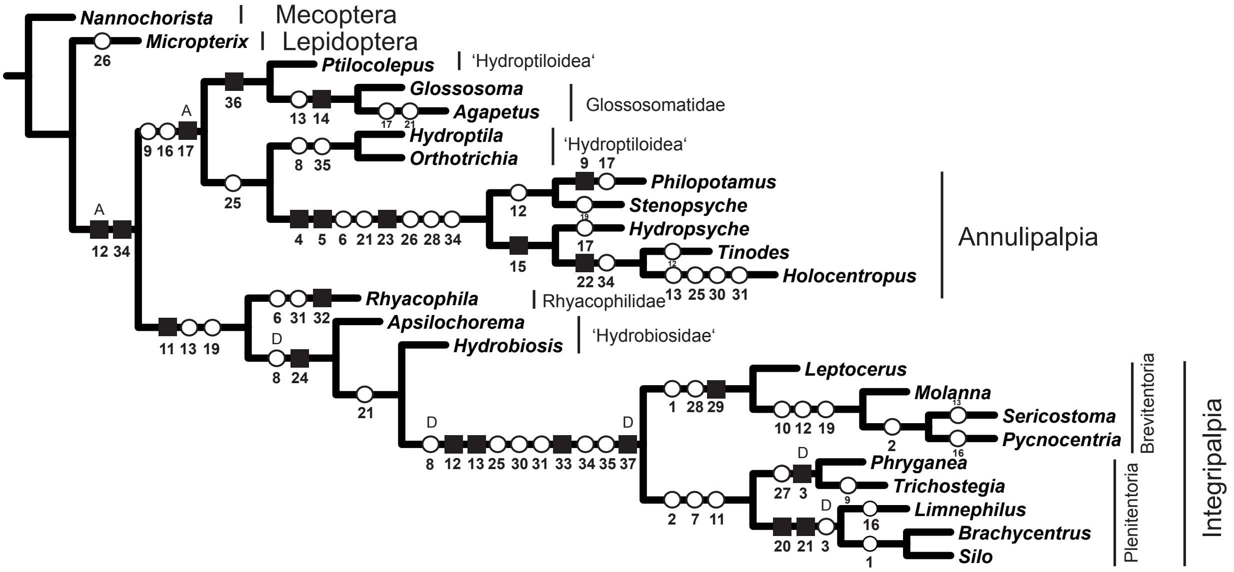

Figure 32: Phylogenetic tree (91 steps, CI = 0.53) obtained in the analysis of the adult and pupal head character data set using Winclada (heuristic search, multiple TBR + TBR, 1000 replicates). Apomorphies mapped on branches, non-homoplasious changes full quadrangles. Apomorphies yielded with ACCTRAN and/or DELTRAN optimization labelled as A/D, respectively.

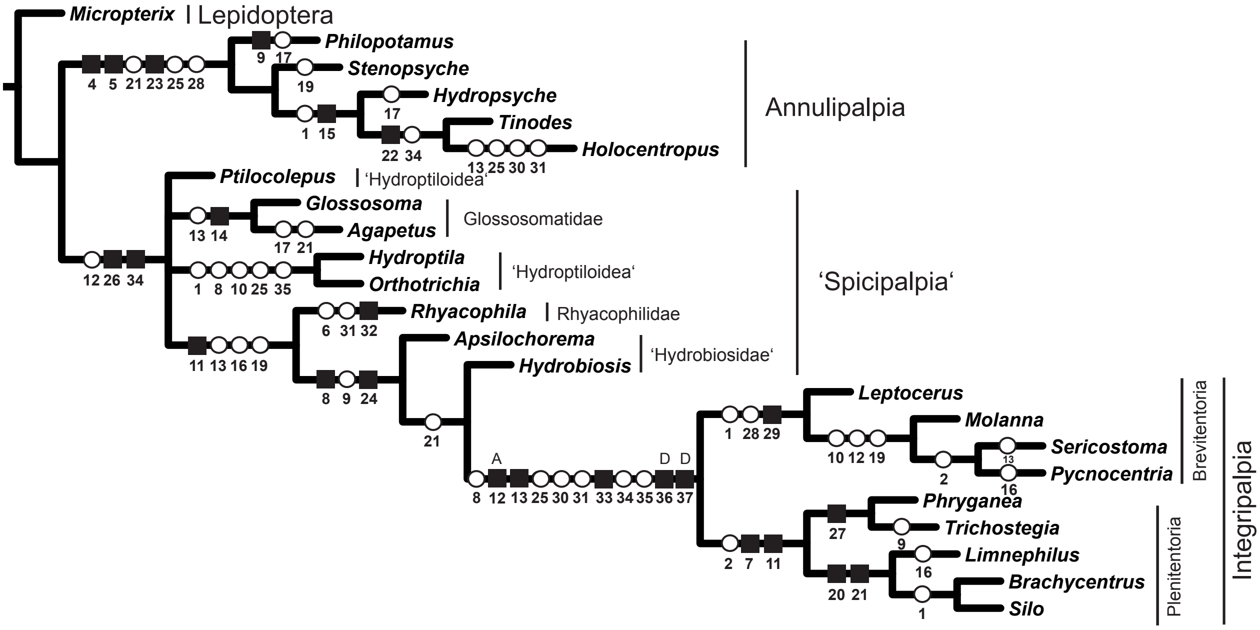

Figure 33: Majority-rule consensus tree for 13 minimum-length trees (86 steps, CI = 0.56) obtained in the analysis of the adult and pupal head character data set using Winclada software (heuristic search, multiple TBR + TBR, 1000 replicates). Apomorphies mapped on branches, non-homoplasious changes full quadrangles. Apomorphies yielded with ACCTRAN and/or DELTRAN optimization labelled as A/D, respectively.

thin, composed of a single fiber; *25.0. M. cranio-pharyngalis posterior absent (also in Hydroptilidae and Integripalpia; reversal in* Holocentropus*)*; *28.1. M. stipito-lacinialis absent (also in Brevitentoria)*.

Hydropsychoidea: *1.1. Ocelli absent (also in Hydroptilidae, Brevitentoria,* Brachycentrus*, and* Silo*)*; 15.1. M. tentorio-scapalis medialis composed of two bundles.

Psychomyioidea: 22.1. M. clypeo-cibarialis dorsalis originates with one bundle at the anterior face of the gena above the non-sclerotized area of the adult mandible; *34.1. M. hypopharyngo-salivarialis forming sphincter of salivarium (also in Integripalpia)*.

***Ptilocolepus* + Glossosomatidae + ‘Hydroptilidae’ + (Rhyacophilidae + [‘Hydrobiosidae’ + Integripalpia]):** *12.2. Laminatentorium strongly developed and heavily sclerotized (reversal in Brevitentoria; also in* Hydropsyche *and* Holocentropus*)*; 26.0. M. cranio-stipitalis absent; 34.2. M. hypopharyngo-salivarialis absent.

Rhyacophilidae + (‘Hydrobiosidae’ + Integripalpia): 11.2. Dorsal tentorial arm not continuous with head capsule; *13.2. M. tentorio-scapalis anterior composed of two bundles (also in* Holocentropus *and Glossosomatidae)*; *16.1. M. tentorio-scapalis lateralis composed of one bundles (also in* Micropterix*; reversal in* Pycnocentria *and* Limnephilus*)*; *19.1. M. tentorio-scapalis posterior originates exclusively from the dorsal tentorial arm (also in* Stenopsyche*; reversal in* Molanna*,* Sericostoma*, and* Pycnocentria*)*.

‘Hydrobiosidae’ + Integripalpia: 8.2. Origin of antennifer at ventrolateral margin of circumantennal sulcus; *9.0. Tentorium Π-shaped (reversal in* Trichostegia*)*; 24.1. M. tentorio-mandibularis absent.

Integripalpia: *8.2. Origin of antennifer at lateral margin of circumantennal sulcus (also in Hydroptilidae)*; 12.1. Laminatentorium small, but strongly sclerotized (ACCTRAN optimization; reversal in *Molanna*, *Sericostoma*, and *Pycnocentria*); 13.2. M. tentorio-scapalis anterior composed of three bundles; *25.0. M. cranio-pharyngalis posterior absent (also in Hydroptilidae and Annulipalpia; reversal in* Holocentropus*)*; *30.1. Longitudinal channels on the anterior surface of haustellum present (also in* Holocentropus*)*; *31.1. Transverse line on the anterior surface of the haustellum present (also in* Rhyacophila *and* Holocentropus*)*; 33.1. Salivary pleat covering the salivary orifice; *34.1. M. hypopharyngo-salivarialis forming sphincter of salivarium (also in* Tinodes *and* Holocentropus*)*; *35.1. Adult mandible vestigial (also in Hydroptilidae)*; 36.0. Pupal mandible without subapical teeth (DELTRAN optimization); 37.1. Pupal mandible small and stout (DELTRAN optimization).

Brevitentoria: *1.1. Ocelli absent (also in Hydroptilidae, Hydropsychoidea,* Brachycentrus*, and* Silo*)*; *28.1. M. stipito-lacinialis absent (also in Annulipalpia)*; 29.1. Lacinia and galea completely inseparable.

Plenitentoria: *2.1. Number of maxillary palpomeres reduced in males (also in* Sericostoma *and* Pycnocentria*)*; 7.1. Anteclypeolabrum remarkably elongated ventrally; 11.2. Dorsal tentorial arm well-developed and continuous with head capsule.

Phryganeoidea: 27.1. M. cranio-cardinalis absent.

Limnephiloidea: 20.1. M. clypeo-epipharyngalis lateralis composed of two bundles; 21.2. M. clypeo-cibarialis dorsalis composed of three bundles.

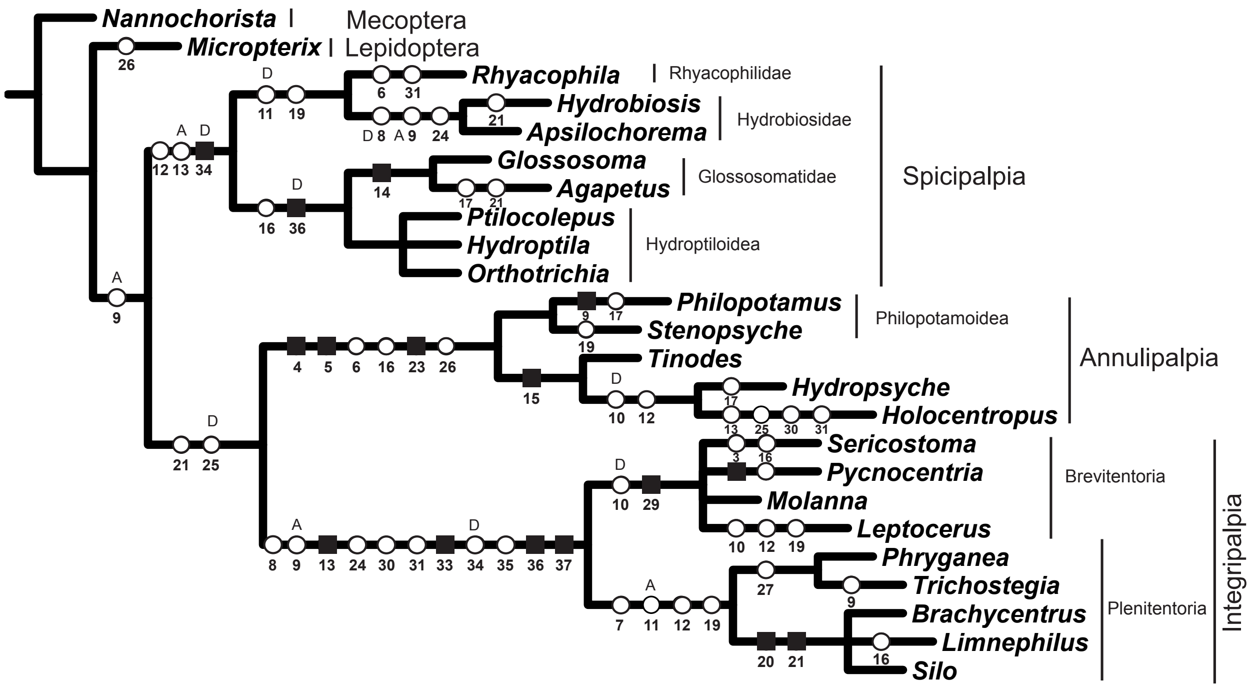

Figure 34: Topology after Wiggins & Wichard (1989: 273, fig. 19). Mapping of the morphological data set in Winclada yielded a tree length of 100 steps (CI = 0.47). Apomorphies mapped on branches, non-homoplasious changes full quadrangles. Apomorphies yielded with ACCTRAN and/or DELTRAN optimization labelled as A/D, respectively.

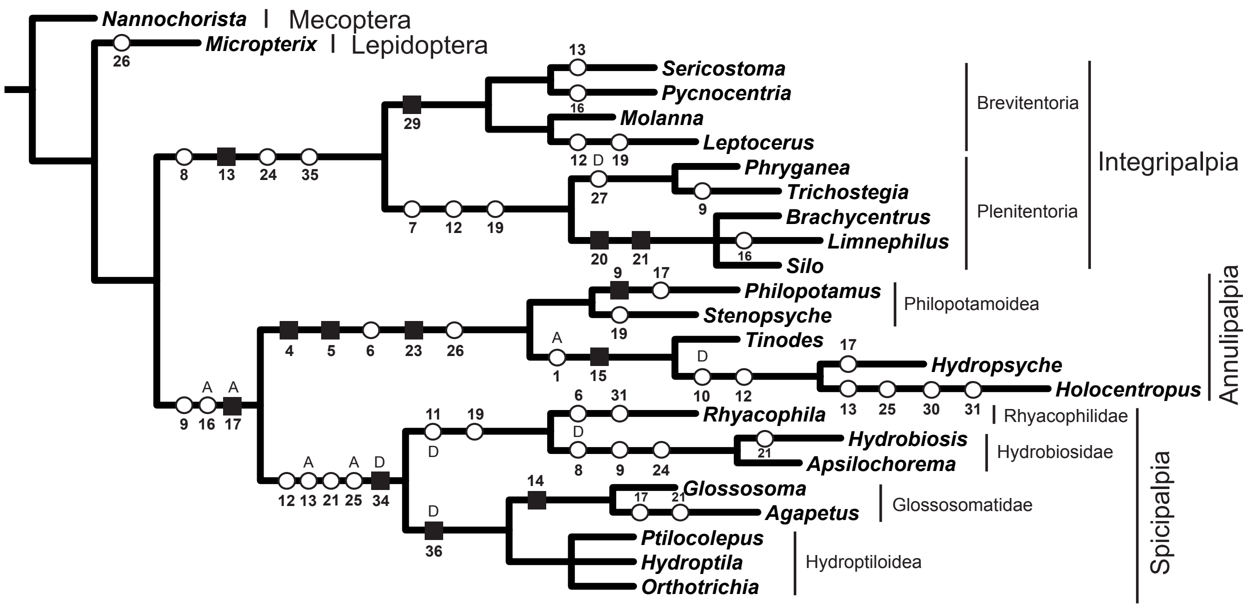

Figure 35: Topology after Weaver & Morse (1986: 154, fig. 3). Mapping of the morphological data set in Winclada yielded a tree length of 103 steps (CI = 0.47). Apomorphies mapped on branches, non-homoplasious changes full quadrangles. Apomorphies yielded with ACCTRAN and/or DELTRAN optimization labelled as A/D, respectively.

3.5.2. Character mapping on phylogenetic hypotheses

The previously defined 37 morphological characters of the adult and pupal head (see above [3.4.]) were interpreted by mapping on eight major phylogenetic hypotheses published during the last decades (Fig. 3; Ross 1967; Weaver & Morse 1986; Wiggins & Wichard 1989; Schmid 1989; Frania & Wiggins 1997; Kjer et al. 2002, 2016; Malm et al. 2013).

In the following quantitative criteria (e.g., tree length, consistency index = CI, retention index = RI) characterizing the data fitting of adult and pupal head characters are provided for each phylogenetic hypothesis. Apomorphies supporting clades are also listed (homoplasious changes in italics) for each topology.

(I) Monophyletic Spicipalpia form the sister group of a clade comprising Annulipalpia and Integripalpia

(Fig. 34; after Wiggins & Wichard 1989)

Number of steps required by mapping morphological characters: 100 (CI: 0.47, RI: 0.76).

Trichoptera: *9.0. Tentorium Π-shaped (ACCTRAN optimization; also in* Trichostegia*; reversal in Hydrobiosidae and Integripalpia).*

Spicipalpia: *12.2. Laminatentorium strongly developed and heavily sclerotized (also in Hydropsychidae and Polycentropodidae)*; *13.2. M. tentorio-scapalis anterior composed of two bundles (ACCTRAN optimization; also in* Holocentropus*; reversal in Hydroptiloidea)*; 34.2. M. hypopharyngo-salivarialis absent (DELTRAN optimization).

Rhyacophilidae + Hydrobiosidae: *11.2. Dorsal tentorial arm not continuous with head capsule (DELTRAN optimization; also in* Leptocerus*)*; *19.1. M. tentorio-scapalis posterior originates exclusively from the dorsal tentorial arm (also in Plenitentoria,* Leptocerus*, and* Stenopsyche*).*

Glossosomatidae + Hydroptiloidea: *16.1. M. tentorio-scapalis lateralis composed of two bundles (also in Annulipalpia,* Pycnocentria*, and* Limnephilus*)*; 36.0. Pupal mandible equipped with two subapical teeth (DELTRAN optimization).

Annulipalpia + Integripalpia: *21.1. M. clypeo-cibarialis dorsalis composed of two bundles (also in* Hydrobiosis*,* Agapetus*)*; *25.1. M. cranio-pharyngalis posterior absent (DELTRAN optimization; reversal in* Holocentropus*; also absent in Hydroptilidae).*

Annulipalpia: 4.1. 5th segment of maxillary palp distinctly elongated; 5.0. Integument of 5th maxillary palpomere with regular cuticular clefts, flexible; *6.0. Labium equipped with small endite labial lobes (also in* Rhyacophila*)*; *16.1. M. tentorio-scapalis lateralis composed of two bundles (also in Glossosomatidae + Hydroptiloidea,* Pycnocentria*, and* Limnephilus*)*; 23.0. M. cranio-pharyngalis anterior extremely thin, composed of a single fiber; *26.0. M. cranio-stipitalis present (also in* Micropterix*).*

Psychomyiidae + (Hydropsychidae + Polycentropodidae): 15.1. M. tentorio-scapalis medialis composed of two bundles.

Hydropsychidae + Polycentropodidae: *10.0. Dorsal tentorial arm absent (DELTRAN optimization; also in Hydroptilidae, Brevitentoria)*; *12.2. Laminatentorium strongly developed and heavily sclerotized (also in spicipalpian taxa).*

Integripalpia: *8.2. Origin of antennifer at*

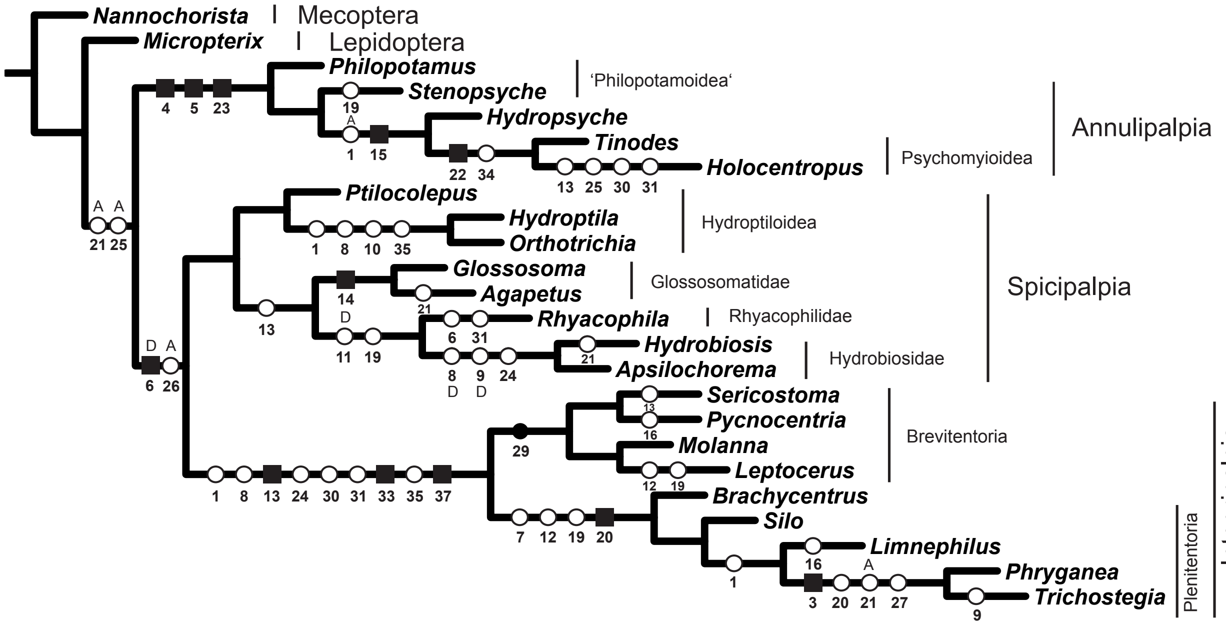

Figure 36: Topology after Kjer et al. (2002: 86, fig. 3). Mapping of the morphological data set in Winclada yielded a tree length of 101 steps (CI = 0.48). Apomorphies mapped on branches, non-homoplasious changes full quadrangles. Apomorphies yielded with ACCTRAN and/or DELTRAN optimization labelled as A/D, respectively.

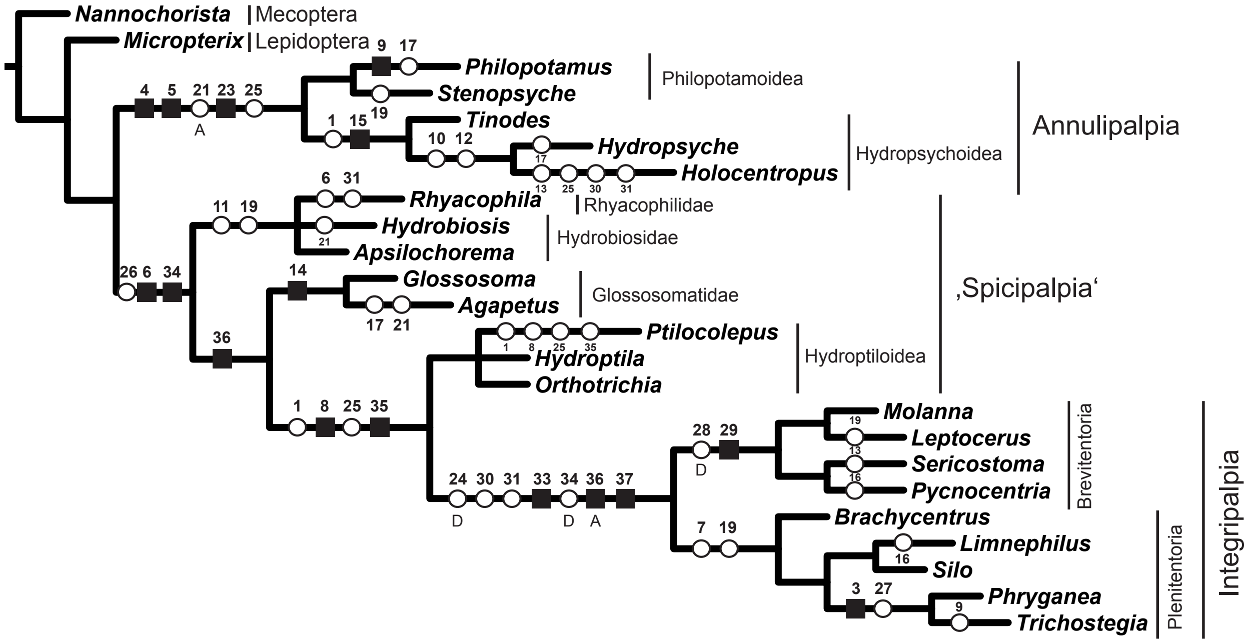

Figure 37: Topology after Ross (1967: 174, fig. 1). Mapping of the morphological data set in Winclada yielded a tree length of 107 steps (CI = 0.45). Apomorphies mapped on branches, non-homoplasious changes full quadrangles. Apomorphies yielded with ACCTRAN and/or DELTRAN optimization labelled as A/D, respectively.

lateral margin of circumantennal sulcus (also in Hydroptilidae); *9.0. Tentorium Π-shaped (ACCTRAN optimization; also in Hydrobiosidae)*; 13.2. M. tentorio-scapalis anterior composed of three bundles; *24.1. M. tentorio-mandibularis absent (also absent in Hydrobiosidae)*; *30.1. Longitudinal channels on the anterior surface of haustellum present (also in* Holocentropus*)*; *31.1. Transverse line on the anterior surface of the haustellum present (also in* Rhyacophila *and* Holocentropus*)*; 33.1. Salivary pleat covering the salivary orifice; *34.1. M. hypopharyngo-salivarialis forming sphincter of salivarium (DELTRAN optimization; also in* Tinodes *and* Holocentropus*)*; *35.1. Adult mandible vestigial (also in Hydroptilidae)*; 36.4. Subapical teeth of pupal mandible absent; 37.1. Pupal mandible small and stout.

Brevitentoria: *10.0. Dorsal tentorial arm absent (DELTRAN optimization; reversal in* Leptocerus*; also absent in Hydroptilidae,* Hydropsyche*, and* Holocentropus*)*; 29.1. Lacinia and galea completely inseparable.

Plenitentoria: *7.1. Anteclypeolabrum remarkably elongated ventrally (also in* Nannochorista*)*; *11.2. Dorsal tentorial arm well-developed and continuous with head capsule (ACCTRAN optimization; also in* Nannochorista*)*; *12.1. Laminatentorium comparatively small but strongly sclerotized (also in* Leptocerus*)*; *19.1. M. tentorio-scapalis posterior originates exclusively from the dorsal tentorial arm (also in* Leptocerus*,* Stenopsyche*, and Hydrobiosidae + Rhyacophilidae)*.

Phryganeoidea: *27.1. M. cranio-cardinalis absent (also in* Nannochorista*)*.

Limnephiloidea: 20.1. M. clypeo-epipharyngalis lateralis composed of two bundles; 21.2. M. clypeo-cibarialis dorsalis composed of three bundles.

(II) Monophyletic Spicipalpia and Annulipalpia form the sister group of Integripalpia

(Fig. 35; after Weaver & Morse 1986)

Number of steps required by mapping morphological characters: 103 (CI: 0.47, RI: 0.76).

Integripalpia: *8.2. Origin of antennifer at lateral margin of circumantennal sulcus (also in Hydroptilidae)*; 13.2. M. tentorio-scapalis anterior composed of three bundles (reversal in *Sericostoma*); *24.1. M. tentorio-mandibularis absent (also in Hydrobiosidae)*; *35.1. Adult mandible vestigial (also in Hydroptilidae)*.

Brevitentoria: 29.1. Lacinia and galea completely inseparable.

Plenitentoria: *7.1. Anteclypeolabrum remarkably elongated ventrally (also in* Nannochorista*)*; *12.1. Laminatentorium comparatively small, but strongly sclerotized (also in* Leptocerus*)*; *19.1. M. tentorio-scapalis posterior originates exclusively from the dorsal tentorial arm (also in* Leptocerus*,* Stenopsyche*, and Hydrobiosidae + Rhyacophilidae)*.

Limnephiloidea: 20.1. M. clypeo-epipharyngalis lateralis composed of two bundles; 21.2. M. clypeo-cibarialis dorsalis composed of three bundles.

Phryganeoidea: *27.1. M. cranio-cardinalis absent (DELTRAN optimization; also absent in* Nannochorista*)*.

Annulipalpia + Spicipalpia: *9.1. Tentorium H-shaped (also in* Trichostegia*; reversal in Hydrobiosidae)*; *16.1. M. tentorio-scapalis lateralis composed of two bundles (ACCTRAN optimization; also in* Pycnocentria*,* Limnephilus*; reversal in Rhyacophilidae + Hydrobiosidae)*; 17.1. Bundles of M. tentorio-scapalis lateralis originate separately on the head capsule and

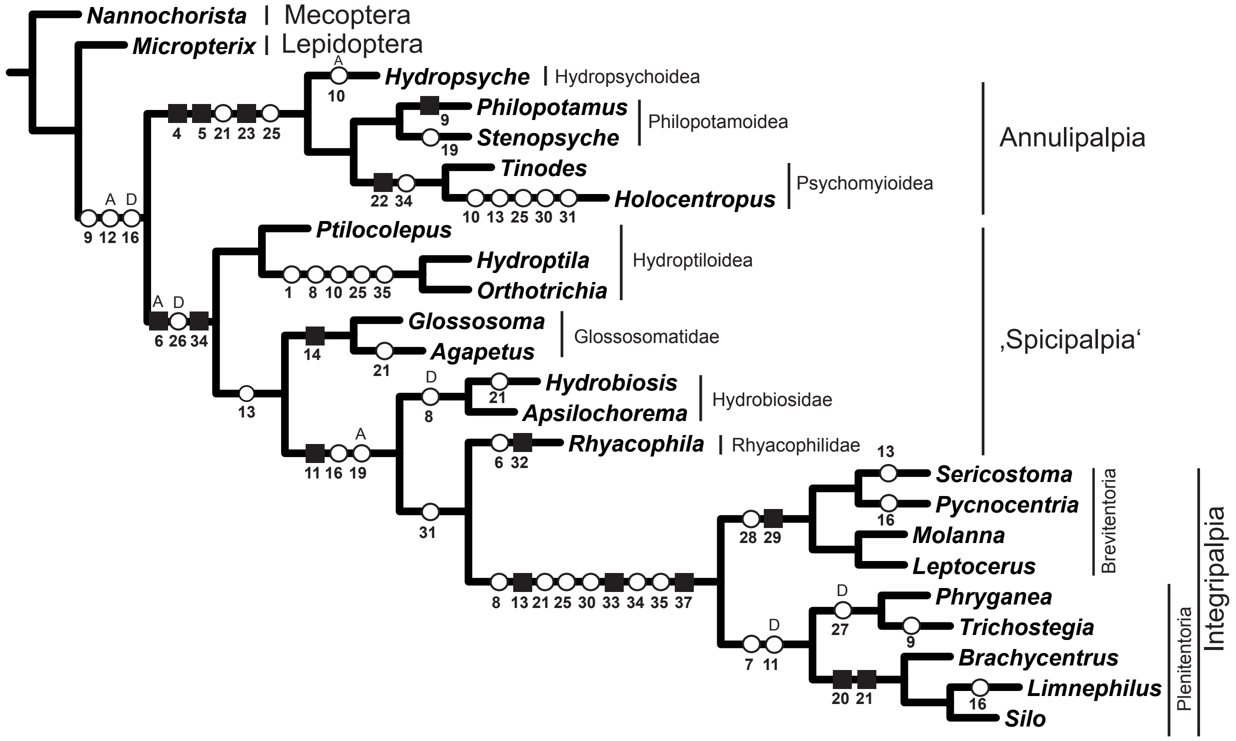

Figure 38: Topology after Kjer et al. (2016: 250, fig. 1) (RAxML analysis of combined DNA data). Mapping of the morphological data set in Winclada yielded a tree length of 100 steps (CI = 0.49). Apomorphies mapped on branches, non-homoplasious changes full quadrangles. Apomorphies yielded with ACCTRAN and/or DELTRAN optimization labelled as A/D, respectively.

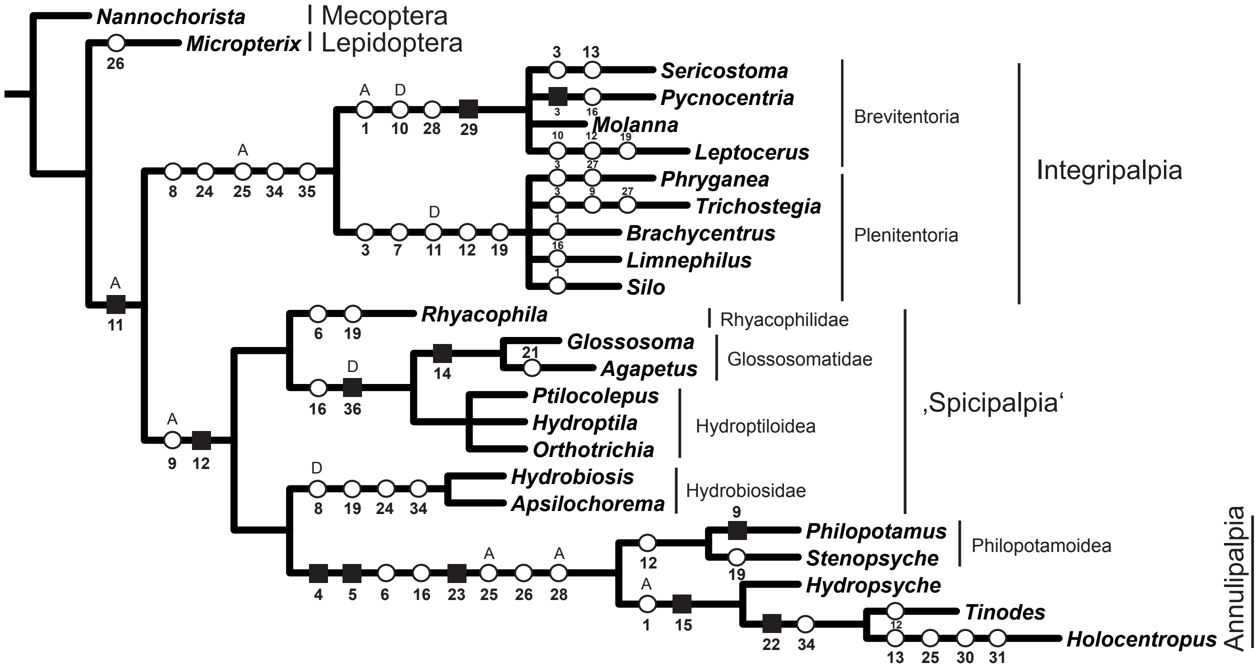

Figure 39: Topology after Schmid (1989: 23, fig. 33) (based on morphological features). Mapping of the morphological data set in Winclada yielded a tree length of 114 steps (CI = 0.42). Apomorphies mapped on branches, non-homoplasious changes full quadrangles. Apomorphies yielded with ACCTRAN and/or DELTRAN optimization labelled as A/D, respectively.

on the tentorium (ACCTRAN optimization; reversal in *Philopotamus*, *Hydropsyche*, and *Agapetus*).

Annulipalpia: 4.1. 5th segment of maxillary palp distinctly elongated; 5.0. Integument of 5th maxillary palpomere with regular cuticular clefts, flexible; *6.0. endite lobes of labium present (also in Rhyacophilidae)*; 23.0. M. cranio-pharyngalis anterior extremely thin, composed of a single fiber; *26.0. M. cranio-stipitalis present (also in* Micropterix*)*.

Hydropsychoidea (= Psychomyiidae + Hydropsychidae + Polycentropodidae): *1.1. Ocelli absent (ACCTRAN optimization; also in Integripalpia and Hydroptiloidea)*; 15.1. M. tentorio-scapalis medialis composed of two bundles.

Hydropsychidae + Polycentropodidae: *10.0. Dorsal tentorial arm absent (DELTRAN optimization; also absent in* Leptocerus*,* Pycnocentria*,* Molanna*, and Hydroptilidae)*; *12.2. Laminatentorium strongly developed and heavily sclerotized (also in Spicipalpia)*.

Spicipalpia: *12.2. Laminatentorium strongly developed and heavily sclerotized (also in Hydropsychidae and Polycentropodidae)*; *13.2. M. tentorio-scapalis anterior composed of two bundles (ACCTRAN optimization; also in* Holocentropus*; reversal in Hydroptiloidea)*; *25.0. M. cranio-pharyngalis posterior present (ACCTRAN optimization; also in* Holocentropus*; reversal in Hydroptilidae)*; 34.2. M. hypopharyngo-salivarialis absent (DELTRAN optimization).

Rhyacophilidae + Hydrobiosidae: *11.2. Dorsal tentorial arm not continuous with head capsule (DELTRAN optimization; also in* Leptocerus*)*; *19.1. M. tentorio-scapalis posterior originates exclusively from the dorsal tentorial arm (also in Plenitentoria,* Leptocerus*,* Stenopsyche*)*.

Glossosomatidae + Hydroptiloidea: 36.0. Pupal mandible equipped with two subapical teeth (DELTRAN optimization).

(III) Monophyletic Spicipalpia and Integripalpia form the sister group of Annulipalpia

(Fig. 36; after Kjer et al. 2002)

Number of steps required by mapping morphological characters: 101 (CI: 0.48, RI: 0.77).

Trichoptera: *21.1. M. clypeo-cibarialis dorsalis composed of two bundles (ACCTRAN optimization; reversal in Spicipalpia; also in* Agapetus*,* Hydrobiosis*)*; *25.1. M. cranio-pharyngalis posterior absent (ACCTRAN optimization; reversal in Spicipalpia and* Holocentropus*; also absent in Hydroptilidae)*.

Annulipalpia: 4.1. 5th segment of maxillary palp distinctly elongated; 5.0. Integument of 5th maxillary palpomere with regular cuticular clefts, flexible; 23.0. M. cranio-pharyngalis anterior extremely thin, composed of a single fiber.

Hydropsychoidea (= Hydropsychidae + Psychomyioidea): *1.1. Ocelli absent (ACCTRAN optimization; also in Integripalpia and Hydroptiloidea)*; 15.1. M. tentorio-scapalis medialis composed of two bundles.

Psychomyioidea: 22.1. M. clypeo-cibarialis dorsalis originates with one bundle at the anterior face of the gena above the non-sclerotized area of the adult mandible; *34.1. M. hypopharyngo-salivarialis forming sphincter of salivarium (also in Integripalpia)*.

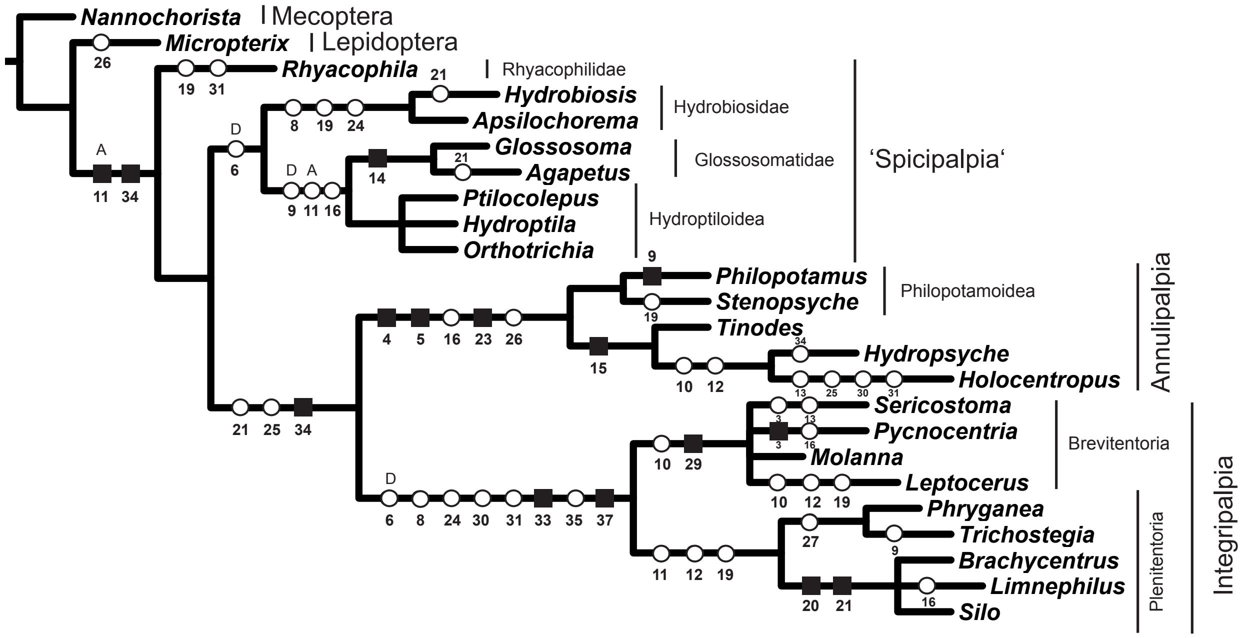

Figure 40: Topology after Malm et al. (2013: 8, fig. 4). Mapping of the morphological data set in Winclada yielded a tree length of 103 steps (CI = 0.44). Apomorphies mapped on branches, non-homoplasious changes full quadrangles. Apomorphies yielded with ACCTRAN and/or DELTRAN optimization labelled as A/D, respectively.

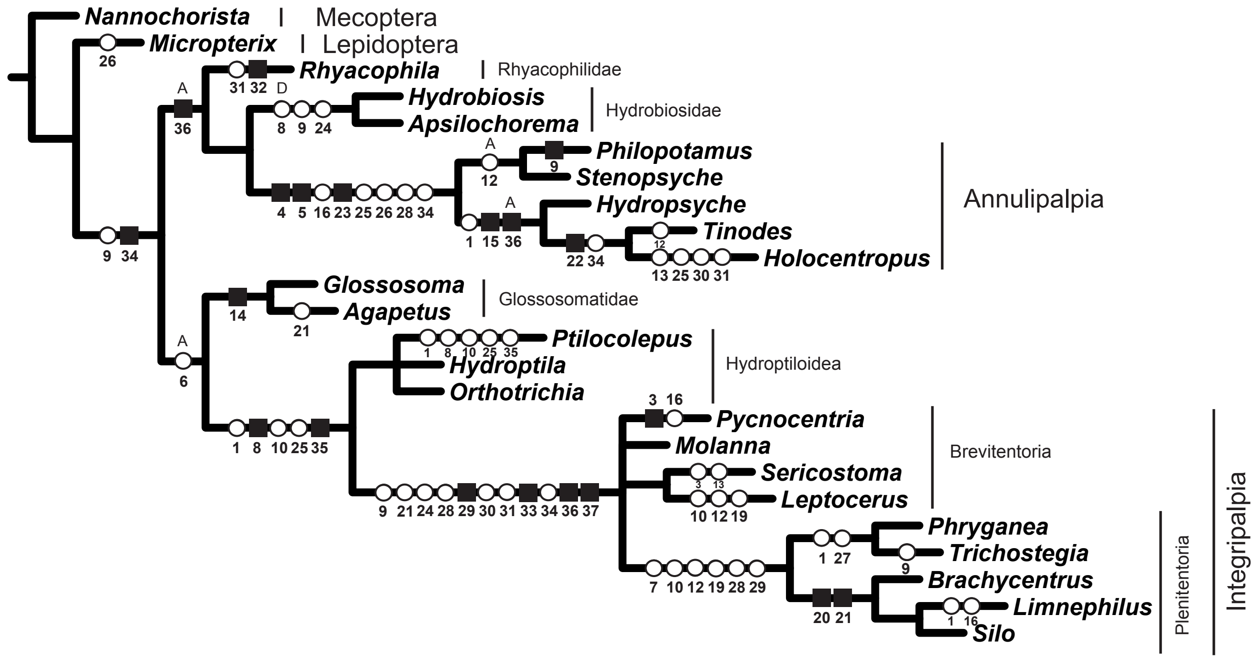

Figure 41: Topology after Frania & Wiggins (1997: fig. 24). Mapping of the morphological data set in Winclada yielded a tree length of 110 steps (CI = 0.44). Apomorphies mapped on branches, non-homoplasious changes full quadrangles. Apomorphies yielded with ACCTRAN and/or DELTRAN optimization labelled as A/D, respectively.

Spicipalpia + Integripalpia: 6.1. Endite lobes of labium absent (DELTRAN optimization; reversal in *Rhyacophila*); *26.1. M. cranio-stipitalis absent (ACCTRAN optimization; also in* Nannochorista*)*.

Glossosomatidae + (Rhyacophilidae + Hydrobiosidae): *13.1. M. tentorio-scapalis anterior composed of two bundles (also in* Holocentropus*)*.

Rhyacophilidae + Hydrobiosidae: *11.2. Dorsal tentorial arm not continuous with head capsule (DELTRAN optimization; also in* Leptocerus*)*; *19.1. M. tentorio-scapalis posterior originates exclusively from the dorsal tentorial arm (also in Plenitentoria,* Leptocerus*,* Stenopsyche*)*.

Integripalpia: *1.0. Ocelli absent (reversal in Limnephiloidea)*; *8.2. Origin of antennifer at lateral margin of circumantennal sulcus (also in Hydroptilidae)*; 13.2. M. tentorio-scapalis anterior composed of three bundles; *24.1. M. tentorio-mandibularis absent (also absent in Hydrobiosidae)*; *30.1. Longitudinal channels on the anterior surface of haustellum present (also in* Holocentropus*)*; *31.1. Transverse line on the anterior surface of the haustellum present (also in* Rhyacophila *and* Holocentropus*)*; 33.1. Salivary pleat covering the salivary orifice; *35.1. Adult mandible vestigial (also in Hydroptilidae)*; 37.1. Pupal mandible small and stout.

Brevitentoria: 29.1. Lacinia and galea completely inseparable.

Plenitentoria: *7.1. Anteclypeolabrum remarkably elongated ventrally (also in* Nannochorista*)*; *12.1. Laminatentorium comparatively small, but strongly sclerotized (also in* Leptocerus*)*; *19.1. M. tentorio-scapalis posterior originates exclusively from the dorsal tentorial arm (also in* Leptocerus*,* Stenopsyche*, and Hydrobiosidae + Rhyacophilidae)*; *20.1. M. clypeo-epipharyngalis lateralis composed of two bundles (reversal in Phryganeoidea)*.

Limnephilidae + Phryganeoidea: *1.0. Three ocelli present (also in Philopotamoidea, Spicipalpia)*.

Phryganeoidea: 3.1. maxillary palp in males 4-segmented; *20.0. M. clypeo-epipharyngalis lateralis composed of a single bundle (also in Annulipalpia, Spicipalpia, and Brevitentoria)*; *21.1. M. clypeo-cibarialis dorsalis composed of two bundles (ACCTRAN optimization; also in Annulipalpia,* Agapetus*,* Hydrobiosis*, Plenitentoria)*; *27.1. M. cranio-cardinalis absent (also absent in* Nannochorista*)*.

(IVa) Paraphyletic 'Spicipalpia' and Integripalpia form the sister group of Annulipalpia

(Fig. 37; after Ross 1967)

Number of steps required by mapping morphological characters: 107 (CI: 0.45, RI: 0.74).

Annulipalpia: 4.1. 5th segment of maxillary palp distinctly elongated; 5.0. Integument of 5th maxillary palpomere with regular cuticular clefts, flexible; *21.1. M. clypeo-cibarialis dorsalis composed of two bundles (ACCTRAN optimization; also in* Hydrobiosis*,* Agapetus*, and Integripalpia)*; 23.0. M. cranio-pharyngalis anterior extremely thin, composed of a single fiber; *25.1. M. cranio-pharyngalis posterior absent (reversal in* Holocentropus; *also absent in Hydroptilidae and Integripalpia)*.

Hydropsychoidea (= Psychomyiidae + [Hydropsychidae + Polycentropodidae]): *1.0. Ocelli absent (reversal in Hydroptilidae and Integripalpia)*; 15.1. M. tentorio-scapalis medialis composed of two bundles.

(Rhyacophilidae + ‘Hydrobiosidae‘) + (Glossosomatidae + [Hydroptiloidea + Integripalpia]): 6.1. Labial endite lobes absent (reversal in *Rhyacophila*); *26.1. M. cranio-stipitalis absent (also absent in* Nannochorista*)*; 34.2. M. hypopharyngo-salivarialis absent (reversal in Integripalpia).

Rhyacophilidae + ‘Hydrobiosidae‘: *11.2. Dorsal tentorial arm not continuous with head capsule (also in* Leptocerus*)*; *19.1. M. tentorio-scapalis posterior originates exclusively from the dorsal tentorial arm (also in Plenitentoria,* Leptocerus*,* Stenopsyche*)*.

Glossosomatidae + (Hydroptiloidea + Integripalpia): 36.0. Pupal mandible equipped with two subapical teeth.

Hydroptiloidea + Integripalpia: *1.1. Ocelli absent (also in Hydropsychoidea; reversal in* Ptilocolepus*, Phryganeoidea, and* Limnephilus*)*; 8.2. Origin of antennifer at lateral margin of circumantennal sulcus (reversal in *Ptilocolepus*); *25.1. M. cranio-pharyngalis posterior absent (also absent in Annulipalpia; reversal in* Ptilocolepus*)*; 35.1. Adult mandible vestigial (reversal in *Ptilocolepus*).

Integripalpia: *24.1. M. tentorio-mandibularis absent (DELTRAN optimization; also absent in Hydrobiosidae)*; *30.1. Longitudinal channels on the anterior surface of haustellum present (also in* Holocentropus*)*; *31.1. Transverse line on the anterior surface of the haustellum present (also in* Rhyacophila *and* Holocentropus*)*; 33.1. Salivary pleat covering the salivary orifice; *34.1. M. hypopharyngo-salivarialis forming sphincter of salivarium (also in* Tinodes *and* Holocentropus*)*; 36.0. Pupal mandible without subapical teeth; 37.1. Pupal mandible small and stout.

Brevitentoria: *28.1. M. stipito-lacinialis absent (also absent in Annulipalpia)*; 29.1. Lacinia and galea completely inseparable.

Plenitentoria: *7.1. Anteclypeolabrum remarkably elongated ventrally (also in* Nannochorista*)*; *19.1. M. tentorio-scapalis posterior originates exclusively from the dorsal tentorial arm (also in* Leptocerus*,* Rhyacophila*,* Stenopsyche*, and Hydrobiosidae)*.

Phryganeoidea: 3.1. Maxillary palp composed of four palpomeres in males; *27.1. M. cranio-cardinalis absent (DELTRAN optimization; also in* Nannochorista*)*.

(IVb) Paraphyletic ‘Spicipalpia’ and Integripalpia form the sister group of Annulipalpia

(Fig. 38; after Kjer et al. 2016)

Number of steps required by mapping morphological characters: 100 (CI: 0.49, RI: 0.77).

Trichoptera: *9.1. Tentorium H-shaped (reversal in Hydrobiosidae and Integripalpia*; *also in* Trichostegia*)*; *12.2. Laminatentorium massive and strongly developed (also in* Holocentropus*; reversal in Annulipalpia*, *Integripalpia)*; *16.2. M. tentorio-scapalis lateralis composed of two bundles (also in* Pycnocentria*,* Limnephilus*; reversal in Hydrobiosidae + (Rhyacophilidae + Integripalpia))*.

Annulipalpia: 4.1. 5th segment of maxillary palp distinctly elongated; 5.0. Integument of 5th maxillary palpomere with regular cuticular clefts, flexible; *21.1. M. clypeo-cibarialis dorsalis composed of two bundles (also in* Agapetus*,* Hydrobiosis*, and Integripalpia)*; 23.0. M. cranio-pharyngalis anterior extremely thin, composed of a single fiber; *25.1. M. cranio-pharyngalis posterior absent (reversal in* Holocentropus*)*.

Hydropsychoidea (= Hydropsychidae): *10.0. Dorsal tentorial arm absent (ACCTRAN* *optimization; also in* Holocentropus*, Hydroptilidae, and Brevitentoria)*.

Psychomyioidea (= Psychomyiidae + Polycentropodidae): 22.1. M. clypeo-cibarialis dorsalis originates with at least one bundle at the gena above the sclerotized area of the mandible; *34.1. M. hypopharyngo-salivarialis forming sphincter of salivarium (also in Integripalpia)*.

Hydroptiloidea + (Glossosomatidae + Hydrobiosidae + [Rhyacophilidae + Integripalpia]): 6.1. Labial endite lobes absent (ACCTRAN optimization; reversal in *Rhyacophila*); *26.1. M. cranio-stipitalis absent (DELTRAN optimization; also in* Nannochorista*)*; 34.2. M. hypopharyngo-salivarialis absent (reversal in Integripalpia).

Glossosomatidae + (Hydrobiosidae + [Rhyacophilidae + Integripalpia]): *13.1. M. tentorio-scapalis anterior composed of two bundles (reversal in Sericostomatidae; also in* Holocentropus*)*.

Hydrobiosidae + (Rhyacophilidae + Integripalpia): 11.1. Dorsal tentorial arm not continuous with head capsule; *16.0. M. tentorio-scapalis lateralis composed of one bundle (reversal in* Pycnocentria *and* Limnephilus*)*; *19.1. M. tentorio-scapalis posterior originates from the dorsal tentorial arm (ACCTRAN optimization; also in* Stenopsyche *and* Leptocerus*)*.

Rhyacophilidae + Integripalpia: *31.0. Transverse line on anterior surface of haustellum present (also in* Holocentropus*)*.

Integripalpia: *8.2. Origin of antennifer at lateral margin of circumantennal sulcus (also in Hydroptilidae)*; 13.2. M. tentorio-scapalis anterior composed of three bundles; *21.1. M. clypeo-cibarialis dorsalis composed of two bundles (also in Annulipalpia,* Agapetus*, and* Hydrobiosis*)*; *25.1. M. cranio-pharyngalis posterior absent (also in Annulipalpia and Hydroptilidae)*; *30.1. Longitudinal channels on the anterior surface of haustellum present (also in* Holocentropus*)*; 33.1. Salivary pleat covering the salivary orifice; *34.1. M. hypopharyngo-salivarialis forming sphincter of salivarium (also in Psychomyioidea)*; *35.1. Adult mandible vestigial (also in Hydroptilidae)*; 37.1. Pupal mandible small and stout.

Brevitentoria: *28.1. M. stipito-lacinialis absent (also in Annulipalpia)*; 29.1. Lacinia and galea completely inseparable.

Plenitentoria: *7.1. Anteclypeolabrum remarkably elongated ventrally (also in* Nannochorista*)*; *11.2. Dorsal tentorial arm well-developed and continuous with the head capsule (DELTRAN optimization; also in* Nannochorista*)*.

Limnephiloidea: 20.1. M. clypeo-epipharyngalis lateralis composed of two bundles; 21.2. M. clypeo-cibarialis dorsalis composed of three bundles.

Phryganeoidea: *27.1. M. cranio-cardinalis absent (DELTRAN optimization; also in* Nannochorista*)*.

(V) Paraphyletic ‘Spicipalpia’ and Annulipalpia form the sister group of Integripalpia

(Fig. 39; after Schmid 1989)

Number of steps required by mapping morphological characters: 114 (CI: 0.42, RI: 0.71).

Trichoptera: 11.1. Dorsal tentorial arm not continuous with the head capsule (reversal in (ACCTRAN optimization; Glossosomatidae + Hydroptiloidea), Annulipalpia).

Integripalpia: *8.2. Origin of antennifer at lateral margin of circumantennal sulcus (also in Hydroptilidae)*; *24.1. M. tentorio-mandibularis absent (also in Hydrobiosidae)*; *25.1. M. cranio-pharyngalis posterior absent (ACCTRAN optimization; also in Annulipalpia and Hydroptiloidea)*; *35.1. Adult mandible vestigial (also in Hydroptilidae)*; 37.1. Pupal mandible small and stout.

Brevitentoria: *1.0. Ocelli absent (ACCTRAN optimization; also in Hydroptiloidea and Hydropsychoidea + Psychomyioidea)*; *10.0. Dorsal tentorial arm absent (DELTRAN optimization; reversal in* Leptocerus*; also absent in* Hydroptila*,* Orthotrichia*,* Hydropsyche*, and* Holocentropus*)*; *28.1. M. stipito-lacinialis absent (also in Annulipalpia)*; 29.1. Lacinia and galea completely inseparable.

Plenitentoria: *3.2. Maxillary palp 3-segmented in males (also in* Sericostoma*)*; *7.1. Anteclypeolabrum remarkably elongated ventrally (also in* Nannochorista*)*; *11.2. Dorsal tentorial arm well-developed and continuous with the head capsule (DELTRAN optimization; also in* Nannochorista*)*; *12.1. Laminatentorium comparatively small, but strongly sclerotized (also in* Leptocerus*)*; *19.1. M. tentorio-scapalis posterior originates exclusively from the dorsal tentorial arm (also in* Leptocerus*,* Rhyacophila*,* Stenopsyche*, and Hydrobiosidae)*.

(Rhyacophilidae + [Glossosomatidae + Hydroptiloidea]) + (Hydrobiosidae + Annulipalpia): *9.1. Tentorium H-shaped (ACCTRAN optimization; also in* Trichostegia*; reversal in Hydrobiosidae)*; 12.2. Laminatentorium massive and strongly sclerotized (reversal in Philopotamoidea and Psychomyiidae).

Glossosomatidae + Hydroptiloidea: *16.1. M. tentorio-scapalis lateralis composed of two bundles (also in Annulipalpia,* Limnephilus*,* Pycnocentria*)*; 36.0. Pupal mandible equipped with two subapical teeth (DELTRAN optimization).

Annulipalpia: 4.1. 5th segment of maxillary palp distinctly elongated; 5.0. Integument of 5th maxillary palpomere with regular cuticular clefts, flexible; *6.0. endite lobes of labium present (also in Rhyacophilidae)*; *16.1. M. tentorio-scapalis lateralis composed of two bundles (also in (Glossosomatidae + Hydroptiloidea),* Limnephilus*,* Pycnocentria*)*; 23.0. M. cranio-pharyngalis anterior extremely thin, composed of a single fiber; *25.1. M. cranio-pharyngalis posterior absent (ACCTRAN optimization; reversal in* Holocentropus*; also in Integripalpia, Hydroptiloidea)*; *26.0. M. cranio-stipitalis present (also in* Micropterix*)*; *28.1. M. stipito-lacinialis absent (ACCTRAN optimization; also in Brevitentoria and* Nannochorista*)*.

Philopotamoidea: *12.0. Laminatentorium small and weakly sclerotized (also in* Tinodes *and Integripalpia)*.

Hydropsychoidea + Psychomyioidea: *1.1. Three ocelli absent (ACCTRAN optimization; also in Brevitentoria,* Brachycentrus*,* Silo*, and Hydroptiloidea)*; 15.1. M. tentorio-scapalis medialis composed of two bundles.

Psychomyioidea: 22.1. M. clypeo-cibarialis dorsalis originates with at least one bundle at the gena above the sclerotized area of the mandible; *34.1. M. hypopharyngo-salivarialis forming sphincter of salivarium (also in Integripalpia)*.

(VI) Paraphyletic 'Spicipalpia' as sister groups to a clade comprising Annulipalpia and Integripalpia

(Fig. 40; after Malm et al. 2013)

Number of steps required by mapping morphological characters: 103 (CI: 0.44, RI: 0.73).

Trichoptera: 11.1. Dorsal tentorial arm not continuous with the head capsule (reversal in (Glossosomatidae + Hydroptiloidea), Annulipalpia); 34.0. M. hypopharyngo-salivarialis absent.

Hydrobiosidae + (Glossosomatidae + Hydroptiloidea): *6.0. endite lobes of labium absent (DELTRAN optimization; also in Integripalpia)*.

Glossosomatidae + Hydroptiloidea: *9.1. Tentorium H-shaped (DELTRAN optimization; also in Rhyacophilidae, Annulipalpia, and* Trichostegia*);11.0. Dorsal tentorial arm vestigial (ACCTRAN optimization; also in Annulipalpia)*; *16.1. M. tentorio-scapalis lateralis composed of two bundles (also in Annulipalpia,* Limnephilus*,* Pycnocentria*)*.

Annulipalpia + Integripalpia: *21.2. M. clypeo-cibarialis dorsalis composed of two bundles (also in* Hydrobiosis *and* Agapetus*)*; *25.1. M. cranio-pharyngalis posterior absent (reversal in* Holocentropus*; also in Hydroptilidae)*; 34.0. M. hypopharyngo-salivarialis forming sphincter of salivarium (reversal in *Philopotamus* and *Hydropsyche*).

Annulipalpia: 4.1. 5th segment of maxillary palp distinctly elongated; 5.0. Integument of 5th maxillary palpomere with regular cuticular clefts, flexible; *16.1. M. tentorio-scapalis lateralis composed of two bundles (also in (Glossosomatidae + Hydroptiloidea),* Limnephilus*,* Pycnocentria*)*; 23.0. M. cranio-pharyngalis anterior extremely thin, composed of a single fiber; *26.0. M. cranio-stipitalis present (also in* Micropterix*)*.

Psychomyiidae + (Hydropsychidae + Polycentropodidae): 15.1. M. tentorio-scapalis medialis composed of two bundles.

Hydropsychidae + Polycentropodidae: *10.0. Dorsal tentorial arm absent (also absent in Hydroptilidae and Brevitentoria; reversal in* Leptocerus*)*; *12.0. Laminatentorium massive and strongly sclerotized (also in* spicipalpian taxa*)*.

Integripalpia: *6.0. endite lobes of labium absent (DELTRAN optimization; also in Glossosomatidae, Hydrobiosidae, and Hydroptiloidea)*; *8.2. Origin of antennifer at lateral margin of circumantennal sulcus (also in Hydroptilidae)*; *24.1. M. tentorio-mandibularis absent (also in Hydrobiosidae); 30.1. Longitudinal channels on the anterior surface of haustellum present (also in* Holocentropus*)*; *31.1. Transverse line on the anterior surface of the haustellum present (also in* Rhyacophila *and* Holocentropus*)*; 33.1. Salivary pleat covering the salivary orifice; *35.1. Adult mandible vestigial (also in Hydroptilidae)*; 37.1. Pupal mandible small and stout.

Brevitentoria: *10.0. Dorsal tentorial arm absent (reversal in* Leptocerus*; also absent in* Hydroptila*,* Orthotrichia*,* Hydropsyche*, and* Holocentropus*)*; 29.1. Lacinia and galea completely inseparable.

Plenitentoria: *11.2. Dorsal tentorial arm well-developed and continuous with the head capsule (also in* Nannochorista*)*; *12.1. Laminatentorium comparatively small, but strongly sclerotized (also in* Leptocerus*)*; *19.1. M. tentorio-scapalis posterior originates exclusively from the dorsal tentorial arm (also in* Leptocerus*,* Rhyacophila*,* Stenopsyche*, and Hydrobiosidae)*.

Phryganeoidea: *27.1. M. cranio-cardinalis absent (also in* Nannochorista*)*.

Limnephiloidea: 20.1. M. clypeo-epipharyngalis lateralis composed of two bundles; 21.2. M. clypeo-cibarialis dorsalis composed of three bundles.

(VII) Polyphyletic 'Spicipalpia'

(Fig. 41; after FRANIA & WIGGINS 1997)

Number of steps required by mapping morphological characters: 110 (CI: 0.44, RI: 0.73).

Trichoptera: *9.1. Tentorium H-shaped (reversal in Hydrobiosidae and Integripalpia; also in* Trichostegia*)*; 34.2. M. hypopharyngo-salivarialis absent (reversal in Annulipalpia and Integripalpia).

Rhyacophilidae + (Hydrobiosidae + Annulipalpia): 36.2. Pupal mandible equipped with three subapical teeth (ACCTRAN optimization).

Annulipalpia: 4.1. 5th segment of maxillary palp distinctly elongated; 5.0. Integument of 5th maxillary palpomere with regular cuticular clefts, flexible; *16.1. M. tentorio-scapalis lateralis composed of two bundles (also in Glossosomatidae + Hydroptiloidea,* Pycnocentria*,* Limnephilus*)*; 23.0. M. cranio-pharyngalis anterior extremely thin, composed of a single fiber; *25.1. M. cranio-pharyngalis posterior absent (reversal in* Holocentropus*; also absent in Hydroptilidae and Integripalpia)*; *26.0. M. cranio-stipitalis present (also in* Micropterix*)*; *28.1. M. stipito-lacinialis absent (also in Brevitentoria)*; *34.0. M. hypopharyngo-salivarialis connecting hypopharynx and salivarium (also in* Nannochorista*,* Micropterix*; reversal in Psychomyioidea)*.

Philopotamoidea: *12.0. Laminatentorium small and weakly sclerotized (ACCTRAN optimization; also in* Tinodes *and Integripalpia)*.

Hydropsychoidea (= Hydropsychidae + Psychomyioidea): *1.1. Ocelli absent (also in Integripalpia and Hydroptiloidea)*; 15.1. M. tentorio-scapalis medialis composed of two bundles; 36.3. Pupal mandible equipped with four subapical teeth (ACCTRAN optimization).

Psychomyioidea: 22.1. M. clypeo-cibarialis dorsalis originates with one bundle at the anterior face of the gena above the non-sclerotized area of the adult mandible; *34.1. M. hypopharyngo-salivarialis forming sphincter of salivarium (also in Integripalpia)*.

Glossosomatidae + (Hydroptiloidea + Integripalpia): *6.1. Endite lobes of labium absent (ACCTRAN optimization; also in Hydrobiosidae)*.

Hydroptiloidea + Integripalpia: *1.1. Ocelli absent (also in Hydropsychoidea; reversal in* Ptilocolepus*, Phryganeoidea, and* Limnephilus*)*; 8.2. Origin of antennifer at lateral margin of circumantennal sulcus (reversal in *Ptilocolepus*); *10.0. Dorsal tentorial arm absent (also in* Hydropsyche*,* Holocentropus*; reversal in* Ptilocolepus*,* Leptocerus*, and Plenitentoria)*; *25.1. M. cranio-pharyngalis posterior absent (also in Annulipalpia; reversal in* Ptilocolepus*)*; 35.1. Adult mandible vestigial (reversal in *Ptilocolepus*).

Integripalpia: *9.0. Tentorium Π-shaped (also in Hydrobiosidae; reversal in* Trichostegia*)*; *21.1. M. clypeo-cibarialis dorsalis composed of two bundles (also in* Hydrobiosis*,* Agapetus*, and Annulipalpia)*; *24.1. M. tentorio-mandibularis absent (also in Hydrobiosidae)*; *28.1. M. stipito-lacinialis absent (also in Annulipalpia; reversal in Plenitentoria)*; 29.1. Galea and lacinia inseparable (reversal in Plenitentoria); *30.1. Longitudinal channels on the anterior surface of haustellum present (also in* Holocentropus*)*; *31.1. Transverse line on the anterior surface of* *the haustellum present (also in* Rhyacophila *and* Holocentropus*)*; 33.1. Salivary pleat covering the salivary orifice; *34.1. M. hypopharyngo-salivarialis forming sphincter of salivarium (also in Psychomyioidea)*; 36.4. Subapical teeth of pupal mandible absent; 37.1. Pupal mandible small and stout.

Plenitentoria: *7.1. Anteclypeolabrum remarkably elongated ventrally (also in* Nannochorista*)*; *10.1. Dorsal tentorial arm present (also in* Rhyacophila*, Hydrobiosidae, Philopotamoidea,* Tinodes*, Glossosomatidae,* Ptilocolepus*,* Leptocerus*)*; *12.1. Laminatentorium comparatively small, but strongly sclerotized (also in* Leptocerus*)*; *19.1. M. tentorio-scapalis posterior originates exclusively from the dorsal tentorial arm (also in* Leptocerus*,* Stenopsyche*, Hydrobiosidae, Rhyacophilidae)*; *28.0. M. stipito-lacinialis present (also in Hydroptiloidea, Glossosomatidae, Hydrobiosidae, and* Rhyacophila*)*; *29.0. Remnant of lacinia small, but separated from galea (also in Annulipalpia and spicipalpian taxa)*.

Phryganeoidea: *1.0. Three ocelli present (also in* Limnephilus, Ptilocolepus*, Glossosomatidae,* Rhyacophila*, Hydrobiosidae, Philopotamoidea)*; *27.1. M. cranio-cardinalis absent (also in* Nannochorista*)*.

Limnephiloidea: 20.1. M. clypeo-epipharyngalis lateralis composed of two bundles; 21.2. M. clypeo-cibarialis dorsalis composed of three bundles.

4. Discussion

4.1. Morphology and terminology *

The terminology used for the description of sclerites and muscles of the adult head of Trichoptera varies considerably. In the following chapter the different interpretations of trichopteran head structures are rewieved and discussed in terms of homology including also data on Lepidoptera and Mecoptera (see also Tab. 13). Finally, a consistent terminology for so far controversially discussed structures will be proposed. Furthermore, a short overview of features, which were not mentioned in the comparative description of trichopteran head structures is also provided with special reference to Lepidoptera and Mecoptera.

4.1.1. Frontopostclypeus

In *Philopotamus* and all other trichopteran representatives investigated so far externally visible demarcations between frons, clypeus and labrum are absent. In the generalized insect condition frons and clypeus are separated by a frontoclypeal strengthening sulcus (= epistomal sulcus of Snodgrass 1935), laterally demarcated by the anterior tentorial pits. Usually, the frontal region serves as attachment area of dilator muscles of the precerebral pharynx, whereas the cibarial dilators are attached to the clypeus (see Snodgrass 1935, v. Kéler 1955). A frontoclypeal sulcus is absent in all investigated trichopteran representatives. In contrast to Chaudonneret (1990), Demoulin (1960: 4, fig. 1; = clypeo-frontal sulcus) described a frontoclypeal sulcus in *Stenophylax*, which originates from the anterior tentorial pits and curves dorsally towards the antennal bases. This sulcus is not homologous with a frontoclypeal sulcus due to the origin of pharyngeal dilators below the median ocellus, which are attached to the frons in the generalized insect head (Snodgrass 1935). It rather resembles the frontogenal sulcus of Philopotamidae. This conclusion is also applicable to the dorsal demarcation of the 'clypeus' presented by Deoras (1943). A frontoclypeal sulcus is described for the leptocerid species *Ceraclea dissimilis* (Denis & Bitsch 1973: 422) and in *Rhyacophila* (Klemm 1966: 37 [= sulcus epistomalis]). In *Rhyacophila* a horizontal sulcus between the anterior tentorial pits is present, but the dorsal cibarial dilator muscle is attached to the sulcus itself and also to the area above it (pers. obs.). Since the dilator muscles of the prepharyngeal tube are exclusively attached to the clypeus (see v. Kéler 1955) a homology of the horizontal sulcus in *Rhyacophila* to the frontoclypeal sulcus of the generalized insect head can be doubted.

Klemm (1966: fig. 11) described a membranous horizontal furrow ('querfaltige Membran') ventrally adjacent to the horizontal sulcus in *Rhyacophila*. A similar depression is present in many other trichopterans, as for instance in *Philopotamus* (hf, Fig. 4), *Phryganea* (Crichton 1957: unlabeled in fig. 26) and *Hydropsyche*. However, in contrast to *Rhyacophila* the horizontal furrow is not membranous in the other taxa. In all trichopteran representatives investigated so far the dorsal dilator muscles of the prepharyngeal tube originate from the head capsule in the area below the anterior tentorial pits and also above the horizontal furrow, which therefore also cannot be homologous with the frontoclypeal sulcus. Additionally, a ventral cibarial dilator muscle [cl-ci(v)] is attached below the horizontal furrow, rendering this structure as transclypeal. It separates the dorsal frontopostclypeus from a ventral anteclypeolabrum. Based on the origin sites of the cibarial dilator muscles Klemm (1966: 19) and Chaudonneret (1990: 78, fig. 175) correctly termed the area below the horizontal furrow in *Rhyacophila* and *Stenophylax*, respectively, as anteclypeolabrum (see Table 13).

Klemm (1966) considered the area above the frontoclypeal sulcus as the frons and in consequence all attached muscles as dilators of the pharynx. There is no cibarial dilator muscle in *Phryganea* recorded as attaching below the horizontal furrow (Crichton 1957: fig. 26). Hence, Crichton (1957) regarded this lower region as a labrum and the area above the horizontal furrow the frontoclypeus; it accommodates the origins of both cibarial and pharyngeal dilator muscles. In accordance to Crichton's (1957) interpretation it is concluded that the area above the anterior tentorial pits truly represents the frons in Philopotamidae and most other trichopterans, but since the frontoclypeal sulcus is absent no clear border between frons and clypeus is present. Consequently, this composite formation has to be termed as frontoclypeus as proposed by Crichton (1957) and Chaudonneret (1990) (see Table 13).

In *Micropterix* (Hannemann 1956; pers. obs.) and other non-glossatan moths (Kristensen 2003) a frontoclypeal sulcus is well-developed, but absent in all Glossata. Kristensen (2003: 43) linked the absence of a frontoclypeal sulcus to the loss of articulated mandibles in the post-pharate glossatan adults. This is also a plausible explanation for the loss of this structure in most trichopterans.

The frontopostclypeus of Philopotamidae and several other trichopterans (e.g., Polycentropodidae) is dorsally subdivided by the interantennal sulcus, which is also recorded for *Stenophylax* (Chaudonneret 1990: 78, fig. 172, stf), but is absent in *Rhyacophila* (pers. obs.; Klemm 1966) and *Phryganea* (Crichton 1957). A homology with the interantennal sulcus of some lepidopterans (Kristensen 2003: 41) is doubtful.

4.1.2. Anteclypeolabrum

The complete lack of the clypeo-labral articulation and of the fronto-labral muscles in all trichopteran species investigated so far impedes the exact delimitation of the labral and clypeal portions of the anteclypeolabrum. The combined loss of both features occurs in almost all insect taxa with an immobilized labrum (e.g., Friedrich et al. 2013; v. Kéler 1955: 722).

A border between a well-sclerotized proximal part and a membranous apical area is distinctly developed in most trichopterans (e.g., Fig. 4, Klemm 1966: fig. 9). If it represents the anatomical clypeo-labral boundary remains uncertain due to the lack of associated muscles, but seems to be at least possible since the epipharyngeal sclerite is laterally continuous with the anteclypeolabrum in this apical area. The proximal border of the structure described as labrum by Crichton (1957) for *Phryganea* (see above) is in fact the intraclypeal horizontal furrow. His interpretation was likely based on the absence of the ventral clypeo-cibarial dilator muscle. Crichton (1957: 61) assumed that the membranous tip in *Phryganea* is movable by an intrinsic muscle (Crichton 1957: 61). Considering the sclerotization pattern of the labrum, this intrinsic muscle most likely allows only light movements or deformation of the membranous tip. It is most likely that it lifts only the epipharynx. Considering the absence of extrinsic labral muscles Crichton's interpretation has to be regarded as not supported. The interpretation of labrum and clypeus forming a composite anteclypeolabrum by Klemm (1966) and Chaudonneret (1990) is comparable with the condition found in Philopotamidae in most other trichopteran representatives.

In the ground plan of Lepidoptera the labrum is moved by paired frontal retractor muscles and is proximally well delimited by a clypeo-labral hinge (Kristensen 2003).

Generalized insect head Beutel et al. 2014			*Philopotamus* [Philopotamidae, Annulipalpia] present study	*Rhyacophila* [Rhyacophilidae, 'Spicipalpia'] Klemm 1966	*Stenophylax* [Limnephilidae, Integripalpia] Chaudonneret 1990	*Phryganea* [Phryganeidae, Integripalpia] Crichton 1957	*Micropterix* [Micropterigidae, Lepidoptera] Hannemann 1956
cranium	occiput		+	+	région occipitale	+	+
	vertex		+	-	-	-	+
	gena		+	+	+	+	+
	postgena		+	+	+	+	+
'face'	frons		frontpostclypeus	+	clypéofrons + aire postérieure du frons	frontoclypeus	+
	clypeus	postclypeus		clypeolabrum			+
		anteclypeus	anteclypeolabrum		clypéo-labre		
	labrum					+	+
maxilla	cardo		cardo + basistipes	+	+	+	+
	stipes	basistipes		+	+	+	+
		dististipes	+				
	lacinia		+	+	-	+	+
	galea		+	-	+	-	+
labium	postlabium		-	-	+	-	-
	postmentum		-	+		-	-
	submentum		-	-	-	-	+
	mentum		-	-	-	-	+
	prementum		+	+	+	+	+
	palpiger		+	-	+	distal labial sclerite	-
	paraglossa		endite lobes of labium	-	-	-	+
	glossa			-	-	-	+
	haustellar sclerites		-	+	+ (1, 2)	+ (1–3)	-

← **Table 13:** Overview of the morphological terminology applied to sclerites of the adult head capsule (cranium/'face') and to selected mouthpart structures (maxilla and labium) in Amphiesmenoptera compared with the generalized insect head (after Beutel et al. 2014). Abbreviations: **+** = term used as the general sense, **–** = structure not mentioned by the respective author (this does not indicate that the respective structure is absent in the taxon!).

4.1.3. Gena and occiput

The gena is anteriorly delimited from the frontopostclypeus by the distinct frontogenal sulcus. The latter extends from the ventral margin of the circumantennal sulcus towards the anterior tentorial pit in Trichoptera; the corresponding internal ridge is of variable size (Klemm 1966; Neboiss 1991; pers. obs.).

In Lepidoptera a frontogenal sulcus (= laterofacial sulcus of Kristensen 2003) is usually well-developed in the glossatan lineages, but joins the circumantennal sulcus dorsolaterally.

It has been shown in other insect groups that the length and connections of the circumantennal and frontogenal sulci can strongly vary even between closely related taxa, depending on other anatomical features (see Klass & Eulitz 2007). A well-sclerotized clypeogenal sulcus as described by Crichton (1957) for *Phryganea* could not be observed in any trichopteran species within this study and is also absent in *Rhyacophila* (Klemm 1966: 37).

A typical feature of the trichopteran head capsule is the elongation of the ventral edge of the gena forming a subgenal process. This process is also a typical feature of Mecoptera (Mickoleit 1971; Friedrich et al. 2013) and basal lepidopterans (Kristensen 2003). As described for *Philopotamus* (see above) the postgena is continuous with the occiput in all other investigated trichopterans (Klemm 1966; Crichton 1957; pers. obs.) while it is distinct in *Micropterix* (Hannemann 1956; pers. obs.) and other lepidopteran lineages (Kristensen 2003). Frontal and coronal sulci are generally present in Trichoptera (e.g., *Philopotamus*, *Hydropsyche*, and *Phryganea* [pers. obs.], *Rhyacophila* [= sulcus mediocranialis of Klemm 1966], and *Stenophylax* [Demoulin 1960]).

The postfrontal sulcus described for *Philopotamus* and *Stenophylax* (Demoulin 1960) are most probably homologues to the mediolateral reinforcement lines described by Klemm (1966: 8) and the postinterocellar sulcus described by Hannemann (1956) for *Micropterix*. These sulci are completely absent in *Phryganea* (pers. obs.). Interocellar sulci occurring in some lepidopteran lineages (Kristensen 2003) are not known from Trichoptera.

4.1.4. Tentorium

Features of the adult trichopteran tentorium are comparatively described in previous chapters (see above [3.2.1.]).

Similar conditions of major tentorial structures (e.g., weakly and well-developed dorsal arms) as described for Trichoptera are also present in Lepidoptera (see Kristensen 2003).

The terminology applied to its features is quite consistent throughout Trichoptera and Lepidoptera and is therefore not discussed herein (see e.g., Hannemann 1956; Crichton 1957; Klemm 1966; Neboiss 1991; Kristensen 2003).

4.1.5. Setal warts

A specific feature of the trichopteran head is the presence of numerous, bulged setal warts equipped with numerous large trichoid sensilla. The homology of these areas is uncertain due to the high variability in presence and location in different trichopteran lineages (see Oláh & Johanson [2007]). In previous descriptions these structures were often neglected or at least insufficiently described (see Crichton 1957; Klemm 1966). Detailed comparative studies are not available.

4.1.6. Photoreceptors

The compound eye of Philopotamidae is irregularly covered by a few interommatidial setae. The number of setae as well as their distribution on the compound eye varies among caddisfly families (see Schmid 1998), and can even be species specific (pers. obs.: *Philopotamus* and *Wormaldia* [Philopotamidae]). Neither Crichton (1957) nor Klemm (1966) mentioned the presence of interommatidial setae in Rhyacophilidae and Phryganeidae, respectively, although they are visible in light microscopy and are commonly present in Trichoptera (pers. obs.) and in Lepidoptera (Kristensen 2003).

Furthermore, in *Philopotamus* the ommatidial cornea shows a specific surface texture of rounded corneal nipples (absent along the interommatidial space), a common feature of the insect compound eye in order to reduce reflection artifacts (Bernhard & Miller 1962; Bernhard et al. 1970). These extremely minute structures are not mentioned by Crichton (1957) and Klemm (1966), likely due to technical constraints. The structure of corneal outgrowths varies among insects from knob-like nipples to parallel sulci (Meyer-Rochow & Stringer 1993). Evidence for the presence of corneal nipples of the knob-like type among 15 different caddisfly families (including Philopotamidae) was provided by Bernhard et al. (1970). A textured surface of the ommatidial cornea is also commonly found in Lepidoptera (Kristensen 2003) and Mecoptera (Bernhard et al. 1970).

The occurrence of ocelli is quite variable among trichopteran lineages (see Malicky 1973; pers. obs.). This is also true for the lateral ocelli in Lepidoptera; the median one reduced in all groups (Kristensen 2003).

Histological sections show that the ocelli in *Philopotamus* have a comparatively thin corneal lens of the convexo-concave type (after Hallberg & Hagberg 1986), whereas the haemocoelic space is voluminous (pers. obs.; Ehnbom 1948). A similar condition was described for limnephilids by Ehnbom (1948) and Hallberg & Hagberg (1986), and is also found in the micropterigid moths (Ehnbom 1948; Kristensen 2003). The corneal lens is much thicker (biconvex type), and underlain by an epidermal layer in phryganeids (pers. obs.: *Phryganea*; Ehnbom 1948; Hallberg & Hagberg 1986). This is also the common condition in most heteroneuran lepidopterans (Ehnbom 1948; Kristensen 2003). Eriocraniidae are different in having the haemocoelic space filled up by a multicellular formation (see Kristensen 2003) not known from any other amphiesmenopteran insect.

An imaginal stemma consisting of numerous heavily pigmented retinula cells is attached to the optical lobe in all investigated Trichoptera (pers. obs.: e.g., *Philopotamus*, *Rhyacophila*; Ehnbom 1948; Hagberg 1986). Initially, this formation which represents a remnant of the larval eyes in the adult stage was described for phryganeids by Ehnbom (1948). Its appearance is variable on family level. Usually each stemma consists of numerous retinula cells associated to at least one crystalline body (see Ehnbom 1948; Hagberg 1986: fig. 2). They are common features of the endopterygote adult head and can be found in various insect groups (i.e., Lepidoptera [Hagberg 1986; Kristensen 2003]; Megaloptera [*Sialis*, Ehnbom 1948]).

In Lepidoptera the imaginal stemma is located inside the lobus opticus, whereas it is found outside, behind the optic lobe in caddisflies and most other holometabolous insect orders (e.g., Megaloptera, Neuroptera, and Mecoptera, see Ehnbom 1948). Hagberg (1986) concluded that these sensory organs are associated with cranial areas of glabrous, translucent cuticle. A small glabrous, bulged field near the lateral ocelli in *Philopotamus* might be comparable. If this structure and the stemma are functionally correlated cannot be assessed with final certainty because they are distinctly separated in *Philopotamus* and other lineages of Trichoptera.

4.1.7. Antenna

The length of the antenna varies remarkably among Trichoptera (see above [3.2.2.]).

The antenna bears numerous sense organs, which mainly function as chemical receptors. These sense organs vary considerably in their shape among Trichoptera (see Faucheux 2004; Melnitsky & Ivanov 2011; pers. obs.) and Lepidoptera (Kristensen 2003; Faucheux 2004). In Philopotamidae and Stenopsychidae the number of fungiform pseudoplacoid sensilla along the antenna is remarkably high (pers. obs.), but this type of sense organs can be found regularly among Trichoptera (Melnitsky & Ivanov 2011).

In Trichoptera the antenna (i.e., the scapus) is usually moved by four extrinsic muscles originating mainly from the tentorium or with at least one bundle from the cranium (see above [3.2.2.]).

This corresponds with the number and origin pattern of extrinsic antennal muscles in Lepidoptera. In contrast, only three or two are present in Mecoptera (e.g., Friedrich et al. 2013). The remaining parts of the antenna are moved by two intrinsic muscles arising from the scapus with several bundles. Maybe these bundles belong to more than two muscles as in the ground plan condition of Lepidoptera (Kristensen 2003), but with the data at hand the homology of these muscles remains unclear.

4.1.8. Mandible

The size and the level of sclerotization vary considerably among the major trichopteran groups (see above [3.2.5.]).

Furthermore, the conditions of the mandibular musculature also distinctly differ in the published studies on trichopteran species (e.g., Crichton 1957; Klemm 1966). Crichton (1957: 60, 7 in fig. 25) described a pair of remarkably thin mandibular muscles, which are composed of only a few fibers in the integripalpian family Phryganeidae. In contrast, Klemm (1966: 10, 1admd and abmd in fig. 5) reported well-developed mandibular muscles filling up large parts of the head capsule in the spicipalpian representative Rhyacophilidae. Own observations (see App. 1) also show remarkable differences in the size of the mandibular muscles between not closely related taxa.

In spite of the remarkable differences between the major groups of caddisflies in size of the mandibular sclerite, sclerotization and musculature development, all post-pharate imagines lack any cranio-mandibular articulations (pers. obs.; Chaudonneret 1990; Kristensen 1997). Hence, the mandible is most likely never functional for the processing of solid food (see also Crichton 1957).

As highlighted by Hinton (1946) the mandibular muscles of adult endopterygote insects with decticous pupae operate the pupal mandibles when the pharate imago hatches from the cocoon. In the post-pharate stage of caddisflies and glossatan moths these muscles are functionless and therefore may become atrophied over time. Differences in the age of the investigated specimen resulting in different grades of muscular atrophy are possible explanations for the variation found in descriptions (Crichton 1957; Klemm 1966).

In order to proof the highly speculative assumption of Hinton (1946), a detailed investigation of the development of the adult mandibular musculature during aging was performed for Limnephilidae (Integripalpia; Pinkernell 2014) and Hydropsychidae (Annulipalpia: Loosmann 2014). Larvae were reared and adults fixed for morphological analyses after defined time intervals after hatching. Measurements of the mandibular muscles clearly showed a distinct decrease in the muscle volume over time in both trichopteran lineages (Pinkernell 2014; Loosmann 2014). Considering these results and in agreement with the hypothesis of Hinton (1946) it is evident that specimen of different age caught in the wild have resulted in competitive morphological descriptions in the literature (Crichton 1957; Klemm 1966).

4.1.9. Preoral cavity and mouth opening

The interpretations of the facial areas (see above [4.1.1.]) mainly depend on the demarcation of the anatomical mouth opening. According to Snodgrass (1935) the border between the prepharyngeal tube (= cibarium) and the pharynx is usually marked by the frontal ganglion. Accordingly, in *Philopotamus* all muscles inserting below the frontal ganglion are termed prepharyngeal (= cibarial) dilators, whereas muscles attached above the frontal ganglion are regarded as pharyngeal dilators.

The prepharyngeal tube is encircled by ring musculature and clearly contributes to a large cibarial-pharyngeal pumping chamber, which represents a composite structure in *Philopotamus* and all other trichopterans.

Klemm (1966) regarded this part as the cibarium and determined the morphological mouth opening at the anterior border of the pharyngeal ring musculature. He considered the muscles above this border either as cibarial dilators or as pharyngeal dilators depending on the origin site below or above the horizontal sulcus (his sulcus epistomalis, see above). It seems not appropriate to separate the preoral cavity into a proximal cibarium enclosed by pharyngeal circulatory musculature and a distal part without ring musculature as proposed by Klemm (1966) since the sitophore plate (i.e. the sclerotized section of the hypopharynx) is a continuous structure and clearly forms the bottom of the composite pumping chamber.

In lepidopterans the ring musculature is located behind the frontal ganglion, but the roof of the cibarium is only covered by semicircular and longitudinal muscle fibers (Kristensen 2003). This semicircular type of cibarial pump musculature is so far not known from any trichopteran species.

The surface of the sitophore plate lacks any chemoreceptors in *Philopotamus* and other trichopterans (Crichton 1957; Klemm 1966; pers. obs.). In Lepidoptera the sitophore is usually equipped with numerous chemoreceptors (Nielsen & Kristensen 1996).

4.1.10. Maxilla

In Trichoptera the base of the maxilla is formed by one sclerite, which is intermitted by a transstipital sulcus. This sulcus was usually misinterpreted as a border between 'cardo' and 'stipes' (e.g., Crichton 1957; Matsuda 1965; Klemm 1966).

In Lepidoptera the proximal maxillary sclerite (apparent 'cardo') is subdivided into two sections by an internal sulcus and delimited from the stipes (dististipes) by a small membranous area (Hannemann 1956: 191; Kristensen & Nielsen 1979: 117). In none trichopteran representative investigated so far, a membranous subdivision of the basal maxillary sclerite could be observed. A strong horizontal sulcus delimits the apparent cap-like cardo and the stipes. Intriguingly a couple of extrinsic muscles of the maxillary palp originate from the putative cardo. A cardo-palpal muscle is not present in any other insect group (see e.g., Wipfler et al. 2011; v. Kéler 1955), and therefore it is more plausible to assume that these muscles are homologues to the stipito-palpal muscle of the insect ground plan (e.g., Snodgrass 1935: 143). The insertion of these palpal muscles to the basalmost maxillary piece in both amphiesmenopteran lineages led to the interpretation that this sclerite represents a combination of cardo and basistipes (Hinton 1958; Kristensen & Nielsen 1979; Kristensen 2003). Accordingly, the horizontal sulcus present in Trichoptera does not demarcate the border between 'cardo' and 'stipes' as suggested by several authors (e.g., Klemm 1966; Chaudonneret 1990), but forms a transstipital border between a basal piece (cardo + basistipes) and the dististipes. The inclusion of a cardinal portion in the basal piece is well proven by the presence of the cranio-cardinal muscle (cr-ca).

In Philopotamidae and most other trichopteran lineages (e.g., Rhyacophilidae [Klemm 1966; pers. obs.] and Glossosomatidae [Chaudonneret 1990: *Agapetus*; pers. obs.]) the maxilla bears two proximally fused inner appendages: a distinct, flattened outer lobe and a comparatively small, sclerotized inner lobe. In *Philopotamus* this composite structure is moved by a cranial flexor muscle, which might be homologous to the cranio-lacinial muscle of generalized insects (v. Kéler 1955: M.19). Additionally, Klemm (1966: 18) described for Rhyacophilidae a stipito-lacinial muscle inserting at the small inner lobe. A stipito-lacinial muscle is also present in all other lineages of 'Spicipalpia' as well as in Integripalpia-Plenitentoria. In contrast, it is absent in Annulipalpia (e.g., Philopotamidae) and in Integripalpia-Brevitentoria. In some Integripalpia (e.g., *Leptocerus* [Integripalpia-Brevitentoria]) the maxillary endite lobe is a single structure without any subdivision. In these groups only a single lacinial flexor muscle is present (i.e., M. cranio-lacinialis). This led several authors to regard this clearly composite lobe of Trichoptera as the lacinia, an interpretation which cannot be accepted considering the conditions in basal representatives. Furthermore, as discussed by Kristensen (2003: 53) and Beutel et al. (2014: 21) the lacinia is usually distinctly stronger sclerotized and less equipped with sensilla (chemoreceptors) than the galea. Therefore, it seems also appropriate to consider the membranous outer maxillary lobe, which bears numerous basiconic sensilla as the galea as suggested by Chaudonneret (1990: 80) and only the small inner piece as the remnants of the lacinia, which is largely (e.g., Rhyacophilidae) or completely incorporated (e.g., Brevitentoria-Leptoceridae) into the outer lobe, which therefore should be regarded as a galeolacinia.

4.1.11. Haustellum

The origin of the trichopteran haustellum was a subject of controversy for decades. Several authors homologized the whole haustellum with the fused inner and outer lobes of the labium, i.e., the ligula (Lucas 1893; Deoras 1943; Despax 1951; Handlirsch & Beier 1936). The small inner labial lobes present in annulipalpians (pers. obs.) and *Rhyacophila* (Klemm 1966) most likely represent remnants of these labial appendages. This renders the hypothesis of the haustellum being a modified ligula very unlikely.

A second hypothesis favored by Cummings (1914), Tillyard (1923), and Klemm (1966) considered the haustellum as a ventral outgrowth of the hypopharynx. Indeed, the salivary orifice is located on the lower anterior (e.g., *Philopotamus*) or posterior (e.g., *Stenophylax* [Chaudonneret 1990]) surface of the haustellum. Usually it marks the border between the hypopharynx and the labium (Moulins 1971; Beutel et al. 2014: 22). Therefore, at least the upper anterior part of the haustellum must be of hypopharyngeal derivation.

Crichton (1957) showed that the haustellum in *Phryganea* is innervated by a branch of the mandibular nerve, but also receives a branch of the labial nerve. He concluded that the lower section of the haustellum is most likely formed by the labium, whereas the hypopharynx contributed to the upper part of this composite structure. The investigation of *Philopotamus* showed that the haustellum as well as the salivarium is only innervated by branches of the labial nerve.

In conclusion a composite nature of the haustellum seems to be well supported by the location of the salivary orifice and by its innervation by different nerve tracts. However, the latter seems not to be consistent throughout all trichopteran lineages and needs further detailed research.

In most trichopterans (e.g., Philopotamidae, Rhyacophilidae; pers. obs.) the haustellum is a completely membranous, highly flexible structure distinctly separated from the sclerotized prementum. Sclerites are absent. Small, distinctive basal haustellar sclerites were described only for some integripalpians by Crichton (1957) and Chaudonneret (1990). These sclerites serve as attachment areas of the labial palp muscles and represent most likely derivatives of the prementum in the generalized insect condition (e.g., Snodgrass 1935: 147).

4.1.12. Salivarium

In all Trichoptera investigated the salivarium orifice is located on the surface of the haustellum, distinctly below the preoral cavity. In *Philopotamus* it is located on the anterior surface of the haustellum, but on its hind face in *Rhyacophila* (Klemm 1966).

In Lepidoptera and most other endopterygote insects the salivary orifice is located at the distal end of the hypopharynx, and distinctly opens into the preoral cavity (Kristensen 2003).

In Trichoptera the salivarium forms a longitudinal, sclerotized channel with U-shaped cross-section. A pair of extrinsic dilator muscles (M. hypopharyngo-salivarialis and M. praemento-salivarialis) inserts on its dorsal wall in *Philopotamus* and *Rhyacophila*. In contrast, in other pterygote insects M. praemento-salivarialis inserts ventrally on the floor of the salivarium (e.g., v. Kéler 1955; Snodgrass 1935; Röber 1942 [Megaloptera]; Kristensen 2003 [Lepidoptera: Acanthopteroctetidae]). Therefore, it seems to be at least possible that the sclerite on which these muscles originate is a derivate of the hypopharyngeal suspensorium of the generalized insect condition and hence the muscle may constitute a displaced bundle of M. hypopharyngo-salivarialis. Extrinsic dilators of the salivarium originating from the prementum are absent in most mecopterid lineages like Lepidoptera (with the exception of Acanthopteroctetidae; Kristensen 2003: 60) and Mecoptera (e.g., Grell 1938; Friedrich et al. 2013).

In most trichopterans a strong longitudinal muscle along the roof of the salivarium is present. This intrinsic salivary muscle is absent in Philopotamidae and other holometabolan lineages (Röber 1942 [Neuropterida: Megaloptera]; Kristensen 2003 [Lepidoptera]; Schneeberg & Beutel 2011 [Diptera]). Instead, a well-developed extrinsic dilator muscle originates from the floor of the hypopharynx (hy-sa) in the annulipalpian groups or from the premental ligula in other holometabolan taxa (e.g., Megaloptera [Röber 1942]). As all trichopterans with intrinsic longitudinal salivary muscles lack the extrinsic hypopharyngeal muscle it is logical to assume the potential homology of these muscles of the salivary roof.

4.1.13. Labium

The labium of the generalized insect head is composed of a proximal postmentum and a distal prementum, which bears the labial palps and the inner endite lobes (e.g., Beutel et al. 2014). In Lepidoptera the labium is usually separated into three distinct sclerotized areas (postlabium, proximal prelabium and prementum) distinguishable either by membranous segregation or by muscle insertion (see Kristensen 2003).

In Philopotamidae and other trichopteran lineages both elements are largely fused forming a weakly sclerotized labial plate bearing the labial palps. In contrast, Crichton (1957), Klemm (1966), and Chaudonneret (1990) described the presence of distinct labial sclerites in Integripalpia and Rhyacophilidae (see Table 13). Unfortunately, the identification of these structures is complicated by the absence of a postlabio-premental muscle in all trichopterans investigated so far. Hence, a pre- or postmental derivation of these labial sclerites cannot be proven with any certainty. For a thorough interpretation of these structures comprehensive studies are needed.

The labium bears small inner lobes in all annulipalpians (e.g., *Philopotamus*, *Hydropsyche* [pers. obs.; Crichton 1957]) and in Rhyacophilidae (pers. obs.; Klemm 1966), whereas these are absent in Integripalpia (e.g., Crichton 1957; Chaudonneret 1990; pers. obs.). The formation of a ‘ligula’ (fused glossae after Kristensen 2003: 57) is a common feature in Lepidoptera. Distinct paraglossae retained only in Micropterigidae (Kristensen 2003).

In Trichoptera the inner lobe lack any musculature and therefore its homology remains uncertain. However, considering the potential contribution of the ‘ligula’ to the haustellum it cannot be excluded that this lobe indeed represents a remnant of the paraglossa.

The labial palp of Trichoptera is usually three-segmented (four-segmented only in *Paduniella* [Psychomyiidae]) in both sexes (Malicky 1973). In Lepidoptera it is three-segmented in some lower groups, but reduction in number of palpomeres occurs several times within the group (Kristensen 2003).

4.1.14. Nervous system

In Trichoptera the cephalic ganglia (brain and suboesophageal ganglion; Fig. 20) are usually distinctly separated by long circumoesophageal connectives (in Hydroptilidae exceptionally short [Ehnbom 1948]).

The brain is divided into a large dorsal protocerebrum, well-developed anterior olfactory lobes (deutocerebrum) and a small ventral tritocerebrum, which is continuous with the other parts of the brain (pers. obs., Ehnbom 1948). Usually frontal and labral nerves have a common root at the frontal connectives and split later into separate frontal (median) and labral (lateral) tracts (pers. obs.; Ehnbom 1948). Only in Hydroptilidae and Lepidoptera both nerves show discrete origins (Ehnbom 1948).

The nervous system of Hydroptilidae and Lepidoptera share also other remarkable similarities as for instance the penetration of the cephalic aorta by the nervus recurrens. Both structures are distinctly separated in all other trichopterans (Ehnbom 1948; pers. obs.). The shape of the suboesophageal ganglion varies considerably among Trichoptera (Ehnbom 1948). Usually, three pairs of nerves (mandibular, maxillary and labial) originate ventrally in both, Trichoptera and Lepidoptera (Ehnbom 1948). An occipital nerve originating from the dorsal wall of the suboesophageal ganglion is a specific formation of Trichoptera.

Paired glands of the hypocerebral complex, the corpora cardiaca and corpora allata are located behind the brain on both sides of the pharynx in Trichoptera and in Lepidoptera (Ehnbom 1948). However, comparative investigations showed considerable differences in shape and localization of the corpora cardiaca between different groups of caddisflies (Ehnbom 1948). In *Philopotamus* they are close to the hind face of the brain and ellipsoidally shaped as it is also described for *Hydropsyche* and *Agraylea* (Hydropsychidae, Hydroptilidae [Ehnbom 1948]). In Limnephilidae the corpora cardiaca are rather slender and distinctly separated from the brain (Ehnbom 1948). In *Philopotamus* the corpora allata are quite prominent (several times larger than the corpora cardiaca) and characterized by a considerably irregular glandular structure (pers. obs.; Ehnbom 1948). This condition is unique among trichopterans, but resembles the condition found in most lepidopterans (Ehnbom 1948).

The cervical connectives are well separated from each other in Trichoptera and Mecoptera (*Panorpa* [Ehnbom 1948]). A different pattern is described for Hydroptilidae in which the cervical connectives being almost completely fused (Ehnbom 1948). This resembles the common condition in Lepidoptera excluding Micropterigidae (Ehnbom 1948).

4.2. Phylogenetic implications

The character mapping (see above [3.6.]) revealed remarkable variations in data fitting of adult and pupal head characters to different phylogenetic hypotheses (Figs. 34–41).

The number of required steps, i.e., the accumulated number of character changes of the tree, is used as quantitative criterion of the data fitting to the respective topology. On the basis of the parsimony criterion, the tree with the lowest number of steps is interpreted as best supported by the characters.

The morphological data set strongly supports the tree topologies published by Wiggins & Wichard (1989; Fig. 34) and Kjer et al. (2016; Fig. 38). The mapping of the morphological data set yielded a tree length of 100 steps for both scenarios.

Based on the analysis of pupal cocoon structures Wiggins & Wichard (1989) intuitively proposed monophyletic Spicipalpia forming the sister group to a clade comprising Annulipalpia and Integripalpia. However, a sister group relationship of Annulipalpia and Integripalpia is quite weakly supported in the present analysis without non-homoplasious apomorphies (Fig. 34).

A monophyletic placement of Spicipalpia was also proposed by Weaver & Morse (1986) based on the analysis of feeding strategies of trichopteran larvae. In particular, these authors postulated a sister group relationship of Spicipalpia and Annulipalpia, and both being the sister group of Integripalpia. The close relationship of Spicipalpia and Annulipalpia is supported by two homoplasious and one non-homoplasious character (char. 17: origin of M. tentorio-scapalis lateralis on head capsule and tentorium; Fig. 35).

A further monophyletic placement of Spicipalpia, but as sister group to Integripalpia was revealed by Kjer et al. (2002) based on the analysis of molecular data. The mapping of adult and pupal head characters on this topology yielded support for the respective clade by one homoplasious and one non-homoplasious character (char. 6: absence of labial endite lobes; Fig. 36).

Kjer et al. (2016) provided an alternative hypothesis rendering the spicipalpian families paraphyletic. The proposed topology comprises a clade with paraphyletic spicipalpians at the base of Integripalpia, together forming the sister group to Annulipalpia. A clade comprising paraphyletic spicipalpians and Integripalpia is well supported by two non-homoplasious characters (char. 6: absence of labial endite lobes; char. 34: M. hypopharyngo-salivarialis absent; Fig. 38). It is noteworthy that the topology of Kjer et al. (2016) yielded the highest consistency index (CI: 0.49) of all analyzed hypotheses, which means the lowest amount of homoplasy within the data set. It requires only nine steps more than the most parsimonious tree obtained in the cladistic analysis of the adult and pupal head data set. A quite similar hypothesis was proposed by Ross (1967) based on a limited number of morphological and behavioral data of adults and larvae. Likewise, his topology (paraphyletic spicipalpians at the base of Integripalpia) is supported by the same three characters as the respective clade in Kjer et al. (2016) (see Fig. 37).

A further hypothesis with spicipalpians being paraphyletic, but with respect to Annulipalpia was postulated by Schmid (1989). This clade is supported in the present analysis by one homoplasious and one non-homoplasious character (char. 12: laminatentorium strongly developed; Fig. 39). Nonetheless, the topology of Schmid (1989) seems to be poorly supported by quantitative criteria of data fitting (i.e., 114 steps; CI: 0.42), but this is most likely caused by the mainly unsolved terminal branching pattern. Unfortunately, Schmid (1989) did not provide any information to resolve the polytomy in the major clades of his preferred topology.

Malm et al. (2013) analyzed a molecular data set and revealed a placement of paraphyletic spicipalpians at the base of a clade comprising both, Annulipalpia and Integripalpia. The mapping of the present morphological data set did not result in any character supporting a clade comprising spicipalpians (without Rhyacophilidae) as sister group to a clade formed by Annulipalpia and Integripalpia (Fig. 40). However, the monophyly of the clade comprising the latter two groups is supported by two homoplasious and one non-homoplasious character (char. 34: M. hypopharyngo-salivarialis forming sphincter of salivarium; Fig. 40).

A polyphyletic placement of the spicipalpian taxa was proposed by Frania & Wiggins (1997) based on the analysis of larval and adult characters. According to these authors Glossosomatidae and Hydroptilidae are closely related to Integripalpia, whereas Rhyacophilidae and Hydrobiosidae are associated with Annulipalpia. A sister group relationship of Rhyacophilidae with a clade comprising Hydrobiosidae and Annulipalpia was supported in the analysis of Frania & Wiggins (1997) by three larval characters (e.g., all instars with prominent anal proleg). The present analysis yielded one non-homoplasious character supporting this clade (char. 36: pupal mandible equipped with three subapical teeth; Fig. 41). Frania & Wiggins (1997) provided no supporting characters for a clade comprising Glossosomatidae as sister group to a clade of Hydroptilidae and Integripalpia. The analysis of the present data set did also not deliver supporting characters for this clade.

In contrast, Frania & Wiggins (1997) provided one larval character supporting a sister group relationship of Hydroptilidae and Integripalpia (anterior sclerite 3 of mesonotum with more than 2 setae). In the present analysis this clade is well-supported by three homoplasious and two non-homoplasious characters of the adult and pupal head (char. 8: origin of antennifer at lateral margin of circumantennal sulcus; char. 35: adult mandible vestigial).

The cladistic analysis of adult and pupal head features (see above [3.5.]) also reveals polyphyletic spicipalpians (Fig. 32). In contrast to Frania & Wiggins (1997), Glossosomatidae (plus *Ptilocolepus*) form the sister group of a clade comprising Hydroptilidae and Annulipalpia. This clade is supported by one non-homoplasious character (char. 17: origin of M. tentorio-scapalis lateralis from head capsule and tentorium; Fig. 32). Furthermore, the topology Rhyacophilidae + (Hydrobiosidae + Integripalpia) is supported by one non-homoplasious character (char. 11: dorsal tentorial arm well-developed, but not continuous with head capsule; Fig. 32).

However, the cladistic analysis also revealed that the character conditions present in the outgroup taxon *Nannochorista* seem to strongly influence the results. The polyphyletic placement of the spicipalpian taxa was not observed when *Nannochorista* was excluded from the analysis (Fig. 33). A detailed review on the character polarity assessment and distribution showed that several convergent modifications are present in *Nannochorista* and trichopteran subgroups. Especially the loss of muscles (e.g., char. 26: M. cranio-stipitalis; char. 28: M. stipito-lacinialis) and of structures of the mouthparts (e.g., char. 6: terminal lobes of the labium) occurs in the not closely related mecopteran and some trichopteran taxa, whereas these features are present in the amphiesmenopteran outgroup Micropterigidae and also some trichopterans. Without *Nannochorista*, paraphyletic spicipalpians are exclusively placed as sister groups to Integripalpia (and not to Annulipalpia), which is well supported by non-homoplasious characters (char. 26: M. cranio-stipitalis absent; char. 34: M. hypopharyngo-salivarialis absent) as it was also revealed by mapping on the topologies of Kjer et al. (2016) and Ross (1967).

Several trichopteran groups are consistently recovered as monophyletic in all phylogenetic hypotheses investigated. Despite different interrelationships were proposed for these groups, the evaluation of the head characters resulted in similar sets of potential apomorphies. These features are shortly discussed in the following.

The monophyly of Integripalpia is well-supported by several apomorphic features (e.g., mesonotum of larva completely sclerotized; female genitalia blunt with abdominal segments X and XI reduced) and was never discussed controversially (see Weaver 1984; Morse 1997). The analysis of the own data revealed several additional apomorphic characters (e.g., char. 13: M. tentorio-scapalis anterior composed of three bundles; char. 33: salivary pleat covers the salivary orifice; char. 37: pupal mandible short and stout) strongly corroborating the traditional view.

The subdivision of Integripalpia into the major lineages Brevitentoria and Plenitentoria was initially proposed by Ross (1956) based on external features of the adult head (e.g., number of maxillary palpomeres in males).

The analyses presented here provide several new apomorphies for both taxa (e.g., Brevitentoria, char. 29: lacinia and galea inseparably fused; Plenitentoria, char. 7: anteclypeolabrum remarkably elongated ventrally; char. 11: dorsal tentorial arm well developed and continuous with head capsule) (see also characters in Figs. 31–36).

Within Plenitentoria, the subgroup Limnephiloidea is strongly supported by two unique characters (char. 20: M. clypeo-epipharyngalis lateralis composed of two bundles; char. 21: M. clypeo-cibarialis dorsalis composed of three bundles). Until now the widely accepted taxon was lacking well-defined and evaluated apomorphies.

Characters supporting the brevitentorian subgroups Sericostomatoidea and Leptoceroidea were not revealed in the present study.

The monophyly of Annulipalpia is well supported by several apomorphic characters of the adult head (e.g., chars. 4 and 5: elongated and flexible 5th maxillary palpomere with a regular system of cuticular clefts; char. 23: M. cranio-pharyngalis anterior extremely thin). Especially, the quite distinctive external structure of the 5th maxillary palpomere was already recognized as a unique feature of Annulipalpia by several authors (e.g., Martynov 1924; Ross 1956, 1967; Weaver 1984). In contrast, the remarkable reduction in size of M. cranio-pharyngalis anterior was never proposed before.

Within Annulipalpia the monophyly of Philopotamoidea is well argued by molecular (Malm et al. 2013; Kjer et al. 2016) and morphological data (e.g., female genitalia without lateral papillae adjacent to the cerci, see Weaver 1984; larval head elongate, see Ross 1967). A paraphyletic placement was only proposed by Kjer et al. (2002) based on the analysis of a molecular data set. Nonetheless, the analysis of adult and pupal head characters did not reveal supporting characters for both, monophyly or paraphyly of the taxon.

The monophyly of Psychomyioidea is well supported by the present data set by one homoplasious (char. 34: M. hypopharyngo-salivarialis forming sphincter of salivarium) and one non-homoplasious character (char. 22: lateral bundle of M. clypeo-cibarialis dorsalis attached to the gena). It is noteworthy that the taxon was not regarded as monophyletic in several studies (e.g., Ross 1967; Wiggins & Wichard 1989; Malm et al. 2013). The monophyly of Psychomyioidea was proposed based on the analysis of molecular (Kjer et al. 2002, 2016) and morphological data (e.g., Schmid 1989; Frania & Wiggins 1997 [e.g., pronotum of larva with tergal ridge]) in others.

A paraphyletic placement of the psychomyioidean lineages within Hydropsychoidea was proposed by Weaver & Morse (1986) and Malm et al. (2013). Both authors postulated a close relationship between Hydropsychidae and Polycentropodidae and both forming the sister group of Psychomyiidae. The analysis of the present data set did not reveal non-homoplasious characters supporting a potential paraphyly of the psychomyioidean families.

The monophyly of the superordinate taxon Hydropsychoidea is also well supported by non-homoplasious adult head features (e.g., char. 15: M. tentorio-scapalis medialis composed of two bundles; char. 36: pupal mandible equipped with four subapical teeth). Based on molecular data Kjer et al. (2016) postulated a sister group relationship between Hydropsychidae and all other annulipalpian taxa. The present analysis of adult and pupal head characters did not reveal any apomorphies supporting this topology.

Only a limited number of studies revealed the ‘Spicipalpia’ as monophyletic (e.g., Weaver & Morse 1986; Kjer et al. 2002; Malm et al. 2013). The monophyly is mainly supported by the analysis of structural features of the trichopteran cocoon (Wiggins & Wichard 1989), larval behavior (Weaver & Morse 1986), and by one molecular study (Kjer et al. 2002).

Despite the monophyly of Spicipalpia is widely negated in recent discussions (see e.g., Morse 1997; Kjer et al. 2016), it is supported by the absence of M. hypopharyngo-salivarialis (char. 34) in the present study when the group forms the sister to all remaining trichopterans or to Annulipalpia. In contrast, monophyletic Spicipalpia as sister to Integripalpia as postulated by Kjer et al. (2002) is not supported by adult and pupal head features.

Within the spicipalpian lineages a close relationship of the free-living representatives Rhyacophilidae and Hydrobiosidae is favored by several authors (e.g., Ross 1956, 1967; Weaver & Morse 1986; Wiggins & Wichard 1989; Kjer et al. 2002; Malm et al. 2013). Furthermore, both families were summarized within Rhyacophilidae in older contributions (e.g., Ross 1956). In the adult head characters provide some support for this clade (e.g., char. 10: dorsal tentorial arms well-developed, but not continuous with the head capsule; char. 19: M. tentorio-scapalis posterior originates exclusively at the dorsal tentorial arm). However, these conditions convergently occur also in other groups of Trichoptera.

Based on a comprehensive morphological data set of mainly larval features Frania & Wiggins (1997) postulated a sister group relationship of Rhyacophilidae to a clade comprising Hydrobiosidae + Annulipalpia. The presence of three subapical teeth in the pupal mandible is a potential autapomorphy of the proposed clade (char. 36; see Fig. 36).

A sister group relationship of Rhyacophilidae and Integripalpia (Kjer et al. 2016,) is only weakly supported by a transverse line on the anterior surface of the haustellum, a feature not exclusively restricted to this clade (char. 31; Fig. 32–41).

The monophyly of a clade comprising Ptilocolepidae and Hydroptilidae (= Hydroptiloidea) is still an unsolved question (e.g., Malicky 2000; Holzenthal et al. 2007b; Kjer et al. 2016). Precisely, the monophyly is recovered only by the molecular analyses of Kjer and co-workers (Kjer et al. 2002, 2016). The adult and pupal head features presented here do not support this clade. Apart from that the monophyly of Hydroptilidae is supported by several apomorphic, but mainly homoplasious characters of the adult and pupal head (see Figs. 32, 38).

In conclusion, it has been shown that adult and pupal head structures are a pivotal source of informative characters addressing the internal relationships within the major trichopteran lineages Annulipalpia and Integripalpia. Furthermore, it became evident that the morphological features presented here best support the paraphyly of ‘Spicipalpia’ as hypothesized in the most recent higher level phylogeny of Kjer et al. (2016).

Additionally, the data favor Integripalpia as sister group to this spicipalpian assemblage. Several new apomorphic features of the adult and pupal head support these relationships. Nonetheless, a serious part of the supporting characters are reductions and several morphological features also support conflicting phylogenetic hypotheses. Therefore, the impact of this single character system should not be overestimated.

The presented data clearly show that detailed comparative investigations, especially on the internal anatomy of trichopterans, are very valuable help in the ongoing discussion of the higher level phylogeny of the group. It is also evident, that data based on this single character system are not sufficient to solve the problem of the systematic position of the enigmatic spicipalpian taxa.

Therefore, further character systems should be investigated in detail. It could be clearly demonstrated in several studies (e.g., Friedrich et al. 2008 [Coleoptera]; Friedrich & Beutel 2010a; Friedrich & Beutel 2010b [Mecoptera]) that thoracic structures or the insect postabdomen (e.g., Hünefeld et al. 2012) are quite useful to obtain characters, which help to address major questions in the higher level phylogeny of several endopterygote insect groups.

For a final evaluation, the presented data will be therefore added to a large morphological data matrix covering all life stages and body parts of Trichoptera generated in the framework of the DFG-founded project 'Trichopteran morphology in the age of phylogenomics' (FR3062/2-1).

The analysis of this comprehensive data set will very likely result in a better understanding of the basal branching pattern within Trichoptera.

4.3. Ground plan reconstruction

With the present study of skeletal features and the soft-tissue anatomy of 22 trichopteran representatives information for all major lineages of Trichoptera is now available.

The present data set shows remarkable intraordinal heterogeneity in several character complexes. Additionally, the still mainly unresolved phylogeny of Trichoptera impedes a thorough interpretation of the structural evolution within the group.

Nevertheless, the current state of knowledge allows for evaluation of the trichopteran and amphiesmenopteran ground plan condition for several head characters.

In Trichoptera the labrum and clypeus are inseparably fused forming a composite formation, the anteclypeolabrum (see above [4.1.2.]). In contrast, both structures are clearly separated in the lepidopteran lineage Micropterigidae (Hannemann 1956; Kristensen 2003). Consequently, the composite anteclypeolabrum of Trichoptera has to be regarded as an ground plan feature of the order.

Several lineages of Trichoptera are equipped with three ocelli (e.g., Philopotamidae), while ocelli are absent in several not closely related groups (e.g., Polycentropodidae; Brachycentridae; Malicky 2004). Ocelli are also a typical feature of most lepidopteran representatives (Kristensen 2003) and are therefore part of the amphiesmenopteran ground plan. Furthermore, the reduction of the median ocellus is a ground plan autapomorphy of Lepidoptera (Kristensen 2003). In contrast, with only one known exception (*Zumatrichia*, Malicky 1973) all trichopteran representatives are equipped with three ocelli. Consequently, the presence of three ocelli is a ground plan feature of Trichoptera and also of Amphiesmenoptera.

The tentorium of most trichopterans is Π-shaped (Neboiss 1991; pers. obs.), a condition also present in the 'basal' lepidopteran family Micropterigidae and which can therefore be interpreted as a plesiomorphic ground plan feature of Trichoptera (see also Kristensen 2003). In contrast, a plate-like corpotentorium is only present in Philopotamidae and most likely represents an autapomorphy of this annulipalpian lineage, which is paralleled in the non-glossatan lepidopteran families Agathiphagidae and Heterobathmiidae (Kristensen 2003).

The very short dorsal tentorial arms of Annulipalpia and some spicipalpian groups (Glossosomatidae and Hydroptilidae) most likely represent the ground plan condition of Amphiesmenoptera since the same condition is also present in primitive non-glossatan Lepidoptera (see KRISTENSEN 2003). Considering this, the well-developed and sclerotized dorsal tentorial arms of the integripalpian lineage Plenitentoria represent a secondary specialization of the group.

The ventral outgrowths of the anterior tentorial arm (= laminatentoria) are well developed and heavily sclerotized in several not closely related trichopteran taxa (e.g., Hydropsychidae; Hydrobiosidae). Nonetheless, the laminatentorium is only weakly developed in most annulipalpian representatives and lower lepidopterans (e.g., Micropterigidae; HANNEMANN 1956) indicating that this condition belongs to the amphiesmenopteran ground plan.

In the ground plan of Amphiesmenoptera (as in most other insects [WIPFLER et al. 2011]) the antenna is moved by four extrinsic muscles, primarily originating from the anterior tentorial arms. This pattern is retained in the ground plan of Trichoptera. Only M. tentorio-scapalis medialis (te-sc(m)) is completely reduced in the spicipalpian lineage Glossosomatidae. The loss of this muscle most likely represents a potential autapomorphy of the group.

Although the number of antennal muscles is quite constant among Trichoptera, shifts of the origin sites towards the head capsule occur in several taxa. These secondary modifications were found in distantly related taxa (e.g., Hydropsychidae [Annulipalpia] and Hydroptilidae [‘Spicipalpia’]) and are therefore regarded as independent developments (homoplasies). The shift of the origin site of M. tentorio-scapalis posterior towards the dorsal tentorial arm in all studied species of Plenitentoria (pers. obs.; CRICHTON 1957) very likely represents a secondary specialization and a further autapomorphy of this integripalpian group.

The antenna (i.e., scapus) articulates with the antennifer at the ventral margin of the antennal foramen in Annulipalpia and most spicipalpian representatives. A similar condition is present in the lower lepidopteran lineages (e.g., Micropterigidae) and therefore has to be regarded as a potential ground plan feature of Amphiesmenoptera. The ventrolateral and lateral position of the antennifer in other lineages of Trichoptera most likely represent secondary modifications. The ventrolateral position of the antennifer in Hydrobiosidae might represent a potential autapomorphy of this family.

The adult mandibular sclerite in the ground plan of Trichoptera is moderately sized and sclerotized, but it is certainly not suitable to process solid food (see above [4.1.8.]). This condition is retained in Annulipalpia and in the spicipalpian lineages (e.g., Rhyacophilidae). The mandibular sclerite is extremely reduced in size and sclerotization in Integripalpia (see CRICHTON 1957; pers. obs.), showing a distinct trend to the reduction of this chewing mouthpart within Trichoptera. It is assumed that the loss of the feeding function of the mandible is the reason for this reduction.

Although the adult mandible is not suitable to process solid food it is equipped with three well-developed pairs of mandibular muscles in all trichopteran lineages. The presence of these muscles of the mandible clearly represents a ground plan feature of Trichoptera. Furthermore, it could be demonstrated in the present study that the large adductor and abductor muscles are remarkably reduced during aging of the adults in distantly related groups (e.g., Hydropsychidae; Limnephilidae; see also Loosmann 2014; Pinkernell 2014). This reduction of the mandibular musculature during aging is also interpreted as an trichopteran ground plan feature.

Beneath the large cranial adductor and abductor muscles, a thin tentorio-mandibular muscle is present in several trichopteran lineages. The loss of this muscle in the integripalpian groups (e.g., Limnephilidae) can be interpreted as an autapomorphy of Integripalpia or one of its subgroups. Otherwise it may be a result of independent reductions.

The morphology of the digestive tract and its associated musculature is quite uniform throughout Trichoptera. Differences occur in the origin of the ventral cibarial dilators from below or from above the intraclypeal sulcus. The data at hand speak for an origin below the intraclypeal sulcus as the plesiomorphic condition in Trichoptera.

Furthermore, the postcerebral pharynx is equipped with a lateral dilator muscle, M. cranio-pharyngalis posterior in most spicipalpian lineages and the annulipalpian representative Polycentropodidae. The muscle is absent in Integripalpia and the remaining annulipalpians. Nonetheless, it is well developed in other endopterygote insect groups (e.g., Lepidoptera, Kristensen 2003; Mecoptera, Beutel & Baum 2008) and is added to the trichopteran ground plan.

The presence of a maxillary lobe comprising a large, chemoreceptive galea and a small median lacinia is part of the amphiesmenopteran ground plan (see also Kristensen 2003). These features are widely retained in the trichopteran ground plan (present in Rhyacophilidae and Annulipalpia), except for the loss of a free, well-developed lacinia.

A dististipital adductor originating from the anterior tentorial arm is present in almost all trichopteran lineages studied to date. As the muscle is regularly present in basal lepidopterans and other holometabolan insects (e.g., Hannemann 1956; Friedrich et al. 2013; Randolf el al. 2014) its occurrence in Trichoptera is plesiomorphic and part of the ordinal ground plan. Its absence in Phryganeidae might be autapomorphic for this family.

Furthermore, the presence of a cranio-stipital adductor muscle is a typical feature of the maxilla in Annulipalpia. It is also well developed in lower lepidopterans and is therefore assigned to the amphiesmenopteran ground plan. The muscle is independently reduced in several distantly related taxa of Trichoptera.

A stipito-lacinial flexor can also be assumed to be part of the ground plan of Amphiesmenoptera since it is well-developed in the non-glossatan moth lineage Micropterigidae (Hannemann 1956; Kristensen 2003) and in the majority of trichopteran lineages.

The number of maxillary palpomeres in the ground plan of Amphiesmenoptera is five (see Kristensen 2003) as it is in all Annulipalpia and ‘Spicipalpia’. The number of maxillary palpomeres is convergently reduced in males throughout Integripalpia (e.g., Plenitentoria: Limnephilidae, Phryganeidae, Brachycentridae; Brevitentoria: Sericostomatidae [Malicky 1973, 2004]).

The terminal segment of the maxillary palp is remarkably elongated in Annulipalpia. It is only slightly longer than the preceding fourth (i.e., second last) segment in other lineages of Trichoptera. In contrast, the terminal segment of the maxillary palp is much shorter than the preceding ones in lower lepidopterans (e.g., Micropterigidae; Hannemann 1956; Kristensen 2003). Considering the present data at hand it might be possible that the slightly elongated configuration present in spicipalpian and integripalpian lineages represents the trichopteran ground plan condition. Consequently, a quite elongated and flexible terminal segment of the maxillary palp might be a potential autapomorphy of annulipalpians. Nonetheless, it could not be excluded at all that the configuration observed in all annulipalpian lineages might represent the plesiomorphic condition in Trichoptera and hence a ground plan feature, which is convergently modified in spicipalpian and integripalpian lineages. This might be an plausible explanation since the maxillary palp of Ledipoptera seems to be quite dissimilar with the terminal segment being by far the shortest palpomere (see Hannemann 1956; Kristensen 2003). Additionally, the surface structure of the terminal segment in Annulipalpia is characterized by deep cuticular clefts resulting in an annulate appearance of this segment remarkably reminiscent to the surface structure of the second last segment in non-glossatan lepidopterans (see Kristensen 2003). Since these cuticular modifications appear on different palp segments they most likely represent independant secondary modifications in representatives of both insect groups.

The composite haustellum represents the only unequivocal trichopteran ground plan autapomorphy (see Kristensen 1997). The surface structure, i.e., the arrangement of microtrichia, varies notably between the major trichopteran lineages (see e.g., Klemm 1966; Crichton 1957; Neboiss 1991). Representatives of Integripalpia and Polycentropodidae exhibit longitudinal channels (Crichton 1957; Engvall 1993), whereas the spicipalpian lineages Hydroptilidae and Glossosomatidae show a more transverse arrangement (Kristensen 1997). The latter condition was interpreted as the ground plan condition of Trichoptera by Kristensen (1997), because a very similar arrangement of spines was observed in the infrabuccal pouches of non-glossatan moths. However, the condition of the annulipalpian haustellum does not fit well in this scenario. At the present state of knowledge it is uncertain if the annulipalpian small, granulose haustellum lost the channels secondarily (potential autapomorphy of Annulipalpia) or represents the plesiomorphic condition in Trichoptera. Detailed comparative studies on the haustellum, especially of the fine structure of the channels are needed to infer the homology of these structures in Amphiesmenoptera and to reconstruct the ground plan of Trichoptera.

The flexible roof of the salivarium, moved against the floor by a hypopharyngo-salivary dilator muscle, is usually present in all holometabolan lineages, where it originates from the hypopharynx (most Lepidoptera [Kristensen 2003], Neuroptera [Randolf et al. 2014], many dipterans [Schneeberg & Beutel 2011]) or from the ligula (Megaloptera; Röber 1942). Within Trichoptera this condition is only described for Philopotamidae and Hydropsychidae, but represents a plesiomorphic ground plan feature of the order. In other trichopteran lineages the origin site of the muscle is remarkably modified. It forms an intrasalivarial muscle running longitudinally along the roof of the salivarium in Integripalpia and Rhyacophilidae. A similar condition is also known from many mecopteran groups (e.g., Heddergott 1938; Grell 1938; Friedrich et al. 2013).

A further potential autapomorphy of Trichoptera is the insertion of the premental dilator muscle dorsally on the roof of the salivarium. The usual attachment sites of this muscle in other holometabolan insects (e.g., Neuropterida [Röber 1942, Randolf et al. 2014]; Hymenoptera [Vilhelmsen 1996]) are the lateral wall or the floor of the salivarium. As the muscle is absent in Lepidoptera (Hannemann 1956; Kristensen 2003) it cannot be assigned to the ground plan of Amphiesmenoptera.

The paired endite lobes of the labium are distinctly developed in Annulipalpia and Rhyacophilidae. Even though the homology to the lepidopteran paraglossa or ligula (Kristensen 2003) remains unclear (see above [4.1.13.]), the appendages certainly represent a trichopteran ground plan feature. In contrast, the loss of endite lobes in integripalpian lineages is the derived condition and maybe an apomorphy of the suborder.

4.4. Evolution of head structures in Trichoptera

In the trichopteran adult head several features of the generalized insect head (e.g., galea and lacinia; Snodgrass 1935) are inseparably fused. Especially the mouthparts are rather 'simple' from a functional point of view with major parts of mandibles and maxillae remarkably reduced. This fact is obviously correlated with the lifestyle of adult caddisflies. Usually, adults of Trichoptera life only for few weeks and the feeding activity is restricted to the uptake of liquids.

Within the trichopteran lineage most striking evolutionary trends are well visible in the haustellum, which is used for the uptake of liquid food (Malicky 1973; Crichton 1957). It is comparatively small and rather granulose in basalmost annulipalpians. In contrast, it is highly specialized in the integripalpian lineages showing quite derived character conditions like a regular system of haustellar channels enhancing the flow of liquids towards the preoral cavity. It is noteworthy that several representatives of Integripalpia (e.g., Limnephilidae) live for several months in order to overcome droughts during the summer time (e.g., Malicky 1973). Hence, in the evolutionary history of these groups the protrusible haustellum became remarkably enlarged and was equipped with a regular system of channels formed by microtrichia allowing them to feed on liquids. In contrast, many annulipalpian and spicipalpian representatives are quite short living with a haustellum being rather small and lack any channels on the surface of the haustellum.

Nonetheless, all Trichoptera possess a large precerebral pumping chamber equipped with several well-developed dilator muscles allowing for the uptake of liquid food. Additionally, trends in size reduction occur in the adult mandible with the mandibular sclerite being comparatively large and moderately sclerotized in the basalmost annulipalpian (e.g., Philopotamidae) and spicipalpian (e.g., Rhyacophilidae) lineages showing the plesiomorphic condition. The adult mandible is not used by the adult to process solid food and is therefore much reduced in size and level of sclerotization in several lineages of Integripalpia showing highly derived conditions in several character complexes.

Apart from its rather 'simple' mouth parts the trichopteran adult head is equipped with prominent antennae varying considerably in length between distantly related groups. The antenna is an important feature of the adult head since it is equipped with numerous sensory organs and most likely plays an important role in terms of swarming and mating behavior. Differences in the length of the antenna are obviously correlated with structural complexes of the antennal base between the major groups of Trichoptera.

Representatives of Integripalpia are equipped with a comparatively long antenna (e.g., three times longer than the forewing in leptocerids). Consequently, the extrinsic muscles of the antenna are strongly developed. The tentorium mainly serves as origin site of these muscles and is also massively developed and strongly sclerotized in many spicipalpian and especially in integripalpian representatives. Furthermore, the dorsal tentorial arm becomes strongly developed in Integripalpia and 'Spicipalpia'. It is even continuous with the head capsule in representatives of the integripalpian lineage Plenitentoria. Evolutionary modifications of the antennal complex also concern the cranio-scapal articulation. In most 'primitive' trichopterans (e.g., Polycentropodidae) the antennifer is located at the ventral margin of the antennal foramen, whereas it is positioned at the lateral margin in the integripalpian lineages representing the derived condition. Several evolutionary transformations occur in the antennal complex indicating a quite important role of this head appendage in the life of adult caddisflies information on its function are almost completely lacking. The absence of behavioral and ecological data in adults greatly impedes the interpretation of major evolutionary trends in adult head structures.

In the past studies on behavior and ecological preferences in Trichoptera are mainly focused on the larval stage (e.g., WEAVER & MORSE 1986; WARINGER & GRAF 2011). Accordingly, studies on the function of major structural complexes as well as behavioral data of adult caddisflies are strongly needed for a deeper understanding of evolutionary transformations in adults of Trichoptera.

5. Summary

Adult head structures of 22 caddisfly representatives covering all major trichopteran lineages were examined by using a combination of morphological techniques as histology, light microscopy, confocal laser scanning microscopy, scanning electron microscopy, and micro-computed tomography in combination with computer-based 3D-reconstruction.

In the first part of this dissertation, internal and external cephalic features of the annulipalpian representative *Philopotamus ludificatus* McLachlan, 1878 were described and illustrated in detail. Based on this description, comparative anatomical investigations on the other representatives were carried out leading to the largest set of morphological data for adult head structures within Trichoptera. This allowed for the first time to evaluate the homology of several sclerites and muscles, which were discussed over decades, but without final decision due to the lack of reliable information. The widely fused and inseparable sclerites of maxilla and labium led to different homology hypotheses. Further, intensively discussed are the identity of the maxillary endite lobes (galea or lacinia), the composition of the basal maxillary sclerites and the origin of the haustellum. Considering the literature, the detailed descriptions presented here allow for a thorough evaluation of these structures and a critical discussion of their complex identity.

Subsequently, a list of adult and pupal head structures is presented and analyzed cladistically. Furthermore, the data set is mapped on eight major phylogeny hypotheses published during the last decades.

The parsimony analysis of adult and pupal head features best supports the paraphyly of the spicipalpian lineages. Precisely, the spicipalpian families are closely related to Integripalpia, together forming the sister group of Annulipalpia. The monophyly of both, Annulipalpia and Integripalpia is well supported by the present data set. A series of new potential apomophies was identified.

Within Annulipalpia, Psychomyioidea (Psychomyiidae + Polycentropodidae) is supported by the unique origin of parts of the dorsal cibarial dilator muscle from the gena. A sister group relationship of Hydropsychidae + Psychomyioidea is also well supported (Musculus tentorio-scapalis medialis composed of two bundles; pupal mandible equipped with four subapical teeth). In contrast, the monophyly of Philopotamoidea (Philopotamidae + Stenopsychidae) is very weakly supported by adult and pupal head features.

Within Integripalpia, the present data set shows strong support for the monophyly of Plenitentoria and Brevitentoria, for which several new apomorphies were obtained. Sericostomatoidea and Leptoceroidea, subordinate taxa within the brevitentorian clade, are not supported herein. In contrast, within Plenitentoria the monophyly of Limnephiloidea (Brachycentridae + Goeridae + Limnephilidae) is strongly supported by several very unique characters of the adult head (M. clypeo-epipharyngalis lateralis composed of two bundles, M. clypeo-cibarialis dorsalis composed of three bundles). The monophyly of Phryganeoidea is only weakly supported by homoplasious characters. Among the spicipalpian lineages the frequently discussed Hydroptiloidea comprising Ptilocolepidae + Hydroptilidae is not supported by the present data set. The monophyly of Glossosomatidae (Glossosomatinae + Agapetinae) (absence of M. tentorio-scapalis medialis), Rhyacophilidae (labium equipped with small endite lobes), and Hydrobiosidae (Hydrobiosinae + Apsilochoreminae) (antennifer small and positioned at the ventrolateral edge of the circumantennal margin) are well-supported by adult and pupal head features.

The ground plan conditions of the

adult and pupal head in Trichoptera and Amphiesmenoptera are reconstructed for several characters.

The trichopteran ground plan contains a Π-shaped tentorium with short dorsal tentorial arms, moderately sized mandibles equipped with three well-developed muscles, a small but distinct lacinia, five-segmented maxillary palps, a small haustellum, and a falciform pupal mandible equipped with several subapical teeth. Additionally, the unusual configuration of the extrinsic dilator muscles of the salivarium is regarded as a potential autapomorphy of Trichoptera.

Adult head structures observed in the annulipalpian family Philopotamidae show a remarkable number of presumably plesiomorphic features, moderately developed and sclerotized, but functionless mandibles, a small protrusible haustellum without channels on its surface, extrinsic antennal muscles originating exclusively from the tentorium, a small lacinia closely associated with the mainly membranous galea (i.e., galeolacinia), extrinsic dorsal muscles of the salivarium originating from the hypopharynx and from the premental sclerite, respectively, and small labial endite lobes. Although, the comprehensive morphological data set of adult and pupal head structures allows for a thorough evaluation of cephalic ground plan features in Trichoptera for the first time, its impact to address major questions in the higher level phylogeny in Trichoptera is limited.

6. Zusammenfassung

Von insgesamt 22 Köcherfliegen-Vertretern, die alle Großgruppen der Köcherfliegen abdecken, wurden die Kopfstrukturen erwachsener Tiere mit Hilfe eines kombinierten Ansatzes unterschiedlicher Methoden wie beispielsweise Histologie, Lichtmikroskopie, konfokaler Laser-Scanning Mikroskopie, Rasterelektronenmikroskopie und Computertomographie in Kombination mit computergestützter 3D-Rekonstruktion analysiert.

Im ersten Abschnitt der Dissertation werden die inneren und äußeren Kopfstrukturen eines Vertreters der Annulipalpia (*Philopotamus ludificatus* McLachlan, 1878) ausführlich beschrieben und grafisch dargestellt. Basierend auf dieser Beschreibung werden vergleichend-anatomische Untersuchungen für die übrigen Vertreter durchgeführt, mit dem Ziel, einen umfangreichen morphologischen Datensatz von Kopfstrukturen der Köcherfliegen zu erstellen. Dies ermöglicht es zum ersten Mal, die Homologie verschiedener Sklerite und Muskeln zu klären, die über Jahrzehnte kontrovers diskutiert wurden. Jedoch gab es bisher keine abschließende Klärung aufgrund des Mangels verlässlicher Datengrundlagen.

Die einzelnen Sklerite von Maxille und Labium sind in mehreren Fällen miteinander verschmolzen und können nicht mehr eindeutig von einander getrennt werden, was zu verschiedenen Homologiehypothesen geführt hat.

Weiterhin wird die Identität der inneren Anhänge der Maxille als Galea oder Lacinia, die genaue Zusammensetzung der Sklerite an der Basis der Maxille und die Homologisierung des Haustellums diskutiert. Unter Einbezug der verfügbaren Literatur ermöglicht die äußerst genaue Beschreibung der einzelnen Strukturen eine tiefgreifende und umfassende morphologische Einordnung dieser Strukturen sowie nachfolgend eine kritische Diskussion ihrer Homologie.

Im Anschluss erfolgt die Herausarbeitung von Merkmalen des Erwachsenen- und Puppenkopfes, welche im Anschluss kladistisch analysiert werden. Diese Merkmale werden nachfolgend auf Grundlage von acht phylogenetischen Hypothesen zur Großgruppenphylogenie der Köcherfliegen, die innerhalb der letzten Jahrzehnte publiziert wurden, phylogenetisch analysiert.

Die durchgeführte Parsimonie-Analyse stützt hierbei vor allem eine Hypothese, die von einer paraphyletischen Stellung der ‚Spicipalpia‘ innerhalb der Köcherfliegen ausgeht. Demnach werden die paraphyletischen Familien der ‚Spicipalpia‘ in einer Stammlinie zusammen mit den monophyletischen Integripalpia vereint. Beide Gruppen bilden somit die Schwestergruppe zu den Annulipalpia. Durch den vorliegenden Datensatz wird eine monophyletische Stellung der Großgruppen Annulipalpia und Integripalpia sehr gut unterstützt. Weiterhin konnte eine Reihe neuer Apomorphien herausgearbeit und definiert werden.

Innerhalb der Annulipalpia ist die monophyletische Stellung des Taxons Psychomyioidea (Psychomyiidae + Polycentropodidae) durch den innerhalb der Köcherfliegen einzigartigen Ursprung des lateralen Muskelbündels des dorsalen cibarialen Dilator-Muskels von der vorderen Wand der Gena, direkt über der größtenteils membranösen Basis der Mandibel, sehr gut begründet. Weiterhin ist auch ein Schwestergruppenverhältnis zwischen den Annulipalpia-Taxa Hydropsychidae und Psychomyioidea sehr gut unterstützt (der Antennenmuskel Musculus tentorio-scapalis medialis besteht in dieser Gruppe aus zwei Bündeln und die Puppenmandibel weist insgesamt vier subapikale Zähnchen auf). Im Gegensatz dazu wird die monophyletische

Stellung des Taxons Philopotamoidea (Philopotamidae + Stenopsychidae) durch Merkmale der Kopfstrukturen im Erwachsenen- und Puppenstadium nur sehr schwach gestützt.

Und auch innerhalb der Großgruppe der Integripalpia lassen sich apomorphe Merkmale finden, die eine monophyletische Stellung der untergeordneten Taxa wie Plenitentoria und Brevitentoria sehr gut unterstützen. Innerhalb des Monophylums Brevitentoria lassen sich in der vorliegenden Studie hingegen keine apomorphen Merkmale, die die untergeordneten Taxa Sericostomatoidea und Leptoceroidea begründen würden, finden. Hingegen wird innerhalb der Schwestergruppe Plenitentoria das untegeordnete Taxon Limnephiloidea (Brachycentridae, Goeridae, Limnephilidae) sehr gut auf Grundlage apomorpher Merkmale des Erwachsenen- und Puppenkopfes begründet (der Muskel M. clypeo-epipharyngalis lateralis besteht aus zwei Bündeln und der Muskel M. clypeo-cibarialis dorsalis besteht innerhalb der Limnephiloidea aus drei Bündeln). Die Monophylie des Taxon Phryganeoidea wird hingegen nur schwach durch konvergente Merkmale unterstützt.

Durch den analysierten Datensatz wird innerhalb der ‚Spicipalpia'-Gruppen eine gemeinsame Abstammungslinie, die die Familien Ptilocolepidae und Hydroptilidae (Hydroptiloidea) umfasst, nicht unterstützt. Jedoch scheint der monophyletische Status der übrigen Familien wie den Glossosomatidae (Glossosomatinae + Agapetinae) (der Muskel M. tentorio-scapalis medialis ist komplett reduziert), Rhyacophilidae (das Labium trägt hier kleine innere Fortsätze zwischen der Basis der Labialpalpen) und den Hydrobiosidae (Hydrobiosinae + Apsilochoreminae) (der Antennifer ist hier vergleichsweise klein und entspringt in der ventrolateralen Ecke des die Antennenbasis umgebenden Randes der Kopfkapsel) auf Grundlage der untersuchten Kopfmerkmale sehr gut begründbar.

Weiterhin wird eine Rekonstruktion des Grundmusters von Kopfstrukturen des Erwachsenen- und Puppenstadiums von Köcherfliegen aber auch des übergeordneten Taxons Amphiesmenoptera für mehrere Merkmale vorgenommen.

Das Grundmuster der Köcherfliegen enthält demnach ein der Form nach dem griechischen Buchstaben Π ähnelndes Tentorium, welches mit relativ kurzen dorsalen Tentorialarmen ausgestattet ist. Die adulten Mandibeln sind vorhanden, aber nur mäßig entwickelt, sie sind mit jeweils drei gut entwickelten Muskeln ausgestattet. Weiterhin umfasst das Grundmuster des Köcherfliegenkopfes eine kleine aber deutlich erkennbare Lacinia als kleinen mesalen Fortsatz der Galeolacinia, einen fünf Segmente umfassenden Maxillarpalpus, ein vergleichsweise kleines Haustellum und eine sichelförmige Puppenmandibel, die mit mehreren subapikalen Zähnchen besetzt ist.

Weiterhin scheint die ungewöhnliche Anordnung der extrinsischen Dilator-Muskeln des Salivariums eine potentielle Synapomorphie des Taxons Trichoptera darzustellen. Insbesondere die Kopfstrukturen des Erwachsenstadiums der Familie Philopotamidae weisen eine erstaunliche Anzahl vermutlich ursprünglicher Merkmalszustände auf.

Hierzu zählen mäßig entwickelte und sklerotisierte aber funktionslose Mandibeln, ein kleines ausstülpbares Haustellum, das jedoch keine Kanälchen aufweist und extrinsische Antennenmuskeln, die in ihrem Ursprung ausschließlich auf das Tentorium beschränkt sind. Weiterhin weisen Vertreter der Familie Philopotamidae eine kleine Lacinia auf, die sehr eng mit der hauptsächlich membranösen Galea verbunden ist, sowie extrinsische dorsale Muskeln des Salivariums, die zum einen entlang des Hypopharynx und zum anderen auf dem Praementalsklerit entspringen als auch weiterhin kleine Fortsätze des Labiums, die zwischen der Basis der Labialpalpen entspringen. Zwar ermöglicht die vorliegende, umfangreiche Analyse von Kopfmerkmalen im Erwachsenen- und Puppenstadium die Herleitung des Grundmusters zahlreicher Kopfmerkmale der Köcherfliegen, jedoch erscheint die Eignung der herausgearbeiteten Merkmale zur Beantwortung von Fragen zur Großgruppenphylogenie der Köcherfliegen nur eingeschränkt geeignet.

7. References

Badcock, R.M. (1961): The morphology of some parts of the head and maxillo-labium in larval Trichoptera, with special reference to the Hydropsychidae. Transactions of the Royal Entomological Society of London **113** (10): 217–248.

Barnard, P., Ross, E. (2012): The adult Trichoptera (caddisflies) of Britain and Ireland. In: Wilson, M., Cymru, A. (Eds.): Handbooks for the Identification of British Insects, Volume 1, Part 17. FSC Publications, Telford: 192 pp.

Becker, G. (2005): Life cycle of *Agapetus fuscipes* (Trichoptera, Glossosomatidae) in a first-order upland stream in central Germany. Limnologica **35** (1–2): 52–60.

Beckmann, F., Donath, T., Fischer, J., Dose, T., Lippmann, T., Lottermoser, L., Martins, R.V., Schreyer, A. (2006): New developments for synchrotron-radiation-based microtomography at DESY. Proceedings of SPIE **6318**: 1–10.

Beckmann, F., Herzen, J., Haibel, A., Müller, B., Schreyer, A. (2008): High density resolution in synchrotron-radiation-based attenuation-contrast microtomography. Proceedings of SPIE **7078**: D-1–10.

Bernhard, C.G., Gemne, G., Sällström, J. (1970): Comparative ultrastructure of corneal surface topography in insects with aspects on phylogenesis and function. Zeitschrift für Vergleichende Physiologie **67**: 1–25.

Bernhard, C.G., Miller, W.H. (1962): A corneal nipple pattern in insect compound eyes. Acta Physiologica Scandinavica **56** (3–4): 385–386.

Beutel, R.G., Baum, E. (2008): A longstanding entomological problem finally solved? Head morphology of *Nannochorista* (Mecoptera, Insecta) and possible phylogenetic implications. Journal of Zoological Systematics and Evolutionary Research **46** (4): 346–367.

Beutel, R.G., Friedrich, F., Ge, S.-Q., Yang, X.-K. (2014): Insect Morphology and Phylogeny. Walter de Gruyter Berlin, Boston: 516 pp.

Beutel, R.G., Friedrich, F., Whiting, M.F. (2008): Head morphology of *Caurinus* (Boreidae, Mecoptera) and its phylogenetic implications. Arthropod Structure and Development **37**: 418–433.

Beutel, R.G., Vilhelmsen, L. (2007): Head anatomy of Xyelidae (Hexapoda: Hymenoptera) and phylogenetic implications. Organisms, Diversity and Evolution **7**: 207–230.

Blanke, A., Wipfler, B., Letsch, H., Koch, M., Beckmann, F., Beutel, R.G., Misof, B. (2012): Revival of Palaeoptera – head characters support a monophyletic origin of Odonata and Ephemeroptera (Insecta). Cladistics **28**: 560–581.

Busck, A., Böving, A. (1914): On *Mnemonica auricyanea* Walsingham. Proceedings of the Entomological Society of Washington **16**: 151–163.

Chamorro, M.L., Holzenthal, R.W. (2011): Phylogeny of Polycentropodidae Ulmer, 1903 (Trichoptera: Annulipalpia: Psychomyioidea) inferred from larval, pupal and adult characters. Invertebrate Systematics **25**: 219–253.

Chaudonneret, J. (1990): Les Piéces Buccales des Insectes. Thème et Variations. Édition hors Série du Bulletin Scientifique de Bourgogne. 255 pp.

Chuluunbat, S., Morse, J.C., Lessard, J.L., Benbow, M.E., Wesener, M.D., Hudson, J. (2010): Evolution of terrestrial habitat in *Manophylax* species (Trichoptera: Apataniidae), with a new species from Alaska. Journal of the North American Benthological Society **29** (2): 413–430.

Cowley, D.R. (1976): Family characteristics of the pupae of New Zealand Trichoptera. New Zealand Journal of Zoology **3**: 99–109.

Crichton, M.I. (1957): The structure and function of the mouth parts of adult caddis flies (Trichoptera). Philosophical Transactions of the Royal Society of London, Series B, Biological Sciences **241** (677): 45–91.

Crichton, M.I. (1989): A scanning electron microscope study of the mouth parts of adult *Phryganea grandis* (L.) (Trichoptera). Pp. 329–333. In: Tomaszewski, C. (Ed.): Proceedings of the 6th International Symposium on Trichoptera. Adam Mickiewicz Press, Poznan: 479 pp.

Crichton, M.I. (1992): A scanning electron microscope study of the mouth parts of some adult Limnephilidae (Trichoptera). Pp. 45–48. In: Otto, C. (Ed.): Proceedings of the 7th International Symposium on Trichoptera. Backhuys Publishers, Leiden: 312 pp.

Cummings, B.F. (1914): Note on the characters of the head and mouthparts in the genera *Plectrotarsus* and *Æthaloptera* (Trichoptera). Annals and Magazine of Natural History **14** (8): 22–31.

Deans, A.R., Mikó, I., Wipfler, B., Friedrich, F. (2012): Evolutionary phenomics and the emerging enlightenment of arthropod systematics. Invertebrate Systematics 26: 323–330.

De Moor, F.C., Ivanov, V.D. (2008): Global diversity of caddisflies (Trichoptera: Insecta) in freshwater. Hydrobiologia **595**: 393–407.

Demoulin, G. (1960): Quelques remarques sur la composition segmentaire de la tete des Insectes. Part I: Varations de la capsule céphalique de la larve à l'adulte, chez quelques insectes mécoptéroides. Bulletin Institut Royal des Sciences Naturelles de Belgique **36** (18): 1–12.

Denis, J.R., Bitsch, J. (1973): Morphologie de la tête des insectes. In: Grassé, P.P. (Ed.): Traité de Zoologie VIII(1). Masson et Cie, Paris: 593 pp.

Deoras, P.J. (1943): On the comparative morphology and evolution of adult Trichoptera. Part I: external Morphology. Indian Journal of Entomology **5**: 177–188.

Despax, R. (1951): Ordre des Trichoptères. Pp. 125–173. In: Grassé, P.P. (Ed.): Traité de Zoologie X(1–2). Masson et Cie, Paris: 1048 pp.

Dressler, C., Beutel, R.G. (2010): The morphology and evolution of the adult head of Adephaga (Insecta: Coleoptera). Arthropod Systematics and Phylogeny **68** (2): 239–287.

Drilling, K., Klass, K.-D. (2010): Surface structures of the antenna of Mantophasmatodea (Insecta). Zoologischer Anzeiger **249**: 121–137.

Durand, J.-B. 1955: Contribution a l'etude des Trichopteres de la Cote-d'Or. Travaux du Laboratoire de Zoologie et de la Station

Aquicole Grimaldi de la Faculté des Sciences de Dijon **9**: 1–45.

Ehlert, T. (2009): Flugaktivität, Eiablage und Habitatbindung von Köcherfliegen (Trichoptera) an Fließgewässern. Essener ökologische Schriften **27**: 169 pp.

Ehnbom, K. (1948): Studies on the central and sympathetic nervous system and some sense organs in the head of neuropteroid insects. Opuscula Entomologica Supplementum **8**: 1–162.

Engvall, M. (1993): Morphology of the Trichoptera haustellum. Unpublished project study under supervision of Kristensen, N.P. and Dahl, C. at Department of Zoology, Uppsala and Zoologisk Museum Copenhagen: 35 pp.

Faucheux, M.J. (2004): Antennal sensilla of Trichoptera and Lepidoptera: Phylogenetic considerations. Bulletin de l'Institut Royal des Sciences Naturelles de Belgique, Entomologie **74**: 69–71.

Flint, O.S. (1958): The larva and terrestrial pupa of *Ironoquia parvula* (Trichoptera, Limnephilidae). Journal of the New York Entomological Society **66** (1/2): 59–62.

Fotius-Jaboulet, M.-C. (1961): Squelette et Musculature Cephaliques de la Larva de *Drusus trifidus* Mac Lachlan (Trichoptera-Limnophilidae). Travaux du Laboratoire de Zoologie et de la Station Aquicole Grimaldi de la Faculté des Sciences de Dijon **40**: 1–54.

Frania, H.E., Wiggins, G.B. (1997): Analysis of morphological and behavioural evidence for the phylogeny and higher classification of Trichoptera (Insecta). Royal Ontario Museum Life Sciences Contributions **160**: 1–67.

Friedrich, F., Beutel, R.G. (2010a): Goodbye Halteria? The thoracic morphology of Endopterygota (Insecta) and its phylogenetic implications. Cladistics **26**: 1–34.

Friedrich, F., Beutel, R.G. (2010b): The thoracic morphology of *Nannochorista* (Nannochoristidae) and its implications for the phylogeny of Mecoptera and Antliophora. Journal of Zoological Systematics and Evolutionary Research **48** (1): 50–74.

Friedrich, F., Farrell, B.D., Beutel, R.G. (2008): The thoracic morphology of Archostemata and the relationships of the extant suborders of Coleoptera (Hexapoda). Cladistics **24**: 1–37.

Friedrich, F., Pohl, H., Beckmann, F., Beutel, R.G. (2013): The head of *Merope tuber* (Meropeidae) and the phylogeny of Mecoptera (Hexapoda). Arthropod Structure and Development **42**: 69–88.

Friedrich, F., Schulz, J., Kubiak, M., Beckmann, F., Wilde, F. (2015): The larval head anatomy of *Rhyacophila* (Rhyacophilidae) with discussion on mouthpart homology and the ground plan of Trichoptera. Journal of Morphology **276**: 1505–1524.

Graf, W., Murphy, J., Dahl, J., Zamora-Muńoz, C., López-Rodríguez, M. (2008): Volume 1. Trichoptera. In: Schmidt-Kloiber, A., Hering, D. (Eds.): Distribution and Ecological Preferences of European Freshwater Organisms. Pensoft Publishers, Sofia: 388 pp.

Grell, K.G. (1938): Der Darmtraktus von *Panorpa communis* L. und seine Anhänge bei der Larve und Imago (Ein Beitrag zur Anatomie und Histologie der Mecopteren). Zoologische Jahrbücher, Abteilung für

Anatomie und Ontogenie der Tiere **64**: 1–86.

Greving, I., Wilde, F., Ogurreck, M., Herzen, J., Hammel, J. U., Hipp, A., Friedrich, F., Lottermoser, L., Dose, T., Burmester, H., Müller, M., Beckmann, F. (2014): P05 Imaging Beamline at Petra III – First Results. Proceedings of SPIE 9212: 92120O-1–O-8.

González, M.A., Vieira-Lanero, R., Cobo, F. (2000): The immature stages of *Ptilocolepus extensus* McLachlan, 1884 (Trichoptera: Hydroptilidae: Ptilocolepinae) with notes on biology. Aquatic Insects **22** (1): 27–38.

Grimaldi, D., Engel, M.S. (2005): Evolution of the Insects. Cambridge University Press, New York: 755 pp.

Hagberg, M. (1986): Ultrastructure and central projections of extraocular photoreceptors in caddisflies (Insecta: Trichoptera). Cell and Tissue Research **245**: 643–648.

Hallberg, E., Hagberg, M. (1986): Ocellar fine structure in *Caenis robusta* (Ephemeroptera), *Trichostegia minor*, *Agrypnia varia*, and *Limnephilus flavicornis* (Trichoptera). Protoplasma **135**: 12–18.

Handlirsch, A., Beier, M. (1936): Trichoptera oder Köcherfliegen. Pp. 1491–1548. In: Kükenthal, W., Krumbach, T. (Eds.): Handbuch der Zoologie. IV. Band: Arthropoda – 2. Hälfte: Insecta. 2. Teil: Spezielles. Walter de Gruyter, Berlin, New York.

Hannemann, H.J. (1956): Die Kopfmuskulatur von *Micropteryx calthella* L. (Lep.). Morphologie und Funktion. Zoologische Jahrbücher, Abteilung für Anatomie und Ontogenie der Tiere **75**: 177–206.

Heddergott, H. (1938): Kopf und Vorderdarm von *Panorpa communis* L. Zoologische Jahrbücher, Abteilung für Anatomie und Ontogenie der Tiere **65**: 229–294.

Hennig, W. (1969): Die Stammesgeschichte der Insekten. Verlag von Waldemar Kramer, Frankfurt/M.: 436 pp.

Hickin, N.E. (1967): Caddis Larvae. Larvae of the British Trichoptera. Hutchinson & Co. Ltd., London: 476 pp.

Hinton, H.E. (1946): A new classification of insect pupae. Journal of Zoology **116** (2): 282–328.

Hinton, H.E. (1949): On the function, origin, and classification of pupae. Proceedings and Transactions of the South London Entomological and Natural History Society 1947–48: 111–154.

Hinton, H.E. (1958): The phylogeny of the panorpoid orders. Annual Review of Entomology **3**: 118–206.

Holzenthal, R.W., Blahnik, R.J., Prather, A.L., Kjer, K.M. (2007a): Order Trichoptera Kirby, 1813 (Insecta), Caddisflies. Zootaxa **1668**: 639–698.

Holzenthal, R.W., Blahnik, R.J., Kjer, K.M., Prather, A.L. (2007b): An update on the phylogeny of caddisflies (Trichoptera). Pp. 143–153. In: Bueno-Soria, J., Barba-Alvarez, R., Armitage, B. (Eds.): Proceedings of the 12th International Symposium on Trichoptera. The Caddis Press, Columbus, Ohio: 378 pp.

Holzenthal, R.W., Morse, J.C., Kjer, K.M. (2011): Trichoptera Kirby, 1813. In: Zhang, Z.-Q. (Ed.): Animal biodiversity: An outline of higher-level classification and survey of taxonomic richness. Zootoxa **3148**:

237 pp.

Hünefeld, F., Missbach, C., Beutel, R.G. (2012): The morphology and evolution of the female postabdomen of Holometabola (Insecta). Arthropod Structure and Development **41** (4): 361–371.

Ivanov, V.D. (1993): Principles of sexual communication in caddisflies (Insecta, Trichoptera). Pp. 609–626. In: Wiese, K., Gribakin, F.G., Popov, A.V., Renninger, G. (Eds.): Sensory Systems of Arthropods. Birkhäuser Verlag, Basel: 682 pp.

Ivanov, V.D. (1997): Rhyacophiloidea – a paraphyletic taxon. Pp. 189–193. In: Holzenthal, R.W., Flint Jr., O.S. (Eds.): Proceedings of the 8th International Symposium on Trichoptera. Ohio Biological Survey, Columbus: 496 pp.

Ivanov, V.D. (2002): Contribution to the Trichoptera phylogeny: new family tree with consideration of Trichoptera-Lepidoptera relations. Pp. 277–292. In: Mey, W. (Ed.): Proceedings of the 10th International Symposium on Trichoptera. Nova Supplementa Entomologica, Keltern **15**: 664 pp.

Ivanov, V.D., Kozlov, M.V. (1987): Comparative analysis of pterothoracic musculature of caddisflies (Insecta, Trichoptera). Zoologicheskii Zhurnal **66**: 1484–1497.

Johanson, K.A., Pham, H.-T. (2011): Three new species of *Helicopsyche* (Trichoptera, Helicopsychidae) from northern Vietnam, with a key to *Helicopsyche* species of Vietnam. European Journal of Taxonomy **6**: 1–10.

Kéler, S. von (1955): Entomologisches Wörterbuch mit besonderer Berücksichtigung der morphologischen Terminologie. Akademie-Verlag, Berlin: 679 pp.

Kirby, W. (1815): Strepsiptera, a new order of insects proposed and the characters of the order with those of its genera laid down. Transactions of the Linnean Society of London **11**: 86–122.

Kjer, K.M., Blahnik, R.J., Holzenthal, R.W. (2001): Phylogeny of Trichoptera (Caddisflies): Characterization of Signal and Noise Within Multiple Datasets. Systematic Entomology **50**: 781–816.

Kjer, K.M., Blahnik, R.J., Holzenthal, R.W. (2002): Phylogeny of caddisflies (Insecta, Trichoptera). Zoologica Scripta **31**: 83–91.

Kjer, K.M., Thomas, J.A., Zhou, X., Frandsen, P.B., Prendini, E., Holzenthal, R.W. (2016): Progress on the phylogeny of caddisflies (Trichoptera). Zoosymposia **10**: 248–256.

Klass, K.-D., Eulitz, U. (2007): The tentorium and anterior head sulci in Dictyoptera and Mantophasmatodea (Insecta). Zoologischer Anzeiger **246**: 205–234.

Kleinteich, T., Beckmann, F., Herzen, J., Summers, A. P., Haas, A. (2008): Applying X-ray tomography in the field of vertebrate biology: form, function, and evolution of the skull of caecilians (Lissamphibia: Gymnophiona). Proceedings of SPIE 7078: 70780D-1–D10.

Klemm, N. (1966): Die Morphologie des Kopfes von *Rhyacophila* Pict. (Trichoptera). Zoologische Jahrbücher, Abteilung für Anatomie und Ontogenie der Tiere **83**: 1–51.

Krafka, J. (1923): Morphology of the head of trichopterous larvæ as a basis for the revision of the family relationships. Journal of the New York Entomological Society **31** (1): 31–52.

Kristensen, N.P. (1981): Phylogeny of insect orders. Annual Review of Entomology **26**: 135–157.

Kristensen, N.P. (1991): Phylogeny of extant Hexapods. A textbook for students and research workers. Pp. 125–140. In: CSIRO (Ed.): The Insects of Australia. Second Edition, Volume 1. Cornell University Press, Ithaca, NY: 542 pp.

Kristensen, N.P. (1997): Early evolution of the Lepidoptera + Trichoptera lineage: phylogeny and the ecological scenario. In: Grandcolas, P. (Ed.): The Origin of Biodiversity in Insects: Phylogenetic Tests of Evolutionary Scenarios. Mémoires du Muséum d'Histoire Naturelle **173**: 253–271.

Kristensen, N.P. (1999): Phylogeny of endopterygote insects, the most successful lineage of living organisms. European Journal of Entomology **96**: 237–253.

Kristensen, N.P. (2003): Skeleton and muscles: adults. Pp. 39–131. In: Kristensen, N.P. (Volume Ed.): Handbuch der Zoologie. Band IV: Arthropoda: Insecta. Teilband 36: Lepidoptera, Moths and Butterflies. Volume 2: Morphology, Physiology, and Development. Walter de Gruyter, Berlin, New York: 564 pp.

Kristensen, N.P., Nielsen, E.S. (1979): A new subfamily of micropterigid moths from South America. A contribution to the morphology and phylogeny of the Micropterigidae, with a generic catalogue of the family (Lepidoptera: Zeugloptera). Steenstrupia **5** (7): 69–147.

Kubiak, M., Beckmann, F., Friedrich, F. (2015): The adult head of the annulipalpian caddisfly *Philopotamus ludificatus* McLachlan, 1878 (Philopotamidae), mouthpart homologies, and implications on the ground plan of Trichoptera. Arthropod Systematics and Phylogeny **73** (3): 351–384.

Lepneva, S.G. (1964): Trichoptera (Rucheiniki). Larvae and pupae of Annulipalpia. In: Pavlovskii, E.N. (Ed.): Fauna of the U.S.S.R. (Fauna SSSR). Volume II, No. 1. Zoological Institute of the Academy of Sciences of the USSR, Moskva, Leningrad. English in: Israel Program for Scientific Translations, Jerusalem (1970): 638 pp.

Lepneva, S.G. (1966): Trichoptera (Rucheiniki). Larvae and pupae of Integripalpia. In: Bykhovskii, B.E. (Ed.): Fauna of the U.S.S.R. (Fauna SSSR). Volume II, No. 2. Zoological Institute of the Academy of Sciences of the USSR, Moskva, Leningrad. English in: Israel Program for Scientific Translations, Jerusalem (1971): 700 pp.

Loosmann, L.M. (2014): Untersuchungen zur Entwicklung der postlarvalen Mandibelmuskulatur von *Hydropsyche pellucidula*. Unpublished Bachelor thesis at the University of Hamburg: 38 pp.

Lucas, R. (1893): Beiträge zur Kenntnis der Mundwerkzeuge der Trichoptera. Archiv für Naturgeschichte **59**: 285–330.

Macan, T.T., Worthington, C.J. (1973): A Key to the Adults of the British Trichoptera. Freshwater Biological Association Scientific Publication **28**: 151 pp.

Mackay, R.J., Wiggins, G.B. (1979): Ecological diversity in Trichoptera. Annual Review Entomology **24**: 185–208.

MADDISON, W.P., MADDISON, D.R. (2011): Mesquite: A Modular System for Evolutionary Analysis. Version 3.0.4. http://mesquiteproject.org.

MAKI, T. (1938): Studies on the thoracic musculature of insects. Memoirs of the Faculty of Science and Agriculture, Taihoku Imperial University **24**: 1–65.

MALICKY, H. (1973): Trichoptera (Köcherfliegen). In: HELMCKE, J.-G., STARK, D., WERMUTH, H. (Eds.): Handbuch der Zoologie. IV. Band: Arthropoda – 2. Hälfte: Insecta. 2. Teil: Spezielles. Walter de Gruyter, Berlin, New York: 114 pp.

MALICKY, H. (2000): Notes on the taxonomy of *Rhadicoleptus*, *Ptilocolepus* and *Pseudoneureclipsis*. Braueria **28**: 19–20.

MALICKY, H. (2004): Atlas of European Trichoptera. Second Edition. Springer Dordrecht, Norwell: 359 pp.

MALICKY, H. (2005): Ein kommentiertes Verzeichnis der Köcherfliegen (Trichoptera) Europas und des Mediterrangebietes. Linzer Biologische Beiträge **37** (1): 533–596.

MALICKY, H. (2010): Atlas of Southeast Asian Trichoptera. Biology Department, Faculty of Science, Chiang Mai University, Chiang Mai: 346 pp.

MALM, T., JOHANSON, K.A., WAHLBERG, N. (2013): The evolutionary history of Trichoptera (Insecta): A case of successful adaptation to life in freshwater. Systematic Entomology **38** (3): 459–473.

MARTYNOV, A.V. (1924): Rucheiniki. In: BOGDANOVA-KAT'KOVA, N.N. (Ed.): Prakticheskaya Entomologiya **5**: 384 pp.

MATSUDA, R. (1965): Morphology and evolution of the insect head. Memoirs of the American Entomological Institute **4**: 1–240.

MELNITSKY, S.I., IVANOV, V.D. (2011): Structure and localization of sensilla on antennae of caddisflies (Insecta: Trichoptera). Journal of Evolutionary Biochemistry and Physiology **47** (6): 593–602.

MEYER-ROCHOW, V.B., STRINGER, I. (1993): A system of regular ridges instead of nipples on a compound eye that has to operate near the diffraction limit. Vision Research **33** (18): 2645–2647.

MICHELS, J. (2007): Confocal laser scanning microscopy: using cuticular autofluorescence for high resolution morphological imaging in small crustaceans. Journal of Microscopy **238**: 95–101.

MISOF, B., LIU, S., MEUSEMANN, K., PETERS, R.S., DONATH, A., MAYER, C., FRANDSEN, P.B., WARE, J., FLOURI, T., BEUTEL, R.G., NIEHUIS, O., PETERSEN, M., IZQUIERDO-CARRASCO, F., WAPPLER, T., RUST, J., ABERER, A.J., ASPÖCK, U., ASPÖCK, H., BARTEL, D., BLANKE, A., BERGER, S., BÖHM, A., BUCKLEY, T.R., CALCOTT, B., CHEN, J., FRIEDRICH, F., FUKUI, M., FUJITA, M., GREVE, C., GROBE, P., GU, S., HUANG, Y., JERMIIN, L. S., KAWAHARA, A.Y., KROGMANN, L., KUBIAK, M., LANFEAR, R., LETSCH, H., LI, Y., LI, Z., LI, J., LU, H., MACHIDA, R., MASHIMO, Y., KAPLI, P., MCKENNA, D.D., MENG, G., NAKAGAKI, Y., NAVARRETE-HEREDIA, J.L., OTT, M., OU, Y., PASS, G., PODSIADLOWSKI, L., POHL, H., VON REUMONT, B.M., SCHÜTTE, K., SEKIYA, K., SHIMIZU, S., SLIPINSKI, A., STAMATAKIS, A., SONG, W., SU, X., SZUCSICH, N.U., TAN, M., TAN, X., TANG, M., TANG, J., TIMETHALER, G., TOMIZUKA, S., TRAUTWEIN, M., TONG, X., UCHIFUNE, T., WALZL, M.G., WIEGMANN, B.M., Wilbrandt, J., Wipfler, B., Wong, T.K.F., Wu, Q., Wu, G., Xie, Y., Yang, S., Yang, Q., Yeates, D.K., Yoshizawa, K., Zhang, Q., Zhang, R., Zhang, W., Zhang, Y., Zhao, J., Zhou, C., Zhou, L., Ziesmann, T., Zou, S., Li, Y., Xu, X., Zhang, Y., Yang, H., Wang, J., Wang, J., Kjer, K.M., Zhou, X. (2014): Phylogenomics resolves the timing and pattern of insect evolution. Science **346** (6210): 763−767.

Mickoleit, G. (1971): Das Exoskelett von *Notiothauma reedi* MacLachlan, ein Beitrag zur Morphologie und Phylogenie der Mecoptera (Insecta). Zeitschrift für Morphologie der Tiere **69**: 318–362.

Moretti, G. (1983): Tricotteri (Trichoptera). Guide per il riconoscimento delle specie animali delle acque interne italiane **19**: 1–155.

Moretti, G.P., Corallini Sorcetti, C., Gattaponi, P. (1981): Trichoptera in the intestinal content of certain fish species. Pp. 243–247. In: Moretti, G.P. (Ed.): Proceedings of the 3rd International Symposium on Trichoptera. Dr. W. Junk Publishers, The Hague, Boston, London: 472 pp.

Morse, J.C. (1997): Phylogeny of Trichoptera. Annual Review of Entomology **42**: 427–450.

Moulins, M. (1971): La cavité préorale de *Blabera craniifer* Burm. (Insecte, Dictyoptére) et son innervation: Etude anatomo-histologique de l'epipharynx et l'hypopharynx. Zoologische Jahrbücher, Abteilung für Anatomie und Ontogenie der Tiere **88** (4): 527–586.

Neboiss, A. (1986): Atlas of Trichoptera of the SW Pecific – Australian Region. Dr. W. Junk Publishers, Dordrecht, Boston, Lancaster: 286 pp.

Neboiss, A. (1991): Comparative study of tentorial structures in caddisflies (Trichoptera). Pp. 283–290. In: Tomaszewski, C. (Ed.): Proceedings of the 6th International Symposium on Trichoptera. Adam Mickiewicz University Press, Poznań: 479 pp.

Nielsen, E.S., Kristensen, N.P. (1996): The Australian moth family Lophocoronidae and the basal phylogeny of the Lepidoptera-Glossata. Invertebrate Taxonomy **10**: 1199–1302.

Nixon, K.C. (1999-2002): WinClada ver. 1.000. Published by the author, Ithaca, NY, USA.

Novak, K., Sehnal, F. (1963): The development cycle of some species of the genus *Limnephilus* (Trichoptera). Acta Societatis Entomologicae Cechosloveniae **60**: 68–80.

Oláh, J., Johanson, K.A. (2007): Trinominal terminology for cephalic setose warts in Trichoptera (Insecta). Braueria **34**: 43–50.

Pinkernell, A. (2014): Entwicklung der postlarvalen Mandibelmuskulatur von *Limnephilus flavicornis*. Unpublished Bachelor thesis at the University of Hamburg: 41 pp.

Pitsch, T. (1993): Zur Larvaltaxonomie, Faunistik und Ökologie mitteleuropäischer Fließwasser-Köcherfliegen (Insecta: Trichoptera). Landschaftsentwicklung und Umweltforschung – Schriftenreihe des Fachbereichs Landschaftsentwicklung – Sonderheft S 8, Technische Universität Berlin: 316 pp.

Pohl, H. (2010): A scanning electron microscopy specimen holder for viewing different angles of a single specimen. Microscopy Research and Technique **73**: 1073–1076.

Pryor, M.G.M. (1951): On the abdominal appendages of larvae of Trichoptera, Neuroptera, and Lepidoptera, and the origin of jointed limbs. Quarterly Journal of Microscopical Science **42**: 351–376.

Randolf, S., Zimmermann, D., Aspöck, U. (2014): Head anatomy of adult *Nevrorthus apatelios* and basal splitting events in Neuroptera (Neuroptera: Nevrorthidae). Arthropod Systematics and Phylogeny **72** (2): 111–136.

Resh, V.H., Flynn, T.S., Lamberti, G.A., McElravy, E.P., Sorg, K.L., Wood, J.R. (1981): Responses of the sericostomatid caddisfly *Gumaga nigricula* (McL.) to environmental disruption. Pp. 311–318. In: Moretti, G.P. (Ed.): Proceedings of the 3rd International Symposium on Trichoptera. Dr. W. Junk Publishers, The Hague, Boston, London: 472 pp.

Riek, E.F. (1976): The marine caddisfly family Chathamiidae (Trichoptera). Australian Journal of Entomology **15** (4): 405–419.

Ross, H.H. (1956): Evolution and Classification of the Mountain Caddisflies. The University of Illinois Press, Urbana: 213 pp.

Ross, H.H. (1964): Evolution of caddisworm cases and nets. American Zoologist **4**: 209–220.

Ross, H.H. (1967): The evolution and past dispersal of the Trichoptera. Annual Review of Entomology **12**: 169–206.

Röber, H. (1942): Morphologie des Kopfes und des Vorderdarmes der Larve und Imago von *Sialis flavilatera*. Zoologische Jahrbücher, Abteilung für Anatomie und Ontogenie der Tiere **67**: 61–118.

Schmid, F. (1980): Les Insectes et Arachnides du Canada. Partie 7. Genera des Trichoptéres du Canada et des États adjacents. Agriculture Canada, Publication **1692**: 296 pp.

Schmid, F. (1989): Les Hydrobiosids (Trichoptera, Annulipalpia). Bulletin de l'Insitut Royal des Sciences Naturelles de Belgique, Entomologie **59** Supplement: 154 pp.

Schmid, F. (1998): Genera of the Trichoptera of Canada and Adjoining or Adjacent United States. In: Haynes, R.H. (Ed.): The Insects and Arachnids of Canada. Part 7. NRC Research Press, Ottawa, Ontario, Canada: 319 pp.

Schneeberg, K., Beutel, R.G. (2011): The adult head structures of Tipulomorpha (Diptera, Insecta) and their phylogenetic implications. Acta Zoologica **92**: 316–343.

Silvenius, A.J. (1906): Über den Laich der Trichopteren. Acta Societatis pro Fauna et Flora Fennica **28**: 1–128.

Snodgrass, R.E. (1935): Principles of Insect Morphology. McGraw-Hill Book Company, New York, London: 667 pp.

Snodgrass, R.E. (1963): A contribution toward an encyclopedia of insect anatomy. Smithsonian Miscellaneous Collections **146**: 1–48.

Spangenberg, R., Friedemann, K., Weirauch, C., Beutel, R.G. (2013): The head morphology of the potentially basal heteropteran lineages Enicocephalomorpha and Dipsocoromorpha (Insecta: Hemiptera: Heteroptera). Arthropod Systematics and Phylogeny **71** (2): 103–136.

Spinelli Batta, G., Moretti, G.P. (1987): The clinging apparatus of Trichoptera pupae: number, structure, and SEM observations of the denticulations on the urotergal plates. Pp. 11–17. In: Bournaud, M., Tachet, H. (Eds.): Proceedings of the 5th International Symposium on Trichoptera. Dr. W. Junk Publishers, Dordrecht, Boston, Lancaster: 397 pp.

Tillyard, R.J. (1923): On the mouth parts of the Micropterygoidea (Lep.). Transactions of the Entomological Society of London 1923: 181–206.

Tindall, A.R. (1963): The skeleton and musculature of the thorax and limbs of the larva of *Limnephilus* sp. (Trichoptera: Limnephilidae). Transactions of the Royal Entomological Society of London **115**: 409–477.

Tindall, A.R. (1964): The skeleton and musculature of the larval thorax of *Triaenodes bicolor* Curtis (Trichoptera: Leptoceridae). Transactions of the Royal Entomological Society of London **116**: 151–210.

Tindall, A.R. (1965): The functional morphology of the thorax of *Limnophilus marmoratus* Curtis (Trichoptera: Limnephilidae). Transactions of the Royal Entomological Society of London **117**: 127–166.

Unzicker, J.D., Resh, V.H., Morse, J.C. (1982): Trichoptera. Pp. 1–138. In: Brigham, A.R., Brigham, W.U., Gnilka, A. (Eds.): Aquatic Insects and Oligochaetes of North and South Carolina 9. Midwest Aquatic Enterprises, Mahomet: 837 pp.

Vilhelmsen, L. (1996): The preoral cavity of lower Hymenoptera (Insecta): comparative morphology and phylogenetic significance. Zoologica Scripta **25** (2): 143–170.

Wagner, R. (1990): A laboratory study on the life cycle of *Sericostoma personatum* (Kirby & Spence), and light dark-dependent food consumption. Hydrobiologica **208** (3): 201–212.

Wallace, I.D., Wallace, B., Philipson, G.N. (2003): Keys to the case-bearing caddis larvae of Britain and Ireland. Freshwater Biological Association Scientific Publication **61**: 259 pp.

Waringer, J., Graf, W. (2011): Atlas der mitteleuropäischen Köcherfliegenlarven. Erik Mauch Verlag, Dinkelscherben: 468 pp.

Weaver III, J.S. (1984): The evolution and classification of Trichoptera. Part I: The groundplan of Trichoptera. Pp. 413–419. In: Morse, J.C. (Ed.): Proceedings of the 4th International Symposium on Trichoptera. Dr. W. Junk Publishers, The Hague: 486 pp.

Weaver III, J.S. (1992a): Remarks on the evolution of Trichoptera: a critique of Wiggins and Wichard's classification. Cladistics **8**: 171–180.

Weaver III, J.S. (1992b): Further remarks on the evolution of Trichoptera: a reply to Wiggins. Cladistics **8**: 187–190.

Weaver III, J.S., Morse, J.C. (1986): Evolution of feeding and case-making behavior in Trichoptera. Journal of the North American Benthological Society **5**: 150–158.

Wenk, P. (1953): Der Kopf von *Ctenocephalus canis* (Curt.) (Aphaniptera). Zoologische Jahrbücher Abteilung für Anatomie und Ontogenie der Tiere **73**: 103–164.

Wiggins, G.B., Gall, W.K. (1992): The Asian caddisfly family Phryganopsychidae:

phylogenetic novelty or relict? Pp. 149–154. In: Otto, C. (Ed.): Proceedings of the 7th International Symposium on Trichoptera. Backhuys Publishers, Leiden: 312 pp.

Wiggins, G.B. (1992): Comments on the phylogeny of pupation behavior in Trichoptera: a response to Weaver. Cladistics **8**: 171–185.

Wiggins, G.B. (2004): Caddisflies. The Underwater Architects. NRC Research Press, Toronto, Buffalo, London: 291 pp.

Wiggins, G.B., Weaver III, J.S., Unzicker, J.D. (1985): Revision of the caddisfly family Uenoidae (Trichoptera). The Canadian Entomologist **117** (6): 763–800.

Wiggins, G.B., Wichard, W. (1989): Phylogeny of pupation in Trichoptera, with proposals on the origin and higher classification of the order. Journal of the North American Benthological Society **8**: 260–276.

Wichard, W. (1989): Anpassung der Köcherfliegen (Trichoptera) an periodische Gewässer. Verhandlungen Westdeutscher Entomologentag 1988: 79–88.

Wichard, W. (1991): The evolutionary effect of overcoming osmosis in Trichoptera. Pp. 337–342. In: Tomaszewski, C. (Ed.): Proceedings of the 6th International Symposium on Trichoptera. Adam Mickiewicz University Press, Poznań: 479 pp.

Wichard, W., Arens, W., Eisenbeis, G. (1995): Atlas zur Biologie der Wasserinsekten. Gustav Fischer Verlag Stuttgart, Jena, New York: 338 pp.

Wichard, W., Klein, H.P., Herter, P. (1997): Pupal cocoon of Amphiesmenoptera (Lepidoptera + Trichoptera) with evolutionary considerations of the Trichoptera. Pp. 475–480. In: Holzenthal, R.W., Flint Jr., O.S. (Eds.): Proceedings of the 8th International Symposium on Trichoptera. Ohio Biological Survey, Columbus: 496 pp.

Wichard, W., Schmidt, H.H., Wagner, R. (1993): The semipermeabilty of the pupal cocoon of *Rhyacophila* (Trichoptera: Spicipalpia). Pp. 25–27. In: Otto, C. (Ed.): Proceedings of the 7th International Symposium on Trichoptera. Backhuys Publishers, Leiden: 312 pp.

Wichard, W., Wagner, R. (2015): Die Köcherfliegen (Trichoptera) – Die Neue Brehm-Bücherei 512. 4., vollständig überarbeitete und erweiterte Auflage. VerlagsKG Wolf, Magdeburg: 180 pp.

Wilde, F., Ogurreck, M., Greving, I., Hammel, J.U., Beckmann, F., Hipp, A., Lottermoser, L., Khokhriakov, I., Lytaev, P., Dose, T., Burmester, H., Müller, M., Schreyer, A. (2016): Micro-CT at the Imaging Beamline P05 at PETRA III. AIP Conference Proceedings **1741**, 030035 (2016); doi: 10.1063/1.4952858: 4 pp.

Winkler, D. (1959): Die Muskulatur der Larve von *Limnophilus flavicornis* Fabr. (Trichopt., Limnophilidae). Deutsche Entomologische Zeitschrift **6** (1–3): 112–128.

Winterbourn, M.J., Anderson, N.H. (1980): The life history of *Philanisus plebejus* Walker (Trichoptera: Chathamiidae), a caddisfly whose eggs were found in a starfish. Ecological Entomology **5**: 293–303.

Wipfler, B., Machida, R., Müller, B., Beutel, R.G. (2011): On the head morphology of Grylloblattodea (Insecta) and the systematic position of the order, with a new nomenclature for the head muscles of Dicondylia. Systematic Entomology **36** (2): 241–266.

8. Acknowledgements

First of all I am very grateful to Dr. Frank Friedrich (University of Hamburg) for his great supervision during the last years. It's been a great honor for me and I appreciated the fact that you always took time to discuss homology concepts as well as major issues in the phylogeny of Trichoptera with me. And, of course, for all the other fruitful discussions beside the Trichoptera. Furthermore, I thank you really much for your technical advice and guidance in morphological techniques and methods, your dedication in getting financial support for the present study and your tremendous efforts in improving the manuscript of head structures of *Philopotamus*, as well as your helpful comments during the preparation of my conference presentations.

I am also deeply grateful to Prof. Dr. Susanne Dobler (University of Hamburg) for her great supervision during the last years since I began to study topics of evolutionary biology in her lab almost eight years ago. I really thank you for opening me the great opportunity to work on the fascinating topic of my dissertation at the University of Hamburg and your enormous help in getting a grant in the early stage of the present project.

I deeply acknowledge the great support of Dr. Ralph S. Peters (University of Bonn) during the preparation of the major concept of the present project and his tremendous involvement in getting financial support.

I am very grateful to Univ.-Prof. Dr. Hans Malicky (Lunz am See, Austria) for his help during the collecting of *P. ludificatus* and also for providing me additional material from his valuable collection. Prof. Dr. Niels Peder Kristensen (†) (University of Copenhagen) helped to improve the manuscript of head structures of *Philopotamus* during numerous fruitful discussions about the morphology of Amphiesmenoptera. His outstanding contribution is greatly acknowledged. Furthermore, I thank Dr. Wolfram Mey (Museum für Naturkunde, Berlin), Brian J. Smith (National Institute of Water and Atmospheric Research, Hamilton, New Zealand), Alice Wells (Department of Sustainability, Water, Population and Communities, Canberra, Australia), and Prof. Dr. Karl Kjer (University of California, Davis) for providing me with valuable caddisfly voucher material. I thank Dr. Klaus-Dieter Klass (Senckenberg Naturhistorische Sammlungen, Dresden) and Dr. Benjamin Wipfler (University of Jena) for helpful comments which greatly improved the manuscript of head structures of *Philopotamus*.

The technical assistance of Rommy Petersohn (University of Jena) and Sabine Gaude (University of Hamburg) for the preparation of histological section series, and Renate Walter (University of Hamburg) for the preparation of SEM samples and her help with the digitalization of histological section series is greatly acknowledged.

I also thank the team of the entomology and arachnology section (Dr. Martin Husemann, Dr. Danilo Harms, Dr. Markus Koch (now University of Bonn), Dr. Hossein Rajaei (now Staatliches Museum für Naturkunde, Stuttgart), Dr. Andreas Wessel (now Museum für Naturkunde, Berlin), Dr. Nikola Szucsich (now Naturhistorisches Museum Wien), Dr. Frank Wieland (now Pfalzmuseum für Naturkunde, Bad Dürkheim), Dr. Hieronymus Dastych, Kai Schütte, Thure Daalsgard, and Ilona Rehmann) for technical assistance and for offering me a pleasant working atmosphere at the University of Hamburg.

Furthermore, I am grateful to our undergraduate students Annika Pinkernell, Lena M. Loosmann, and Johannes Schulz for being part of the project and for providing us useful morphological data on head structures in Trichoptera.

The technical support by the DESY facility, Hamburg (Dr. Felix Beckmann, Dr. Fabian Wilde, Dr. Jörg U. Hammel, and Dr. Imke Greving) (project numbers: I-20070032; I-20100317; I-20120676; I-20140725) for obtaining high quality SR-µCT-data at storage ring DORIS III and PETRA IV is greatly acknowledged.

I thank Prof. Dr. Rolf G. Beutel (University of Jena) for offering me the opportunity to use Bitplane Imaris software in his lab.

Dr. Martin Husemann and Prof. Dr. Patrick Danley (Baylor University, Waco, USA) corrected the English version of the text. This is also highly appreciated.

The financial support by the European Commission's (FP 7) Integrated Infrastructure Initiative programme SYNTHESYS (DK-TAF-4052) which offered me the possibility to travel to Copenhagen for a research stay in the lab of Prof. Dr. Niels Peder Kristensen (†) is kindly appreciated.

The financial support for the project provided by the Deutsche Forschungsgemeinschaft (DFG) (FR 3062/2-1) is also greatly acknowledged.

I am very grateful to my former housemate, Dr. Christiane Bramer (University of Göttingen) for supporting me with technical assistance, but especially with numerous appreciative discussions and for being a good and faithful friend outside the University.

I am very grateful to Swantje Grabener for being always a reliable, great support and for having always a sympathetic ear for all the trichopteran stuff of my dissertation, especially during the last months.

Thank you Swantje, that you are every day a non-equalled source of inspiration to my work and my life! Last but not least I really want to thank my friends and especially my family for their tremendous support during the time of my thesis by offering me a lot of patience and appreciation.

Declaration on oath [Eidesstattliche Versicherung]

I hereby declare, on oath, that I have written the present dissertation by my own and have not used other than the acknowledged resources and aids.

Hamburg 13-10-2016

[Hiermit erkläre ich an Eides statt, dass ich die vorliegende Dissertationsschrift selbst verfasst und keine anderen als die angegeben Quellen und Hilfsmittel benutzt habe.]

Hamburg, den 13. Oktober 2016

Furthermore, I declare that parts of the present thesis have already been published (marked by an asterisk* in the heading) (Appendix 8). I declare that I have written the first version of the manuscript on my own and further contributions to the paper have been: collection of the material, data acquisition, literature research, data analysis, and writing the of the manuscript. My total contribution to the publication are approximately 70 %, whereas the other authors Dr. Frank Friedrich (data acquisition, contributing to the manuscript, proof reading) and Dr. Felix Beckmann (data acquisition, proof reading) contributed with ca. 25 % and 5 %, respectively.

Hamburg 13-10-2016

Außerdem erkläre ich hiermit, dass Teile der vorliegenden Arbeit bereits publiziert wurden (gekennzeichnet durch ein hochgestelltes Sternchen*) (Appendix 8). Ich versichere, dass ich die erste Manuskriptfassung selbst geschrieben habe und mein Beitrag zur Arbeit umfasst die Materialbeschaffung, die Datenerhebung, die Datenanalyse sowie das Schreiben der des Manuskripts. Mein Gesamtbeitrag entspricht ungefähr 70 %. Die anderen Autoren Dr. Frank Friedrich (Unterstützung und Anleitung bei der Datenerhebung und -auswertung, Schreiben des Manuskripts, Korrekturlesen) und Dr. Felix Beckmann (Datenerhebung, Korrekturlesen) trugen je ca. 25 % und 5 % dazu bei.

Hamburg, den 13. Oktober 2016

BAYLOR
UNIVERSITY

date: October 4, 2016

recipient:
Universität Hamburg
Biozentrum Klein Flottbek
Studienbüro Biologie
z.H. Frau Sült-Wüpping
Ohnhorststr. 18
22609 Hamburg

Subject: Native speaker confirmation

To whom it may concern,

I hereby confirm that I have read the dissertation of Martin Kubiak from the University of Hamburg with the title '*The morphology and evolution of adult head structures in Trichoptera (Insecta)*'. I am a native speaker in English and Associate Professor in the Department of Biology at Baylor University (Waco, Texas, USA) and I have checked the correctness of the English spelling and grammar.

Kind regards,

Patrick Danley

DEPARTMENT OF BIOLOGY
One Bear Place #97388 • Waco, TX 76798-7388 • (254) 710-2911 • FAX (254) 710-2969

List of Appendices

Appendix 1: Head musculature of representatives of Trichoptera, Lepidoptera, and Mecoptera

Appendix 2: Detailed description of the antennal musculature of adult Trichoptera

Appendix 3: Description of the epipharyngeal and hypopharyngeal musculature of adult Trichoptera

Appendix 4: Detailed description of the pharyngeal musculature of adult Trichoptera

Appendix 5: Detailed description of the musculature of the maxilla in adult Trichoptera

Appendix 6: Detailed description of the musculature of the labium and salivarium in adult Trichoptera

Appendix 7: Character state matrix of the trichopteran adult and pupal head

Appendix 8: Publication: The adult head of the annulipalpian caddisfly *Philopotamus ludificatus* McLachlan, 1878 (Philopotamidae), mouthpart homologies, and implications on the ground plan of Trichoptera

Appendix 1: Head musculature of representatives of Trichoptera, Lepidoptera, and Mecoptera. Full names of muscles are presented in Tab. 4. Abbreviations: **bdl.** – bundle; **n.a.** – not applicable; **+** – present; **-** – absent; **?** – uncertain; [1] – see Klemm 1966.

Species	**fr-lb** (K: M8; Wi: 0lb1)	**lb-eph** (K: M7; Wi: 0lb5)	**fr-eph** (K: M9; Wi: 0lb2)	**cl-eph(m)** (K: M43; Wi: 0ci1, 0lb2 (?))	**cl-eph(l)** (K: M43; Wi: 0ci1)	**cl-ci(v)** (K: M44 (?); Wi: 0bu1 (?))	**cl-ci(d)** (K: M44; Wi: 0bu1)	**te-si** (K: M48; Wi: 0bu5)	**fr-ph(a)** (K: M45; Wi: 0bu2)
Philopotamus ludificatus McLachlan, 1878	-	-	-	+ (1 bdl.)	+ (1 bdl.)	+ (1 bdl.)	+ (2 bdl.)	+ (1 bdl.)	+ (1 bdl.)
Stenopsyche marmorata Navas, 1920	-	-	-	+ (1 bdl.)	+ (1 bdl.)	+ (1 bdl.)	+ (1 bdl.) [?]	+ (1 bdl.)	+ (1 bdl.)
Hydropsyche angustipennis (Curtis, 1834)	-	-	-	+ (1 bdl.)	+ (1 bdl.)	+ (1 bdl.)	+ (2 bdl.)	+ (1 bdl.)	+ (1 bdl.)
Tinodes dives (Pictet, 1834)	-	-	-	+ (1 bdl.)	+ (1 bdl.)	+ (1 bdl.)	+ (2 bdl.)	+ (1 bdl.)	+ (1 bdl.)
Holocentropus dubius (Rambur, 1842)	-	-	-	+ (1 bdl.)	+ (1 bdl.)	+ (2 bdl.)	+ (2 bdl.)	+ (1 bdl.)	+ (1 bdl.)
Rhyacophila obliterata McLachlan, 1863	-	-	+ (?) [1]	+ (1 bdl.)	+ (1 bdl.)	+ (2 bdl.)	+ (1 bdl.)	+ (1 bdl.)	+ (1 bdl.)
Apsilochorema sutshanum Martynov, 1934	-	-	-	+ (1 bdl.)	+ (1 bdl.)	+ (2 bdl.)	+ (1 bdl.)	+ (1 bdl.)	+ (1 bdl.)
Hydrobiosis styracine McFarlane, 1960	-	-	-	+ (1 bdl.)	+ (1 bdl.)	+ (1 bdl.)	+ (2 bdl.)	+ (1 bdl.)	+ (1 bdl.)
Glossosoma spinosum Morse et Yang, 2005	-	-	-	+ (1 bdl.)	+ (1 bdl.)	+ (2 bdl.)	+ (1 bdl.)	+ (1 bdl.)	+ (2 bdl.)
Agapetus fuscipes Curtis, 1834	-	-	-	+ (1 bdl.)	+ (1 bdl.)	+ (1 bdl.)	+ (2 bdl.)	+ (1 bdl.)	+ (1 bdl.)
Ptilocolepus granulatus (Pictet, 1834)	-	-	-	+ (1 bdl.)	+ (1 bdl.)	+ (1 bdl.)	+ (1 bdl.)	+ (1 bdl.)	+ (1 bdl.)
Hydroptila scamandra Neboiss, 1977	-	-	-	+ (1 bdl.)	+ (1 bdl.)	+ (1 bdl.)	+ (1 bdl.)	+ (1 bdl.)	+ (1 bdl.)
Orthotrichia atraseta Wells, 1979	-	-	-	+ (1 bdl.)	+ (1 bdl.)	+ (1 bdl.)	+ (1 bdl.)	+ (1 bdl.)	+ (1 bdl.)
Phryganea grandis Linnaeus, 1758	-	-	-	+ (1 bdl.)	+ (1 bdl.)	+ (1 bdl.)	+ (2 bdl.)	+ (1 bdl.)	+ (1 bdl.)
Trichostegia minor (Curtis, 1834)	-	-	-	+ (1 bdl.)	+ (1 bdl.)	+ (1 bdl.)	+ (2 bdl.)	+ (1 bdl.)	+ (1 bdl.)
Sericostoma personatum Kirby et Spence, 1826	-	-	-	+ (1 bdl.)	+ (1 bdl.)	+ (1 bdl.)	+ (2 bdl.)	+ (1 bdl.)	+ (1 bdl.)
Brachycentrus subnubilus Curtis, 1834	-	-	-	+ (1 bdl.)	+ (2 bdl.)	+ (1 bdl.)	+ (3 bdl.)	+ (1 bdl.)	+ (1 bdl.)
Limnephilus flavicornis (Fabricius, 1787)	-	-	-	+ (1 bdl.)	+ (2 bdl.)	+ (1 bdl.)	+ (3 bdl.)	+ (1 bdl.)	+ (1 bdl.)
Silo nigricornis (Pictet, 1834)	-	-	-	+ (1 bdl.)	+ (2 bdl.)	+ (1 bdl.)	+ (3 bdl.)	+ (1 bdl.)	+ (1 bdl.)
Pycnocentria evecta McLachlan, 1868	-	-	-	+ (1 bdl.)	+ (1 bdl.)	+ (1 bdl.)	+ (2 bdl.) [?]	+ (1 bdl.)	+ (1 bdl.)
Molanna angustata Curtis, 1834	-	-	-	+ (1 bdl.)	+ (1 bdl.)	+ (1 bdl.)	+ (2 bdl.)	+ (1 bdl.)	+ (1 bdl.)
Leptocerus tineiformis Curtis, 1834	-	-	-	+ (1 bdl.)	+ (1 bdl.)	+ (1 bdl.)	+ (2 bdl.)	+ (1 bdl.)	+ (1 bdl.)
Micropterix clathella (L., 1761) [Hannemann 1956]	+	+	+	+	+	-	+ [?]	+	+ [?]
Nannochorista sp. [Beutel and Baum 2008]	-	-	-	+	+	+	+	-	-

Appendix 1: Continued.

Species	**fr-ph(p)** (K: M46; Wi: 0bu3)	**te-ph(l)** (K: M47 (?); Wi: 0hy2 (?))	**te-ph(a)** (K: 50; Wi: 0bu6)	**te-ph(p)** (K: 52, 54 (?); Wi: 0ph2 (?))	**cr-ph(a)** (K: 51; Wi: 0ph1)	**cr-ph(p)** (K: 51, 53 (?); Wi: 0ph3 (?))	**an-ci** (K: 67; Wi: 0hy9)	**an-ph** (K: 68; Wi: 0st1)
Philopotamus ludificatus McLachlan, 1878	+ (2 bdl.)	+ (1 bdl.)	+ (2 bdl.)	+ (1 bdl.)	+ (1 bdl.)	-	+	+
Stenopsyche marmorata Navas, 1920	+ (1 bdl.) [?]	+ (1 bdl.)	+ (1 bdl.)	- [?]	- [?]	-	+	+
Hydropsyche angustipennis (Curtis, 1834)	+ (3 bdl.)	+ (1 bdl.)	+ (2 bdl.)	+ (1 bdl.)	+ (1 bdl.)	-	+	+
Tinodes dives (Pictet, 1834)	+ (2 bdl.)	+ (1 bdl.)	+ (2 bdl.)	+ (1 bdl.)	+ (1 bdl.)	-	+	+
Holocentropus dubius (Rambur, 1842)	+ (2 bdl.)	+ (1 bdl.)	+ (2 bdl.)	+ (1 bdl.)	+ (1 bdl.)	+ (1 bdl.)	+	+
Rhyacophila obliterata McLachlan, 1863	+ (2 bdl.)	+ (1 bdl.)	+ (2 bdl.)	+ (1 bdl.)	+ (1 bdl.)	+ (1 bdl.)	+	+
Apsilochorema sutshanum Martynov, 1934	+ (2 bdl.)	+ (2 bdl.)	+ (2 bdl.)	+ (1 bdl.)	+ (1 bdl.)	+ (2 bdl.)	+	+
Hydrobiosis styracine McFarlane, 1960	+ (3 bdl.)	+ (2 bdl.)	+ (2 bdl.)	+ (1 bdl.)	+ (1 bdl.)	+ (2 bdl.) [?]	+	+
Glossosoma spinosum Morse et Yang, 2005	+ (2 bdl.)	+ (2 bdl.)	+ (2 bdl.)	+ (1 bdl.)	+ (1 bdl.)	+ (2 bdl.) [?]	+	+
Agapetus fuscipes Curtis, 1834	+ (1 bdl.) [?]	+ (2 bdl.)	+ (2 bdl.)	- [?]	+ (1 bdl.)	+ (1 bdl.) [?]	+	+
Ptilocolepus granulatus (Pictet, 1834)	+ (2 bdl.)	+ (2 bdl.)	+ (2 bdl.)	+ (1 bdl.)	+ (1 bdl.)	+ (1 bdl.)	+	+
Hydroptila scamandra Neboiss, 1977	+ (2 bdl.) [?]	+ (1 bdl.)	+ (2 bdl.)	+ (1 bdl.)	-	-	+	+
Orthotrichia atraseta Wells, 1979	+ (3 bdl.) [?]	+ (1 bdl.)	+ (2 bdl.)	+ (1 bdl.)	-	-	+	+
Phryganea grandis Linnaeus, 1758	+ (2 bdl.)	+ (1 bdl.)	+ (2 bdl.) [?]	+ (1 bdl.)	+ (1 bdl.)	-	+	+
Trichostegia minor (Curtis, 1834)	+ (2 bdl.)	+ (1 bdl.)	+ (2 bdl.)	+ (1 bdl.)	+ (1 bdl.)	-	+	+
Sericostoma personatum Kirby et Spence, 1826	+ (2 bdl.)	+ (3 bdl.) [?]	+ (2 bdl.)	+ (1 bdl.)	+ (1 bdl.)	-	+	+
Brachycentrus subnubilus Curtis, 1834	+ (2 bdl.)	+ (1 bdl.)	+ (2 bdl.)	+ (1 bdl.)	+ (1 bdl.)	-	+	+
Limnephilus flavicornis (Fabricius, 1787)	+ (2 bdl.)	+ (1 bdl.)	+ (2 bdl.)	+ (1 bdl.)	+ (1 bdl.)	-	+	+
Silo nigricornis (Pictet, 1834)	+ (2 bdl.) [?]	+ (1 bdl.)	+ (2 bdl.) [?]	+ (1 bdl.)	+ (1 bdl.)	-	+	+
Pycnocentria evecta McLachlan, 1868	+ (2 bdl.) [?]	+ (1 bdl.)	+ (1 bdl.) [?]	+ (1 bdl.)	+ (1 bdl.)	-	+	+
Molanna angustata Curtis, 1834	+ (2 bdl.)	+ (1 bdl.)	+ (2 bdl.)	+ (1 bdl.)	+ (1 bdl.)	-	+	+
Leptocerus tineiformis Curtis, 1834	+ (2 bdl.)	+ (1 bdl.)	+ (1 bdl.)	- [?]	+ (1 bdl.)	-	+	+
Micropterix clathella (L., 1761) [Hannemann 1956]	+	+ [?]	+	+	+	+	+	+
Nannochorista sp. [Beutel and Baum 2008]	-	-	-	+	+	-	+	+

Appendix 1: Continued.

Species	**lo-ph** (K: 69; Wi: 0st2)	**te-sc(a)** (K: M1; Wi: 0an1)	**te-sc(p)** (K: M2; Wi: 0an2)	**te-sc(l)** (K: M3; Wi: 0an3)	**te-sc(m)** (K: M4; Wi: 0an4)	**sc-pe(l)** (K: M5; Wi: 0an6)	**sc-pe(m)** (K: M6; Wi: 0an7)	**cr-md(m)** (K: M11; Wi: 0md1)
Philopotamus ludificatus McLachlan, 1878	+	+ (1 bdl.)	+ (1 bdl.)	+ (2 bdl.)	+ (1 bdl.)	+	+	+ (several bdl.)
Stenopsyche marmorata Navas, 1920	+	+ (1 bdl.)	+ (1 bdl.)	+ (2 bdl.)	+ (1 bdl.)	+	+	+ (several bdl.)
Hydropsyche angustipennis (Curtis, 1834)	+	+ (1 bdl.)	+ (1 bdl.)	+ (2 bdl.)	+ (2 bdl.)	+	+	+ (several bdl.)
Tinodes dives (Pictet, 1834)	+	+ (1 bdl.)	+ (1 bdl.)	+ (2 bdl.)	+ (2 bdl.)	+	+	+ (several bdl.)
Holocentropus dubius (Rambur, 1842)	+	+ (2 bdl.)	+ (1 bdl.)	+ (2 bdl.)	+ (2 bdl.)	+	+	(-) [?]
Rhyacophila obliterata McLachlan, 1863	+	+ (2 bdl.)	+ (1 bdl.)	+ (1 bdl.)	+ (1 bdl.)	+	+	+ (several bdl.)
Apsilochorema sutshanum Martynov, 1934	+	+ (2 bdl.)	+ (1 bdl.)	+ (1 bdl.)	+ (1 bdl.)	+	+	(-) [?]
Hydrobiosis styracine McFarlane, 1960	+	+ (2 bdl.)	+ (1 bdl.)	+ (1 bdl.)	+ (1 bdl.)	+	+	+ (several bdl.)
Glossosoma spinosum Morse et Yang, 2005	+	+ (2 bdl.)	+ (1 bdl.)	+ (2 bdl.)	-	+	+	+ (several bdl.)
Agapetus fuscipes Curtis, 1834	+	+ (2 bdl.)	+ (1 bdl.)	+ (2 bdl.)	-	+	+	+ (several bdl.)
Ptilocolepus granulatus (Pictet, 1834)	+	+ (1 bdl.)	+ (1 bdl.)	+ (2 bdl.)	+ (1 bdl.)	+	+	+ (several bdl.)
Hydroptila scamandra Neboiss, 1977	+	+ (1 bdl.)	+ (1 bdl.)	+ (2 bdl.)	+ (1 bdl.)	+	+	(-) [?]
Orthotrichia atraseta Wells, 1979	+	+ (1 bdl.)	+ (1 bdl.)	+ (2 bdl.)	+ (1 bdl.)	+	+	+ (several bdl.)
Phryganea grandis Linnaeus, 1758	+	+ (3 bdl.)	+ (1 bdl.)	+ (1 bdl.)	+ (1 bdl.)	+	+	(-) [?]
Trichostegia minor (Curtis, 1834)	+	+ (3 bdl.)	+ (1 bdl.)	+ (1 bdl.)	+ (1 bdl.)	+	+	+ (several bdl.)
Sericostoma personatum Kirby et Spence, 1826	+	+ (1 bdl.)	+ (1 bdl.)	+ (1 bdl.)	+ (1 bdl.)	+	+	+ (several bdl.)
Brachycentrus subnubilus Curtis, 1834	+	+ (3 bdl.)	+ (1 bdl.)	+ (1 bdl.)	+ (1 bdl.)	+	+	+ (several bdl.)
Limnephilus flavicornis (Fabricius, 1787)	+	+ (3 bdl.)	+ (1 bdl.)	+ (2 bdl.)	+ (1 bdl.)	+	+	(-) [?]
Silo nigricornis (Pictet, 1834)	+	+ (3 bdl.)	+ (1 bdl.)	+ (1 bdl.)	+ (1 bdl.)	+	+	+ (several bdl.)
Pycnocentria evecta McLachlan, 1868	+	+ (3 bdl.)	+ (1 bdl.)	+ (2 bdl.)	+ (1 bdl.)	+	+	+ (several bdl.)
Molanna angustata Curtis, 1834	+	+ (3 bdl.)	+ (1 bdl.)	+ (2 bdl.)	+ (1 bdl.)	+	+	+ (several bdl.)
Leptocerus tineiformis Curtis, 1834	+	+ (3 bdl.)	+ (1 bdl.)	+ (2 bdl.)	+ (1 bdl.)	+	+	+ (several bdl.)
Micropterix clathella (L., 1761) [Hannemann 1956]	+	+	+	+	+	+	+	+
Nannochorista sp. [Beutel and Baum 2008]	+	+	+	-	+	+	+	-

Appendix 1: Continued.

Species	cr-md(l) (K: M12; Wi: 0md3)	te-md (K: M14; Wi: 0md6)	hy-md (K: M13; Wi: 0md4)	te-cd (K: M17; Wi: 0mx3)	te-st (K: M18; Wi: 0mx4)	cr-cd (K: M15; Wi: 0mx1)	cr-st (K: M16; Wi: 0mx1)	cr-lc (K: M19; Wi: 0mx2)
Philopotamus ludificatus McLachlan, 1878	+ (several bdl.)	+ (1 bdl.)	-	+ (1 bdl.)	+ (1 bdl.)	+ (1 bdl.)	+ (1 bdl.)	+ (1 bdl.)
Stenopsyche marmorata Navas, 1920	+ (several bdl.)	- [?]	-	+ (1 bdl.)	+ (1 bdl.)	+ (1 bdl.)	+ (1 bdl.)	+ (1 bdl.)
Hydropsyche angustipennis (Curtis, 1834)	+ (several bdl.)	+ [?]	-	+ (1 bdl.)	+ (1 bdl.)	+ (1 bdl.)	+ (1 bdl.)	+ (1 bdl.)
Tinodes dives (Pictet, 1834)	+ (several bdl.)	+	-	+ (1 bdl.)	+ (1 bdl.)	+ (1 bdl.)	+ (1 bdl.)	+ (1 bdl.)
Holocentropus dubius (Rambur, 1842)	(-) [?]	+	-	+ (1 bdl.)	+ (1 bdl.)	+ (1 bdl.)	+ (1 bdl.)	+ (1 bdl.)
Rhyacophila obliterata McLachlan, 1863	+ (several bdl.)	+	-	+ (1 bdl.)	+ (1 bdl.)	+ (1 bdl.)	-	+ (1 bdl.)
Apsilochorema sutshanum Martynov, 1934	(-) [?]	(-) [?]	-	+ (1 bdl.)	+ (1 bdl.)	+ (1 bdl.)	-	+ (1 bdl.)
Hydrobiosis styracine McFarlane, 1960	+ (several bdl.)	- [?]	-	+ (1 bdl.)	+ (1 bdl.)	+ (1 bdl.)	-	+ (1 bdl.)
Glossosoma spinosum Morse et Yang, 2005	+ (several bdl.)	+ [?]	-	+ (1 bdl.)	+ (1 bdl.)	+ (1 bdl.)	-	+ (1 bdl.)
Agapetus fuscipes Curtis, 1834	+ (several bdl.)	+	-	+ (1 bdl.)	+ (1 bdl.)	+ (1 bdl.)	-	+ (1 bdl.)
Ptilocolepus granulatus (Pictet, 1834)	+ (several bdl.)	+	-	+ (1 bdl.)	+ (1 bdl.)	+ (1 bdl.)	-	+ (1 bdl.)
Hydroptila scamandra Neboiss, 1977	(-) [?]	(-) [?]	-	+ (1 bdl.)	+ (1 bdl.)	+ (1 bdl.)	-	+ (1 bdl.)
Orthotrichia atraseta Wells, 1979	+ (several bdl.)	+	-	+ (1 bdl.)	+ (1 bdl.)	+ (1 bdl.)	-	+ (1 bdl.)
Phryganea grandis Linnaeus, 1758	(-) [?]	(-) [?]	-	+ (1 bdl.)	-	+ (1 bdl.)	-	+ (1 bdl.)
Trichostegia minor (Curtis, 1834)	+ (several bdl.)	(-) [?]	-	+ (1 bdl.)	-	+ (1 bdl.)	-	+ (1 bdl.)
Sericostoma personatum Kirby et Spence, 1826	+ (several bdl.)	(-) [?]	-	+ (1 bdl.)	+ (1 bdl.)	+ (1 bdl.)	-	+ (1 bdl.)
Brachycentrus subnubilus Curtis, 1834	+ (several bdl.)	(-) [?]	-	+ (1 bdl.)	+ (1 bdl.)	+ (1 bdl.)	-	+ (1 bdl.)
Limnephilus flavicornis (Fabricius, 1787)	(-) [?]	(-) [?]	-	+ (1 bdl.)	+ (1 bdl.)	+ (1 bdl.)	-	+ (1 bdl.)
Silo nigricornis (Pictet, 1834)	+ (several bdl.)	(-) [?]	-	+ (1 bdl.)	+ (1 bdl.)	+ (1 bdl.)	-	+ (1 bdl.)
Pycnocentria evecta McLachlan, 1868	+ (several bdl.)	(-) [?]	-	+ (1 bdl.)	+ (1 bdl.)	+ (1 bdl.)	-	+ (1 bdl.)
Molanna angustata Curtis, 1834	+ (several bdl.)	(-) [?]	-	+ (1 bdl.)	+ (1 bdl.)	+ (1 bdl.)	-	+ (1 bdl.)
Leptocerus tineiformis Curtis, 1834	+ (several bdl.)	(-) [?]	-	+ (1 bdl.)	+ (1 bdl.)	+ (1 bdl.)	-	+ (1 bdl.)
Micropterix clathella (L., 1761) [Hannemann 1956]	+	-	-	+	+	+	+	+
Nannochorista sp. [Beutel and Baum 2008]	-	-	+	+	+	-	-	+

Appendix 1: Continued.

Species	**st-lc** (K: M20; Wi: 0mx6)	**st-ga** (K: M21; Wi: 0mx7)	**cd-mp(d)** -	**st/cd-mp(v)** (K: M22; Wi: 0mx8)	**st-mp(d)** (K: M23; Wi: 0mx10)	**mp1-mp2(m)** (K: M24 (?); Wi: 0mx12)	**mp1-mp2(l)** (K: M24; Wi: 0mx12)	**mp2-mp3** (K: M25; Wi: 0mx13)
Philopotamus ludificatus McLachlan, 1878	-	-	+ (1 bdl.)	+ (1 bdl.)	+ (1 bdl.)	+ (1 bdl.)	+ (1 bdl.)	+ (1 bdl.)
Stenopsyche marmorata Navas, 1920	-	-	+ (1 bdl.)	+ (1 bdl.)	+ (1 bdl.)	+ (1 bdl.)	+ (1 bdl.)	+ (1 bdl.)
Hydropsyche angustipennis (Curtis, 1834)	-	-	+ (1 bdl.)	+ (1 bdl.)	+ (1 bdl.)	+ (1 bdl.)	+ (1 bdl.)	+ (2 bdl.)
Tinodes dives (Pictet, 1834)	-	-	+ (1 bdl.)	+ (1 bdl.)	+ (1 bdl.)	+ (1 bdl.)	+ (1 bdl.)	+ [?] (1 bdl.)
Holocentropus dubius (Rambur, 1842)	-	-	+ (1 bdl.)	+ (1 bdl.)	+ (1 bdl.)	n.a.	n.a.	n.a.
Rhyacophila obliterata McLachlan, 1863	+ (1 bdl.)	-	+ (1 bdl.)	+ (1 bdl.)	+ (1 bdl.)	+ (1 bdl.)	+ (1 bdl.)	+ (2 bdl.)
Apsilochorema sutshanum Martynov, 1934	+ (1 bdl.)	-	+ (1 bdl.)	+ (1 bdl.)	+ (1 bdl.)	+ (1 bdl.)	+ (1 bdl.)	+ (2 bdl.)
Hydrobiosis styracine McFarlane, 1960	+ (1 bdl.)	-	+ (1 bdl.)	+ (1 bdl.)	+ (1 bdl.)	+ (1 bdl.)	+ (1 bdl.)	n.a.
Glossosoma spinosum Morse et Yang, 2005	-	-	+ (1 bdl.)	+ (1 bdl.)	+ (1 bdl.)	+ (1 bdl.)	+ (1 bdl.)	+ (1 bdl.)
Agapetus fuscipes Curtis, 1834	+ (1 bdl.)	-	+ (1 bdl.)	+ (1 bdl.)	+ (1 bdl.)	+ (1 bdl.)	+ (1 bdl.)	+ (2 bdl.)
Ptilocolepus granulatus (Pictet, 1834)	+ (1 bdl.)	-	+ (1 bdl.)	+ (1 bdl.)	+ (1 bdl.)	+ (1 bdl.)	+ (1 bdl.)	+ (2 bdl.)
Hydroptila scamandra Neboiss, 1977	+ (1 bdl.)	-	+ (1 bdl.)	+ (1 bdl.)	- [?]	+ (1 bdl.)	+ (1 bdl.)	+ (2 bdl.)
Orthotrichia atraseta Wells, 1979	+ (1 bdl.)	-	+ (1 bdl.)	+ (1 bdl.)	+ (1 bdl.)	+ (1 bdl.)	+ (1 bdl.)	+ (2 bdl.)
Phryganea grandis Linnaeus, 1758	+ (1 bdl.)	-	+ (1 bdl.)	+ (1 bdl.)	+ (1 bdl.)	+ (1 bdl.)	+ (1 bdl.)	+ (1 bdl.)
Trichostegia minor (Curtis, 1834)	+ (1 bdl.)	-	+ (1 bdl.)	+ (1 bdl.)	+ (1 bdl.)	+ (1 bdl.)	+ (1 bdl.)	+ (1 bdl.)
Sericostoma personatum Kirby et Spence, 1826	-	-	+ (1 bdl.)	+ (1 bdl.)	+ (1 bdl.)	+ [?] (1 bdl.)	+ [?] (1 bdl.)	-
Brachycentrus subnubilus Curtis, 1834	+ (1 bdl.)	-	+ (1 bdl.)	+ (1 bdl.)	+ (1 bdl.)	+ (1 bdl.)	+ (1 bdl.)	+ (1 bdl.)
Limnephilus flavicornis (Fabricius, 1787)	+ (1 bdl.)	-	+ (1 bdl.)	+ (1 bdl.)	+ (1 bdl.)	+ (1 bdl.)	+ (1 bdl.)	+ (2 bdl.)
Silo nigricornis (Pictet, 1834)	+ (1 bdl.)	-	+ (2 bdl.)	- [?]	- [?]	+ (1 bdl.)	+ (1 bdl.)	+ (1 bdl.)
Pycnocentria evecta McLachlan, 1868	-	-	+ (1 bdl.)	+ (1 bdl.)	+ (1 bdl.)	-	-	-
Molanna angustata Curtis, 1834	-	-	+ (1 bdl.)	+ (1 bdl.)	+ (1 bdl.)	+ (1 bdl.)	+ (1 bdl.)	+ (1 bdl.)
Leptocerus tineiformis Curtis, 1834	-	-	+ (1 bdl.)	+ (1 bdl.)	+ (1 bdl.)	+ (1 bdl.)	+ (1 bdl.)	n.a.
Micropterix clathella (L., 1761) [Hannemann 1956]	+	+	-	+	+	+	+	+
Nannochorista sp. [Beutel and Baum 2008]	-	-	-	+	-	n.a.	+	-

Appendix 1: Continued.

Species	**mp3-mp4** (K: M26; Wi: 0mx14)	**mp4-mp5** (K: M27; Wi: 0mx15)	**hy-sa** (K: M37; Wi: 0hy12)	**i-sa** (K: M37 (?); Wi: -)	**prm-sa** (K: M38/39; Wi: 0hy7, 0hy8 (?))	**cr-prm(m)** (K: M30; Wi: 0la6)	**cr-prm(l)** (K: M29; Wi: 0la5)	**smt-pmt** (K: M28; Wi: 0la8)
Philopotamus ludificatus McLachlan, 1878	+ (1 bdl.)	+ (1 bdl.)	+ (1 bdl.)	-	+ (1 bdl.)	+ (2 bdl.)	+ (1 bdl.)	-
Stenopsyche marmorata Navas, 1920	+ (1 bdl.)	+ (1 bdl.)	- [?]	-	+ (1 bdl.)	+ (1 bdl.) [?]	+ (1 bdl.)	-
Hydropsyche angustipennis (Curtis, 1834)	+ (2 bdl.)	n.a.	+ (1 bdl.)	-	+ (2 bdl.)	+ (2 bdl.)	+ (1 bdl.)	-
Tinodes dives (Pictet, 1834)	n.a.	n.a.	-	-	+ (2 bdl.)	+ (2 bdl.)	+ (1 bdl.)	-
Holocentropus dubius (Rambur, 1842)	n.a.	n.a.	-	+ (1 bdl.)	-	+ (2 bdl.)	+ (1 bdl.)	-
Rhyacophila obliterata McLachlan, 1863	+ (1 bdl.)	n.a.	-	+ (1 bdl.)	+ (1 bdl.)	+ (2 bdl.)	+ (1 bdl.)	-
Apsilochorema sutshanum Martynov, 1934	+ (1 bdl.)	n.a.	-	-	+ (1 bdl.)	+ (2 bdl.)	+ (1 bdl.)	-
Hydrobiosis styracine McFarlane, 1960	n.a.	n.a.	-	-	+ (1 bdl.)	+ (2 bdl.)	+ (1 bdl.)	-
Glossosoma spinosum Morse et Yang, 2005	+ (1 bdl.)	+ (1 bdl.)	-	-	+ (1 bdl.)	+ (2 bdl.)	+ (1 bdl.)	-
Agapetus fuscipes Curtis, 1834	n.a.	n.a.	-	-	+ (1 bdl.)	+ (2 bdl.)	+ (1 bdl.)	-
Ptilocolepus granulatus (Pictet, 1834)	n.a.	n.a.	-	-	+ (1 bdl.)	+ (2 bdl.)	+ (1 bdl.)	-
Hydroptila scamandra Neboiss, 1977	+ (1 bdl.)	n.a.	-	-	+ (1 bdl.)	+ (2 bdl.)	+ (1 bdl.)	-
Orthotrichia atraseta Wells, 1979	n.a.	n.a.	-	-	+ (1 bdl.)	+ (2 bdl.)	+ (1 bdl.)	-
Phryganea grandis Linnaeus, 1758	n.a.	n.a.	-	+ (1 bdl.) [?]	+ (1 bdl.)	+ (2 bdl.)	+ (1 bdl.)	-
Trichostegia minor (Curtis, 1834)	+ (1 bdl.)	n.a.	-	+ (1 bdl.) [?]	+ (1 bdl.)	+ (2 bdl.)	+ (1 bdl.)	-
Sericostoma personatum Kirby et Spence, 1826	-	-	-	- [?]	+ (1 bdl.)	+ (2 bdl.)	+ (1 bdl.)	-
Brachycentrus subnubilus Curtis, 1834	+ (1 bdl.)	n.a.	-	+ (1 bdl.)	- [?]	+ (2 bdl.)	+ (1 bdl.)	-
Limnephilus flavicornis (Fabricius, 1787)	+ (1 bdl.)	n.a.	-	+ (1 bdl.) [?]	- [?]	+ (2 bdl.)	+ (1 bdl.)	-
Silo nigricornis (Pictet, 1834)	n.a.	n.a.	-	+ (1 bdl.) [?]	- [?]	+ (2 bdl.)	+ (2 bdl. [?])	-
Pycnocentria evecta McLachlan, 1868	-	-	-	-	+ (1 bdl.)	+ (2 bdl.)	+ (1 bdl.)	-
Molanna angustata Curtis, 1834	+ (1 bdl.)	+ (1 bdl.)	-	+ (1 bdl.)	+ (1 bdl.)	+ (2 bdl.)	+ (1 bdl.)	-
Leptocerus tineiformis Curtis, 1834	n.a.	n.a.	-	-	+ (1 bdl.)	+ (2 bdl.) [?]	+ (1 bdl.)	-
Micropterix clathella (L., 1761) [Hannemann 1956]	+	+	+	-	-	+	+	+
Nannochorista sp. [Beutel and Baum 2008]	+	-	+	n.a.	-	+	-	-

Appendix 1: Continued.

Species	**prm-pgl** (K: M31; Wi: 0la11)	**prm-gl** (K: M32; Wi: 0la12)	**prm-lp(m)** (K: M33; Wi: 0la13)	**prm-lp(l)** (K: M34; Wi: 0la14)	**lp1-lp2(a)** (K: M35; Wi: 0la16)	**lp1-lp2(p)** (K: M35 (?); Wi: 0la16)	**lp2-lp3** (K: M36; Wi: 0la17)
Philopotamus ludificatus McLachlan, 1878	-	-	+ (1 bdl.)	+ (1 bdl.)	+ (1 bdl.)	+ (1 bdl.)	+ (1 bdl.)
Stenopsyche marmorata Navas, 1920	-	-	+ (1 bdl.)	+ (1 bdl.)	+ (1 bdl.) [?]	+ (1 bdl.) [?]	+ (1 bdl.)
Hydropsyche angustipennis (Curtis, 1834)	-	-	+ (1 bdl.)	+ (1 bdl.)	+ (1 bdl.)	+ (1 bdl.)	+ (1 bdl.)
Tinodes dives (Pictet, 1834)	-	-	+ (1 bdl.)	+ (1 bdl.)	n.a.	n.a.	n.a.
Holocentropus dubius (Rambur, 1842)	-	-	+ (1 bdl.)	+ (1 bdl.)	+ (1 bdl.)	+ (1 bdl.)	+ (1 bdl.)
Rhyacophila obliterata McLachlan, 1863	-	-	+ (1 bdl.)	+ (1 bdl.)	n.a.	n.a.	n.a.
Apsilochorema sutshanum Martynov, 1934	-	-	+ (1 bdl.)	+ (1 bdl.)	+ (1 bdl.)	+ (1 bdl.)	+ (1 bdl.)
Hydrobiosis styracine McFarlane, 1960	-	-	+ (1 bdl.)	+ (1 bdl.)	+ (1 bdl.)	+ (1 bdl.)	+ (1 bdl.)
Glossosoma spinosum Morse et Yang, 2005	-	-	+ (1 bdl.)	+ (1 bdl.)	+ (1 bdl.)	+ (1 bdl.)	+ (1 bdl.)
Agapetus fuscipes Curtis, 1834	-	-	+ (1 bdl.)	+ (1 bdl.)	+ (1 bdl.)	- [?]	+ (1 bdl.)
Ptilocolepus granulatus (Pictet, 1834)	-	-	+ (1 bdl.)	+ (1 bdl.)	+ (1 bdl.)	+ (1 bdl.)	n.a.
Hydroptila scamandra Neboiss, 1977	-	-	+ (1 bdl.)	+ (1 bdl.)	+ (1 bdl.)	+ (1 bdl.)	+ (1 bdl.)
Orthotrichia atraseta Wells, 1979	-	-	+ (1 bdl.)	+ (1 bdl.)	+ (1 bdl.)	+ (1 bdl.)	n.a.
Phryganea grandis Linnaeus, 1758	-	-	+ (1 bdl.)	+ (1 bdl.)	+ (1 bdl.)	+ (1 bdl.)	n.a.
Trichostegia minor (Curtis, 1834)	-	-	+ (1 bdl.)	+ (1 bdl.)	+ (1 bdl.)	+ (1 bdl.)	+ (1 bdl.)
Sericostoma personatum Kirby et Spence, 1826	-	-	+ (1 bdl.)	+ (1 bdl.)	+ (1 bdl.)	+ (1 bdl.)	+ (1 bdl.)
Brachycentrus subnubilus Curtis, 1834	-	-	+ (1 bdl.)	+ (1 bdl.)	+ (1 bdl.)	+ (1 bdl.)	+ (1 bdl.)
Limnephilus flavicornis (Fabricius, 1787)	-	-	+ (1 bdl.)	+ (1 bdl.)	+ (1 bdl.)	+ (1 bdl.)	+ (1 bdl.)
Silo nigricornis (Pictet, 1834)	-	-	+ (1 bdl.)	+ (1 bdl.)	+ (1 bdl.)	+ (1 bdl.)	+ (1 bdl.)
Pycnocentria evecta McLachlan, 1868	-	-	+ (1 bdl.)	+ (1 bdl.)	+ (1 bdl.)	+ (1 bdl.)	+ (1 bdl.)
Molanna angustata Curtis, 1834	-	-	+ (1 bdl.)	+ (1 bdl.)	+ (1 bdl.)	+ (1 bdl.)	+ (1 bdl.)
Leptocerus tineiformis Curtis, 1834	-	-	+ (1 bdl.)	+ (1 bdl.)	+ (1 bdl.)	+ (1 bdl.)	+ (1 bdl.)
Micropterix clathella (L., 1761) [Hannemann 1956]	+	+	+	+	+	+	-
Nannochorista sp. [Beutel and Baum 2008]	-	-	+	+	-	-	-

Appendix 2: Detailed description of the antennal musculature of adult Trichoptera. Abbreviations: **acl** – anteclypeolabrum, **ata** – anterior tentorial arm, **atf** – antennifer, **atp** – anterior tentorial pit, **bdl.** – bundle, **cpe** – compound eye, **dta** – dorsal tentorial arm, **fgs** – frontogenal sulcus, **fpc** – frontopostclypeus, **ge** – gena, **gp** – subgenal process, **hf** – horizontal furrow, **I** – insertion, **lt** – laminatentorium, **md(m)** – membranous part of mandible, **O** – origin, **ocs** – occipital sulcus, **sca** – scapus, **te** – tendon, **te-sc(a)** – M. tentorio-scapalis anterior, **te-sc(l)** – M. tentorio-scapalis lateralis, **te-sc(m)** – M. tentorio-scapalis medialis, **te-sc(p)** – M. tentorio-scapalis posterior, ? – uncertain.

Taxon	te-sc(a)		te-sc(p)		te-sc(l)		te-sc(m)	
	O	I	O	I	O	I	O	I
	1 bdl. (te-sc(a))		1 bdl. (te-sc(p))		2 bdl. (te-sc(l)-v, te-sc(l)-d)		1 bdl. (te-sc(m))	
Philopotamus ludificatus McLachlan, 1878	mesal side of **ata** and **lt**	ventromesally at the scapal base with strong **te**	**ata**	posterior basal margin of scapal base	both at the lateral face of **ata** and **lt**	both together ventrolaterally at the scapal base; posterior bundle with short **te**	dorsally on **ata** close to the head capsule	mesal margin of scapal base
	1 bdl. (te-sc(a))		1 bdl. (te-sc(p))		2 bdl. (te-sc(l)-v, te-sc(l)-d)		1 bdl. (te-sc(m))	
Stenopsyche marmorata Navas, 1920	mesally at **ata** and base of **dta** [?]	at anterior basal margin of **sca**	**dta**	posterior basal margin of scapal base	te-sc(l)-v at anterior wall of **ge** ventrolateral to **atp,** te-sc(l)-d laterally at **ata**	both at lateral basal margin of **sca** directly above **atf**	dorsomesally at **ata** [?] close to the head capsule	mesal margin of scapal base
	1 bdl. (te-sc(a))		1 bdl. (te-sc(p))		2 bdl. (te-sc(l)-v, te-sc(l)-d)		2 bdl. (te-sc(m)-v, te-sc(m)-d)	
Hydropsyche angustipennis (Curtis, 1834)	mesal face of **ata** and inner **lt** (mesal to te-sc(l)-d)	ventrally at the scapal base with strong **te** (mesal to **atf**)	dorsally at lateral projection of **ata**	posterior basal margin of scapal base without **te**	te-sc(l)-d at mesal face of inner **lt**; te-sc(l)-v laterally at lateral projection of **ata**	both together laterally at (dorsally to **atf**) scapal base with short **te**	te-sc(m)-v at head capsule (**fpc**) dorsomesally to **atp**; te-sc(m)-d at mesal face of inner **lt**	both together with strong **te** at mesal margin of scapal base
	1 bdl. (te-sc(a))		1 bdl. (te-sc(p))		2 bdl. (te-sc(l)-v, te-sc(l)-d)		2 bdl. (te-sc(m)-v, te-sc(m)-d)	
Tinodes dives (Pictet, 1834)	mesal face of **ata** and inner **lt** (mesal to te-sc(l)-d)	ventrally at the scapal base (mesal to **atf**)	laterally at **ata**	posterior basal margin of scapal base without **te**	te-sc(l)-v at anterior wall of **ge** ventrolateral to **atp,** te-sc(l)-d laterally at **ata**	both at lateral basal margin of **sca** directly above **atf**	te-sc(m)-v at head capsule (**fpc**) dorsomesally to **atp**; te-sc(m)-d at mesal face of inner **lt**	both together with strong **te** at mesal margin of scapal base

Appendix 2: Continued.

Taxon	te-sc(a)		te-sc(p)		te-sc(l)		te-sc(m)	
	O	I	O	I	O	I	O	I
	2 bdl. (te-sc(a)-v, te-sc(a)-d)		**1 bdl. (te-sc(p))**		**2 bdl. (te-sc(l)-v, te-sc(l)-d)**		**2 bdl. (te-sc(m)-v, te-sc(m)-d)**	
Holocentropus dubius (Rambur, 1842)	te-sc(a)-v dorsomesally at **ata**, te-sc(a)-d dorsomesally at **ata** and **lt** directly posterior to te-sc(a)-v	both together ventrally at basal margin of **sca** (mesal to **atf**) with long **te**	dorsolaterally at **ata**	dorsolateral margin of scapal base without **te**	te-sc(l)-d ventrolaterally at **ata**; te-sc(l)-v laterally at head capsule (gena above **gp**)	both together laterally at (dorsally to atf) scapal base with strong tendon	te-sc(m)-v mesally at head capsule (**fpc**) above **hf**; te-sc(m)-d dorsomesally at **ata** and mesal face of **lt**	both together with strong **te** at mesal margin of scapal base
	2 bdl. (te-sc(a)-v, te-sc(a)-d)		**1 bdl. (te-sc(p))**		**1 bdl. (te-sc(l))**		**1 bdl. (te-sc(m))**	
Rhyacophila obliterata McLachlan, 1863	te-sc(a)-v dorsally at **ata**, te-sc(a)-d mesally at **ata** and mainly at mesal face of **lt**	at anterior basal margin of **sca** with short, distinct **te's**, te-sc(a)-v mesad **atf** and te-sc(a)-d; te-sc(a)-d between **atf** and te-sc(a)-v	at the base of the small, membranous **dta**	posterior basal margin of **sca**	lateral face of **lt** and **ata**	lateral basal margin of **sca** directly above **atf** with long **te**	mesal face of **lt**	mesally at the anterior basal margin of scapal base with short **te**
	2 bdl. (te-sc(a)-v, te-sc(a)-d)		**1 bdl. (te-sc(p))**		**1 bdl. (te-sc(l))**		**1 bdl. (te-sc(m))**	
Hydrobiosis styracine McFarlane, 1960	te-sc(a)-v mesally at **ata** and **lt**; te-sc(a)-d dorsomesally at **ata** in front of **dta** and base of **dta**	both bdl. anterolaterally at basal margin of **sca** (directly below **atf**)	apically at the mambranuous tip of **dta**	posteromesally at the basal margin of scapal base	lateral face of **lt**	lateral basal margin of **sca** directly above **atf** with short, strong **te**	dorsomesally at **ata** near head capsule	at anterior basal margin of scapus mesal to te-sc(a)-v/d
	2 bdl. (te-sc(a)-v, te-sc(a)-d)		**1 bdl. (te-sc(p))**		**1 bdl. (te-sc(l))**		**1 bdl. (te-sc(m))**	
Apsilochorema sutshanum Martynov, 1934	te-sc(a)-v mesally at **ata** and **lt**; te-sc(a)-d dorsomesally at **ata** in front of **dta** and base of **dta**	both bdl. anterolaterally at basal margin of **sca** (directly below **atf**)	apically at the mambranuous tip of **dta**	posteromesally at the basal margin of scapal base	lateral face of **lt**	lateral basal margin of **sca** directly above **atf** with short, strong **te**	dorsomesally at **ata** near head capsule	at anterior basal margin of scapus mesal to te-sc(a)-v/d
	2 bdl. (te-sc(a)-v, te-sc(a)-d)		**1 bdl. (te-sc(p))**		**2 bdl. (te-sc(l)-v, te-sc(l)-d)**		**-**	
Glossosoma spinosum Morse et Yang, 2005	te-sc(m)-v mesally at **ata** near head capsule; te-sc(a)-d dorsomesally at **ata** and **lt**	both bdl. anterolaterally at basal margin of **sca** (directly below **atf**)	dorsally at **ata** near head capsule	posteromesally at the basal margin of scapal base with short **te**	te-sc(l)-d ventrolaterally at **ata**; te-sc(l)-v laterally at head capsule (gena above **gp**)	both together laterally at (dorsally to atf) scapal base with strong tendon		

Appendix 2: Continued.

Taxon	te-sc(a)		te-sc(p)		te-sc(l)		te-sc(m)	
	O	I	O	I	O	I	O	I
	2 bdl. (te-sc(a)-v, te-sc(a)-d)		**1 bdl. (te-sc(p))**		**2 bdl. (te-sc(l)-v, te-sc(l)-d)**		**-**	
Agapetus fuscipes Curtis, 1834	te-sc(m)-v mesally at **ata** near head capsule; te-sc(a)-d dorsomesally at **ata** and **lt**	both bdl. anterolaterally at basal margin of **sca** (directly below **atf**)	dorsomesally at **ata** and **lt**	posteromesally at the basal margin of scapal base without **te**	te-sc(l)-v dorsolaterally at the small **dta**, te-sc(l)-d ventrolaterally at **ata** and **lt**	both together at lateral basal margin of sca (lateral/above **atf**), te-sc(l)-v with short **te**		
	1 bdl. (te-sc(a))		**1 bdl. (te-sc(p))**		**2 bdl. (te-sc(l)-v, te-sc(l)-d)**		**1 bdl. (te-sc(m))**	
Ptilocolepus granulatus (Pictet, 1834)	dorsally at **ata** close to head capsule	at anterior basal margin of **sca** (mesal to atf) with short **te**	dorsolaterally at **ata** and the small **dta**	posterior basal margin of scapal base without **te**	te-sc(l)-v anterolaterally at head capsule between **atp** and base of mandible, te-sc(l)-d laterally at **ata**	both at lateral basal margin of **sca** (lateral/above **atf**) with distinct **te**'s	mesally at head capsule (**fpc**) directly above **atp**	mesal margin of scapal base with long **te**
	1 bdl. (te-sc(a))		**1 bdl. (te-sc(p))**		**2 bdl. (te-sc(l)-v, te-sc(l)-d)**		**1 bdl. (te-sc(m))**	
Hydroptila scamandra Neboiss, 1977	dorsomesally at **ata**	ventrally at the scapal base (mesal to **atf**)	dorsally at **ata**	posterolaterally at the basal margin of scapal base with short **te**	te-sc(l)-v anterolaterally at **ge**, te-sc(l)-d dorsolaterally at **ata**	both at lateral basal margin of **sca** (lateral/above **atf**) with distinct **te**'s	mesally at ata	mesal margin of scapal base
	1 bdl. (te-sc(a))		**1 bdl. (te-sc(p))**		**2 bdl. (te-sc(l)-v, te-sc(l)-d)**		**1 bdl. (te-sc(m))**	
Orthotrichia atraseta Wells, 1979	dorsomesal wall of **ata**	ventral margin of scapal base (mesal to **atf**)	dorsally at **ata**	posterior basal margin of scapal base	te-sc(l)-v anterolaterally at **ge**, te-sc(l)-d dorsolaterally at **ata**	both at lateral basal margin of **sca** (lateral/above **atf**) with distinct **te**'s	mesally at **ata**	anterior basal margin of scapal base
	3 bdl. (te-sc(a)-l, te-sc(a)-v, te-sc(a)-m)		**1 bdl. (te-sc(p))**		**1 bdl. (te-sc(l))**		**1 bdl. (te-sc(m))**	
Phryganea grandis Linnaeus, 1758	te-sc(a)-m near the base of **dta**; te-sc(a)-v dorsolaterally at **ata**; te-sc(a)-l dorsally at **ata**	te-sc(a)-m at anterior basal margin of sca closely adjacent to te-sc(a)-v with long **te**; te-sc(a)-v close to te-sc(a)-m ; te-sc(a)-l at anterior basal margin of **sca** with short **te**	**dta** close to the base of the antenna	mesally at posterior basal margin of scapal base with short **te**	laterally at **ata** and **lt**	at lateral basal margin of **sca** directly above **atf** with short **te**	dorsomesally at **ata**	mesally at basal margin of **sca** with long **te**

Appendix 2: Continued.

Taxon	te-sc(a)		te-sc(p)		te-sc(l)		te-sc(m)	
	O	I	O	I	O	I	O	I
	3 bdl. (te-sc(a)-l, te-sc(a)-v, te-sc(a)-m)		**1 bdl. (te-sc(p))**		**1 bdl. (te-sc(l))**		**1 bdl. (te-sc(m))**	
Trichostegia minor (Curtis, 1834)	te-sc(a)-l at lateral face of **ata** and **lt**; te-sc(a)-v dorsolaterally at **ata**; te-sc(a)-m **dta** above te-sc(p)	te-sc(a)-l ventrolaterally at basal margin of **sca**; te-sc(a)-v at anterior basal margin of **sca** between te-sc(a)-l and te-sc(a)-m; te-sc(a)-m anterior basal margin of **sca**	**dta**	posterior basal margin of scapal base with short **te**	lateral face of **ata** and **lt**	lateral basal margin of **sca** with short **te**, directly above **atf**	dorsomesally at **ata**	mesally at basal margin of **sca** with short **te**
	3 bdl. (te-sc(a)-l, te-sc(a)-v, te-sc(a)-m)		**1 bdl. (te-sc(p))**		**1 bdl. (te-sc(l))**		**1 bdl. (te-sc(m))**	
Brachycentrus subnubilus Curtis, 1834	te-sc(a)-l at dorsal face of **lt** and **fgs**; te-sc(a)-v anterolaterally at **fpc** directly above **md(m)**; te-sc(a)-m at the base of **dta**	te-sc(a)-l anterolaterally at basal margin of **sca** (below **atf**); te-sc(a)-v at anterior basal margin of **sca**; te-sc(a)-m at anterior basal margin of **sca** mesal to te-sc(a)-v	anterior face of **dta**	posterior basal margin of scapal base without **te**	at lateral face of **ata** and **lt**	posterolaterally at basal margin of **sca** with short **te**	at **ata** (**fgs**) close to head capsule and at **fpc** lateral to **atp**	mesal margin of scapal base with short **te**
	3 bdl. (te-sc(a)-l, te-sc(a)-v, te-sc(a)-m)		**1 bdl. (te-sc(p))**		**2 bdl. (te-sc(l)-v, te-sc(l)-d)**		**1 bdl. (te-sc(m))**	
Limnephilus flavicornis (Fabricius, 1787)	te-sc(a)-l dorsolaterally at **lt**; te-sc(a)-v dorsomesally at **ata** and **lt**; te-sc(a)-m at **dta**	te-sc(a)-l at lateral basal margin of **sca** (below **atf**); te-sc(a)-v ventrolaterally at basal margin of **sca**, between te-sc(a)-l and te-sc(a)-m; te-sc(a)-m at anterior basal margin of **sca**	laterally at the base of **dta**	posterior basal margin of scapal base without **te**	te-sc(l)-v at **ata** behind the base of **dta**; te-sc(l)-d dorsolaterally at **lt** and **ata**	both together posterolaterally at basal margin of **sca** with short **te**	at anterior face of **ge** (dorsolateral to **atp**)	mesally at anterior basal margin of **sca** with short **te**
	3 bdl. (te-sc(a)-l, te-sc(a)-v, te-sc(a)-m)		**1 bdl. (te-sc(p))**		**1 bdl. (te-sc(l))**		**1 bdl. (te-sc(m))**	
Silo nigricornis (Pictet, 1834)	te-sc(a)-l laterally at ata; te-sc(a)-v anterolaterally at **ge** (above **md(m)**), directly above te-sc(l); te-sc(a)-m dorsolaterally at **ata**	te-sc(a)-l anterolaterally at basal margin of **sca** (directly below **atf**); te-sc(a)-v anterior basal margin of **sca**, between te-sc(a)-l and te-sc(a)-m; te-sc(a)-m at anterior basal margin of **sca**	at the basal half of **dta**	at the posterior basal margin of **sca** with short **te**	anterolaterally at **ge** (above **md(m)**) and at **gp**	lateral basal margin of sca with short **te**, directly above **atf**	anterior face of **ge** (lateral to **atp**)	mesal basal margin of scapal base with strong **te**
	1 bdl. (te-sc(a))		**1 bdl. (te-sc(p))**		**1 bdl. (te-sc(l))**		**1 bdl. (te-sc(m))**	
Sericostoma personatum Kirby et Spence, 1826	dorsomesally at **ata** and **lt** (directly adjacent to te-sc(p))	at anterior basal margin of **sca** without **te**	dorsally at **ata** closely adjacent to te-sc(a)	posterolaterally at basal margin of **sca** with short **te**	ventrally at **ge** near **cpe** and at **ocs**	lateral basal margin of **sca** directly above **atf**	anterior face of **ge** (at and behind subgenal process)	mesally at basal margin of **sca** with long **te** (intersects with te-sc(a))

Appendix 2: Continued.

Taxon	te-sc(a)		te-sc(p)		te-sc(l)		te-sc(m)	
	0	I	0	I	0	I	0	I
	3 bdl. (te-sc(a)-l, te-sc(a)-v, te-sc(a)-m)		**1 bdl. (te-sc(p))**		**2 bdl. (te-sc(l)-v, te-sc(l)-d)**		**1 bdl. (te-sc(m))**	
Pycnocentria evecta McLachlan, 1868	te-sc(a)-l dorsolaterally at **ata**; te-sc(a)-v ventrolaterally at ge below cpe; te-sc(a)-m dorsally at **ata** and **lt**	te-sc(a)-l ventrolaterally at basal margin of **sca** (below **atf**); te-sc(a)-v at anterior basal margin of **sca** between te-sc(a)-l and te-sc(a)-m; te-sc(a)-m anterior basal margin of **sca**	terally at posterior half of **at**	at posterior basal margin of scapal base with short **te**	te-sc(l)-d at **ge** between **cpe and ocs** (lateral to te-sc(l)-v); te-sc(l)-v at **ge** below **cpe** mesally to te-sc(l)-d	both together at lateral basal margin of **sca** with short **te**, directly above **atf**	dorsomesally at **ata** and **lt**	ventromesally at scapal base with short **te**
	3 bdl. (te-sc(a)-l, te-sc(a)-v, te-sc(a)-m)		**1 bdl. (te-sc(p))**		**1 bdl. (te-sc(l))**		**1 bdl. (te-sc(m))**	
Molanna angustata Curtis, 1834	te-sc(a)-l anterior face of **ge** above **md(m)**; te-sc(a)-v at **ata** and **fpc** lateral to **atp**; te-sc(a)-m dorsomesally at **ata**	te-sc(a)-l laterally at anterior basal margin of **sca** (directly below **atf**); te-sc(a)-v anterior basal margin of **sca**, between te-sc(a)-l and te-sc(a)-m; te-sc(a)-m at anterior basal margin of **sca**	dorsally at **ata**	at the posterior basal margin of **sca** without **te**	laterally at **ata** and **lt**	posterolaterally at basal margin of **sca** with short **te**	ventral face of **fpc** (dorsolaterally to **atp**)	anteromesally at basal margin of **sca** without **te**
	3 bdl. (te-sc(a)-l, te-sc(a)-v, te-sc(a)-m)		**1 bdl. (te-sc(p))**		**1 bdl. (te-sc(l))**		**1 bdl. (te-sc(m))**	
Leptocerus tineiformis Curtis, 1834	te-sc(a)-l dorsally at **ata**, inner **lt** and **dta**; te-sc(a)-v laterally at **ata** and outer **lt**; te-sc(a)-m dorsomesally at inner **lt**	te-sc(a)-l anterolaterally at basal margin of **sca** (closely adjacent to te-sc(a)-v) (below **atf**); te-sc(a)-v anterolaterally at basal margin of **sca**; te-sc(a)-m at anterior basal margin of **sca**	at the tip of the incomplete **dta**	at the posterior basal margin of **sca** with short **te**	lateral basal margin of **sca** (above **atf**) with long **te**	at posterior face of **pge**	dorsomesally at **ata** and inner **lt** in front of te-sc(a)	mesal basal margin of scapal base without **te**

Appendix 3: Description of the epipharyngeal and hypopharyngeal musculature of adult Trichoptera. Abbr.: **acl** – anteclypeolabrum, **ata** – anterior tentorial arm, **atp** – anterior tentorial pit, **bdl.** – bundle, **cl-ci(d)** – M. clypeo-cibarialis dorsalis, **cl-ci(v)** – M. clypeo-cibarialis ventralis, **cl-eph(l)** – M. clypeo-epipharyngalis lateralis, **cl-eph(m)** – M. clypeo-epipharyngalis medialis, **eph** – epipharynx, **fg** – ganglion frontale, **fpc** – frontopostclypeus, **ge** – gena, **hf** – horizontal furrow, **I** – insertion, **lt** – laminatentorium, **md(m)** – membr. part of mandible, **O** – origin, poc – preoral cavity, **ppt** – prepharyngeal tube, **sit** – sitophore plate, **tb** – tentorial bridge, **te-si** – M. tentorio-sitophorialis.

Taxon	cl-eph(m)		cl-eph(l)		cl-ci(v)		cl-ci(d)		te-si	
	O	I	O	I	O	I	O	I	O	I
	1 compact muscle		1 compact muscle		1 bdl.		2 distinct bdl.		1 bdl.	
Philopotamus ludificatus McLachlan, 1878	central at the beginning of the sclerotized part of **acl**	median at the distal end of **eph**	laterally at proximal half of **acl** (between **cl-eph(m)** and **hf**)	mesally at **eph** dorsad **cl-eph(m)**	dorsolaterally at **acl** (dorsally of **cl-eph(l)**)	**poc** at the ventralmost part of **ppt**	mesally and laterally at **fpc** dorsally to **hf**	proximal edge of membr. part of **ppt** directly below **fg**	paramedian on ventral side of **tb** (between the **ata**)	dorsal end of sitophore plate, opposite to **cl-ci(v)**
	1 compact muscle		1 compact muscle		1 bdl.		1 bdl. [?]		1 bdl.	
Stenopsyche marmorata Navas, 1920	centrally at the sclerotized part of **acl**	median at **eph** (directly below **cl-eph(l)**)	directly dorsal to **cl-eph(m)**)	mesally at proximal half of **eph**	mesally [?] at **fpc** above **hf**	**poc** at the ventralmost part of **ppt**	laterally [?] at **fpc** above **hf**	**ppt** directly below **fg** [?]	paramedian on ventral side of **tb** (between the **ata**)	dorsal end of sitophore plate, opposite to **cl-ci(v)**
	1 compact muscle		1 bdl. on each side		1 bdl.		2 distinct bdl.		1 bdl.	
Hydropsyche angustipennis (Curtis, 1834)	central at the sclerotized part of **acl** between both bdl.'s of **cl-eph(l)**	median at the distal end of **eph** (below **cl-eph(l)**)	laterally at proximal half of **acl**	both bdl. together mesally at proximal half of **eph**	laterally at **fpc** above **hf** between lateral and ventral bdl. of **cl-ci(d)**	**poc** at the ventralmost part of **ppt**	mesally and laterally at **fpc** directly above **hf**	membr. part of **ppt** distinctly below **fg**	paramedian on ventral side of **tb** (between the **ata**)	dorsal end of sitophore plate, below dorsal process of **sit**
	1 compact muscle		1 bdl. on each side		1 bdl.		2 distinct bdl.		1 bdl.	
Tinodes dives (Pictet, 1834)	central at the sclerotized part of **acl** between both bdl.'s of **cl-eph(l)**	median at the distal end of **eph** (below **cl-eph(l)**)	laterally at sclerotized proximal half of **acl**	both bdl. together mesally at proximal half of **eph**	mesally at **fpc** distinctly dorsal to **hf**	**poc** at the ventralmost part of **ppt**	laterally at **fpc** above **hf** (dorsal bdl.); at **ge** above **md(m)** (ventral bdl.)	both bdl. laterally at **ppt** directly below **fg**	paramedian on ventral side of **tb** (between the **ata**)	proximal end of **sit**
	1 compact muscle		1 bdl. on each side		2 distinct bdl.		2 distinct bdl.		1 bdl.	
Holocentropus dubius (Rambur, 1842)	central at the sclerotized part of **acl** below both bdl.'s of **cl-eph(l)**	median at the distal end of **eph** (below **cl-eph(l)**)	laterally at sclerotized proximal half of **acl**	both bdl. together mesally at proximal half of **eph**	both bdl. mesally at **fpc** directly dorsal to **hf**	ventral bdl. ventrally at **ppt**, lateral bdl. below **fg** at **ppt**	laterally at **fpc** above **hf** (dorsal bdl.); at **ge** above **md(m)** (ventral bdl.)	both laterally at **ppt,** ventral bdl. together with ventral bdl. of **cl-ci(v)**	paramedian on ventral side of **tb** (between the **ata**)	dorsal end of sitophore plate, below dorsal process of **sit**

Appendix 3: Continued.

Taxon	cl-eph(m)		cl-eph(l)		cl-ci(v)		cl-ci(d)		te-si	
	O	I	O	I	O	I	O	I	O	I
	1 compact muscle		**1 bdl. on each side**		**2 distinct bdl.**		**1 bdl.**		**1 bdl.**	
Rhyacophila obliterata McLachlan, 1863	central at the sclerotized part of **acl** below **cl-eph(l)**	median at the distal end of **eph** (distinctly below **cl-eph(l)**)	laterally at sclerotized proximal half of **acl**	both bdl. together mesally at proximal half of **eph**	dorsolaterally at **acl** (directly posterior to **cl-eph(l)**)	dorsally at **poc** at the ventralmost part of **ppt**	laterally at **fpc** directly above **hf**	**ppt** directly below **fg** [?]	paramedian on ventral side of **tb** (between the **ata**)	dorsal end of sitophore plate
	1 compact muscle		**1 compact muscle**		**1 bdl.**		**2 distinct bdl.**		**1 bdl.**	
Hydrobiosis styracine McFarlane, 1960	central at the beginning of the sclerotized part of **acl**	median at the distal end of **eph**	laterally at **acl** (between **cl-eph(m)** and **hf**)	mesally at **eph** dorsad **cl-eph(m)**	dorsolaterally at **acl** (dorsally of **cl-eph(l)**)	**poc** at the ventralmost part of **ppt**	mesally and laterally at **fpc** dorsally to **hf**	proximal edge of membr. part of **ppt** directly below **fg**	ventrally at mesal wall of the large **lt**	dorsal end of sitophore plate
	1 compact muscle		**1 bdl. on each side**		**2 distinct bdl.**		**1 bdl.**		**1 bdl.**	
Apsilochorema sutshanum Martynov, 1934	central at the sclerotized part of **acl** below **cl-eph(l)**	median at the distal end of **eph** (distinctly below **cl-eph(l)**)	dorsolaterally at sclerotized proximal half of **acl**	both bdl. together mesally at proximal half of **eph**	dorsolaterally at **acl** (both directly posterior to **cl-eph(l)**)	both bdl. dorsally at **poc** at the ventralmost part of **ppt**	laterally at **fpc** directly above **hf**	**ppt** directly below **fg**	paramedian on ventral side of **tb** (between the **ata**)	dorsal end of sitophore plate
	1 compact muscle		**1 compact muscle**		**2 distinct bdl.**		**1 bdl.**		**1 bdl.**	
Glossosoma spinosum Morse et Yang, 2005	central at the distal half of **acl**	median at the distal end of **eph**	laterally and mesally at **acl** (between **cl-eph(m)** and **hf**)	mesally at **eph** distinctly dorsad **cl-eph(m)**	dorsolaterally at **acl** (both directly posterior to **cl-eph(l)**)	both bdl. dorsally at **poc** at the ventralmost part of **ppt**	laterally at **fpc** directly above **hf**	**ppt** directly below **fg**	paramedian on ventral side of **tb** (between the **ata**)	dorsal end of sitophore plate
	1 compact muscle		**1 bdl. on each side**		**1 bdl.**		**2 distinct bdl.**		**1 bdl.**	
Agapetus fuscipes Curtis, 1834	mesally at the distal half of the sclerotized part of **acl**	median at the distal end of **eph**	laterally at **acl** (between **cl-eph(m)** and **hf**)	mesally at **eph** dorsad **cl-eph(m)**	dorsolaterally at **acl** (dorsolaterally of **cl-eph(l)**)	**poc** at the ventralmost part of **ppt**	mesally and laterally at **fpc** dorsally to **hf**	proximal edge of membr. part of **ppt** directly below **fg**	paramedian on ventral side of **tb** (between the **ata**)	dorsal end of sitophore plate
	1 compact muscle		**1 compact muscle**		**1 bdl.**		**1 bdl.**		**1 bdl.**	
Ptilocolepus granulatus (Pictet, 1834)	central at the distal half of **acl**	median at the distal end of **eph**	laterally and mesally at **acl** (between **cl-eph(m)** and **hf**)	mesally at **eph** directly dorsad **cl-eph(m)**	dorsolaterally at **acl** (dorsolaterally of **cl-eph(l)**)	**poc** at the ventralmost part of **ppt**	mesally at **fpc** directly above **hf**	**ppt** directly below **fg**	paramedian on **tb** (between the **ata**)	dorsal end of sitophore plate

Appendix 3: Continued.

Taxon	cl-eph(m)		cl-eph(l)		cl-ci(v)		cl-ci(d)		te-si	
	O	I	O	I	O	I	O	I	O	I
	1 compact muscle		**1 bdl. on each side**		**1 bdl.**		**1 bdl.**		**1 bdl.**	
Hydroptila scamandra Neboiss, 1977	in the middle of **acl** (composed of 4 fibers)	median at the distal end of **eph**	laterally at **acl** (between **cl-eph(m)** and **cl-ci(v)**) (only 2 fibers)	mesally at **eph** dorsad **cl-eph(m)**	dorsomesally at **acl** (dorsolaterally of **cl-eph(l)**)	**poc** at the ventralmost part of **ppt**	laterally at **fpc** directly above **hf**	**ppt** directly below **fg**	paramedian on **tb** (between the **ata**)	dorsal end of sitophore plate
	1 fiber on each side		**2 fibers on each side**		**1 bdl.**		**1 bdl.**		**1 bdl.**	
Orthotrichia atraseta Wells, 1979	laterally in the proximal half of **acl** (only 1 fiber)	median at the distal end of **eph**	one fiber laterally and one fiber meseally at **acl** (only 2 fibers)	mesally at **eph** dorsad **cl-eph(m)**	dorsolaterally at **acl** (dorsolaterally of **cl-eph(l)**)	**poc** at the ventralmost part of **ppt**	laterally at **fpc** directly above **hf**	**ppt** directly below **fg**	paramedian on **tb** (between the **ata**)	dorsal end of sitophore plate
	1 compact muscle		**1 compact muscle**		**1 bdl.**		**2 distinct bdl.**		**1 bdl.**	
Phryganea grandis Linnaeus, 1758	in the distal half of **acl** (small and short)	median at the distal end of **eph**	mesally at **acl** (above **cl-ci(m)**) with broad attach. area	mesally at **eph** distinctly dorsad **cl-eph(m)**	mesally at **fpc** (directly above **hf**)	**poc** at the ventralmost part of **ppt**	mesally and laterally at **fpc** directly above **hf**	**ppt** directly below **fg**	paramedian on ventral side of **tb** (between the **ata**)	dorsal end of sitophore plate
	1 compact muscle		**1 compact muscle**		**1 bdl.**		**2 adjacent bdl.**		**1 bdl.**	
Trichostegia minor (Curtis, 1834)	mesally in the distal half of **acl**	median at the distal end of **eph**	mesally at **acl** (above **cl-ci(m)**) with broad attach. area	mesally at **eph** above **cl-eph(m)**	mesally at **fpc** (directly above **hf**)	**poc** at the ventralmost part of **ppt**	mesally and laterally at **fpc** directly above **hf**	**ppt** directly below **fg**	paramedian on ventral side of **tb** (between the **ata**)	dorsal end of sitophore plate, below dorsal process of **sit**
	1 compact muscle		**2 compact bundles**		**1 bdl.**		**3 distinct bdl.**		**1 bdl.**	
Brachycentrus subnubilus Curtis, 1834	mesally in the distal half of **acl**	median at the distal end of **eph**	both mesally and laterally at **acl** (above **cl-ci(m)**) with distinct O	both mesally at **eph** above **cl-eph(m)**, distinctly separated	laterally at **acl** (directly below **hf**)	**poc** at the ventralmost part of **ppt**	mesally (dorsal bdl.), laterally (ventral bdl.'s) at **fpc** above **hf**	**ppt** distinctly below **fg**	paramedian on ventral side of **tb** (between the **ata**)	dorsal end of sitophore plate
	1 compact muscle		**2 compact bundles**		**1 bdl.**		**3 distinct bdl.**		**1 bdl.**	
Limnephilus flavicornis (Fabricius, 1787)	mesally in the distal half of **acl**	median at the distal end of **eph**	both mesally and laterally at **acl** (above **cl-ci(m)**) with distinct O	both mesally at **eph** above **cl-eph(m)**, distinctly separated	laterally at **acl** (distinctly below **hf**)	**poc** at the ventralmost part of **ppt**	mesally (dorsal bdl.), laterally (ventral bdl.'s) at **fpc** above **hf**	**ppt** distinctly below **fg**	paramedian on ventral side of **tb** (between the **ata**)	dorsal end of sitophore plate, below dorsal process of **sit**

Appendix 3: Continued.

Taxon	cl-eph(m)		cl-eph(l)		cl-ci(v)		cl-ci(d)		te-si	
	O	I	O	I	O	I	O	I	O	I
	1 compact muscle		**2 compact bundles**		**1 bdl.**		**3 distinct bdl.**		**1 bdl.**	
Silo nigricornis (Pictet, 1834)	mesally in the distal half of **acl**	median at the distal end of **eph**	both mesally and laterally at **acl** (above **cl-ci(m)**) with distinct O	both mesally at **eph** above **cl-eph(m)**, distinctly separated	laterally at **fpc** (directly above **hf**)	**poc** at the ventralmost part of **ppt**	mesally (dorsal bdl.), laterally (ventral bdl.'s) at **fpc** above **hf**	**ppt** distinctly below **fg**	paramedian on ventral side of **tb** (between the **ata**)	dorsal end of sitophore plate, below dorsal process of **sit**
	1 compact muscle		**1 compact muscle**		**1 bdl.**		**2 adjacent bdl.**		**1 bdl.**	
Sericostoma personatum Kirby et Spence, 1826	mesally in the distal half of **acl**	median at the distal end of **eph**	mesally and laterally at **acl** (above **cl-ci(m)**)	mesally at **eph** above **cl-eph(m)**	mesally at **acl** (directly below **hf** and above **cl-eph(l)**)	**poc** at the ventralmost part of **ppt**	mesally and laterally at **fpc** directly above **hf**	**ppt** directly below **fg**	paramedian on ventral side of **tb** (between the **ata**)	dorsal end of sitophore plate
	1 compact muscle		**1 compact muscle**		**1 bdl.**		**2 distinct bdl. [?]**		**1 bdl.**	
Pycnocentria evecta McLachlan, 1868	centrally in the proximal half of **acl**	median at the distal end of **eph**	mesally and laterally at **acl** (above **cl-ci(m)**)	mesally at **eph** above **cl-eph(m)**	dorsolaterally at **acl** (directly below **hf** and above **cl-eph(l)**)	**poc** at the ventralmost part of **ppt**	laterally at **fpc** directly above **hf**	**ppt** directly below **fg**	paramedian on ventral side of **tb** (between the **ata**)	dorsal end of sitophore plate
	1 compact muscle		**1 compact muscle**		**1 bdl.**		**2 distinct bdl.**		**1 bdl.**	
Molanna angustata Curtis, 1834	centrally in the distal half of **acl**	median at the distal end of **eph**	mesally and laterally at **acl** (above **cl-ci(m)**)	mesally at **eph** above **cl-eph(m)**	mesally at **fpc** (directly above **hf**)	**poc** at the ventralmost part of **ppt**	mesally and laterally (below **atp**) at **fpc** directly above **hf**	**ppt** directly below **fg**	paramedian on ventral side of **tb** (between the **ata**)	dorsal end of sitophore plate
	1 compact muscle		**1 compact muscle**		**1 bdl.**		**2 distinct bdl.**		**1 bdl.**	
Leptocerus tineiformis Curtis, 1834	centrally in the distal half of **acl**	median at the distal end of **eph**	mesally and laterally at **acl** (above **cl-ci(m)**)	mesally at **eph** above **cl-eph(m)**	laterally at **fpc** (directly above **hf**)	**poc** at the ventralmost part of **ppt**	mesally and laterally at **fpc** directly above **hf**	**ppt** distinctly below **fg**	paramedian on ventral side of **tb** (between the **ata**)	dorsal end of sitophore plate, below dorsal process of **sit**

Appendix 4: Detailed description of the pharyngeal musculature of adult Trichoptera. Abbr.: **ata** – anterior tentorial arm, **atp** – anterior tentorial pit, **bdl.** – bundle, **br** – brain, **cr-ph(a)** – M. cranio-pharyngalis anterior, **cr-ph(p)** – M. cranio-pharyngalis posterior, **fg** – ganglion frontale, **fgs** – frontogenal sulcus, **fpc** – frontopostclypeus, **fr-ph(a)** – M. fronto-pharyngalis anterior, **fr-ph(p)** – M. fronto-pharyngalis posterior, **I** – insertion, **ias** – interantennal sulcus, **loc** – lateral ocellus, **te-ph(l)** – M. tentorio-pharyngalis lateralis, **O** – origin, **ppc** – precerebral pumping chamber, **pph** – postpharynx, **pta** – posterior tentorial arm, **tb** – tentorial bridge, **te-ph(a)** – M. tentorio-pharyngalis anterior, **te-ph(p)** – M. tentorio-pharyngalis posterior, **te-si** – M. tentorio-sitophorialis.

Taxon	fr-ph(a)		fr-ph(p)		te-ph(l)		te-ph(a)		te-ph(p)		cr-ph(a)		cr-ph(p)	
	O	I	O	I	O	I	O	I	O	I	O	I	O	I
	1 bdl.		**2 distinct bdl.**		**1 bdl.**		**2 distinct bdl.**		**1 bdl.**		**1 bdl.**		**-**	
Philopotamus ludificatus McLachlan, 1878	central region of **fpc**, between the **atp**	mesally at the anterolateral corner of the **ppc**, behind **fg**	both at frons, mesally of **ias**	dorsally at the posterodorsal face of the **ppc**, in front of the **br**	broad area of the distal half of **ata**	dorsolaterally at the **ppc**	mesally on the base of **ata**	ventrally at the posterior end of **ppc**, opposite to **fr-ph(p)**	**pta**	ventrally at pph, slightly behind the **br**, opposite to **cr-ph(a)**	vertex, mesally of postgenal sulcus (posteriorly of **loc**)	dorsally on **pph**, directly behind the **br**		
	1 bdl.		**1 bdl. [?]**		**1 bdl.**		**1 bdl.**		**- [?]**		**- [?]**		**- [?]**	
Stenopsyche marmorata Navas, 1920	mesally at **fpc**	mesally at the anterior wall of the **ppc**, behind **fg**	at frons between **ias**	dorsally at the posterodorsal wall of **ppc**, in front of **br**	mesally at the distal end of **ata**	lateral wall of **ppc**	mesally on the base of **ata** directly behind **te-si**	ventrally at the posterior end of **ppc**						
	1 bdl.		**3 distinct bdl.**		**1 bdl.**		**2 distinct bdl.**		**1 bdl.**		**1 bdl.**		**-**	
Hydropsyche angustipennis (Curtis, 1834)	dorsally at bulged part of **fpc**	dorsomesally at **ppc**, distinctly behind **fg**	all at frons, between the bases of the antennae	dorsally at the posterodorsal face of the **ppc**	mesally at the distal end of **ata**	at the lateral wall of **ppc**	dorsomesally on the base of **ata**	ventrally at the posterior end of **ppc,** slightly behind **te-si**	**tb/pta**	ventrally at pph, slightly behind the **br**, opposite to **cr-ph(a)**	vertex, mesally of postgenal sulcus	dorsally on **pph**, directly behind the **br**		
	1 bdl.		**2 distinct bdl.**		**1 bdl.**		**2 distinct bdl.**		**1 bdl.**		**1 bdl.**		**-**	
Tinodes dives (Pictet, 1834)	dorsolaterally at **fpc** directly in front of te-ph(l)	dorsomesally at **ppc**, directly above **fg**	both at frons, between the bases of the antennae	dorsally at the posterodorsal face of the **ppc**	dorsomesally at **fpc** near **ata**	at the lateral wall of **ppc**	mesally on the base of **ata**	ventrally at the posterior end of **ppc,** opposite to **fr-ph(p)**	dorsally at **pta**	ventrally at pph, slightly behind the **br**	vertex, mesally of postgenal sulcus, between bdl. of cr-md(m)	dorsally on **pph**, directly behind the **br**		
	1 bdl.		**2 distinct bdl.**		**1 bdl.**		**2 distinct bdl.**		**1 bdl.**		**1 bdl.**		**1 bdl.**	
Holocentropus dubius (Rambur, 1842)	centrally at **fpc**	dorsomesally at **ppc**, directly above **fg**	both at frons, between the bases of the antennae	dorsally at the posterodorsal face of the **ppc**, in front of **br**	mesally at **ata** and **fgs** near **fpc**	at the lateral wall of **ppc**	mesally on the base of **ata**	ventrally at the posterior end of **ppc**	dorsally at **pta**	ventrally at pph, below the **br**	vertex, mesally of postgenal sulcus	dorsally on **pph**, directly below the **br**	dorsally at **pta** **directly** behind te-ph(p)	at proximal half of **pph**, below **tb**

Appendix 4: Continued.

Taxon	fr-ph(a)		fr-ph(p)		te-ph(l)		te-ph(a)		te-ph(p)		cr-ph(a)		cr-ph(p)	
	O	I	O	I	O	I	O	I	O	I	O	I	O	I
	1 bdl.		**2 distinct bdl.**		**1 bdl.**		**2 distinct bdl.**		**1 bdl.**		**1 bdl.**		**1 bdl.**	
Rhyacophila obliterata McLachlan, 1863	centrally at **fpc**	dorsomesally at **ppc**, directly above **fg**	both at frons, directly in front of **moc**	dorsally at the posterodorsal face of the **ppc**, in front of **br**	mesally at **ata** and **fgs** near **fpc**	at the lateral wall of **ppc**	mesally on the base of **ata** and at **tb**	ventrally at the posterior end of **ppc**, ventrally at **pph**	dorsally at **ata** directly in front of the base of **pta**	ventrally at pph, below the **br**, opposite to **cr-ph(a)**	vertex, mesally of postgenal sulcus	dorsally on **pph**, directly below the **br**	posterolateral at head capsule, directly above **pta**	laterally at posterior half of **pph**
	1 bdl.		**2 distinct bdl.**		**2 distinct bdl.**		**2 adjacent bdl.**		**1 bdl.**		**1 bdl.**		**2 distinct bdl.**	
Hydrobiosis styracine McFarlane, 1960	mesally at **fpc**	dorsomesally at **ppc**, directly above **fg**	both dorsally at frons, directly in front of **moc**	dorsally at the posterodorsal face of the **ppc**, in front of **br**	dorsolaterally at **fpc,** directly above **atp** and distally at **fgs/ata** near **hc**	laterally at **ppc** directly behind **fg**	mesally on the base of **ata** and at **tb**	ventrally at the posterior end of **ppc**	dorsally at **pta**	ventrally at pph, opposite to **cr-ph(a)**	laterally at vertex, behind **loc**	dorsally on **pph**, directly below/behind the **br**	**pta**	dorsolaterally at posterior half of **pph**
	1 bdl.		**3 distinct bdl.**		**2 distinct bdl.**		**2 distinct bdl.**		**1 bdl.**		**1 bdl.**		**2 distinct bdl. [?]**	
Apsilochorema sutshanum Martynov, 1934	centrally at **fpc** with broad attachment area	dorsomesally at **ppc**, directly above **fg**	dorsally and laterally at frons	dorsal and dorsolateral face of **ppc**	dorsolaterally at **fpc** above **atp** and lateral wall of **fgs**/**ata**	laterally at **ppc** directly behind **fg**	mesally on the base of **ata** and at **tb** (mesal protuberance)	ventrally at the posterior end of **ppc**, ventrally at **pph**	dorsolaterally at **tb**	ventrolaterally at pph, opposite to **cr-ph(a)**	laterally at vertex, behind **loc**	dorsally on **pph**, directly below/behind the **br**	posterodorsally at **pta**	dorsolaterally at posterior half of **pph**
	2 distinct bdl.		**2 distinct bdl.**		**2 distinct bdl.**		**2 distinct bdl.**		**1 bdl.**		**1 bdl.**		**2 adjacent bdl. [?]**	
Glossosoma spinosum Morse et Yang, 2005	centrally at **fpc** with broad attachment area	dorsomesally at **ppc**, directly above **fg**	dorsomesally at frons	dorsal face of **ppc**	dorsolaterally at **fpc** above **atp** and lateral wall of **fgs/ata**	laterally at **ppc** directly behind **fg**	mesally on the base of **ata**	ventrally at the posterior end of **ppc**	dorsally at **tb**	ventrolaterally at pph, opposite to **cr-ph(a)**	laterally at vertex, behind **loc**	dorsally on **pph**, between bundles of **cr-md(m)**	posterodorsally at **pta**	dorsolaterally at posterior half of **pph**
	1 bdl.		**1 bdl. [?]**		**2 distinct bdl.**		**2 distinct bdl.**		**- [?]**		**1 bdl.**		**1 bdl. [?]**	
Agapetus fuscipes Curtis, 1834	centrally at **fpc** with broad attachment area	dorsomesally at **ppc**, directly above **fg**	dorsomesally at frons directly in front of **moc**	dorsal face of **ppc** in front of **br**	dorsolaterally at **fpc** above **atp** and lateral wall of **fgs/ata**	dorsolaterally at **ppc** directly behind **fg**	mesally on the base of **ata** and at **tb**	ventrally at the posterior end of **ppc**			laterally at vertex	dorsally on **pph**	posterolaterally at head capsule (lateral to base of **pta**)	ventrolaterally at posterior half of **pph**
	1 bdl.		**2 adjacent bdl.**		**2 adjacent bdl.**		**2 distinct bdl.**		**1 bdl.**		**1 bdl.**		**1 bdl.**	
Ptilocolepus granulatus (Pictet, 1834)	dorsomesally at **fpc**	dorsomesally at **ppc**	mesally at frons directly in front of **moc**	dorsal face of **ppc** in front of **br**	dorsolaterally at **fpc** above **atp**	dorsolaterally at **ppc** directly behind **fg**	mesally on the base of **ata**	both closely adjacent ventrally at the posterior end of **ppc**	ventromesally at the base of **ata**	ventrolaterally at pph	laterally at vertex	dorsally on **pph** directly behind the **br**	posterolaterally at head capsule (lateral to base of **pta**)	ventrolaterally at posterior half of **pph**

Appendix 4: Continued.

Taxon	fr-ph(a)		fr-ph(p)		te-ph(l)		te-ph(a)		te-ph(p)		cr-ph(a)		cr-ph(p)	
	O	**I**	**O**	**I**	**O**	**I**	**O**	**I**	**O**	**I**	**O**	**I**	**O**	**I**
	1 bdl.		**2 adjacant bdl. [?]**		**1 bdl.**		**2 distinct bdl.**		**1 bdl.**		**-**		**-**	
Hydroptila scamandra Neboiss, 1977	dorsolaterally at **fpc**	dorsomesally at **ppc**, directly above **fg**	mesally at frons between the bases of the antennae	dorsal face of **ppc** in front of **br**	mesally at **ata** near **fpc**	at the lateral wall of **ppc**	mesally on the base of **ata** and at **tb**	ventrally at the posterior end of **ppc**	posterodorsally at **ata**	ventrolaterally at pph, below **br**				
	1 bdl.		**3 adjacant bdl. [?]**		**1 bdl.**		**2 distinct bdl.**		**1 bdl. [?]**		**-**		**-**	
Orthotrichia atraseta Wells, 1979	dorsolaterally at **fpc**	dorsomesally at **ppc**, directly above **fg**	mesally at vertex (?) distinctly behind the bases of the antennae	dorsal face of **ppc** in front of **br**	mesally at **fpc** mesal to **atp**	at the lateral wall of **ppc**	mesally on the base of **ata** and at **tb**	ventrally at the posterior end of **ppc**	posterodorsally at **ata**	ventrolaterally at pph, below **br**				
	1 bdl.		**2 adjacent bdl.**		**1 bdl.**		**2 distinct bdl. [?]**		**1 bdl.**		**1 bdl.**		**-**	
Phryganea grandis Linnaeus, 1758	mesally at **fpc**	dorsomesally at **ppc**, directly above **fg**	mesally at frons between the bases of the antennae	dorsal face of **ppc** in front of **br**	laterally at **fpc** mesal to **atp**	at the dorsolateral wall of **ppc**	mesally on the base of **ata** and at **tb**	ventrally at the posterior end of **ppc**	dorsally at **pta**	ventrally at **pph**, behind the **br**, opposite to **cr-ph(a)**	laterally at vertex	dorsally on **pph** directly behind the **br**		
	1 bdl.		**2 adjacent bdl.**		**1 bdl.**		**2 distinct bdl.**		**1 bdl.**		**1 bdl.**		**-**	
Trichostegia minor (Curtis, 1834)	mesally at **fpc**	dorsomesally at **ppc**, directly above **fg**	mesally at frons between the bases of the antennae	dorsal face of **ppc** in front of **br**	laterally at **fpc** mesal to **atp**	at the dorsolateral wall of **ppc**	mesally on the base of **ata** and at **tb**	ventrally at the posterior end of **ppc**	dorsally at **pta**	ventrally at **pph**, behind the **br**, opposite to **cr-ph(a)**	laterally at vertex	dorsally on **pph** directly behind the **br**		
	1 bdl.		**2 adjacent bdl.**		**1 bdl.**		**2 distinct bdl.**		**1 bdl.**		**1 bdl.**		**-**	
Brachycentrus subnubilus Curtis, 1834	laterally at central face of **fpc**	dorsomesally at **ppc**, directly above **fg**	mesally at frons	dorsal face of **ppc** in front of **br**	distinctly lateral at **fpc** above **atp**	at the lateral wall of **ppc**	anteromesally at the **tb**	ventrally at the posterior end of **ppc**	dorsally at the short **pta**	ventrally at **pph**, behind the **br**, opposite to **cr-ph(a)**	laterally at vertex	dorsally on **pph** directly behind the **br**		
	1 bdl.		**2 adjacent bdl.**		**1 bdl.**		**2 distinct bdl.**		**1 bdl.**		**1 bdl.**		**-**	
Limnephilus flavicornis (Fabricius, 1787)	at central face of **fpc**	dorsomesally at **ppc**, directly above **fg**	mesally at frons directly in front of **moc**	dorsal face of **ppc** in front of **br**	laterally at **fpc** distinctly above **atp**	at the lateral wall of **ppc**	anteromesally at the **tb** and at the lateral base of **pta**	ventrally at the posterior end of **ppc**	dorsally at the short **pta**	ventrally at **pph**, behind the **br**, opposite to **cr-ph(a)**	posterolaterally at vertex	dorsally on **pph** directly behind the **br**		

Appendix 4: Continued.

Taxon	fr-ph(a)		fr-ph(p)		te-ph(l)		te-ph(a)		te-ph(p)		cr-ph(a)		cr-ph(p)	
	O	I	O	I	O	I	O	I	O	I	O	I	O	I
	1 bdl.		**2 adjacent bdl. [?]**		**1 bdl.**		**2 distinct bdl. [?]**		**1 bdl.**		**1 bdl.**		**-**	
Silo nigricornis (Pictet, 1834)	laterally at **fpc** distinctly above **atp**, and adjacent but above **te-ph(l)**	dorsolaterally at **ppc**, directly above **fg**	mesally at frons	dorsal face of **ppc** in front of **br**	laterally at **fpc** distinctly above **atp**, but slightly below **fr-ph(a)**	dorsolaterally at **ppc**, directly above **fg**, behind **fr-ph(a)**	mesally at the mesal base of ata	ventrally at the posterior end of **ppc**	dorsally at the short **pta**	ventrally at **pph**, behind the **br**, opposite to **cr-ph(a)**	posterolaterally at vertex	dorsally on **pph** directly behind the **br**		
	1 bdl.		**2 adjacent bdl.**		**3 adjacent bdl. [?]**		**2 distinct bdl.**		**1 bdl.**		**1 bdl.**		**-**	
Sericostoma personatum Kirby et Spence, 1826	mesally at **fpc** directly mesal to **atp**	dorsolaterally at **ppc**, directly above **fg**	mesally at frons	dorsal face of **ppc** in front of **br**	laterally at **fpc** above (2 bdl.) and below (1 bdl.) **atp**	laterally at **ppc**, directly above **fg**	anteromesally at **tb**	ventrally at the posterior end of **ppc**	dorsally at the short **pta**	lateroventrally at **pph**, behind the **br**, opposite to **cr-ph(a)**	posterolaterally at vertex	dorsally on **pph** directly behind the **br**		
	1 bdl.		**2 adjacent bdl. [?]**		**1 bdl.**		**1 bdl. [?]**		**1 bdl.**		**1 bdl.**		**-**	
Pycnocentria evecta McLachlan, 1868	mesally at **fpc**	dorsolaterally at **ppc**	mesally at frons	dorsal face of **ppc** in front of **br**	laterally at **fpc** above directly above **atp**	laterally at **ppc**	anteromesally at the base of **ata**	ventrally at the posterior end of **ppc**	dorsally at the short **pta**	lateroventrally at **pph**, behind the **br**, opposite to **cr-ph(a)**	posterolaterally at vertex	dorsally on **pph** directly behind the **br**		
	1 bdl.		**2 adjacent bdl.**		**1 bdl.**		**2 distinct bdl.**		**1 bdl.**		**1 bdl.**		**-**	
Molanna angustata Curtis, 1834	mesally at **fpc** directly above **fg**	dorsolaterally at **ppc**	mesally at frons	dorsal face of **ppc** in front of **br**	mesally at ata near head capsule	laterally at **ppc**	mesally at **tb** and the base of **ata**	ventrally at the posterior end of **ppc**	dorsally at the short **pta**	lateroventrally at **pph**, behind the **br**, opposite to **cr-ph(a)**	posterolaterally at vertex	dorsally on **pph** directly behind the **br**		
	1 bdl.		**2 adjacent bdl.**		**1 bdl.**		**1 bdl. [?]**		**- [?]**		**1 bdl.**		**-**	
Leptocerus tineiformis Curtis, 1834	laterally at **fpc** (mesal to **atp**) directly above **fg**	dorsolaterally at **ppc**	mesally at frons	dorsal face of **ppc** in front of **br**	mesally at ata near head capsule	laterally at **ppc**	mesally at **tb**	ventrally at the posterior end of **ppc** in fron of **br**			posterolaterally at vertex	dorsally on **ppc** directly in front of the **br**		

Appendix 5: Detailed description of the musculature of the maxilla in adult Trichoptera. Abbr.: **ata** – anterior tentorial arm, **bdl.** – bundle, **cd-mp(d)** – M. cardo-palpalis dorsalis, **cd/st-mp(v)** – M. cardo/stipito-palpalis ventralis, **cr-cd** – M. cranio-cardinalis, **cr-lc** – M. cranio-lacinialis, **cr-prm(l)** – M. cranio-praementalis lateralis, **cr-prm(m)** – M. cranio-praementalis medialis, **cr-st** – M. cranio-stipitalis, **dst** – dististipes, **I** – insertion, **lt** – laminatentorium, **O** – origin, **ocs** – occipital sulcus, **pge** – postgena, **pta** – posterior tentorial arm, **ptp** – posterior tentorial pit, **st-lc** – M. stipito-lacinialis, **st-mp(d)** – M. stipito-palpalis dorsalis, **te-cd** – M. tentorio-cardinalis, **te-st** – M. tentorio-stipitalis, **?** – uncertain, **-** – absent.

Taxon	te-cd		te-st		cr-cd		cr-st		cr-lc		st-lc		cd-mp(d)		cd/st-mp(v)		st-mp(d)	
	O	I	O	I	O	I	O	I	O	I	O	I	O	I	O	I	O	I
	1 bdl.		1 bdl.		1 bdl.		1 bdl.		1 bdl.		-		1 bdl.		1 bdl.		1 bdl.	
Philopotamus ludificatus McLachlan, 1878	laterally at the mid part of **ata**	mesally at the distal margin of the cardostipital sclerite	broadly at the ventral face of **lt**	distal process of mesal dististipital margin	ventrolaterally at **pge**, mesally to **ocs**	ventromesally at the proximal margin of cardostipital	**pge**, ventrally of base of the **pta**	distal process of mesal dististipital margin	**pge**, dorsally to **cr-cd**	laterally at the small inner lobe of galeolacinia			proximomesal angle of the cardostipital sclerite	dorsolaterally at the base of the 1st palpomere	cardostitpital sclerite, laterally of **cd-mp(d)**	ventral margin of 1st palpomere (opposite **cd-mp(d)**)	mesally on the proximal half of **dst**	mesally at the dorsal margin of the 1st palpmere
	1 bdl.		1 bdl.		1 bdl.		1 bdl.		1 bdl.		-		1 bdl.		1 bdl.		1 bdl.	
Stenopsyche marmorata Navas, 1920	ventrolaterally at the mid part of **ata** and **lt** directly behind **te-st**	mesally the cardostipital sclerite	ventrally at **ata** and **lt** directly in front of **te-cd**	mesal margin of **dst**	ventrolaterally at **pge**, mesally to **ocs**	ventrally at proximal margin of cardostipital sclerite	**pge**, directly lateral to the base of **pta**	mesally at dististipital margin [?]	posteriorly at **pge**, directly lateral to **cr-prm(m)**	laterally at galeolacinia			dorsolaterally at cardostipital sclerite	dorsolaterally at the base if the 1st palpomere	cardostitpital sclerite, in front of **cd-mp(d)**	ventral margin of 1st palpomere (opposite **cd-mp(d)**)	mesally on the proximal half of **dst**	mesally at the dorsal margin of the 1st palpmere
	1 bdl.		1 bdl.		1 bdl.		1 bdl.		1 bdl.		-		1 bdl.		1 bdl.		1 bdl.	
Hydropsyche angustipennis (Curtis, 1834)	ventrolaterally at the mid part of **ata** and **lt** directly behind **te-st**	mesally at the distal margin of the cardostipital sclerite	ventrolaterally at **ata** and **lt** directly in front of **te-cd**	mesally at distal margin of **dst**	mesal wall of **ocs** (**pge**)	ventromesally at the cardostipital sclerite	mesally at **pge**, lateral to **ptp**, mesal to **cr-prm(m)** and **cr-prm(l)**	mesal margin of **dst**	mesal wall of **ocs** in front of **cr-cd**	anterolaterally at galeolacinia			laterally at posterior wall of cardostipital sclerite	dorsally at the basal margin of 1st palpomere	laterally at cardostipital scl. with broad attachment area	ventrally at the basal margin of 1st palpomere	mesally on the proximal half of **dst**	mesally at the dorsal margin of the 1st palpmere
	1 bdl.		1 bdl.		1 bdl.		1 bdl.		1 bdl.		-		1 bdl.		1 bdl.		1 bdl.	
Tinodes dives (Pictet, 1834)	ventrolaterally at the mid part of **ata** directly behind **te-st**	mesally at the distal margin of the cardostipital sclerite	ventrolaterally at **ata** and **lt** directly in front of **te-cd**	mesally at distal margin of **dst**	mesal wall of **ocs** (**pge**)	ventromesally at the cardostipital sclerite	dorsally on **pta**	mesal margin of **dst**	mesal wall of **ocs** in front of **cr-cd**	anterolaterally at the small galeolacinia			laterally at posterior wall of cardostipital sclerite	dorsally at the basal margin of 1st palpomere	laterally at cardostipital sclerite	ventrally at the basal margin of 1st palpomere	mesal margin of **dst**	mesally at the dorsal margin of the 1st palpmere
	1 bdl.		1 bdl.		1 bdl.		1 bdl.		1 bdl.		-		1 bdl.		1 bdl.		1 bdl.	
Holocentropus dubius (Rambur, 1842)	ventral face of **ata** (mid part)	mesally at the proximal margin of the cardostipital sclerite	ventromesally at **lt** of **ata**	anteromesally at distal margin of **dst**	ventrolaterally at **pge**	ventrally at proximal margin of cardostipital sclerite	posterolaterally at **pge** mesal to **cr-prm(l)** and **cr-prm(m)**	mesal margin of **dst**	**pge**, dorsally to **cr-cd**	mesally at proximal margin of galeolacinia			proximomesal angle of the cardostipital sclerite	dorsolaterally at the base of the 1st palpomere	cardostitpital sclerite, mesally of **cd-mp(d)**	ventral margin of 1st palpomere	mesal margin of **dst**	mesally at the dorsal margin of the 1st palpmere

Appendix 5: Continued.

Taxon	te-cd		te-st		cr-cd		cr-st		cr-lc		st-lc		cd-mp(d)		cd/st-mp(v)		st-mp(d)	
	O	I	O	I	O	I	O	I	O	I	O	I	O	I	O	I	O	I
	1 bdl.		1 bdl.		1 bdl.		-		1 bdl.		1 bdl.		1 bdl.		1 bdl.		1 bdl.	
Rhyacophila obliterata McLachlan, 1863	ventrolaterally at the mid part of **ata** and **lt** directly behind **te-st**	posteriorly at the mesal margin of the cardostipital sclerite	ventromesally at **lt** of **ata**	anteromesally at distal margin of **dst**	ventrolaterally at **pge**, mesally to **ocs**	laterally at proximal margin of cardostipital sclerite			posteriorly at **pge**, distinctly separated from **cr-cd**	laterally at proximal margin of galeolacinia	mesally at **dst**	laterally at proximal edge of galeolacinia	posterior basal margin of cardostipital sclerite	dorsolaterally at the base of the 1st palpomere	mesally at proximal half of cardostipital sclerite	ventrally at the basal margin of 1st palpomere	mesal margin of **dst**	mesally at the dorsal margin of the 1st palpmere
	1 bdl.		1 bdl.		1 bdl.		-		1 bdl.		1 bdl.		1 bdl.		1 bdl.		1 bdl.	
Hydrobiosis styracine McFarlane, 1960	ventrolaterally at **lt** (proximal part of **ata**) directly behind **te-st**	posteriorly at the mesal margin of the cardostipital sclerite	ventromesally at **lt** of **ata**	anteromesally at distal margin of **dst**	ventrally at central part of **pge**	laterally at proximal margin of cardostipital sclerite			posteriorly at **pge**, distinctly separated from **cr-cd**	laterally at proximal margin of galeolacinia	mesally at **dst**	laterally at proximal edge of galeolacinia	posterior basal margin of cardostipital sclerite	dorsolaterally at the base of the 1st palpomere	mesally at proximal half of cardostipital sclerite	ventrally at the basal margin of 1st palpomere	mesal margin of **dst**	mesally at the dorsal margin of the 1st palpmere
	1 bdl.		1 bdl.		1 bdl.		-		1 bdl.		1 bdl.		1 bdl.		1 bdl.		1 bdl.	
Apsilochorema sutshanum Martynov, 1934	ventromesally at the anterior half of **ata** and **lt** directly behind **te-st**	posteriorly at the mesal margin of the cardostipital sclerite	ventrolaterally at **ata**	anteromesally at distal margin of **dst**	mesally at mid part of **pge**	laterally at proximal margin of cardostipital sclerite			posteriorly at **pge**, distinctly separated from **cr-cd**	laterally at proximal margin of galeolacinia	mesally at **dst**	postero-mesally at proximal edge of galeolacinia	posterior basal margin of cardostipital sclerite	dorsolaterally at the base of the 1st palpomere	mesally at proximal half of cardostipital sclerite	ventrally at the basal margin of 1st palpomere	mesal margin of cardostipital sclerite [?]	mesally at the dorsal margin of the 1st palpmere
	1 bdl.		1 bdl.		1 bdl.		-		1 bdl.		-		1 bdl.		1 bdl.		1 bdl.	
Glossosoma spinosum Morse et Yang, 2005	ventromesally at **ata** and **lt** directly behind **te-st**	posteriorly at the mesal margin of the cardostipital sclerite	ventromesally at **lt**	anteromesally at distal margin of **dst**	anteromesally at **pge**	mesally at proximal margin of cardostipital sclerite			laterally at **pge**, closely behind the posterior margin of **cpe**	laterally at proximal margin of galeolacinia			laterally at posterior wall of cardostipital sclerite	dorsally at the basal margin of 1st palpomere	mesally at proximal half of cardostipital sclerite	ventrally at the basal margin of 1st palpomere	mesally on the proximal half of **dst**	mesally at the dorsal margin of the 1st palpmere
	1 bdl.		1 bdl.		1 bdl.		-		1 bdl.		1 bdl.		1 bdl.		1 bdl.		1 bdl.	
Agapetus fuscipes Curtis, 1834	ventrally at **lt** directly behind **te-st**	posteriorly at the mesal margin of the cardostipital sclerite	ventromesally at **lt**	anteromesally at distal margin of **dst**	anteromesally at **pge**	mesally at proximal margin of cardostipital sclerite			laterally at **pge** and mainly at mesal wall of **ocs**	mesally at sclerotized inner lobe of galeolacinia	anteromesally at **dst**, at insertion site of **te-st**	postero-laterally at proximal edge of galeolacinia	mesally at posterior wall of cardostipital sclerite	dorsally at the basal margin of 1st palpomere	laterally at proximal half of cardostipital sclerite	ventrally at the basal margin of 1st palpomere	mesally at **dst**	mesally at the dorsal margin of the 1st palpmere
	1 bdl.		1 bdl.		1 bdl.		-		1 bdl.		1 bdl.		1 bdl.		1 bdl.		1 bdl.	
Ptilocolepus granulatus (Pictet, 1834)	ventrally at **ata** directly behind **te-st**	posteriorly at the mesal margin of the cardostipital sclerite	ventrally at **ata**	anteromesally at distal margin of **dst**	**pge**, mesal face of **ocs**	dorsolaterally at cardostipital sclerite			centrally at **pge**, mesal to **ocs**	laterally at proximal margin of galeolacinia	anteromesally at **dst**, at insertion site of **te-st**	postero-laterally at proximal edge of galeolacinia	mesally at posterior wall of cardostipital sclerite	dorsally at the basal margin of 1st palpomere	mesally at proximal half of cardostipital sclerite	ventrally at the basal margin of 1st palpomere	mesally at **dst**	mesally at the dorsal margin of the 1st palpmere

Appendix 5: Continued.

Taxon	te-cd		te-st		cr-cd		cr-st		cr-lc		st-lc		cd-mp(d)		cd/st-mp(v)		st-mp(d)	
	O	I	O	I	O	I	O	I	O	I	O	I	O	I	O	I	O	I
	1 bdl.		1 bdl.		1 bdl.		-		1 bdl.		1 bdl.		1 bdl.		1 bdl.		- [?]	
Hydroptila scamandra Neboiss, 1977	ventrally at **ata** directly behind **te-st**	posteriorly at the mesal margin of the cardostipital sclerite	ventrally at **ata**	anteromesally at distal margin of **dst**	anteromesally at **pge**	dorsolaterally at cardostipital sclerite			laterally at **pge** directly mesal to **ocs**	laterally at sclerotized inner lobe of galeolacinia	anteromesally at **dst**, at insertion site of te-st	postero-laterally at proximal edge of galeolacinia	mesally at posterior wall of cardostipital sclerite	dorsally at the basal margin of 1st palpomere	mesally at proximal half of cardostipital sclerite	ventrally at the basal margin of 1st palpomere		
	1 bdl.		1 bdl.		1 bdl.		-		1 bdl.		1 bdl.		1 bdl.		1 bdl.		1 bdl.	
Orthotrichia atraseta Wells, 1979	ventrally at **ata** directly behind **te-st**	posteriorly at the mesal margin of the cardostipital sclerite	ventrally at **ata**	anteromesally at distal margin of **dst**	anteromesally at **pge**	dorsolaterally at cardostipital sclerite			laterally at **pge** directly mesal to **ocs**	laterally at sclerotized inner lobe of galeolacinia	anteromesally at **dst**, at insertion site of te-st	postero-laterally at proximal edge of galeolacinia	mesally at posterior wall of cardostipital sclerite	dorsally at the basal margin of 1st palpomere	at proximal half of cardostipital sclerite	ventrally at the basal margin of 1st palpomere	mesally at **dst**	mesally at the dorsal margin of the 1st palpmere
	1 bdl.		-		1 bdl.		-		1 bdl.		1 bdl.		1 bdl.		1 bdl.		1 bdl.	
Phryganea grandis Linnaeus, 1758	anteroventrally in the proximal half of **ata** and at **lt**	posteriorly at the mesal margin of the cardostipital sclerite			laterally at **pge**, below **cpe**	dorsomesally at cardostipital sclerite			posterolaterally at **pge**	mesally at the base of galeolacinia	mesally at **dst**	laterally at posterior margin of galeolacinia	mesally at cardostipital sclerite	dorsolaterally at the base of the 1st palpomere	cardostitpital sclerite, laterally of **cd-mp(d)**	ventral margin of 1st palpomere (opposite **cd-mp(d)**)	mesally on the proximal half of **dst**	mesally at the dorsal margin of the 1st palpmere
	1 bdl.		-		1 bdl.		-		1 bdl.		1 bdl.		1 bdl.		1 bdl.		1 bdl.	
Trichostegia minor (Curtis, 1834)	anteroventrally in the proximal half of **ata** and at **lt**	posteriorly at the mesal margin of the cardostipital sclerite			laterally at **pge**, below **cpe**	dorsomesally at cardostipital sclerite			posterolaterally at **pge**	mesally at the base of galeolacinia	mesally at **dst**	laterally at posterior margin of galeolacinia	mesally at cardostipital sclerite	dorsolaterally at the base of the 1st palpomere	cardostitpital sclerite, laterally of **cd-mp(d)**	ventral margin of 1st palpomere (opposite **cd-mp(d)**)	mesally on the proximal half of **dst**	mesally at the dorsal margin of the 1st palpmere
	1 bdl.		1 bdl.		1 bdl.		-		1 bdl.		1 bdl.		1 bdl.		1 bdl.		1 bdl.	
Brachycentrus subnubilus Curtis, 1834	anteroventrally in the proximal half of **ata** and at **fgs** in front of **te-st**	mesally at distal margin of cardostipital sclerite	ventromesally at **ata** directly behind **te-cd**	anteromesally at distal margin of **dst**	mesal wall of **ocs** in front of **cr-lc**	dorsomesally at cardostipital sclerite			laterally at **pge** and mesal wall of **ocs**	dorsomesally at the base of galeolacinia	mesally at **dst**	laterally at posterior margin of galeolacinia	mesally at cardostipital sclerite	dorsolaterally at the base of the 1st palpomere	cardostitpital sclerite, laterally of **cd-mp(d)**	ventral margin of 1st palpomere (opposite **cd-mp(d)**)	mesally on the proximal half of **dst**	mesally at the dorsal margin of the 1st palpmere
	1 bdl.		1 bdl.		1 bdl.		-		1 bdl.		1 bdl.		1 bdl.		1 bdl.		1 bdl.	
Limnephilus flavicornis (Fabricius, 1787)	ventrally at **ata** and **lt** directly behind **te-st**	mesally at distal margin of cardostipital sclerite	ventromesally at **lt** directly in front of **te-cd**	anteromesally at distal margin of **dst**	at **pge** mesal to **ocs**	dorsomesally at cardostipital sclerite			at mesal wall of **ocs**	dorsomesally at the base of galeolacinia	mesally at **dst**	laterally at posterior margin of galeolacinia	mesally at cardostipital sclerite	dorsolaterally at the base of the 1st palpomere	cardostitpital sclerite, laterally of **cd-mp(d)**	ventral margin of 1st palpomere (opposite **cd-mp(d)**)	mesally on the proximal half of **dst**	mesally at the dorsal margin of the 1st palpmere

Appendix 5: Continued.

Taxon	te-cd		te-st		cr-cd		cr-st		cr-lc		st-lc		cd-mp(d)		cd/st-mp(v)		st-mp(d)	
	O	I	O	I	O	I	O	I	O	I	O	I	O	I	O	I	O	I
	1 bdl.		**1 bdl.**		**1 bdl.**		**-**		**1 bdl.**		**1 bdl.**		**2 bdl.**		**- [?]**		**- [?]**	
Silo nigricornis (Pictet, 1834)	ventrally at **ata** and **lt** directly lateral to **te-st**	mesally at distal margin of cardostipital sclerite	ventromesally at **ata**	anteromesally at distal margin of **dst**	at **pge** mesal wall of **ocs**	dorsomesally at cardostipital sclerite			at mesal wall of **ocs**	dorsally at the lateral wall of galeolacinia	mesally at the proximal half of cardostipital sclerite	laterally at posterior margin of galeolacinia	mesally at posterior margin of cardostipital sclerite	dorsolaterally at the base of the 1st palpomere				
	1 bdl.		**1 bdl.**		**1 bdl.**		**-**		**1 bdl.**		**-**		**1 bdl.**		**1 bdl.**		**1 bdl.**	
Sericostoma personatum Kirby et Spence, 1826	ventrolaterally at **ata** directly lateral to **te-st**	mesally at distal margin of cardostipital sclerite	ventromesally at **ata** and **lt**	anteromesally at distal margin of **dst**	posterolaterally at **pge**	dorsomesally at cardostipital sclerite			posterolaterally at **pge**	dorsomesally at the base of galeolacinia			mesally at cardostipital sclerite	dorsally at the base of the 1st palpomere	cardostitpital sclerite, laterally of **cd-mp(d)**	ventral margin of 1st palpomere	mesally on the proximal half of **dst**	mesally at the dorsal margin of the 1st palpmere
	1 bdl.		**1 bdl.**		**1 bdl.**		**-**		**1 bdl.**		**-**		**1 bdl.**		**1 bdl.**		**1 bdl.**	
Pycnocentria evecta McLachlan, 1868	ventromesally at **ata** and **lt**	mesally at distal margin of cardostipital sclerite	ventromesally at **ata** and **lt**	anteromesally at distal margin of **dst**	laterally at **pge** directly below **cpe**	dorsomesally at cardostipital sclerite			centrally at **pge**	dorsally at the lateral wall of galeolacinia			mesally at cardostipital sclerite	dorsally at the base of the 1st palpomere	cardostitpital sclerite, laterally of **cd-mp(d)**	ventral margin of 1st palpomere	mesally on the proximal half of **dst**	mesally at the dorsal margin of the 1st palpmere
	1 bdl.		**1 bdl.**		**1 bdl.**		**-**		**1 bdl.**		**-**		**1 bdl.**		**1 bdl.**		**1 bdl.**	
Molanna angustata Curtis, 1834	ventromesally at **ata** and **lt** directly lateral to **te-st**	mesally at distal margin of cardostipital sclerite	ventromesally at **ata**	anteromesally at distal margin of **dst**	posterolaterally at **pge**	dorsomesally at cardostipital sclerite			posterolaterally at **pge**	dorsomesally at the base of galeolacinia			proximomesal angle of the cardostipital sclerite	dorsolaterally at the base of the 1st palpomere	cardostitpital sclerite, laterally of **cd-mp(d)**	ventrolateral margin of 1st palpomere (opposite **cd-mp(d)**)	mesally on the proximal half of **dst**	mesally at the dorsal margin of the 1st palpmere
	1 bdl.		**1 bdl.**		**1 bdl.**		**-**		**1 bdl.**		**-**		**1 bdl.**		**1 bdl.**		**1 bdl.**	
Leptocerus tineiformis Curtis, 1834	ventrally at **ata** and **lt**	mesally at distal margin of cardostipital sclerite	ventrally at **ata** and **lt**	anteromesally at distal margin of **dst**	laterally at **pge**	dorsomesally at cardostipital sclerite			posterolaterally at **pge**	dorsomesally at the base of galeolacinia			proximomesal angle of the cardostipital sclerite	dorsolaterally at the base of the 1st palpomere	cardostitpital sclerite, laterally of **cd-mp(d)**	ventrolateral margin of 1st palpomere (opposite **cd-mp(d)**)	mesally on the proximal half of **dst**	mesally at the dorsal margin of the 1st palpmere

Appendix 6: Detailed description of the musculature of the labium and salivarium in adult Trichoptera. Abbr.: **bdl.** – bundle, **cr-prm(l)** – M. cranio-prementalis lateralis, **cr-prm(m)** – M. cranio-prementalis medialis, **cr-st** – M. cranio-stipitalis, **hst** – haustellum, **hy-sa** – M. hypopharyngo-salivarialis, **I** – insertion, **i-sa** – M. intra-salivarialis, **O** – origin, **pge** – postgena, **ppg** – palpiger, **prm** – prementum, **prm-lp(l)** – M. praemento-palpalis lateralis, **prm-lp(m)** – M. praemento-palpalis medialis, **prm-sa** – M. praemento-salivarialis, **pta** – posterior tentorial arm, **ptp** – posterior tentorial pit, **sal** – salivarium, **sit** – sitophore plate, **?** – uncertain, **-** – absent.

Taxon	hy-sa		i-sa		prm-sa		cr-prm(m)		cr-prm(l)		prm-lp(m)		prm-lp(l)	
	O	I	O	I	O	I	O	I	O	I	O	I	O	I
	1 bdl.		**-**		**1 bdl.**		**2 adjacent bdl.**		**1 bdl.**		**1 bdl.**		**1 bdl.**	
Philopotamus ludificatus McLachlan, 1878	laterally at the ventral half of **sit**, close to the base of the galeolacinia	proximally on the roof of **sal**			ventral part of the prementum (close to **prm-lp(m)**)	proximal half of the roof of **sal**	both bdl. closely adjacent mesally at the **pge**	distal part of the prementum	**pge**, ventrally of **ptp** and directly mesally of **cr-st**	lateral rim of **ppg**	mesally at the dorsal face of the prementum (close to the base of **hst**)	laterally at the proximal margin of palpomere 1	proximolaterally on **ppg**	laterally at the proximal margin of palpomere 1
	- [?]		**-**		**1 bdl. [?]**		**1 bdl. [?]**		**1 bdl.**		**1 bdl. [?]**		**1 bdl. [?]**	
Stenopsyche marmorata Navas, 1920					ventral part of the prementum	proximal half of the roof of **sal**	posteromesallly at the **pge** directly mesal to **cr-st**	distal part of the prementum	**pge** near (lateral) the **pta**	lateral rim of **ppg** [?]	mesally at the dorsal face of the prementum	laterally at the proximal margin of palpomere 1 [?]	proximolaterally on **ppg**	laterally at the proximal margin of palpomere 1
	1 bdl.		**-**		**2 distinct bdl.**		**2 distinct bdl.**		**1 bdl.**		**1 bdl.**		**1 bdl.**	
Hydropsyche angustipennis (Curtis, 1834)	laterally at the ventral half of **sit**	proximally on the roof of **sal**			at antero-ventral edge and lateral wall of **prm**	proximal half of the roof of **sal**	**pge**, directly lateral to **cr-prm(l)** and **cr-st**	both distinctly separated at prementum lateral to **cr-prm(l)**	posteriorly at **pge**, between **cr-prm(m)** and **cr-st**	lateral margin of **ppg**	mesally at the dorsal face of the prementum	laterally at the proximal margin of palpomere 1	proximolaterally on **ppg**	laterally at the proximal margin of palpomere 1
	-		**-**		**2 distinct bdl.**		**2 adjacent bdl.**		**1 bdl.**		**1 bdl.**		**1 bdl.**	
Tinodes dives (Pictet, 1834)					at antero-ventral edge and lateral wall of **prm**	proximal half of the roof of **sal**	mesally at the **pge**, lateral to **cr-prm(l)**	distal part of the prementum	mesally at **pge**, mesal to **cr-prm(m)**	laterally at **ppg**	posteromesally at the basal margin of **ppg**	laterally at the proximal margin of palpomere 1	laterally on **ppg**	mesally at the proximal margin of palpomere 1
	-		**1 bdl.**		**-**		**2 distinct bdl.**		**1 bdl.**		**1 bdl.**		**1 bdl.**	
Holocentropus dubius (Rambur, 1842)			roof of **sal**	roof of **sal**			laterally at **pge**, directly lateral to **cr-prm(l)** and **cr-st**	both distinctly separated at prementum anteromesally to **cr-prm(l)**	posteriorly at **pge**, between **cr-prm(m)** and **cr-st**	laterally at prementum near the base of **ppg**	laterally at the dorsal face of the prementum	dorsolaterally at the proximal margin of palpomere 1	laterally on **ppg**	laterally at the proximal margin of palpomere 1

Appendix 6: Continued.

Taxon	hy-sa		i-sa		prm-sa		cr-prm(m)		cr-prm(l)		prm-lp(m)		prm-lp(l)	
	O	I	O	I	O	I	O	I	O	I	O	I	O	I
	-		1 bdl.		1 bdl.		2 distinct bdl.		1 bdl.		1 bdl.		1 bdl.	
Rhyacophila obliterata McLachlan, 1863			roof of **sal**	roof of **sal**	laterally at prementum	mesally at the proximal half of the roof of **sal**	mesally at **pge**, lateral to **cr-prm(l)** near the base and at the base of **pta**	both distinctly separated at prementum posteromesally to **cr-prm(l)**	at the base of **pta**, mesal to **cr-prm(m)**	laterally at prementum near the base of **ppg**	laterally at the proximal wall of **ppg** [?]	dorsolaterally at the proximal margin of palpomere 1	laterally on **ppg**	laterally at the proximal margin of palpomere 1
	-		-		1 bdl.		2 distinct bdl.		1 bdl.		1 bdl.		1 bdl.	
Hydrobiosis styracine McFarlane, 1960					laterally at prementum in front of anterior bdl. of **cr-prm(m)**	mesally at the proximal half of the roof of **sal**	mesally at **pge**, lateral to **cr-prm(l)** and near the base of **pta**	both anteriorly at prementum (closely adjacent)	**pge** near the base of **pta**, mesal to **cr-prm(m)**	laterally at prementum	laterally at the proximal face of the prementum	dorsolaterally at the proximal margin of palpomere 1	proximolaterally on **ppg**	laterally at the proximal margin of palpomere 1
	-		-		1 bdl.		2 distinct bdl.		1 bdl.		1 bdl.		1 bdl.	
Apsilochorema sutshanum Martynov, 1934					laterally at prementum	mesally at the proximal half of the roof of **sal**	mesally at **pge**, and at posterior half of **ata**	both together anteriorly at prementum	at the posterior half of **ata**	mesally at prementum near the base of **ppg**	laterally at the dorsal face of the prementum	dorsolaterally at the proximal margin of palpomere 1	laterally on **ppg**	laterally at the proximal margin of palpomere 1
	-		-		1 bdl.		2 distinct bdl.		1 bdl.		1 bdl.		1 bdl.	
Glossosoma spinosum Morse et Yang, 2005					laterally at prementum in front of anterior bdl. of **cr-prm(m)**	mesally at the proximal half of the roof of **sal**	laterally at **pge** and at **pta**	distal part of the prementum	at the anterior base of **pta**	laterally at prementum near the base of **ppg**	mesally at the dorsal face of the prementum	laterally at the proximal margin of palpomere 1	proximolaterally on **ppg**	laterally at the proximal margin of palpomere 1
	-		-		1 bdl.		2 distinct bdl.		1 bdl.		1 bdl.		1 bdl.	
Agapetus fuscipes Curtis, 1834					laterally at prementum in front of anterior bdl. of **cr-prm(m)**	mesally at the proximal half of the roof of **sal**	mesally at **pge**, but lateral to **cr-prm(l)**	both together anteriorly at prementum	mesally at **pge** near base of **pta**	lateral rim of **ppg**	mesally at the dorsal face of the prementum	laterally at the proximal margin of palpomere 1	proximal at **ppg**	laterally at the proximal margin of palpomere 1
	-		-		1 bdl.		2 distinct bdl.		1 bdl.		1 bdl.		1 bdl.	
Ptilocolepus granulatus (Pictet, 1834)					laterally at prementum in front of anterior bdl. of **cr-prm(m)**	mesally at the proximal half of the roof of **sal**	both at **pge**, posterior bundle near base of **pta**	distal part of the prementum	**pge** near the base of **pta**	lateral rim of **ppg**	mesally at the dorsal face of the prementum	dorsolaterally at the proximal margin of palpomere 1	proximal at **ppg**	laterally at the proximal margin of palpomere 1

Appendix 6: Continued.

Taxon	hy-sa		i-sa		prm-sa		cr-prm(m)		cr-prm(l)		prm-lp(m)		prm-lp(l)	
	O	I	O	I	O	I	O	I	O	I	O	I	O	I
	-		**-**		**1 bdl.**		**2 distinct bdl.**		**1 bdl.**		**1 bdl.**		**1 bdl.**	
Hydroptila scamandra Neboiss, 1977					laterally at prementum in front of anterior bdl. of **cr-prm(m)**	mesally at the proximal half of the roof of **sal**	laterally (anterior bdl.) and mesally (posterior bdl.) at **pge**	distal part of prementum slightly behind origin of **prm-sa**	at **pge** near base of **pta**, lateral to posterior bdl. of **cr-prm(m)**	laterally at the base of **ppg**	mesally at prementum	dorsolaterally at the proximal margin of palpomere 1	at lateral wall of **ppg**	laterally at the proximal margin of palpomere 1
	-		**-**		**1 bdl.**		**2 distinct bdl.**		**1 bdl.**		**1 bdl.**		**1 bdl.**	
Orthotrichia atraseta Wells, 1979					laterally at prementum in front of anterior bdl. of **cr-prm(m)**	mesally at the proximal half of the roof of **sal**	laterally (anterior bdl.) and mesally (posterior bdl.) at **pge**	distal part of prementum slightly behind origin of **prm-sa**	at **pge** near base of **pta**, lateral to posterior bdl. of **cr-prm(m)**	laterally at the base of **ppg**	mesally at prementum	dorsolaterally at the proximal margin of palpomere 1	at lateral wall of **ppg**	laterally at the proximal margin of palpomere 1
	-		**1 bdl. [?]**		**1 bdl.**		**2 distinct bdl.**		**1 bdl.**		**1 bdl.**		**1 bdl.**	
Phryganea grandis Linnaeus, 1758			roof of **sal**	roof of **sal**	laterally at prementum [?]	mesally at the proximal half of the roof of **sal**	laterally at **pge** [?]	proximal part of prementum	laterally at **pge** [?]	laterally at prementum near the base of **ppg**	mesally at prementum	dorsolaterally at the proximal margin of palpomere 1	at lateral wall of **ppg**	laterally at the proximal margin of palpomere 1
	-		**1 bdl. [?]**		**1 bdl.**		**2 distinct bdl.**		**1 bdl.**		**1 bdl.**		**1 bdl.**	
Trichostegia minor (Curtis, 1834)			roof of **sal**	roof of **sal**	laterally at prementum in front of anterior bdl. of **cr-prm(m)**	mesally at the proximal half of the roof of **sal**	laterally (anterior bdl.) and mesally (posterior bdl.) at **pge**	proximal part of prementum slightly behind origin of **prm-sa**	laterally at **pge** mesal to both bundles of **cr-prm(m)**	laterally at prementum near the base of **ppg**	mesally at prementum	dorsolaterally at the proximal margin of palpomere 1	at lateral wall of **ppg**	laterally at the proximal margin of palpomere 1
	-		**1 bdl.**		**- [?]**		**2 distinct bdl.**		**1 bdl.**		**1 bdl.**		**1 bdl.**	
Brachycentrus subnubilus Curtis, 1834			roof of **sal**	roof of **sal**			mesally at posterior half of **pge** (lateral to **cr-prm(l)**)	proximal part of prementum	mesally at **pge** near base of **pta**	laterally at prementum near the base of **ppg**	mesally at prementum	dorsolaterally at the proximal margin of palpomere 1	at lateral wall of **ppg**	laterally at the proximal margin of palpomere 1
	-		**1 bdl. [?]**		**- [?]**		**2 distinct bdl.**		**1 bdl.**		**1 bdl.**		**1 bdl.**	
Limnephilus flavicornis (Fabricius, 1787)			roof of **sal**	roof of **sal**			mesally at posterior half of **pge** (lateral to **cr-prm(l)**)	both bdl. together at proximal part of prementum	postero-mesally at **pge**	laterally at prementum near the base of **ppg**	mesally at prementum	dorsolaterally at the proximal margin of palpomere 1	at lateral wall of **ppg**	laterally at the proximal margin of palpomere 1

Appendix 6: Continued.

Taxon	hy-sa		i-sa		prm-sa		cr-prm(m)		cr-prm(l)		prm-lp(m)		prm-lp(l)	
	O	I	O	I	O	I	O	I	O	I	O	I	O	I
	-		**1 bdl. [?]**		**- [?]**		**2 distinct bdl.**		**2 adjacent bdl. [?]**		**1 bdl.**		**1 bdl.**	
Silo nigricornis (Pictet, 1834)			roof of **sal**	roof of **sal**			mesally at posterior half of **pge** (lateral to **cr-prm(l)**)	both bdl. together at proximal part of prementum	postero-mesally at **pge**	both together laterally at prementum near the base of **ppg**	mesally at prementum	dorsolaterally at the proximal margin of palpomere 1	at lateral wall of **ppg**	laterally at the proximal margin of palpomere 1
	-		**- [?]**		**1 bdl.**		**2 distinct bdl.**		**1 bdl.**		**1 bdl.**		**1 bdl.**	
Sericostoma personatum Kirby et Spence, 1826					laterally at prementum in front of **cr-prm(m)**	mesally at the proximal half of the roof of **sal**	mesally at posterior half of **pge** (lateral to **cr-prm(l)**)	both bdl. together at proximal part of prementum	postero-mesally at **pge**, lateral to the base of **pta**	laterally at prementum near the base of **ppg**	mesally at prementum	dorsolaterally at the proximal margin of palpomere 1	at lateral wall of **ppg**	laterally at the proximal margin of palpomere 1
	-		**-**		**1 bdl.**		**1 bdl.**		**1 bdl.**		**1 bdl.**		**1 bdl.**	
Pycnocentria evecta McLachlan, 1868					anterolaterally at prementum in front of **cr-prm(m)**	mesally at the proximal half of the roof of **sal**	laterally at posterior half of **pge** (lateral to **cr-prm(l)**)	both bdl. together at proximal part of prementum	postero-mesally at **pge**	laterally at prementum near the base of **ppg**	mesally at prementum	dorsolaterally at the proximal margin of palpomere 1	at lateral wall of **ppg**	laterally at the proximal margin of palpomere 1
	-		**1 bdl.**		**1 bdl.**		**2 adjacent bdl.**		**1 bdl.**		**1 bdl.**		**1 bdl.**	
Molanna angustata Curtis, 1834			roof of **sal**	roof of **sal**	laterally at prementum in front of **cr-prm(m)**	mesally at the proximal half of the roof of **sal**	mesally at posterior half of **pge** (lateral to **cr-prm(l)**)	both bdl. together at proximal part of prementum	postero-mesally at **pge**, lateral to the base of **pta**	laterally at prementum near the base of **ppg**	mesally at prementum	dorsolaterally at the proximal margin of palpomere 1	at lateral wall of **ppg**	laterally at the proximal margin of palpomere 1
	-		**-**		**1 bdl.**		**2 adjacent bdl. [?]**		**1 bdl.**		**1 bdl.**		**1 bdl.**	
Leptocerus tineiformis Curtis, 1834					laterally at prementum in front of **cr-prm(m)**	mesally at the proximal half of the roof of **sal**	mesally at posterior half of **pge** (lateral to **cr-prm(l)**)	both bdl. together at proximal part of prementum	postero-mesally at **pge**, lateral to the base of **pta**	laterally at prementum near the base of **ppg**	mesally at prementum	dorsolaterally at the proximal margin of palpomere 1	at lateral wall of **ppg**	laterally at the proximal margin of palpomere 1

Appendix 7: Character state matrix. Abbreviations: ? – uncertain, - – not applicable.

Character No. **Taxon**	**1**	**2**	**3**	**4**	**5**	**6**	**7**	**8**	**9**	**10**	**11**	**12**	**13**	**14**	**15**	**16**	**17**	**18**	**19**	**20**	**21**	**22**	**23**	**24**	**25**	**26**	**27**	**28**	**29**	**30**	**31**	**32**	**33**	**34**	**35**	**36**	**37**
Philopotamus ludificatus McLachlan, 1878	0	0	0	1	0	0	0	0	2	1	0	0	0	0	0	1	0	-	0	0	1	0	0	0	1	0	0	1	0	0	0	-	0	0	0	2	0
Stenopsyche marmorata Navas, 1920	0	0	0	1	0	0	0	0	1	1	0	0	0	0	0	1	1	0	1	0	?	0	0	?	1	0	0	1	0	0	?	-	0	?	0	?	?
Hydropsyche angustipennis (Curtis, 1834)	1	0	0	1	0	0	0	0	1	0	-	2	0	0	1	1	0	-	0	0	1	0	0	0	1	0	0	1	0	0	0	-	0	0	0	3	0
Tinodes dives (Pictet, 1834)	1	0	0	1	0	0	0	0	1	1	0	0	0	0	1	1	1	0	0	0	1	1	0	0	1	0	0	1	0	0	0	-	0	1	0	?	?
Holocentropus dubius (Rambur, 1842)	1	0	0	1	0	0	0	0	1	0	-	2	1	0	1	1	1	0	0	0	1	1	0	0	0	0	0	1	0	1	1	1	0	1	0	?	?
Rhyacophila obliterata McLachlan, 1863	0	0	0	0	1	0	0	0	1	1	1	2	1	0	0	0	-	-	1	0	0	0	1	0	0	1	0	0	0	0	1	0	0	2	0	2	0
Apsilochorema sutshanum Martynov, 1934	0	0	0	0	1	1	0	1	0	1	1	2	1	0	0	0	-	-	1	0	0	0	1	1	0	1	0	0	0	0	0	-	0	2	0	?	?
Hydrobiosis styracine McFarlane, 1960	0	0	0	0	1	1	0	1	0	1	1	2	1	0	0	0	-	-	1	0	1	0	1	1	0	1	0	0	0	0	0	-	0	2	0	?	?
Glossosoma spinosum Morse et Yang, 2005	0	0	0	0	1	1	0	0	1	1	0	2	1	1	-	1	1	0	0	0	0	0	1	0	0	1	0	0	0	0	0	-	0	2	0	0	0
Agapetus fuscipes Curtis, 1834	0	0	0	0	1	1	0	0	1	1	0	2	1	1	-	1	0	-	0	0	1	0	1	0	0	1	0	0	0	0	0	-	0	2	0	0	0
Ptilocolepus granulatus (Pictet, 1834)	0	0	0	0	1	1	0	0	1	1	0	-	0	0	0	1	1	0	0	0	0	0	1	0	0	1	0	0	0	0	0	-	0	2	0	0	0
Hydroptila scamandra Neboiss, 1977	1	0	0	0	1	1	0	2	1	0	-	-	0	0	0	1	1	0	0	0	0	0	1	?	1	1	0	0	0	0	0	-	0	2	1	?	?
Orthotrichia atraseta Wells, 1979	1	0	0	0	1	1	0	2	1	0	-	-	0	0	0	1	1	0	0	0	0	0	1	0	1	1	0	0	0	0	0	-	0	2	1	?	?
Phryganea grandis Linnaeus, 1758	0	1	1	0	1	1	1	2	0	1	2	1	2	0	0	0	-	-	1	0	1	0	1	1	1	1	1	0	0	1	1	1	1	1	1	4	1
Trichostegia minor (Curtis, 1834)	0	1	1	0	1	1	1	2	1	1	2	1	2	0	0	0	-	-	1	0	1	0	1	1	1	1	1	0	0	1	1	1	1	1	1	4	1
Brachycentrus subnubilus Curtis, 1834	1	1	2	0	1	1	1	2	0	1	2	1	2	0	0	0	-	-	1	1	2	0	1	1	1	1	0	0	0	1	1	1	1	1	1	4	1
Limnephilus flavicornis (Fabricius, 1787)	0	1	2	0	1	1	1	2	0	1	2	1	2	0	0	1	0	-	1	1	2	0	1	1	1	1	0	0	0	1	1	1	1	1	1	4	1
Silo nigricornis (Pictet, 1834)	1	1	2	0	1	1	1	2	0	1	2	1	2	0	0	0	-	-	1	1	2	0	1	1	1	1	0	0	0	1	1	1	1	1	1	4	1
Sericostoma personatum Kirby et Spence, 1826	1	1	2	0	1	1	0	2	0	0	-	0	0	0	0	0	-	-	0	0	1	0	1	1	1	1	0	1	1	1	1	1	1	?	1	4	1
Pycnocentria evecta McLachlan, 1868	1	1	4	0	1	1	0	2	0	0	-	0	2	0	0	1	2	1	0	0	1	0	1	1	1	1	0	1	1	1	1	1	1	?	1	4	1
Molanna angustata Curtis, 1834	1	0	0	0	1	1	0	2	0	0	-	0	2	0	0	0	-	-	0	0	1	0	1	1	1	1	0	1	1	1	1	1	1	1	1	4	1
Leptocerus tineiformis Curtis, 1834	1	0	0	0	1	1	0	2	0	1	1	1	2	0	0	0	-	-	1	0	1	0	1	1	1	1	0	1	1	1	1	1	1	?	1	4	1
Micropterix clathella (Linnaeus, 1761)	0	0	0	0	1	-	0	0	0	1	0	0	0	0	0	0	-	-	0	0	0	0	1	0	0	0	0	0	0	-	-	-	-	0	0	?	?
Nannochorista sp.	0	0	0	0	1	-	1	1	0	1	2	-	0	0	0	-	-	-	0	0	0	0	1	0	0	1	1	1	0	-	-	-	-	0	0	?	?

ARTHROPOD SYSTEMATICS
& PHYLOGENY

73 (3): 351 – 384
23.12.2015

SENCKENBERG

© Senckenberg Gesellschaft für Naturforschung, 2015.

The adult head of the annulipalpian caddisfly *Philopotamus ludificatus* McLachlan, 1878 (Philopotamidae), mouthpart homologies, and implications on the ground plan of Trichoptera

Martin Kubiak *,[1a,b], Felix Beckmann[2] & Frank Friedrich[1b]

[1a] Centrum für Naturkunde (CeNak) – Zoologisches Museum, Universität Hamburg, Martin-Luther-King-Platz 3, 20146 Hamburg, Germany; Martin Kubiak * [martin.kubiak@uni-hamburg.de] — [1b] Biozentrum Grindel, Universität Hamburg, Martin-Luther-King-Platz 3, 20146 Hamburg, Germany; Frank Friedrich [frank.friedrich@uni-hamburg.de] — [2] Institut für Werkstoffforschung, Helmholtz-Zentrum Geesthacht, Außenstelle am DESY Hamburg, Notkestraße 85, 22607 Hamburg, Germany; Felix Beckmann [felix.beckmann@hzg.de] — * Corresponding author

Accepted 16.iv.2015.

Published online at www.senckenberg.de/arthropod-systematics on 14.xii.2015.

Editor in charge: Klaus-Dieter Klass.

Abstract

Adult head structures of representatives of all major trichopteran lineages were examined by using a combination of well-established morphological techniques as histology, light microscopy, scanning electron microscopy, and micro-computed tomography in combination with computer-based 3D-reconstruction. Internal and external cephalic features of the annulipalpian representative, *Philopotamus ludificatus* McLachlan, 1878, are described and illustrated in detail. The sclerites of maxilla and labium are often fused and inseparable leading to different homology hypotheses in the literature, concerning for instance the identity of the maxillary endite lobes (galea or lacinia), the composition of the basal maxillary sclerites and the origin of the haustellum. The detailed description of the skeleto-muscular system of *Philopotamus* allows for a thorough evaluation of these structures and a critical discussion of their identity. Furthermore, character complexes showing the most relevant variability among the major trichopteran lineages are presented. The ground plan conditions of the adult head in Trichoptera and Amphiesmenoptera are reconstructed for several characters. The trichopteran ground plan contains a Π-shaped tentorium with short dorsal arms, moderately sized mandibles equipped with three well-developed muscles, a small but distinct lacinia, five-segmented maxillary palps and a small haustellum. Additionally, the unusual configuration of the extrinsic dilator muscles of the salivarium is regarded as a potential autapomorphy of Trichoptera. Adult head structures observed in the annulipalpian family Philopotamidae show a remarkable number of presumably plesiomorphic features, as moderately developed and sclerotized but functionless mandibles, a small protrusible haustellum without channels on its surface, extrinsic antennal muscles originating exclusively from the tentorium, a small lacinia closely associated with the mainly membranous galea (i.e., galeolacinia), extrinsic dorsal muscles of the salivarium originating from the hypopharynx and from the premental sclerite, respectively, and small labial endite lobes.

Key words

Head morphology, skeleton, musculature, nervous system, Amphiesmenoptera, Integripalpia, Spicipalpia, Rhyacophilidae, Phryganeidae.

1. Introduction

Trichoptera (caddisflies) are comprised of two lineages, the suborder Annulipalpia (fixed-retreat makers, app. 5,500 spp.) and the suborder Integripalpia (tube-case makers, app. 5,200 spp.), plus the families Rhyacophilidae, Hydrobiosidae (both free-living), Glossosomatidae (saddle-case makers), Hydroptilidae, and Ptilocolepidae (both purse-case makers), collectively containing app. 4,000 species (Malicky 2001; Holzenthal et al. 2011).

These families have been combined in a third suborder 'Spicipalpia', or cocoon-makers, established by Weaver (1984). 'Spicipalpia' are likely not monophyletic and the taxon was not recognized in the most recent classification of the order (Holzenthal et al. 2011). The phylogenetic position of the spicipalpian families is still unresolved, and a major question in trichopteran phylogenetic research (Ross 1956; Wiggins & Wichard 1989; Schmid 1989; Ivanov 1997; Kjer et al. 2002; Holzenthal et al. 2007a,b; Malm et al. 2013). The unresolved basal branching pattern within the order also impedes the reconstruction of the trichopteran anatomical ground plan conditions. The reconstruction of the last common ancestor of the extant species is a crucial issue in phylogenetics and the necessary basis for the interpretation of evolutionary transformations in any group (see e.g., Beutel et al. 2011; Peters et al. 2014). As emphasized by Kristensen (1997), the reconstruction of the trichopteran ground plan is also impeded by the scarcity of detailed and comparative morphological and behavioral data. Especially the soft-tissue anatomy is seriously understudied for all tagmata and life stages (Friedrich & Beutel 2010; Beutel et al. 2011).

Insect head structures are a valuable source for phylogenetic information (see analyses in Beutel et al. 2011) and internal features are essential for analyzing feeding mechanisms (e.g., feeding of the mecopteran *Merope* in Friedrich et al. 2013). Anatomical data on adult cephalic structures of Trichoptera are scarce. Early investigations focused on a limited number of external features and the published data (e.g., Cummings 1914; Demoulin 1960) are largely insufficient for comparative analyses and phylogenetic evaluation. Very few studies have been devoted to internal features ('soft anatomy') of the adult head. The extensive description of *Phryganea bipunctata* (Retzius, 1783) (Integripalpia-Phryganeidae) by Crichton (1957) provides general information on cephalic features, but as this taxon is apparently deeply subordinate phylogenetically (see e.g., Malm et al. 2013), the usefulness of the data for the reconstruction of the ordinal ground plan is quite limited. The only study of a comparatively 'ancestral' trichopteran is a detailed description of the internal and external morphology of a species of *Rhyacophila* ('Spicipalpia'-Rhyacophilidae) (Klemm 1966). It was apparent that the cephalic ground plan of Trichoptera (e.g., shape and fine structure of the haustellum, musculature of the prepharynx, shape of the tentorium, etc.) could not be reliably reconstructed with the very limited data at hand.

Even though Rhyacophilidae have retained a number of apparently plesiomorphic features, a sistergroup relationship of Annulipalpia to all other trichopteran lineages ('Spicipalpia' + Integripalpia) is supported by both morphological and molecular data (Ross 1956; Frania & Wiggins 1997; Kjer et al. 2002). Malm et al. (2013) identified the spicipalpian lineages as a non-monophyletic group and as basal branches subsequently branching off, with Rhyacophilidae as the sistergroup of all the remaining Trichoptera. Like in the spicipalpian families, more or less extensive sets of potentially ancestral features also occur in Annulipalpia (Ross 1956). The 10 annulipalpian families are recently grouped into the three superfamilies Philopotamoidea (Stenopsychidae and Philopotamidae), Hydropsychoidea (Hydropsychidae), and Psychomyioidea (Kambaitipsychidae, Pseudoneureclipsidae, Psychomyiidae, Ecnomidae, Xiphocentronidae, Polycentropodidae, and Dipseudopsidae) (e.g., Holzenthal et al. 2007b; Chamorro & Holzenthal 2011; Holzenthal et al. 2011). Ross (1956) proposed Philopotamidae as sistergroup to the remaining annulipalpians based on characters of the wing venation and the two-segmented, 'primitive' male genitalia. Additionally, some of the oldest known trichopteran fossils from the Siberian Jurassic belong to this family (†*Archiphilopotamus* Sukatsheva, 1985). With about 1,000 extant species (Holzenthal et al. 2007a) Philopotamidae is also one of the most species rich families of Annulipalpia. Members of Philopotamidae are adapted to cool, running waters and are distributed worldwide (Ross 1956; Holzenthal et al. 2007a). Even though presumptive plesiomorphies (see Ross 1956) and the long evolutionary history suggests Philopotamidae as a key taxon for reconstructing the ground plan of Annulipalpia and the entire Trichoptera, the soft tissue anatomy of species of this family (and other groups of Annulipalpia) is very insufficient known and only limited information on external skeletal features is available (Ross 1956; Frania & Wiggins 1997). Consequently, we choose the philopotamid species *Philopotamus ludificatus* McLachlan, 1878 for the first comprehensive description and documentation of internal and external head structures. For the investigation of soft tissues and the skeleton of the head a combination of traditional and innovative morphological techniques was used (see Friedrich et al. 2014), including micro-computed tomography (SR-µCT), scanning electron microscopy (SEM), histological sectioning and light microscopy.

The findings are compared with own observations and literature based information on other trichopterans (e.g., Klemm 1966; Crichton 1957) and outgroup taxa (e.g., Lepidoptera – Micropterigidae; Hannemann 1956; Kristensen 2003) to discuss the homology of the mouthparts and to reconstruct the trichopteran ground plan. Additionally, character complexes potentially relevant for phylogenetic analyses are presented for further detailed investigations.

2. Material and methods

2.1. List of taxa examined and techniques applied

Annulipalpia, Philopotamidae: *Philopotamus ludificatus* McLachlan, 1878 (male, 70 % ethanol; hist., SR-µCT, SEM, diss.). **Hydropsychidae:** *Hydropsyche angustipennis* (Curtis, 1834) (male, 70 % ethanol; SR-µCT, hist., SEM).

'Spicipalpia', Rhyacophilidae: *Rhyacophila obliterata* McLachlan, 1863 (male, SR-µCT); *Rhyacophila fasciata* Hagen, 1859 (male, 70 % ethanol; SEM, diss.).

Integripalpia, Phryganeidae: *Phryganea grandis* Linnaeus, 1758 (male, 70 % ethanol; SR-µCT, SEM, diss.).

Lepidoptera (outgroup), Micropterigidae: *Micropterix calthella* (Linnaeus, 1761) (male, 70 % ethanol; hist., SEM).

[**Abbreviations:** hist. = histological section series; SR-µCT = synchrotron radiation based micro-computed tomography; SEM = scanning electron microscopy; diss. = dissection]

2.2. Morphological techniques

Synchrotron radiation based micro-computed tomography (SR-µCT). The SR-µCT data for an adult specimen of *Philopotamus* were obtained at beamline BW2 of storage ring DORIS III at the German Electron Synchrotron Facility (DESY), Hamburg (project number: I-20100317). For our studies we used a stable low photon energy beam (8 keV) and absorption contrast (for technical details of micro-tomography at beamline BW2 see Beckmann et al. 2006, 2008). Before the SR-µCT scans were carried out the appendages (wings, antennae, and legs) were cut off from the body proximally resulting in a distinctly reduced field of view. Subsequently, the specimen was dehydrated in an ethanol series and critical point dried (Balzers Critical Point Dryer) to avoid shrinking of soft tissues. The sample was mounted on a metal rod and scanned in 180° rotation (0.25° steps; 720 tomograms). The obtained image stack revealed a physical resolution of 5.68 µm (voxel size app. 2.3 µm) and allowed for easy discrimination of different tissue types. SR-µCT scans of adult specimens of *Hydropsyche*, *Rhyacophila* and *Phryganea* were also performed at the DESY facility using an identical preparations and procedures.

Computer-based 3D-reconstruction. A combination of different software packages (Visage Imaging Amira® 5.4, Bitplane Imaris 6, and Autodesk® Maya 2014) was applied to reconstruct the head morphology of *Philopotamus* based on µCT image data three-dimensionally. Amira software in combination with a Wacom Cintiq 22HD interactive pen display was used for segmentation of raw image data. Due to high density resolution of the SR-µCT scan different types of soft tissue such as muscles, glands, nerves, and also the sclerotization of the skeleton could be easily distinguished. An image stack series was obtained for each segmented structure and subsequently transferred into Bitplane Imaris 6 software for automatic creation of surface objects. Subsequently, for final post processing in Maya 2014 software all surface files (.iv) were converted into object files (.obj) using Transform2 64 bit software (Heiko Stark, Jena, Germany; URL: http://starkrats.de). The modeling of minor surface artifacts, reduction of file size, and surface renderings were processed in Maya 2014 software (for details see Friedrich et al. 2013).

Histology. Heads of *Philopotamus* and *Hydropsyche* were embedded in Araldite resin and cut at 1 µm with a Microm Microtome (HM 360) with diamond knife. The obtained cross section series were stained with toluidin blue and fuchsin. Digitalization was carried out using a Leica DM6000 microscope with slide scanning option (based on MetaMorph software). The photographed sections were automatically aligned and processed using Visage Imaging Amira 5.4® software.

Light microscopy imaging. Light microscopy imaging represents a useful tool for the documentation of coloration pattern and allows for easy discrimination of membranous and well-sclerotized areas of the insect body. The head of a male of *Philopotamus* was dehydrated in an ethanol series and critical point dried (Balzers Critical Point Dryer). Subsequently, it was glued on a small insect pin for imaging in standard morphological views. Photographs were taken using a Passport II system built by Visionary Digital™, equipped with a Canon EOS 6D digital camera and a 65 mm Canon compact macro-lens. Helicon Focus Pro X64 was used to combine the partially focused images.

Scanning electron microscopy (SEM). The fine structure of the external head capsule and its appendages was studied and documented by using SEM imaging. The head of a male of *Philopotamus* was dehydrated in an ethanol series, critical point dried (Balzers Critical Point Dryer), glued on a pin, and finally fixed to a specimen holder following the methods of Pohl (2010). The sample was evenly coated with platinum using a Polaron SC7650 Sputter Coater. SEM images were taken with a LEO 1525 scanning electron microscope at 5 or 10 keV.

Terminology. The terminology of the skeleton is mainly based on Snodgrass (1935) and Beutel et al. (2014). Sensilla are named and homologized after Melnitsky & Ivanov (2011). The names of muscles are designated by the areas of their origin and insertion sites (abbreviations used in the text: O = origin, I = insertion). If this alone is ambiguous, the topographical orientation (e.g., ventralis vs. dorsalis, etc.) is added. They are homologized with the terminologies used by Hannemann (1956), v. Kéler (1955), and Wipfler et al. (2011) (see Table 1). The musculature of other trichopteran species investigated in the present study or taken from the literature (Crichton 1957; Klemm 1966) is also summarized in Table 1.

The systematics follows Holzenthal et al. (2011). Nomenclature for Trichoptera taxa is adopted from Malicky (2005).

Fig. 1. *Philopotamus ludificatus* McLachlan, 1878: head, light-microscopic images, anterior view. — ***Abbreviations***: acl(d) – distal part of anteclypeolabrum, acl(p) – proximal part of anteclypeolabrum, as – antennal socket, atf – antennifer, atp – anterior tentorial pit, cpe – compound eye, cs – coronal sulcus, fcsw – frontoclypeal setal wart, fgs – frontogenal sulcus, fl – flagellomere, fo – fossa of subgenal process, fpc – frontopostclypeus, fs – frontal sulcus, fsw – frontal setal wart, ge – gena, gp – subgenal process, hf – horizontal furrow between frontopostclypeus and anteclypeolabrum, hst – haustellum, ias – interantennal sulcus, lap – labial palp, loc – lateral ocellus, md(m) – membranous part of mandible, md(s) – mandibular sclerite, moc – median ocellus, mxp – maxillary palp, ped – pedicellus, pfs – postfrontal sulcus, sca – scapus, srts – smooth ribbed trichoid sensillum, ve – vertex, vsw(a) – anterior setal wart of vertex, vsw(p) – posterior setal wart of vertex, I–V – number of palpomere. (Scale bar: 250 µm)

3. Results

3.1. General appearance

The mean body length of adults of *P. ludificatus* is 8.2 mm (6.2 – 10.2 mm; n = 25) for males and 9.9 mm (8.0 – 11.7 mm; n = 25) for females. The body color of the adults is dark brown. The ovate forewings are brown with large, evenly distributed yellowish to ochre spots. The hindwings are uniformly light brown. The wings are held roof-like folded above the abdomen when the living insect is at rest. Large parts of the body and especially the forewings have a dense vestiture of setae and microtrichia. The tibia of all three pairs of legs bear large, ochre spurs (spur formula 2,4,4).

3.2. Head capsule

The head is orthognathous and largely covered by a dense vestiture of minute microtrichia (Fig. 6A,B). The margin

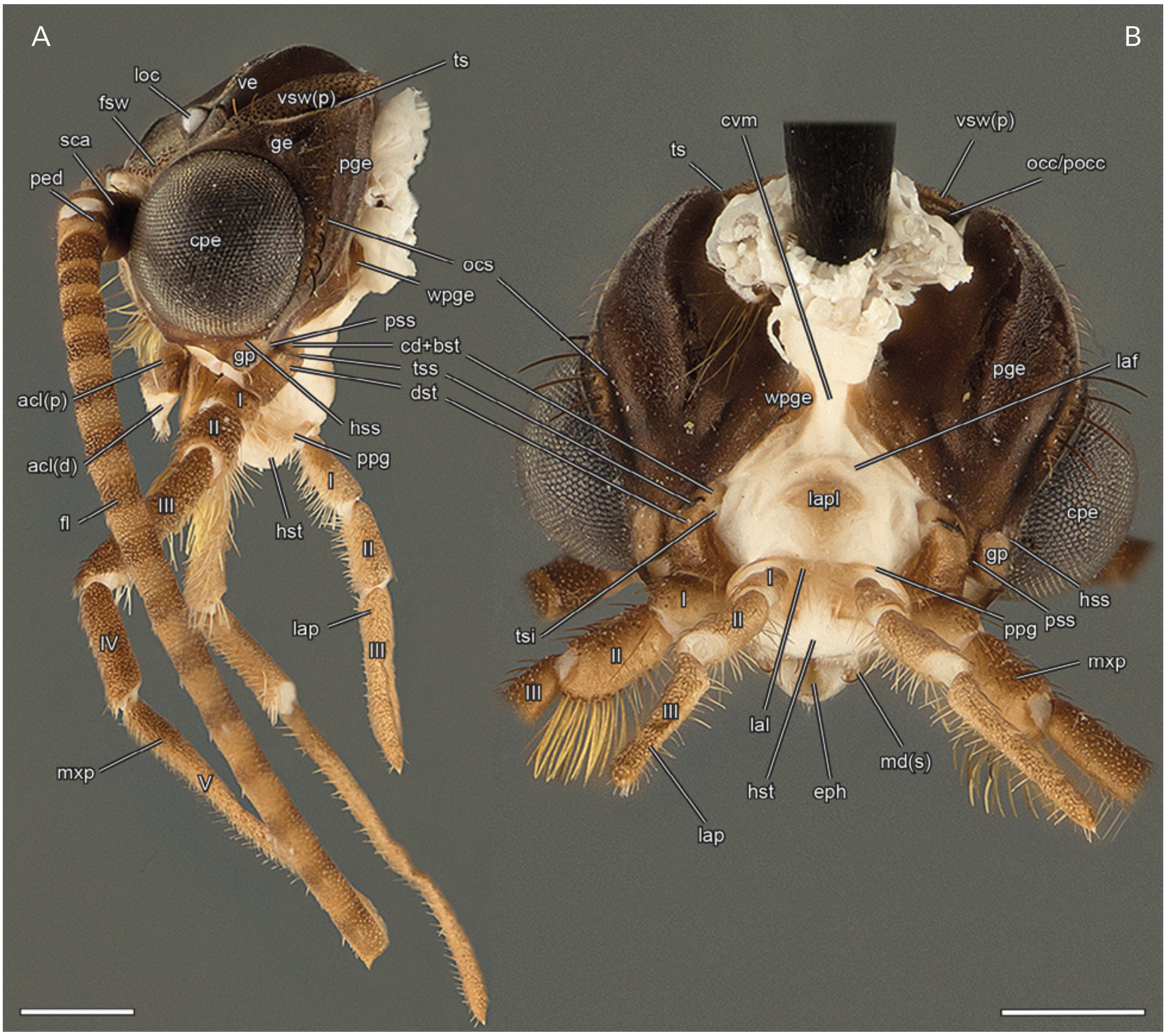

Fig. 2. *Philopotamus ludificatus* McLachlan, 1878: head, light-microscopic images. **A**: lateral view, **B**: posterior view. — ***Abbreviations***: acl(d) – distal part of anteclypeolabrum, acl(p) – proximal part of anteclypeolabrum, bst – basistipes, cd – cardo, cpe – compound eye, cvm – cervical membrane, dst – dististipes, eph – epipharynx, fl – flagellomere, fsw – frontal setal wart, ge – gena, gp – subgenal process, hss – hypostomal sulcus, hst – haustellum, laf – semicircular fold of labium, lal – labial lobe, lap – labial palp, lapl – central plate of labium, loc – lateral ocellus, md(s) – mandibular sclerite, mxp – maxillary palp, occ – occiput, ocs – occipital sulcus, ped – pedicellus, pge – postgena, pocc – postocciput, ppg – palpiger, pss – pleurostomal sulcus, sca – scapus, ts – temporal sulcus, tsi – triangular membranous incision of stipes, tss – transstipital sulcus, ve – vertex, vsw(p) – posterior setal wart of vertex, wpge – wing-shaped extension of postgena, I–V – number of palpomere. (Scale bars: 250 µm)

of the antennal foramen is slightly reinforced by the circumantennal sulcus[1] ('antennal socket' sensu Snodgrass 1935, as in Fig. 1). The antennal socket is ventrally suspended by a large extension (antennifer, atf in Figs. 1, 6A) which is continuous with the dorsal end of the strong frontogenal sulcus (fgs in Fig. 1), interconnecting the ventral margin of the antennal socket and the base of the anterior tentorial arm (= anterior tentorial pit, atp in Figs. 1, 6A). The frontal sulci (fs) diverge anteriorly from the median coronal sulcus (cs) directly behind the median ocellus (Fig. 1). They run ventrolaterad in a straight line toward the antennal socket (obliterated at level of the frontal setal warts [fsw in Fig. 1]; see below). The coronal sulcus extends backwards toward the occipital foramen. The dorsal part of the head capsule represents the vertex (ve in Fig. 1). It is not distinctly bordered laterally, but continuous with the gena (ge in Fig. 2A) and the occiput (occ in Fig. 12B). Halfway between the lateral ocelli and the occiput a postfrontal sulcus (pfs in Fig. 1) arises from the coronal sulcus, runs laterad of the lateral ocellus anteriorly and meets the antennal socket dorsally.

---

[1] The term 'sulcus' refers to any line of cuticular inflection forming internal ridges. In contrast, the term 'suture' is only used for unsclerotized lines between two adjacent sclerotized areas, which are not present in the adult head capsule of caddisflies (see Snodgrass 1963: 9; Kristensen 2003: 39).

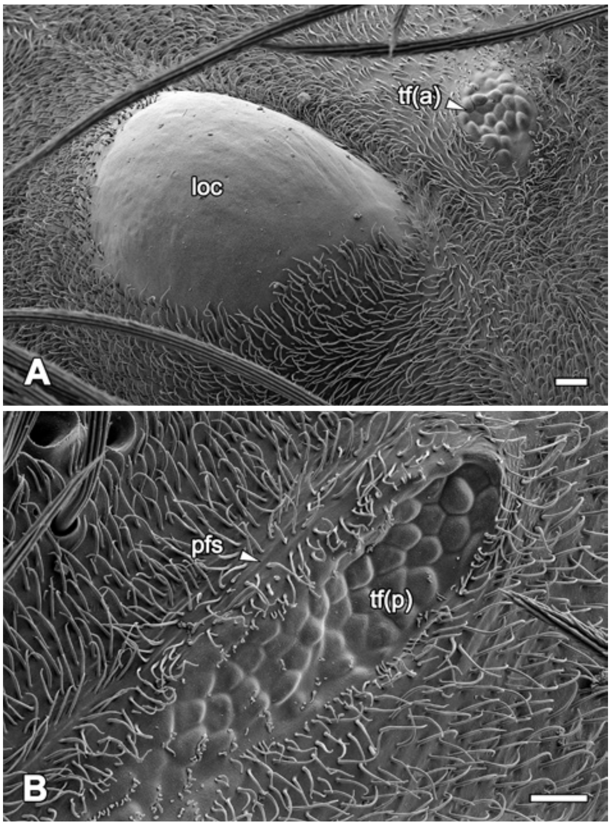

Fig. 3. *Philopotamus ludificatus* McLachlan, 1878: details of head capsule, SEM images. **A**: dorsal view on lateral ocellus with adjacent tubercular field (tubercular field marked by arrow head), **B**: detail of tubercular field behind the postfrontal sulcus (postfrontal sulcus marked by arrow head). — ***Abbreviations***: loc – lateral ocellus, pfs – postfrontal sulcus, tf(a) – anterior tubercular field of vertex, tf(p) – posterior tubercular field of vertex. (Scale bars: 10 µm)

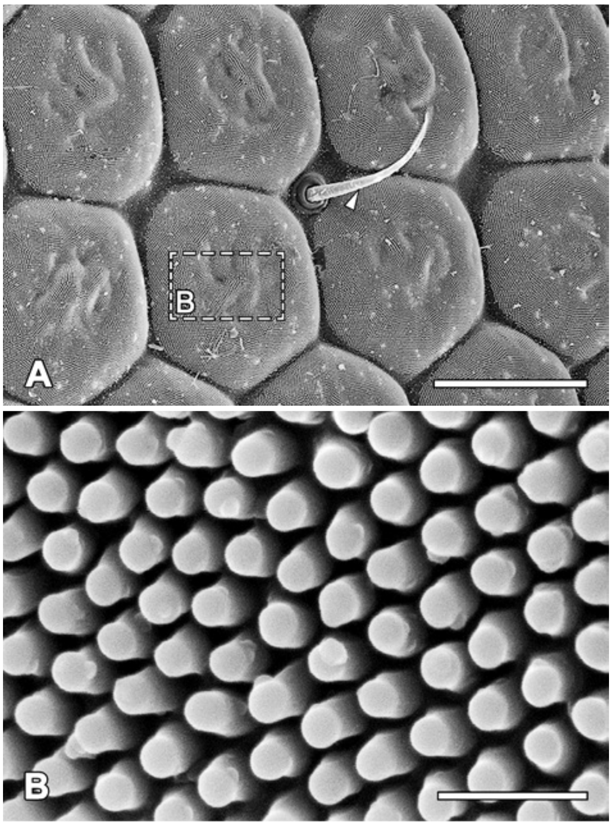

Fig. 4. *Philopotamus ludificatus* McLachlan, 1878: details of compound eye, SEM images. **A**: ommatidia with interommatidial sensillum (marked by arrow head), **B**: ultrastructure of ommatidial surface with corneal nipples. (Scale bars: A: 5 µm; B: 300 nm)

Below the median ocellus a very distinct, curved interantennal sulcus (ias in Fig. 1) runs ventrolaterad toward the frontoclypeal setal wart (see below) (Fig. 1).

The triangular facial area dorsally and laterally delimited, respectively, by the frontal sulcus and the frontogenal sulcus is a frontopostclypeus without any external demarcation of a frontoclypeal boundary (i.e., epistomal sulcus) (Fig. 1); the area above a line connecting the anterior tentorial pits bears a smooth median depression.

The lower facial region is subdivided into ante- and postclypeus by a conspicuous horizontal furrow (hf in Figs. 1, 12A); the head capsule areas adjacent to the latter are less pigmented than elsewhere, and since muscle origins indicate their clypeal nature and the apical (/ventral) area must include a labral component, they can conveniently be termed postclypeus (i.e., frontopostclypeus, fpc in Fig. 1) and anteclypeolabrum (acl(p)/acl(d) in Fig. 1), respectively. The upper/dorsal part (acl(p)) of the anteclypeolabrum has a sparse vestiture of strong smooth ribbed trichoid sensilla and a few placoid sensilla (Fig. 7A), while the lower/apical part (acl(d)) is weakly sclerotized and pigmented (Fig. 1).

The lateral parts of the head capsule, enclosing the compound eyes, are formed by the genae (ge in Fig. 2A). The gena bears a row of five strong dentate and ribbed trichoid sensilla behind the compound eye (Fig. 2A,B). Three basiconic sensilla (bs in Fig. 6A) are located on its anterior surface between the frontogenal sulcus and the anterior margin of the compound eye. Posteriorly, the gena is delimited from the postgenal region by an incomplete occipital sulcus (ocs in Fig. 2A,B). This sulcus dissappears dorsally (behind the compound eye) but ventrally splits into an anterior pleurostomal sulcus (pss) and a posterior hypostomal sulcus (hss) (both in Fig. 2A,B). The two latter sulci demarcate the dorsal margin of the small subgena, which forms a strong, heavily sclerotized process lateral to the base of the mandible. The subgenal process (gp in Figs. 1, 2A,B) is enforced by a strong sulcus and bears an oval fossa (fo in Fig. 1) apically. This structure forms the articular surface of the posterior joint of the pupal mandible.

The posteroventral parts of the head capsule are formed by the postgenae (pge in Fig. 2A,B), which are dorsally delimited from the occiput/postocciput by a strong sulcus ('sulcus temporalis' sensu Klemm 1966, ts in Fig. 2A). The mesal halves of the postgenae are bent posterad and form wing-shaped extensions (wpge in Fig. 2B) connected with the extensive cervical membrane (cvm in Fig. 2B). A ventral closure of the head capsule (e.g., postgenal bridge, gula) is absent (Fig. 2B). Occipital and postoccipital regions are inseparable. Dorsolateral to the tentorial bridge a prominent process forming the median margin of the postoccipital component of the composite occipital and postoccipital region ('condylus occipitalis' sensu Snodgrass 1935, cocc in Fig. 12B) is developed on each side of the occipital foramen, articulating with the lateral cervical sclerite.

The foramen occipitale is divided by the tentorial bridge into a broad, trapezoid upper part (app. ⅔ of the opening) and a smaller lower part (app. ⅓ of the opening). The lower opening has the margins reinforced by a strong sulcus laterally, but is ventrally just closed by the cervical membrane (Fig. 12B).

The head capsule bears a vestiture of strong dentate ribbed trichoid sensilla densely clustered on bulged setal warts (after Oláh & Johanson 2007). One slightly raised frontoclypeal setal wart (fcsw in Figs. 1, 6A) is located on the lateral frontopostclypeal region (fpc in Fig. 1) between the anterior tentorial pit and the antennal socket (Fig. 6A). Three closely adjacent setal warts (two lateral and one median) are arranged in a broad w-shaped pattern in the frontal region (= frontal setal wart, fsw in Figs. 1, 6A) bordered anteriorly by the median ocellus, laterally by the postfrontal sulcus and posteriorly by the frontal sulcus and the lateral ocelli. A pair of large triangular setal warts (= anterior setal wart of vertex, vsw(a) in Fig. 1) is located on the vertex between the lateral ocelli and the meeting point of coronal sulcus and postfrontal sulcus. The posterolateral regions of the vertex bear extremely large, strongly bulged setal warts (= posterior setal wart of vertex, vsw(p) in Figs. 2A, 12B). These areas are posteriorly reinforced by strong internal sulci at their anterior and lateral margins. A shallow furrow (tf(p) in Fig. 3B) is located directly behind the dorsal setal wart of the vertex. Its surface is tubercular and bare of microtrichia. A similarly structured but slightly bulged field (tf(a) in Fig. 3A) is located laterally behind the lateral ocellus. The nature of these fields (secretionary or sensory) could not be identified in histological sections.

3.3. Tentorium

The tentorium is X-shaped with very short but stout posterior tentorial arms (pta in Fig. 14A,B) enforcing the ventrolateral margin of the alaforamen toward the condyli occipitales (Fig. 12B). The posterior tentorial pit (ptp in Fig. 12B) is located in the postoccipital sulcus. It is directed laterad (Fig. 12B). A stout tentorial bridge (tb in Fig. 14A,B) connects the posterior tentorial arms. The posterior most parts of the anterior tentorial arms are mesally fused, forming a plate-like corpotentorium (cot in Fig. 14A,B) posteriorly continuous with the tentorial bridge. The anterior tentorial arm (ata in Fig. 14A,B) is well-developed and originates in a large, rounded anterior tentorial pit which is located about half the distance between the base of the antenna and the anteclypeolabrum (atp in Figs. 1, 12A). The part of the anterior arm directly adjacent to the head capsule or the tentorial bridge is well sclerotized. Between these areas the arm becomes medio-laterally flattened with the lateral side weakly sclerotized. In this region a flattened and weakly sclerotized ventromesally directed process (laminatentorium) is developed (lt in Fig. 14A,B). The margin of the anterior tentorial pit is reinforced by the dorsally directed frontogenal sulcus (fgs in Figs. 1, 16A). A dorsal tentorial arm is weakly developed and is represented by a short peak directed dorsad (dta in Fig. 17C).

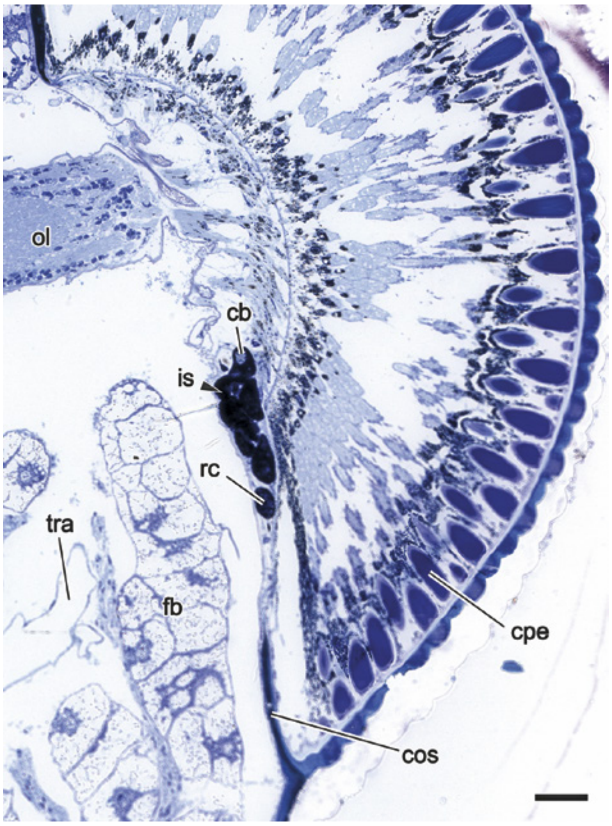

Fig. 5. *Philopotamus ludificatus* McLachlan, 1878: head, cross-section of compound eye and imaginal stemma (marked by arrow head). — ***Abbreviations***: cb – crystalline body, cos – circumocular sulcus, cpe – compound eye, fb – fat body, is – imaginal stemma, ol – optical lobe of protocerebrum, rc – retinula cell, tra – trachea. (Scale bar: 10 µm)

3.4. Eyes

The large, circular compound eye (cpe in Figs. 1, 5) protrudes laterally beyond the head capsule. Along its internal margin it is supported by a well-sclerotized circumocular sulcus (cos in Figs. 5, 16A) with a keyhole-shaped aperture. Each compound eye consists of app. 1,500 ommatidia. The ommatidia are covered by a dense vestiture of very fine, rounded corneal nipples (after Bernhard & Miller 1962) (ca. 130 nm in diameter) (Fig. 4B). Few interommatidial trichoid sensilla are irregularly spread on the surface of the compound eye (arrow head in Fig. 4A). Two lateral ocelli (loc in Fig. 1) are located mesally, slightly behind the midline of the compound eyes. A median ocellus (moc in Fig. 1) is located half the distance

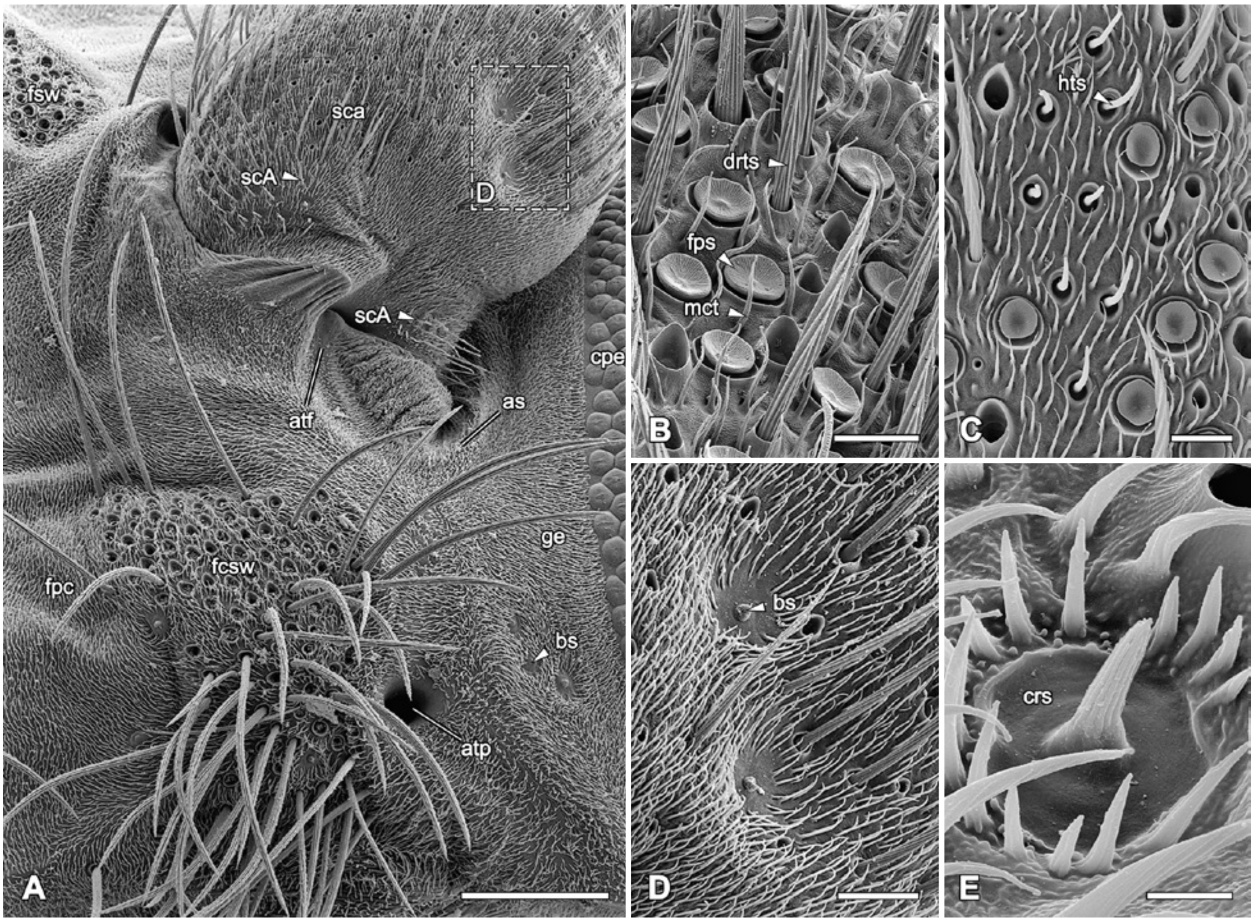

Fig. 6. *Philopotamus ludificatus* McLachlan, 1878: antenna, SEM images. **A**: anterior view on frontoclypeus and antennal base, **B**: detail of antennal sensilla and microtrichia, **C**: detail of sensory field on sixth flagellomere, **D**: detail of scapal sensilla, **E**: detail of sensillum basiconicum surrounded by a ring of microtrichia. — ***Abbreviations***: as – antennal socket, atf – antennifer, atp – anterior tentorial pit, bs – sensillum basiconicum, cpe – compound eye, crs – coronary sensillum, drts – dentate ribbed trichoid sensillum, fcsw – frontoclypeal setal wart, fpc – frontopostclypeus, fps – fungiform pseudoplacoid sensillum, fsw – frontal setal wart, ge – gena, hts – helical trichoid sensillum, mct – microtrichium, sca – scapus, scA – sensillum chaeticum A. (Scale bars: A: 100 µm; D: 20 µm; B, C: 10 µm; E: 2 µm)

between the dorsal antennal edges. An internalized imaginal stemma (is in Fig. 5) is located posteroventrally adjacent to the retinula cells of the compound eye between the optic lobe of the brain (ol in Fig. 5) and the inner edge of the circumocular sulcus (cos in Fig. 5). It is visible as a wedge-shaped assemblage of several pigment cells (rc) and at least one cone cell (cb in Fig. 5).

3.5. Antenna

The filiform antenna is almost as long as the body. It comprises on average 53 antennomeres in both sexes (49 – 55; n = 50). The general coloration is light brown. Scapus (sca), pedicellus (ped) and the first 24 – 27 flagellomeres (fl; all in Fig. 1) show a dark brown band in the proximal half (Figs. 1, 2A). The width of the band decreases along the antenna from proximal to distal. The scapus is the largest antennomere. It is almost as long as wide (sca in Figs. 1, 12A). The pedicellus (ped in Figs. 1, 12A) is the smallest antennomere (half of the size of the scapus). Flagellomeres 1 and 2 are smaller than the remaining flagellomeres. The terminal flagellomere is apically pointed.

All antennomeres except the scapus are irregularly covered by numerous dentate ribbed trichoid (drts) and fungiform pseudoplacoid sensilla (fps) (both in Fig. 6B). Additionally, each flagellomere is equipped with a few and irregularly distributed coronary sensilla (mainly in the proximal half on the dorsal side) (crs in Fig. 6E), numerous helical trichoid sensilla (distal half) (hts in Fig. 6C), and very few small basiconic sensilla (distal half). The ventrolateral side of the scapus is equipped with two basiconic sensilla (Fig. 6D). Proximally, the scapus bears two groups of sensilla chaetica A (after Drilling & Klass 2010; scA in Fig. 6A) which flank the articulation with the antennifer.

The antenna is attached dorsolaterally between the compound eye and the median ocellus. It is articulated with the antennifer situated at the ventral margin of the broad antennal socket (Fig. 6A). Scapus and pedicellus are similarly articulated. A ventromesal process of the scapus corresponds with a small furrow at the base of the pedicellus. The position of this articulation is shifted by 55° in relation to the antennifer (Fig. 1). There are no specific articulations between the flagellomeres, which are separated by very short membranous areas.

Musculature (Figs. 12A, 13A, 16A,B, 17C–F): **M. tentorio-scapalis anterior** [te-sc(a)]: long, together with te-sc(l) the largest antennal muscle, O: mesal side of the anterior tentorial arm and laminatentorium, I: ventromesally at the scapal base with strong tendon (mesal of antennifer); **M. tentorio-scapalis posterior** [te-sc(p)]: slender, O: dorsally at the anterior tentorial arm (between te-sc(a)/(l)), I: dorsomesal margin of the scapal base; **M. tentorio-scapalis lateralis** [te-sc(l)]: two adjacent bundles, O: lateral face of the anterior tentorial arm and the laminatentorium (opposite to te-sc(a)), I: ventrolaterally at the scapal base (lateral of antennifer), posterior bundle with short tendon; **M. tentorio-scapalis medialis** [te-sc(m)]: comparatively short, O: dorsally on the anterior tentorial arm close to the head capsule (close to fr-ph(l)), distinctly anterior to the other antennal muscles, I: mesal margin of the scapal base; **M. scapo-pedicellaris medialis** [sc-pe(m)][2]: comprises three bundles: two lateral: O: dorsal and ventromesal areas of scapal base, I: both bundles together mesally at the pedicellar base (mesal of scapo-pedicellar articulation); one dorsal: O: between the first two bundles on the mesal face of the scapus, I: dorsally at the proximal margin of the pedicellus (almost opposite to scapo-pedicellar articulation); **M. scapo-pedicellaris lateralis** [sc-pe(l)]: two bundles, O: ventromesal and ventrolateral margin of scapal base (enclosing the scapal joint with the head capsule) I: large parts of ventral and ventrolateral margin of the pedicellus (lateral of scapo-pedicellar articulation).

3.6. Labrum

The labrum and anteclypeus together form a structural and functional unit (anteclypeolabrum, acl in Fig. 1; see above); the two components are inseparable since a clypeolabral articulation and the cranial flexor muscle (M. fronto-labralis) of the labrum are absent. The anteclypeolabrum is triangular and divided into a large, strongly sclerotized proximal part (acl(p)) and a short, membranous distal section (acl(d)) forming a rounded tip (Fig. 1).

Musculature: **M. labro-epipharyngalis** [lb-eph]: absent. **M. fronto-labralis** [fr-lb]: absent.

3.7. Mandible

The mandible (md) is largely membranous in its lateral half (md(m) in Figs. 1, 7A) which is mesally continuous with the moderately sclerotized mandibular sclerite (md(s) in Figs. 1, 7A). The short, lobe-like mandibular sclerite is antero-posteriorly flattened and lacks any teeth. The inner rims of the mandibular sclerites form blunt edges, which do not overlap but touch each other at mid-length. Proximally, the mandibular sclerites enclose the bulged mid-part of the hypopharynx (Fig. 16D). The mandibular sclerites are almost completely covered by the anteclypeolabrum and hung into distinct concavities of the latter (Fig. 16D). There are no true articulations with the head capsule. The extensive adductor tendon (adte in Fig. 16C) is largely formed by non-sclerotized cuticle and has a broad origin at the proximomesal edge of the mandible (Fig. 16C); the cuticle is not particularly thickened in this area. The abductor tendon (abte in Fig. 16D) is not connected to the mandibular sclerite but attaches to an invagination, which forms a distinct pit in the lateral mandibular membrane (Fig. 7A). This configuration does not allow notable movements of the mandible in the post-pharate stage (see also Discussion).

Musculature (Figs. 12A,B, 13A,B, 16A–D, 17D,E): **M. cranio-mandibularis medialis** [cr-md(m)]: the largest muscle of the head (fills app. ½ of the head capsule volume), composed of several bundles which aggregate toward the adductor tendon, O: large parts of the dorsal and lateral head capsule (occipital/postoccipital region, postgena and vertex posterior to postfrontal sulcus), I: adductor tendon of the mandible; **M. cranio-mandibularis lateralis** [cr-md(l)]: large but only app. ¼ of cr-md(m), O: with several bundles on the lateral area of the postgena and dorsolateral on gena and circumocular sulcus (partly between attachment areas of cr-md(m)), I: laterally at the membranous part of the mandible (close to the subgenal process) by means of the long abductor tendon; **M. hypopharyngo-mandibularis** [hy-md]: absent; **M. tentorio-mandibularis** [te-md]: extremely thin, composed of 2–3 fibers, closely adjacent with the mandibular nerve, O: anterior tentorial arm, covered by the anterior bundle of te-sc(l), I: mesally on the inner wall of the mandibular sclerite (with a long and very thin tendon).

3.8. Maxilla

The maxilla is composed of a composite basal sclerite (i.e., cardo + basistipes, dististipes), a composite galeolacinia, and a 5-segmented maxillary palp. The small cardo (cd in Figs. 2A,B, 10) forms the basalmost part of the maxilla. Distally, the cardo is completely fused with the considerably larger stipes. A strong oblique sulcus (tss in Figs. 2A,B, 10), externally visible as a dark brown stripe, separates the stipes into a proximal basistipes (bst in Figs. 2A,B, 10) which is continuous with the cardo and an apical dististipes (dst in Figs. 2A,B, 10). The lateral end of this sulcus forms a distinct dorsal apodeme serving as attachment area of the cranial muscle of the stipes, whereas the mesal end is only slightly pointed. The proximolateral angle of the cardo meets the subgena close to the adjacent postgena without forming a distinct articulation.

The proximal margin of the dististipes is almost completely fused with the composite basal piece formed by

---

[2] Lateral and medial reflects the relative position of the muscles to the scapo-pedicellar joint.

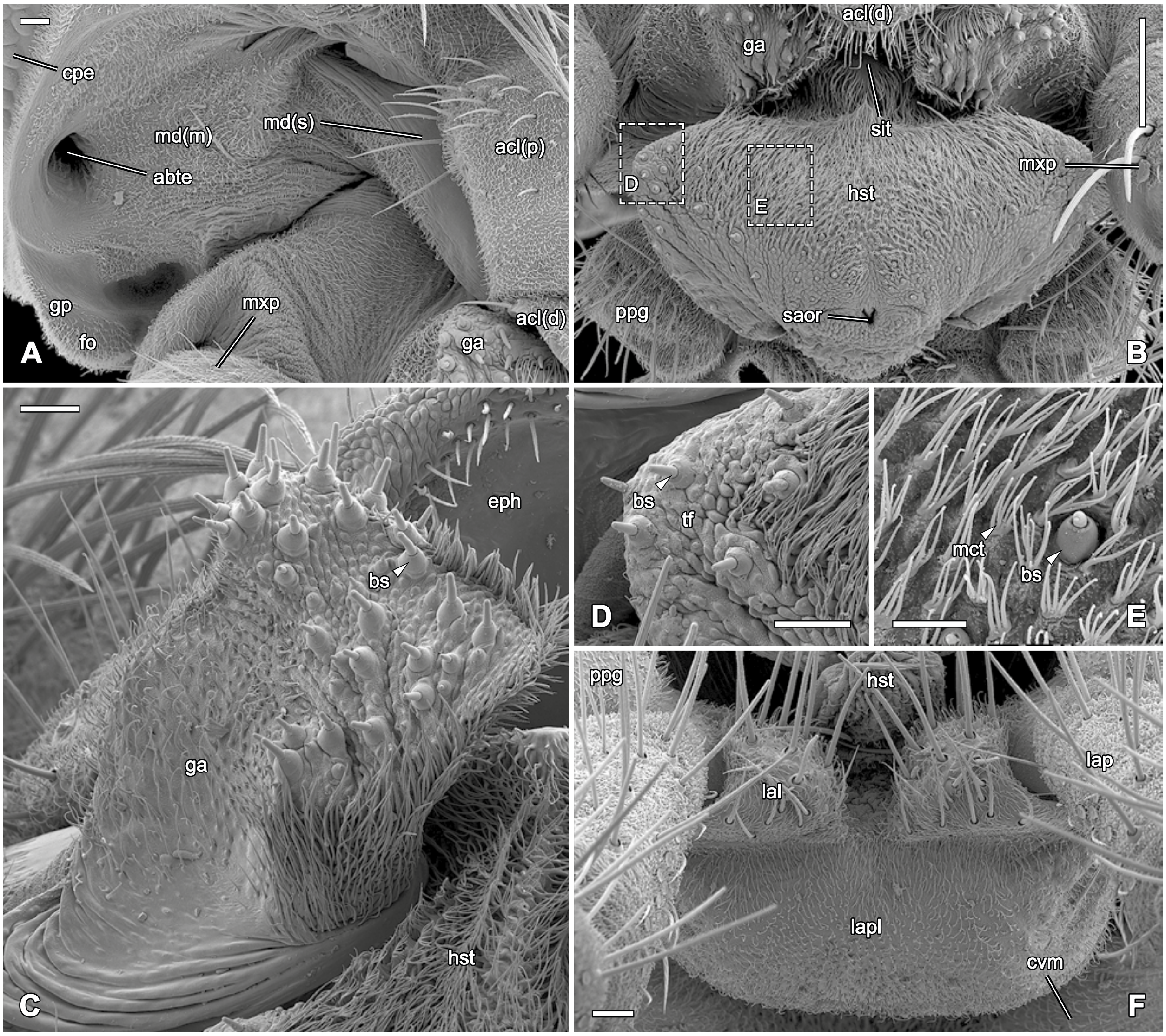

Fig. 7. *Philopotamus ludificatus* McLachlan, 1878: mouthparts, SEM images. **A**: anterior view on base of mandible, **B**: anterior view on haustellum, **C**: anterior view on galeolacinia, **D**: detail of surface of haustellum, **E**: detail of sensilla and microtrichia of haustellum, **F**: anterior view on labium. — ***Abbreviations***: abte – tendon of abductor muscle of mandible (M. cranio-mandibularis lateralis), acl(d) – distal part of anteclypeolabrum, acl(p) – proximal part of anteclypeolabrum, bs – sensillum basiconicum, cpe – compound eye, cvm – cervical membrane, eph – epipharynx, fo – fossa of subgenal process, ga – galea, gp – subgenal process, hst – haustellum, lal – labial lobe, lap – labial palp, lapl – central plate of labium, mct – microtrichium, md(m) – membranous part of mandible, md(s) – mandibular sclerite, mxp – maxillary palp, ppg – palpiger, saor – salivary orifice, sit – sitophore plate, tf – tubercular field. (Scale bars: B: 100 µm; A, C, D, F: 20 µm; E: 10 µm)

the cardo and the basistipes. It is only mesally separated by a short triangular membranous incision (tsi in Fig. 2B). The mesal margin of the trough-shaped stipes is somewhat more strongly sclerotized and forms a short distal process (msp in Fig. 10) at 2/3 of its length. The sclerite slightly widens distally bearing two terminal appendages, the large maxillary palp (mxp in Figs. 1, 2A,B) laterally and an endite lobe which presumably represents a composite structure formed by a galea and a mainly incorporated lacinia mesally (i.e., a galeolacinia, see Discussion). Most parts of the galea (ga in Figs. 8, 9A–C) are weakly sclerotized and quite flexible. Only the lateral margin is more strongly sclerotized. The lobe-like structure is dorso-ventrally flattened and apically blunted (Fig. 8). A membranous area around the base of the galea allows for substantial movements of the appendage (Fig. 7C). A small, slightly bulged lobe is located on the lower inner wall of the galea. It is separated from the latter by a small invagination of comparatively weakly sclerotized cuticle whereas its inner wall is heavily sclerotized (Fig. 9A–C). This inner lobe of the galea may represent the remnants of a lacinia (lac in Figs. 8, 9B, see Discussion), and hence this structure should be termed as a galeolacinia. The galeolacinia is located between the base of the haustellum and the maxillary palp (Fig. 7B). Its surface is densely covered by different types of sensilla. The granulose terminal face lacks microtrichia but bears several large basiconic sensilla (bs in Fig. 7C). The mesal wall is covered by a very dense vestiture of outwards directed microtrichia.

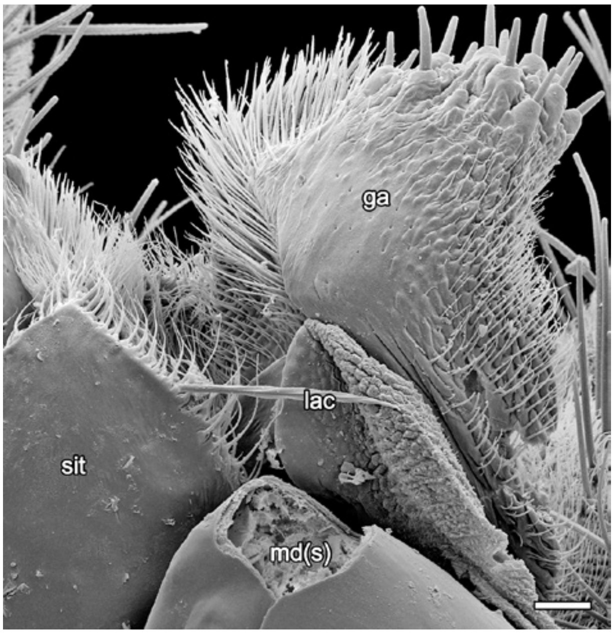

Fig. 8. *Philopotamus ludificatus* McLachlan, 1878: dorsal view on mouthparts with mandible partly removed, SEM image. — ***Abbreviations***: ga – galea, lac – lacinia, md(s) – mandibular sclerite, sit – sitophore plate. (Scale bar: 20 µm)

The large maxillary palp (mxp in Fig. 1) is 5-segmented in both sexes. It is about three times longer than the overall length of the head capsule. The 1st and 2nd palpomeres are comparatively short (together as long as the 3rd). The 3rd and the 4th palpomere are of equal length. The tapering 5th palpomere is by far the longest (almost as long as the other palpomeres together) (Fig. 1). The diameter of the palpomeres constantly decreases toward the apex. All are covered by a dense vestiture of short, dentate ribbed trichoid and fungiform pseudoplacoid sensilla (same condition as in labial palp; drts, fps in Fig. 11A,E). Additionally, the 1st and 2nd palpomeres are equipped with numerous strong, smooth ribbed trichoid sensilla (mainly on the mesal faces) (srts in Figs. 1). The 4th palpomere bears proximomesally a distinctly delimited sensory field which is composed of numerous sensilla with stout, peg-shaped trichoms (ps in Fig. 11C). The 5th palpomere is apically equipped with three basiconic sensilla. A large central sensillum basiconicum (bs) is mesally and laterally flanked by three-time shorter sensilla of this type (same ratio as in labial palp; see Fig. 11D).

Musculature (Figs. 9A,B, 10, 12A,B, 13A, 16E): **M. cranio-cardinalis** [cr-cd]: flattened, fan-shaped, O: ventrolaterally at the postgena, immediately mesally to the occipital sulcus, I: ventromesally at the proximal margin of the cardostipital sclerite (i.e., cardo + basistipes); **M. cranio-stipitalis** [cr-st]: long and slender, intersects with cr-prm(l), O: postgena, ventrally of base of the posterior tentorial arm (between cr-prm(l) and cr-prm(m)), I: distal process of mesal dististipital margin (msp) (together with te-st); **M. tentorio-cardinalis** [te-cd]: strong, slightly tapering, O: laterally at the mid part of the anterior tentorial arm, I: mesally at the distal margin of the cardostipital sclerite (i.e., cardo + basistipes); **M. tentorio-stipitalis** [te-st]: equally sized and shaped as te-cd, O: broadly at the ventral face of the laminatentorium, I: distal process of mesal dististipital margin (msp) (together with cr-st); **M. cranio-lacinialis** [cr-lc]: long and slender, O: postgena (dorsally to cr-cd), I: laterally at the small inner lobe (i.e., lacinia) of the galeolacinia; **M. stipito-lacinialis** [st-lc]: absent; **M. stipito-galealis** [st-ga]: absent; **M. cardo-palpalis dorsalis** [cd-mp(d)]: strong (app. two times stronger than st-mp(d)), O: proximomesal angle of the cardostipital sclerite, I: dorsolaterally at the base of the 1st palpomere; **M. cardo-palpalis ventralis** [cd-mp(v)]: compact, O: cardostipital sclerite, laterally of cd-mp(d), I: ventral margin of the 1st palpomere (opposite cd-mp(d)); **M. stipito-palpalis dorsalis** [st-mp(d)]: compact, O: mesally on the proximal half of the dististipes, I: mesally at the dorsal margin of the 1st palpomere (medially of cd-mp(d)); **M. palpo-palpalis maxillae primus lateralis** [mp1-mp2(l)]: two adjacent bundles, O: mesal margin of the base of palpomere 1, I: ventrolaterally at the proximal margin of palpomere 2; **M. palpo-palpalis maxillae primus medialis** [mp1-mp2(m)]: short, slightly tapering, O: mesal wall of palpomere 1 (distally of mp1-mp2(l)), I: dorsomesally at the base of palpomere 2; **M. palpo-palpalis maxillae secundus** [mp2-mp3]: compact, flattened, O: dorsal wall of palpomere 2, I: dorsolaterally at the base of palpomere 3; **M. palpo-palpalis maxillae tertius** [mp3-mp4]: slender, O: dorsally at the middle of the mesal wall of palpomere 3, I: ventromesally at the base of palpomere 4; **M. palpo-palpalis maxillae quartus** [mp4-mp5]: very thin, O: dorsomesally on the distal half of palpomere 4, I: ventromesally at the base of palpomere 5.

3.9. Labium

The main body of the labium is bulged, pillow-shaped and weakly sclerotized (Figs. 2B, 7F). Posteriorly, it is continuous with the cervical membrane (cvm in Fig. 2B). A non-pigmented central labial plate (lapl in Figs. 2B) is delimited from the cervix by a semicircular fold (laf in Fig. 2B). This fold might represent the posterior margin of the labium, but the homology of the central plate is uncertain (see Discussion). The degree of sclerotization increases from the proximal to the distal parts (Fig. 2B). There are no traces of subdivision. Laterally, it is not distinctly delimited from the surrounding membrane. The distal face of the labial plate bears a small lobe (lal in Fig. 7F) mesally to the base of the labial palp (lap in Figs. 7F, 10). This lobe is covered with several stout smooth ribbed trichoid sensilla and is not equipped with intrinsic muscles. Laterally, the prementum forms a moderately sclerotized palpiger (ppg in Fig. 7B). This sclerite surrounds the base of the labial palp forming the anterolateral edge of the labium. The surface of the palpiger is equipped with stout smooth ribbed trichoid sensilla. The labial palp is 3-segmented in both sexes and located distally on the premental palpiger. Both elements

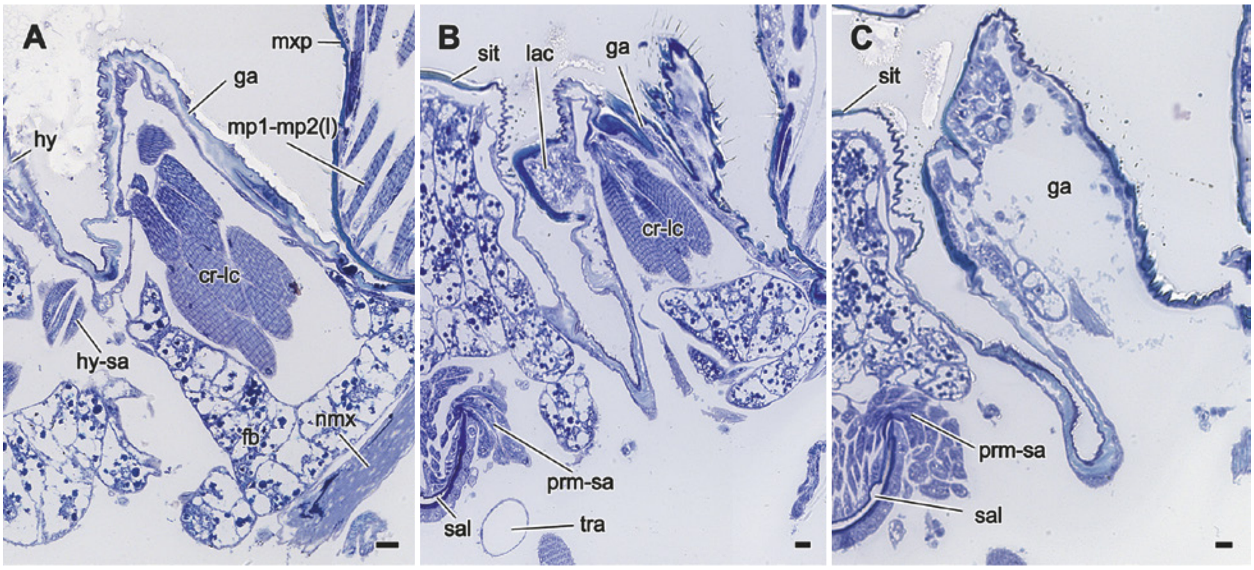

Fig. 9. *Philopotamus ludificatus* McLachlan, 1878: head, histological section of galeolacinia. **A**: proximal part of galea, **B**: galea with incorporated lacinia, **C**: distal part of galea. — ***Abbreviations***: cr-lc – M. cranio-lacinialis, fb – fat body, ga – galea, lac – lacinia, hy – hypopharynx, hy-sa – M. hypopharyngo-salivarialis, mp1-mp2(l) – M. palpo-palpalis maxillae primus lateralis, mxp – maxillary palp, nmx – maxillary nerve, prm-sa – M. praemento-salivarialis, sal – salivarium, sit – sitophore plate, tra – trachea. (Scale bars: 10 µm)

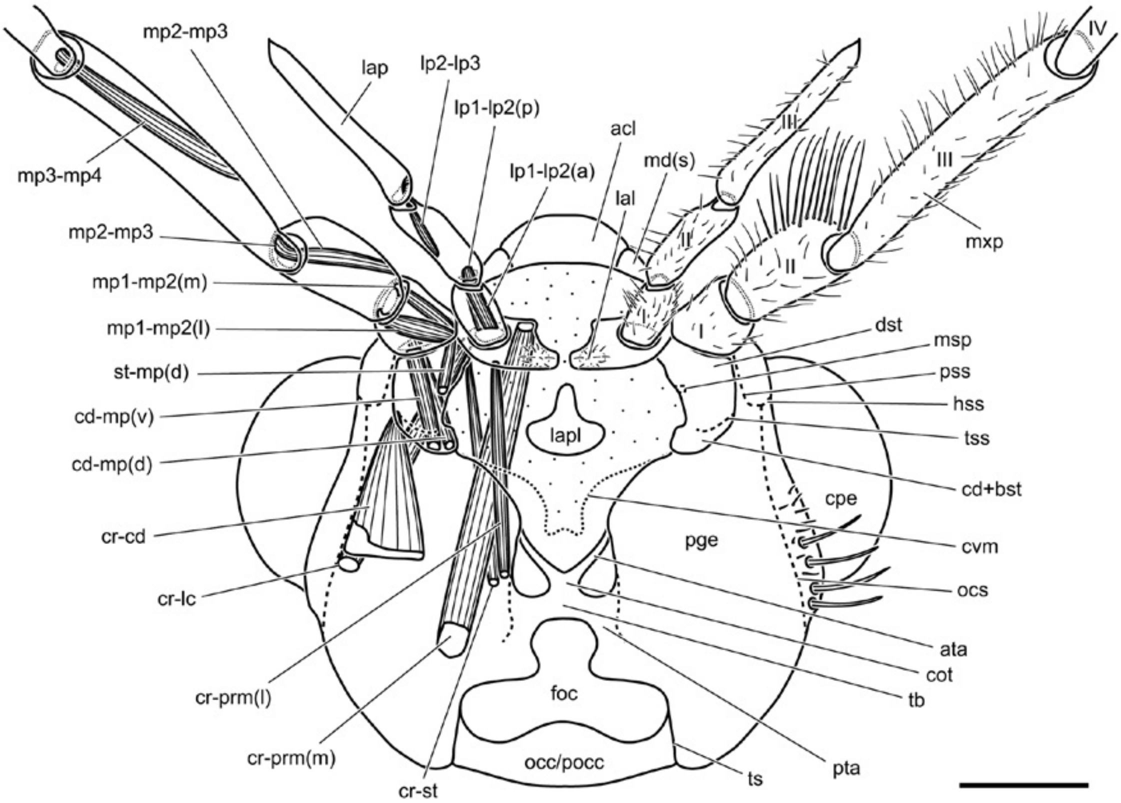

Fig. 10. *Philopotamus ludificatus* McLachlan, 1878: head, posterior view. — ***Abbreviations***: acl – anteclypeolabrum, ata – anterior tentorial arm, bst – basistipes, cd – cardo, cd-mp(d) – M. cardo-palpalis dorsalis, cd-mp(v) – M. cardo-palpalis ventralis, cot – corpotentorium, cpe – compound eye, cr-cd – M. cranio-cardinalis, cr-lc – M. cranio-lacinialis, cr-prm(l) – M. cranio-praementalis lateralis, cr-prm(m) – M. cranio-praementalis medialis, cr-st – M. cranio-stipitalis, cvm – cervical membrane, dst – dististipes, foc – foramen occipitale, hss – hypostomal sulcus, lal – labial lobe, lap – labial palp, lapl – labial plate, lp1-lp2(a) – M. palpo-palpalis labii primus anterior, lp1-lp2(p) – M. palpo-palpalis labii primus posterior, lp2-lp3 – M. palpo-palpalis labii secundus, md(s) – mandibular sclerite, mp1-mp2(l) – M. palpo-palpalis maxillae primus lateralis, mp1-mp2(m) – M. palpo-palpalis maxillae primus medialis, mp2-mp3 – M. palpo-palpalis maxillae secundus, mp3-mp4 – M. palpo-palpalis maxillae tertius, mxp – maxillary palp, msp – mesal process of dististipes, occ – occiput, ocs – occipital sulcus, pge – postgena, pocc – postocciput, pss – pleurostomal sulcus, pta – posterior tentorial arm, st-mp(d) – M. stipito-palpalis dorsalis, tb – tentorial bridge, ts – temporal sulcus, tss – transstipital sulcus, I–IV – number of palpomere. (Scale bar: 250 µm)

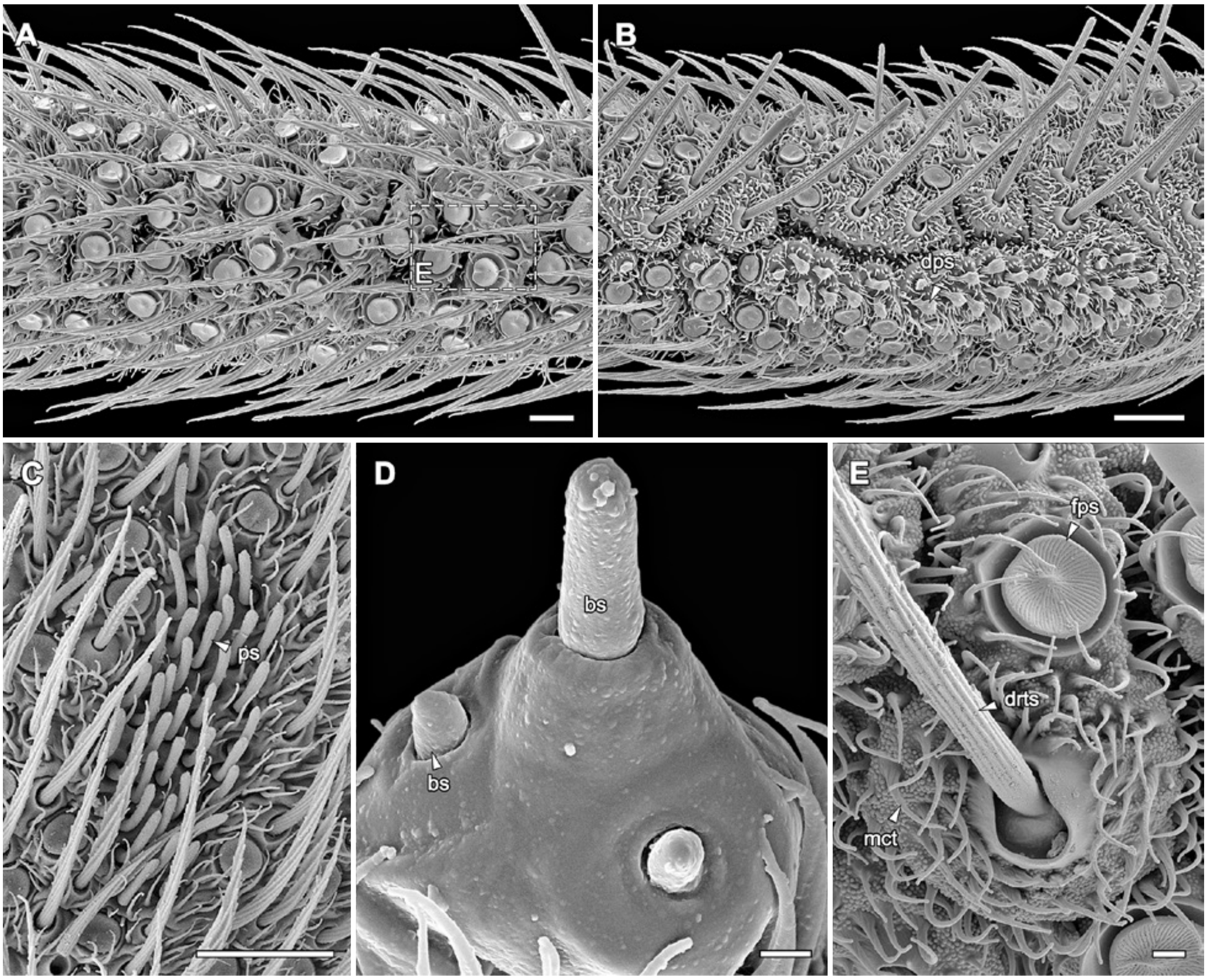

Fig. 11. *Philopotamus ludificatus* McLachlan, 1878: mouthparts, SEM images. **A**: lateral wall of third palpomere of labial palp, **B**: mesal wall of third palpomere of labial palp with sensory field of dentate pseudoplacoid sensilla, **C**: lateral wall of maxillary palp with sensory field of peg-like sensilla, **D**: tip of labial palp with basiconic sensilla, **E**: detail of sensilla and microtrichia of labial palp. — ***Abbreviations***: bs – sensillum basiconicum, dps – dentate pseudoplacoid sensillum, drts – dentate ribbed trichoid sensillum, fps – fungiform pseudoplacoid sensillum, mct – microtrichium, ps – peg-like sensillum. (Scale bars: B, C: 20 µm; A: 10 µm; E: 2 µm; D: 1 µm)

are distinctly separated by an extensive articulary membrane; no specific skeletal articulation is developed. The 2nd palpomere is almost as long as the 1st. The tapering 3rd palpomere is as long as segments 1 and 2 together (Fig. 1). All labial palpomeres are covered by a dense vestiture of short dentate ribbed trichoid and fungiform pseudoplacoid sensilla (drts, fps in Fig. 11A,E). A discrete, elongate sensory field composed of app. 30 dentate pseudoplacoid sensilla is located mesally in the proximal half of the 3rd palpomere (Fig. 11B). The tip of the 3rd palpomere bears four basiconic sensilla: a large central sensillum is surrounded by three smaller ones (Fig. 11D).

Musculature (Figs. 10, 12A,B, 13A,B, 16D–F): **M. cranio-praementalis medialis** [cr-prm(m)]: strong, composed of two more or less distinct bundles, O: both bundles closely adjacent mesally at the postgena (laterally of posterior tentorial pits, dorsolaterally of cr-st), I: broadly at the distal part of the prementum, bundles more or less distinctly separated mesally and laterally of prm-lp(m); **M. cranio-praementalis lateralis** [cr-prm(l)]: long, slender (app. ⅔ thinner as cr-prm(m)), O: postgena, ventrally of posterior tentorial pit and directly mesally of cr-st, I: lateral rim of palpiger; **M. submento-praementalis** [smt-prm]: absent; **M. praemento-paraglossalis** [prm-pgl]: absent; **M. praemento-glossalis** [prm-gl]: absent; **M. praemento-palpalis medialis** [prm-lp(m)]: slender, comparatively long, O: mesally at the dorsal face of the prementum (close to the base of haustellum, between bundles of cr-prm(m)), I: laterally at the proximal margin of palpomere 1; **M. praemento-palpalis lateralis** [prm-lp(l)]: compact, O: proximolaterally on palpiger, I: laterally at the proximal margin of palpomere 1 (close to prm-lp(m)); **M. palpo-palpalis labii primus anterior** [lp1-lp2(a)]: O: anterolaterally at the base of palpomere 1, I: anteriorly at the base of palpomere 2; **M. palpo-palpalis labii primus posterior** [lp1-lp2(p)]: O: posteriorly at the base of palpomere 1, I: posteriorly at the base of palpomere 2; **M. palpo-palpalis labii secundus** [lp2-lp3]: thin, O: anterolaterally at the distal half of palpomere 2, I: laterally at the proximal margin of palpomere 3.

3.10. Epipharynx and hypopharynx

The epipharynx (eph in Figs. 7C, 16D), that is, the inner wall of the anteclypeolabrum, is strongly sclerotized and positioned between the mandibles in its ventral half, forming the roof of the preoral cavity (= cibarium) (poc in Fig. 13B). The narrow, somewhat bulged epipharynx is only continuous with the sclerotized lateral margin of the anteclypeolabrum at its distal end. It is laterally surrounded by membranous regions in the other parts. The epipharyngeal sclerite terminates dorsally at the beginning of the closed prepharyngeal tube (see below).

The hypopharynx is composed of a mainly membranous, ventral section (i.e., anterior surface of the haustellum between the functional mouth opening and the salivary orifice) and the dorsal sitophore plate (sensu Chaudonneret 1990). The ventral part of the sitophore (sit in Figs. 8, 16C) is broadly underlying the distal half of the mandibles (Fig. 16D). It narrows dorsally and bulges between the mandibular bases. Before the beginning of the prepharyngeal tube (i.e., the lateral union of hypo- and epipharynx) (ppt in Figs. 13B, 16C) the sitophore plate is deeply transversely folded and continues toward the anatomical mouth opening (below the frontal ganglion) (Fig. 17F). This part of the sitophore plate forms the sclerotized floor of the prepharynx terminating in a spoon-shaped median process (sps in Fig. 13B), which projects into the prepharyngeal lumen (Figs. 13B, 17F). The sitophore lacks any sensilla (i.e., chemoreceptors) along its entire surface. The membranous roof of the prepharyngeal tube is formed by the epipharynx. The prepharynx is encircled by a thick layer of ring muscle fibers (Fig. 16C).

Musculature (Figs. 12A,B, 13A,B, 16A–C, 17C,D, F,G): **M. clypeo-epipharyngalis medialis** [cl-eph(m)]: compact, fan-shaped, O: central at the beginning of the sclerotized part of the anteclypeolabrum, I: median at the distal end of the epipharynx; **M. clypeo-epipharyngalis lateralis** [cl-eph(l)]: strong, compact, O: laterally at proximal half of the anteclypeolabrum (between cl-eph(m) and horizontal furrow), I: mesally at the epipharynx dorsad cl-eph(m); **M. clypeo-cibarialis ventralis** [cl-ci(v)]: slender, O: dorsolaterally at the anteclypeolabrum (dorsally of cl-eph(l)), I: preoral cavity at the ventralmost part of the prepharyngeal tube (dorsally of epipharyngeal sclerite), between prepharyngeal ring muscle fibers; **M. clypeo-cibarialis dorsalis** [cl-ci(d)]: two distinct bundles, compact median bundle app. two times larger than the slender lateral bundle, O: mesally (median bundle) and laterally (lateral bundle) at the frontopostclypeus, dorsally to the horizontal furrow, I: lateral bundle: proximal edge of the membranous (epipharyngeal) part of the prepharyngeal tube, directly below the ganglion frontale, median bundle: ventromesally of lateral bundle; **M. tentorio-sitophorialis** [te-si]: slender, O: paramedian on the ventral side of the tentorial bridge (between the anterior tentorial arms), I: dorsal end of the sitophore plate (below the spoon-shaped process), opposite to cl-ci(v); **M. anularis cibarialis** [an-ci]: series of ring muscle fibers covering the prepharynx, dorsally not delimited from the pharyngeal ring musculature (an-ph).

3.11. Haustellum

The distal region of the hypopharynx is fused with the labium, forming an extensive, largely membranous and eversible lobe, the haustellum (hst in Figs. 1, 7B,C). The haustellum is located between the galeolaciniae (dorsolateral), the bases of the maxillary and labial palps (ventrolateral) and the labial lobes (posterior) (Figs. 7B, 16F). It is dorsally continuous with the sitophore (see above) and below it forms a keel between the galeolaciniae (Fig. 7C). Behind the galeolaciniae the haustellum extends

→ **Fig. 12.** *Philopotamus ludificatus* McLachlan, 1878: head, 3D-reconstruction based on µCT data. **A**: anterior view, **B**: posterior view. — ***Colors***: blue – skeleton (sclerotized), light blue – eyes, green – gut, orange – musculature, rose – glands, yellow – nervous system. — ***Abbreviations***: acl(d) – distal part of anteclypeolabrum, acl(p) – proximal part of anteclypeolabrum, ata – anterior tentorial arm, atf – antennifer, atp – anterior tentorial pit, br – brain, cco – cervical connective, cd-mp(d) – M. cardo-palpalis dorsalis, cd-mp(v) – M. cardo-palpalis ventralis, cl-ci(d) – M. clypeo-cibarialis dorsalis, cl-ci(v) – M. clypeo-cibarialis ventralis, cl-eph(l) – M. clypeo-epipharyngalis lateralis, cl-eph(m) – M. clypeo-epipharyngalis medialis, cocc – condyli occipitales, cpe – compound eye, cr-cd – M. cranio-cardinalis, cr-lc – M. cranio-lacinialis, cr-md(l) – M. cranio-mandibularis lateralis, cr-md(m) – M. cranio-mandibularis medialis, cr-ph(a) – M. cranio-pharyngalis anterior, cr-prm(l) – M. cranio-praementalis lateralis, cr-prm(m) – M. cranio-praementalis medialis, cr-st – M. cranio-stipitalis, cvm – cervical membrane, foc – foramen occipitale, fg – ganglion frontale, fr-ph(a) – M. fronto-pharyngalis anterior, fr-ph(p) – M. fronto-pharyngalis posterior, ga – galea, gp – subgenal process, hf – horizontal furrow between frontopostclypeus and anteclypeolabrum, hst – haustellum, lap – labial palp, loc – lateral ocellus, lp1-lp2 – M. palpo-palpalis labii primus [lp1-lp2(a) and lp1-lp2(p) together], md(s) – mandibular sclerite, moc – median ocellus, mp1-mp2(l) – M. palpo-palpalis maxillae primus lateralis, mp1-mp2(m) – M. palpo-palpalis maxillae primus medialis, mp2-mp3 – M. palpo-palpalis maxillae secundus, occ – occiput, oes – oesophagus, ped – pedicellus, pocc – postocciput, prm-lp(l) – M. praemento-palpalis lateralis, prm-lp(m) – M. praemento-palpalis medialis, prm-sa – M. praemento-salivarialis, pta – posterior tentorial arm, ptp – posterior tentorial pit, sc-pe(l) – M. scapo-pedicellaris lateralis, sc-pe(m) – M. scapo-pedicellaris medialis, sca – scapus, sd – salivary duct, soeg – suboesophageal ganglion, st-mp(d) – M. stipito-palpalis dorsalis, tb – tentorial bridge, te-cd – M. tentorio-cardinalis, te-md – M. tentorio-mandibularis, te-ph(a) – M. tentorio-pharyngalis anterior, te-ph(l) – M. tentorio-pharyngalis lateralis, te-ph(p) – M. tentorio-pharyngalis posterior, te-sc(a) – M. tentorio-scapalis anterior, te-sc(l) – M. tentorio-scapalis lateralis, te-sc(m) – M. tentorio-scapalis medialis, te-sc(p) – M. tentorio-scapalis posterior, te-si – M. tentorio-sitophorialis, te-st – M. tentorio-stipitalis, tra – trachea, vsw(p) – posterior setal wart of vertex. (Scale bars: 250 µm) (General features of nervous system shown, for details see Fig. 18)

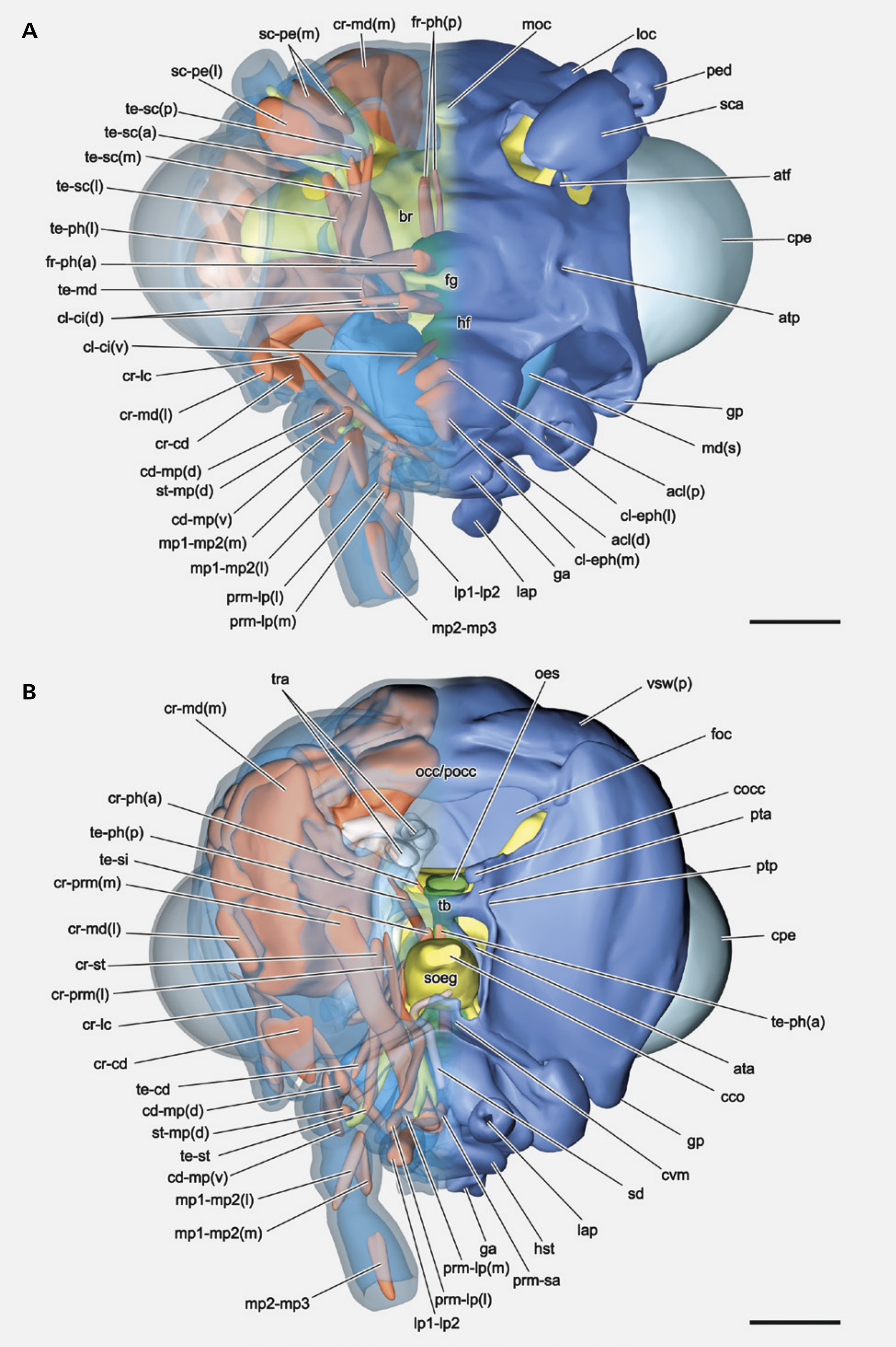
A
sc-pe(m)
cr-md(m)
fr-ph(p)
moc
loc
ped
sca
sc-pe(l)
te-sc(p)
te-sc(a)
te-sc(m)
te-sc(l)
atf
br
cpe
te-ph(l)
fr-ph(a)
fg
te-md
cl-ci(d)
hf
atp
cl-ci(v)
cr-lc
cr-md(l)
gp
cr-cd
md(s)
cd-mp(d)
st-mp(d)
acl(p)
cd-mp(v)
cl-eph(l)
mp1-mp2(m)
acl(d)
mp1-mp2(l)
cl-eph(m)
ga
prm-lp(l)
lp1-lp2
lap
prm-lp(m)
mp2-mp3
B
tra
oes
vsw(p)
cr-md(m)
foc
occ/pocc
cocc
cr-ph(a)
pta
te-ph(p)
te-si
ptp
cr-prm(m)
tb
cr-md(l)
cpe
cr-st
soeg
cr-prm(l)
te-ph(a)
cr-lc
cr-cd
ata
cco
te-cd
cd-mp(d)
gp
st-mp(d)
te-st
cvm
cd-mp(v)
sd
mp1-mp2(l)
mp1-mp2(m)
lap
ga
hst
prm-lp(m)
prm-sa
mp2-mp3
prm-lp(l)
lp1-lp2

laterally till the bases of the maxillary and labial palps. This anterior, upper area is densely covered by multibranched, irregularly distributed microtrichia (mct in Fig. 7E) more or less directed toward the preoral cavity. A regular system of channels on the surface of the haustellum is not present (Fig. 7B–E). The posterior part of the haustellum converges toward the labial lobes (Fig. 7F). Its lower surface is glabrous and tubercular (Fig. 7D). Centrally, on this anterior area terminates the salivarium (see below). A median crest with a moderately dense set of microtrichia connects the salivary orifice and the preoral cavity (Fig. 7C). Basiconic sensilla (bs in Fig. 7E) of different sizes are randomly distributed on the whole face of the haustellum.

3.12. Salivarium

The long, tubular salivary glands (sg in Fig. 17H) extend into the cervical and prothoracic regions. Anteriorly two thin salivary ducts (sd in Fig. 17H) enter the head capsule through the lower section of the occipital foramen (below the suboesophageal ganglion) and unite at the beginning of the unpaired salivarium (sal in Figs. 13B, 17I). The sclerotized salivarium is U-shaped in cross section and rapidly increases its caliber in the proximal half (Fig. 16E,F). The distal part (after the muscle insertion areas) is tapering toward the orifice. Its strongly concave floor (fsal in Fig. 16E,F) is heavily sclerotized. The less sclerotized pestle-like roof (rsal in Fig. 16E,F) sinks into the concavity of the floor. The salivary orifice is located on the lower, anterior edge of the haustellum (saor in Fig. 7B). The opening is surrounded by numerous small, two- to three-branched microtrichia.

Musculature (Figs. 13B, 16E,F, 17I): **M. hypopharyngo-salivarialis** [hy-sa]: compact, slender, O: laterally at the ventral half of the sitophore, close to the base of the galeolacinia, I: proximally on the roof of the salivarium; **M. praemento-salivarialis** [prm-sa]: ventral part of the prementum (close to prm-lp(m) and the mesal bundle of cr-prm(m)), I: proximal half of the roof of the salivarium (immediately laterally and before hy-sa); **M. intra-salivarialis** [i-sa]: absent.

3.13. Cephalic food tract

The cephalic food tract comprises a distinctly widened precerebral pumping chamber (pch in Fig. 18A) (= buccal cavity, i.e. a composite formation of the prepharyngeal tube [ppt] and the precerebral pharynx [pph in Fig. 13B]). The border between both elements, i.e. the anatomical mouth opening, is marked by the position of the ganglion frontale (fg in Figs. 13B, 18A). The precerebral pumping chamber is moved by strong cibarial and pharyngeal dilator muscles. Posteriorly, the pharynx (ph in Fig. 13B) tapers distinctly before passing the tritocerebral commissures (trc in Fig. 18B). The straight intra-/postcerebral pharyngeal regions have a constant, comparatively small width (⅓ of diameter of the precerebral pharynx) (Fig. 13B).

Musculature of the precerebral pharynx (Figs. 12A, 13A,B, 16A–C, 17B,C, 18A): **M. fronto-pharyngalis anterior** [fr-ph(a)]: compact, O: central region of frontopostclypeus, between the anterior tentorial pits, I: mesally at the anterolateral corner of the precerebral pumping chamber, directly behind the ganglion frontale; **M. fronto-pharyngalis posterior** [fr-ph(p)]: two distinct bundles, ventral bundle app. two times larger than dorsal bundle, both bundles are closely associated with the precerebral part of the cephalic aorta, O: frons, mesally of interantennal sulcus, I: dorsally at the posterodorsal face of the pharyngeal pumping chamber, just in front of the brain; **M. tentorio-pharyngalis lateralis** [te-ph(l)]: strong, O: broad area of the distal half of the anterior tentorial arm, I: dorsolaterally at the pharyngeal pumping chamber; **M. tentorio-pharyngalis anterior** [te-ph(a)]: two long and slender bundles, O: mesally on the base of the anterior tentorial arm, I: ventrally at the posterior end of the pharyngeal pumping chamber (opposite to fr-ph(p)).

Musculature of the postcerebral pharynx (Figs. 13B, 16A–C, 18A): **M. tentorio-pharyngalis posterior** [te-ph(p)]: slender, O: posterior tentorial arm, I: ventrally at the postcerebral pharynx, slightly behind the brain, opposite to cr-ph(a); **M. cranio-pharyngalis anterior** [cr-ph(a)]: very thin, composed of very few fibers, O: vertex, mesally of postgenal sulcus (posteriorly of lateral ocellus), I: dorsally on postcerebral pharynx, directly behind the brain; **M. cranio-pharyngalis posterior** [cr-ph(p)]: absent.

Musculature of the entire pharynx (pre- and postcerebral regions) (Figs. 16B,C, 17C,F): **M. anularis pharyngalis** [an-ph]: series of ring muscles covering the surface of the entire pharynx, most heavily developed around the precerebral pharyngeal pumping chamber; forming a distinctly thinner layer along the postcerebral pharynx. **M. longitudinalis pharyngalis** [lo-ph]: series of longitudinal muscle fibers stretching between the surface of the pharynx and an-ph, the layer is of constant thickness in the pre- and postcerebral regions.

3.14. Central nervous system (CNS)

The brain is located in the dorsal half of the head capsule between the large compound eyes. The large protocerebrum forms laterally the optical lobes (ol in Fig. 16A), which are of similar diameter as the rest of the brain (Fig. 18A,B). One compact anteromedian nerve and two posterolateral nerves arising from the dorsal protocerebral surface supply the median ocellus and the lateral ocelli, respectively (Fig. 18A).

The deutocerebral olfactory lobe (dol in Fig. 16A) is located paramedially on the anterodorsal edge of the brain. It is not externally delimited from the deutocerebrum (Figs. 17B, 18A). The strong antennal nerve (nan in Fig. 18A,B) proximally innervates the tentorio-scapal

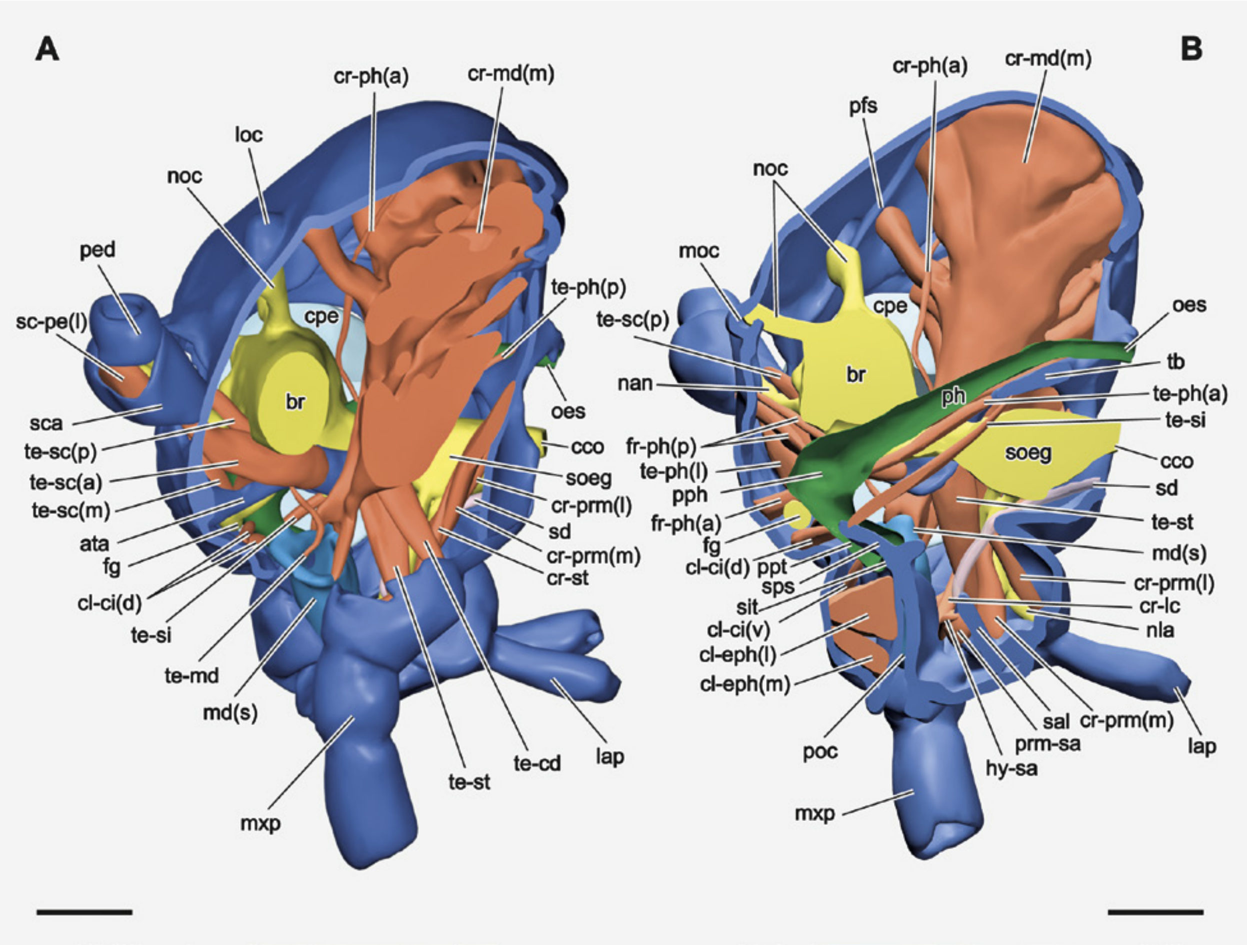

Fig. 13. *Philopotamus ludificatus* McLachlan, 1878: head, 3D-reconstruction based on µCT data. **A**: parasagittal section (level of anterior tentorial pit), **B**: sagittal section. — ***Colors***: blue – skeleton (sclerotized), light blue – eyes, green – gut, orange – musculature, rose – glands, yellow – nervous system. — ***Abbreviations***: ata – anterior tentorial arm, br – brain, cco – cervical connective, cl-ci(d) – M. clypeo-cibarialis dorsalis, cl-ci(v) – M. clypeo-cibarialis ventralis, cl-eph(l) – M. clypeo-epipharyngalis lateralis, cl-eph(m) – M. clypeo-epipharyngalis medialis, cpe – compound eye, cr-lc – M. cranio-lacinialis, cr-md(m) – M. cranio-mandibularis medialis, cr-ph(a) – M. cranio-pharyngalis anterior, cr-prm(l) – M. cranio-praementalis lateralis, cr-prm(m) – M. cranio-praementalis medialis, cr-st – M. cranio-stipitalis, fg – ganglion frontale, fr-ph(a) – M. fronto-pharyngalis anterior, fr-ph(p) – M. fronto-pharyngalis posterior, hy-sa – M. hypopharyngo-salivarialis, lap – labial palp, loc – lateral ocellus, md(s) – mandibular sclerite, moc – median ocellus, mxp – maxillary palp, nan – nervus antennalis, nla – labial nerve, noc – ocellar nerve, oes – oesophagus, ped – pedicellus, pfs – postfrontal sulcus, ph – pharynx, poc – preoral cavity, pph – precerebral pharynx, ppt – prepharyngeal tube, prm-sa – M. praemento-salivarialis, sal – salivarium, sca – scapus, sc-pe(l) – M. scapo-pedicellaris lateralis, sd – salivary duct, sit – sitophore plate, soeg – suboesophageal ganglion, sps – spoon-shaped process of sitophore plate, tb – tentorial bridge, te-cd – M. tentorio-cardinalis, te-md – M. tentorio-mandibularis, te-ph(a) – M. tentorio-pharyngalis anterior, te-ph(l) – M. tentorio-pharyngalis lateralis, te-ph(p) – M. tentorio-pharyngalis posterior, te-sc(a) – M. tentorio-scapalis anterior, te-sc(m) – M. tentorio-scapalis medialis, te-sc(p) – M. tentorio-scapalis posterior, te-si – M. tentorio-sitophorialis, te-st – M. tentorio-stipitalis. (Scale bars: 250 µm) (General features of nervous system shown, for details see Fig. 18)

muscles with thin nerve fibers before entering the scapus. It splits into two equally strong branches at the base of the antenna.

The ventral portion of the brain is formed by the tritocerebrum, which is also not externally delimited from the other parts. The tritocerebrum forms anterior lobes and the circumoesophageal connectives (coc in Fig. 18B) of the CNS. They are interconnected by a short free tritocerebral commissure (trc in Fig. 18B) below the pharynx, extending between the tentorial muscles of the sitophore plate and the ventral pharynx (te-si, te-ph(a)) (Figs. 17F, 18B). A thin nervus tegumentalis emerges from the posterolateral face of the dorsal part of the tritocerebrum. It runs dorsolaterad into the large posterolateral setal wart of the vertex.

The somewhat egg-shaped suboesophageal ganglion (soeg in Figs. 13B, 18B) is located below the postpharynx, between the posterior margin of the brain and the neuroforamen. Its posterior end is continuous with the paired cervical connectives (cco in Fig. 18B). The comparatively thin mandibular nerve arises at its anterior edge. The mandibular nerve (nmd in Fig. 18A,B) passes the mesal side of the anterior tentorial arm (at level of the laminatentorium) and splits into several bundles associat-

Table 1. Terminology and homology of the trichopteran adult head musculature. Muscles are named by their areas of origin and insertion. The musculature described for *Philopotamus* (Annulipalpia) is homologized with muscles described for 'Spicipalpia' (Klemm 1966: *Rhyacophila*), Integripalpia (Crichton 1957: *Phryganea*) and basal lepidopterans (Hannemann 1956: *Micropterix*). General nomenclatures of the insect head muscles (v. Kéler 1955; Wipfler et al. 2011) are also assigned. Squared brackets indicate that the muscle description was extracted from the literature, because it is absent in *Philopotamus*. Abbreviations used: **X** = present, **−** = absent, **?** = uncertain homology, ***** = revised information taken from Kristensen 2003, **n.a.** = no information available.

Name	**Abbrev.**	**Origin**	**Insertion**	**v. Kéler 1955**	**Wipfler et al. 2011**	**Hannemann 1956**	**Klemm 1966**	**Crichton 1957**	**present study**
						Micropterix	*Rhyacophila*	*Phryganea*	*Philopotamus*
M. fronto-labralis	fr-lb	[mesally on frons]	[mesally on outer basal wall of labrum]	8	0lb1	19	–	–	–
M. fronto-epipharyngalis	fr-eph	[mesally on frons]	[basal labral wall]	9	0lb2	–	mlrp (?)	–	–
M. labro-epipharyngalis	lb-eph	[outer wall of labrum]	[epipharynx]	7	0lb5	21	–	–	–
M. clypeo-epipharyngalis medialis	cl-eph(m)	distomedian at anteclypeolabrum	distal at epipharynx	43, 7 (?)	0ci1, 0lb5 (?)	20	1cplr	1	X
M. clypeo-epipharyngalis lateralis	cl-eph(l)	lateral at anteclypeolabrum	epipharynx	43	0ci1	45	2cplr	2	X
M. clypeo-cibarialis ventralis	cl-ci(v)	proximal at anteclypeolabrum	anteroventral at cibarium	44 (?)	0bu1 (?)	–	2dlcb, 1dlcb (?)	21, 22 (?)	X
M. clypeo-cibarialis dorsalis	cl-ci(d)	frontoclypeus, directly below frontal ganglion	anteroventral at cibarium	44	0bu1	49 (?)	1dlphy, 1dlcb (?)	21, 22	X (2 bundles)
M. tentorio-sitophorialis	te-si	tentorial bridge	dorsal margin of sitophore	48	0bu5	46	pdlcb	23	X
M. fronto-pharyngalis anterior	fr-ph(a)	frontoclypeus, directly behind frontal ganglion	dorsal at precerebral pharynx (anterior)	45	0bu2	48 (?)	4dlphy	24	X
M. fronto-pharyngalis posterior	fr-ph(p)	frontoclypeus	dorsal at precerbral pharynx (posterior), in front of supra-oesophageal ganglion	46	0bu3	50	2dlphy	25	X (2 bundles)
M. tentorio-pharyngalis lateralis	te-ph(l)	distal at anterior tentorial arm	lateral at precerbral pharynx	47 (?)	0hy2 (?)	48 (?)	3dlphy	26 (?)	X
M. tentorio-pharyngalis anterior	te-ph(a)	tentorial bridge	ventral at precerbral pharynx	50	0bu6	54	pdlphy1, 2 (?)	23, 28 (?)	X
M. tentorio-pharyngalis posterior	te-ph(p)	tentorial bridge or posterior tentorial arm	ventral / ventrolateral at precerebral pharynx	52, 54 (?)	0ph2 (?)	55	pdlphy 3, 4, 2dlpphy (?)	28 (?)	X
M. cranio-pharyngalis anterior	cr-ph(a)	vertex	dorsal at postcerbral pharynx, behind supraoesophageal ganglion	51	0ph1	51	1dlpphy	27	X
M. cranio-pharyngalis posterior	cr-ph(p)	[posterolateral at cranium]	[dorsolateral at postcerebral pharynx]	51, 53 (?)	0ph1, 0ph3 (?)	52, 53	2dlpphy (?)	28 (?)	–
M. anularis cibarialis	an-ci	ring muscle fibers covering the prepharynx	–	67	0hy9	X (*)	rm	29	X
M. anularis pharyngalis	an-ph	ring muscle fibers covering the entire pharynx	–	68	0st1	X (*)	rm	29	X
M. longitudinalis pharyngalis	lo-ph	longitudinal muscle fibers stretching between the surface of the pharynx and an-ph	–	69	0st2	47	lm	n.a.	X
M. tentorio-scapalis anterior	te-sc(a)	anterior tentorial arm	anterior basal margin of scapus	1	0an1	3	abant2	5	X
M. tentorio-scapalis posterior	te-sc(p)	anterior tentorial arm	posterior basal margin of scapus	2	0an2	4	adant2	3	X
M. tentorio-scapalis lateralis	te-sc(l)	anterior tentorial arm	lateral basal margin of scapus	3	0an3	2	abant1	4	X (2 bundles)
M. tentorio-scapalis medialis	te-sc(m)	anterior tentorial arm	mesal basal margin of scapus	4	0an4	1	adant1	6	X
M. scapo-pedicellaris lateralis	sc-pe(l)	ventrolateral and ventromesal wall of scapus	ventral and ventrolateral basal margin of pedicellus	5	0an6	7, 8	adpde	n.a.	X (2 bundles)
M. scapo-pedicellaris medialis	sc-pe(m)	dorsal and ventromesal wall of scapus	dorsal at proximal margin of pedicellus	6	0an7	5, 6	abpde	n.a.	X (3 bundles)
M. cranio-mandibularis medialis	cr-md(m)	dorsal and lateral head capsule	adductor tendon of mandible	11	0md1	22	1admd	7	X

Table 1 continued.

Name	**Abbrev.**	**Origin**	**Insertion**	**v. Kéler 1955**	**Wipfler et al. 2011**	**Hannemann 1956**	**Klemm 1966**	**Crichton 1957**	**present study**
						Micropterix	*Rhyacophila*	*Phryganea*	*Philopotamus*
M. cranio-mandibularis lateralis	cr-md(l)	lateral at head capsule	abductor tendon of mandible	12	0md3	23	abmd	7	X
M. tentorio-mandibularis	te-md	anterior tentorial arm	mesally at inner wall of mandible	14	0md6	– (*)	2admd	–	X
M. hypopharyngo-mandibularis	hy-md	[hypopharyngeal sclerite]	[inner wall of mandible]	13	0md4	–	–	–	–
M. tentorio-cardinalis	te-cd	anterior tentorial arm	mesal process of ‚cardo‘ (cardo + basistipes)	17	0mx3	26	adcd	9	X
M. tentorio-stipitalis	te-st	anterior tentorial arm	mesal margin of ‚stipes‘ (dististipes)	18	0mx4	27	adst	–	X
M. cranio-cardinalis	cr-cd	postgena	proximolateral process of ‚cardo‘ (cardo + basistipes)	15	0mx1	24	J	8	X
M. cranio-stipitalis	cr-st	postgena	distal process of mesal stipital margin (dististipes)	16	0mx1	25	–	–	X
M. cranio-lacinialis	cr-lc	postgena	laterally at composite endite lobe of maxilla	19	0mx2	29	flcc	10	X
M. stipito-lacinialis	st-lc	[mesal at stipes]	[basal edge of lacinia]	20	0mx6	28	flcs	11	–
M. stipito-galealis	st-ga	[stipes]	[basal edge of galea]	21	0mx7	30	–	–	–
M. cardo-palpalis dorsalis	cd-mp(d)	proximomesal angle of ‚cardo‘ (cardo + basistipes)	dorsolateral at palpomere 1	–	–	–	lplp b	12, 13 (?)	X
M. stipito-palpalis dorsalis	st-mp(d)	mesally at proximal half of ‚stipes‘ (dististipes)	mesal at dorsal margin of palpomere 1	23	0mx10	31	lplp a	12, 13 (?)	X
M. stipito-palpalis ventralis / M. cardo-palpalis ventralis	st-mp(v) / cd-mp(v)	lateral at ‚cardo‘ (cardo + basistipes)	ventral basal margin of palpomere 1	22	0mx8	32	dplp	12, 13 (?)	X
M. palpo-palpalis maxillae primus medialis	mp1-mp2(m)	mesal wall of palpomere 1	dorsomesal at basal margin of palpomere 2	24 (?)	0mx12	33	X	X	X
M. palpo-palpalis maxillae primus lateralis	mp1-mp2(l)	mesal basal margin of palpomere 1	ventrolateral at basal margin of palpomere 2	24	0mx12	33	X	X	X
M. palpo-palpalis maxillae secundus	mp2-mp3	dorsal wall of palpomere 2	dorsolaterally at basal margin of palpomere 3	25	0mx13	34	X	X	X
M. palpo-palpalis maxillae tertius	mp3-mp4	dorsomesally at palpomere 3	ventromesally at basal margin of palpomere 4	26	0mx14	35	X	X	X
M. palpo-palpalis maxillae quartus	mp4-mp5	dorsomesal on distal half of palpomere 4	ventromesally at basal margin of palpomere 5	27	0mx15	36	X	X	X
M. hypopharyngo-salivarialis	hy-sa	lateral at ventral half of hypopharynx	proximally on the roof of the salivarium	37	0hy12	56, 57	–	–	X
M. intra-salivarialis	i-sa	[roof of salivarium]	[roof of salivarium]	37 (?)	–	–	1 (unpaired)	18	–
M. praemento-salivarialis	prm-sa	prementum	proximal half of the roof of the salivarium	38/39	0hy7, 0hy8 (?)	– (*)	2s	17	X
M. cranio-praementalis medialis	cr-prm(m)	postgena (together with cr-st)	mesally at distal part of prementum	30	0la6	39	1ablb, 2adlb	16	X (2 bundles)
M. cranio-praementalis lateralis	cr-prm(l)	mesal at postgena	lateral rim of palpiger	29	0la5	40	rst	16	X
M. submento-praementalis	smt-pmt	[submentum or gula]	[prementum]	28	0la8	41(*)	–	–	–
M. praemento-paraglossalis	prm-pgl	[basal edge of prementum]	[paraglossa]	31	0la11	37	–	–	–
M. praemento-glossalis	prm-gl	[mesally on prementum]	[glossa]	32	0la12	38	–	–	–
M. praemento-palpalis medialis	prm-lp(m)	mesally at dorsal face of prementum	lateral at proximal margin of palpomere 1	33	0la13	42	lplp	19, 20 (?)	X
M. praemento-palpalis lateralis	prm-lp(l)	proximolateral on palpiger	lateral at proximal margin of palpomere 1	34	0la14	43	dplp	19, 20 (?)	X
M. palpo-palpalis labii primus anterior	lp1-lp2(a)	lateral at the base of palpomere 1	anteriorly at the base of palpomere 2	35	0la16	44a (*)	X	X	X
M. palpo-palpalis labii primus posterior	lp1-lp2(p)	posteriorly at the base of palpomere 1	posteriorly at the base of palpomere 2	35 (?)	0la16	44b (*)		X	X
M. palpo-palpalis labii secundus	lp2-lp3	anterolaterally at the distal half of palpomere 2	laterally at the proximal margin of palpomere 3	36	0la17	–	X	X	X

Table 2. Overview of the morphological terminology applied to sclerites of the adult head capsule (cranium/'face') and to selected mouthpart structures (maxilla and labium) in Amphiesmenoptera compared with the generalized insect head (after Beutel et al. 2014). Abbreviations used: + = term used by the author as in the generalized insect head, – = structure not mentioned by the respective author (this does not indicate that the respective structure is absent in the taxon!).

	Generalized insect head		***Philopotamus*** **[Philopotamidae, Annulipalpia]**	***Rhyacophila*** **[Rhyacophilidae, 'Spicipalpia']**	***Stenophylax*** **[Limnephilidae, Integripalpia]**	***Phryganea*** **[Phryganeidae, Integripalpia]**	***Micropterix*** **[Micropterigidae, Lepidoptera]**
	Beutel et al. 2014		present study	Klemm 1966	Chaudonneret 1990	Crichton 1957	Hannemann 1956
cranium	occiput		+	+	région occipitale	+	+
	vertex		+	—	—	—	+
	gena		+	+	+	+	+
	postgena		+	+	+	+	+
'face'	frons		frontopostclypeus	+	clypéofrons + aire postérieure du frons	frontoclypeus	+
	clypeus	postclypeus		clypeolabrum			+
		anteclypeus	anteclypeolabrum		clypéo-labre		
	labrum					+	+
maxilla	cardo		cardo + basistipes	+	+	+	+
	stipes	basistipes		+	+	+	+
		dististipes	+				
	lacinia		+	+	—	+	+
	galea		+	—	+	—	+
	postlabium		—	—	+	—	—
	postmentum		—	+		—	—
labium	submentum		—	—	—	—	+
	mentum		—	—	—	—	+
	prementum		+	+	+	+	+
	palpiger		+	—	+	distal labial sclerite	—
	paraglossa		endite lobes of labium	—	—	—	+
	glossa			—	—	—	+
	haustellar sclerites		—	+	+ (1, 2)	+ (1–3)	—

ed with the mandibular muscles. The thickest branch runs into the mandible closely accompanied by the extremely thin tentorio-mandibular muscle (te-md, see above) (Fig. 17E). The strong maxillary nerve (nmx in Fig. 18A,B) originates from the ventral side of the suboesophageal ganglion, distinctly behind the mandibular nerve. It runs into the maxilla innervating its muscles with very thin branches. The major part of the maxillary nerve forms the sensory branch, which enters the sensilla-rich palps. Shortly behind the maxillary nerve originates its almost equal thick labial counterpart (nla in Fig. 18A,B). It innervates the labial and salivary muscles. Analogous to the conditions of the maxilla, the main part of the labial nerve continue into the labial palp to receive information of the large array of different sensory setae (see above). A smaller branch (nh in Fig. 18A,B) is send to the sensilla of the haustellum.

3.15. Stomatogastric nervous system

The stomatogastric nervous system innervates the preoral and pharyngeal musculature. The moderately sized frontal ganglion is connected with anterior tritocerebral lobes by strong frontal connectives (fco in Figs. 17C, 18A). At the base of each connective originate the labrofrontal nerve, rapidly splitting up into two discrete fine branches. The very thin frontal nerves run downwards, merge each other after a short distance and proceed as an unpaired nervus frontalis (nfr in Fig. 18A) in front of the ganglion frontale downwards. The labral nerve (nlbr in Fig. 18A) runs more laterally, posterior to the ganglion frontale downwards sending branches to the clypeolabral dilator muscles. An unpaired nervus connectivus linking the frontal ganglion with the protocerebrum is absent. The nervus recurrens (nrec in Fig. 18A) originates from the hind face of the frontal ganglion and runs, between the pharyngeal ring musculature and the aorta, backwards below the brain and proceeds into the hypocerebral ganglion which forms together with the corpora cardiaca a somewhat diffuse structure. A thin occipital nerve (nocc in Fig. 18B) supplying the posterior part of the vertex, the occipital/postoccipital region, and the cervix originates from the posterior end of the suboesophageal ganglion, immediately above the cervical connectives.

3.16. Hypocerebral complex

Paired, diffuse neural glands (corpora cardiaca and corpora allata; together ccc in Fig. 16B,D) are situated adjacent to the dorsal face of the postcerebral pharynx and the cephalic aorta with the comparatively small, rounded corpora cardiaca located directly behind the brain. They receive a thin and short nerve tract (nervus corpus cardiacus) from the brain. The considerably voluminous, elongated corpora allata are continuous with the corpora cardiaca and proceed into the neck region after receiving the nervus corpus allatum from the latter. A thin nerve originating laterally from the corpora allata connects it with the strong maxillary nerve.

3.17. Circulatory system

The cephalic aorta (ao in Figs. 16A, 17B) enters the head capsule through the alaforamen, directly dorsal to the pharynx. Its postcerebral part is voluminous but constricts rapidly before the passage through the circumoesophageal connectives. In front of the brain the aorta bents upwards and runs toward the area between the antennal sockets. It adheres to the posterior frontopharyngeal muscle (fr-ph(p)) (Fig. 17B) whose contractions may enhance the haemolymph flow. Between the antennae the aorta widens into a flat unpaired haemolymph sinus, reaching the median ocellus dorsally. Laterally, the sinus extends toward the antennal base, where it is continued as a thin vessel extending into the antenna (av in Fig. 17A). This antennal vessel runs, accompanied by a trachea, into the distal part of the flagellum. Specific dilator muscles of the aorta or the antennal sinus are absent. However, the thickened wall of the sinus lateral to the interantennal sulcus may contain muscle fibers and be contractile (muscle fibers could not be identified with certainty in histological sections at hand).

3.18. Tracheal system

Two pairs of main head tracheae (tra in Fig. 12B) pass through the alaforamen into the head capsule and flank the postcerebral pharynx dorsolaterally. The dorsal pair of stems split into two branches. One runs dorsolaterad and supplies the mandibular muscles whereas the second is almost exclusively associated with the brain and the antenna. The ventral stems proceed anterolaterad and split into numerous thin branches which supply the musculature of the ventral parts of the head capsule (mouthparts, cibarium, precerebral pharynx etc.).

3.19. Fat body

Fat body aggregations take approximately two thirds of the free lumen of the head (space not filled with musculature or the nervous system) (fb in Fig. 16A–D). They are only absent directly around the digestive, circulatory, nervous and tracheal systems. The entire antenna and the distal segments of the maxillary (3rd and following palpomeres) and labial palp (2nd and 3rd palpomere) are also free of fat body.

4. Discussion

4.1. Morphology & terminology

Morphological features of the skeleton and soft tissues of the adult head of *Philopotamus* are compared with conditions found in other trichopteran lineages (e.g., Rhyacophilidae, Phryganeidae), Lepidoptera and Mecoptera. The homology of trichopteran head sclerites and consequences for the terminology applied to head structures in caddisflies are discussed in detail (see also Table 2).

4.1.1. Frontopostclypeus

In *Philopotamus* externally visible demarcations between frons, clypeus and labrum are absent. In the generalized insect condition frons and clypeus are separated by a frontoclypeal strengthening sulcus (= epistomal sulcus of Snodgrass 1935), laterally demarcated by the anterior tentorial pits. Usually, the frontal region serves as attachment area of dilator muscles of the precerebral pharynx whereas the cibarial dilators are attached to the clypeus (see Snodgrass 1935, v. Kéler 1955). A frontoclypeal sulcus is absent in *Philopotamus* and *Hydropsyche*, as in *Phryganea* (Crichton 1957) and *Stenophylax* (Chaudonneret 1990). In contrast to Chaudonneret (1990), Demoulin (1960: 4, fig. 1; = clypeo-frontal sulcus) described a frontoclypeal sulcus in *Stenophylax* which originates from the anterior tentorial pits and curves dorsally toward the antennal bases. This sulcus is not homologous with a frontoclypeal sulcus due to the origin of pharyngeal dilators below the median ocellus which are attached to the frons in the generalized insect head (Snodgrass 1935). It rather resembles the frontogenal sulcus of Philopotamidae. This conclusion is also applicable to the dorsal demarcation of the 'clypeus' presented by Deoras (1943). A frontoclypeal sulcus is described for the leptocerid species *Ceraclea dissimilis* (Denis & Bitsch 1973: 422) and in *Rhyacophila* (Klemm 1966: 37 [= sulcus epistomalis]). In *Rhyacophila* a horizontal sulcus between the anterior tentorial pits is present but the dorsal cibarial dilator muscle is attached to the sulcus itself and also to the area above it (pers. obs.). Since the dilator muscles of the prepharyngeal tube are exclusively attached to the clypeus (see v. Kéler 1955) a homology of the horizontal sulcus in *Rhyacophila* to the frontoclypeal sulcus of the generalized insect head can be doubted.

Klemm (1966: fig. 11) described a membranous horizontal furrow ('querfaltige Membran') ventrally adjacent to the horizontal sulcus in *Rhyacophila*. A similar depression is present in many other trichopterans, as for instance in *Philopotamus* (hf in Fig. 1), *Phryganea* (Crichton 1957: unlabeled in fig. 26) and *Hydropsyche* (pers. obs). However, in contrast to *Rhyacophila* the horizontal furrow is not membranous in the other taxa. In *Philopotamus* the dorsal dilator muscles of the prepharyngeal tube originate from the head capsule in the area below the anterior tentorial pits and also above the horizontal furrow which therefore also cannot be homologous with the frontoclypeal sulcus. Additionally, a ventral cibarial dilator muscle [cl-ci(v)] is attached below the horizontal furrow, rendering this structure as transclypeal. It separates the dorsal frontopostclypeus from a ventral anteclypeolabrum. Based on the origin sites of the cibarial dilator muscles Klemm (1966: 19) and Chaudonneret (1990: 78, fig. 175) correctly termed the area below the horizontal furrow in *Rhyacophila* and *Stenophylax*, respectively, as anteclypeolabrum (see Table 2). Klemm (1966) considered the area above the frontoclypeal sulcus as the frons and in consequence all attached muscles as dilators of the pharynx. There is no cibarial dilator muscle in *Phryganea* recorded as attaching below the horizontal furrow (Crichton 1957: fig. 26). Hence, Crichton (1957) regarded this lower region as a labrum and the area above the horizontal furrow the frontoclypeus; it accommodates the origins of both cibarial and pharyngeal dilator muscles. In accordance to Crichton's (1957) interpretation we conclude that the area above the anterior tentorial pits truly represents the frons in Philopotamidae and most other trichopterans but since the frontoclypeal sulcus is absent no clear border between frons and clypeus is present. Consequently, this composite formation has to be termed as frontoclypeus as proposed by Crichton (1957) and Chaudonneret (1990) (see Table 2). In *Micropterix* (Hannemann 1956) and other non-glossatan moths (Kristensen 2003) a frontoclypeal sulcus is well-developed but absent in all Glossata. Kristensen (2003: 43) linked the absence of a frontoclypeal sulcus to the loss of articulated mandibles in the post-pharate glossatan adults. This is also a plausible explanation for the loss of this structure in most trichopterans.

The frontopostclypeus of *Philopotamus* is dorsally subdivided by the interantennal sulcus which is also present in *Stenophylax* (Chaudonneret 1990: 78, fig. 172, stf) but is absent in *Rhyacophila* (pers. obs.; Klemm 1966) and *Phryganea* (Crichton 1957). A homology with the interantennal sulcus of some lepidopterans (Kristensen 2003: 41) is doubtful.

4.1.2. Anteclypeolabrum

The complete lack of the clypeo-labral articulation and of the fronto-labral muscles in all trichopteran species investigated so far impedes the exact delimitation of the labral and clypeal portions of the anteclypeolabrum. The combined loss of both features occurs in almost all insect taxa with an immobilized labrum (e.g., Friedrich et al. 2013; v. Kéler 1955: 722). A border between a well-sclerotized proximal part and a membranous apical area is distinctly developed in most trichopterans (e.g., Fig. 1, Klemm 1966: fig. 9). If it represents the anatomical clypeo-labral boundary remains uncertain due to the lack of associated muscles but seems to be at least possible since the epipharyngeal sclerite is laterally continuous with the anteclypeolabrum in this apical area. The proximal border of the structure described as labrum by Crichton (1957) for *Phryganea* (see above) is in fact the intraclypeal horizontal furrow. His interpretation was likely based on the absence of the ventral clypeo-cibarial dilator muscle. Crichton (1957: 61) assumed that the membranous tip in *Phryganea* is movable by an intrinsic muscle. Considering the sclerotization pattern of the labrum, this intrinsic muscle most likely allows only light movements or deformation of the membranous tip. It is most likely that it lifts only the epipharynx. Considering the absence of extrinsic labral muscles Crichton's interpretation has to be regarded as not supported. The interpretation of labrum and clypeus forming a composite anteclypeolabrum by Klemm (1966) and Chaudonneret (1990) is comparable with the condition found in Philopotamidae. In the ground plan of Lepidoptera the labrum is moved by paired frontal retractor muscles and is proximally well delimited by a clypeo-labral hinge (Kristensen 2003).

4.1.3. Gena and occiput

The gena is anteriorly delimited from the frontopostclypeus by the distinct frontogenal sulcus. The latter extends from the ventral margin of the circumantennal sulcus toward the anterior tentorial pit in Trichoptera; the corresponding internal ridge is of variable size (Klemm 1966; Neboiss 1991). In Lepidoptera a frontogenal sulcus (= laterofacial sulcus of Kristensen 2003) is usually well-developed in the glossatan lineages but joins the circumantennal sulcus dorsolaterally. It has been shown in other insect groups that the length and connections of the circumantennal and frontogenal sulci can strongly vary even between closely related taxa, depending on other anatomical features (see Klass & Eulitz 2007). A well-sclerotized clypeogenal sulcus as described by Crichton (1957) for *Phryganea* could not be observed in *Philopotamus* and is also absent in *Rhyacophila* (Klemm 1966: 37).

A typical feature of the trichopteran head capsule is the elongation of the ventral edge of the gena forming a subgenal process. This process is also a typical feature of Mecoptera (Mickoleit 1971; Friedrich et al. 2013) and basal lepidopterans (Kristensen 2003). As described for *Philopotamus* the postgena is continuous with the occiput in all other investigated trichopterans (Klemm 1966; Crichton 1957) while it is distinct in *Micropterix* (Hannemann 1956) and other lepidopteran lineages (Kristensen 2003). Frontal and coronal sulci are generally present in Trichoptera (*Philopotamus*, *Hydropsyche*, *Phryganea* [pers. obs.], *Rhyacophila* [= sulcus mediocranialis of Klemm 1966], *Stenophylax* [Demoulin 1960]). The postfrontal sulcus described for *Philopotamus* and *Stenophylax* (Demoulin 1960) are most probably homologues to the medio-lateral reinforcement lines described by Klemm (1966: 8) and the postinterocellar sulcus described by Hannemann (1956) for *Micropterix*. These sulci are completely absent in *Phryganea* (pers. obs.). Interocellar sulci occurring in some lepidopteran lineages (Kristensen 2003) are not known from Trichoptera.

4.1.4. Tentorium

The tentorium of Philopotamidae is characterized by extremely reduced dorsal tentorial arms and a well-developed corpotentorium resulting in an X-shaped configuration of the anterior and posterior tentorial arms. Full developed dorsal tentorial arms appear as a characteristic feature of the integripalpian lineage Plenitentoria (e.g., Phryganeidae [Crichton 1957], Limnephilidae: *Stenophylax* [Demoulin 1960], Goeridae, and Brachycentridae [Neboiss 1991]). They are remarkably weak developed or completely absent in Annulipalpia (see Neboiss 1991), Rhyacophilidae (Klemm 1966) and also in some Integripalpia (e.g., Brevitentoria: Sericostomatidae [see Neboiss 1991]). A similar pattern of weakly and well-developed dorsal arms is found in Lepidoptera (see Kristensen 2003: 44). The X-shaped configuration of the tentorium can also be found in Hydropsychidae (Neboiss 1991). In most other lineages of Trichoptera (e.g., Rhyacophilidae, Glossosomatidae, Psychomyiidae, Leptoceridae) it is H- or Π-shaped (Neboiss 1991) as in Lepidoptera-Micropterigidae (Kristensen 2003). Therefore, a Π-shaped configuration is added to the trichopteran ground plan. The presence of a plate-like corpotentorium in Philopotamidae is a potential autapomorphy of the group (see Neboiss 1991). Similar conditions present in the agathiphagid and heterobathmiid lepidopterans (Kristensen 2003) are very likely convergently developed, because all spicipalpian representatives show other configurations (Neboiss 1991). A large, heavily sclerotized laminatentorium occurs in several not closely related groups (e.g., Hydropsychidae (Annulipalpia), Hydrobiosidae (spicipalpians), and Leptoceridae (Integripalpia) [Neboiss 1991]).

4.1.5. Setal warts

A specific feature of the trichopteran head is the presence of numerous, bulged setal warts equipped with numerous large trichoid sensilla. The homology of these areas is uncertain due to the high variability in presence and location in different trichopteran lineages (see Oláh & Johanson 2007). In previous descriptions these structures were often neglected or at least insufficiently described (see Crichton 1957; Klemm 1966). Detailed comparative studies are not available.

4.1.6. Photoreceptors

The compound eye of Philopotamidae is irregularly covered by a few interommatidial setae. The number of setae as well as their distribution on the compound eye varies among caddisfly families (see Schmid 1998), and can even be species specific (pers. obs.: *Philopotamus* and *Wormaldia* [Philopotamidae]). Neither Crichton (1957) nor Klemm (1966) mentioned the presence of interommatidial setae in Rhyacophilidae and Phryganeidae, respectively, although they are visible in light microscopy and are commonly present in Trichoptera (pers. obs.) and in Lepidoptera (Kristensen 2003).

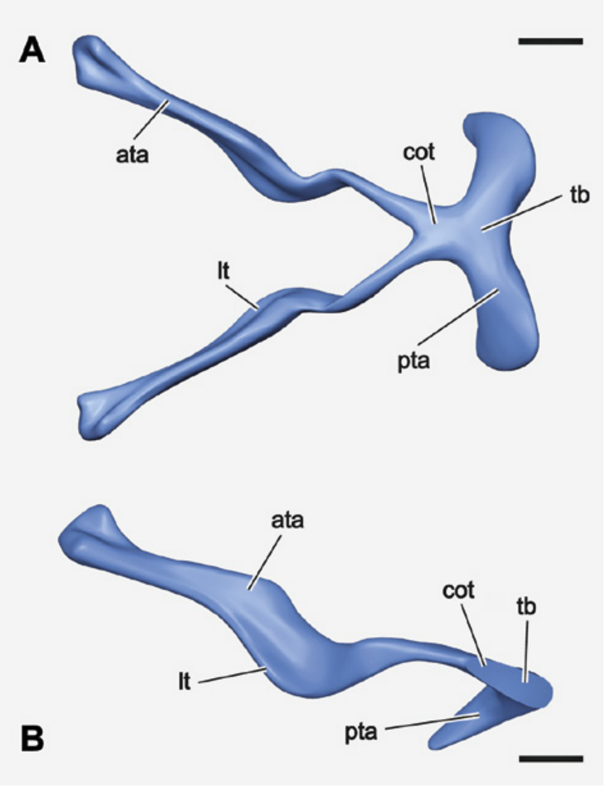

Fig. 14. *Philopotamus ludificatus* McLachlan, 1878: tentorium, 3D-reconstruction based on µCT data. **A**: dorsal view, **B**: sagittal section (dorsal tentorial arm not shown; see Fig. 17C). — ***Abbreviations***: ata – anterior tentorial arm, cot – corpotentorium, lt – laminatentorium, pta – posterior tentorial arm, tb – tentorial bridge. (Scale bars: 100 µm)

Furthermore, in *Philopotamus* the ommatidial cornea shows a specific surface texture of rounded corneal nipples (absent along the interommatidial space), a common feature of the insect compound eye in order to reduce reflection artifacts (Bernhard & Miller 1962; Bernhard et al. 1970). These extremely minute structures are not mentioned by Crichton (1957) and Klemm (1966), likely due to technical constraints. The structure of corneal outgrowths varies among insects from knob-like nipples to parallel sulci (Meyer-Rochow & Stringer 1993). Evidence for the presence of corneal nipples of the knob-like type among 15 different caddisfly families (including Philopotamidae) was provided by Bernhard et al. (1970). A textured surface of the ommatidial cornea is also commonly found in Lepidoptera (Kristensen 2003) and Mecoptera (Bernhard et al. 1970).

Three ocelli are present in *Philopotamus*, *Rhyacophila* (pers. obs.; Klemm 1966) and *Phryganea* (pers. obs.; Crichton 1957) but the occurrence of ocelli is quite variable among trichopteran lineages (see Malicky 1973). This is also true for the lateral ocelli in Lepidoptera; the median one is reduced in all groups (Kristensen 2003).

Histological sections show that the ocelli in *Philopotamus* have a comparatively thin corneal lens of the convexo-concave type (after Hallberg & Hagberg 1986) whereas the haemocoelic space is voluminous (pers.

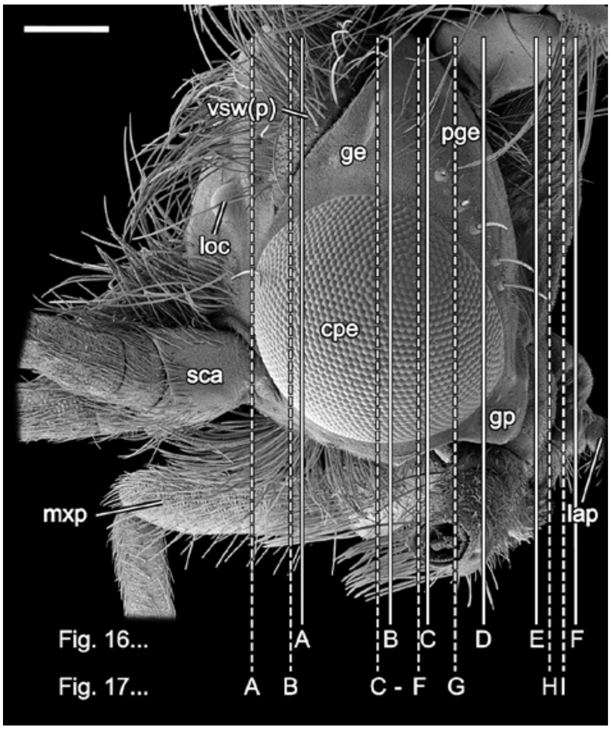

Fig. 15. *Philopotamus ludificatus* McLachlan, 1878: head, SEM image. **A**: lateral view with section planes of Figs. 16 (continuous lines) and 17 (dashed lines) marked. — ***Abbreviations***: cpe – compound eye, ge – gena, gp – subgenal process, lap – labial palp, loc – lateral ocellus, mxp – maxillary palp, pge – postgena, sca – scapus, vsw(p) – posterior setal wart of vertex. (Scale bar: 200 µm)

obs.; Ehnbom 1948). A similar condition was described for limnephilids by Ehnbom (1948) and Hallberg & Hagberg (1986), and is also found in the micropterigid moths (Ehnbom 1948; Kristensen 2003). The corneal lens is much thicker (biconvex type), and underlain by an epidermal layer in phryganeids (pers. obs.: *Phryganea*; Ehnbom 1948; Hallberg & Hagberg 1986). This is also the common condition in most heteroneuran lepidopterans (Ehnbom 1948; Kristensen 2003). Eriocraniidae are different in having the haemocoelic space filled up by a multicellular formation (see Kristensen 2003) not known from any other amphiesmenopteran insect.

An imaginal stemma consisting of numerous heavily pigmented retinula cells is attached to the optical lobe in all investigated Trichoptera (pers. obs.: *Philopotamus*, *Rhyacophila*; Ehnbom 1948; Hagberg 1986). Initially, this formation which represents a remnant of the larval eyes in the adult stage was described for phryganeids by Ehnbom (1948). Its appearance is variable on family level. Usually each stemma consists of numerous retinula cells associated to at least one crystalline body (see Ehnbom 1948; Hagberg 1986: fig. 2). They are common features of the endopterygote adult head and can be found in various insect groups (i.e., Lepidoptera [Hagberg 1986; Kristensen 2003]; Megaloptera [*Sialis*, Ehnbom 1948]). In Lepidoptera the imaginal stemma is located inside the lobus opticus whereas it is found outside, behind the optic lobe in caddisflies and most other holometabolous insect orders (e.g., Megaloptera, Neuroptera, and Mecoptera, see Ehnbom 1948). Hagberg (1986) concluded that these sensory organs are associated with cranial areas of glabrous, translucent cuticle. A small glabrous, bulged field near the lateral ocelli in *Philopotamus* might be comparable. If this structure and the stemma are functionally correlated cannot be assessed with final certainty because they are distinctly separated in *Philopotamus.*

4.1.7. Antenna

The length of the antenna varies remarkably among Trichoptera. In most groups (including Philopotamidae and Limnephilidae) it is as long as the forewing. But it is considerably shorter in Hydroptilidae (app. half of length of forewing) or extremely long as in Leptoceridae (app. three times longer than forewing length), respectively.

→ **Fig. 16.** *Philopotamus ludificatus* McLachlan, 1878: head, cross-sections. **A–F**: Cross-sections in dorsal-ventral sequence. — ***Abbreviations***: abte – tendon of abductor muscle of mandible (M. cranio-mandibularis lateralis), acl(d) – distal part of anteclypeolabrum, acl(p) – proximal part of anteclypeolabrum, adte – tendon of adductor muscle of mandible (M. cranio-mandibularis medialis), an-ci – M. anularis cibarialis, an-ph – M. anularis pharyngalis, ao – aorta, ata – anterior tentorial arm, br – brain, ccc – corpora cardiaca & corpora allata complex, cd-mp(d) – M. cardo-palpalis dorsalis, cd-mp(v) – M. cardo-palpalis ventralis, cl-ci(d) – M. clypeo-cibarialis dorsalis, cl-ci(v) – M. clypeo-cibarialis ventralis, cl-eph(l) – M. clypeo-epipharyngalis lateralis, coc – circumoesophageal commissure, cos – circumocular sulcus, cpe – compound eye, cr-lc – M. cranio-lacinialis, cr-md(l) – M. cranio-mandibularis lateralis, cr-md(m) – M. cranio-mandibularis medialis, cr-ph(a) – M. cranio-pharyngalis anterior, cr-prm(l) – M. cranio-praementalis lateralis, cr-prm(m) – M. cranio-praementalis medialis, cr-st – M. cranio-stipitalis, dol – deutocerebral olfactory lobe, eph – epipharynx, fb – fat body, fgs – frontogenal sulcus, fsal – floor of salivarium, fr-ph(p) – M. fronto-pharyngalis posterior, ga – galea, gp – subgenal process, hst – haustellum, is – immaginal stemma, md(s) – mandibular sclerite, mp1-mp2(l) – M. palpo-palpalis maxillae primus lateralis, mp1-mp2(m) – M. palpo-palpalis maxillae primus medialis, mp2-mp3 – M. palpo-palpalis maxillae secundus, nla – labial nerve, nmx – maxillary nerve, ocs – occipital sulcus, ol – optical lobe of protocerebrum, pch – precerebral pumping chamber, ph – pharynx, poc – preoral cavity, ppg – palpiger, ppt – prepharyngeal tube, prm-lp(l) – M. praemento-palpalis lateralis, prm-lp(m) – M. praemento-palpalis medialis, prm-sa – M. praemento-salivarialis, rsal – roof of salivarium, sit – sitophore plate, soeg – suboesophageal ganglion, st-mp(d) – M. stipito-palpalis dorsalis, tb – tentorial bridge, te-cd – M. tentorio-cardinalis, te-ph(a) – M. tentorio-pharyngalis anterior, te-ph(p) – M. tentorio-pharyngalis posterior, te-sc(a) – M. tentorio-scapalis anterior, te-sc(l) – M. tentorio-scapalis lateralis, te-sc(m) – M. tentorio-scapalis medialis, te-sc(p) – M. tentorio-scapalis posterior, te-si – M. tentorio-sitophorialis, te-st – M. tentorio-stipitalis, tra – trachea, I, and II – number of palpomere of maxillary palp. (Section planes marked in Fig. 15, continuous lines) (Scale bars: A–E: 250 µm; F: 100 µm)

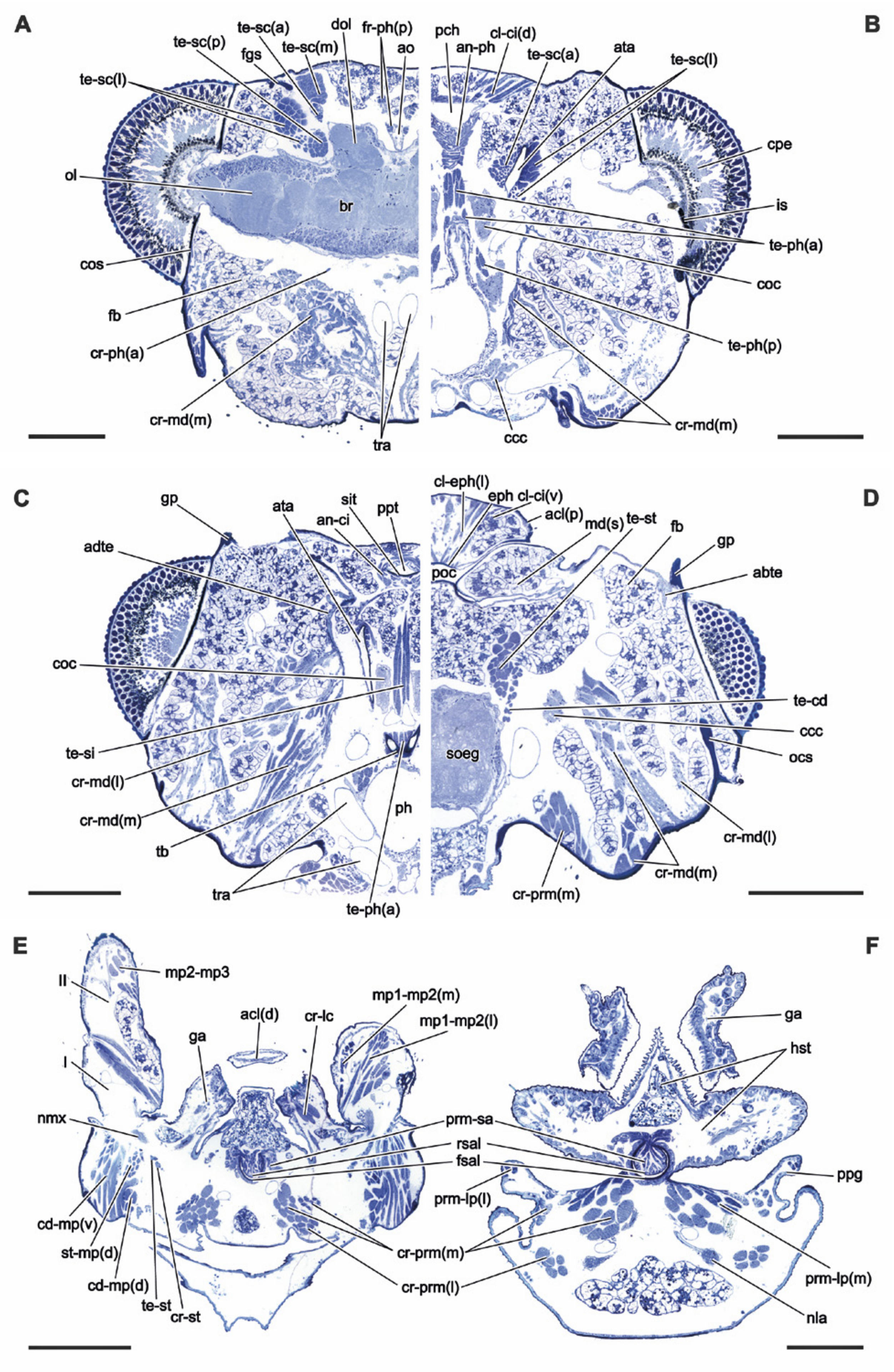
A
te-sc(a)
dol
fr-ph(p)
te-sc(p)
fgs
te-sc(m)
ao
te-sc(l)
ol
br
cos
fb
cr-ph(a)
cr-md(m)
tra
B
pch
cl-ci(d)
an-ph
te-sc(a)
ata
te-sc(l)
cpe
is
te-ph(a)
coc
te-ph(p)
cr-md(m)
ccc
C
gp
ata
sit
ppt
an-ci
adte
coc
te-si
cr-md(l)
cr-md(m)
tb
ph
tra
te-ph(a)
D
cl-eph(l)
eph
cl-ci(v)
acl(p)
md(s)
te-st
fb
gp
poc
abte
te-cd
ccc
soeg
ocs
cr-md(l)
cr-md(m)
cr-prm(m)
E
ll
mp2-mp3
mp1-mp2(m)
acl(d)
cr-lc
mp1-mp2(l)
ga
l
nmx
prm-sa
rsal
fsal
prm-lp(l)
cd-mp(v)
st-mp(d)
cd-mp(d)
te-st
cr-st
cr-prm(m)
cr-prm(l)
F
ga
hst
ppg
prm-lp(m)
nla

→ **Fig. 17.** *Philopotamus ludificatus* McLachlan, 1878: head, cross-sections in dorsal-ventral sequence. **A**: base of antenna with antennal ampulla, **B**: head aorta accompanied by bundles of posterior fronto-pharyngeal muscle (marked by arrow) in front of the brain, **C**: precerebral pharynx at level of the ganglion frontale, **D**: mid part of the anterior tentorial arm with origin of tentorio-antennal muscles and M. tentorio-mandibularis (extremely thin), **E**: region short distance ventrad from (D) with M. tentorio-mandibularis accompanied by mandibular nerve, **F**: prepharyngeal tube below the frontal ganglion with dorsal margin of the sitophore plate, **G**: sitophore plate short distance below (F), **H**: cervical region with salivary glands, **I**: proximal part of salivarium. — ***Abbreviations***: aa – antennal ampulla, an-ci – M. anularis cibarialis, an-ph – M. anularis pharyngalis, ao – aorta, ata – anterior tentorial arm, av – antennal vessel, br – brain, cco – cervical connective, cl-ci(d) – M. clypeo-cibarialis dorsalis, coc – circumoesophageal commissure, cr-prm(m) – M. cranio-praementalis medialis, cvm – cervical membrane, dol – deutocerebral olfactory lobe, dta – dorsal tentorial arm, fb – fat body, fco – frontal connective, fg – ganglion frontale, fr-ph(p) – M. fronto-pharyngalis posterior, hy-sa – M. hypopharyngo-salivarialis, ias – interantennal sulcus, nmd – mandibular nerve, ph – pharynx, ppt – prepharyngeal tube, sal – salivarium, sc-pe(m) – M. scapo-pedicellaris medialis, sd – salivary duct, sg – salivary gland, sit – sitophore plate, te-md – M. tentorio-mandibularis, te-ph(a) – M. tentorio-pharyngalis anterior, te-ph(l) – M. tentorio-pharyngalis lateralis, te-sc(a) – M. tentorio-scapalis anterior, te-sc(l) – M. tentorio-scapalis lateralis, te-sc(m) – M. tentorio-scapalis medialis, te-sc(p) – M. tentorio-scapalis posterior, te-si – M. tentorio-sitophorialis, tra – trachea, trc – tritocerebral commissure, tri – tritocerebrum. (Section planes marked in Fig. 15, dashed lines) (Scale bars: 100 µm)

The antenna bears numerous sense organs which mainly function as chemical receptors. These sense organs vary considerably in their shape among Trichoptera (see Faucheux 2004; Melnitsky & Ivanov 2011) and Lepidoptera (Kristensen 2003; Faucheux 2004). In Philopotamidae and Stenopsychidae the number of fungiform pseudoplacoid sensilla along the antenna is remarkably high (pers. obs.) but this type of sense organs can be found regularly among Trichoptera (Melnitsky & Ivanov 2011).

In Trichoptera the antenna (i.e., the scapus) is moved by four extrinsic muscles originating mainly from the tentorium (e.g., in Philopotamidae, Limnephilidae [pers. obs.]; Phryganeidae [pers. obs.; Crichton 1957], and Rhyacophilidae [Klemm 1966]) or with at least one bundle from the cranium (e.g., in Polycentropodidae and Hydropsychidae [pers. obs.]) but data on this potentially phylogenetically valuable character complex is quite limited. This corresponds with the number and origin pattern of extrinsic antennal muscles in Lepidoptera. In contrast, only three or two are present in Mecoptera (e.g., Friedrich et al. 2013). The remaining parts of the antenna are moved by two intrinsic muscles arising from the scapus with several bundles. Maybe these bundles belong to more than two muscles as in the ground plan condition of Lepidoptera (Kristensen 2003) but with the data at hand the homology of these muscles remains unclear and should be investigated in detail for a larger set of taxa.

4.1.8. Mandible

The mandibular sclerite of *Philopotamus* is moderately sized and sclerotized as it is in *Rhyacophila* (Klemm 1966). In Integripalpia it is less sclerotized and often almost vestigial (*Phryganea* [Crichton 1957]; *Stenophylax* [Demoulin 1960; Chaudonneret 1990: 77, fig. 172]). The conditions of the mandibular musculature distinctly differ in the trichopteran species studied so far. While the adductor muscle is strongly developed in annulipalpians (pers. obs.) and in *Rhyacophila* (Klemm 1966; pers. obs.), it is comparatively small in *Phryganea* (Crichton 1957: 60, fig. 25).

In spite of the remarkable differences between the major groups of caddisflies in size of the mandibular sclerite, sclerotization and musculature development in all post-pharate imagines lack any cranio-mandibular articulations (pers. obs.; Chaudonneret 1990; Kristensen 1997). Hence, the mandible is most likely never functional for the processing of solid food (see also Crichton 1957). As highlighted by Hinton (1946) the mandibular muscles of adult endopterygote insects with decticous pupae operate the pupal mandibles when the pharate imago hatches from the cocoon; in the post-pharate stage of caddisflies and glossatan moths they are functionless and therefore may become atrophied. This might be a possible explanation for descriptions of differently sized mandibular muscles in Trichoptera (Crichton 1957; Klemm 1966). However, a detailed documentation of the development of the mandibular musculature during aging of the imagines is not available.

4.1.9. Preoral cavity and mouth opening

The interpretations of the facial areas (see above) mainly depend on the demarcation of the anatomical mouth opening. After Snodgrass (1935) the border between the prepharyngeal tube (= cibarium) and the pharynx is usually marked by the frontal ganglion. Accordingly, in *Philopotamus* all muscles inserting below the frontal ganglion are termed prepharyngeal (= cibarial) dilators whereas muscles attached above the frontal ganglion are regarded as pharyngeal dilators. The prepharyngeal tube is encircled by ring musculature and clearly contributes to a large cibarial-pharyngeal pumping chamber which represents a composite structure in *Philopotamus*. Klemm (1966) regarded this part as the cibarium and determined the morphological mouth opening at the anterior border of the pharyngeal ring musculature. He considered the muscles above this border either as cibarial dilators or as pharyngeal dilators depending on the origin site below or above the horizontal sulcus (his sulcus epistomalis, see above). It seems not appropriate to separate the preoral cavity into a proximal cibarium enclosed

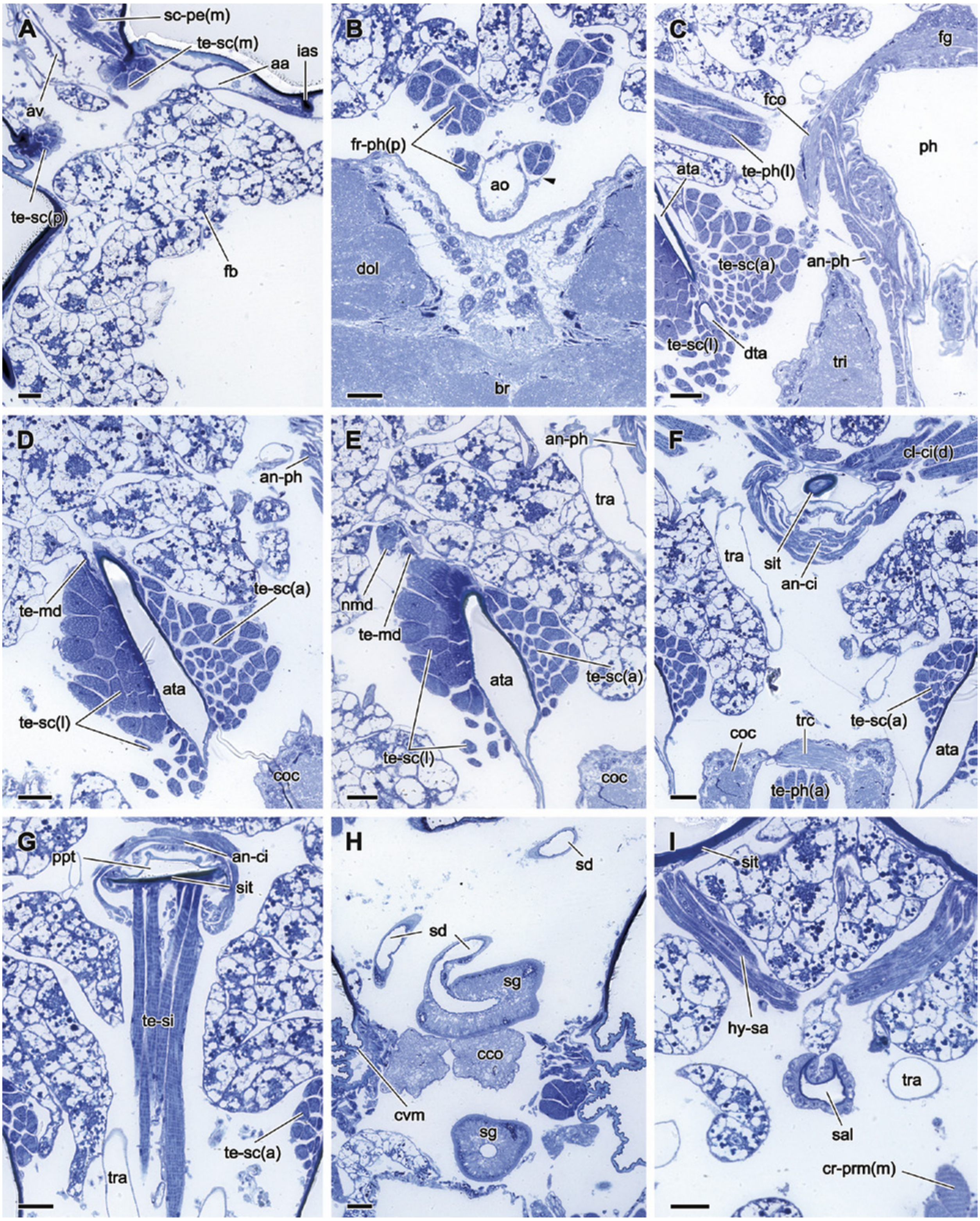

by pharyngeal circulatory musculature and a distal part without ring musculature as proposed by Klemm (1966) since the sitophore plate (i.e. the sclerotized section of the hypopharynx) is a continuous structure and clearly forms the bottom of the composite pumping chamber. In lepidopterans the ring musculature is located behind the frontal ganglion but the roof of the cibarium is only covered by semicircular and longitudinal muscle fibers (Kristensen 2003). This semicircular type of cibarial pump musculature is so far not known from any trichopteran species.

The surface of the sitophore plate lacks any chemoreceptors in *Philopotamus* and the sparse literature (Crichton 1957; Klemm 1966) gives no evidence that sensilla are present along the floor of the preoral cavity in any other trichopteran. In Lepidoptera the sitophore is usually equipped with numerous chemoreceptors (Nielsen & Kristensen 1996).

4.1.10. Maxilla

In Trichoptera the base of the maxilla is formed by one sclerite which is intermitted by a transstipital sulcus. This sulcus was usually misinterpreted as a border between 'cardo' and 'stipes' (e.g., Crichton 1957; Matsuda 1965; Klemm 1966). In Lepidoptera the proximal maxillary sclerite (apparent 'cardo') is subdivided into two sections by an internal sulcus and delimited from the stipes (dististipes) by a small membranous area (Hannemann 1956: 191; Kristensen & Nielsen 1979: 117). In *Philopotamus* as in *Rhyacophila* (Klemm 1966) no membranous subdivision of the basal maxillary sclerite could be observed. A strong horizontal sulcus delimits the apparent cap-like cardo and the stipes. Intriguingly, a couple of extrinsic muscles of the maxillary palp originate from the putative cardo. A cardo-palpal muscle is not present in any other insect group (see e.g., Wipfler et al. 2011; v. Kéler 1955) and therefore it is more plausible to assume that these muscles are homologues to the stipito-palpal muscle of the insect ground plan (e.g., Snodgrass 1935: 143). The insertion of these palpal muscles to the basalmost maxillary piece in both amphiesmenopteran lineages led to the interpretation that this sclerite represents a combination of cardo and basistipes (Hinton 1958; Kristensen & Nielsen 1979; Kristensen 2003). Accordingly, the horizontal sulcus present in Trichoptera does not demarcate the border between 'cardo' and 'stipes' as suggested by several authors (e.g., Klemm 1966; Chaudonneret 1990), but forms a transstipital border between a basal piece (cardo + basistipes) and the dististipes. The inclusion of a cardinal portion in the basal piece is well proven by the presence of the cranio-cardinal muscle (cr-ca).

In Philopotamidae and the spicipalpian families Rhyacophilidae (Klemm 1966) and Glossosomatidae (Chaudonneret 1990: *Agapetus*) the maxilla bears two proximally fused inner appendages: a distinct, flattened outer lobe and a comparatively small, sclerotized inner lobe. In *Philopotamus* this composite structure is moved by a cranial flexor muscle, which might be homologous to the cranio-lacinial muscle of generalized insects (v. Kéler 1955: M.19). Additionally, Klemm (1966: 18) described for Rhyacophilidae a stipito-lacinial muscle inserting at the small inner lobe. This muscle is absent in Philopotamidae. In Integripalpia (e.g., Phryganeidae [Crichton 1957: 63]) the maxillary endite lobe is a single structure without any subdivision, but both the cranio-lacinial and the stipito-lacinial muscle are present. This led several authors to regard this clearly composite lobe of Trichoptera as the lacinia, an interpretation which cannot be accepted considering the conditions in basal representatives. Furthermore, as discussed by Kristensen (2003: 53) and Beutel et al. (2014: 21) the lacinia is usually distinctly stronger sclerotized and less equipped with sensilla (chemoreceptors) than the galea. Therefore, it seems also appropriate to consider the membranous outer maxillary lobe which bears numerous basiconic sensilla as the galea as suggested by Chaudonneret (1990: 80) and only the small inner piece as the remnants of the lacinia, which is largely (e.g., Rhyacophilidae) or completely incorporated (e.g., Phryganeidae) into the outer lobe which therefore should be regarded as a galeolacinia.

4.1.11. Haustellum

The origin of the trichopteran haustellum was a subject of controversy for decades. Several authors homologized the whole haustellum with the fused inner and outer lobes of the labium, i.e., the ligula (Lucas 1893; Deoras 1943; Despax 1951; Handlirsch & Beier 1936). The small inner labial lobes present in annulipalpians (pers. obs.) and *Rhyacophila* (Klemm 1966) most likely represent remnants of these labial appendages. This renders the hypothesis of the haustellum being a modified ligula very unlikely.

A second hypothesis favored by Cummings (1914), Tillyard (1923) and Klemm (1966) considered the haustellum as a ventral outgrowth of the hypopharynx. Indeed, the salivary orifice is located on the lower anterior (e.g., *Philopotamus*) or posterior (e.g., *Stenophylax* [Chaudonneret 1990]) surface of the haustellum. Usually it marks the border between the hypopharynx and the labium (Moulins 1971; Beutel et al. 2014: 22). Therefore, at least the upper anterior part of the haustellum must be of hypopharyngeal derivation.

Crichton (1957) showed that the haustellum in *Phryganea* is innervated by a branch of the mandibular nerve but also receives a branch of the labial nerve. He concluded that the lower section of the haustellum is most likely formed by the labium whereas the hypopharynx contributed to the upper part of this composite structure. The investigation of *Philopotamus* showed that the haustellum as well as the salivarium are only innervated by branches of the labial nerve.

In conclusion a composite nature of the haustellum seems to be well supported by the location of the salivary orifice and by its innervation by different nerve tracts. However, the latter seems not to be consistent throughout all trichopteran lineages and needs further detailed research.

In *Philopotamus* and *Rhyacophila* (pers. obs.) the haustellum is a completely membranous, highly flexible structure distinctly separated from the sclerotized prementum. Sclerites are absent. Small, distinctive basal haustellar sclerites were described for some integripalpians by Crichton (1957) and Chaudonneret (1990). These sclerites serve as attachment areas of the labial palp muscles and represent most likely derivatives of the prementum in the generalized insect condition (e.g., Snodgrass 1935: 147).

The fine structure of the haustellar surface varies considerably between Annulipalpia and Rhyacophilidae on one hand and Integripalpia on the other. The upper surface of the haustellum in *Philopotamus* and *Rhyacophila* (pers. obs.; Klemm 1966) is densely covered by numerous irregularly distributed, multibranched microtrichia. The corresponding microtrichia in Phryganeidae and Limnephilidae are arranged in rows forming a regular system of channels on the surface of the haustellum (Crichton 1957, 1989, 1992; Chaudonneret 1990) which is absent in most annulipalpian groups (Crichton 1992).

4.1.12. Salivarium

In all Trichoptera investigated so far the salivarium orifice is located on the surface of the haustellum, distinctly below the preoral cavity. In *Philopotamus* it is located on the anterior surface of the haustellum but on its hind face in *Rhyacophila* (Klemm 1966) and Integripalpia (Crichton 1957; Chaudonneret 1990). In Lepidoptera and most other endopterygote insects the salivary orifice is located at the distal end of the hypopharynx, and distinctly opens into the preoral cavity (Kristensen 2003).

In Trichoptera the salivarium forms a longitudinal, sclerotized channel with U-shaped cross-section. A pair of extrinsic dilator muscles (M. hypopharyngo-salivarialis and M. praemento-salivarialis) inserts on its dorsal wall in *Philopotamus* and *Rhyacophila*. In contrast, in other pterygote insects M. praemento-salivarialis inserts ventrally on the floor of the salivarium (e.g., v. Kéler 1955; Snodgrass 1935; Röber 1942 [Megaloptera]; Kristensen 2003 [Lepidoptera: Acanthopteroctetidae]). Therefore, it seems to be at least possible that the sclerite on which these muscles originate is a derivate of the hypopharyngeal suspensorium of the generalized insect condition and hence the muscle may constitute a displaced bundle of M. hypopharyngo-salivarialis. Extrinsic dilators of the salivarium originating from the prementum are absent in most mecopterid lineages like Lepidoptera (with the exception of Acanthopteroctetidae; Kristensen 2003: 60) and Mecoptera (e.g., Grell 1938; Friedrich et al. 2013). Furthermore, in *Phryganea* (Crichton 1957), *Rhyacophila* (Klemm 1966), and *Merope* (Mecoptera [Friedrich et al. 2013]) the hypopharyngeal dilator of the salivarium is also absent.

In most trichopterans (Rhyacophilidae [pers. obs., Klemm 1966]; Phryganeidae [Crichton 1957] and Limnephilidae [Chaudonneret 1990]) a strong longitudinal muscle along the roof of the salivarium is present. This intrinsic salivary muscle is absent in Philopotamidae and other holometabolan lineages (Röber 1942 [Neuropterida: Megaloptera]; Kristensen 2003 [Lepidoptera]; Schneeberg & Beutel 2011 [Diptera]). Instead a well-developed extrinsic dilator muscle originates from the floor of the hypopharynx (hy-sa) in the annulipalpian groups or from the premental ligula in other holometabolan taxa (e.g., Megaloptera [Röber 1942]). As all trichopterans with intrinsic longitudinal salivary muscles lack the extrinsic hypopharyngeal muscle it is logical to assume the potential homology of these muscles of the salivary roof.

4.1.13. Labium

The labium of the generalized insect head is composed of a proximal postmentum and a distal prementum which bears the labial palps and the inner endite lobes (e.g., Beutel et al. 2014). In Lepidoptera the labium is usually separated into three distinct sclerotized areas (postlabium, proximal prelabium and prementum) distinguishable either by membranous segregation or by muscle insertion (see Kristensen 2003). In Philopotamidae both elements are largely fused forming a weakly sclerotized labial plate bearing the labial palps. In contrast, Crichton (1957), Klemm (1966), and Chaudonneret (1990) described the presence of distinct labial sclerites in Integripalpia and Rhyacophilidae (see Table 2). Unfortunately, the identification of these structures is complicated by the absence of a postlabio-premental muscle in all trichopterans investigated so far. Hence, a pre- or postmental derivation of these labial sclerites cannot be proven with any certainty. For a thorough interpretation of these structures comprehensive studies are needed.

The labium bears small inner lobes in all annulipalpians (*Philopotamus*, *Hydropsyche* [pers. obs.; Crichton 1957]) and in Rhyacophilidae (pers. obs.; Klemm 1966), whereas these are absent in Integripalpia (e.g., Crichton 1957; Chaudonneret 1990). The formation of a 'ligula' (fused glossae after Kristensen 2003: 57) is a common feature in Lepidoptera. Distinct paraglossae retained only in Micropterigidae (Kristensen 2003). In Trichoptera the inner lobe lack any musculature and therefore its homology remains uncertain. However, considering the potential contribution of the 'ligula' to the haustellum it cannot be excluded that this lobe indeed represents a remnant of the paraglossa.

The labial palp of Trichoptera is usually three-segmented (four-segmented only in *Paduniella* [Psychomyiidae]) in both sexes (Malicky 1973). In Lepidoptera it is three-segmented in some lower groups but reduction in number of palpomeres occurs several times within the group (Kristensen 2003).

4.1.14. Nervous system

In Trichoptera the cephalic ganglia (brain and suboesophageal ganglion; Fig. 18) are usually distinctly separated by long circumoesophageal connectives (in Hydroptilidae exceptionally short [Ehnbom 1948]). The brain is divided into a large dorsal protocerebrum, well-developed anterior olfactory lobes (deutocerebrum) and a small ventral tritocerebrum which is continuous with the other parts of the brain (pers. obs., Ehnbom 1948). Usually frontal and labral nerves have a common root at the frontal connectives and split later into separate frontal (median) and labral (lateral) tracts (pers. obs.; Ehnbom 1948). Only in Hydroptilidae and Lepidoptera both nerves show discrete origins (Ehnbom 1948). The nervous system of Hydroptilidae and Lepidoptera share also other remarkable similarities as for instance the penetration of the cephalic aorta by the nervus recurrens. Both structures are distinctly separated in all other trichopterans (Ehnbom 1948). The shape of the suboesophageal ganglion varies considerably among Trichoptera (Ehnbom 1948). Usually, three pairs of nerves (mandibular, maxillary and labial) origi-

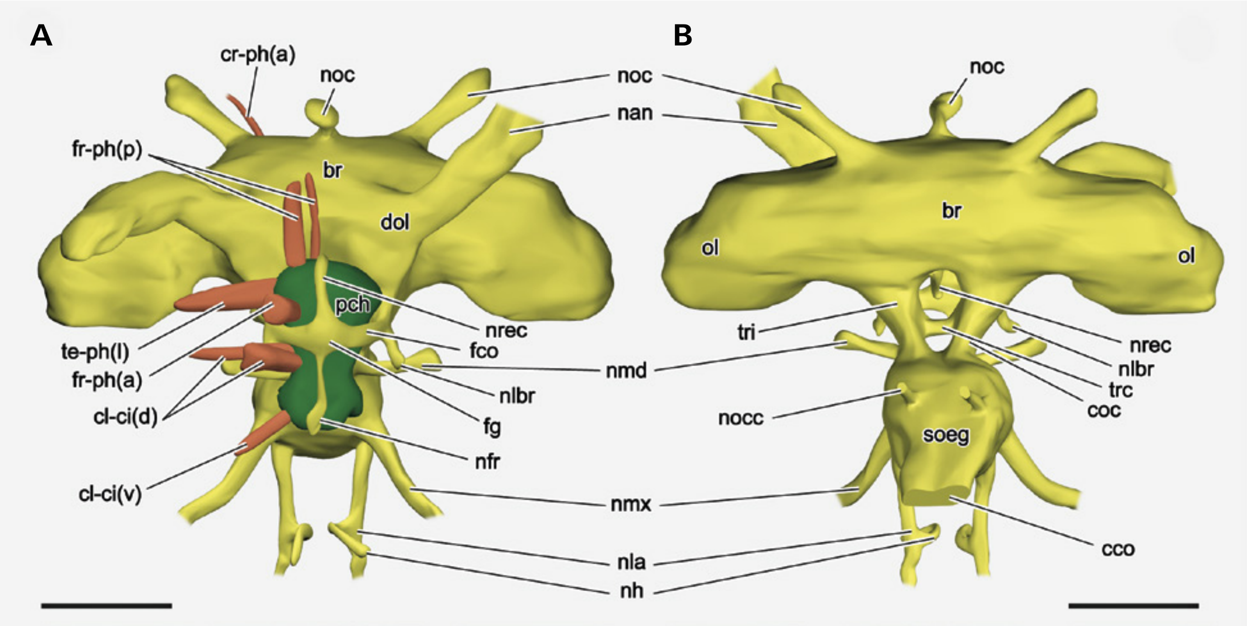

Fig. 18. *Philopotamus ludificatus* McLachlan, 1878: nervous system and gut with attached musculature (removed in B), 3D-reconstruction based on µCT data. **A**: anterior view, **B**: posterior view. — ***Colors***: green – gut, orange – musculature, yellow – nervous system. — ***Abbreviations***: br – brain, cco – cervical connective, cl-ci(d) – M. clypeo-cibarialis dorsalis, cl-ci(v) – M. clypeo-cibarialis ventralis, coc – circumoesophageal commissure, cr-ph(a) – M. cranio-pharyngalis anterior, dol – deutocerebral olfactory lobe, fco – frontal connective, fg – ganglion frontale, fr-ph(a) – M. fronto-pharyngalis anterior, fr-ph(p) – M. fronto-pharyngalis posterior, nan – nervus antennalis, nfr – nervus frontalis, nh – nerve of the haustellum, nla – labial nerve, nlbr – labral nerve, nmd – mandibular nerve, nmx – maxillary nerve, noc – ocellar nerve, nocc – occipital nerve, nrec – nervus recurrens, ol – optical lobe of protocerebrum, pch – precerebral pumping chamber, soeg – suboesophageal ganglion, te-ph(l) – M. tentorio-pharyngalis lateralis, trc – tritocerebral commissure, tri – tritocerebrum. (Scale bars: 250 µm)

nate ventrally in both, Trichoptera and Lepidoptera (Ehnbom 1948). An occipital nerve originating from the dorsal wall of the suboesophageal ganglion in *Philopotamus* is not described for any other trichopteran representative.

Paired glands of the hypocerebral complex, the corpora cardiaca and corpora allata are located behind the brain on both sides of the pharynx in Trichoptera and in Lepidoptera (Ehnbom 1948). However, comparative investigations showed considerable differences in shape and localization of the corpora cardiaca between different groups of caddisflies (Ehnbom 1948). In *Philopotamus* they are close to the hind face of the brain and ellipsoidally shaped as it is also described for *Hydropsyche* and *Agraylea* (Hydropsychidae, Hydroptilidae [Ehnbom 1948]). In Limnephilidae the corpora cardiaca are rather slender and distinctly separated from the brain (Ehnbom 1948). In *Philopotamus* the corpora allata are quite prominent (several times larger than the corpora cardiaca) and characterized by a considerably irregular glandular structure (pers. obs.; Ehnbom 1948). This condition is unique among trichopterans but resembles the condition found in most lepidopterans (Ehnbom 1948).

The cervical connectives are well separated from each other in Trichoptera and Mecoptera (*Panorpa* [Ehnbom 1948]). A different pattern is described for Hydroptilidae in which the cervical connectives being almost completely fused (Ehnbom 1948). This resembles the common condition in Lepidoptera excluding Micropterigidae (Ehnbom 1948).

4.2. Ground plan reconstruction

With this contribution to the soft-tissue anatomy of an annulipalpian species information for all three traditional trichopteran suborders is now available (Spicipalpia paraphyletic; see e.g., Kjer et al. 2002; Holzenthal et al. 2007b). Our data show remarkable intraordinal heterogeneity in several character complexes. As pointed out above, data are only available for few lineages (Rhyacophilidae, Philopotamidae, and Phryganeidae). This situation as well as the unresolved phylogeny of Trichoptera impedes a thorough interpretation of the structural evolution within Trichoptera. Nevertheless, the current state of knowledge allows us to hypothesize the trichopteran ground plan condition for several characters.

The tentorium of most Trichoptera is Π-shaped (Neboiss 1991), a condition which can be interpreted as a plesiomorphic ground plan feature of the group (Kristensen 2003). The X-shaped tentorium of Philopotamidae and Hydropsychidae most likely represents a derived condition in Trichoptera. Furthermore, a plate-like corpotentorium is only present in Philopotamidae (see also Neboiss 1991) and most likely represents an autapomorphy of this annulipalpian lineage, which is paralleled in the non-glossatan Lepidoptera families Agathiphagidae and Heterobathmiidae (Kristensen 2003). The dorsal tentorial arms are very short in Annulipalpia and some spicipalpian groups (Glossosomatidae and Hydroptilidae) (Neboiss 1991). This configuration most likely represents the ground plan condition of Amphiesmenoptera since the same condition is present in primitive non-glossatan Lepidoptera (see Kristensen 2003). Considering this, the well-developed and sclerotized dorsal tentorial arms of the integripalpian lineage Plenitentoria (e.g., Crichton 1957) represent a derived condition and a potential autapomorphy of the group.

In the ground plan of Amphiesmenoptera (as in most other insects [Wipfler et al. 2011]) the antenna is moved by four extrinsic muscles, primarily originating from the anterior tentorial arms. This pattern is retained in the ground plan of Trichoptera. However, shifts of the origin sites toward the head capsule occur in several taxa. These secondary modifications were found in distantly related taxa (e.g., Hydropsychidae [Annulipalpia] and Hydroptilidae ['Spicipalpia']) and are therefore regarded as independent developments (homoplasies). The shift of the origin of M. tentorio-scapalis posterior toward the dorsal tentorial arm in all studied species of Plenitentoria (pers. obs.; Crichton 1957) very likely represents a further autapomorphy of this group.

The adult mandibular sclerite in the ground plan of Trichoptera is moderately sized and sclerotized but it is certainly not suitable to process solid food (see above). This condition is retained in Annulipalpia and in the spicipalpian lineage Rhyacophilidae. The mandibular sclerite is extremely reduced in size and sclerotization in Integripalpia (see Crichton 1957), showing a distinct trend to the reduction of this chewing mouthpart within Trichoptera. We assume that the loss of the feeding function of the mandible is the reason for this reduction. While the evolution of the skeletal elements is clear, the correlated changes in the muscle system are ambiguous. Three well-developed pairs of muscles associated with the mandible can be assumed in the ground plan of Trichoptera. Beneath the large cranial adductor and abductor muscles, a thin tentorio-mandibular muscle is present in the spicipalpian (Klemm 1966) and annulipalpian representatives investigated so far. The loss of this muscle in integripalpian representatives (e.g., *Limnephilus*, pers. obs.) can be interpreted as an apomorphy of Integripalpia or one of its subgroups. Otherwise it may be a result of independent reductions. This aspect cannot be reconstructed with the present data and should be investigated more thoroughly. The dimensions of the cranio-mandibular muscles are very heterogeneous. While for *Philopotamus* (see above) and *Rhyacophila* (Klemm 1966) extensively sized muscles are reported, the musculature of phryganeid species is comparatively small and slender (Crichton 1957). Analog to the mandible itself, this could be interpreted as a trend to size-reduction in the evolution of Trichoptera. Interestingly, Klemm (1966) did not find well-developed muscles in all specimens studied. Thus it is also possible that the recorded morphological differences are caused by individual muscle degenerations in the adult stage after eclosion in all caddisflies as proposed by Hinton (1946). Consequently, the reduction of these mandibular muscles should be interpreted as a ground plan feature of Trichoptera. The main drawback of all anatomical studies is the unknown age of the specimens caught in the wild. Further investigations on the development of the musculature from specimens of exactly defined age are needed to answer this question with quantitative data.

The morphology of the digestive tract and its associated musculature is quite uniform throughout Trichoptera. Differences occur only in the origin of the ventral cibarial dilators from below (Philopotamidae, Rhyacophilidae; pers. obs.; Klemm 1966) or from above (Phryganeidae; Crichton 1957) the intraclypeal sulcus. The data at hand suggest that the origin below the intraclypeal sulcus is the plesiomorphic condition in Trichoptera but further comparative studies are necessary to homologize the clypeal dilators of the prepharyngeal tube and to trace their modifications during the evolution of the group.

The presence of a maxillary lobe comprising a large, chemoreceptive galea and a small median lacinia is part of the amphiesmenopteran ground plan (see also Kristensen 2003). These features are widely retained in the trichopteran ground plan (present in Rhyacophilidae [Klemm 1966] and Annulipalpia), except for the loss of a free, well-developed lacinia. A dististipital adductor originating from the anterior tentorial arm is present in almost all trichopteran lineages studied to date. As the muscle is regularly present in basal lepidopterans and other holometabolan insects (e.g., Hannemann 1956; Friedrich et al. 2013; Randolf el al. 2014) its occurrence in Trichoptera is plesiomorphic. Its absence in Phryganeidae (Integripalpia; Crichton 1957) might be autapomorphic for this family. A stipito-lacinial flexor can also be assumed to be part of the ground plan of Amphiesmenoptera since it is well-developed in the non-glossatan moth lineage Micropterigidae (Kristensen 2003) and in the majority of trichopteran lineages. The known exceptions are the annulipalpian families Hydropsychidae and Philopotamidae (pers. obs.). Due to absence of data it is not known if the loss of this muscle is an autapomorphy of the suborder.

The number of maxillary palpomeres in the ground plan of Amphiesmenoptera is five (see Kristensen 2003) as it is in all Annulipalpia and 'Spicipalpia'. It is convergently reduced in males throughout Integripalpia (e.g., Plenitentoria: Limnephilidae, Phryganeidae, Brachycentridae; Brevitentoria: Sericostomatidae [Malicky 1973, 2004]).

The composite haustellum represents the only unequivocal autapomorphy of Trichoptera (Kristensen 1997). The surface structure, i.e., the arrangement of microtrichia, varies notably between the major trichopteran lineages (see e.g., Klemm 1966; Crichton 1957). Representatives of Integripalpia and Rhyacophilidae exhibit longitudinal channels (Klemm 1966; Crichton 1957), whereas the spicipalpian lineages Hydroptilidae and Glossosomatidae show a more transverse arrangement (Kristensen 1997). The latter condition was interpreted as the ground plan condition of Trichoptera by Kristensen (1997), because a very similar arrangement of spines was observed in the infrabuccal pouches of non-glossatan moths. However, the condition of the annulipalpian haustellum does not fit well in this scenario. At the present state of knowledge it is uncertain if the annulipalpian small, granulose haustellum lost the channels secondarily (potential autapomorphy of Annulipalpia) or represents the plesiomorphic condition in Trichoptera. Detailed comparative studies on the haustellum, especially of the fine structure of the channels are needed to infer the homology of these structures in Amphiesmenoptera and to reconstruct the ground plan of Trichoptera.

The flexible roof of the salivarium, moved against the floor by a hypopharyngo-salivary dilator muscle, is usually present in all holometabolan lineages, where it originates from the hypopharynx (most Lepidoptera [Kristensen 2003], Neuroptera [Randolf et al. 2014], many dipterans [Schneeberg & Beutel 2011]) or from the ligula (Megaloptera; Röber 1942). Within Trichoptera this condition is only described for Philopotamidae, but represents a plesiomorphic ground plan feature of the order. It is unknown if this plesiomorphy is also retained in other annulipalpians. In other trichopteran lineages the origin site of the muscle is remarkably modified. It forms an intrasalivarial muscle running longitudinally along the roof of the salivarium in Integripalpia and Rhyacophilidae. A similar condition is also known from many mecopteran groups (e.g., Heddergott 1938; Grell 1938; Friedrich et al. 2013).

A further potential autapomorphy of Trichoptera is the insertion of the premental dilator muscle dorsally on the roof of the salivarium (Fig. 16E,F; Klemm 1966: 2s). The usual attachment sites of this muscle in other holometabolan insects (e.g., Neuropterida [Röber 1942; Randolf et al. 2014]; Hymenoptera [Vilhelmsen 1996]) are the lateral wall or the floor of the salivarium. As the muscle is absent in Lepidoptera (Kristensen 2003) it cannot be assigned to the ground plan of Amphiesmenoptera.

The paired endite lobes of the labium are distinctly developed in Annulipalpia (e.g., Fig. 7F) and Rhyacophilidae (Klemm 1966). Even though the homology to the lepidopteran paraglossa or ligula (Kristensen 2003) remains unclear (see above), the appendages certainly represent a trichopteran ground plan feature. In contrast, the loss of endite lobes in integripalpian lineages is the derived condition and maybe an apomorphy of the suborder.

As pointed out earlier only the evolution of some features of the adult head in Trichoptera can be reconstructed with the data at hand. The lack of comparative data for the majority of families renders the reconstruction of evolutionary scenarios for the suborders almost impossible. Furthermore, the assignment of anatomical features to the trichopteran ground plan is strongly hampered by the unresolved placement of the 'spicipalpian' families. Additionally, detailed and comprehensive information on internal morphology is also needed for the non-cephalic tagmata of adults and other life stages. The anatomy of an extensive number of trichopteran lineages should be investigated to infer the phylogenetic relationship of the order based on morphological characters, to test phylogenies from molecular data, and to trace the evolution of major morphological and behavioral traits within the order.

5. Acknowledgements

We are very grateful to Univ.-Prof. Dr. Hans Malicky (Lunz am See, Austria) for his help during the collecting of *P. ludificatus* and also for providing additional material from his valuable collection. Prof. Dr. Niels Peder Kristensen (University of Copenhagen) helped to improve the manuscript during numerous fruitful discussions about the morphology of Amphiesmenoptera. His outstanding contribution is greatly acknowledged. Furthermore, we thank Dr. Klaus-Dieter Klass (Senckenberg Naturhistorische Sammlungen Dresden), Dr. Benjamin Wipfler (University of Jena) and one anonymous reviewer for helpful comments which greatly improved the manuscript. We thank Rommy Petersohn (University of Jena) for the preparation of histological section series. Renate Walter (University of Hamburg) prepared SEM samples and helped us with the digitalization of histological section series. This is also greatly acknowledged. We thank the DESY facility, Hamburg (project number: I-20100317) for the possibility to obtain high quality SR-µCT-data at storage ring DORIS III. We thank Prof. Dr. Rolf G. Beutel (University of Jena) for offering us the opportunity to use Bitplane Imaris software in his lab. A research stay of MK in Copenhagen was supported by a grant from the European Commission's (FP 7) Integrated Infrastructure Initiative programme SYNTHESYS (DK-TAF-4052) which is kindly appreciated. The financial support for the project provided by the Deutsche Forschungsgemeinschaft (DFG) (FR 3062/2-1) is greatly acknowledged. The support of Dr. Ralph S. Peters (Forschungsmuseum A. Koenig, Bonn) in this matter is also acknowledged.

6. References

Beckmann F., Donath T., Fischer J., Dose T., Lippmann T., Lottermoser L., Martins R.V., Schreyer A. 2006. New developments for synchrotron-radiation-based microtomography at DESY. – Proceedings of SPIE **6318**: 1–10.

Beckmann F., Herzen J., Haibel A., Müller B., Schreyer A. 2008. High density resolution in synchrotron-radiation-based attenuation-contrast microtomography. – Proceedings of SPIE **7078**: D-1–10.

Bernhard C.G., Gemne G., Sällström J. 1970. Comparative ultrastructure of corneal surface topography in insects with aspects on phylogenesis and function. – Zeitschrift für Vergleichende Physiologie **67**: 1–25.

Bernhard C.G., Miller W.H. 1962. A corneal nipple pattern in insect compound eyes. – Acta Physiologica Scandinavica **56** (3–4): 385–386.

Beutel R.G., Friedrich F., Ge S.-Q., Yang X.-K. 2014. Insect Morphology and Phylogeny. A textbook for students of entomology. – Walter de Gruyter, Berlin, Boston. 516 pp.

Beutel R.G., Friedrich F., Hörnschemeyer T., Pohl H., Hünefeld F., Beckmann F., Meier R., Misof B., Whiting M.F., Vilhelmsen L. 2011. Morphological and molecular evidence converging upon a robust phylogeny of the megadiverse Holometabola. – Cladistics **27**(4): 341–355.

Chamorro M.L., Holzenthal R.W. 2011. Phylogeny of Polycentropodidae Ulmer, 1903 (Trichoptera: Annulipalpia: Psychomyioidea) inferred from larval, pupal and adult characters. – Invertebrate Systematics **25**: 219–253.

Chaudonneret J. 1990. Les Pièces Buccales des Insectes. Thème et Variations. – Édition hors Série du Bulletin Scientifique de Bourgogne. 255 pp.

Crichton M.I. 1957. The structure and function of the mouth parts of adult caddis flies (Trichoptera). – Philosophical Transactions of the Royal Society B **241**: 45–91.

Crichton M.I. 1989. A scanning electron microscope study of the mouth parts of adult *Phryganea grandis* (L.) (Trichoptera). Pp. 329–333 in: Tomaszewski C. (ed.), Proceedings of the 6th International Symposium on Trichoptera. – Adam Mickiewicz Press, Poznan.

Crichton M.I. 1992. A scanning electron microscope study of the mouth parts of some adult Limnephilidae (Trichoptera). Pp. 45–48 in: Otto C. (ed.), Proceedings of the 7th International Symposium on Trichoptera. – Backhuys Publishers, Leiden.

Cummings B.F. 1914. Note on the characters of the head and mouthparts in the genera *Plectrotarsus* and *Æthaloptera* (Trichoptera). – Annals and Magazine of Natural History **14**(8): 22–31.

Demoulin G. 1960. Quelques remarques sur la composition segmentaire de la tete des Insectes. Part I: Variations de la capsule céphalique de la larve à l'adulte, chez quelques insectes mécoptéroides. – Bulletin Institut Royal des Sciences Naturelles de Belgique **36**(18): 1–12.

Denis J.R., Bitsch J. 1973. Morphologie de la tête des insectes. In: Grassé P.P. (ed.), Traité de Zoologie VIII(1). – Masson et Cie, Paris. 593 pp.

Deoras P.J. 1943. On the comparative morphology and evolution of adult Trichoptera. Part I: External morphology. – Indian Journal of Entomology **5**: 177–188.

Despax R. 1951. Ordre des Trichoptères. In: Grassé P.P. (ed.), Traité de Zoologie X(1). – Masson et Cie, Paris. pp. 125–173.

Drilling K., Klass K.-D. 2010. Surface structures of the antenna of Mantophasmatodea (Insecta). – Zoologischer Anzeiger **249**: 121–137.

Ehnbom K. 1948. Studies on the central and sympathetic nervous system and some sense organs in the head of neuropteroid insects. – Opuscula Entomologica Supplementum **8**: 1–162.

Faucheux M.J. 2004. Antennal sensilla of Trichoptera and Lepidoptera: Phylogenetic considerations. – Bulletin de l'Institut Royal des Sciences Naturelles de Belgique, Entomologie **74**: 69–71.

Frania H.E., Wiggins G.B. 1997. Analysis of morphological and behavioural evidence for the phylogeny and higher classification of Trichoptera (Insecta). – Royal Ontario Museum Life Sciences Contributions **160**: 1–67.

Friedrich F., Beutel R.G. 2010. Goodbye Halteria? The thoracic morphology of Endopterygota (Insecta) and its phylogenetic implications. – Cladistics **26**(6): 579–612.

Friedrich F., Pohl H., Beckmann F., Beutel R.G. 2013. The head of *Merope tuber* (Meropeidae) and the phylogeny of Mecoptera (Hexapoda). – Arthropod Structure & Development **42**(1): 69–88.

Friedrich F., Matsumura Y., Pohl H., Bai M., Hörnschemeyer T., Beutel R.G. 2014. Insect morphology in the age of phylogenomics: innovative techniques and its future role in systematics. – Entomological Science **17**(1): 1–24.

Grell K.G. 1938. Der Darmtraktus von *Panorpa communis* L. und seine Anhänge bei Larve und Imago (Ein Beitrag zur Anatomie und Histologie der Mecopteren). – Zoologische Jahrbücher, Abteilung für Anatomie und Ontogenie der Tiere **64**: 1–86.

Hagberg M. 1986. Ultrastructure and central projections of extraocular photoreceptors in caddisflies (Insecta: Trichoptera). – Cell and Tissue Research **245**: 643–648.

Hallberg E., Hagberg M. 1986. Ocellar fine structure in *Caenis robusta* (*Ephemeroptera*), *Trichostegia minor*, *Agrypnia varia*, and *Limnephilus flavicornis* (*Trichoptera*). – Protoplasma **135**: 12–18.

Handlirsch A., Beier M. 1936. Trichoptera oder Köcherfliegen. Pp. 1491–1548 in: Kükenthal W., Krumbach T. (eds), Handbuch der Zoologie IV. Band: Arthropoda – 2. Hälfte: Insecta. 2. Teil: Spezielles. – Walter de Gruyter, Berlin, New York.

Hannemann H.J. 1956. Die Kopfmuskulatur von *Micropteryx calthella* L. (Lep.). Morphologie und Funktion. − Zoologische Jahrbücher, Abteilung für Anatomie und Ontogenie der Tiere **75**: 177–206.

Heddergott H. 1938. Kopf und Vorderdarm von *Panorpa communis* L. – Zoologische Jahrbücher, Abteilung für Anatomie und Ontogenie der Tiere **65**: 229−294.

Hinton H.E. 1946. A new classification of insect pupae. − Journal of Zoology **116**(2): 282−328.

Hinton H.E. 1958. The phylogeny of the panorpoid orders. – Annual Review of Entomology **3**: 118−206.

Holzenthal R.W., Blahnik R.J., Prather A.L., Kjer K.M. 2007a. Order Trichoptera Kirby, 1813 (Insecta), Caddisflies. – Zootaxa **1668**: 639–698.

Holzenthal R.W., Blahnik R.J., Kjer K.M., Prather A.P. 2007b. An update on the phylogeny of caddisflies (Trichoptera). Pp. 143–153 in: Bueno-Soria J., Barba-Alvarez R., Armitage B. (eds), Proceedings of the 12th International Symposium on Trichoptera. – The Caddis Press, Columbus, Ohio.

Holzenthal R.W., Morse J.C., Kjer K.M. 2011. Order Trichoptera Kirby, 1813. In: Zhang Z.-Q. (ed.), Animal biodiversity: An outline of higher-level classification and survey of taxonomic richness. – Zootaxa **3148**: 209–211.

Ivanov V.D. 1997. Rhyacophiloidea: a paraphyletic taxon. Pp. 189–193 in: Holzenthal R.W., Flint Jr. O.S. (eds), Proceedings of the 8th International Symposium on Trichoptera. – Ohio Biological Survey, Columbus, Ohio.

Kéler S. von 1955. Entomologisches Wörterbuch mit besonderer Berücksichtigung der morphologischen Terminologie. – Akademie-Verlag, Berlin. 679 pp.

Kjer K.M., Blahnik R.J., Holzenthal R.W. 2002. Phylogeny of caddisflies (Insecta, Trichoptera). – Zoologica Scripta **31**: 83–91.

Klass K.-D., Eulitz U. 2007. The tentorium and anterior head sulci in Dictyoptera and Mantophasmatodea (Insecta). – Zoologischer Anzeiger **246**: 205–234.

Klemm N. 1966. Die Morphologie des Kopfes von *Rhyacophila* Pict. (Trichoptera). – Zoologische Jahrbücher, Abteilung für Anatomie und Ontogenie der Tiere **83**: 1–51.

Kristensen N.P. 1997. Early evolution of the Lepidoptera + Trichoptera lineage: phylogeny and the ecological scenario. In: Grandcolas P. (ed.), The Origin of Biodiversity in Insects: Phylogenetic Tests of Evolutionary Scenarios. – Mémoires du Muséum National d'Histoire Naturelle **173**: 253–271.

Kristensen N.P. 2003. Skeleton and muscles: adults. Pp. 39–131 in: Kristensen N.P. (volume ed.), Handbuch der Zoologie. Band IV: Arthropoda: Insecta. Teilband 36: Lepidoptera, Moths and Butterflies. Volume 2: Morphology, Physiology, and Development. – Walter de Gruyter, Berlin, New York. 564 pp.

Kristensen N.P., Nielsen E.S. 1979. A new subfamily of micropterigid moths from South America. A contribution to the morphology and phylogeny of the Micropterigidae, with a generic catalogue of the family (Lepidoptera: Zeugloptera). – Steenstrupia **5**(7): 69–147.

Lucas R. 1893. Beiträge zur Kenntnis der Mundwerkzeuge der Trichoptera. – Archiv für Naturgeschichte **59**: 285–330.

Malicky H. 1973. Trichoptera (Köcherfliegen). In: Helmcke J.-G., Starck D., Wermuth H. (eds), Handbuch der Zoologie. IV. Band: Arthropoda – 2. Hälfte: Insecta. 2. Teil: Spezielles. – Walter de Gruyter, Berlin, New York. 114 pp.

Malicky H. 2001. Notes on the taxonomy of *Rhadicoleptus*, *Ptilocepus* and *Pseudoneureclipsis*. – Braueria **28**: 19–20.

Malicky H. 2004. Atlas der Europäischen Köcherfliegen. Second Edition. – Springer Verlag, Dordrecht. 359 pp.

Malicky H. 2005. Ein kommentiertes Verzeichnis der Köcherfliegen (Trichoptera) Europas und des Mediterrangebietes. – Linzer Biologische Beiträge **37**(1): 533–596.

Malm T., Johanson K.A., Wahlberg N. 2013. The evolutionary history of Trichoptera (Insecta): A case of successful adaptation to life in freshwater. – Systematic Entomology **38**(3): 459–473.

Matsuda R. 1965. Morphology and evolution of the insect head. – Memoirs of the American Entomological Institute **4**: 1–240.

Melnitsky S.I., Ivanov V.D. 2011. Structure and localization of sensilla on antennae of caddisflies (Insecta: Trichoptera). – Journal of Evolutionary Biochemistry and Physiology **47**(6): 593–602.

Meyer-Rochow V.B., Stringer I. 1993. A system of regular ridges instead of nipples on a compound eye that has to operate near the diffraction limit. – Vision Research **33**(18): 2645–2647.

Mickoleit G. 1971. Das Exoskelett von *Notiothauma reedi* Mac Lachlan, ein Beitrag zur Morphologie und Phylogenie der Mecoptera (Insecta). – Zeitschrift für Morphologie der Tiere **69**: 318–362.

Moulins M. 1971. La cavité préorale de *Blabera craniifer* Burm. (Insecte, Dictyoptère) et son innervation: Etude anatomo-histologique de l'epipharynx et l'hypopharynx. – Zoologische Jahrbücher, Abteilung für Anatomie und Ontogenie der Tiere **88**(4): 527–586.

Neboiss A. 1991. Comparative study of tentorial structures in caddis-flies (Trichoptera). Pp. 283–290 in: Tomaszewski C. (ed.), Proceedings of the 6th International Symposium on Trichoptera. – Adam Mickiewicz University Press, Poznań.

Nielsen E.S., Kristensen N.P. 1996. The Australian moth family Lophocoronidae and the basal phylogeny of the Lepidoptera-Glossata. – Invertebrate Taxonomy **10**: 1199–1302.

Oláh J., Johanson K.A. 2007. Trinominal terminology for cephalic setose warts in Trichoptera (Insecta). – Braueria **34**: 43–50.

Peters R.S., Meusemann K., Petersen M., Mayer C., Wilbrandt J., Ziesmann T., Donath A., Kjer K.M., Aspöck U., Aspöck H., Aberer A., Stamatakis A., Friedrich F., Hünefeld F., Niehuis O., Beutel R.G., Misof B. 2014. The evolutionary history of holometabolous insects inferred from transcriptome-based phylogeny and comprehensive morphological data. – BMC Evolutionary Biology **14**: 52.

Pohl H. 2010. A scanning electron microscopy specimen holder for viewing different angles of a single specimen. – Microscopy Research and Technique **73**: 1073–1076.

Randolf S., Zimmermann D., Aspöck U. 2014. Head anatomy of adult *Nevrorthus apatelios* and basal splitting events in Neuroptera (Neuroptera: Nevrorthidae). – Arthropod Systematics and Phylogeny **72**(2): 111−136.

Ross H.H. 1956. Evolution and Classification of the Mountain Caddisflies. – The University of Illinois Press, Urbana. 213 pp.

Röber H. 1942. Morphologie des Kopfes und des Vorderdarmes der Larve und Imago von *Sialis flavilatera*. – Zoologische Jahrbücher, Abteilung für Anatomie und Ontogenie der Tiere **67**: 61–118.

Schmid F. 1989. Les Hydrobiosides (Trichoptera, Annulipalpia). – Bulletin de l'Institut Royal des Sciences Naturelles de Belgique, Entomologie **59** Supplement: 154 pp.

Schmid F. 1998. Genera of the Trichoptera of Canada and adjoining or adjacent United States. In: Haynes R.H. (ed.), The Insects and Arachnids of Canada. Part 7. – NRC Research Press, Ottawa. 319 pp.

Schneeberg K., Beutel R.G. 2011. The adult head structures of Tipulomorpha (Diptera, Insecta) and their phylogenetic implications. – Acta Zoologica **92**: 316–343.

Snodgrass R.E. 1935. Principles of Insect Morphology. – McGraw-Hill Book Company, New York, London. 667 pp.

Snodgrass R.E. 1963. A contribution toward an encyclopedia of insect anatomy. – Smithsonian Miscellaneous Collections **146**: 1–48.

Tillyard R.J. 1923. On the mouth parts of the Micropterygoidea (Lep.). – Transactions of the Entomological Society of London 1923: 181–206.

Vilhelmsen L. 1996. The preoral cavity of lower Hymenoptera (Insecta): comparative morphology and phylogenetic significance. – Zoologica Scripta **25**(2): 143–170.

Weaver III J.S. 1984. The evolution and classification of Trichoptera, Part I: The ground plan of Trichoptera. Pp. 413−419 in: Morse J.C. (ed.), Proceedings of the 4th International Symposium on Trichoptera. – Dr. W. Junk Publishers, The Hague, Boston, Lancaster.

Wipfler B., Machida R., Müller B., Beutel R.G. 2011. On the head morphology of Grylloblattodea (Insecta) and the systematic position of the order, with a new nomenclature for the head muscles of Dicondylia. – Systematic Entomology **36**(2): 241–266.

Wiggins G.B., Wichard W. 1989. Phylogeny of pupation in Trichoptera, with proposals on the origin and higher classification of the order. – Journal of the North American Benthological Society **8**: 260–276.